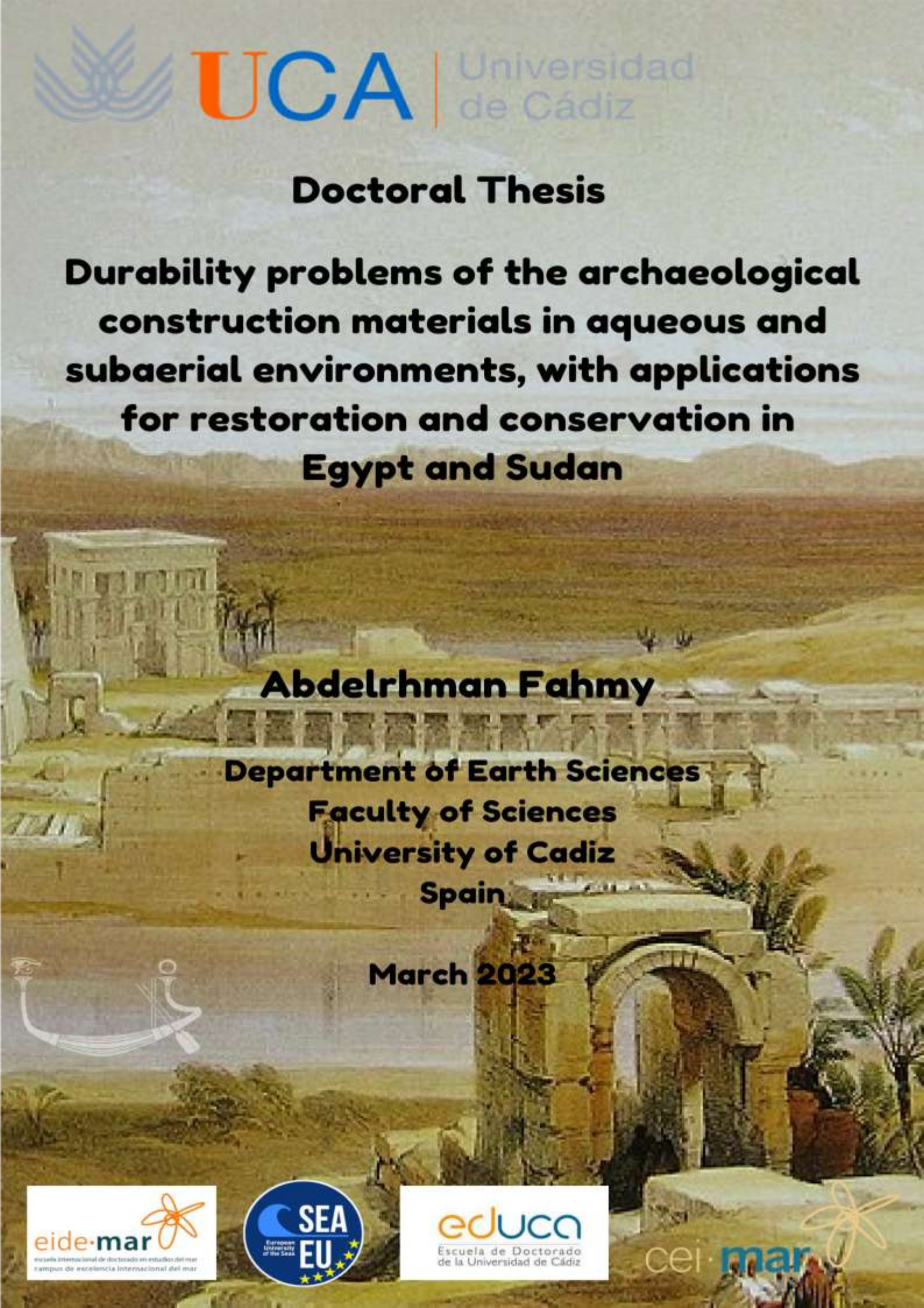
UCA | Universidad de Cádiz

Doctoral Thesis

Durability problems of the archaeological construction materials in aqueous and subaerial environments, with applications for restoration and conservation in Egypt and Sudan



Abdelrhman Fahmy

Department of Earth Sciences
Faculty of Sciences
University of Cadiz
Spain

March 2023

eide·mar
escuela internacional de doctorado en estudios del mar
campus de excelencia internacional del mar

SEA EU
European University of the Seas

educa
Escuela de Doctorado de la Universidad de Cádiz

cei·mar

Durability problems of the archaeological construction materials in aqueous and subaerial environments, with applications for restoration and conservation in Egypt and Sudan

Tesis Doctoral (Doctoral thesis)
El autor (Author): Abdelrhman Fahmy

Tesis Doctoral (Doctoral Thesis)

Durability problems of the archaeological construction materials in aqueous and subaerial environments, with applications for restoration and conservation in Egypt and Sudan.

Problemas de durabilidad de los materiales de construcción arqueológicos en ambientes acuosos y subaéreos, con aplicaciones a la restauración y conservación en Egipto y Sudán.

Autor (Author): Abdelrhman Muhamed Fahmy Sayed Ahmed

Directores (Directors): Salvador Domínguez Bella and Eduardo Molina Piernas

Faculty of Sciences

Department of Earth Sciences

University of Cadiz

Spain

March-2023

Durability problems of the archaeological construction materials in aqueous and subaerial environments, with applications for restoration and conservation in Egypt and Sudan

Tesis Doctoral (Doctoral thesis)
El autor (Author): Abdelrhman Fahmy

Validación de la Tesis Doctoral

Salvador Domínguez Bella, Catedrático del Departamento de Ciencias de la Tierra de la Universidad De Cádiz, y Eduardo Molina Piernas, Doctor del Departamento de Ciencias de la Tierra de la Universidad De Cádiz.

HACEN CONSTAR: que la presente Tesis Doctoral titulada "Problemas de durabilidad de los materiales arqueológicos de construcción en ambientes acuosos y subaéreos, con aplicaciones a la restauración y conservación en Egipto y Sudán", elaborada por D. Abdelrhman Muhamed Fahmy Sayed Ahmed, pasaporte A20325343, con máster en Ciencias de la Conservación y Restauración Arqueológica, ha sido realizada bajo nuestra dirección en el Departamento de Ciencias de la Tierra de la Universidad de Cádiz y que, hallándose concluida, autorizamos su presentación a fin de que pueda ser evaluada por el tribunal correspondiente.

Y para que así conste, expedimos y firmamos el presente informe en Puerto Real, Cádiz, a 18 de enero de 2023.

Salvador Domínguez Bella

Fdo:



Eduardo Molina Piernas

Fdo:



UCA Universidad de Cádiz DEPARTAMENTO DE CIENCIAS DE LA TIERRA

Abdelrhman Muhamed Fahmy Sayed Ahmed

Fdo:



Durability problems of the archaeological construction materials in aqueous and subaerial environments, with applications for restoration and conservation in Egypt and Sudan

Tesis Doctoral (Doctoral thesis)
El autor (Author): Abdelrhman Fahmy

Validation of the Doctoral Thesis

Salvador Domínguez Bella, Professor at the Department of Earth Sciences of the University of Cádiz, and Eduardo Molina Piernas, Doctor at the Department of Earth Sciences of the University of Cádiz.

THEY CERTIFY that the Doctoral Thesis entitled "Durability problems of the archaeological construction materials in aqueous and subaerial environments, with applications for restoration and conservation in Egypt and Sudan", written by Mr. Abdelrhman Muhamed Fahmy Sayed Ahmed, Passport A20325343, with a Master's degree in the Archaeological Conservation and Restoration Sciences, has been carried out under our direction in the Department of Earth Sciences of the University of Cádiz. We authorize its submission in order to the University committee can evaluate it.

In witness thereof, we sign this report in Puerto Real, Cádiz, on January 18, 2023.

Salvador Domínguez Bella

Signature:



Eduardo Molina Piernas

Signature:



UCA
Universidad de Cádiz
DEPARTAMENTO DE
CIENCIAS DE LA TIERRA

Abdelrhman Muhamed Fahmy Sayed Ahmed

Signature:



Durability problems of the archaeological construction materials in aqueous and subaerial environments, with applications for restoration and conservation in Egypt and Sudan

Tesis Doctoral (Doctoral thesis)
El autor (Author): Abdelrhman Fahmy

The International Doctorate

The thesis was peer-reviewed by international experts in archaeology and heritage science from France and Portugal as follows:

1. **Patricia Vázquez**

Full Professor. University of Reims Champagne-Ardenne (URCA), 2 esplanade Roland Garros, 51100 Reims, France.

E-mail: patricia.vazquez@univ-reims.fr

ORCID ID: 0000-0002-5392-6451

2. **Carlos Fabião**

Associate professor of Archaeology. Lisbon University, Centro de Arqueologia da Faculdade de Letras da Universidade de Lisboa (Uniarq)

E-mail: cfabiao@campus.ul.pt

http://lisboa.academia.edu/CarlosFabi%C3%A3o

Ciência ID: 4718-7C15-D7C1

ORCID ID: 0000-0001-6588-3930

Durability problems of the archaeological construction materials in aqueous and subaerial environments, with applications for restoration and conservation in Egypt and Sudan

Tesis Doctoral (Doctoral thesis)
El autor (Author): Abdelrhman Fahmy

The International Mention

The researcher carried out an international research stay at the School of Archaeology and Ancient History, University of Leicester, The United Kingdom. The research stay certificate is attached as follows:

UNIVERSITY OF LEICESTER

School of Archaeology and Ancient History
University of Leicester
University Road
Leicester
LE1 7RH
United Kingdom

12/12/2022

Certificate of attendance

School of Archaeology and Ancient History (SAAH) at University of Leicester certifies that Abdelrhman Muhamed Fahmy Sayed Ahmed with NIE Number: Y8196167Q and Passport Number: A20325343 has carried out his research stay as doctoral visiting Scholar from 01/09/2022 to 12/12/2022.

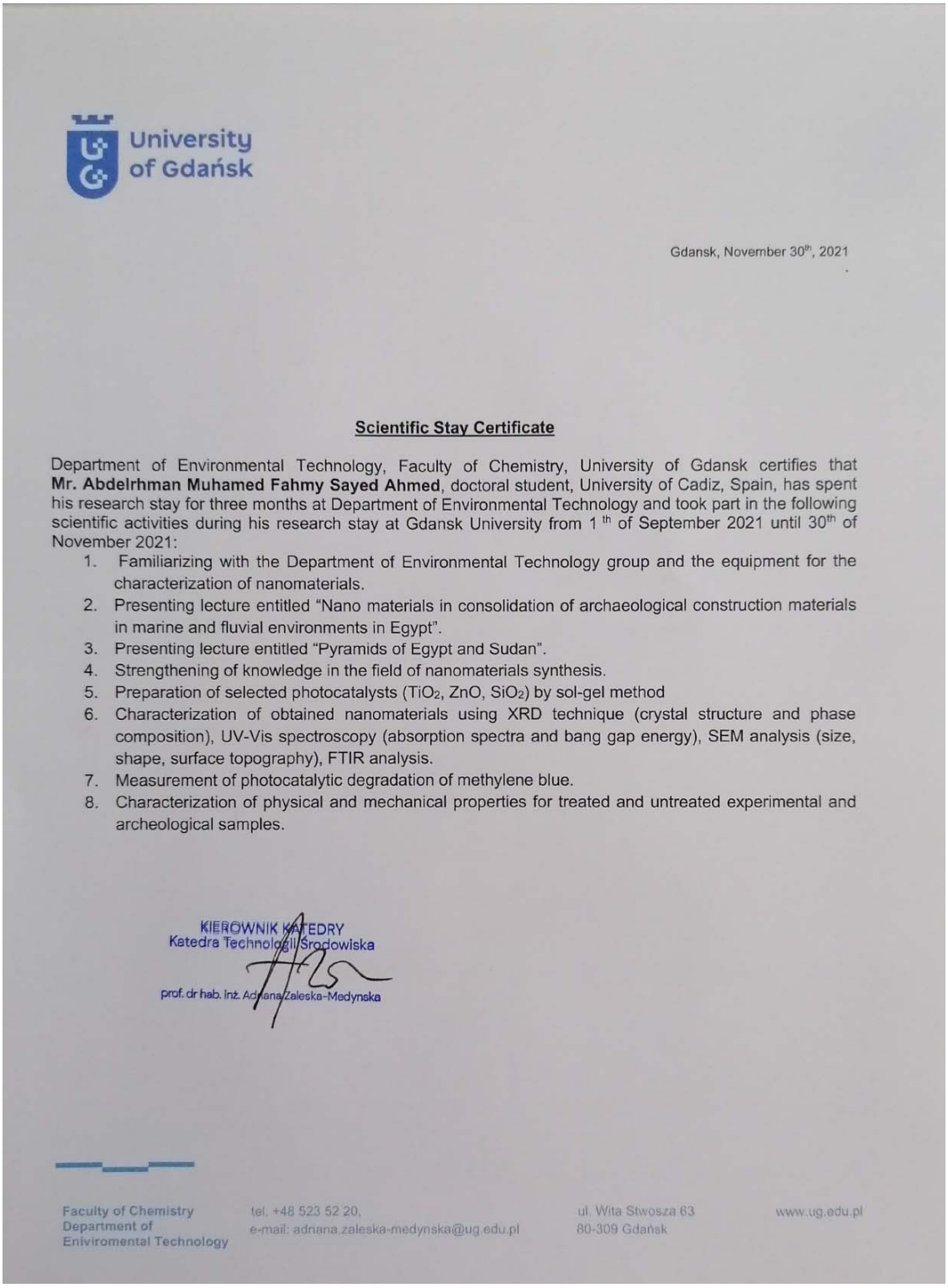
Professor Ruth Young
Director of Research
School of Archaeology & Ancient History

UNIVERSITY OF LEICESTER
School of Archaeology and Ancient History

Durability problems of the archaeological construction materials in aqueous and subaerial environments, with applications for restoration and conservation in Egypt and Sudan

Tesis Doctoral (Doctoral thesis)
El autor (Author): Abdelrhman Fahmy

As well as, the researcher conducted another research stay at the Department of Environmental Technology, Faculty of Chemistry, University of Gdansk, Poland. The certificate of this research stay is enclosed as follows:



University of Gdańsk

Gdansk, November 30th, 2021

Scientific Stay Certificate

Department of Environmental Technology, Faculty of Chemistry, University of Gdansk certifies that **Mr. Abdelrhman Muhamed Fahmy Sayed Ahmed**, doctoral student, University of Cadiz, Spain, has spent his research stay for three months at Department of Environmental Technology and took part in the following scientific activities during his research stay at Gdansk University from 1 th of September 2021 until 30th of November 2021:

1. Familiarizing with the Department of Environmental Technology group and the equipment for the characterization of nanomaterials.
2. Presenting lecture entitled "Nano materials in consolidation of archaeological construction materials in marine and fluvial environments in Egypt".
3. Presenting lecture entitled "Pyramids of Egypt and Sudan".
4. Strengthening of knowledge in the field of nanomaterials synthesis.
5. Preparation of selected photocatalysts (TiO_2, ZnO, SiO_2) by sol-gel method
6. Characterization of obtained nanomaterials using XRD technique (crystal structure and phase composition), UV-Vis spectroscopy (absorption spectra and bang gap energy), SEM analysis (size, shape, surface topography), FTIR analysis.
7. Measurement of photocatalytic degradation of methylene blue.
8. Characterization of physical and mechanical properties for treated and untreated experimental and archeological samples.

KIEROWNIK KATEDRY
Katedra Technologii Środowiska
prof. dr hab. Inż. Adriana Zaleska-Medynska

Faculty of Chemistry
Department of
Enviromental Technology

tel. +48 523 52 20,
e-mail: adriana.zaleska-medynska@ug.edu.pl

ul. Wita Stwosza 63
80-309 Gdańsk

www.ug.edu.pl

Durability problems of the archaeological construction materials in aqueous and subaerial environments, with applications for restoration and conservation in Egypt and Sudan

Tesis Doctoral (Doctoral thesis)
El autor (Author): Abdelrhman Fahmy

CERTIFICADO DE PARTICIPACIÓN

D.FIDEL MARÍA ECHEVARRÍA NAVAS, Delegado del Rector para la Universidad Europea de los Mares y Coordinador General de la Alianza,

INFORMA

que **ABDELRHMAN MUHAMED FAHMY** ha realizado una estancia en la Universidad de Gdansk a través de las Becas Talento en el "*estudio de las aplicaciones de la nanotecnología en la protección de superficies de piedra arqueológica*", celebrado entre los días **1 a 30 de septiembre de 2021**.

Fdo.: D. Fidel Mª Echevarría Navas

Delegado del Rector para la Universidad Europea de los Mares

Fecha de emisión: **22/11/2021**

CERTIFICATE OF COMPLETION

Mr. FIDEL MARÍA ECHEVARRÍA NAVAS, Rector's Delegate for the European University of the Seas and General Coordinator of SEA-EU

INFORMS

that: **ABDELRHMAN MUHAMED FAHMY** has made a stay in the University of Gdansk through the Becas Talento in "*the study of the applications of nanotechnology in the protection of archaeological stone surfaces*", held between **September 1 to 30, 2021**

Signed: Mr. Fidel Mª Echevarría Navas

Delegate of the Rector for the European University of the Seas

Issue date: **22/11/2021**

CSV (Código de Verificación Segura)	IV7F2O72BPRTQT6MBQNSD52BGU	Fecha	24/11/2021 11:08:54
Normativa	Este documento incorpora firma electrónica reconocida de acuerdo a la ley 6/2020, de 11 de noviembre, reguladora de determinados aspectos de los servicios electrónicos de confianza	Validez del documento	Original
Firmado por	FIDEL MARIA ECHEVARRIA NAVAS		
Url de verificación	https://sede.uca.es/verifirma/code/IV7F2O72BPRTQT6MBQNSD52BGU	Página	6/6

Durability problems of the archaeological construction materials in aqueous and subaerial environments, with applications for restoration and conservation in Egypt and Sudan

Tesis Doctoral (Doctoral thesis)
El autor (Author): Abdelrhman Fahmy

In addition, the researcher conducted a research stay (ERASMUS+ KA107) Between Cairo University (Egypt) and University of Cadiz (Spain). The completion certificate is attached as follows:

Vicerrectorado de Internacionalización
Vice-rectorate for Internationalization

Hospital Real
Plaza Falla, 8 | 11003 Cádiz
Tlfno. 956 015066
vicerrectorado.internacionalizacion@uca.es
https://internacional.uca.es/

CERTIFICADO DE ESTANCIA

Certificate of Attendance

UNIVERSIDAD DE CADIZ, España

University of Cadiz, Spain

E CADIZ01

CERTIFICA QUE:/ **This is to certify that:**

Mr Abdelrhman Muhamed FAHMY SAYED

Número de pasaporte/**Passport Number** A20325343

Área de estudios/ **Field of studies** Earth sciences

Universidad de origen / **Home University**: UNIVERSIDAD DE EL CAIRO

EGIPTO

realizó una estancia por estudios en el marco del programa ERASMUS+ KA107 SMS IN en nuestra institución entre/ **performed a Student Mobility for Studies specified under the ERASMUS+ KA107 SMS IN programme at our institution between**

2020-09-22 and 2021-02-07**

en la Facultad/Escuela/ **at the Faculty/Schoo**l: ESCUELA INTERN. DOCTORADO ESTUDIOS MAR.

2021-02-22

Fecha/Date (*)

(*) La fecha de firma no debería de ser anterior a la fecha de la finalización de la estancia/ The date of signature should not be before the date of departure

RAFAEL JIMENEZ CASTAÑEDA

VICERRECTOR DE INTERNACIONALIZACIÓN

**Debido al estado de alarma provocado por el COVID-19, la Universidad de Cádiz implantó la teledocencia y practicas presenciales a partir del 10 de noviembre y hasta el final de semestre./ Due to the COVID-19 alarm, the University of Cádiz has used the online learning for lessons and face to face for practical parts from 10th November until the end of the semester.

Código Seguro de verificación:7Paj4fJubah3v3UkTzN5hQ==. Permite la verificación de la integridad de una copia de este documento electrónico en la dirección: https://verificarfirma.uca.es
Este documento incorpora firma electrónica reconocida de acuerdo a la Ley 59/2003, de 19 de diciembre, de firma electrónica.

FIRMADO POR	RAFAEL JIMENEZ CASTAÑEDA		FECHA	27/02/2021
ID. FIRMA	angus.uca.es	7Paj4fJubah3v3UkTzN5hQ==	PÁGINA	1/1

7Paj4fJubah3v3UkTzN5hQ==

Durability problems of the archaeological construction materials in aqueous and subaerial environments, with applications for restoration and conservation in Egypt and Sudan

Tesis Doctoral (Doctoral thesis)
El autor (Author): Abdelrhman Fahmy

Furthermore, the researcher conducted a research stay at the Faculty of Geology and Geography, University of Sofia, Bulgaria. The certificate of this research stay is enclosed as follows:

СОФИЙСКИ УНИВЕРСИТЕТ
„СВ. КЛИМЕНТ ОХРИДСКИ"
ГЕОЛОГО-ГЕОГРАФСКИ
ФАКУЛТЕТ

SOFIA UNIVERSITY
ST. KLIMENT OHRIDSKI
FACULTY OF
GEOLOGY AND GEOGRAPHY

CERTIFUCATE

The Faculty of Geology and Geography at the Sofia University "St, Kliment Ohridski" confirms that the PhD student Abdelrhman Muhamed Fahmy Sayed Ahmed from Cadiz University Spain took part in the following activities during the visit in Sofia from 1th of May to 30th of July:

1. Microscopic observation of thin sections from archeological artefacts and microphotographs with polarizing microscope Leica 750P.
2. X-ray diffraction of archeological samples with X-ray Brucker facility.
3. SEM investigation and photography under high magnification with LYRA\TESCAN microscope
4. Taking part in archeological excavations in the area of Pliska (NE Bulgaria)

July, 26 2021

Dean of the Faculty:

(Assoc. Prof. Dr. Kliment Naydenof)

България, София 1504, бул. Цар Освободител 15
тел.: +359 2 846 7057; факс: +359 2 944 6487
www.uni-sofia.bg; decanat@gea.uni-sofia.bg

Bulgaria, 1504 Sofia, 15 Tsar Osvoboditel Blvd.
phone: +359 2 846 7057; fax: +359 2 944 6487
www.uni-sofia.bg; decanat@gea.uni-sofia.bg

Durability problems of the archaeological construction materials in aqueous and subaerial environments, with applications for restoration and conservation in Egypt and Sudan

Tesis Doctoral (Doctoral thesis)
El autor (Author): Abdelrhman Fahmy

At last, the researcher carried out an international mobility (online mode) at the International relations office - Worcester International (University of Worcester, the United Kingdom). The certificate of this research stay is enclosed as follows:

compostela GROUP OF UNIVERSITIES GRUPO DE UNIVERSIDADES

CGU Stella Junior 2021

Mobility and training programme for students

Programa de movilidad y formación para estudiantes

STELLA JUNIOR CERTIFICATE / CERTIFICADO STELLA JUNIOR

Ms M.ª Teresa Carballeira Rivera, Executive Secretary of the Compostela Group of Universities (CGU), recognised as an association of public benefit, with CIF G15520307 and registered in the Spanish National Register for Associations under the number 145.292, hereby	Doña M.ª Teresa Carballeira Rivera, secretaria ejecutiva del Grupo Compostela de Universidades (GCU), entidad declarada de utilidad pública, con CIF G15520307 e inscrita en el Registro Nacional de Asociaciones con el número 145.292, por el presente,
DECLARES	CERTIFICA
That, within the programme *Stella Junior* of the CGU,	Que, en el marco del programa *Stella Junior* del GCU,

Mr/D. Abdelrhman Muhamed Fahmy Sayed AHMED, pasaporte/passport A20325343

has successfully completed a professional internship, in virtual mode, at the International Experience Team – Worcester International (University of Worcester, United Kingdom), from 14/09/2021 to 22/10/2021.	ha completado con éxito sus prácticas profesionales, en modalidad virtual, en el Equipo de Experiencia Internacional – Worcester International (Universidad de Worcester, Reino Unido), entre el 14/09/2021 y el 22/10/2021.
And so it is stated, and to take effects on the applicant's curriculum vitae, this document is issued in Santiago de Compostela, on 2 February 2022.	Y para que conste y surta los oportunos efectos en el currículo del solicitante, se extiende el presente documento en Santiago de Compostela, el 2 de febrero de 2022.

Signature/Firma:

32632621Z MARIA TERESA CARBALLEIRA (R: G15520307)

Firmado digitalmente por 32632621Z MARIA TERESA CARBALLEIRA (R: G15520307)
Nombre de reconocimiento (DN): 2.5.4.3=#0c4533323633323132...
TERESA, sn=CARBALLEIRA RIVERA, cn=32632621Z MARIA TERESA CARBALLEIRA (R: G15520307), 2.5.4.97=VATES-G15520307, o=74205-46 R.JPO COMPOSTELA DE UNIVERSIDADES, c=ES
Fecha: 2022.02.02 11:21:29 +01'00'

Compostela Group of Universities · Casa da Cuncha, Rúa da Conga, 1, P.C.: E-15782 Santiago de Compostela
Tel.: +34 881 812 931/4/5 Fax: +34 881 812 932 · grupo.compostela@usc.es / www.gcompostela.org

Durability problems of the archaeological construction materials in aqueous and subaerial environments, with applications for restoration and conservation in Egypt and Sudan

Tesis Doctoral (Doctoral thesis)
El autor (Author): Abdelrhman Fahmy

Assessment of the committee (Defence date: 31st/03/2023)

1. **Myriam Seco Álvarez (President)**

Associate Professor of Archaeology at the Department of Prehistory and Archaeology, University of Seville, Spain.

Signature:

2. **Macarena Lara Medina (Secretary)**

Interim university professor of Archaeology at the Faculty of History, Geography, and Philosophy, University of Cadiz, Spain.

Signature:

3. **Laura Sophie Basell (Member)**

Professor of Archaeology at the School of Archaeology and Ancient History, University of Leicester, the United Kingdom.

Signature:

Durability problems of the archaeological construction materials in aqueous and subaerial environments, with applications for restoration and conservation in Egypt and Sudan

Tesis Doctoral (Doctoral thesis)
El autor (Author): Abdelrhman Fahmy

Dedication

To my beloved dad (Muhamed Fahmy) and mom (Fatma Muhamed).

To my whole family.

To all people who supported and helped me in my personal and life career,

and to my homeland Egypt.

Durability problems of the archaeological construction materials in aqueous and subaerial environments, with applications for restoration and conservation in Egypt and Sudan

Tesis Doctoral (Doctoral thesis)
El autor (Author): Abdelrhman Fahmy

Acknowledgments

I acknowledge the University of Cadiz for its support and facilities provided to me. In addition, I acknowledge SCiCYT and UGEA-PHAM at the University of Cadiz for carrying out the main part of the archaeometric analysis and access to the laboratories. I would love to acknowledge Professor Salvador Dominguez Bella and his wife Ana who received and hosted me very well and with all kindness. I can consider Salvador the best professor in the world. I acknowledge my friend Dr. Eduardo Molina Piernas who was patient with me, I have learned so much from him about scientific research writing, and he was a professional tutor and reviewer during my doctoral phase. Special thanks to professor Javier Martínez López and Ángel Sánchez Bellón for their helping and supporting me during my doctorate. Many thanks to all department members of Earth sciences at University Cadiz.

Durability problems of the archaeological construction materials in aqueous and subaerial environments, with applications for restoration and conservation in Egypt and Sudan

Tesis Doctoral (Doctoral thesis)
El autor (Author): Abdelrhman Fahmy

Table of contents

Highlights i

Abstract iii

Resumen v

Keywords / Palabras clave vii

Chapter 1: Introduction 1

1.1. Introduction 3

1.2 Research gap 13

1.3 Hypotheses 15

1.4 Objectives. 17

1.5 Significance 19

1.6 Research organization. 21

1.7 References 23

Chapter 2: Cases of study, materials, and methodology 31

2. Study cases and geological context 33

2.1. Archaeological sites in Egypt and Sudan 33

1.1.1. Aswan (Egypt): Abaton temple of Osiris, Philae complex 34

2.1.2. Alexandria (Egypt): Al-Anfushi Necropolis 37

2.1.3. Abusir (Giza, Egypt): Sahure's pyramid 40

2.1.4. El-Ashmonein archaeological site (Minia, Egypt: Nero's Temple) 41

2.1.5. Al Bagrawiya archaeological site (Sudan): Pyramids of Meroe 42

2.2. Regional geological context of the selected sites 43

2.2.1. Aswan (Egypt) 46

2.2.2. Alexandria (Egypt) 47

2.2.3. Abusir (Giza, Egypt) 48

2.2.4. El-Ashmonein archaeological site, Minia (Egypt) 49

2.2.5. Al Bagrawiya archaeological site (Sudan) 51

2.3. Materials 52

2.4. Methodology 57

2.4.1. Chemical and mineralogical, and microscopic analysis 58

2.4.2. Tests 60

2.5. List of Publications (Thesis) 65

2.6. References 75

Chapter 3: Results and discussion 79

Part I: Characterization of construction building materials in aqueous environments 79

3.1. Coastal environment impact on the construction materials of Anfushi's Necropolis (Pharos's Island) in Alexandria, Egypt 81

Highlights 81

Abstract 83

1. Introduction 84

2. The Geographical and Archaeological Context of Anfushi's Necropolis 87

3. Geological Context and Ancient Quarries in Alexandria 92

4. Coastal Geodynamics Context 94

4.1. Sea Level Rise 94

4.2. Earthquakes and Land Subsidence 97

4.3. Environmental Factors 98

4.3.1. Storminess 98

4.3.2. Flooding 99

4.3.3. Meteorological Context 100

4.4. Anthropogenic Damage 102

5. Materials and Methods 102

6. Results 104

6.1. In-Situ Recordings 104

6.2. Sea Level Rise Impact (SRL) and Future Scenarios 109

6.3. Construction Materials Characterization 111

6.3.1. Petrographic description 111

6.3.2. Mineralogical and chemical characterization 114

6.3.3. Macroscopic and microscopic investigation 115

6.4. Digital Mapping 120

7. Discussion 123

8. Conclusions 129

Acknowledgments 130

9. References 131

3.2. Multianalytical diagnostic approaches for the assessment of materials and decay of the archaeological sandstone of Osiris Temple (The Abaton) in Bigeh Island, Philae (Aswan, Egypt) 143

Highlights 143

Graphical abstract 145

Abstract 147

1. Introduction 148

2. Aim of the paper 150

3. Geomorphological and geological context of the quarries and Temple 150

4. Historical and architectural description 153

5. Materials and methods 155

6. Results 157

6.1. Decay patterns of the construction material 157

6.2. Macroscopic and microscopic investigation 159

6.3. Chemical and mineralogical analysis 164

6.4. Physical properties of sandstone 166

7. Discussion and conclusions 167

Acknowledgments 171

8. References 172

Part II: Characterization of construction building materials in subaerial environments 181

3.3. Geoenvironmental investigation of Sahure's pyramid, Abusir Archeological site, Giza, Egypt. 183

Highlights 183

Abstract 185

1. Introduction 186

2. Sahure's pyramid context 191

2.1. Description of Sahure's pyramid 191

2.2. Geological context 193

2.3. Stone quarries and pyramids construction materials..... 195

2.4. Geoenvironmental context..... 196

2.5. Intrinsic factors 200

2.6. Geodynamic factors 201

3. Materials and methods..... 202

4. Results..... 205

4.1. In situ investigation..... 205

4.2. Macro and microscopic description..... 207

4.3. Mineralogical and chemical studies..... 211

4.4. Physical properties..... 216

5. Discussion 217

6. Preservation proposal for the pyramid 222

7. Conclusions..... 223

Acknowledgments 224

8. References..... 225

3.4. Salt weathering impact on Nero/Ramses II Temple at El-Ashmonein archaeological site (Hermopolis Magna), Egypt. 237

Highlights 237

Graphical abstract..... 239

Abstract 241

1. Introduction 242

2. Location, archaeological, and site context 244

3. Materials and methods 247

4. Results 251

4.1. In-situ observation 251

4.2. Petrological study 253

4.3. Mineralogical and elemental analysis of the construction materials 257

4.4. Microscopic investigation 261

5. Discussion 267

6. Conclusions 272

Acknowledgments 274

7. References 275

3.5. Sand dunes movement and flooding risk analysis for the pyramids of Meroe, Al Bagrawiya archaeological site, Sudan 283

Highlights 283

Abstract 285

1. Introduction 286

2. Al Bagrawiya Pyramids' studied area 288

3. Geological and climate context 292

4. Methodology 295

5. Results and discussion 296

5.1. Destruction of the pyramids 296

5.2. Sand dunes and wind impacts 297

5.3. Heavy rains and flash flooding risks 304

5.4. Damage rate and decay patterns of the pyramids 306

6. Conclusion 312

Acknowledgments 312

7. References 313

Part III: Consolidation 321

3.6. Multi-functional monodispersed SiO_2-TiO_2 NPs and TEOS in the consolidation of archaeological lime mortars surfaces. 323

Graphical abstract 325

Abstract 325

Abbreviations and symbols 328

1. Introduction 329

2. Ancient lime mortar decay 333

3. Materials and methods 335

4. Results and discussion 344

4.1. Characterization of the NPs 344

4.2. Physical properties 348

4.3. Spectrophotometric measurements 351

4.4. Hydrophobic properties 351

4.5. Methylene Blue Test (self-cleaning and Photocatalytic test 353

4.6. Mechanical tests 355

4.6.1. Nano-indentation test 355

4.6.2. Uniaxial compressive strength (UCS 357

4.7. Durability assessment 357

4.7.1. Salt crystallization test 357

4.7.2. Thermal aging 359

4.7.3. UV aging 360

5. Conclusion 362

Acknowledgments 363

6. References 364

Chapter 4: General conclusions, original contributions, and future perspectives 373

4.1. General conclusions 375

4.2. Original contributions 379

4.3. Future perspectives 381

Appendixes 383

Annex 1: Supplementary materials for Chapter 3.1 387

Annex 2: Supplementary materials for Chapter 3.2 404

Annex 3: Scientific activities 421

Annex 4: List of publications and contributions 473

Annex 5: Plan of the Investigation 497

Index of Figures

Figure No.	Caption	Page
Chapter 1	**Introduction**	1-30
Fig 1.1	Map of Egypt and its archaeological sites.	7
Fig.1.2	Map of Sudan and its archaeological sites.	8
Chapter 2	**Cases of study, materials and methodology**	31-78
Fig 2.1	The locations of the selected archaeological sites in Egypt (Anfushi Necropolis, Sahure pyramid, Nero Temple and Abaton Temple) and Sudan (Pyramids of Meroe).	34
Fig 2.2	(A) Osiris temple (The Abaton) in Aswan (Bigeh Island) referred in the yellow square (B). (C) Represents the semi- submerged Osiris Temple in in the Nile River (UNESCO archives).	36
Fig 2.3	Map of the archaeological site of Philae temple and Abaton temple of Osiris in Aswan and Nile water surrounding and covering parts of the archaeological buildings such as Abaton temple of Osiris, (Blue: Nile water; yellow and red: dry rocks).	37
Fig 2. 4	Al Anfushi tombs, A) Google Earth image for the location of Al Anfushi tombs (White square), B) General view of Al Anfushi tombs, C) and D) durability problems (salt decay) of the elements and the construction materials of Al Anfushi tombs.	39
Fig 2.5	(A) Location of the site on global earth map. (B) The map of Abusir area (Blue rectangle) and its monuments. (C) General view for Sahure pyramid.	40
Fig 2. 6	(A) Location of El-Ashmonein site on Egypt map. (B) General view for Nero's Temple.	41
Fig 2.7	(A) Green pin is the location of Al Bagrawiya archaeological site. (B) General view for the pyramids of Meroe (The case study).	42

Fig 2. 8	Geological map of Egypt.	44
Fig 2.9	Geological map of Sudan.	45
Fig 2.10	Regional geological setting of Philae area, Aswan.	46
Fig 2.11	Geomorphological units of Alexandria and its lithology.	47
Fig 2.12	General Map of Egypt including the geological setting of the studied area in Abusir in the red circle.	48
Fig 2.13	Geological map of El Minia (from Ibrahim and Lyons, 2017). The yellow rectangle is Mellawy center that includes El-Ashmonein archaeological site.	50
Fig 2.14	Geological map of the studied area is in the yellow circle.	51
Fig 2.15	The collected samples from selected monuments. A) Anfushi's Necropolis, 1 and 2 refers to stone building materials and 3 refer to mortars and plaster. B) Abaton temple in Aswan, 1 and 2 sandstone building materials. C) Sahure pyramid, 1 casing stone, 2 core stone and 3 mortar. D) Nero/Ramses II Temple, 1 stone building material, 2 mortar and 3 Roman Mortar.	54
Fig 2.16	(A) The experimental samples of the prepared lime mortars. (B) Presentation of the used chemicals as raw materials and reagents for the synthesis of SiO_2 and SiO_2-TiO_2 NPs. (C) Various concentrations of SiO_2-TiO_2 NPs which added to 20% TEOS and dispersed in Ethanol.	55
Fig 2.17	Scheme of the current research methodology.	58
Chapter 3	**Results and discussion** **Part I: Characterization of construction building materials in aqueous environments**	79-180
Chapter 3.1	**3.1 Coastal environment impact on the construction materials of Anfushi's Necropolis (Pharos's Island) in Alexandria, Egypt**	79-141

Fig 3.1.1	(A) The geographical location of Anfushi's Necropolis on the coast of the Mediterranean Sea. (B) The general view and the current state of preservation of Anfushi's Necropolis. (C) Ancient Egyptian-style scene.	89
Fig 3.1.2	(A) General map of the endangered coastal archaeological sites in North Africa and the Middle East. (B)Zoomed risk map for the delta (including Alexandria), and the green pin shows the case study of Anfushi's Necropolis as an endangered coastal archaeological site in North Africa, Egypt (Alexandria). (C) Zoomed map for endangered Anfushi's Necropolis and its surrounding coastal environment.	90
Fig 3.1.3	(A) Schematic plans for the five tombs of Anfushi's Necropolis and their architectural elements of the rock-cut tombs and their elements. (B) General view the ground level of the tomb No 4 leads to the burial units and attached rooms. Numbers and red rectangles refer to the image (C). (C) Cross-section for mortar of the tombs, which consists of the support wall (bedrock), coarse rendering mortar [2], and fine rendering mortar for painting [1].	91
Fig 3.1.4	(A) Geological map of Egypt, black rectangle refers to Alexandria, from [**39**]. Detailed maps for soil units (B) and geological map (C) of Alexandria, edited after [**43**]. Black rectangles refer to the study area.	93
Fig 3.1.5	Ancient quarries in Alexandria (green and red stars) with an example of the light-coloured limestone outcrop.	94
Fig 3.1.6	(A-D) Satellite images for the average monthly sea-level rise variations; the pink rectangle refers to Alexandria. From https://climate.nasa.gov/ accessed 13 May 2022.	95

Fig 3.1.7	(A and B) Two scenarios for possible water increases of 0.5 m and 1 m, respectively, and their impact on the territory. Alexandria and the research area are represented in the green dotted square, after [**29**]. (C) Longitudinal profile for the flood line, safe and risk zones for the SLR scenario of 1.5 m. The study area is represented in black rectangular as a risk zone, after [**28**].	96
Fig 3.1.8	(A) General disruption of the historical record of earthquakes in Egypt (2200 BC to 2015 AD). (B) Map of historical earthquakes with their magnitudes from 2200 BC to 1989 AD, after [**61**]. Red squares represent the Alexandria area.	98
Fig 3.1.9	Hyetographs for the meteorological data in Alexandria 2021. After https://www.weather-atlas.com/en/egypt/alexandria-climate Accessed 19 May 2022.	101
Fig 3.1.10	**(**A and B**)** Rare snow falls over Alexandria in December 2021.	102
Fig 3.1.11	(A-B) Construction stones (casing + bedrock). (C) Coarse and fine rendering mortars.	103
Fig 3.1.12	(A and B) Structural damage aspects due to earthquakes. (A) The red rectangle refers to the deformations in the structures. (B) The red arrows refer to the collapse, displacement for the blocks and opened joints, and the red square refers to the damage to walls with chipping. (C) Water intrusion impact on the architectural and structural elements Anfushi's Necropolis. Red arrows refer to biological growth, salt accumulation, and degradation of the stone and painting layers. (D) Geotechnical problems, unconsolidated bedrock with many cavities as shown by the red arrows. (E) Dampness impact over the structural and decorative elements of Tomb No 5(burial unit) at Anfushi's Necropolis. Red arrows refer to	107

	flaking, salt erosion and biological attack on the tomb construction materials [77].	
Fig 3.1.13	(A-C) Different kinds of decay patterns due to the marine environment for the walls. (A) The red rectangle refers to areas with efflorescence, subflorescence, edge eroding, flaking and loss of the painting layer in the courtyard of Tomb No 4. (B) The red arrows refer to flaking, exfoliation, salt erosion, surface disintegration and loss of the painting layer in the courtyard of Tomb No 4. (C) Red squares refer to honeycomb and loss of material decay patterns, and black arrows refer to salt precipitation and loss of the painting layer in the corridor to the burial units of Tomb No 4. (D) A ritual scene in the necropolis and its state of preservation state in 2010from Tomb No. 2 (back wall of the burial chamber) (from https://mapsus.net/EG/necropolis-of-anfushi-5577). (E) The same ritual scene after 8 years, with a worsened state of preservation, where a large loss of the painting layer and renderings occurred due to the salt attack (from https://www.meretsegerbooks.com/gallery/581/anfushi-necropolis).	109
Fig 3.1.14	(A-C) Different decay patterns for various architectural elements of Anfushi's Necropolis, where salt erosion is the main decay pattern on the surfaces in the Tomb No 2 rooms 1 and 2.	110
Fig 3.1.15	(A-F) Various scenarios for SLR influence on Anfushi's Necropolis.	111
Fig 3.1.16	Photomicrographs of the geological and archaeological prepared thin sections. (A and B) Bedrock (BR) oolitic limestone with recrystallized sparitic calcite cement and sand-sized spheres (ooids/oosparite). (C and D) Casing stone (CS), creamy fossiliferous micritic limestone and calcite embedded in a micrite matrix rich in	114

	benthic foraminifera. (E and F) Coarse-grained rendering mortar (CRM) with quartz grains poorly sorted, polycrystalline, and angular to subangular, grains embedded in a micritic matrix with rock fragments. (G and H) Fine-grained rendering mortar (FRM) has well-sorted quartz grains, subangular to rounded, and these grains are embedded in a micritic matrix.	
Fig 3.1.17	(A-D) Photomicrographs under a binocular microscope for the bedrock (BR), casting stone (CS), coarse-grained rendering mortar (CRM) and fine-grained rendering mortar (FRM). Black arrows and rectangles show the ooids, quartz grains, disintegration and salt crusts on different samples. Apparently, salt erosion is the main feature of deterioration for all samples.	117
Fig 3.1.18	Micromorphological features of the construction building materials of Anfushi's Necropolis. (A and B) The oolitic limestone (BR, bedrock) surface texture with halite cubic crystals and needle-like gypsum. (C and D) The fossiliferous micritic limestone (CS, casing stone) morphological texture with halite crystal perceptions, pores and microfissures. (E - H) The coarse-grained rendering mortar (CRM) textural features with disintegrated grains, precipitation of halite (cubes), gypsum (needles), and detection of gaps and pitting. (I and J) Fine-grained rendering mortar (FRM) textural aspects with depositing halite mixed with needle-like crystals of gypsum, in addition to gaps and pitting. Red squares and rectangles refer to the disintegration feature of the samples due to salt weathering impact. Scales are expressed in microns.BR: bedrock; CS casting stone; CRM: coarse-grained rendering mortar; FRM: fine-grained rendering mortar; Hl: halite; Cal: calcite; Qz: quartz; Gp: gypsum.	119

Fig 3.1.19	(A) Micromorphological feature of (BR, bedrock) with halite cubic crystals and needle-like gypsum and the red squares were analyzed elementally using EDS. (B and C) EDS, elemental anylsis results for halite and gypusm salts for one of selected samples from bedrock of the necropolis.	120
Fig 3.1.20	(A-D) Digital restoration for some selected structural and architectural elements in Anfushi's Necropolis (Walls of Tomb No 2, rooms 1 and 2) using AutoCAD 2020.	122
Fig 3.1.21	(A and B) show two satellite images (2012 and 2013) confirming the submergence of the ancient structures. (C)Old photo (1916) of the same area before the submergence of the ancient structures, from [**83**], and a recent Google Earth image (D) for the same area with nourishment interventions.	124
Chapter 3.2	**3.2. Multianalytical diagnostic approaches for the assessment of materials and decay of the archaeological sandstone of Osiris Temple (The Abaton) in Bigeh Island, Philae (Aswan, Egypt)**	143-180
Fig 3.2.1	(A) General map of the study area and the position of Aswan's Old and New Dam (red circles 1 and 3, respectively) and Osiris Temple (red circle 2). (B) Geological features of the area surrounding Osiris Temple, where black squares are the quarries Gebel El Silsila and green squares are quarries of Girtass in Aswan. (C) Digital elevation model and geomorphological features for Aswan, as well as showing Nubian sandstone formations such as the Kurkur Formation. The black dotted rectangle represents the area surrounding the Osiris temple. From [**38**].	152
Fig 3.2.2	(A) General map of Philae monuments, where circles represent the original location of Philae temples (in red), recent place of transferred temples from the original location to the Island of	154

	Agilkia (in blue) and Osiris Temple (Abaton Temple, in yellow). (B) The current state of the temple and its plan section. Modified after [**42**].	
Fig 3.2.3	Hand-samples of the yellow (A) and pink (B) sandstones.	155
Fig 3.2.4	(A) Front and back views of Osiris Temple and their current preservation state and (B) degradation patterns for building materials of the temple**.**	158
Fig 3.2.5	Samples of yellow (S1 and S2) and pink (S3 and S4) sandstones under a digital microscope (DM, left row), polarized optical microscope (POM, two rows in the middle under plane and cross-polarized light, respectively), and scanning electron microscope (SEM, right row) for macro-and microtextural investigation. Dotted blue rectangles refer to the disintegration areas of the sandstone. The blue and yellow arrows show the disintegration, soiling layer, black patina, pores and microfractures and fissures as decay patterns for the sandstones. Legends: (Qz) Quartz; (Cal) Calcite. The mineral legend according to [**46**]**.**	162
Fig 3.2.6	(A) Cross-section of the sandstone (S3) and (B) a detail photography of the black patina by means of digital microscope.SEM photomicrographs of the black patina, where (C) shows a homogeneous distribution of the organic matter, (D) algae filaments (red arrows), and (E-H) different species of fluvial diatoms.	163
Fig 3.2.7	(A) Diffraction patterns for clay minerals after separation and oriented aggregate (OA) preparation of the clay fraction for yellowish and pinkish sandstones. In the black line (untreated OA), red line (OA treated with dimethyl-sulfoxide, +DMS, note the displacement of the kaolinite peak from 7.18 to 11.1 Å), and blue	166

	line (OA heating at 550 °C). (B) Raman spectrum for the four construction sandstones (S1-S4). Legend: Kln: kaolinite; Qz: quartz; Cal: calcite; Hem: hematite; Or: orthoclase.The mineral legend according to [**46**]**.**	
Fig 3.2.8	(A) Old paintings and photos showing the preservation state of the temple in 1838, 1909, and 1970 from left to right, respectively. (B)Water level around the Philae temples and Osiris Temple after building Aswan's Old and New Dams. Modified after [**39**]**.**	169
Chapter 3	**Part II: Characterization of construction building materials in subaerial environments**	181-319
Chapter 3.3	**Geoenvironmental investigation of Sahure's pyramid, Abusir Archeological site, Giza, Egypt**	183-235
Fig 3.3.1	(a) General map of Egypt and location of the Abusir archaeological site in Giza. (b) Pyramids at the Abusir archaeological site and specifically the Sahure's pyramid (edited after http://www.narmer.pl/map/abusir_en.htm). (c) General view of Sahure's pyramid from the causeway of the pyramid. (d) The preservation state of the pyramid.	190
Fig 3.3.2	(a) Cross section and (b) Plan of the Sahure's pyramid. The colors in cross-section represent the white fossiliferous limestone from the Tura quarry (casing stone, in white); the body of the pyramid made by laminated sandy argillaceous limestone (marl, in white gray); granite (casing for entrance and some parts in the corridor, in red); and bedrock from limestone (in dark gray). Edited after [**35**].	192
Fig 3.3.3	(a) General geological map of the Memphis area and (b) a simplified geological map of the Abusir area. As shown in the legend, the	195

	pyramid is connected to the Mokattam formation and Maddi formation. Sahure's pyramid is located on Nile deposits/silt that was deposited directly to cover the Eocene bedrock. Edited after [39].	
Fig 3.3.4	Map of ancient Egyptian quarries (gray squares). The yellow circle refers to the Widan El-Faras quarry, the red circle refers to the Tura and Massara quarries as the source for casting blocks, and the blue circle is the local quarry of the Abusir site as the source for core blocks.	197
Fig 3.3.5	(a) General map of Egypt, where the red square marks the Abusir zone, referring to the Abusir archaeological site in an orange circle (b). (c) The treated satellite image on the NASA Terra satellite (May 2010) explains the dust and sandstorms over Egypt spirally in blue, which extends strongly from the red sea and Nile River to the Mediterranean Sea. The amount of sand and dust thickly exists and results in the total hiding of the land surface below (edited after https://earthobservatory.nasa.gov/images). (d) The treated satellite image from the NASA Terra satellite (April 2012) explains the dust and sandstorms in blue, which extends strongly from north-northeast to south-southwest. The amount of sand and dust is high, resulting in the total hiding of the land surface below (edited after https://earthobservatory.nasa.gov/images).	199
Fig 3.3.6	(a) Image from Google Earth map showing the representative sampling areas for the construction material of the pyramid near Abusir village. The red circle refers to the local quarry from which the core blocks of the pyramid were extracted, and in the blue circle, the place where some fragments were collected from fallen and highly weathered fragments/samples. These fragments	203

	represent the fossiliferous limestone as casing stone and sandy limestone as core building material (b) and the mortar fragment (c).	
Fig 3.3.7	Features of damage and degradation of Sahure's pyramid building materials. (a) Collapsed blocks from core and casing stones due to earthquakes and environmental impacts (blue rectangle). (b) Structural cracks and crumbling of stone blocks due to earthquakes (blue rectangle). (c) Exfoliation and detachments of the stone blocks (red rectangle). (d) Scaling, powdering, and differential weathering of sandy limestone blocks (red rectangle). (e) Alveolar weathering. (f) Weakening and splitting of stone blocks.	206
Fig 3.3.8	Microphotographs under the digital microscope for the construction materials of Sahure's pyramid. (a and b) Core stone, grains of quartz admixed with calcite, fractures, laminations, and microcracks are detected. (c and d) Unweathered casing limestone is a very white stone, microveinlets filled with calcite and quartz are observed, and comb texture is observed in some microveinlets. (e and f) Weathered casing limestone of the pyramid with clear irregular pore spaces present in the carbonate matrix of the stone and comb texture is observed. (g and h) Sample of mortar with a significant number of microfossils and fossil fragments are observed in the carbonate samples and in the groundmass, and several irregular interparticle pores are detected in the mortar. Legend: Cal (calcite), Qz (quartz), and Ba (basalt rock fragments).	208
Fig 3.3.9	(a) Thin section for the core stone investigated under the polarizing microscope. The sample shows the pore spaces, channels (microcracks), and dolomite presented as alteration minerals after calcite (dolomitization process). (b) The casing stone under a polarizing microscope. The stone is cut by microveinlets filled with secondary calcite and traces of quartz. Quartz presents as a	212

	secondary replacement mineral over carbonates, especially microfossils. (c) The decayed casing stone under a polarizing microscope. Secondary quartz replaces calcite both in the matrix and in some microfossils. Secondary gypsum replaces calcite and partially fills cavities and pore spaces. (d) Observed stone fragments are of sedimentary (fossiliferous limestone, gypsum (chemical alteration byproduct), feldspathic graywacke, and ironstone) and igneous (porphyritic basalt and rhyolite) origin (e) in basaltic mortar. Gypsum rock fragments are composed of a network of very fine-grained irregular gypsum crystals, and this texture is characteristic of secondary gypsum after anhydrite. (f) Some grains of quartz are polycrystalline, feldspar (anorthite) occurs as fine-grained euhedral to subhedral crystals scattered in the matrix, calcite occurs as very fine-grained (micrite), iron oxides and opaque minerals occur as very fine to medium-grained, gypsum occurs as fibrous aggregates to needle-like crystals, and some irregular pore spaces and fine channels are detected.	
Fig 3.3.10	X-ray diffraction patterns of the construction materials of Sahure's pyramid. Legend: CS, core stone; UWsC, unweathered casing stone; WcS, weathered casing stone; BM, basaltic mortar; Gyp, gypsum; Qz, quartz; Cal, calcite; An, anorthite; Dol, dolomite (according to [**70**]).	214
Fig 3.3.11	X-ray diffraction patterns of the clay fraction from the core stone sample, where the main peak observed corresponds to swellable clays. The AO sample (black line) corresponds to oriented aggregates without treatment, AO-DM (red line) after treatment with dimethyl sulfoxide, and finally, AO-550 (blue line) treated thermally at 550 °C.	215

Chapter 3.4	**Salt weathering impact on Nero/Ramses II Temple at El-Ashmonein archaeological site (Hermopolis Magna), Egypt**	237-282
Fig 3.4.1	(A) General map of Egypt. Black square refers to Minia and the black star refers to El-Ashmonein archaeological site. (B) El-Ashmonein archaeological site and its location regarding the Minia limestone quarries and water sources. (C) El-Ashmonein archaeological site and its monuments; the black square refers to Nero's Temple. (D) Plan of the Nero's Temple. (E) Cross-section and the system of construction for the walls, indicating the architectural elements with dimensions of the stone blocks. (F) The cross-section for the construction materials confirms the reuse of stone blocks from Ramses II and using Roman red bricks and Roman mortar admixed together in one construction building near Nero's Temple.	246
Fig 3.4.2	Cross-section of the geological and geohydrological features of Minia, including the study area (dotted black square refers to Al-Ashmonein archaeological site). Edited after [**39**].	247
Fig 3.4.3	(A) Google Earth view, Nero's Temple in yellow pin and yellow arrows represent the sampling places. (B) The samples of the study temple, where NT1 and NT3 represent the surface crust, NT2 altered construction stone, NT4, and NT5 represent the structural mortar and NT6 represents the structural roman mortar.	250
Fig 3.4.4	(A) Nero's Temple and the contaminated water sources. Green, red and blue arrows refer to canal water, houses, and agricultural lands, respectively. (B) The preservation state of the temple in 1983. The Blue arrow refers to the near houses and the yellow arrow indicates the gathered water, from [**43**]**.** (C-E) The current state of preservation in 2022 for Nero's Temple with its decayed	252

	and damaged elements due to salt weathering. Red rectangles refer to the degradation and deformation of the temple's architectural and structural elements. The blue arrow refers to the houses near the temple.	
Fig 3.4.5	Deterioration maps for the remaining parts of Nero's Temple. (A) Refers to the general deterioration aspects (soiling layer, salt erosion, and loss of material) of the remaining column. (B) Refers to the focused deteriorated part with a high rate of decay in the column that shows the figure of Emperor Nero. (C) Refers to the severe decay of the important cartouche of Ramses II king	253
Fig 3.4.6	Thin section photomicrographs of limestone and mortars of Nero's Temple. (NT1, NT3) crust sections with significant amounts of pores are existed due to the dissolution and weathering processes of original carbonate minerals. (NT2) Altered biomicrite limestone as fine- to medium-grained; anhedral, sutured interlocked crystals. (NT4, NT5) Structural mortar with very fine to coarse grains and mainly composed of sand, lime, and gypsum. (NT6) Roman mortar is composed of sand with angular single grains of quartz, pottery fragments, and crushed limestone.	256
Fig 3.4.7	Raman spectra for NT1 and NT3 (Crust) NT2 (altered stone), NT4 and NT5 (structural mortar), and NT6 (structural roman mortar). Legend: Anh (anhydrite); Hl (halite); Cal (Calcite); Gp (gypsum); Brt (brushite); Qz (quartz). Minerals symbols after [**44**] except for Brt (brushite).	260
Fig 3.4.8	Microphotographs for the construction elements to detect the texture features of decayed stones and mortars. NT1 (crust), NT2 (altered stone), NT3 (crust), NT4 (mortar), NT5 (mortar) and NT6	263

	(mortar). Salts precipitation and disintegration are dominant decay patterns for all samples.	
Fig 3.4.9	General morphological view of the six samples (NT1-NT6). In NT1 to NT4, the halite (light gray) and Ca and K sulfates (dark grey) crusts are shown, with some calcium-phosphate crystals (in white) and black organic particles. NT5 shows a crust composed mainly of layered and mesostructured gypsum with traces of Na and Cl (halite) and sulfates. In NT6, there is a pore with a quartz grain with signs of corrosion and a film with acicular-planar halite crystals, and a matrix composed of calcite and a mixture of calcium silicates, halite, sulfates, and calcium-phosphate. Legends: Legend: Hl (halite); Gp (gypsum); Anh (anhydrite); Brt (brushite); Qz (quartz); Hbe (humberstonite); Ugm (ungemachite). Minerals symbols after [**44**] except for Brt (brushite).	265
Fig 3.4.10	EDS results of detailed points and areas (dots and rectangles areas, respectively) for the temple construction materials. In sample NT1, (A) refers to sulfates, (B) refers to chlorides, and (C) refers to phosphates. In NT2 (D) and NT3 (E), the red rectangles refer to two types of salt attack (sulfates and chlorides). In NT4 (F), quartz grains of the mortar surrounded by halite can be distinguished. NT5 (G) shows an example of a salt attack of sulfates of structural mortar and NT6 (H) shows a different kind of salt attack (phosphates and chlorides) over the Roman mortar.	267
Fig 3.4.11	Salt decay mechanism and salts migration to the construction materials of Nero's Temple	269
Chapter 3.5	**Sand dunes movement and flooding risk analysis for the pyramids of Meroe, Al Bagrawiya archaeological site, Sudan**	283-319

Fig 3.5.1	Map of Sudan and location of the pyramids of Meroe at Al Bagrawiya (red point). (B) The pyramids of Meroe at Al Bagrawiya and their general view.	290
Fig 3.5.2	(A) General map with plans for the pyramids at Al Bagrawiya (edited after [**31**]). (B) Elevation and plan view of the Pyramid number 10 and its architectural and structural elements (edited after [**30**]).	291
Fig 3.5.3	(A) Lithological map of the study area. (B) Ancient Meroitic quarries in the northwest sector.	293
Fig 3.5.4	Thermal map (up-left) and chart of temperature(up-right) over Sudan monthly. (Down) Historical temperature recordsfrom 1901 to 2020.	295
Fig 3.5.5	(A) Map of Sudan's rainfalls (after [**43**]). (B) Map of affected areas by flooding in Sudan (after [**50**]). White stars present the case study.	296
Fig 3.5.6	(A) Barchan sand dunes components and movement. (B) Schematic formation of barchan sand dunes around pyramids	297
Fig 3.5.7	(A and B) Captured satellite images for sandstorm over Sudan in 9 May 2009 (from https://earthobservatory.nasa.gov/images/38459/dust-storm-over-sudan). (C and D) A sandstorm over the archaeological site of Al Bagrawiya in 14 May 2013 (from https://earthobservatory.nasa.gov/images/81127/dust-storm-in-sudan). Yellow arrows in (D) refer to the wind directions. (E) General view of the pyramids of Meroe and the impact of the sand dunes over the building materials of the pyramids. Taken by Martchan/Shutterstock(https://www.theafricandream.net/sudan-forgotten-pyramids-are-more-than-egypt/).	298

Fig 3.5.8	(A) Images for monitoring the movement of sand dunes around the pyramids from Google Earth. (B) Treated images to clearly see this movement around the pyramids. Images of 2004 to 2021 are in grey colour, except for 2014 is in RGB colour.	299
Fig 3.5.9	(A) Base map for the studied area. (B) Coloured estimation for the sand dunes coverage around the pyramids and their variations from 2004 to 2021. (C) Linear outlines for the variations of sand dunes coverage from 2004 to 2021.	301
Fig 3.5.10	The coverage rates of the accumulated sands over the studied pyramids in the years of 2004, 2010, 2014 to 2021.	302
Fig 3.5.11	(A) Mechanism of sands accumulation around the pyramids. (B) Three possible phases for the sands as external forces on pyramids structures.	304
Fig 3.5.12	Aerial satellite image to show the heavy rains over the case study in July 2007. From https://earthobservatory.nasa.gov/images	305
Fig 3.5.13	(A) The impact of flooding in Sudan. From https://dailynewsegypt.com/2020/09/06/egypt-dispatches-urgent-aid-to-flood-hit-sudan/. (B) Satellite image for the flooding over Atbara and near to Al Bagrawiya archaeological site	306
Fig 3.5.14	Damage rate for the pyramids in 2004, 2010, 2014 and 2021.	308
Fig 3.5.15	(A-F) Degradation maps for the construction materials for the pyramids of Meroe.	309
Fig 3.5.15	(C and D) cont.	310
Fig 3.5.15	(E and F) cont.	311
Chapter 3.6	**Part III: Consolidation**	321-372

Chapter 3.6	**Multi-functional monodispersed SiO_2-TiO_2 NPs and TEOS in the consolidation of archaeological lime mortars surfaces.**	323-372
Fig 3.6.1	The degradations of the ancient lime mortar (structural joint material) and lime rendering from various archaeological sites in Egypt. (A) Temple of Ramses II, Al-Ashmounien archeological site, Egypt, where the joint mortar between blocks was disintegrated as shown in the black arrow. (B) Abusir archaeological site, Giza, Egypt, where the lime mortar between blocks was decomposed and disintegrated as referred to as the black arrow. (C and D) The salt weathering of lime rendering is shown in the rectangles, of Anfushi's necropolis, Alexandria, Egypt.	334
Fig 3.6.2	(A) The used proportion in preparation of lime mortar. (B) The preparation process of the mortar. (C and D) Presentation of experimental casted lime mortar samples.	335
Fig 3.6.3	(A) Contact angle test equipment**.** (B) Glass surfaces supplied with 3%, 5% and 7% of SiO_2-TiO_2 NPs/TEOS. (C) During test operation and droplets releasing.	338
Fig 3.6.4	(A and B) Prepared UV chamber for the self-cleaning test.	340
Fig 3.6.5	(A-B) Indentations were taken by Nano test equipment. (C) The prepared samples for the Nano-test.	342
Fig 3.6.6	(A) XRD patterns of nano-SiO_2 and SiO_2-TiO_2 NPs. (B) UV–Vis diffuse reflectance spectra of nano-SiO_2 and SiO_2-TiO_2NPs.	346
Fig 3.6.7	Micrograph under SEM for the nano-SiO_2 particles with characteristic spherical shape (A) and SiO_2-TiO_2NPs (B).	346
Fig 3.6.8	(A) Untreated lime mortar sample with inhomogeneous textural details as shown in the blue square. (B) Surface consolidation of the lime mortar by 3% of SiO_2-TiO_2 NPs/TEOS. Black square presents the coating layer of consolidate. (C) Microstructure features of the	349

	consolidated surface by 5% of SiO_2-TiO_2 NPs/TEOS. The black square shows the homogenous texture and binding of the surface after consolidation. (D) The surface cohesion after consolidation by 7% of SiO_2-TiO_2 NPs/TEOS as seen in the black square. (E and F) Elemental analysis results by EDS for the treated (mainly Si and Ti) and untreated mortar (mainly Ca) surfaces.	
Fig 3.6.9	(A-C) Physical properties and average values of experimental lime mortars before and after consolidation (3%, 5% and 7% of SiO_2-TiO_2 NPs/TEOS) for assessment the porosity (A), water absorption (B), and density (C).	350
Fig 3.6.10	(A) Static contact angle values for 3%, 5% and 7% SiO_2-TiO_2 NPs/TEOS over glass slides. (B and C) The monitoring of the consolidates behaviors and changes detection over the surfaces after one hour of droplets releasing. 3% and 5% SiO_2-TiO_2 NPs/TEOS maintained their hydrophobic activity, meanwhile, the 7% SiO_2-TiO_2 NPs/TEOS consolidate and converted into a hydrophilic phase.	352
Fig 3.6.11	(A-C) Photocatalytic activity of 3%, 5% and 7% SiO_2-TiO_2 NPs/TEOS and their efficacy in staining degradation.	354
Fig 3.6.12	Distribution results of Nano-indentation Hardness and Young Modulus for the untreated lime mortars (A) and treated lime mortars with SiO_2-TiO_2 NPs /TEOS with concentration 3% (B), 5% (C), and 7% (D).	355
Fig 3.6.13	Micrographs of the untreated (A) and treated surfaces after salt weathering (B-D).	358
Fig 3.6.14	(A) Micrograph of the treated surface with 3% SiO_2-TiO_2 NPs/TEOS after thermal aging without change detection. (B) Micrograph of the treated surface with 5% SiO_2-TiO_2 NPs/TEOS after thermal	360

	aging with moderate durability. (C) Micrograph of the treated surface with 7% SiO_2-TiO_2 NPs/TEOS after thermal aging with low resistance and noticed changes in the surface.	
Fig 3.6.15	Micrographs for the untreated (A) and treated lime mortar surfaces with 3% (B), 5% (C), and 7% (D) SiO_2-TiO_2 NPs /TEOS after UV aging. (A and D) Pores and micro-cracks were observed (black rectangles), which (B and C) no changes were detected.	361
	Annex 1: Supplementary materials for Chapter 3.1 titled "Coastal environment impact on the construction materials of Anfushi's Necropolis (Pharos's Island) in Alexandria, Egypt".	385-403
SM1. Fig 1	(A) Ruins of collapsed structures and displacements. (B) Gaps in the bedrocks indicate the geotechnical problems of the Anfushi's Necropolis. (C) Crumbling and deformations in the walls and vaults. (D) Loss of materials and loss of rendering layers. (E) Collapsed parts from bedrock and chipped blocks.	385
SM1. Fig 2	(A) Alveolar weathering (honeycomb), crack in the blocks, chipped blocks, salt erosion, flaking, and pittings. (B) Loss of painting layer due to salt erosion. (C) Flaking, scaling, chipped blocks, and salt crystallization. (D) Salt erosion (efflorescence and sub fluorescence).	386
SM1. Fig 3	(A) Green arrows refer to fallen parts from the bedrock, salt erosion, dampness due to water gathering, and plant growth. (B) Blue arrows show the gaps in the bedrock, chipping patterns, salt erosion, and eroded parts from the structure of the tomb. (C) Missing rendering layers. (D) Layering for the surface, bulking of the wall, and salt erosion. (E) Loss of painting layer and delamination. (F) blistering, flaking and loss of materials.	387

SM1. Fig 4	(A) The dotted blue rectangular and squares refer to the salt erosion on the surfaces of Anfushi's Necropolis. (B and C) shows the flaking and layering patterns, blue arrow refers to recent restoration for filling a gap. (D) Significant graffiti and endangered with salt crystallization.	388
SM1. Fig 5	(A-R) Various decay patterns for the building materials of the Anfushi's Necropolis due to the marine dynamic impact. The most dominant patterns are salt erosion, loss of materials, loss of rendering layers, discoloration, pittings, alveolar weathering, flaking, cracks and layering.	389-398
SM1. Fig 6	(A-E) Reconstruction and retouching for the architectural and structural elements of the Anfushi's Necropolis.	399-403
	Annex 2: **Supplementary materials for Chapter 3.2 titled "Multianalytical diagnostic approaches for the assessment of materials and decay of the archaeological sandstone of Osiris Temple (The Abaton) in Bigeh Island, Philae (Aswan, Egypt)"**	404-419
SM2. Fig 1	Digital elevation model and geomorphological features for Aswan as well as it shows Nubian sandstone formations such as Kurkur formation, the blue dotted circle represents the surrounding area of Osiris temple.	404
SM2. Fig 2	Osiris Temple (the Abaton) current plan. Those drawn remains are underwater and some parts above the water. A, B and C represent columns.	405
SM2. Fig 3	(A-E) General views for the Osiris temple and surrounding environment.	406
SM2. Fig 4	Different photographs document the dominant black crust and general decay state of Osiris temple stone surfaces.	407

SM2. Fig 5	Different photographs document the structural instability of the temple (Structural cracks in black rectangular patches).	408
SM2. Fig 6	(A and B) General sketches of preservation state for Osiris Temple.	409
SM2. Fig 7	(A-U) the detailed degradation patterns and problems for building materials of the Osiris temple. Each figure has its own scale and legend.	410

Index of tables

Table No.	Caption	Page
Chapter 3	**Results and discussion** **Part I: Characterization of construction building materials in aqueous environments**	79-180
Chapter 3.1	**3.1 Coastal environment impact on the construction materials of Anfushi's Necropolis (Pharos's Island) in Alexandria, Egypt**	79-141
Table 3.1.1	Some recorded heavy storms in Alexandria with expected dates and durations. From [**65**].	99
Table 3.1.2	Wind dynamics in Alexandria.	101
Table 3.1.3	Mineralogical analysis of Anfushi's Necropolis samples. BR: bedrock; CS casting stone; CRM: coarse-grained rendering mortar; FRM: fine-grained rendering mortar; Cal: calcite; Qz: quartz; Gp: gypsum; Ar: aragonite and Hal: halite (+++ Very Abundant; ++ Abundant; + Rare).	115
Table 3.1.4	Elemental analysis of major and minor elements, expressed in oxides (wt. %), for the Anfushi's Necropolis samples. BR: bedrock; CS casting stone; CRM: coarse-grained rendering mortar; FRM: fine-grained rendering mortar.	116
Chapter 3.2	**3.2. Multianalytical diagnostic approaches for the assessment of materials and decay of the archaeological sandstone of Osiris Temple (The Abaton) in Bigeh Island, Philae (Aswan, Egypt)**	143-180
Table 3.2.1	Summary table with the main characteristics observed by polarizing microscopy in the studied sample. According to	162

	[47]. Legends: (Qz) Quartz; (Or) Orthoclase; (Ms) Muscovite; (Tur) Tourmaline; (Hem) Hematite; (Grt) Garnet; (Cal) Calcite; (Kln) Kaolinite; (Zrn) Zircon, according to [46].	
Table 3.2.2	Mineralogical content of Osiris Temple construction material samples (S1-S4). Legends: (Qz) Quartz; (Cal) Calcite; (Kln) Kaolinite; (Hem) Hematite; (Or) Orthoclase; (Apt) Apatite; (Nit) Nitratine; +++ = high; + = low; tr = traces. Mineral legend according to [46].	164
Table 3.2.3	Results of elemental analysis of sandstone construction material. Major and minor elements are expressed in oxides (wt. %).	166
Table 3.2.4	Physical properties testing for Osiris Temple building material. Legend: ρ is density (in g/cm^3), Po is open porosity (in %), and A_w is the water absorption coefficient (in %).	167
Chapter 3	**Part II: Characterization of construction building materials in subaerial environments**	181-319
Chapter 3.3	**Geoenvironmental investigation of Sahure's pyramid, Abusir Archeological site, Giza, Egypt**	183-235
Table 3.3.1	Examples of historical earthquakes with their approximate latitudes and intensities. Edited after [58].	201
Table 3.3.2	XRD results of the core, casing, and basaltic mortar/concrete of the pyramid. Legend: CS, core stone; UWsC, unweathered casing stone; WcS, weathered casing stone; BM, basaltic mortar; "-", a mineral phase not registered; Cal, calcite; Dol, dolomite; Qz, quartz; Gyp, gypsum; An, anorthite (according to [70]).	213

Table 3.3.3	Chemical composition of the core stone, unweathered and weathered casing stones, and basaltic mortar from Sahure's pyramid. Major and minor elements are expressed in wt. %. Legend: CS, core stone; WCS, weathered casing stone; UWCS, unweathered casing stone; BM, basaltic mortar.	216
Table 3.3.4	Results of the petrophysical properties for the core stone (sandy limestone) of the pyramid. Legend: L, length (in cm); W, width (in cm); H, height (in cm); V, volume (in cm^3); M, mass (in g); NW, natural weight (in g); DW, dry weight (in g); SW, saturated weight (in g); MC, moisture content (in %); WA, water absorption (in %); D, density (g/cm^3); UW, unit weight ($g.mm.s^2$); SG, specific gravity (g/cm^3); Po, open porosity (in %).	217
Chapter 3.4	**Salt weathering impact on Nero/Ramses II Temple at El-Ashmonein archaeological site (Hermopolis Magna), Egypt**	237-282
Table 3.4.1	Semi-quantitative mineralogical analysis of the samples, where NT1 and NT3 represent the surface crust, NT2 altered construction stone, NT4, and NT5 represent the structural mortar and NT6 represents the structural roman mortar. Legends: (Cal) calcite; (Hl) halite; (It) illite; (Hbe) humberstonite; (Ugm) ungemachite; (Gp) gypsum; (Anh) anhydrite; (Bas) bassanite; (Brt) brushite; (Qz) quartz; (Na) natron; (Mc) microcline; (Sep) sepiolite; (Nah) nahcolite; (Stk) starkeyite; (Stg) strengite; (Syl) sylvite; x, scarce; xx, abundant; xxx, very abundant. Minerals symbols after [**44**] except for (It) illite; (Hbe) humberstonite; (Bas) bassanite; (Brt) brushite; (Na) natron; (Nah) nahcolite; (Stk) starkeyite; (Stg) strengite; (Syl) sylvite.	259

Table 3.4.2	Chemical composition of the six construction materials. Major and minor elements are expressed in wt. % oxides.	261
Chapter 3.6	**Multi-functional monodispersed SiO_2-TiO_2 NPs and TEOS in the consolidation of archaeological lime mortars surfaces.**	323-372
Table 3.6.1	Colorimetric parameters for the lime mortars before and after consolidation at 3%, 5%, and 7% of SiO_2-TiO_2 NPs/TEOS.	351
Table 3.6.2	Color change values ΔE* for 3%, 5% and 7% SiO_2-TiO_2 NPs/TEOS and their chromatic behaviors during the self-cleaning test.	354
Table 3.6.3	Average values for untreated lime mortars and for the treated lime mortars with 3%, 5%, and 7% SiO_2-TiO_2 NPs /TEOS under uniaxial compressive strength (Rc, in MPa).	357
Table 3.6.4	Measurement of the salt resistance (mass loss) of the treated samples. Legends: (M_0, in g) mass of the dried samples in grams, (M_n, in g) mass of the dried specimen after exposure cycles and (ΔM, in %) percentage of mass loss.	359

Durability problems of the archaeological construction materials in aqueous and subaerial environments, with applications for restoration and conservation in Egypt and Sudan

Tesis Doctoral (Doctoral thesis)
El autor (Author): Abdelrhman Fahmy

Durability problems of the archaeological construction materials in aqueous and subaerial environments, with applications for restoration and conservation in Egypt and Sudan

Tesis Doctoral (Doctoral thesis)
El autor (Author): Abdelrhman Fahmy

Highlights

- Sahure's pyramid casing stone is limestone and the inner core is sandy limestone.
- Basaltic mortar as the first trial for green concrete manufacturing in the Egyptian Old Kingdom, Fifth Dynasty was revealed.
- Mineralogical content in the construction materials was an intrinsic problem of Sahure's pyramid.
- Geoenvironmental conditions affected the architectural, structural, and engineering stability of Sahure's pyramid.
- The sources of the contaminated water around Nero's Temple are canals, houses, and agriculture.
- Sulphates and chlorides were identified as the main damaging components of the salts in Nero's Temple.
- Conservation plan is needed considering the prevention of saline water flowing in Nero's Temple.
- The bedrock of Anfushi's Necropolis is oolitic limestone and the casing stone is micritic limestone.
- Probabilistic risk of sea level rises and its impact on the submergence of Anfushi's Necropolis.
- The structural deficiencies of Anfushi's Necropolis were caused by the effect of the earthquake.
- Osiris Temple wasn't rescued during the UNESCO saving campaign for Aswan temples.
- Yellowish and pinkish sandstones are the building materials of the Osiris Temple.
- Fluctuations in the Nile water level decayed the Osiris Temple building materials severely.
- Main intrinsic decay factors are the clayed matrix of sandstones of the Osiris Temple.
- Nubian sandstone is the main building material of the pyramids of Meroe.
- Wind is considered the main catalytic force for the damage to the pyramids of Meroe.
- Sand dunes along with heavy rains and flooding are the main decay factors for the pyramids of Meroe.

- 3% and 5% SiO_2-TiO_2 NPs /TEOS enhanced the lime mortar surfaces multifunctionally.
- 3% and 5% are suitable consolidates for lime mortar surfaces without leaving chromatic changes.
- 7% SiO_2-TiO_2 NPs /TEOS did not enhance the lime mortars physically and mechanically.

Abstract

The main objective of the study was to identify and assess the conservation problems of the building materials of each case study and compare the aggressive impacts of each environment on the sustainability of the construction materials. Carefully, the construction materials (limestone, sandy limestone, sandstone, lime mortars, gypsum, hydraulic lime mortar/roman mortar) were selected from different archaeological sites with different environmental conditions in Egypt and Sudan (desert: Sahure's pyramid and pyramids of Meroe; urban/agricultural: Nero/Ramses II Temple; coastal: Anfushi's Necropolis; and fluvial: Abaton/Osiris Temple). To achieve this goal, field observations, analytical (X-ray diffraction, X-ray fluorescence, Raman spectroscopy, UV-Vis spectrometry), microscopic (binocular microscope, polarizing microscope and scanning electron microscope), mapping (AutoCAD, ArcMap 10.8, SeaDAS, QGIS), and physical and mechanical testing investigations were carried out. Furthermore, open-access satellite lenses were used for the detection and assessment of the archaeological sites and their risks, and, the deterioration patterns of each case study were recorded through decay mappings. Finally, to preserve the lime mortar surfaces, a newly synthesized nanomaterial of SiO_2-TiO_2 NPs/TEOS was applied and tested. The results showed the severity of each factor on the construction materials. In this sense, Sahure's pyramid was affected mainly by climatic and environmental factors, earthquakes and the inner composition of the building materials. Nero/Ramses II Temple showed its susceptivity mainly from the salt attack which came from the contaminated sources of water around the temple. Water intrusion, earthquakes, storms, and heavy rains factors attacked Anfushi's Necropolis severely. Abaton/Osiris Temple was decayed because of Nile water fluctuations impact and the inner weakness of the temple sandstones. In Sudan, the pyramids of Meroe were damaged because of the sand dunes and wind forces, in addition to the flooding risks. Finally, and concerning to the heritage conservation, the research exhibited the efficacy of the multifunctional 3% and 5% SiO_2-TiO_2 NPs/TEOS in the consolidation and improvement of the physical and mechanical ancient lime mortars.

Resumen

El objetivo principal del estudio fue identificar y evaluar los problemas de conservación y durabilidad de los materiales de construcción de cada caso de estudio y el impacto de cada entorno. Los materiales de construcción (calizas, calizas arenosas, areniscas, morteros de cal, yeso, mortero de cal hidráulica/mortero romano) fueron seleccionados de distintos sitios arqueológicos expuestos a diferentes condiciones ambientales en Egipto y Sudán (desierto: Pirámide de Sahure y pirámides de Meroe; urbano/agrícola: Templo de Nerón/Ramsés II; costero: Necrópolis de Anfushi; y fluvial: Templo de Abaton/Osiris). Para lograrlo, se llevaron a cabo observaciones de campo y se realizaron mediciones analíticas (difracción de rayos X, fluorescencia de rayos X, espectroscopías Raman y Espectrometría UV-Vis), microscópicas (lupa binocular, microscopio polarizador y microscopio electrónico de barrido), cartográficas (AutoCAD, ArcMap 10.8, SeaDAS, QGIS), y pruebas físicas y mecánicas. Además, se utilizaron imágenes satelitales de acceso abierto para la detección y evaluación de los sitios arqueológicos y sus riesgos, así como el registro patrones de deterioro de cada caso de estudio a través de mapeos de deterioro en detalle. Por último, para mejorar la preservación de las superficies de los morteros de cal, se aplicó y probó un nano-material recién sintetizado de nanopartículas de SiO_2-TiO_2 y TEOS. Los resultados mostraron la severidad con la que cada factor ha actuado sobre los materiales de construcción. En este sentido, la pirámide de Sahure se vio afectada principalmente por factores climáticos y ambientales, los terremotos y la composición interna de los materiales de construcción. El Templo de Nerón/Ramsés II mostró su susceptibilidad principalmente por el ataque de sal que provenía de las fuentes de agua contaminadas de alrededor. La intrusión de agua marina, los terremotos, las tormentas y las fuertes lluvias han afectado intensamente a la Necrópolis de Anfushi. El Templo de Abaton/Osiris se deterioró debido al impacto de las fluctuaciones del agua del Nilo y la debilidad interna de los sillares de arenisca. En Sudán, las pirámides de Meroe resultaron dañadas por las dunas de arena y la fuerza del viento, además de los riesgos de inundaciones. Finalmente, y en cuanto a la conservación de morteros de cal históricos y actuales, la investigación mostró la eficacia del tratamiento multifuncional a base de nanopartículas de SiO_2-TiO_2 y TEOS al 3% y 5% en la consolidación y mejora de las propiedades físicas y mecánicas de los morteros de cal.

Keywords / Palabras clave

English	Spanish
Sahure's pyramid	Pirámide de Sahure
Nero/Ramses II Temple	Templo de Nerón/Ramses II
Abaton/ Osiris Temple	Templo de Abaton/Osiris
Pyramids of Meroe	Pirámides de Meroe
Anfushi's Necropolis	Necrópolis de Anfushi
Durability	Durabilidad
Decay	Deterioro
Degradation	Degradación
Construction materials	Materiales de construcción
Archaeological sites	Sitios arqueológicos
Environments	Ambientes
Geoenvironmental	Geoambiental
Natural stone	Piedra natural
Limestone	Caliza
Sandstone	Arenisca
Sandy limestone	Caliza arenosa
Lime mortar	Mortero de cal
Hydraulic lime/Roman mortar	Cal hidráulica/mortero romano
Gypsum mortar	Mortero de yeso
Weathering	Meteorización
Salt weathering	Meteorización salina
Nanotechnology	Nanotecnología
Nano silica/SiO_2	Nano sílice/SiO_2
Nano titanium/TiO_2	Nano titanio/TiO_2
Consolidation	Consolidación
Conservation	Conservación
Restoration	Restauración

Chapter 1

Introduction

1.1. Introduction

The ancient cultural heritage is part of who we are as it is the memory of our past; it leads us to a better future. In addition, heritage and history influence how we develop, and transfer knowledge to the next generations and provide a basis for tradition and value [**1, 2**]. In this regard, we must safeguard the cultural heritage with scientific studies and investigation to understand the cultural materials and manage us to preserve and restore it scientifically.

Underwater cultural heritage (UCH) has become a day talk globally, especially in excavations, finding of archaeological finds, and preservation of this type of archaeology. Many authors and international organizations in archaeology and marine sciences presented a great effort to publish many international reports, charters, papers, and books about the excavation works in oceans and seas, materials, and preservation of this kind of heritage. In this sense, e.g. [**3**] illustrated the environmental impacts of underwater cultural heritage. Khakzad, [**4**] studied the damage assessment and conservation of UCH relics in Belgium and suggested an excellent presentation in her case study. In 1987, Florida started to develop underwater parks to show shipwrecks and other historic sites. The preserved shipwreck has become popular attraction for skin and scuba diving visitors to witness a part of Florida's history first-hand [**5**]. In 2014, UNESCO issued a conference book to present the underwater cultural heritage from the First World War and their threats and challenges as a step for taking initiatives and programs to protect them for the next generations [**6**]. In a step towards preserving the underwater cultural heritage International Center of Archaeology in cooperation with other authors and UNESCO, they issued a code of ethics for drivers to protect the underwater heritage from damage [**7**]. Hassan et al. [**8**] presented a study on underwater cultural heritage, conservation management for marine artifacts and shipwrecks, pollution and erosion impacts on coastal heritage and remote sensing in marine archaeology in Alexandria. Maarleveld *et al.* [**9**] authored a manual book with guidelines to present conservation and site management plans, documentation techniques and impacts of offshore activities on underwater cultural heritage. [**10, 11**] presented a study on safeguarding underwater cultural heritage by mapping projects and programs and

identifying the gaps to be addressed in order to strengthen the underwater cultural heritage UCH protection for sustainable development. By protecting underwater cultural heritage, we can achieve so many benefits from the economic and tourism point of view, as well as achieving urban and sustainable development for the site. Prott [**12**] explained the natural and human impacts on underwater cultural heritage and showed simple and cheap methods to protect the underwater cultural heritage. [**13**, **14**] presented a management study for coastal cultural heritage with potentials and obstacles. Carper [**15**] presented proceedings for underwater archaeology in geophysical investigations to find the Wreck of an iconic Upper Missouri River Mountain Packet Steamboat, Wood Analysis from the Spring Break Wreck, Launching the Submerged Heritage Monitoring Scouts Florida Program, Using Archaeological Lenses and Conservation Assessment Tools to Influence Curation and in Situ Digital Documentation of the 1559 Emanuel Point Shipwrecks. Schwarz [**16**] presented a study on the safeguarding of the underwater cultural heritage in the Pacific: report on good practice in the protection and management of World War II. Hairy [**17**] presents a significant study about Qaitbay underwater site at Alexandria with surveying methodology for the site using GIS and photogrammetry. Tallet and Gregory [**18**] reported that the French mission had discovered the harbour of king Khufu on the red seacoast with so much stone blocks (anchors), potteries and papyrus. Abd-el-Maguid [**19**] presented a study on underwater archaeology in Egypt and its protection and mentioned the various international and local institutes and missions who have worked in underwater archaeology in Egypt such as Institut European d'Archéologie Sous-Marine, Centre d'Études Alexandrines, Institute of Nautical Archaeology, Hellenic Institute of Ancient and Mediaeval Alexandrian Studies, In Situ Institute, University of Torino, DUA's foundation and Nile Archaeological Mapping Project (NAMP).

In subaerial archaeology, the archaeological sites and their construction building materials are susceptible to various endangered factors leading to degradation and destruction [**20-24**]. In Egypt and Sudan, archaeological sites are exposed to daily bleeding, degradations, and deformations due to external factors such as climate change, pollution, water impact, winds, heavy rains, flooding, or earthquakes. In addition, there are also many intrinsic

factors affecting the durability of the construction building materials such as mineral composition, stone quality, bedding position, kind of mortar, plasters, etc. Anthropogenic factors are considered a third driving threat that affects the buildings of archaeological sites due to lack of maintenance, conservation problems, and low funding resources [**25-27**].

Many experts and researchers conducted many studies related to the assessment of endangered archaeology using different traditional and advanced techniques to study decayed building materials. Lazzari and Cano [**28**] informed that only environmental pressures do not cause damage to cultural heritage materials. In addition, war and vandalism, urban development, changing architectural styles, or poor restoration contribute to the damage. Binda et al. [**29**] added that the durability of the construction building materials is highly affected not only by aggressive environments but also by the choice and combination of constituents within the masonry. For instance, Tsipoyura and Michopoulos [**30**] reported that the decay forms of sandstone could be caused by intrinsic and environmental (extrinsic) indices. Internally, the main intrinsic factors of decay could be the high porosity, the pore size distribution, the matrix of the stone and mineralogical composition, especially the presence of swelling clay minerals. Externally, the damage of the stone can be affected by environmental conditions such as water (floods, subsurface water, and rains), pollution, and biological attack. Danese et al. [**31**] and Lerma et al. [**32**] used Infrared thermography (IRT) or thermal imaging to find out the various defects in the archaeological buildings. Using this technique, it gives us the possibility to assess the conservation problems in the construction materials and thier causes of deterioration and decay. As well as, it helps in carrying out a thermal mapping for the deformations and the patterns that appear in the architectural and structural elements. Veniale and Lodola [**33**] reported that an “ad hoc” computerized system (12) based on visual inspection and the photogrammetric survey was used to map the construction materials of the Pisa Tower and make degradation maps (black crust, efflorescence, patinas, insulation damage “scorching” damage, detachment and abrasion). Furthermore, this system is powerful in identifying mechanical resistance (compression, wind force, temperature fluctuations, flooding, and seismic actions) by knowing the dimensions and spatial orientation of the construction

material. Casula et al. [**34**] utilized combined destructive and non-destructive techniques (Photogrammetry (CRP), and low frequency (24 kHz) ultrasonic tomography combined with petrographical analysis) in decay detection such as exfoliation and pulverization. Furthermore, Lopez et al. [**35**] carried out moisture measurements, ultrasonic velocity propagation and water absorption tests. As well as they used polarized light and fluorescence optical microscopy, mercury intrusion porosimetry, ion chromatography and X-ray diffraction analyses in order to determine the origin and the degree of stone decay. Finally, Donato et al. [**36**] discussed that the type, intensity, and weathering forms are considered important parameters for the evaluation, quantification, and rating of stone damages.

Egypt is located in the north-eastern of the African continent and south-western of Asia with coordinates 27°N, 30°E, occupies an area of 1 million km^2 and is bordered by the Mediterranean Sea in the north, Sudan in the south, Libya in the west and red sea in the east (**Fig. 1.1**). Egypt has very significant archaeological sites above the ground and underwater heritage, containing one of the world's notable and old sites such as the great pyramid that is one of the seven world's wonders. Egypt has two kinds of sunken or submerged monuments one of them related to seawater in the Mediterranean Sea and Red Sea and the second kind with the Nile River (freshwater) from south to north of Egypt. In fact, plenty of archaeological artifacts and built heritage are underwater such as old cities and old harbours. For example, Wadi Al–Jarf port, Qaitbay fort, Al-Shatby, Mamoura Bay, Saadana Island, Eastern harbour, Abu Quir Bay and Aswan. In addition, to mnay rock cut and subaerial archaeological sites such as Giza pyramids, the Temple of Luxor, Temple of Hatshepsut, the Valley of Nobles, Beni Hassan Tombs, etc. On the other hand, Sudan is located between Egypt and Eritrea (north-eastern of Africa). It is bordered by the Red Sea in the northeast, Libya in the northwest, Chad in the west, the Central African Republic in the southwest, South Sudan in the south and Ethiopia in the southeast (**Fig. 1.2**). Sudan contains many significant archaeological sites and monuments such as the pyramids of Meroe, Temple of Amun, Old Dongola, Nuri Pyramids, Jebel Barkal, etc. Most of the buildings are in the desert and urban environments.



Fig. 1.1. Map of Egypt and its archaeological sites.



Fig. 1.2. Map of Sudan and its archaeological sites.

In Egypt, many studies were brought off in order to investigate the external and internal decay factors for the construction materials in the archaeological sites and in different environmental approaches. In the desert environment, Hanafy and Holail [**37**] presented a diagnosis study of the middle Eocene "nummulite bank" of the Giza Pyramid Plateau and

explained that the early diagenetic alteration of the rock matrix was followed by partial to complete dolomitization of the limestone matrix and nummulite grain. Furthermore, Emery [**38**] studied the weathering conditions on the Great Pyramid and revealed four types of limestone used to build it, such as gray hard dense limestone, soft gray limestone, gray shaly limestone, and yellow limy shaly sandstone. Reader [**39**] studied the weathering problems and erosion on Sphinx and presented a geomorphological study for Giza Necropolis. USAID of Egypt [**40**] presented an assessment report to study the environmental impacts on the Giza plateau and suggested a methodology for groundwater lowering. In addition, Gandah [**41**] studied and discussed the environmental impacts of rain, wind, and salts on the pyramid of Khufu and presented hypotheses for restoration and conservation. Franc [**42**] studied and gave us the opportunity to see the construction materials of the Great Pyramid in his study through the petrography observations of the building stones. Kukela [**43**] studied the degradation patterns for the step pyramid of Saqqara and showed isometric deterioration maps for the pyramid. Furthermore, Khalil et al. [**44**] showed the effects of strong ground shaking on the stability of the step pyramid and showed that there are many earthquakes in Greater Cairo with low magnitudes but with accumulative effects for the long term on the pyramid.

In urban and agricultural environments, salt aggressiveness is considered the main degradation force for construction materials. In this sense and from the literature review, salt attack from chlorides, nitrates, and sulfates are the most common salts that attack Egyptian stone building materials [**45-47**]. Bradley and Middleton [**48**] studied the soluble salt's effect on ancient Egyptian limestone due to the changes in relative humidity that decreased the durability of the stones. Tombs and ancient Egyptian monuments in Thebes were affected by salt efflorescence because of natural weathering, and human impacts [**49, 50**]. Aboushook et al. [**51**] evaluated the surrounding local environment's impact on the Egyptian stone monuments, and the quantification of the deterioration process was carried out through digital image processing. They explained that black crusts in the middle and upper parts of stone walls were formed mainly by gypsum salt and soot from vehicles and the whitish crusts in the lower parts of stone walls were formed mainly by halite.

In the coastal environment, the construction materials are very susceptible to many destruction and decay inducers such as earthquakes, climatic changes, flooding, sea level rising, heavy rains, storms, winds and water intrusions. In this regard, El-Raey [**52**] carried out an assessment study using GIS maps and remote sensing to evaluate the impact of SLR on Egypt. He reported that many historical sites would be affected and flooded when the water reaches 50 cm up. Elsharkawy et al. [**53**] conducted a study on SLR impacts and observed that SLR can increase soil salinity due to saltwater intrusion in the Delta and Alexandria. In this sense, SLR affected the library of Alexandria, one of Alexandria's landmarks, in 2005. Moreover, Bekheet et al. [**54**] and El-Raey and RCDRR [**55**] mentioned that Egypt is considered among the top five countries that will be in danger due to SLR with 1 m, specifically in Alexandria, which is considered among the 20 top cities in the world that will be in danger due to SLR. In addition, they explained that permanent coastal flooding results in the loss of dry land and saltwater intrusion into the surface and groundwater by submergence. Furthermore, Abdelnaby and Elnashai [**56**] studied the impact of the historical earthquake of 1303 AD in damaging the historical buildings in Alexandria, concluding that the historical earthquakes felt in Alexandria caused structural cracks, failures, and partial and total collapse of most of the ancient buildings in Alexandria.

In the fluvial environment, the impact of Nile water on the construction building materials was not studied before, except for a few types of research that had been addressed to study the impact of groundwater and flooding on archaeological sites in southern Egypt [**57, 59**].

In Sudan, there are many endangered archaeological sites mainly because of flash flooding, sand dunes, wind force, and temperature variations. In this context, Sweek et al. [**60**] carried out a conservation project for the Amun Temple because the architectural elements of the temple were affected by different kinds of decay mechanisms due to the poor quality of sandstone and heavy rains. Osman et al. [**61**] studied several properties of the Nubian formations and their geotechnical problems because these formations were the sources of construction materials in different archaeological buildings in Sudan. The governmental report of Sudan in March 2021 [**62**] mentioned different vulnerabilities that threaten the archaeological sites in Sudan. Among these vulnerabilities are natural encroachments such

as strong winds, earthquakes, flash flooding, and Nile flooding. They explained that wind power could transport the sand particles and weaken the sandstone building materials of the archaeological buildings. In addition, the floods affected many archaeological sites, especially the Island of Meroe. Onderka and Vrtal [**63**] showed the damage to the red brick and mud-brick structures in Wad Ben Naga's archaeological site is due to the seasonal heavy rains. Fahmi et al. [**64**] studied the challenges of Sudanese heritage and mentioned that around 150 pyramids near to Nile River were affected during the recent flooding.

Nowadays, to protect the construction materials surfaces from different environmental actions, novel nano-based materials are develpoing for consolidation and protection of archaeological stones surfaces and joint mortars. In this regard, [**65**] prepared SiO_2-TiO_2 and PDMS compound which was used as coating material. This compound gave a good performance as photocatalytic and superhydrophobic material. SiO_2 is considered the support for TiO_2 that prevents the formation of large clusters of TiO_2 and create nano TiO_2 colloidal with high catalytic activity for different applications [**66**]. [**67**] Carried out an experimental study to evaluate SiO_2-TiO_2 nano-composite as anti-fouling and anti-microbial applied on historic Roman mortar. They discussed the efficient role of SiO_2-TiO_2 integration as a durable coating material for the preservation of the mortar surface.

From previous literature, it can be concluded that although many studies have been carried out, there are still many gaps and lackage in topics of archaeometrical studies because most of the studies only focus on archaeological excavations for the underwater findings without looking after the archaeological matters and their characteristics, problems and conservation, especially for the stone-based monuments and existed in underwater conditions. Furthermore, most studies have focused or continue to focus on coastal, marine and oceanic archeological sites, but for river underwater archaeology there is hardly any study. In this sense, in Egypt, all archaeological studies are concentrated in the Mediterranean Sea and the Red Sea but related to the Nile River still without any archaeometrical studies for underwater findings and buildings along with the comparison with subaerial environments at El Ashmoenin archaeological site (Nero Temple, Egypt), Abusir archaeological site (Sahure pyramid, Egypt) and Al Bagrawyia archeological site

(Pyramids of Meroe, Sudan). That is why; the present research is entitled “Durability problems of the archaeological construction materials in aqueous and subaerial environments, with applications for restoration and conservation in Egypt and Sudan”.

1.2. Research gap

According to the mentioned literature review previously, it is observed that there is no study to compare two or more different environments risks on the archaeological construction materials, especially in comparing the impact of the fluvial, coastal, urban and desert envoirmments on the construction materials. The fluvial water impact on the archaeological building materials is missing, especially in Egypt. In addition, the assessment and creation of multifunctional Nano-materials is needed and novel. In Sudan, it is noticed that there are very few articles discussing the conservation problems on some sites that indicates the gap of the research in this country, especially in the conservation and restoration field. In this regard, the current study was carried out to study different kinds of archaeological construction materials and their conservation problems in various environments in Egypt. The research was conducted on some selected archaeological buildings such as Sahure's pyramid (desert environment) at Abusir (Giza, Memphis), Nero/Ramses II Temple (Urban and agricultural environment) at El-Ashmonein archaeological site (Minia), Anfushi's Necropolis (Coastal environmental) in Alexandria, Abaton/Osiris Temple (Fluvial environment) (Aswan, south of Egypt) and the pyramids of Meroe in (desert environment) at Al Bagrawiya archaeological site (Sudan). On the other hand, synthesizing new multifunctional Nano-based material was addressed using a series of advanced techniques to assess 3%, 5% and 7 % of SiO_2-TiO_2 NPs/TEOS and to select the most efficient percentage in the consolidation of the ancient lime mortars surfaces with multifunctional properties. To conduct the research, field observations and monitoring, analytical (X-ray diffraction, X-ray fluorescence, Raman spectroscopy, UV-Vis spectrometry), microscopic (binocular microscope, polarizing microscope, and scanning electron microscope), mapping (AutoCAD, ArcMap 10.8, SeaDAS, QGIS), testing (physical and mechanical) investigations were carried out. Finally, open-access satellite lenses were used for the detection and assessment for the archaeological sites and their risks.

1.3. Hypotheses

The main scientific questions to answer and hypotheses are:

- Nile river water has an effective role in damaging underwater construction materials or contact with water.

Hypothesis 1: The archaeometrical studies through examination, investigation, and analysis will be carried out to evaluate the influence of Nile River water upon the total and partially submerged archaeological building.

- What is the coastal environment's influence on archaeological building characteristics adjacent to the sea?

Hypothesis 2: Saline water influences the physical (porosity and density) and mechanical (compressive strength) properties of construction materials due to the salt attack from the sea (the Mediterranean Sea at Alexandria) and this assessment study is going to be carried out throughout investigative, analytical, and testing studies.

- Is the desert environment aggressive to archaeological construction materials?

Hypothesis 3: The geoenvironmental impact of the desert can be aggressive, especially the variations of temperature degrees, wind and rains on the construction materials. The research will address monitoring studies for the climate and environmental data in the sites and their impact on the building materials through analysis and microscopic studies.

- What is the impact of the urban environment on the durability of the construction materials?

Hypothesis 4: The urban environments can affect the construction materials, especially through the subsurface water coming from near houses and agricultural activities. The assessment of the urban area will be conducted through the analysis of the construction materials and their alteration.

- Are there preservation strategies that should be done to protect the archaeological underwater stone construction materials?

Hypothesis 5: The research is going to present conservation, restoration, and management plan for the cultural heritage in different environmental sites through development some nanomaterials that used in protection of stone surfaces subjected to water and development of structural pins to repair the damaged stone block of the underwater archaeological buildings.

1.4. Objectives

The main objective is to compare and assess the durability problems of the selected archaeological buildings related to aqueous ambient (Nile River and the Mediterranean Sea), compared with aerial ambient (desert and urban environment) from Egypt and Sudan. In this context, the specific objectives are:

1. Identify and characterize the construction materials chemically, physically and mechanically from the selected monuments.
2. Investigate the microstructure of the construction building materials.
3. Study the the geonvironmental impact on the selected archaeological sites and their built heritage.
4. Detect both the external and internal decay factors and instability of the construction materials.
5. Map the decay patterns in the structural and architectural elements
6. Discuss the mechanisms of decay and degradations for the various construction material in each site.
7. Create multifunctional nano-based material to consolidate the lime mortars surface of the archaeological buildings in the selected sites.

1.5. Significance

The most significant outputs of the doctoral research are 1) contributing to understanding how can aqueous and subaerial environments affecting the Egyptian cultural heritage; 2) getting new information for the construction materials used for the selected submerged building in Aswan; 3) evaluating the impact of different water environments upon selected archaeological buildings; 4) study the construction materials and their decay in the urban and desert environments as well; 5) creating new nano-composite multifunctional materials for mortar surfaces protection from water and environmental impacts; and, finally, 6) contributing to the preservation of world cultural heritage in different environmental challenges.

1.6. Research organization

This Thesis is classified into six chapters and provided 81 figures and 19 tables, and the organization of each chapter of the results section has been done according to the publication system of a paper:

1. Title
2. Highlights
3. Graphical abstract
4. Abstract
5. Keywords
6. Introduction
7. Aim of the study
8. Archaeological, architectural, geographical, geological, hydrological, climatic and/or environmental context for each case study
9. Materials and Methods
10. Results
11. Discussion
12. Conclusion
13. References

1.7. References

[1] Timmermans D, Guérin U. Heritage for peace and reconciliation: safeguarding underwater cultural heritage of the First World War;manual for teachers. Français.2015 https://unesdoc.unesco.org/ark:/48223/pf0000231426

[2] Viejo-Rose D. Cultural heritage and memory: untangling the ties that bind. *Culture & History Digital Journal*.2015; *4*(2), e018. https://doi.org/10.3989/chdj.2015.018

[3] Mann H. The Appearance of New Bacteria (titanic bacterium) and Metal Corrosion. *UNESCO Scientific Colloquium on Factors Impacting Underwater Cultural Heritage*.2011; *December*,44–51. https://www.academia.edu/7243168/UNESCO_SCIENTIFIC_COLLOQUIUM_ON_FACTORS_IMPACTING_UNDERWATER_CULTURAL_HERITAGE?email_work_card=view-paper

[4] Khakzad S. *Conservation, and Presentation of Underwater Cultural Heritage to the Public Case study: The current projects in Belgium Leuven*. 2008;146. https://www.academia.edu/3677467/Underwater_Cultural_Heritage_Conservation_and_Presentation_to_the_Public_Master_Thesis?email_work_card=view-paper

[5] Florida Department of State. https://dos.myflorida.com/historical/archaeology/underwater/underwater-preserves/ accessed on 07/01/2023.

[6] UNESCO. Underwater Cultural Heritage from World War I. In *Scientific conference on the occasion of the centenary of World War I*. 2014; Issues 26 & 27 June. https://www.academia.edu/13991579/The_Underwater_Cultural_Heritage_of_World_War_I._Proceedings_of_the_Scientific_Conference_on_the_Occasion_of_the_Centenary_of_World_War_I_Bruges_Belgium_26_and_27_June_2014?email_work_card=minimal-title

[7] Ferenčić N, Brugman F, Villegas T, Dromgoole S, Sataloff R T, Johns M M, Kost K M, UNESCO, Guérin U, SCHWARZ G, VV AA, Favis R L, Manders M R, Underwood C J, Goter P W, Mann H, Body T A, Williams S. *International Journal of Nautical Archaeology*. 2015; *152*(2), 1–6.

[8] Hassan M, Grimal N, Nakashima D. *Underwater Archaeology and Coastal Management focus on Alexandria*.2000. ISSN: 9231037307, UNESCO.

[9] Maarleveld T J, Guérin U, Egger B. *Manual for Activities directed at Underwater Cultural Heritage, Guidelines to the Annex of the UNESCO 2001 Convention, in Arabic*. 2016. www.unesco.org/en/underwater-cultural-heritage

[10] Craig F, Bill J. *Underwater cultural heritage (UCH) related legislation and programme review in the five countries in Micronesia - UNESCO Biblioteca Digital.pdf*. 2018. (UNESCO).

[11] Body T A. *The Benefit of the Protection of Underwater Cultural Heritage for Sustainable Growth, Tourism and Urban Development*.2001. https://www.scubatravel.co.uk/unesco-underwater-tourism.pdf

[12] Prott L. Underwater Cultural Heritage at Risk: Managing Natural and Human Impacts. In *International Journal of Nautical Archaeology.2007;* Vol. 36, Issue 2, pp. 429–431. https://doi.org/10.1111/j.1095-9270.2007.163_2.x

[13] Khakzad S. Integrated Approach in Management of Coastal Cultural Heritage. *Dissertation*. 2015; *June*, 236. https://kuleuven.limo.libis.be/discovery/search?query=any,contains,lirias1727535&tab=LIRIAS&search_scope=lirias_profile&vid=32KUL_KUL:Lirias&foolmefull=1

[14] Khakzad S, Pieters M, Van Balen K. Coastal cultural heritage: A resource to be included in integrated coastal zone management. *Ocean and Coastal Management*.2015; *118*, 110–128. https://doi.org/10.1016/j.ocecoaman.2015.07.032

[15] Carper R G. Underwater Archaeology. *Current Anthropology*.2007; *48*(6), 779–779. https://doi.org/10.1086/521536

[16] Schwarz G. Safeguarding Underwater Cultural Heritage in the Pacific: report on good practice in the protection and management of World War II-related underwater cultural heritage. In *International Journal of Nautical Archaeology.* 2018; Vol. 47, Issue 2, pp. 495–496. https://doi.org/10.1111/1095-9270.12315

[17] Hairy I. *The Qaitbay Underwater Site at Alexandria, Egypt: The evolution of surveying techniques*. 2020. https://doi.org/10.33583/utm2020.11

[18] Pierre T, Gregory M. The harbor of Khufu on the Red Sea Coast at Wadi al-Jarf, Egypt. *Near Eastern Archaeology.2014; 77*(1), 4-14. doi:10.5615/neareastarch.77.1.0004.

[19] Abd-el-Maguid M M. Underwater Archaeology in Egypt and the Protection of its Underwater Cultural Heritage. *Journal of Maritime Archaeology*.2012; *7*(1), 193–207. https://doi.org/10.1007/s11457-012-9098-5

[20] English Heritage. Practical building conservation. Stone. https://historicengland.org.uk/images-books/publications/stone-conservation/stone-marketing-spreads/ accessed on 06/01/2023.

[21] https://australia.icomos.org/resources/australia-icomos-heritage-toolkit/stone-conservation-of/ Accessed on 06/01/2023.

[22] Rabasa D E. Forma y construcción en piedra: de la cantería medieval a la estereotomía del siglo XIX. Madrid: Akal. 2000.ISBN 84-460-1542-0.

[23] Price MT. Decorative stone: the complete sourcebook. London: Thames & Hudson.2007. ISBN 978-0-500-51341-5.

[24] Meyhofer D. Set in stone : rethinking a timeless material. Berlin: Braun. 2009. ISBN 978-3-938780-64-0.

[25] Charola AE. Stone Deterioration Characterization For its Conservation. 2016;24(2):16–20.

[26] Liu X, Koestler RJ, Warscheid T, Katayama Y, Gu J. Conservation of stone monuments and buildings. Nature Sustainability [Internet]. 2020;3(December). Available from: http://dx.doi.org/10.1038/s41893-020-00602-5

[27] Basu S, Orr SA. A Geological Perspective on Climate Change and Building Stone Deterioration in London : Implications for Urban Stone-Built Heritage Research and Management. Atmosphere 2020, 11, 788; doi:10.3390/atmos11080788.

[28] Lazzari M, Cano E. Science and Technology Conservation of Cultural Heritage. 2013. https://doi.org/10.1201/b15577

[29] Binda L, Giuliana C, Elsa G. Study of Decay of Historic Masonry Due to Salt Crystallization: A Systematic Approach.2011;1–4. https://www.irbnet.de/daten/iconda/CIB22294.pdf

[30] Tsipoura-Vlachou M. Michopoulos K. Characterization and causes of the building stone decay at the Artemis temple, Brauron, E. Attica, Greece. Bulletin of the Geological Society of Greece.2007; 40(4), 1859–1873. https://doi.org/10.12681/bgsg.17146

[31] Danese M, Demšar U, Masini N, Charlton M. Investigating material decay of historic buildings using visual analytics with multi-temporal infrared thermographic data.. 2010;3(April 2009):482–501.

[32] Lerma C, Mas Á, Gil E, Vercher J, Peñalver MJ. Pathology of building materials in historic buildings. Relationship between laboratory testing and infrared thermography. 2014; 64(313):1–11.

[33] Veniale F, Lodola MSS. Datos y perspectivas Diagnosing stone decay in built heritage. Facts and perspectives. 2008; 58: 11–32.

[34] Casula G, Fais S, Cuccuru F, Bianchi MG, et al. Decay Detection in an Ancient Column with Combined. 2021;1–17.

[35] Lopez-arce P, Navarro A, Zornoza-indart A, Gómez D. Identification and cause of decay of building materials used in the architectural heritage of Bizerte city (Tunisia). 2017;19:2017.

[36] Donato A, Randazzo L, Ricca M, Rovella N, Collina M, Ruggieri N, et al. Decay Assessment of Stone-Built Cultural Heritage: The Case Study of the Cosenza Cathedral Façade (South Calabria, Italy). 2021; 1–17.

[37] Hanafy H M. Diagenesis of the middle Eocene "nummulite bank" of The Giza pyramids plateau, Egypt: petrologic and 18°/16° evidence, Qatar Univ. Sci. J. 1994;14 (I): 146-152.

[38] Emery KO. Weathering of the Great Pyramid. J. Sediment. Res.1960;30(1):140–143. https://doi.org/10.1306/74D709DE-2B21-11D7-8648000102C1865D

[39] Reader CD. A Geomorphological Study of the Giza Necropolis, with Implications for the Development of the Site. Archaeometry. 2001;43(1):149–65. https://doi.org/10.1111/1475-4754.00009

[40] Pyramids Plateau Groundwater Lowering Activity. Environmental Assessment Report, United States Agency for International Development. USAID Egypt, 2010. https://pdf.usaid.gov/pdf_docs/PA00HS7G.pdf Accessed 25 Feb 2022.

[41] Gandah AF. The Conservation Status of the Pyramid of Khufu. Hist.R.L.2015; 26:12–22. https://www.iiste.org/Journals/index.php/HRL/article/viewFile/26963/27646

[42] Franc Z. Petrographic Observations of the Building Stones of the Great Pyramid of Giza. J. Eng. Geol. 2017; 28;5(4). 10.17265/2328-2193/2017.04.002

[43] Kukela A. Assessment of Stone Material Deterioration of the Exposed Surfaces of the Step Pyramid in Saqqara. Earth Sci. Eng. 2013; 3:238-244.

[44] Khalil AE, Abdel Hafiez HE, Girgis M, Taha MA. Earthquake ground motion simulation at Zoser pyramid using the stochastic method: A step toward the preservation of an ancient Egyptian heritage. NRIAG J. Astron. 2017; 6(1):52–9. https://doi.org/10.1016/j.nrjag.2016.11.003

[45] Ahmed AA, Fogg GE. Journal of African Earth Sciences The impact of groundwater and agricultural expansion on the archaeological sites at Luxor, Egypt. J. African Earth Sci. 2014; 93–104. https://doi.org/10.1016/j.jafrearsci.2014.02.007

[46] Aly N, Heras MG, Hamed A, Buergo M.A, Soliman F. *The influence of temperature in a capillary imbibition salt weathering simulation test on Mokattam limestone*. 2015; 65(317). Available from: https://materconstrucc.revistas.csic.es/index.php/materconstrucc/article/view/1682

[47] Aly N, Hamed A. The impact of salt crystallization on the building stones of Al-Azhar Mosque. 2020;11(4):895–904. Available from: https://ijcs.ro/public/IJCS-20-65_Aly.pdf Accessed 10 April 2022.

[48] Bradley SM, Middleton AP. A Study of the Deterioration of Egyptian Limestone Sculpture. *J. Am. Inst. Conserv.*1988; *27*(2): 64–86. https://doi.org/10.2307/3179403

[49] Wu RAJ, Schlu C. *The Origin of Soluble Salts in Rocks of the Thebes Mountains, Egypt: The Damage Potential to Ancient Egyptian Wall Art*. 2000; 1161–1172. https://doi.org/10.1006/jasc.1999.0550

[50] Mahmoud HM, Kantiranis N, Stratis JA. *Salt Damage on the Wall Paintings of the Festival Temple of Thutmosis III, Karnak Temples Complex, Upper Egypt*. *Int. J. Environ. Sci.* 2010;1(3): 133-142.

[51] Aboushook M, Park HD, Gouda M, Mazen O, El-Sohby M. Determination of durability of some Egyptian monument stones using digital image analysis, Proceedings of the 10th IAEG Congress – Engineering Geology for Tomorrow`s Cities, Nottingham, UK, The Geological Society of London, 2006, Paper Number: 80, pp.1-10. Available from: https://kau.edu.sa/Files/135/Researches/59046_29391.PDF Accessed 18 April 2022.

[52] El-Raey M. Vulnerability assessment of the coastal zone of the Nile delta of Egypt, to the impacts of sea level rise. 1998; 37(1), 29–40. https://doi.org/10.1016/S0964-5691(97)00056-2

[53] Elsharkawy H, Rashed H, Rached I. *Climate Change: The Impacts of Sea Level Rise on Egypt*. 2009, 1–11. Available from: https://www.isocarp.net/data/case_studies/1456.pdf Accessed 03 May 2022.

[54] Bekheet R A, Raey M El, Yassin A. The crest line approach for assessing the development of coastal flooding due to sea level rise. *Mitigation and Adaptation Strategies for Global Change*. *October* 2017. https://doi.org/10.1007/s11027-016-9717-9

[55] El-Raey M, Regional Center for Disaster Risk Reduction (RCDRR). Impact of sea level rise on the Arab Region. UNDP Regional Bureau for the Arab States (UNDP-RBAS), Cairo, Egypt. 2010. Available from: https://research.fit.edu/media/site-specific/researchfitedu/coast-

climate-adaptation-library/africa/morocco-algeria-tunisia/El-Raey.-2010.-SLR-Impacts-on-Arab-Region.pdf Accessed 05 May 2022.

[56] Abdelnaby A E, Elnashai A S. Integrity assessment of the Pharos of Alexandria during the AD 1303 earthquake Integrity assessment of the Pharos of Alexandria during the AD 1303 earthquake. *Engineering Failure Analysis*. 2013, *33*(October 2017), 119–138. https://doi.org/10.1016/j.engfailanal.2013.04.013

[57] Ahmed A A, Fogg G E. Journal of African Earth Sciences The impact of groundwater and agricultural expansion on the archaeological sites at Luxor, Egypt. Journal of African Earth Science.2014; 95, 93–104. https://doi.org/10.1016/j.jafrearsci.2014.02.007

[58] Hemeda S, Fahmy A, Moustafa A, Abd M, Hafez E. The Early Basilica Church, El-Ashmonein Archaeological Site, Minia, Egypt: Geo-Environmental Analysis and Engineering Characterization of the Building Materials. 2019, 157–186. https://doi.org/10.4236/ojg.2019.93011

[59] Ahmed E A. Investigation of environmental impacts on sandstone blocks at Luxor temple and concepts for conservation. 2016; 1 (1), 23–45. https://dx.doi.org/10.21608/jguaa2.2016.3893

[60] Sweek T, Anderson J R, Tanimoto S. Architectural Conservation of an Amun Temple in Sudan. 2012;10(2), 8–16. http://doi.org/10.5334/jcms.1021202

[61] Osman M A, Ali E M, Elhaj O B. A Study on Geotechnical Properties of Weak Rocks in Sudan Abstract. 2014; 17, 13–27. https://doi.org/10.53332/jbrr.v17i.597

[62] Government of Sudan. Report: Sudan Rapid Post Disaster Needs and Recovery Assessment (Rapid PDNRA). 2021. Available from: https://www.gfdrr.org/sites/default/files/Sudan_RPDNRA-English_HighRes.pdf

[63] Onderka P, Vrtal V. Preliminary report on the nineteenth excavation season of the archaeological expedition. 2021; 145–163. https://doi.org/10.37520/anpm.2021.012

[64] Fahmi M M, Ahmad Y, Hashim H. The Challenges for Preserving Glorious Heritage of Sudan: Status and Solutions. 2022;9(2), 25–38. Available from: https://www.informaticsstudies.org/index.php/informatics/article/download/334/434

[65] Wang X, Ding H, Sun S, Zhang H, Zhou R, Li Y, Liang Y, Wang J. Preparation of a temperature-sensitive superhydrophobic self-cleaning SiO2-TiO2@PDMS coating with photocatalytic activity. *Surface and Coatings Technology*. 2021; *408* (December 2020), 126853. https://doi.org/10.1016/j.surfcoat.2021.126853

[66] Kim D, Noh W, Jo S, Lee TS. Electrospun mesoporous silica nanofibers decorated with titanium dioxide nanoparticles for a repeatable photocatalysis. *Molecular Crystals and Liquid Crystals*.2021; *730*(1), 85–100. https://doi.org/10.1080/15421406.2021.1956761

[67] Gemelli G M C, Luna M, Zarzuela R, Gil Montero M L A, Carbú M, Moreno-Garridol, Mosquera M J. 4-Year in-situ assessment of a photocatalytic TiO2/SiO2 antifouling treatment for historic mortar in a coastal city. *Building and Environment*.2022; *225*, 109627. https://doi.org/https://doi.org/10.1016/j.buildenv.2022.109627

Chapter 2

Cases of study, materials and methodology

2. Study cases and geological context

2.1. Archaeological sites in Egypt and Sudan

Fig. 2.1 displays the different locations of the selected archaeological sites in Egypt: Necropolis of Anfushi (Alexandria), Sahure Pyramid (Abusir), Nero Temple (Minia, El Ashmoenin archaeological site), and Abaton Temple (Aswan) in Sudan, the Pyramids of Meroe (Al Bagrawyia archeological site). The present research is an analytical and comparative study between different selected sites in Alexandria (Al-Anfushy tombs) exposed to the coastal environment, and the second located in Aswan (Abaton temple of Osiris near to Philae temple) as (river environment) partially submerged cultural heritage. On the other hand, subaerial environments, Sahure Pyramid (Abusir) and Pyramids of Meroe (Al Bagrawyia archeological site) were selected as desert environment, Nero Temple (Minia, El Ashmoenin archaeological site) as urban environment. The coastal environment represents the subaerial marine archaeology causes many erosions impacts on the archaeological buildings contact with the marine environments due to saline water action and salt decay. On the other hand, the river environments also have different impact upon the archaeological buildings totally or partially submerged in Nile River. Furthermore, the desert environment shows the geoenvironmental impacts on the durability of the construction material and in the urban environment; the subsurface water is the main hazard of the building materials decay. Generally, this study is a pioneer study because all previous archaeometrical studies were upon aerial stone archaeological buildings in the deserts or above the ground.

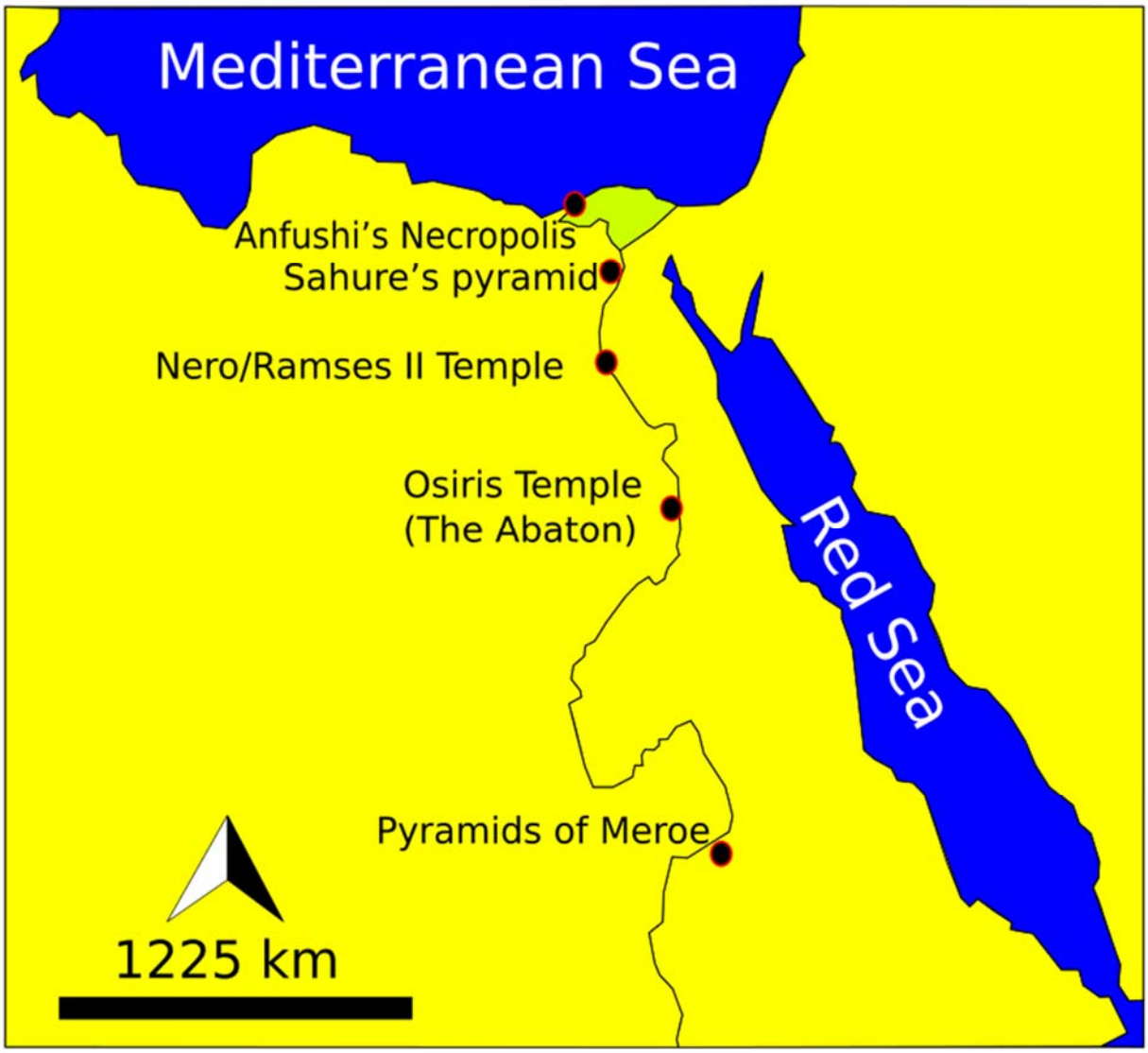


Fig. 2.1. The locations of the selected archaeological sites in Egypt (Anfushi Necropolis, Sahure pyramid, Nero Temple and Abaton Temple) and Sudan (Pyramids of Meroe).

2.1.1. Aswan (Egypt): Abaton temple of Osiris, Philae complex

Aswan is a big city in south of Egypt with coordinates 24°05'20"N / 32°53'59"E and 194 m.a.s.l., and it is considered the border between Egypt and Sudan. A lot of fascinating archaeological sites are existing in Aswan such as Wadi Allaqui, Abu Simbel, Elephantine, Philae, El Nabatat Island, Kalabsha temple, Tombs of nobles, Nubia, Banu Kanz and Coptic Diocese of Syene, among others.

Our case study is related to Abaton temple of Osiris related and near to Philae complex (**Fig. 2.1**) which it is located on Agilkia Island on Nile River. Nile river is the world's longest river, the Nile runs 6,695 km from its source in Burundi, in Central Africa, to the Mediterranean Sea, most of the water contributed to the Nile comes from the Blue Nile, which originates at Lake Tana in Ethiopia, the average flow of the Nile River is about 50 million cubic meters per day., During the rainy season, however, the three branches of the Nile River increase their flow to just over 700 million cubic meters per day [**1**]. The research focuses on the Abaton temple of Osiris, south to Philae complex that is situated on north side of Aswan dam (**Fig. 2-2**). Abaton temple of Osiris is a very clear example for the effects of freshwater environment (Nile River) and atmospheric environment. **Fig. 3** shows the effects of Nile River oscillation levels upon archaeological buildings in Aswan, where the bluish and reddish colors mean the Nile River and rocks around, respectively.

This temple was constructed by ancient Egyptians under *Ptolemaic* era and was devoted as mausoleum to the Osiris god (God of fertility, agriculture, after life and death), considered as the most important sacred place in Egypt because it was the tomb of Osiris. This current remained gate was constructed in the entrance of this tomb and now is located in Bigeh Island but previously was situated in west side of Philae Island (**Fig. 3**).

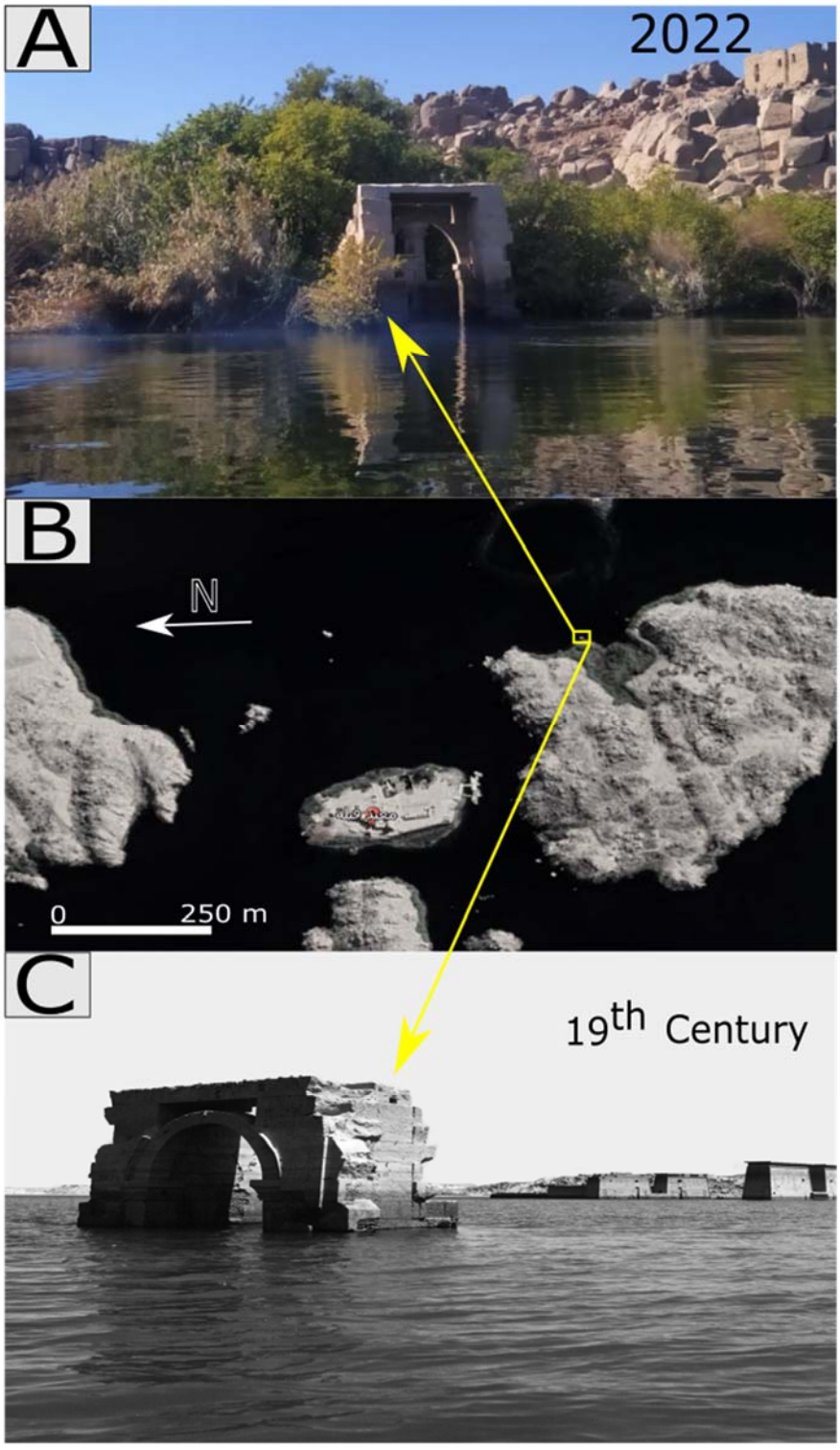


Fig. 2.2. (A) Osiris temple (The Abaton) in Aswan (Bigeh Island) referred in the yellow square (B). (C) Represents the semi- submerged Osiris Temple in in the Nile River (UNESCO archives).

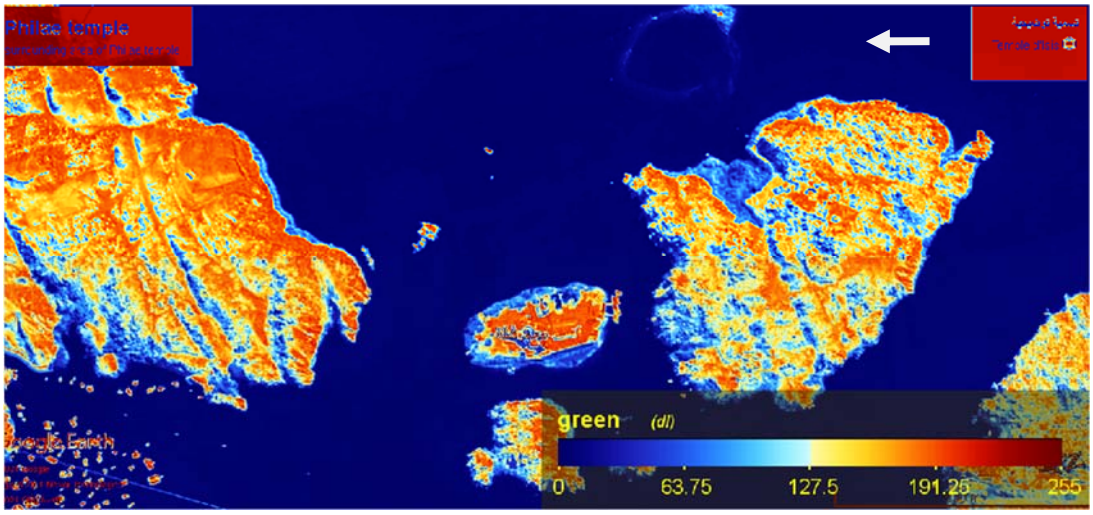


Fig. 2.3. Map of archaeological site of Philae temple and Abaton temple of Osiris in Aswan and Nile water surrounding and covering parts of the archaeological buildings such as Abaton temple of Osiris, (Blue: Nile water; yellow and red: dry rocks).

2.1.2. Alexandria (Egypt): Al-Anfushi Necropolis

The research will focus on the marine archaeological buildings exposed to saline water environment in Alexandria, such as Al-Anfushi Necropolis. In 1901, Giuseppe Botti who is the director of the Greco-Roman Museum discovered the Anfushi Tombs, he was the first to discover the tombs and publish about them. After his death, in 1903, Evaristo Breccia and Achille Adriani, his successors in the directorship of the museum, continued the work of Botti. Only five tombs from the overall complex are visible today, dating from the mid of second century, from these tombs, Anfushi I, II, and V will be studied. Each of them consists of two burial units, both approached directly by the court, having also subsidiary rooms. The main characteristic of these tombs is the bilingual character of its decoration, which emerged with the redecoration of the tomb. During this process, Greek decorative elements were retained in the anteroom, while Egyptian elements were added, probably onto plaster previously unpainted, we should also be aware of the fact that the necropolis was located in a district where the majority of the population was Egyptian. In addition, Anfushi II was the only structure of a Ptolemaic Alexandrian tomb with Egyptian-style views, such as the

priest painted in the mural painting of the stairs headed to the court. A comparison with other types of material evidence indicates the important role of Egyptian priesthood throughout the Ptolemaic Period [**2-4**].

In this necropolis, the study will focus on archaeometrical and petrophysical studies for the construction materials of those tombs and their durability problems due to the coastal environment and effect of subsurface water which led to severe degradation and decay to the structural, architectural and decoration elements of the tombs, with advanced techniques for analysis and investigation to assess the durability of the stone construction material (**Fig. 2.4**).

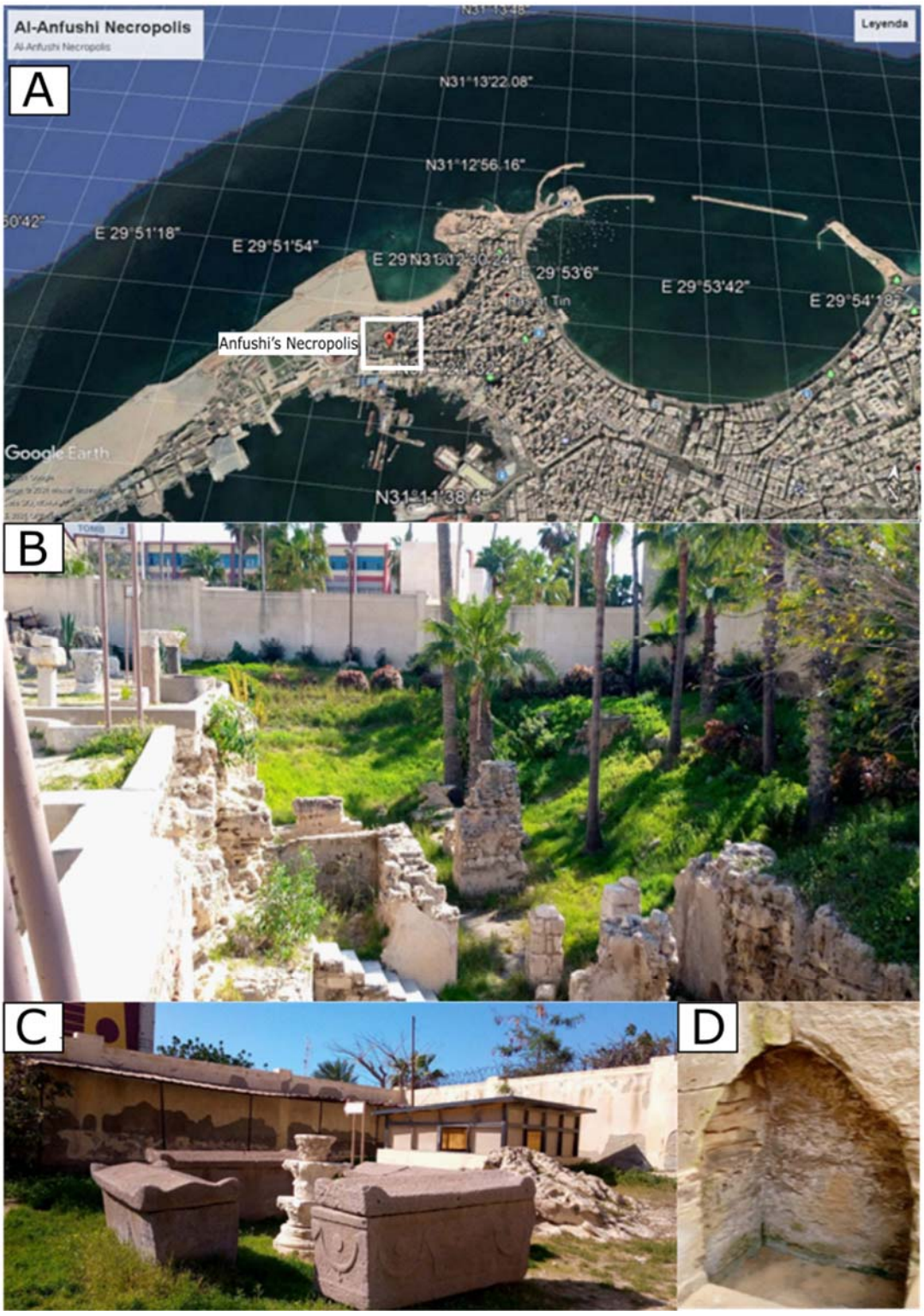


Fig. 2.4. Al Anfushi tombs, A) Google Earth image for the location of Al Anfushi tombs (White square), B) General view of Al Anfushi tombs, C) and D) durability problems (salt decay) of the elements and the construction materials of Al Anfushi tombs.

2.1.3. Abusir (Giza, Egypt): Sahure's pyramid

Of the sixty villages named Abusir in Egypt, only one is an archaeological site of first-class importance. It is located in the southern direction of the Giza Plateau and north of the Saqqara archaeological site and is considered one of the most enriched archaeological sites of the Memphis necropolis (**Fig. 2.5**). The ancient name of Abusir is called Busiri "the house or temple of the Osiris". In this site, the work will focus on the study of the archaeological construction materials of Sahure's pyramids and their durability.



Fig. 2.5. (A) Location of the site on global earth map. (B) The map of Abusir area (Blue rectangle) and its monuments. (C) General view for Sahure's pyramid.

2.1.4. El-Ashmonein archaeological site (Minia, Egypt: Nero Temple)

El-Ashmonein is a small village located in Mellway District of Minia governate, which is about 246 km from Cairo, situated on the western bank of the Nile River, 27 m elevation and one of the ancient Egyptian metropolis capitals of the fifteenth century of Upper Egypt is called the "hare". In this site, we will study the impact of the agricultural and urban environment on the archaeological construction materials of Nero's temple (**Fig. 2.6**).

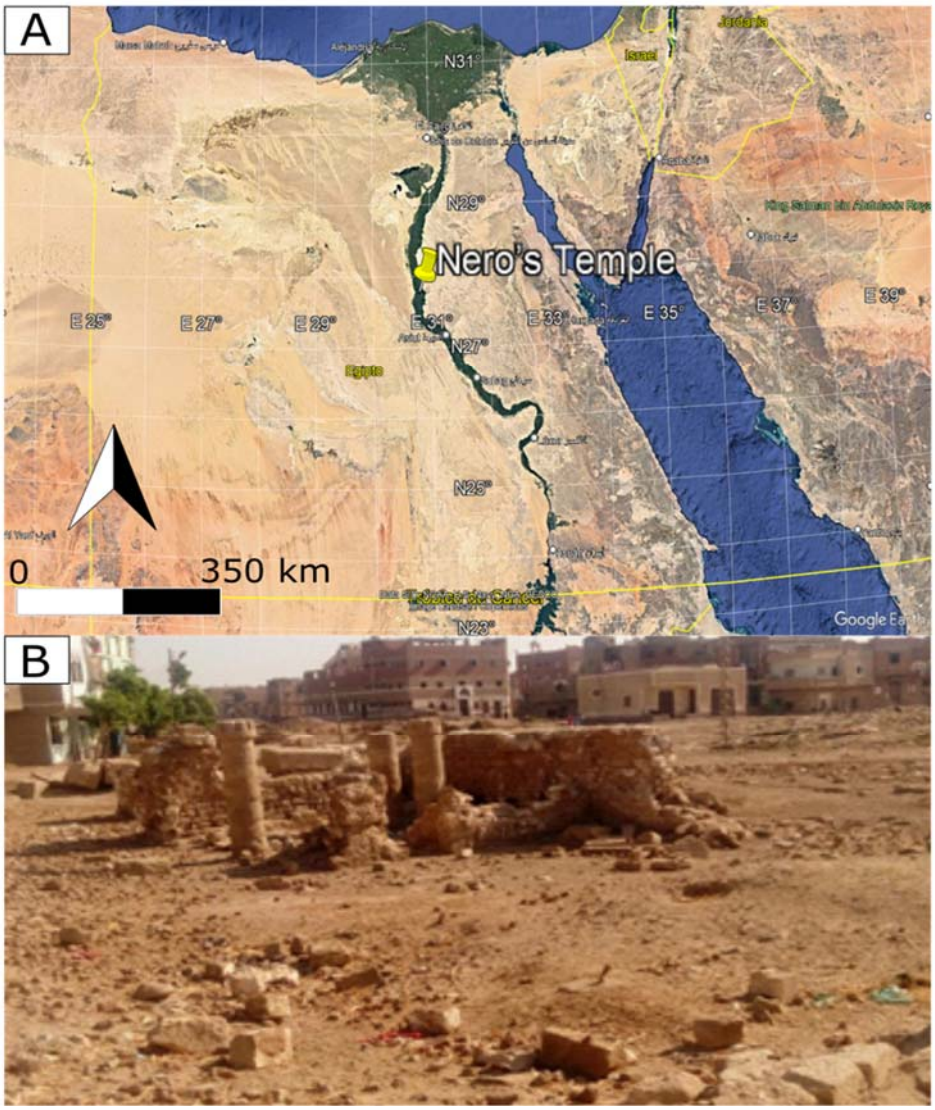


Fig.2. 6. (A) Location of El-Ashmonein site on Egypt map. (B) General view for Nero's Temple.

2.1.5. Al Bagrawiya archaeological site (Sudan): Pyramids of Meroe

Al Bagrawiya archaeological site is a World Heritage Site with significant pyramid-shaped structures of the Meroe kingdom. Meroe was an ancient city in Sudan, and it was the seat of the government and the royal palace. The pyramids of Meroe back to the kingdom of Kush, between the 8th century BC and 4th century AD and were devoted as a necropolis site for the kings and queens of Meroe (**Fig. 2.7**). In this part, the impact of sand dunes and flooding on the pyramids of Meroe will be carried out.

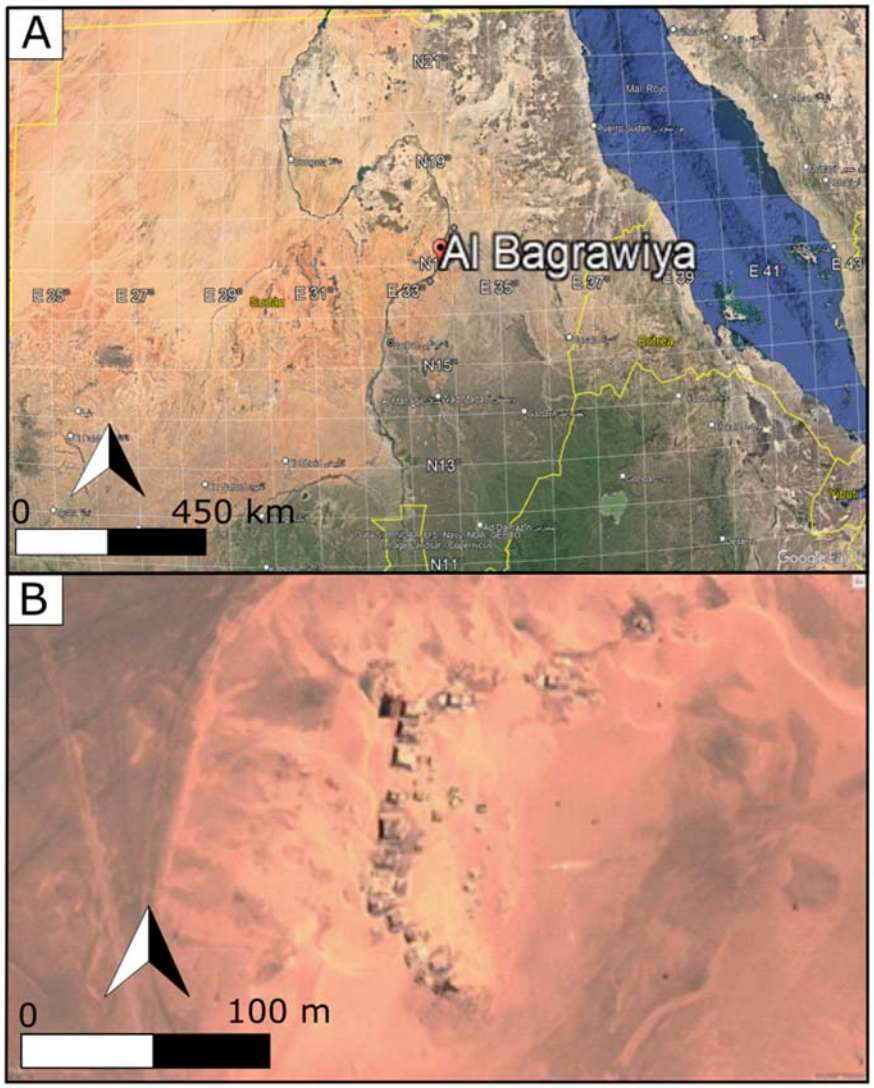


Fig.2.7. (A) Green pin is the location of Al Bagrawiya archaeological site. (B) General view for the pyramids of Meroe (The case study).

2.2. Regional and specific geological context of the selected sites

Egypt covers 1000000 km^2 and it is classified into four major physical regions: Nile Valley and Nile Delta, Western Desert, Eastern Desert and the Sinai Peninsula. Geologically, In Egypt there are mainly 5 types of lithologies in addition to unconsolidated Quaternary sediments (**Fig. 2.8**), Egypt is composed of thick deposits of loose sediments mainly sand dunes in the western desert, flood plain, silty and clay in the Nile valley and sand and gravel in the eastern desert and Sinai, in the northwest is mainly composed of sandstone and conglomerate, western and eastern desert are mainly composed of limestone with some formations in the eastern and western desert with main sandstone of upper cretaceous age and little formations in the southwestern desert are mainly from sandstone and shale and basement rocks and basement complex, are terms that are commonly applied to igneous and metamorphic rocks, overlaid by sedimentary strata. In the eastern and southeastern deserts, there are crystalline basements from igneous and metamorphic rocks [**5,6**].

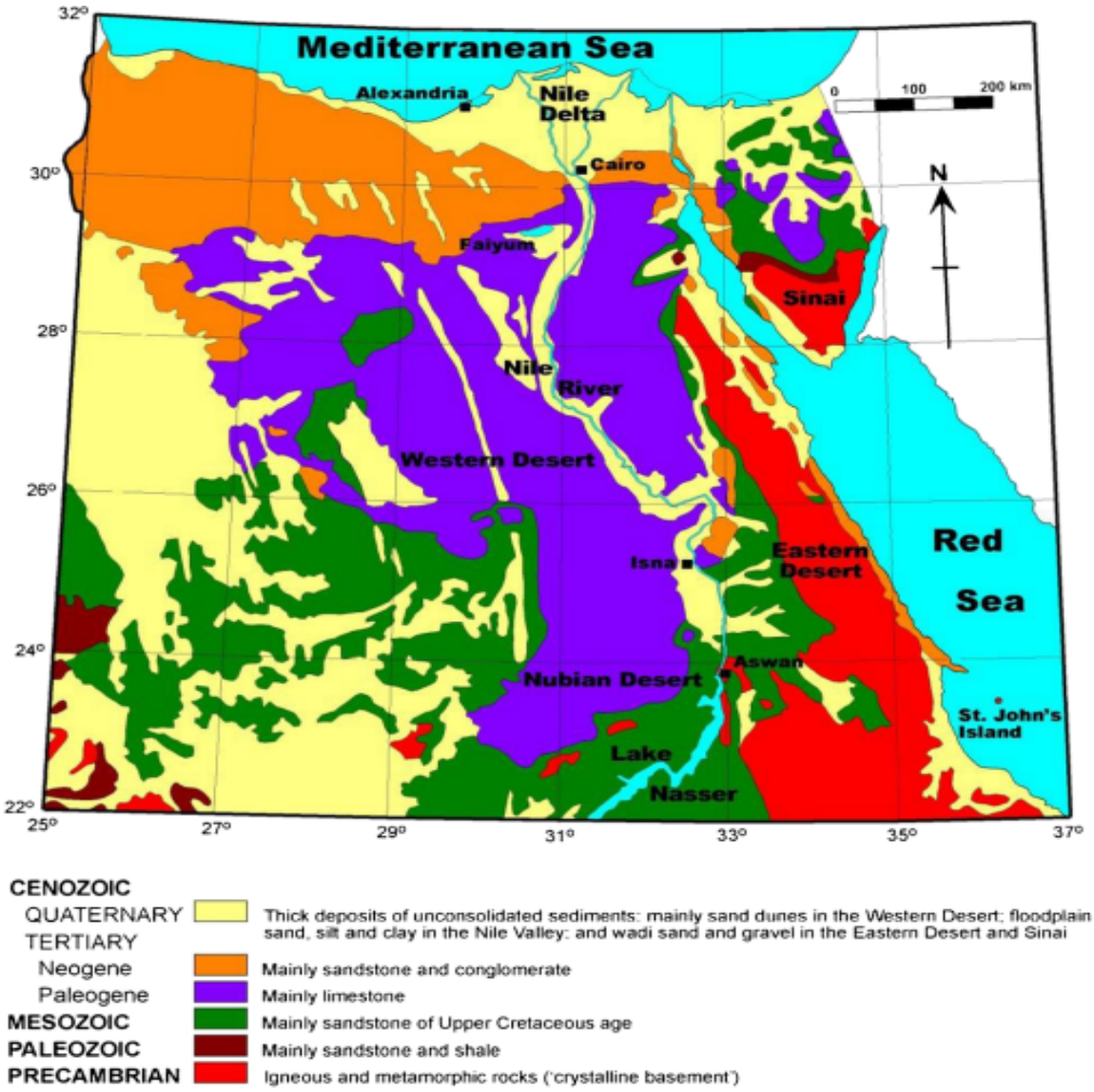


Fig. 2.8. Geological map of Egypt (from [5]).

On the other hand, Sudan occupies 1,886,068 km^2 and its geological features range from Precambrian crystalline basement rocks to Quaternary unconsolidated alluvial deposits. The lithology of Sudan consists of Unconsolidated sedimentary deposits (Quaternary and Late Tertiary to Quaternary), Igneous Volcanic (Tertiary), Mesozoic Sedimentary Rocks - mainly Cretaceous (Upper Jurassic to Lower Cenozoic, mainly Cretaceous) and Precambrian Basement (Precambrian) [7] (**Fig. 2.9**).

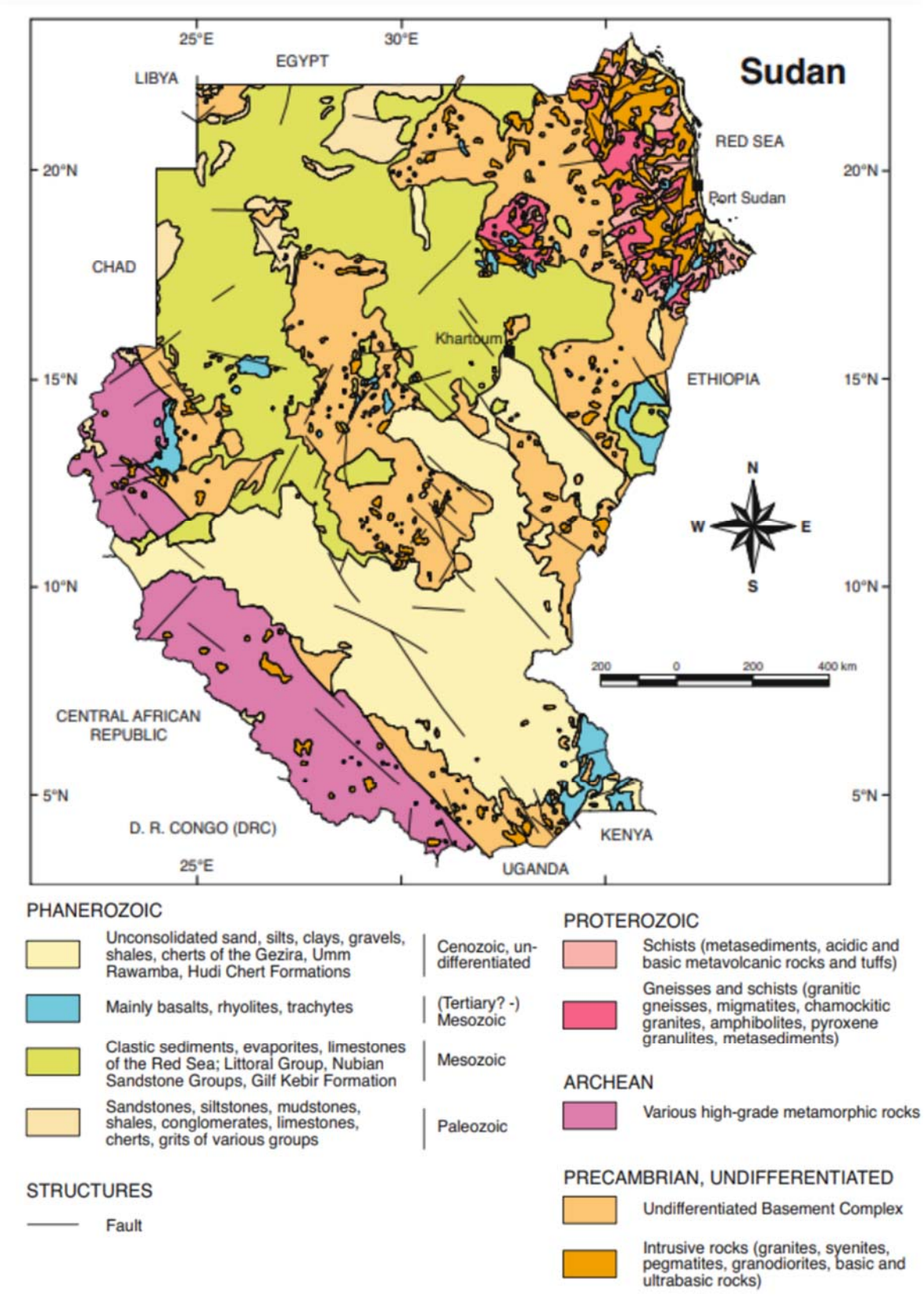


Fig.2.9. Geological map of Sudan (from [8]).

2.2.1. Aswan (Egypt)

Abaton temple of Osiris is situated at a short distance upstream from the First Cataract of the Nile, about 9 kilometers to the South of Aswan town. The underground of this region is formed by various rocks belonging to the Basement Complex, for instance granites, schists and gneisses, meta dolerites, aplites, pegmatites, and late minor dykes and neck intrusions, the coarse variety of the granite is the famous ornamental and building stone, the quarrying of which started more than 5000 years ago during the fourth dynasty of ancient Egypt. The Basement Complex is overlaid by sandstones of the Nubian formation (Upper Cretaceous) [9] (**Fig. 2.10**).

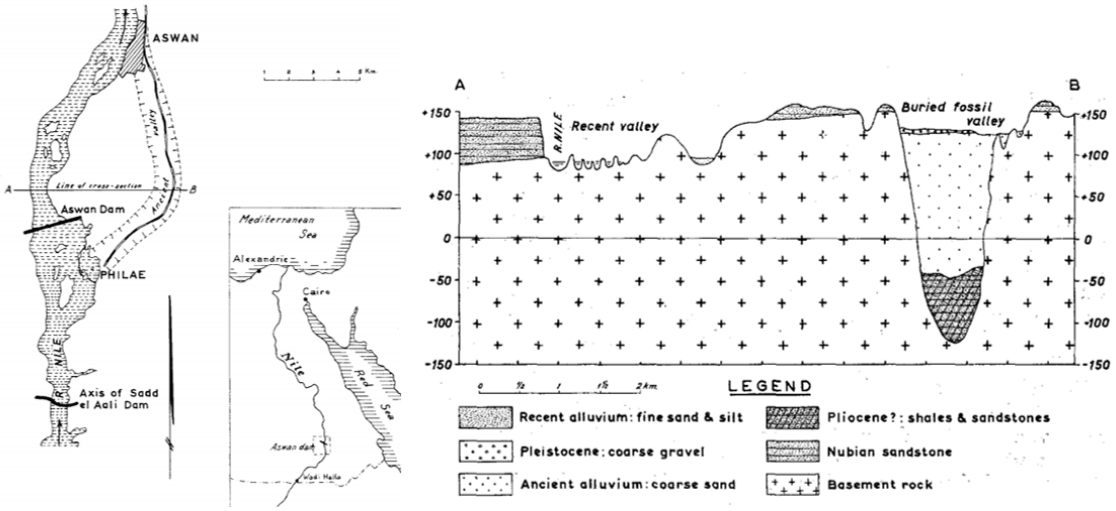


Fig. 2.10. Regional geological setting of Philae area, Aswan (from [6]).

2.2.2. Alexandria (Egypt)

Lithographically, Alexandria's coastline is featured an unconformity surface and is composed of soil sediments, oolitic sand and clay, oolitic limestone, grey shelly dolomite, marly dolomite, oncolitic limestone and dolomite, shelly limestone and core sections comprise largely bioclastic (shelly) and muddy carbonate sand strata interbedded with fine-grained sandy silt, silty mud, and dark organic-rich layers [**10,11**] (**Fig. 2.11**).

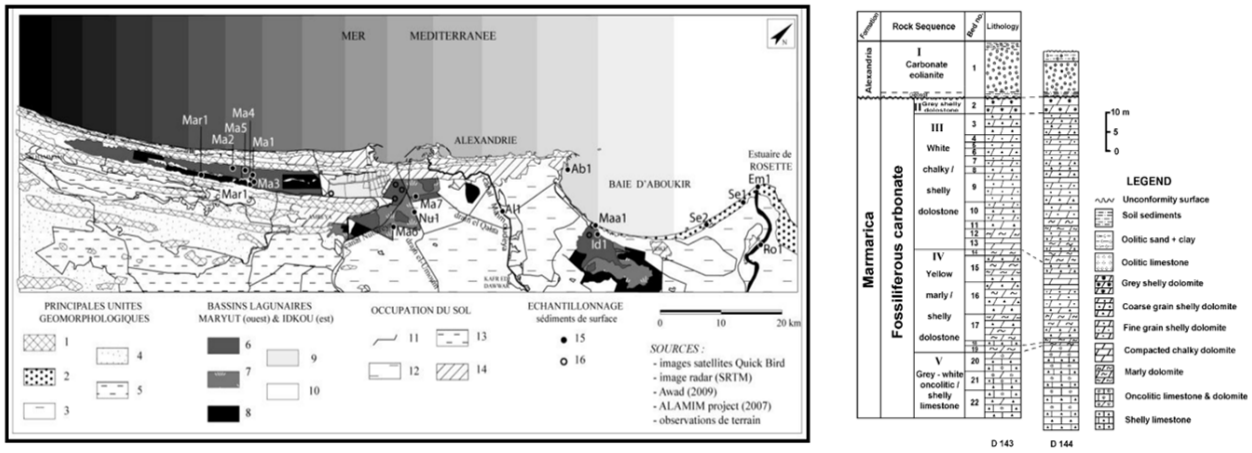


Fig. 2.11. Geomorphological units of Alexandria and its lithology (from [**10**, **12**]).

2.2.3. Abusir (Giza, Egypt)

Generally, the Memphis area consists of different geological features, such as Nile silts, which are located on the eastern and western sides of the Nile River and adjacent to the archaeological sites in Memphis, Wadi (Valley). In addition, deposits include neonile deposits, pronile deposits, undifferentiated pronile deposits, limestone intercalated with shale stones and Cretaceous formations [**13**] (**Fig. 2.12**). Specifically, Abusir geological formations are considered from the Late Eocene, and Maadi limestone, clay-limestone, and marls crop out (tafla).

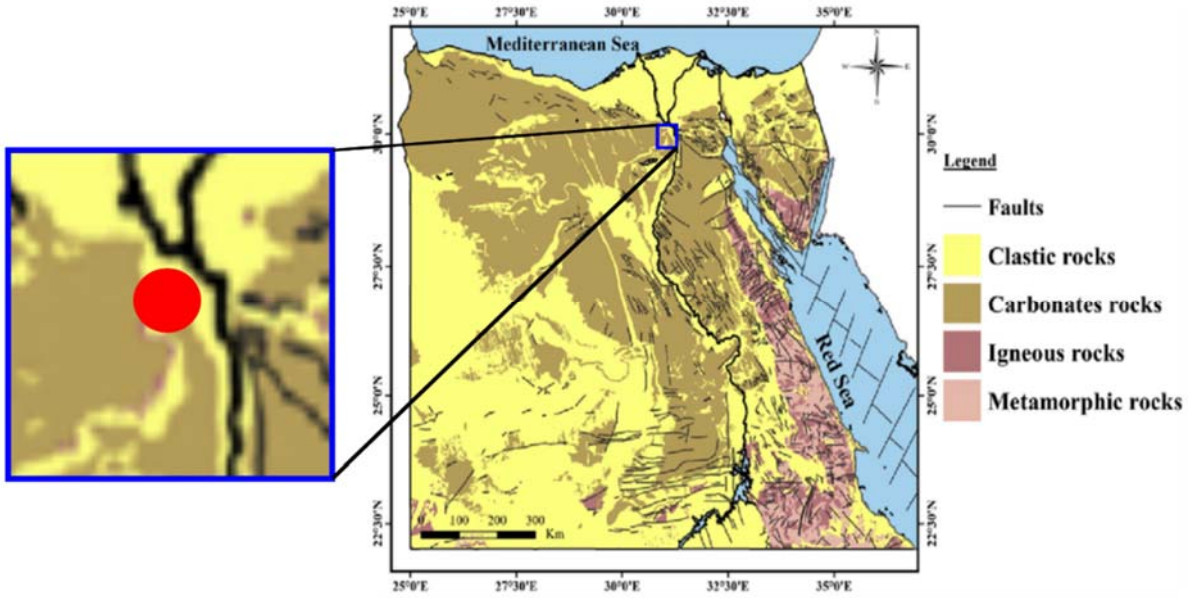


Fig. 2.12. General Map of Egypt including the geological setting of the studied area in Abusir in red circle (edited after [**14**]).

2.2.4. El-Ashmonein archaeological site, Minia (Egypt)

Minia is featured by sedimentary successions geologically. The sedimentary boundaries range from the Middle Eocene to Pleistocene and Holocene (**Fig. 2.13**). Limestone (fissured, chalky, silicified, and nummulitic belong to Eocene rocks. In addition, Oligocene sands and gravels, Pliocene dark clays, Pleistocene alluvial deposits (sand, gravel) and Holocene Nile silt belong to post-Eocene deposits [**15**]. Geomorphologically, the El-Ashmonein archaeological site is formed by the annual deposition of river sediments (mud and silt) during flooding events between August and October. This type of soil represents most of the territory of Minia governorate and its villages near the border of the eastern highlands and western desert, while the calcareous soil covers the land available for eastern highlands, near Maghagha and Bani Mazar cities [**16**].

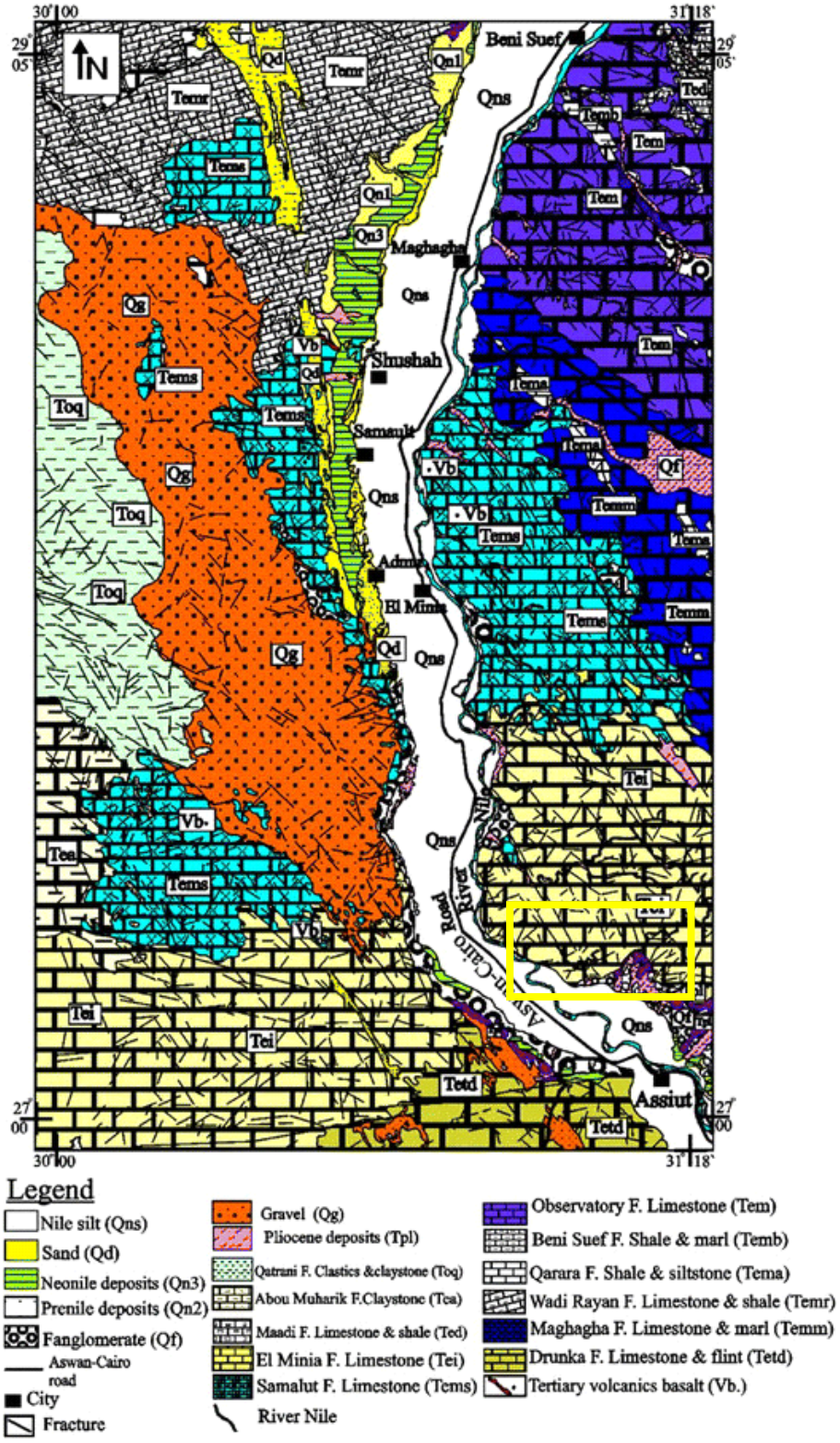


Fig. 2.13. Geological map of El Minia (from [**15**]). The yellow rectangle is Mellawy center that includes El-Ashmonein archaeological site.

2.2.5. Al Bagrawiya archaeological site (Sudan)

The Sudan plain consists of dark clays and red-brown sands [17]. The general geological column of Sudan is composed of coastal plain deposits, Nubian formations, Paleozoic sandstone formations, and a basement complex (mainly Precambrian). Deposition of the fluvial and marine sediments overlying the amalgamated terranes, from the Cambrian onwards was because of the erosion of the Trans- Gondwanan Mountain belt and subsequent recycling of the eroded detritus during later inversion tectonics [18]. The geology of Al Bagrawiya archaeological site consists mainly of four formations: 1) the basement complex; 2) the Nubian series; 3) the alluvium; and 4) the surface deposits of wind-blown sand [17] (**Fig. 2.14**).

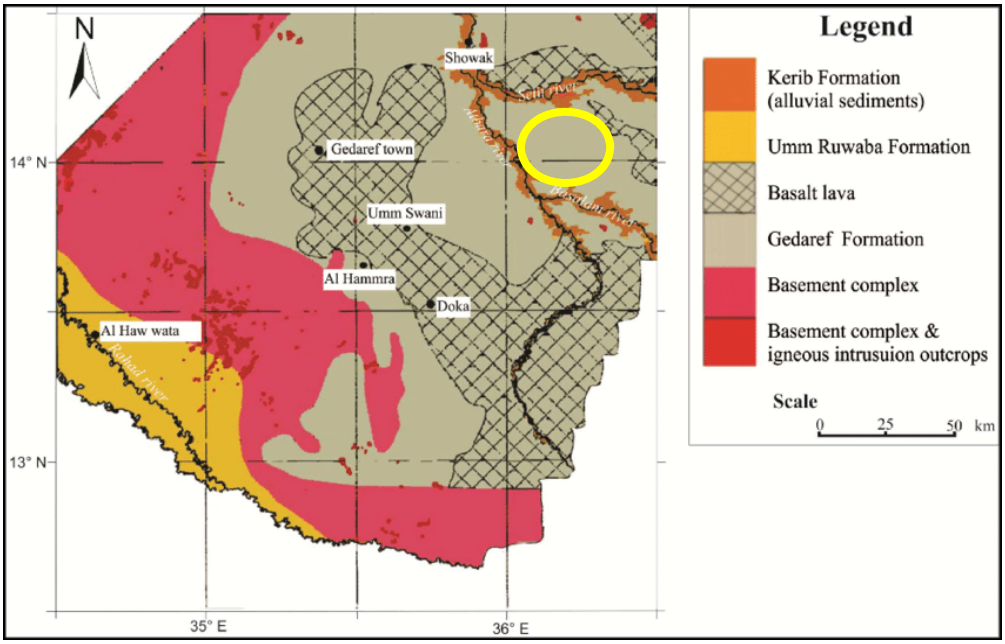


Fig. 2.14. Geological map of studied area is in the yellow circle (from [19]).

2.3. Materials

Sampling in the field was carefully carried out in order to select representative's specimens for the construction building materials and their decayed parts. To evaluate the impact of environmental dynamics in Alexandria over Anfushi's Necropolis, highly weathered fallen archaeological samples were collected from the different parts of Anfushi's Necropolis (natural stones and rendering mortars) to carry out the assessment study of the decay through analysis and microscopic examination from the construction. Samples of the construction materials were divided into samples from the casing stone and the bedrock with light color and crust over the surface. The rendering mortar samples were coarse and fine mortars from the first and second layers with blackish and yellowish colors, respectively. The samples ranged from 3 cm to 7 cm^3 in size. In addition, some of the samples had been ground to be ready for analysis purposes (**Fig. 2.15-A**).

For Abaton temple in Aswan, the main building materials noted in this temple are sandstones, and two main groups could be chromatically differentiated: one yellowish to brown–yellow color and the other represented by a pinkish color. All samples were representative of the building materials used in the temple. They were taken from archaeological fallen and highly weathered fragments and parts for analysis, examination, and physical testing. The collected fragments were coded with S from 1 to 4, where 1 and 2 represented yellowish sandstone and 3 and 4 represented pinkish sandstone. Three cubes of 3×3×3 cm in size were also prepared for both sandstone groups to measure the physical properties (**Fig. 2.15-B**).

In addition, In Abusir and in order to characterize the durability problems of the Sahure pyramid, some fragments of limestone (casing stone) and sandy limestone (core stone) were collected for analysis from the original quarries to use in the analysis and identification of physical properties. Highly weathered fallen parts were collected for analysis and examination purposes. In this sense, samples taken from the quarry are referred to in the text as "unweathered", while those taken from the fallen blocks of the pyramid are called "weathered". Finally, a fragment of mortar was taken from highly weathered fallen parts for its analysis and investigation (**Fig. 2.15-C**).

Furthermore, fragments were collected from Nero/Ramses II Temple. These samples carry six codes in Nero's Temple (NT), where NT1 (crust) was taken from a fallen highly weathered part that represents the crust. NT2 (stone) was collected from fallen parts on the ground that represents the altered stone. NT3 (crust) was taken from fallen highly weathered parts in different locations that represent the crust. NT4 (mortar) was collected from the fallen parts on the ground and represents the joint mortar of the temple. Finally, NT5 (mortar) and NT6 (mortar) were taken from the fallen parts on the ground that represent the Roman mortar. The samples were about 10 cm and thickness of 4 cm. The samples were prepared in a solid and powered state for analysis and examination purposes (**Fig. 2.15-D**).

Finally, for conservation and restoration purposes and to assess the efficacy of 3%, 5% and 7% of SiO_2-TiO_2 NPs/TEOS in the conservation of lime mortars multifunctionally, a well-mixed lime mortar with a mix proportion of around 1:3 (lime: sand) were prepared (**Fig. 2.16-A**). Additionally, some chemicals had been prepared as raw materials and reagents for the synthesis of SiO_2 and SiO_2-TiO_2 NPs such as ammonia (NH_4OH), tetraethoxysilane (TEOS) (Si $(C_2H_5)_4$), tetrabutytitanate (TBOT)($CH_2CH_2CH_2CH_3$), acetylacetone ($C_5H_8O_2$), ethanol (C_2H_6O) and Distilled water (**Fig. 2.16-B**). The needed grams of 3%, 5% and 7% of SiO_2-TiO_2 NPs were 1.5 g, 2.5 g and 3.5 g, respectively. Moreover, the required TEOS was 10.8 ml and 63.38 ml of Ethanol in all cases. At last, different concentrations of SiO_2-TiO_2 NPs were added to 20% TEOS and dispersed in Ethanol (**Fig. 2.16-C**).

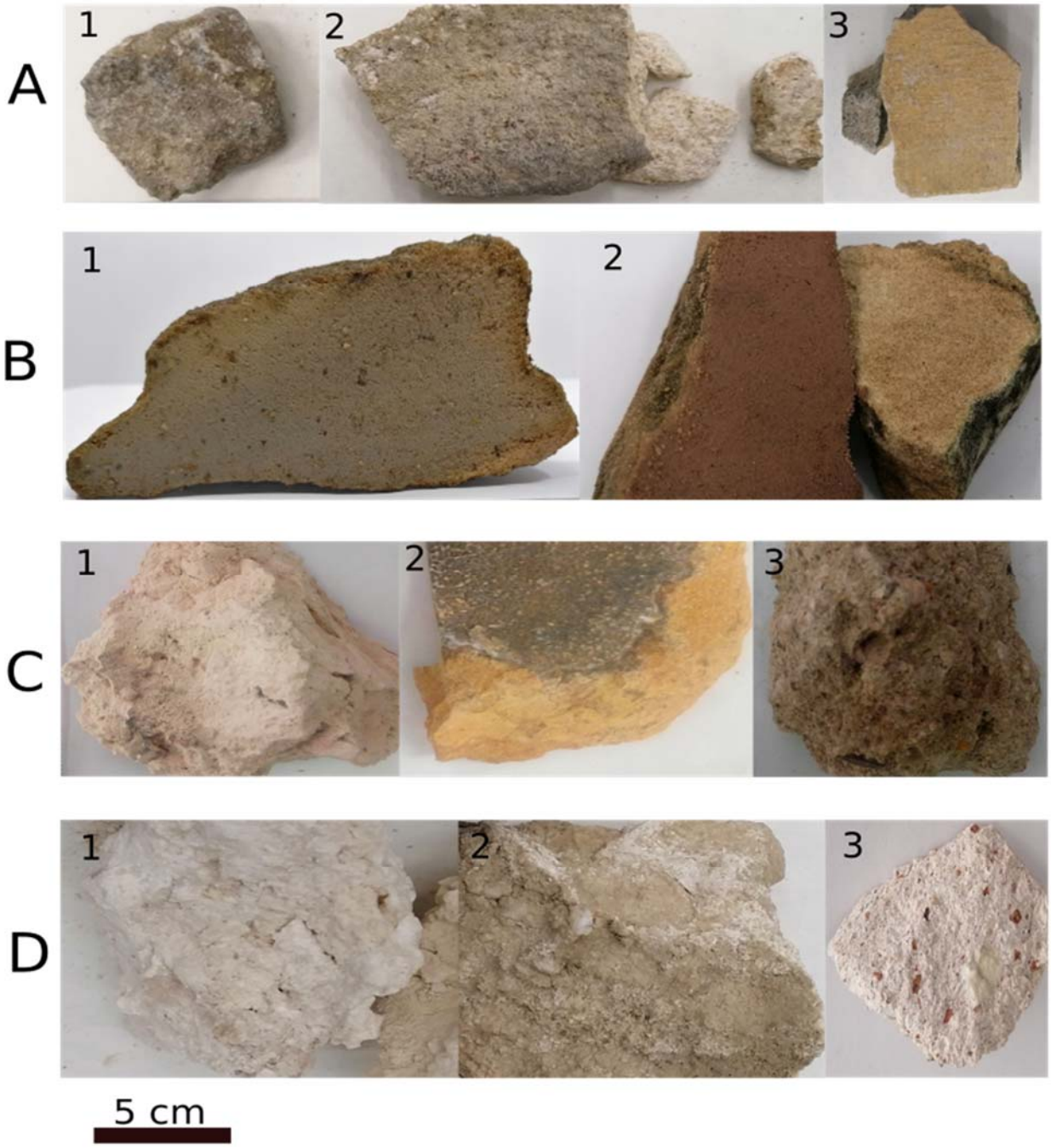


Fig. 2.15. The collected samples from selected monuments. A) Anfushi's Necropolis, 1 and 2 refers to stone building materials and 3 refer to mortars and plaster. B) Abaton temple in Aswan, 1 and 2 sandstone building materials. C) Sahure pyramid, 1 casing stone, 2 core stone and 3 mortar. D) Nero/Ramses II Temple, 1 stone building material, 2 mortar and 3 Roman Mortar.

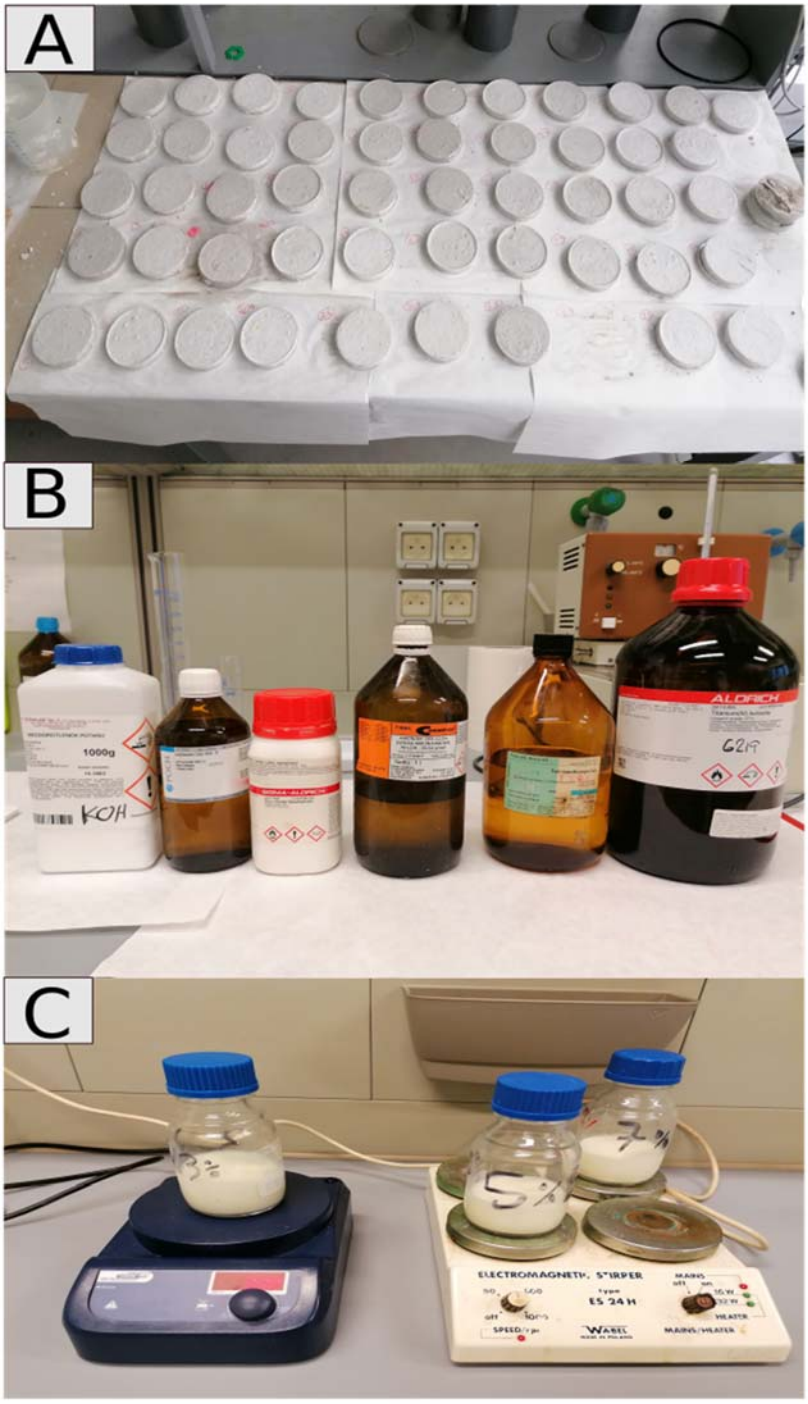


Fig. 2.16. (A) The experimental samples of the prepared lime mortars. (B) Presentation of the used chemicals as raw materials and reagents for the synthesis of SiO_2 and SiO_2-TiO_2 NPs. (C) Various concentrations of SiO_2-TiO_2 NPs which added to 20% TEOS and dispersed in Ethanol.

2.4. Methodology

The scientific methodology for the research relied on analytical, testing and experimental studies with destructive (DT) and non-destructive techniques (NDT) for evaluation/assessment of construction materials of the selected archaeological buildings and their decay patterns. The thesis was conducted through field, analytical, mapping, testing and experimental methodology (**Fig. 2.17**). The in-situ observation was carried out through regular visits to the archaeological sites to monitor the construction materials conditions by taking digital photographs, doing measurements and sampling. Moreover, chemical, microstructure and engineering characterizations were carried out using series of analytical, microscopic and testing instruments. Finally, experimental work was achieved to assess the synthesized nano-based materials (3%, 5% and 7% SiO_2-TiO_2 NPs/TEOS) in the consolidation of the casted lime mortars samples in the laboratory. Practically all of these equipment and techniques are found in both the laboratory of Geoarchaeology and Archaeometry (UGEA-PHAM) at Department of Earth Sciences, INHARMAR and SCiCYT, Faculty of Sciences, University of Cadiz. In addition, mechanical testing and nano-testing were performed at University of Gdansk.

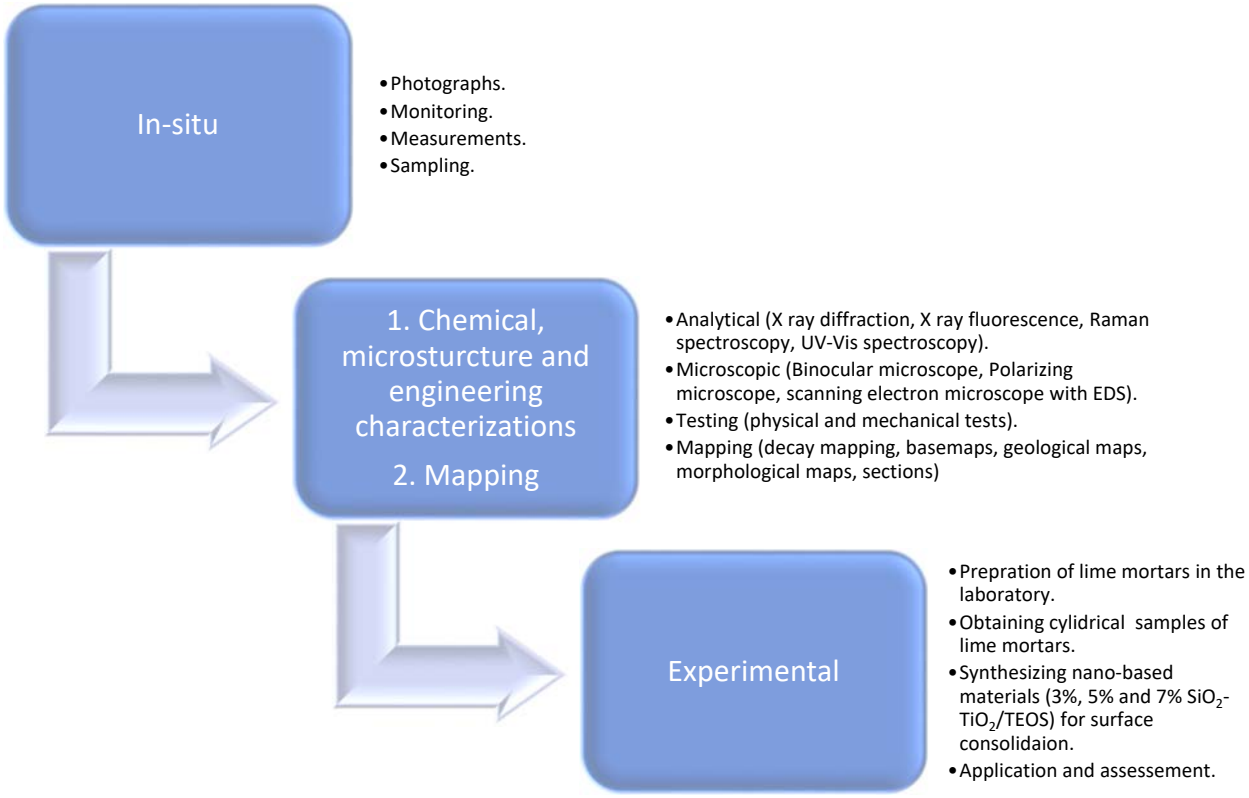


Fig. 2.17. Scheme of the current research methodology.

2.4.1 Chemical, mineralogical, and microscopic analysis

A. X-Ray Fluorescence (XRF)

A.1 X-Ray micro-fluorescence (mXRF)

A.2 Portable X-ray fluorescence (pXRF)

X-ray florescence is a usual chemical elemental analysis for the archaeological (inorganic) materials. X-ray micro-fluorescence is a quantitative elemental analysis for the identification of major and some trace elements. The presence of some elements can be the responsible for the chemical alteration of the archaeological stone blocks in the Nile River or in coastal environment or to detect the by-products as result of chemical reactions between the substrate and environment. In the current study, XRF portable is going to be used as an advanced and non-destructive tool especially for the archaeological matters. In this regard, a Bruker AXS M-4 Tornado sequential dispersive wave X-ray spectrometer with

a Rh tube operating at 4000 W was used to identify the elemental composition of the samples.

B. X-ray diffraction (XRD)

X-Ray Diffraction is a qualitative analytical technique, and it is an important tool in archaeometric studies to identify the mineral compositions of the archaeological matters and detect different original minerals of the substrate and altered minerals of as result of alterations and weathering impacts upon the archaeological underwater buildings. For this purpose, a Bruker D-8 Advance ECO diffractometer equipped with a Lynx-Eye high-speed measurement detector was used under the following conditions: CuKα radiation filtered by Ni, graphite monocromator and fixed slots, 2theta 5° to 60° scanning angle; diffractograms were interpreted with the software EVA (Bruker-AXS).

C. Micro Raman spectroscopy (portable)

Raman spectroscopy is a quantitative powerful non-destructive technique for determination of the chemical compositions of the archaeological materials and give more information about phase, polymorphs, crystallinity, and molecular interactions of the archaeological matters. For this, a portable Raman spectroscopy (i-Raman Pro, BW TEK) BW475-532S model equipped with a 785 nm laser was used.

D. UV-Vis spectroscopy

UV-Vis spectroscopy is an analytical method that measures the amount of various wavelengths of UV or visible light that are absorbed by or transmitted through a specific sample in comparison to a reference or blank sample. In the study, an equipment model Shimadzu UV-2600, within the wavelength range of 200 to 800 nm was utilized to recognize the reflectance and absorbance of the synthesized SiO_2-TiO_2 NPs. This analysis was hosted by University of Gdansk.

E. Optical binocular

Simple optical or digital binocular is perfect tool for examining the morphology of the stone surfaces and detect the problems and weathering aspects and decay forms of the natural stones submerged in water or subjected to water environment. In this context, A binocular microscope (USB digital microscope with stand), magnification between 20 and 400×, and equipped with a digital camera of 1.3 Mpx was used to survey the morphological characteristics of the samples and to detect different kinds of degradation aspects.

F. Optical polarized-light microscope

It is a petrological microscope used with transmitted light to identify the minerals and the alteration products as well. Petrological study enhances the archaeometrical studies of the archaeological stone buildings and identify their intrinsic and extrinsic interactions. Thin sections were prepared and studied using an Olympus BH-2 polarized optical microscope (POM) to identify the different minerals and altered phases of the samples.

G. Scanning electron microscope (SEM)

It uses a focused high energy of electrons over the samples to scan the surface and to see morphological and compositional aspects of the grains and their problems related with decay in perfect due to salt and their crystallizations processes. SEM with EDX detector will be used as elemental analysis for the samples. In the research, (Quanta 200), the voltage between 200 V to 30 kV, resolution 3.0 nm at 30 kV and 10 nm at 3 kV, and supplied with EDAX 60 mm 2 Octane Super EDS detector was utilized.

2.4.2. Tests

H. Physical properties

H.1. Bulk and apparent density

Density, as applied to any kind of homogeneous monophasic material of mass (M) and volume (V), is expressed as the ratio of M to V. Under specified conditions, this definition leads to unique values that represent a well-defined property of the material. For heterogeneous and multiphasic materials, such as porous media, however, application of this definition can lead to different results, depending on the exact way the mass and

volume of the system are defined [20]. Density gives an indication to the degradation state of the stone-built heritage. In this regard, the density of the stone indicates the unit weight of the stone and is calculated by dividing mass up by the total volume of the stone according to the formula D = m/v according to IS: 2386 (Part III) [21] and ASTM C97 [22].

H.2. Spectrophotometry (Color analysis)

This is a basic process to measure and detect the change in colors of the archaeological stone heritage visually. Naturally, the minimum inhomogeneity depends on color diversity of the scanned material, spatial distribution of this diversity (soft, long-range transitions or sharp, abrupt color changes), rock texture, color, and size of embedded grains, but also of shape and size of the sampling window and the number of "bins" used during data aggregation. Generally, the inhomogeneity is "sufficient" as long as the peaks remain above the significance lines ("white noise" lines) of the Lomb periodogram (90–95%) [23]. In this context, This CIE Lab values were carried out at National institute of standards (NIS) Cairo, Egypt. In this system, L*= brightness coordinate (100 = white, 0 = black), a* = red–green coordinate (positive sign = red, negative sign = green) and b*= yellow–blue coordinate (positive sign = yellow, negative sign = blue). It can be calculated as the Euclidean distance between two points in CIELAB color space and the Commission Internationale de l' Éclairage (CIE) agreed upon this measurement in 1976.

I. Hydric properties

I.1. Water absorption

Water absorption (WA) is considered an important hydric attribute/test of stone-built heritage, WA reflects the mechanical and physical characteristics of the stone-built heritage and generally the durability of the natural stones. Lower water absorption generally correlates to a greater durability, as it restricts the passage of deleterious solutions, but a larger pore size can assist with durability by reducing the pressure applied by salt or ice crystallization on the walls of the pore, in order to better evaluate the water absorption of stones and drying features, the samples should first tested for real density, apparent density and open and total porosity [24]. In this regard, and according to according to IS:

2386 (Part III) [21] and ASTM C97 [22], water absorption is expressed as the percent weight change due to absorbed water and calculated according to the formula WA=(M_{wet}−M_{dry}) /M_{dry}×100%.

I.2. Porosity

Porosity is the percentage of void space in a rock. It is defined as the ratio pore space divided by volume n= v (volume of the voids)/v (total volume). The porosity of a rock depends on many factors, including the rock type and how the grains of a rock are arranged. For example, crystalline rock such as granite has a very low porosity (<1%) since the only pore spaces are the tiny, long, thin cracks between the individual mineral grains. On the other hand, sandstones, typically, have much higher porosities (10–35%) because the individual sand or mineral grains do not fit together closely, allowing larger pore spaces [25]. In this sense, porosity is measured according to the formula Po = V_V/V_T and according to IS: 2386 (Part III) [21] and ASTM C97 [22].

I.3. Contact angle test

This test was carried out in order to evaluate the efficacy of the nano materials regarding to their wettability behaviours. In this regard, three different concentrations 3%, 5% and 7 % of SiO_2-TiO_2 NPs/TEOS were applied on the glass surfaces to be tested using the OCA 15EC package. This package is supplied with a movable table for the samples, 6x parfocal zoom lens, video measuring, led lighting and the software module SCA 20-contact angle. Faculty of Chemistry, Gdańsk University of Technology, Poland, hosted this test.

J. Mechanical properties

J.1. Nano-indentation test

This Nano-indentation tool is used to identify the hardness and Young's modulus of the mortar samples and it is considered as pioneer application to be used in the conservation field and archaeological science for nano materials assessment. In addition, it contributes to assess the behaviours of nano treatment in enhancing the mechanical properties of the lime. Each sample for nano-indentation test was included into a resin and tested on Nano-

Test Vantage Nan-oindentation measurement system in temperature 20 °C according to ISO 14577 and ASTM 2546. The number of measurements for each sample was 10 indentations with 5s dwell at maximum electromagnetic load equaled 5 mN with2 nN load resolution, 0.1 mN limit stop load, 0.002 nm displacement resolution, 50 s loading time, 50s unloading time, no more than 0.4 µm repositioning accuracy and 1 µN contact surface loading and 1 min of exchange time. The distance between two following indentations was 15 µm (counted from the most distant points of two indentations). The distance between the most distant points of the first indentation and the last (tenth) indentation was 1.35 mm. During each testing following parameters were measured: maximum depth [nm], plastic depth [nm], nano-indentation hardness [GPa] and young's modulus [GPa]. The nanoindentation test was performed at the Faculty of Mechanical Engineering and Ship Technology, Gdansk University of Technology, Poland.

J.2. Uniaxial compressive test (UCS)

The compressive load was applied to evaluate the compressive strength of the untreated and treated samples. In addition, on the base of results of this test the most efficient percentage of the Nano-treatments for consolidation of the lime mortars (3%, 5%, and 7 % of SiO_2-TiO_2 NPs) was identified. To carry out this test, 6 samples were prepared with 8.5 cm (diameter) × 1.5 cm (height) (three untreated samples and three treated for each (3%, 5%, and 7%). Static tensile test was performed on testing machine INSTRON 8503 (500 kN) in temperature 20 °C by using equipment for compressive testing. The UCS test was performed at the Faculty of Mechanical Engineering and Ship Technology, Gdansk University of Technology, Poland.

K. Laboratory weathering

K.1. Salt weathering

To evaluate the salt resistance of the treated and untreated samples (expiermtals lime mortars samples), salt of NaCl had been used in salt weathering with 25% concentration, and the experimental consolidated samples with three different concentrations of 3%, 5%, and 7% of SiO_2-TiO_2 NPs/TEOS had been exposed to the sodium chloride for 2 hours then

subjecting to normal chamber conditions for 28 hours at 25 ºC and 40% RH according to European standard [**26**]. Then, the samples were put in the oven for 16 hours at 105 ºC for repeated 15 cycles. Moreover, to calculate the salt resistance, the loss of mass was calculated according to the European standard [**27**] from the formula $\Delta M = (M_O - M_n/M_o) \times 100\%$, where M_O means initial weight and M_n means Dried weight. This test was hosted at the laboratories of the Department of Environmental Technology, Faculty of Chemistry, University of Gdansk, Poland.

K.2. Thermal aging

In order to evaluate the efficacy and durability of the treated samples with SiO_2-TiO_2 NPs/TEOS against variations of the temperature degrees, the samples were subjected to 18 hours of total immersion in water and then 6 h in a temperature inside a controlled oven at 105 ºC. In this study, 30 cycles of the subjection (variations of the temperature degrees) had been conducted according to [**28**]. This test was carried out at the laboratories of the Department of Environmental Chemistry, Faculty of Chemistry, University of Gdansk, Poland.

K.3. UV aging

UV accelerated aging test (weathering test) was performed to assess the durability and the performance against UV of the untreated and treated samples with SiO_2-TiO_2 NPs/TEOS. In this sense, a bench UV lamp with the ultraviolet light of 365 nm x 40 W BLB Tubes 120 V was used at a distance of 20 cm from the samples according to the recommendation described in (www.micomlab.com).

2.5. List of publications (Thesis)

A. Abdelrhman Fahmy, Eduardo Molina-Piernas, Javier Martínez-López, Philip Machev, and Salvador Domínguez-Bella. 2022. "Coastal Environment Impact on the Construction Materials of Anfushi's Necropolis (Pharos's Island) in Alexandria, Egypt". *Minerals* 12, no. 10: 1235. https://doi.org/10.3390/min12101235

minerals MDPI

Article

Coastal Environment Impact on the Construction Materials of Anfushi's Necropolis (Pharos's Island) in Alexandria, Egypt

Abdelrhman Fahmy [1,2,*], Eduardo Molina-Piernas [1], Javier Martínez-López [1], Philip Machev [3] and Salvador Domínguez-Bella [1]

[1] Department of Earth Sciences, Faculty of Sciences, University of Cadiz, Campus Rio San Pedro, 11519 Puerto Real, Spain
[2] Conservation Department, Faculty of Archaeology, Cairo University, Giza 12613, Egypt
[3] Faculty of Geology & Geography, St. Kliment Ohridski University, 1504 Sofia, Bulgaria
* Correspondence: abdelrhman.fahmy@uca.es or abdelrhmanmuhammedfahmy@gmail.com; Tel.: +34-655138576

Abstract: The only example and reference of Ptolemaic Alexandrian tombs, with clear integrations of Egyptian-style scenes and decorations, is considered an endangered archaeological site due to different coastal environmental risks in Alexandria and the absence of maintenance. Anfushi's Necropolis is located near the western harbour (Island of Pharos) and dates back to the 2nd century BC. Sea level rises, earthquakes, flooding, storminess, variations in temperature, rainfall, and wind are the factors that have the largest effect on the destruction and decay of Anfushi's Necropolis building materials. This paper's main objectives were to characterize this necropolis's building materials and assess its durability problems and risks regarding the coastal environment. Additionally, the vector mapping of its architectural and structural elements was applied for documentation and recording purposes for the necropolis. To achieve these aims, field (recording and photographs), desk (engineering drawing and mapping), and laboratory works (X-ray diffraction, X-ray fluorescence, binocular microscopy, polarizing microscopy, and scanning electron microscopy) were carried out. The results confirmed the probabilistic risk of sea level rises and its impact on the submergence of Anfushi's Necropolis. The structural deficiencies of the tombs were caused by the effect of earthquake tremors along with anthropogenic factors. In addition, chemical and microscopic investigations showed that salt weathering (halite and gypsum) induced the decay of the building materials.

Keywords: Anfushi's Necropolis; Alexandria; building materials; mortar; coastal environment; SLR; stone decay; salt erosion; vector mapping

check for updates

Citation: Fahmy, A.; Molina-Piernas, E.; Martínez-López, J.; Machev, P.; Domínguez-Bella, S. Coastal Environment Impact on the Construction Materials of Anfushi's Necropolis (Pharos's Island) in Alexandria, Egypt. *Minerals* **2022**, *12*, 1235. https://doi.org/10.3390/min12101235

Academic Editor: Donatella Barca

Received: 1 September 2022
Accepted: 25 September 2022
Published: 28 September 2022

Publisher's Note: MDPI stays neutral with regard to jurisdictional claims in published maps and institutional affiliations.

Copyright: © 2022 by the authors. Licensee MDPI, Basel, Switzerland. This article is an open access article distributed under the terms and conditions of the Creative Commons Attribution (CC BY) license (https://creativecommons.org/licenses/by/4.0/).

1. Introduction

The resilience and durability of historical buildings near marine areas are reduced due to the dynamics of coastal environments [1]. Due to the importance of preserving heritage, for example, in 2022, a database was constructed for 213 natural and 71 cultural African heritage sites affected by coastal environmental changes for their sustainable management. In this regard, by 2050, the number of archaeological sites that will be subjected to severe effects due to coastal flooding and erosion will increase more than three times [2]. Sea level rise (SLR), coastal flooding, coastal erosion, extreme rainfall, high winds, storm surge, temperatures, and soil moisture are the most relevant issues related to the sustainability problems of archaeological buildings near coasts [3]. Sea level rise is considered a major threat to coastal areas and is recognized as a powerful indicator of climate change and coastal dynamics [4,5]. Sea level rise occurs due to increasing global mean temperature, leading to oceanic thermal expansion and the loss of continental ice [6]. Accordingly, global sea levels will rise between 1 and 5 m by 2100, submerging most archaeological sites worldwide [7].

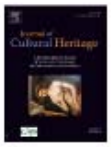
B. Abdelrhman Fahmy, Javier Martínez-López, Ángel Sánchez-Bellón, Salvador Domínguez-Bella, and Eduardo Molina-Piernas. 2022. "Multianalytical Diagnostic Approaches for the Assessment of Materials and Decay of the Archaeological Sandstone of Osiris Temple (the Abaton) in Bigeh Island, Philae (Aswan, Egypt)." Journal of Cultural Heritage 58 (November): 167–78. https://doi.org/10.1016/j.culher.2022.09.025

Journal of Cultural Heritage 58 (2022) 167–178

Contents lists available at ScienceDirect

Journal of Cultural Heritage

journal homepage: www.elsevier.com/locate/culher



VSI: Geomaterials in CH

Multianalytical diagnostic approaches for the assessment of materials and decay of the archaeological sandstone of Osiris Temple (The Abaton) in Bigeh Island, Philae (Aswan, Egypt)

Abdelrhman Fahmy[a,b,c,*], Javier Martínez-López[a], Ángel Sánchez-Bellón[a], Salvador Domínguez-Bella[a], Eduardo Molina-Piernas[a]

[a] Department of Earth Sciences, Faculty of Sciences, University of Cadiz, Campus Río San Pedro, 11510 Puerto Real, Cadiz, Spain
[b] Conservation Department, Faculty of Archaeology, Cairo University, 12613, Giza, Egypt
[c] Doctoral scholar at the Department of Earth Sciences, Faculty of Sciences, University of Cadiz, Spain

ARTICLE INFO

Article history:
Received 14 March 2022
Accepted 30 September 2022
Available online 17 October 2022

Keywords:
Osiris Temple
Abaton
Nile River
Sandstone
Water effect
Decay

ABSTRACT

The ancient Osiris Temple at Philae/Aswan, also known as Abaton, was considered one of the most sacred and mysterious temples in Egypt. In 1960, UNESCO rescued Philae temples because the rise of the water level after the construction of the Old and New Dam of Aswan caused the submergence of all temples underwater. Rescue camping was performed to protect all Aswan temples. Unfortunately, Osiris Temple was not rescued and was forgotten in its original place on Bigeh Island. Currently, this temple is subjected to Nile water effects and is partially submerged underwater due to Nile water level changes. This study aims to unravel and assess the conservation state of the temple sandstone-building material through multianalytical and examination techniques (X-ray diffraction, X-ray fluorescence, Raman spectroscopy, polarizing microscopy, binocular microscopy, and scanning electron microscopy). Furthermore, in situ records were obtained, and degradation maps were drawn to establish the patterns of damage and decay of the building material of the Osiris temple. The results showed that blackening, soiling, and disintegration are the dominant decay patterns in the building material of the temple. In addition, the Nile water as an extrinsic factor severely affected the conservation state of the temple due to the continuous exposure to water force. The mineralogical composition of sandstone played an important role in its degradation as an intrinsic decay factor due to mainly dispersion of clayed and/or carbonate matrix dissolution, quartz hydrolysis, and feldspar alteration.

© 2022 Consiglio Nazionale delle Ricerche (CNR). Published by Elsevier Masson SAS. All rights reserved.

Introduction

Ancient Egyptians used sandstones for their workability, accessibility, and affordability in construction as structural and architectural elements in their buildings, such as tombs and temples [1–3]. Many of the buildings of the Egyptians were erected in the vicinity of the course of the Nile River, so the flooding of the land caused by the construction of reservoirs threatens their preservation. For this reason,in March 1960, UNESCO called for a rescue campaign from financial and research points of view to protect Aswan temples from damage due to the building of the New Dam of Aswan (111 m above the Nile bed level) impounding water in a lake extending three hundred miles south of the first waterfall with a storage capacity of 164 billion cubic meters [4,5]. To preserve the Aswan temples from permeant submergence, the campaign performed extensive geological and geotechnical studies on the construction materials of the Aswan temples. Moreover, determination of the internal stresses and places of cracks and fissures in the sandstone blocks and rocks, tests on cutting of sandstones, tests on physical and mechanical properties of sandstone, and hydrology studies were performed [6,7]. Unfortunately, Osiris Temple was the only temple not rescued during the saving campaign of Aswan temples. In this regard, the motive behind leaving Osiris Temple without rescuing could be because the level of the Osiris Temple was higher than the opposite Temples of Philae and the water impact was not as significant as today's condition. However, the real motive behind ignoring Osiris Temple is not generally known. According to Willcock's report [8], during the building of the Aswan dam, taking up the Philae temples stone by stone and reconstructing them on the island of Bigeh, this suggestion was not welcomed because this action would cause damage to the Osiris Temple, and

* Corresponding author.
E-mail addresses: abdelrhmanmuhammedfahmy@gmail.com, abdelrhman.fahmy@uca.es (A. Fahmy).

C. Abdelrhman Fahmy, Eduardo Molina-Piernas, Salvador Domínguez-Bella, Javier Martínez-López, and Fatma Helmi. 2022. "Geoenvironmental Investigation of Sahure's Pyramid, Abusir Archeological Site, Giza, Egypt." Heritage Science 10 (1). https://doi.org/10.1186/s40494-022-00699-1

Fahmy et al. Heritage Science (2022) 10:61
https://doi.org/10.1186/s40494-022-00699-1

Heritage Science

RESEARCH ARTICLE Open Access

Geoenvironmental investigation of Sahure's pyramid, Abusir archeological site, Giza, Egypt

Abdelrhman Fahmy[1*], Eduardo Molina-Piernas[1], Salvador Domínguez-Bella[1], Javier Martínez-López[1] and Fatma Helmi[2]

Abstract

Abusir is the name of an elaborate burial area in Egypt, dotted with 19 pyramids and other temples, stretching on the western side of the Nile from the south of the Giza Plateau to the northern rim of Saqqara. It seems to have been created as the resting site for the Pharaohs dated from 2494 to 2345 BC. The name Abusir, originally spoken as Busiri, means "Temple of Osiris". Over time, the name has become so popular because more than 60 villages now carry this name, but only one is the archaeological site. This paper focused on one of its most important pyramids from the Abusir archaeological area, Sahure's pyramid, since it is one of Egypt's little-known but heavily damaged treasures. Field and laboratory studies have been carried out to investigate and understand the durability problems and construction materials of this pyramid, leading to results that confirmed the impact of the geoenvironmental conditions on the pyramid's architectural, structural, and engineering stability. Moreover, the results showed that mineralogical content in the construction materials was an intrinsic problem due to the presence of swellable (expansive) clays, which are considered responsible for pyramid decay and damage. In addition to external factors such as the effect of temperature variations, rain, pollutants, wind, and earthquakes and their interactions with intrinsic building material defects. Finally, this paper revealed a new discovery for basaltic mortar as the first trial for green concrete manufacturing in the Egyptian Old Kingdom, Fifth Dynasty.

Keywords: Abusir archaeological site, Sahure's pyramid, Geoenvironmental factors, Petrological characterization, Petrophysical properties, Geochemistry, Stone decay, Sandy limestone, Mortar

Introduction

Studies on the impact of geoenvironmental conditions and how external agents affect construction materials are a recurring topic in new construction but are especially important in the materials of historical and archaeological heritage since its understanding will allow better preservation of this cultural heritage [1]. There are several previous studies on stone weathering; for example, Charola et al. [2] explained salt weathering for porous building materials and showed some related deterioration patterns on archaeological stone masonry because of environmental conditions such as fissures, granular disintegration, splitting in building materials, and salt efflorescence. Fitzner and Heinrichs [3] presented a study about weathering impacts on monumental stones and their forms and rates. In addition, they showed the nonvisible/nanoscale deterioration patterns of archaeological stones, visible deterioration in micro- and meso/macroscale-like mass loss, and structural stability. Grossi et al. [4] studied the effect of air pollution, salt weathering, and climate change on the durability of archaeological stones, showing that the blackening of the stones returned to high levels of sulfate deposition, diesel soot, and nitrogen deposition from vehicular sources around the archaeological buildings. Additionally, Figueiredo et al. [5] studied the degradation factors that affected

*Correspondence: abdelrhman.fahmy@uca.es; abdelrhmanmuhammedfahmy@gmail.com
[1] Department of Earth Sciences, Faculty of Sciences, University of Cadiz, Campus Río San Pedro, 11510 Puerto Real, Spain
Full list of author information is available at the end of the article

Springer Open

© The Author(s) 2022. **Open Access** This article is licensed under a Creative Commons Attribution 4.0 International License, which permits use, sharing, adaptation, distribution and reproduction in any medium or format, as long as you give appropriate credit to the original author(s) and the source, provide a link to the Creative Commons licence, and indicate if changes were made. The images or other third party material in this article are included in the article's Creative Commons licence, unless indicated otherwise in a credit line to the material. If material is not included in the article's Creative Commons licence and your intended use is not permitted by statutory regulation or exceeds the permitted use, you will need to obtain permission directly from the copyright holder. To view a copy of this licence, visit http://creativecommons.org/licenses/by/4.0/. The Creative Commons Public Domain Dedication waiver (http://creativecommons.org/publicdomain/zero/1.0/) applies to the data made available in this article, unless otherwise stated in a credit line to the data.

D. Abdelrhman Fahmy, Eduardo Molina-Piernas, Javier Martínez-López, and Salvador Domínguez-Bella. 2022. "Salt Weathering Impact on Nero/Ramses II Temple at El-Ashmonein Archaeological Site (Hermopolis Magna), Egypt". Heritage Science 10 (1). https://doi.org/10.1186/s40494-022-00759-6

Fahmy et al. Heritage Science (2022) 10:125
https://doi.org/10.1186/s40494-022-00759-6

Heritage Science

RESEARCH Open Access

Salt weathering impact on Nero/Ramses II Temple at El-Ashmonein archaeological site (Hermopolis Magna), Egypt

Abdelrhman Fahmy[1,2*], Eduardo Molina-Piernas[1], Javier Martínez-López[1] and Salvador Domínguez-Bella[1]

Abstract

Nero's Temple at El-Ashmonein archaeological site, in Minia (middle of Egypt), is considered one of the most important of all temples of Nero. This temple dates back to 1520 BC–1075 BC in the New Kingdom and was reused in the era of Nero (the Fifth Emperor of Rome). The temple construction materials are severely decayed from surrounding environmental impacts, especially contaminated water sources. The main objective of this paper is to identify the construction materials of Nero's Temple and their decay by-products. To achieve them, X-ray diffraction, micro X-ray fluorescence spectrometry, and portable Raman spectroscopy were utilized to identify the compositions and alteration by-products/degradation compounds (mainly saline efflorescence and crusts) from the construction materials, such as limestone walls, and structural mortars of the temple. In addition, a polarizing microscope was used to identify the minerals inside the construction materials and reveal the alteration of the minerals because of decay. Digital microscopy and scanning electron microscopy with EDS were used to detect decayed materials' morphological features. Finally, results showed that the main decay factor is salt attack (chlorides, sulfates, phosphates, nitrates, carbonates, and bicarbonates) for all architectural and structural elements of the temple, which have been carried to the construction materials from various sources of contaminated water (canal, sewage, and agricultural water).

Keywords: Nero's Temple, El-Ashmonein archaeological site, Salt attack, Contaminated water, Building stone, Mortar, Decay, Weathering

*Correspondence: abdelrhman.fahmy@uca.es; abdelrhmanmuhammedfahmy@gmail.com

[1] Department of Earth Sciences, Faculty of Sciences, University of Cadiz, Campus Río San Pedro, 11510 Puerto Real, Spain
Full list of author information is available at the end of the article

SpringerOpen

© The Author(s) 2022. **Open Access** This article is licensed under a Creative Commons Attribution 4.0 International License, which permits use, sharing, adaptation, distribution and reproduction in any medium or format, as long as you give appropriate credit to the original author(s) and the source, provide a link to the Creative Commons licence, and indicate if changes were made. The images or other third party material in this article are included in the article's Creative Commons licence, unless indicated otherwise in a credit line to the material. If material is not included in the article's Creative Commons licence and your intended use is not permitted by statutory regulation or exceeds the permitted use, you will need to obtain permission directly from the copyright holder. To view a copy of this licence, visit http://creativecommons.org/licenses/by/4.0/. The Creative Commons Public Domain Dedication waiver (http://creativecommons.org/publicdomain/zero/1.0/) applies to the data made available in this article, unless otherwise stated in a credit line to the data.

E. Abdelrhman Fahmy, Eduardo Molina-Piernas, Javier Martínez-López, and Salvador Domínguez-Bella. Sand dunes movement and flooding risk analysis for the pyramids of Meroe, Al Bagrawiya archaeological site, Sudan. (**Under revision**, submitted to International Journal of Architectural Heritage).

F. Abdelrhman Fahmy, Anna Gołąbiewska, Wiktoria Wojnicz, Alicja Stanisławska, Jakub Kowalski, Justyna Łuczak, Adriana Zaleska-Medynska, Salvador Domínguez-Bella, Javier Martínez-López and Eduardo Molina-Piernas. Multi-functional monodispersed SiO_2-TiO_2 NPs and TEOS in the consolidation of archaeological lime mortars surfaces. (**Under revision**, submitted to Journal of Construcrion and Building materials).

2.6. References

[1] Stephenson J. People and Place. *Planning Theory and Practice*.2010; *11*(1), 9–21. https://doi.org/10.1080/14649350903549878

[2] Kyriakos S. The Polyvalent Nature of the Alexandrian Elite Hypogea: a case study in the Greco-Egyptian Cultural Interaction in the Hellenistic and Roman Periods.Porto.2013.https://digitalis-dsp.uc.pt/jspui/bitstream/10316.2/36162/1/AlexandreaAegyptum_artigo7.pdf

[3] Kyriakos S. *Alexandrea in Aegypto. The Role of the Egyptian Tradition in the Hellenistic and Roman Periods: Ideology, Culture, Identity, and Public Lif*. Ph.D. Thesis. Faculty of Archaeology. University of Leiden. 2011. https://scholarlypublications.universiteitleiden.nl/handle/1887/16395

[4] http://www.alexandria.gov.eg/Alex/english/ANFUSHY%20NECOPOLIS.html Accessed on 07/01/2023.

[5] Hosny A, Ali S M, Abed A. Study of the 26 December 2011 Aswan earthquake, Aswan area, South of Egypt. *Arabian Journal of Geosciences*. 2014; *7*(11), 4553–4562. https://doi.org/10.1007/s12517-013-1098-8

[6] El-Sharkawi M. History of the Geological Research in Egypt. In: Hamimi Z., El-Barkooky A., Martínez Frías J., Fritz H., Abd El-Rahman Y. (eds) The Geology of Egypt. Regional Geology Reviews. Springer, Cham. 2020. https://doi.org/10.1007/978-3-030-15265-9_1

[7] Worrall G A. A simple introduction to the geology of the Sudan. Sudan Notes and Records.1957; 38, 2–9. http://www.jstor.org/stable/41710729

[8] Schlüter T. Geological Atlas of Africa. Springer Berlin, Heidelberg.2008. https://doi.org/10.1007/978-3-540-76373-4

[9] Voûte C. Some geological aspects of the conservation project for the Philae Temples in the Aswan Area. *Geologische Rundschau*.1963; *52*(2), 665–675. https://doi.org/10.1007/BF01821149

[10] Ibrahim M I A, Mansour A M S. Biostratigraphy and palaeoecological interpretation of the Miocene–Pleistocene sequence at El-Dabaa, northwestern Egypt. *Journal of Micropalaeontology*. 2002; *21*(1), 51–65. https://doi.org/10.1144/jm.21.1.51

[11] Stanley J D, Jorstad TF, Goddio F. Human impact on sediment mass movement and submergence of ancient sites in the two harbours of Alexandria, Egypt. *Norsk Geologisk Tidsskrift*. 2006; *86*(3), 337–350.

[12] Torab M M. Paleo-geomorphological map of Alexandria site, Egypt by using submerged archaeological and other evidence. *International Conference on Agriculture, Science and Engineering*. 2013; 16.

[13] Bárta M. Abusir in the Third Millennium BC. 2015. https://cegu2.ff.cuni.cz/en/research/projects/field-projects/abusir/abusir-in-the-third-millennium-bc/ . Accessed 08 Mar 2022.

[14] Abdel Zaher M, Elbarbary S, El-Shahat A, Mesbah H, Embaby A. Geothermal resources in Egypt integrated with GIS-based analysis. *Journal of Volcanology and Geothermal Research*.2018;*365*,1–12. https://doi.org/https://doi.org/10.1016/j.jvolgeores.2018.09.013

[15] Ibrahim RGM, Lyons WB. Assessment of the Hydrogeochemical Processes Affecting Groundwater Quality in the Eocene Limestone Aquifer at the Desert Fringes of El Minia Governorate, Egypt. Aquat Geochem. 2017;23, 33–52. https://doi.org/10.1007/s10498-016-9298-y

[16] Moneim AAA, Fernández-Álvarez JP, Abu El Ella EM, Masoud AM. Groundwater management at West El-Minia Desert Area, Egypt using numerical modelling. J Geosci Environ Prot. 2016; 04:66–76. https://doi.org/10.4236/gep.2016.47008.

[17] Whiteman AJ. Geology and Scenery of the Sudan. Sudan Notes and Records. 1966;vol. 47. pp. 137–44, http://www.jstor.org/stable/44947310. Accessed 25 Apr. 2022.

[18] Fielding L, Najman Y, Millar I, Butterworth P, Ando S, Padoan M, Barfod D, Kneller B. A detrital record of the Nile River and its catchment. Journal of the Geological Society.2016; 174(2), 301–317. https://doi.org/10.1144/jgs2016-075

[19] Osman A F I, Ibrahim A, Abuobida Y, Eisawi A A M, Alhadi M. *Sedimentary Facies and Depositional Environment of the Gedaref Formation, Eastern Sudan*.2016. https://doi.org/10.13140/RG.2.1.4000.5521

[20] Sataloff R T, Johns M M, Kost KM. *data collection handbook to support modelling impacts of radioactive material in soil and building structures, environmental science division*Argonne national laborator.USA .2015.

[21] Bureau of Indian Standards. Method of Test for Aggregate for Concrete. IS 2386- Part III - Specific Gravity, Density, Voids, Absorption and Bulking (1963) New Delhi.1963 (Reaffirmed 2002). Available from: https://law.resource.org/pub/in/bis/S03/is.2386.1.1963.pdf

[22] ASTM. C97/C97 M-18 Standard Test Methods for Absorption and Bulk Specific Gravity of Dimension Stone. ASTM International, West Conshohocken, PA. 2018. www.astm.org

[23] Halász A, Halmai Á. *The color analysis method applied to homogeneous rocks*. 2015; *4*, 233–239. https://doi.org/10.1515/logos-2015-0019

[24] Ozcelik Y, Ozguven A. Water absorption and drying features of different natural building stones. *Construction and Building Materials*.2014; *63*, 257–270. https://doi.org/10.1016/j.conbuildmat.2014.04.030

[25] Wisconsin rocks. https://wgnhs.wisc.edu/maps-data/data/rock-properties/understanding-porosity-density/ . Accessed on 12/05/2022.

[26] UNE-EN 12370. https://www.une.org/encuentra-tu-norma/busca-tu-norma/norma?c=N0064854 . Accessed on 10/12/2022.

[27] UNE-EN 14147. https://www.une.org/encuentra-tu-norma/busca-tu-norma/norma?c=N0031620 . Accessed on 12/12/2022.

[28] UNE-EN 14066. https://www.une.org/encuentra-tu-norma/busca-tu-norma/norma?c=N0052555. Accessed on 16/12/2022.

Chapter 3

Results and discussion

Part I: Characterization of construction building materials in aqueous environments

3.1 Coastal environment impact on the construction materials of Anfushi's Necropolis (Pharos's Island) in Alexandria, Egypt

Abdelrhman Fahmy, Eduardo Molina-Piernas, Javier Martínez-López, Philip Machev, and Salvador Domínguez-Bella. 2022. "Coastal Environment Impact on the Construction Materials of Anfushi's Necropolis (Pharos's Island) in Alexandria, Egypt". *Minerals* 12, no. 10: 1235. https://doi.org/10.3390/min12101235

3.2 Multianalytical diagnostic approaches for the assessment of materials and decay of the archaeological sandstone of Osiris Temple (The Abaton) in Bigeh Island, Philae (Aswan, Egypt)

Abdelrhman Fahmy, Javier Martínez-López, Ángel Sánchez-Bellón, Salvador Domínguez-Bella, and Eduardo Molina-Piernas. 2022. "Multianalytical Diagnostic Approaches for the Assessment of Materials and Decay of the Archaeological Sandstone of Osiris Temple (the Abaton) in Bigeh Island, Philae (Aswan, Egypt)". Journal of Cultural Heritage 58 (November): 167–78. https://doi.org/10.1016/j.culher.2022.09.025

3.1. Coastal environment impact on the construction materials of Anfushi's Necropolis (Pharos's Island) in Alexandria, Egypt

Highlights:

- The bedrock of Anfushi's Necropolis is oolitic limestone and the casing stone is micritic limestone.
- Probabilistic risk of sea level rises and its impact on the submergence of Anfushi's Necropolis.
- The structural deficiencies of the tombs were caused by the effect of earthquake.
- Salt weathering (halite and gypsum) induced the decay of the building materials.

Abstract

The only example and reference of Ptolemaic Alexandrian tombs, with clear integrations of Egyptian-style scenes and decorations, is considered an endangered archaeological site due to different coastal environmental risks in Alexandria and the absence of maintenance. Anfushi's Necropolis is located near the western harbour (Island of Pharos) and dates back to the 2nd century BC. Sea level rises, earthquakes, flooding, storminess, variations in temperature, rainfall, and wind are the most affected factors in the destruction and decay of Anfushi's Necropolis building materials. This paper's main objectives were to characterize this necropolis's building materials and assess its durability problems and risks regarding the coastal environment. Additionally, vector mapping of its architectural and structural elements was applied for documentation and recording purposes for the necropolis. To achieve these aims, field (recording and photographs), desk (engineering drawing and mapping), and laboratory works (X-ray diffraction, X-ray fluorescence, binocular microscope, polarizing microscope, and scanning electron microscope) were carried out. The results confirmed the probabilistic risk of sea level rises and its impact on the submergence of Anfushi's Necropolis. The structural deficiencies of the tombs were caused by the effect of earthquake tremors along with anthropogenic factors. In addition, chemical and microscopic investigations showed that salt weathering (halite and gypsum) induced the decay of the building materials.

Keywords: Anfushi's necropolis, Alexandria, building materials, mortar, coastal environment, SLR, stone decay, salt erosion, vector mapping.

1. Introduction

The resilience and durability of historical buildings near marine areas are reduced due to the dynamics of the coastal environment [1]. Due to the importance of preserving heritage, for example, in 2022, a database was constructed for 213 natural and 71 cultural African heritage sites affected by coastalenvironmental changes for their sustainable management. In this regard, by 2050, the number of archaeological sites that will be subjected to severe effects due to coastal flooding and erosion will increase more than three times [2]. Sea level rise (SLR), coastal flooding, coastal erosion, extreme rainfall, high winds, storm surge, temperatures, and soil moisture are the most relevant issues related to the sustainability problems of archaeological buildings near coasts [3]. Sea level rise is considered a major threat to coastal areas and is recognized as a powerful indicator of climate change and coastal dynamics [4, 5]. Sea level rise occurs due to increasing global mean temperature, leading to oceanic thermal expansion and the loss of continental ice [6]. Accordingly, global sea levels will rise between 1 and 5 m by 2100, submerging most archaeological sites worldwide [7].

Globally, many desktop and field studies have been performed to evaluate and assess the threats and sustainability problems of archaeological sites and their built heritage sites in the coastal context [8-11]. In New Zealand, the heritage sites in Whangarei District near the harbor have been destroyed due to sea level rises, extreme rainfall, and storminess [12]. In Ireland, Westley et al. [13] studied and assessed the impact of coastal erosion on archaeological sites and showed the collapse of archaeological buildings at Derryoge town due to cliff erosion. In the United States, Anderson et al. [14] studied the impact of SLR on the archaeological sites, buildings, and cultural landscapes of the Gulf and Atlantic coasts of the southeastern United States, reporting that a 1 m rise in sea level will lead to the loss of over >13,000 recorded archaeological sites there. In the United Kingdom, Harkin et al. [15] mentioned that the rate of regional sea-level rise is between 1 and 2 mm according to tide gauge records, which causes potential damage to the heritage on its coastline. In Cyprus, Andreou [16] studied endangered areas using the Digital Shoreline Analysis System (DSAS) to monitor the area's most vulnerable to coastal erosion and flooding. Accordingly,

archaeological sites in the south-central zone are experiencing a high rate of coastal erosion. Furthermore, Andreou et al. [17] started to work on endangered coastalarchaeological sites in the Middle East and North Africa to show that sea waves and storm effects produced coastal erosion and damage to archaeological buildings in Libya, Yemen, and Jordan.

On the other hand, sea spray (marine aerosol), rising dampness, and coastal/flash flooding can cause salt decay in archaeological building materials near the marine environment [18]. In this context, Morillas et al. [19] said that one of the most aggressive deterioration aspects of sea spray is salt precipitation, which is composed of inorganic salts (sulfates, nitrates, and mainly chlorides) and organic matter. In addition, sea spray existed in a range of particles named in different terms because of their physical characteristics, such as film drops, jet drops, seawater drops, brine drops, hygroscopic salt drops, sea salt nuclei, and sea salt particles. These drops are composed of bubbles where a large amount of air and water are blended and they reflect the chemical context in the atmosphere [18, 20, 21]. Sea spray could cause accumulative deposition of ions on the stones surfaces and penetrates inside the stone pores through ionic diffusion leading to degeneration [22]. Moreover, wind can increase the possibility for the aggressiveness of sea spray impact on the stone by carrying the sea spray and deposited it on the stone surfaces directly [23]. Cardell et al. [24] demonstrated that most of the decayed stones in their case studies (SW coast of France) were noticed on the medium-high parts of the buildings because the stones did not receive saline water from groundwater, but the stones received salts from sea spray. Therefore, the mechanism of the salt crystallization of sea spray is different from the salt crystallization from groundwater through capillary action. In this sense, salts from sea spray and groundwater can be considered significant factors in the decay of building stones near coasts [25].

In Egypt, some studies have been conducted to evaluate climate changes and marine environmental impacts on archaeological sites, including Alexandria. For instance, El-Raey [26] carried out an assessment study using GIS maps and remote sensing to evaluate the impact of SLR on Egypt. He reported that many historical sites will be affected and flooded when the water reaches 50 cm up. Elsharkawy et al. [27] conducted a study on SLR impacts and observed that SLR can increase soil salinity due to saltwater intrusion in the Delta and

Alexandria. In this sense, SLR affected the library of Alexandria, one of Alexandria's landmarks, in 2005. Moreover, Bekheet et al. [**28**] and El-Raey and RCDRR [**29**] mentioned that Egypt is considered among the top five countries that will be in danger due to SLR with 1 m, specifically in Alexandria, which is considered among the 20 top cities in the world that will be in danger due to SLR. In addition, they explained that permanent coastal flooding results in the loss of dry land and saltwater intrusion into the surface and groundwater by submergence. The European Institute of Underwater Archaeology (EIUA) allowed us to see the submerged port structures of the Great Harbor of Alexandria using new methods (sonar scanning and magnetic surveys) [**30**]. Ivanov [**31**] revealed the remains of the submerged ancient breakwater using historical satellite images at Anfushi, which reflects the sea level rise impact in Alexandria. Furthermore, Abdelnaby and Elnashai [**32**] studied the impact of the historical earthquake of 1303 AD in damaging the historical buildings in Alexandria, concluding that the historical earthquakes felt in Alexandria caused structural cracks, failures, and partial and total collapse of most of the ancient buildings in Alexandria. Hemeda et al. [**33**] studied the geohazards problems for the necropolis of Mustafa Kamil in Alexandria and showed how the susceptibility of the necropolis rocks with regard to saline water and the seismic analysis response upon the necropolis revealed that the tombs are not structurally safe for PGA (peak ground acceleration) values greater than 0.07-0.08 G. Moreover, Hemeda [**34**] studied climate change at the archaeological sites in Alexandria using satellite images and geotechnical modelling and concluded that flooding is a key factor in the damage to the most built heritage in Alexandria. According to a recent study [**35**], the Qaitbay Citadel is the most vulnerable site to SLR after carrying out four SLR scenarios based on representative concentration pathways (RCPs) and shared socioeconomic pathways (SSPs).

The present study is conducted to evaluate the coastal environment's impact on Anfushi's Necropolis and the building materials' decay sources, which led to severe damage to the structural and architectural elements of the tombs. To achieve these aims, satellite images and Google Earth maps were integrated into the research paper to evaluate the vulnerability of Anfushi's Necropolis to coastal dynamics (SLR, earthquakes, flooding, and climate). In addition, multianalytical techniques (X-ray diffraction, X-ray fluorescence,

Raman spectroscopy, digital microscopy, optical polarizing microscopy, and scanning electron microscopy) were applied to assess the durability and sustainability problems of Anfushi's Necropolis building materials in the context of the coastal environment.

2. The geographical and archaeological context of Anfushi's Necropolis

Anfushi's Necropolis is located on the island of Pharos (western harbor), north of Marriot Lake and 300 m from the Mediterranean Sea with coordinates N 31^0 12' and E 29^0 52' (**Fig. 3.1.1-A** and **B**). The necropolis is situated around 1 m above the sea level and around 3 m from the ground level of the tombs to the soil surface. Anfushi's Necropolis is considered one of the endangered coastal archaeological sites in North Africa that had not been studied before from a material characterization and problems of conservation point of view. **Fig. 3.1.2** (**A**) presents a general risk map for all marine archaeological sites in North Africa, and **Fig. 3.1.2** (**B** and **C**) shows the study area (zoomed risk map) as part of these endangered sites due to the coastal environment. Giuseppe Botti, who was the director of the Greco-Roman Museum in Alexandria, revealed Anfushi's Necropolis in 1901. After Giuseppe's death, Evaristo Breccia and Achille Adriani continued their work on this archaeological site and published about it [**36**]. Anfushi's Necropolis is considered an elite Egyptian tomb for a blessed afterlife and represents a distinguished style for the tombs that emerged from the 2nd century B.C. This Necropolis shows the only example and reference of a Ptolemaic Alexandrian tomb with extensive integrations of Egyptian-style scenes and decorations; it was also the right place for a mummified body to be preserved and resurrected (**Fig. 3.1.1-C)** [**36**]. The architectural features of the necropolis's tombs reflected the mentioned importance and role of the necropolis, which consists of only five tombs from the overall complex that is visible currently in a bad state of preservation (**Fig. 3.1.1-B**). Each tomb consists of an open courtyard with burial units with attached rooms for burial purposes and descending stairs from the ground level to the underground court (**Fig. 3.1.3-A**). The first room of the burial unit showed depicted scenes in the Egyptian style. For instance, represents the dead person wearing as an Egyptian priest between Horus god Pharaonic couple, standing in front of the enthroned Osiris to offer him a jar as a clear effect of Egyptian art. From the previous room, we can see a doorframe in Egyptian style leading us

to the burial chamber and Egyptian motif interrupted by larger tiles with painted Egyptian crowns (**Fig. 3.1.1-C**). As shown in **Fig. 3.1.3** (**A-B**)**,** tombs were engraved in the bedrock of the Pharos Island ridge and were covered with two plastering layers (coarse and fine) as preparation layers for the painting (**Fig. 3 C**). Some Egyptian scenes may have been over Greek decorative plastered elements [**37, 38**].

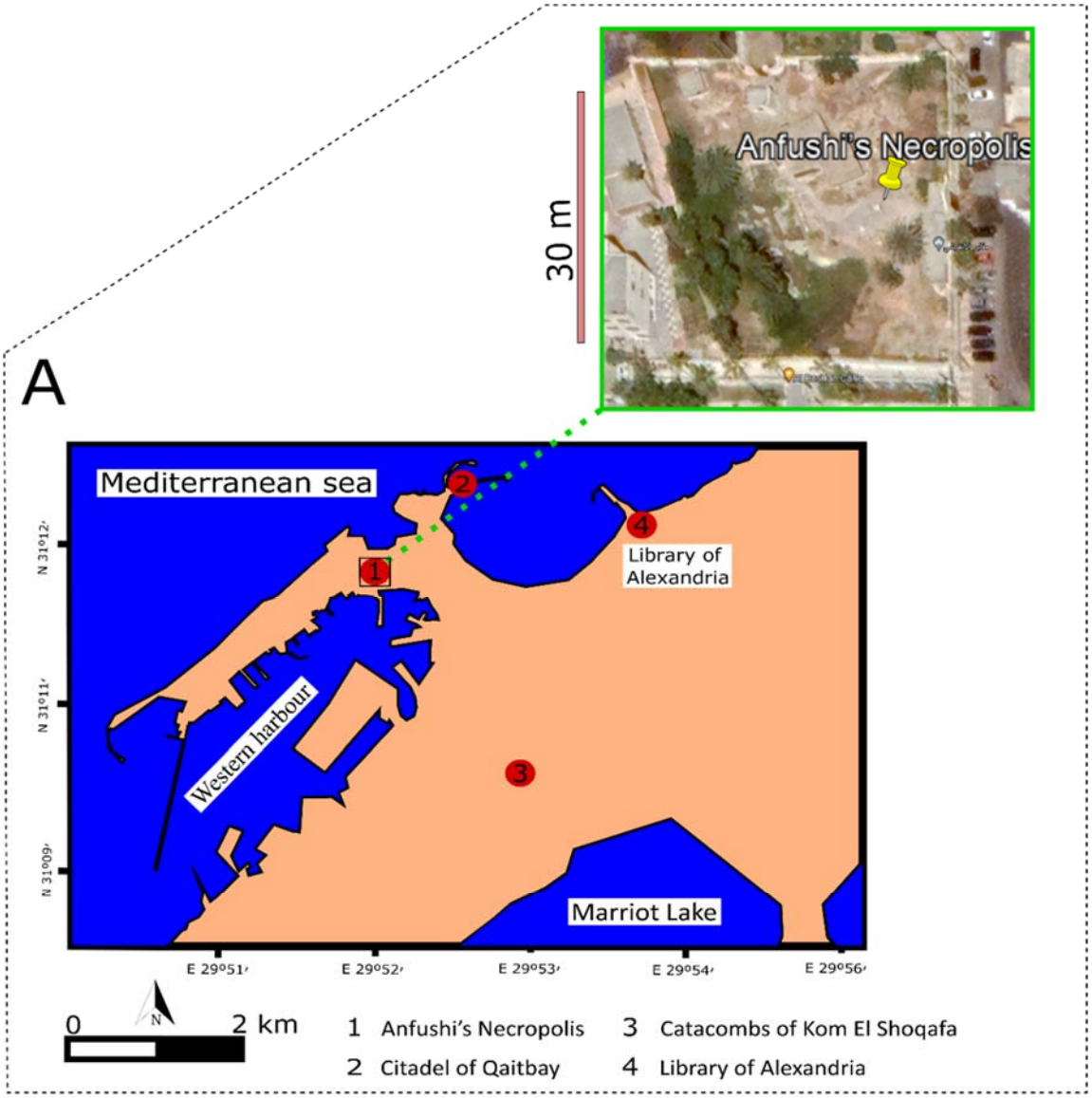




Fig. 3.1.1. (A) The geographical location of Anfushi's Necropolis on the coast of the Mediterranean Sea. (B) The general view and the current state of preservation of Anfushi's Necropolis. (C) Ancient Egyptian-style scene.

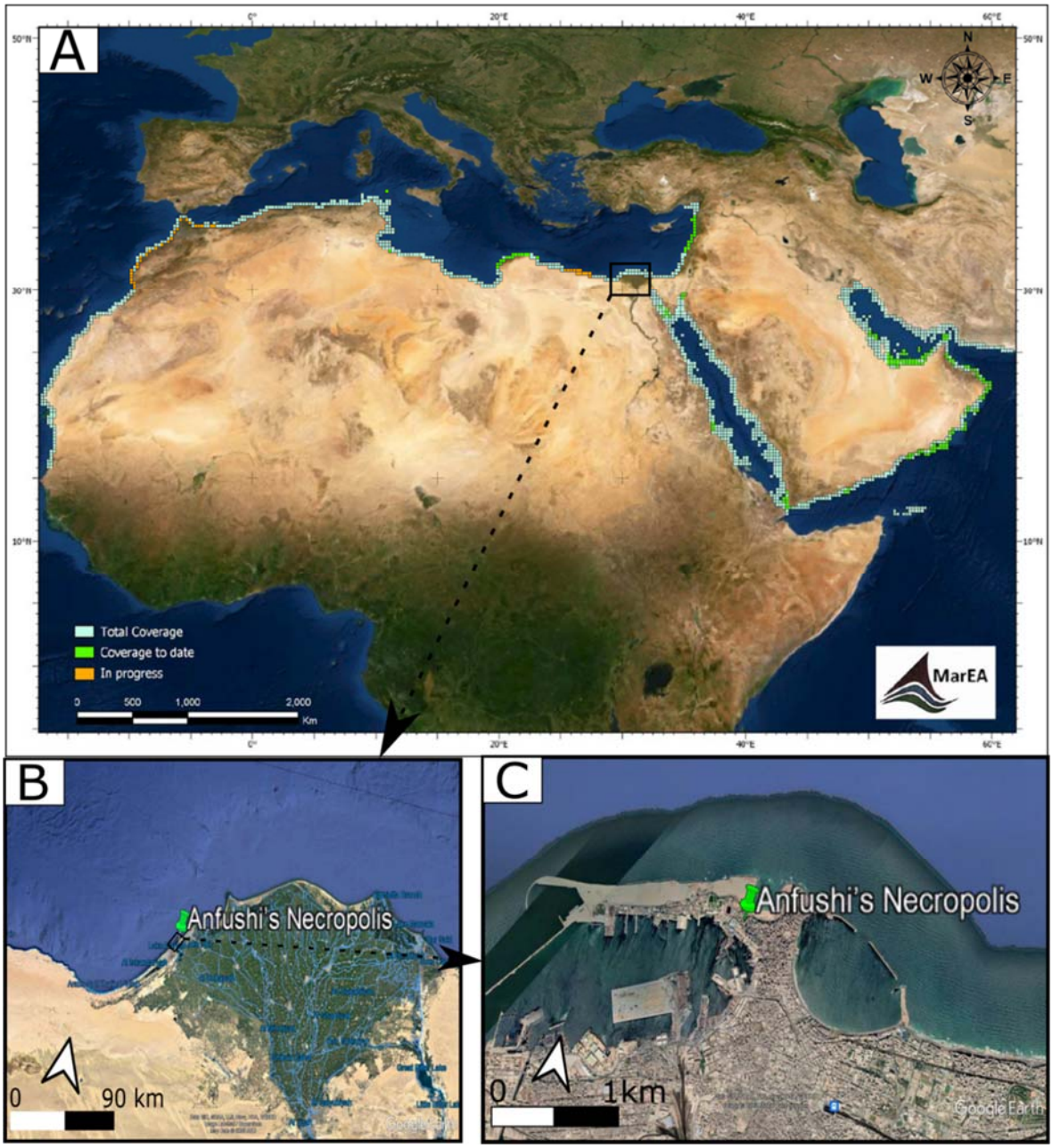


Fig. 3.1.2. (A) General map of the endangered coastal archaeological sites in North Africa and the Middle East. From [**17**]. (B) Zoomed risk map for the delta (including Alexandria), and the green pin shows the case study of Anfushi's Necropolis as an endangered coastal archaeological site in North Africa, Egypt (Alexandria). (C) Zoomed map for endangered Anfushi's Necropolis and its surrounding coastal environment.

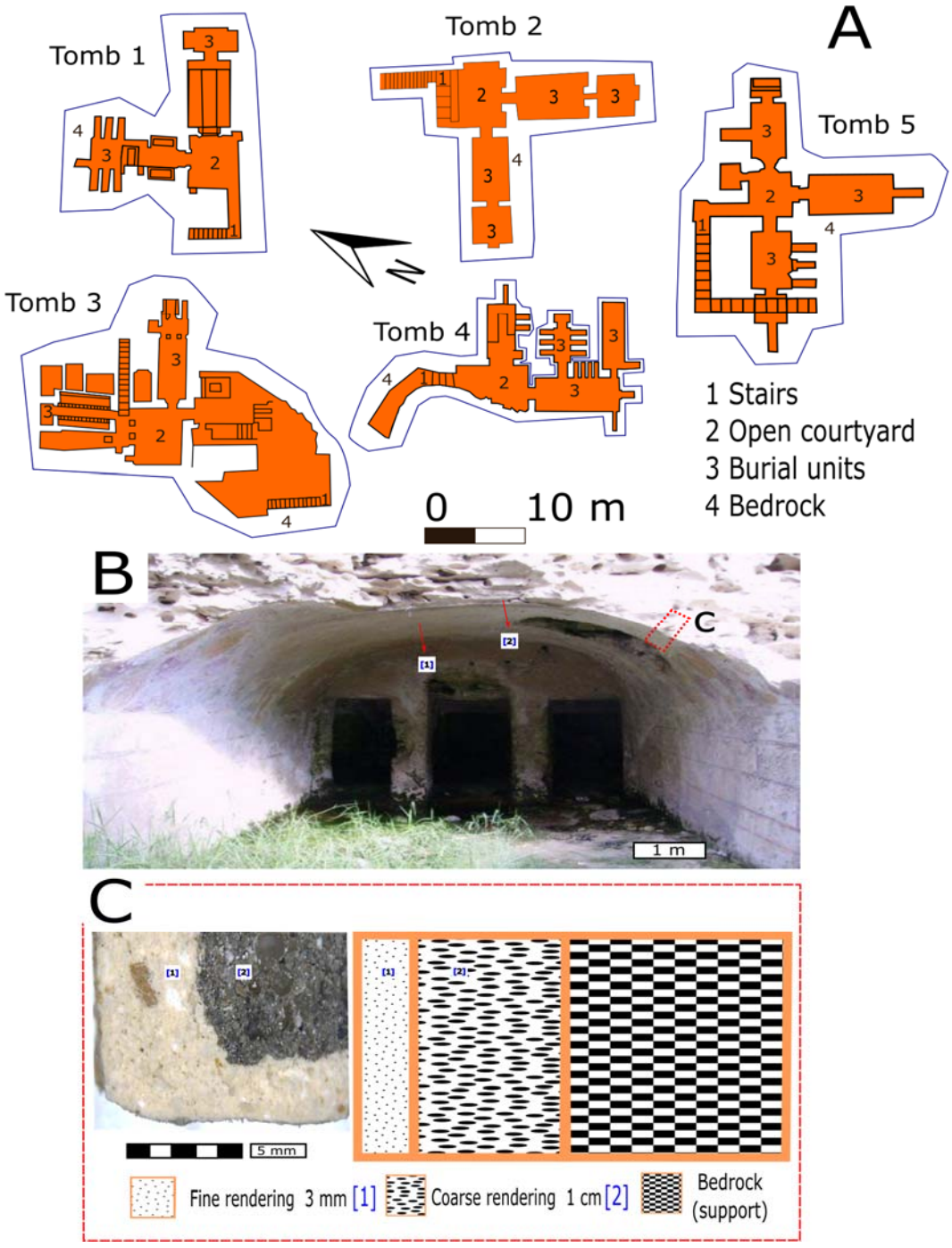


Fig. 3.1.3. (A) Schematic plans for the five tombs of Anfushi's Necropolis and their architectural elements of the rock-cut tombs and their elements. (B) General view the ground level of the tomb No 4 leads to the burial units and attached rooms. Numbers and red rectangles refer to the image (C). (C) Cross-section for mortar of the tombs, which consists of the support wall (bedrock), coarse rendering mortar [2], and fine rendering mortar for painting [1].

3. Geological context and ancient quarries in Alexandria

Egypt covers 1,000,000 km^2 and consists of four major morphological regions: Nile Valley and Nile Delta, Western Desert, Eastern Desert, and the Sinai Peninsula. Geologically, Egypt is mainly composed of five kinds of lithologies with unconsolidated Quaternary sediments (**Fig. 3.1.4 A)** [**39**]. The western desert is composed of thick deposits of loose sediments, mainly sand dunes, while the Nile valley is composed of floodplains, silt, and clay. The eastern desert and Sinai are composed of mainly sand and gravel, while the northwest is composed of sandstone and conglomerate. Moreover, the western and eastern deserts are mainly composed of limestone with some formations of sandstone from the Upper Cretaceous age and sandstone, shale, and basement rocks. In the eastern and southeastern deserts, there are crystalline basements from igneous and metamorphic rocks [**39**, **40**]. The coastline of Alexandria is characterized as an unconformity surface composed of soil sediments, oolitic sand and clay, oolitic limestone (Middle Miocene), gray shelly dolomite, marly dolomite, oncolitic limestone and dolomite, and shelly limestone. In addition, it comprises largely bioclastic (shelly) and muddy carbonate sand strata interbedded with fine-grained sandy silt (Arid Loamy soil), silty mud, and dark organic-rich layers (**Fig. 3.1.4. B and C**) [**41**-**44**]. On the other hand, the ridge of the Abusir between southwestern Alexandria to Abu Kir in the east dates back to the Pleistocene age, which reaches a height of 35 m in its western part and 6 m in Abu Kir, and it was formed by poorly to moderately cemented sandy carbonate [**45**]. The island of Pharos is formed of limestone (the bedrock ofAnfushi's Necropolis). A thin layer of clay with different thicknesses and consolidation states is overlaid on the slopes of this limestone ridge [**46**].

Ancient Egyptians used different kinds of stones (limestone, sandstone, granite, basalt, etc.) from different quarries along Egypt, from south to north and from east to west. The extracted stone blocks were used to build temples and tombs in different periods in Egypt for architectural and ornamental purposes [**47-49**]. Alexandria was a source of quarried limestone blocks from Quaternary ages along the Nile Delta's Mediterranean coast [**50**]. Abusir and Al Max west of Alexandria are considered quarries that were used from the Ptolemaic era to the Roman era (**Fig. 3.1.5**). The limestone of these quarries is light-

coloured, and their deposits belong to the Pleistocene Alexandria Formation. Ancient and recent quarries are observed on the Alexandria-Marsa Matrouh Road in a 21 km area [**51, 52**].

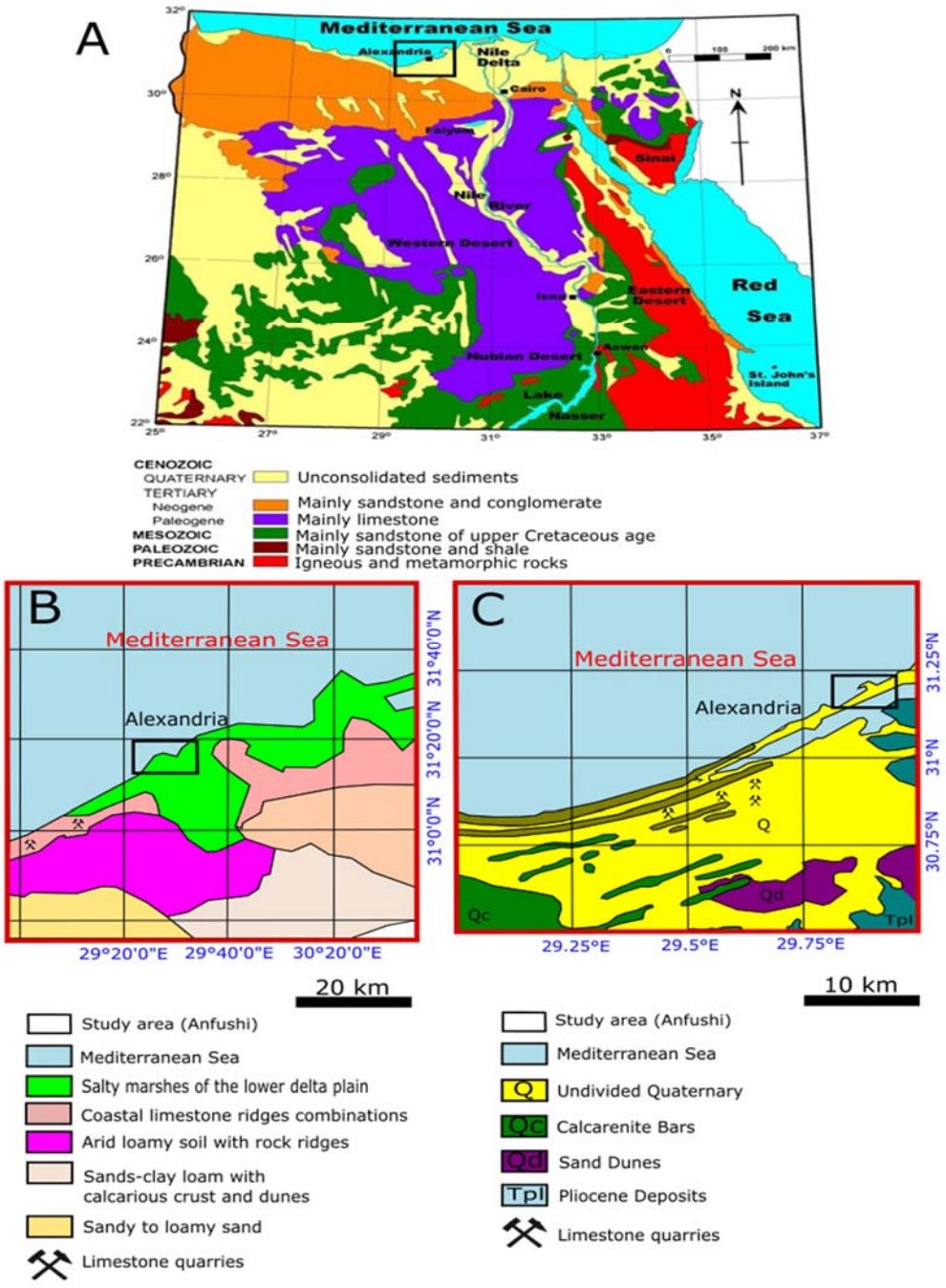


Fig.3.1.4. (A) Geological map of Egypt, black rectangle refers to Alexandria, from [**39**]. Detailed maps for soil units (B) and geological map (C) of Alexandria, edited after [**43**]. Black rectangles refer to the study area.

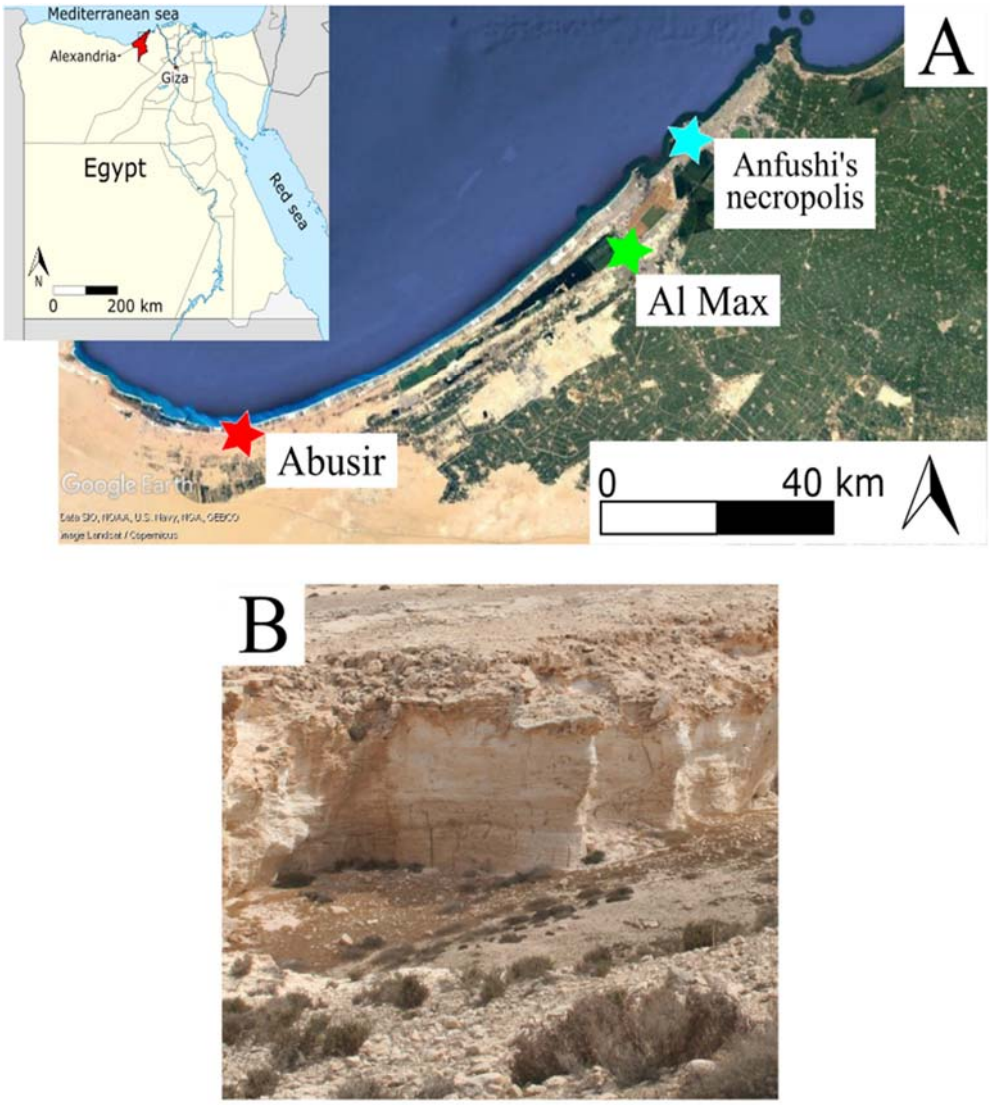


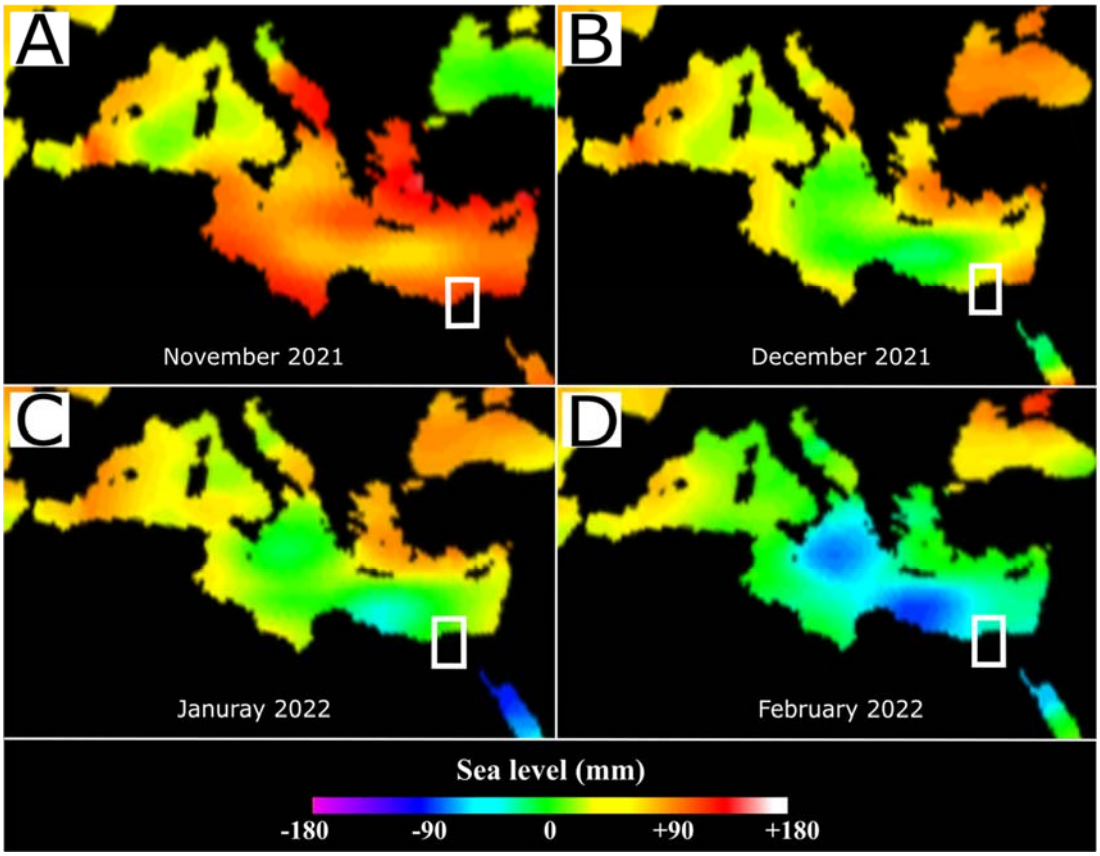
Fig. 3.1.5. Ancient quarries in Alexandria (green and red stars) with an example of the light-coloured limestone outcrop.

4. Coastal geodynamics context

4.1. Sea level rise

Globally, sea levels are rising due to global warming, and from 1995 to 2020, the water has risen to approximately 102.3 mm, and in January 2022, it reached 102 ± 4 mm according to satellite sea level observations [**53**]. Alexandria is susceptible to the SLR effect as one of the marine dynamics. From 1906 to 2020, the annual linear SLR in Alexandria was 2.6 mm/year; from 1906 to 1980, the SLR increased by 51%; from 1981 to 2000, the SLR increased by 20%;

and from 2001 to 2020, the SLR increased by 78% [54]. **Fig.3.1 6** shows the change in the average water level from November 2021 to February 2022. In November 2021, sea-level rise reached +88 mm (maximum), but in February 2022, sea-level rise returned to -88 mm (minimum), which reflects the considerable variation in the sea level in Alexandria.



(The caption is in the next page)

Fig. 3.1.6. (A-D) Satellite images for the average monthly sea-level rise variations; the pink rectangle refers to Alexandria. From https://climate.nasa.gov/ accessed 13 May 2022.

Furthermore, Alexandria is also vulnerable to SLR because of its low elevation and local land subsidence. The land in front of the sea approximately 50 km is less than 2 m from the sea's water level, and a sand belt formed by sediments charged from Nile branches protects this land with its buildings. After building a high dam, the discharge of these sediments decreased, and the safe sand belt started to be eroded [55]. El-Raey and RCDRR [29] studied two scenarios for SLR impact on loss of land and socioeconomic activities in Alexandria and the whole delta after [56, 57]. In this regard, they proposed that an SLR of 0.5 m would

affect 3.8 million people and 1,800 km^2 of land while assuming an increase of 1.0 m SLR would influence 6.1 million people and 4,500 km^2 of land use (**Fig. 3.1.7 A and B**). Another scenario has been studied with a 1.5 m SLR, which put Anfushi Bay (approximately 300 meters from Anfushi's Necropolis) in the risk zone of the future SLR (**Fig. 3.1.7 C**) [**28**].

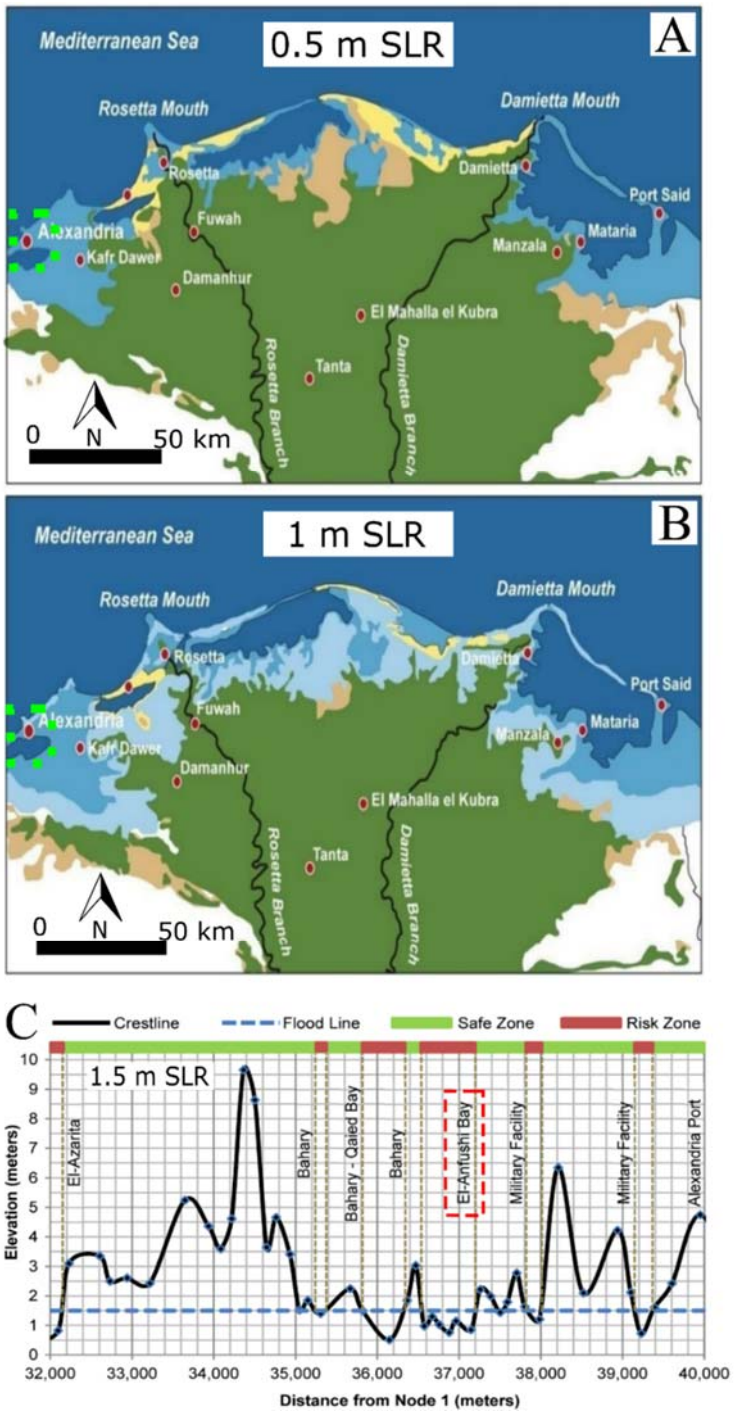


Fig. 3.1.7. (A and B) Two scenarios for possible water increases of 0.5 m and 1 m, respectively, and their impact on territory. Alexandria and the research area are represented in the green dotted square, after [**29**]. (C) Longitudinal profile for the flood line, safe and risk zones for the SLR scenario of 1.5 m. The study area is represented in black rectangular as a risk zone, after [**28**].

4.2. Earthquakes and land subsidence

Generally, Egypt has many seismotectonic sources, such as those in the Gulf of Suez-Northern Eastern Desert, Southwest Cairo (Dahshour), Northern Red Sea, Gulf of Aqaba, and Aswan zones [**58**]. Historically, Alexandria was subjected to 25 severe earthquakes between 320-2000 AD with large and moderate magnitudes. Alexandria was subjected to a very strong earthquake that affected the ancient buildings in 702 AD, and the earthquake of 726 AD caused the collapse of many structures, especially the lighthouse of Alexandria [**43**]. A recent study confirmed that the historical record of earthquakes in Egypt is from 2200 BC to 1889 AD. Recently, there have been various earthquakes of different sizes, such as the Aswan earthquake in 1981 (moderate magnitude, 5.8), Cairo earthquake in 1992 (moderate magnitude, 5.8), Aqaba earthquake in 1995 (great magnitude, 7.2), and El Alamein earthquake in 2015 (moderate magnitude, 4.5), and most earthquake activities are focused in northern Egypt. In this regard, the Hellenic Arc, Red Sea, and Aqaba earthquakes gave less than 100 cm/sec^2 peak ground acceleration with a duration of more than 3 minutes, which affected the ancient building in Alexandria [**59-61**]. In addition, **Fig. 3.1.8** (**A**) presents the distributions of historical earthquakes in Egypt from 2200 BC to 2015 AD. Due to their closeness to the two major faults, Egypt's Eastern Mediterranean–Cairo–Fayoum fault and Suez–Cairo–Alexandria fault have severely affected the ancient buildings of Alexandria. The second reason for Alexandria's vulnerability to earthquakes is the mechanical and physical characterizations of the soil [**60**]. In **Fig. 3.1.8** (**B**), the historical epicenters in Egypt are shown, and most of these earthquake epicenters affected many buildings structurally in Alexandria with magnitudes from 4.5 to 6.5, since with a magnitude of 6.7, the offshore area gives a peak ground acceleration up to 300 cm/sec^2 [**59**].

Additionally, Alexandria's land subsidence ranges from zero to -5 mm yearly. From 2017 to 2020, the vertical displacement/deformations in Alexandria were -60 mm with average -12.5 mm and a mean displacement rate of -1.73 mm/yr [**62**]. Moreover, another study suggested that Alexandria was subjected to 0.4 mm/yr on average and up to 2 mm/yr locally over the last decade after analysis using GPS and persistent scattered interferometry data [**63**]. It was mentioned that the subsidence rate in Alexandria during the last 60 years was

2 mm/year. In addition, the average rates of land subsidence in Alexandria from 0.9–4.3 mm/year, from west to the east along the northern Delta coast, vary irregularly with an average of ~2.5 mm/year [45]. SLR, earthquakes and other natural hazards from the Ptolemaic era until the Arabic era caused land subsidence and affected the archaeological landscape, such as the ancient Royal Port in Alexandria, which is 1 km from Anfushi's Necropolis [61].

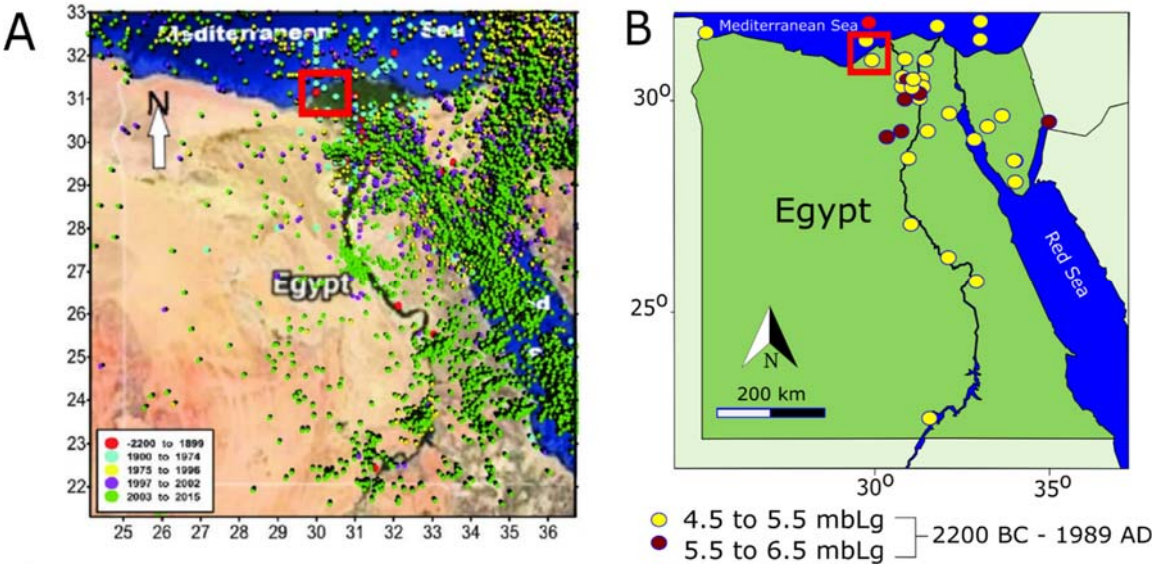


Fig. 3.1.8. (A) General disruption of the historical record of earthquakes in Egypt (2200 BC to 2015 AD). (B) Map of historical earthquakes with their magnitudes from 2200 BC to 1989 AD, after [61]. Red squares represent the Alexandria area.

4.3. Environmental factors

4.3.1. Storminess

Alexandria experiences approximately 16 strong storms yearly with strong winds, high waves, and heavy rains, especially in the winter season [65]. In 2010, storm waves were measured with heights of 7.7 and 6.8 m [63]. Most heavy storms (Nawat, local name) occur between September and March each year, with a minimum of two days and a maximum of eight days (**Table 3.1.1**).

Table 3.1.1. Some recorded heavy storms in Alexandria with expected dates and durations. From [65].

No	Storm Name	Expected date	Approximate duration
1	Nawat El-Saliba	September	3 days
2	Nawat El- Maknassa	November	3 days
3	Nawat Kassem and El- Fida	December	5 days
4	Nawat El-Ghatas, El- Fida El-Kabira and El-Karam	January	10 days
5	Nawat El-Hosoum, El- Shams El-Kabira and El- Aowa	March	16 days

4.3.2. Flooding

Heavy rainfall and tidal actions are the main reasons for flash and coastal flooding in Alexandria [67]. On 25 October and 4 November 2015, Alexandria practiced a rare rainfall storm with 100 mm/h, which led to the worst flooding for decades because 60% of the city was covered by water from 0.5 to 1 m [68]. Accordingly, Alexandria is considered one of the five coastal cities that have the risk of flash flooding and coastal flooding [69]. Young [70] said that rainfalls with a 50 mm event would have a higher severity, as well as rainfalls with a 20 mm rainfall, resulting in significant flooding. In 2020, the maximum tide in Alexandria occurred on 1 January at 0.40m, and the minimum tide occurred on February 29 at 0.25 m. In 2022, the minimum tidal action was 0.03 cm, and the maximum was 0.29 cm from 18 May to 31 May 2022 (https://www.seatemperatu.re/middle-east/egypt/alexandria/tides.html). Flooding in Alexandria occurs each winter and has an insufficient drainage system and infrastructure [71]. For this reason, the archaeological sites in Alexandria will be under the permanent impact of wetting and flooding each year as well.

4.3.3. Meteorological context

Alexandria is considered warm, arid, and clear in the summer, but it is cool, rainy, and windy in the winter. In the summer, the average temperature degree is above 30 °C from June to the end of September. On the other hand, the temperature in the winter is a 5 °C minimum and 18 °C maximum from December to mid-March (**Fig. 3.1.9 A**) [**72**]. From the automated weather station at Western Harbor (approximately 1 km from Anfushi's Necropolis), the maximum relative humidity from 2007 to 2018 was 99%, and the minimum relative humidity was 11% [**73**]. In 2021, the maximum relative humidity was 71%, and the minimum relative humidity was 65% (**Fig. 3.1.9 B**). Furthermore, the average rainfall in the summer is approximately 30 mm, while the average rainfall in the winter is 166 mm [**68**]. Hafez [**72**] said that the average annual rainfall is approximately 200 mm but can reach more than 400 mm. **Fig. 3.1.9** (**C**) shows the average days of rainfall in Alexandria, and **Fig. 3.1.9** (**D**) shows the monthly average rainfall in Alexandria in 2021. Due to rapid climatic change, Alexandria has only two seasons: a hot summer from April to September and a moderate winter from October to March. Daytime temperature and wind patterns are the main factors for the difference between the two seasons [**74**]. Eventually, in 2021, the maximum wind speed was 44 km/h or 24 kts (strong), and the minimum speed was 7 km/h or 3.78 kts (weak). Wind forces represent 70% of the total dynamic in both sea level, and current and tidal actions represent 30% of the sea level and its current energy (**Table 3.1.2**) [**75**]. Currently, snow is part of the marine dynamics in Alexandria that affect ancient building materials. For decades, Alexandria was subjected to snowfall in December 2021 and was considered a rare snow occurrence (**Fig. 3.1.10 A** and **B**). However, from time to time, Egypt is experiencing a cold snap with low temperatures reaching 2 °C. The bibliographical studies for snowfalls in Egypt and Alexandria are not available; however, it said that Egypt experienced snowfalls in 1639, 1855, and 1934.

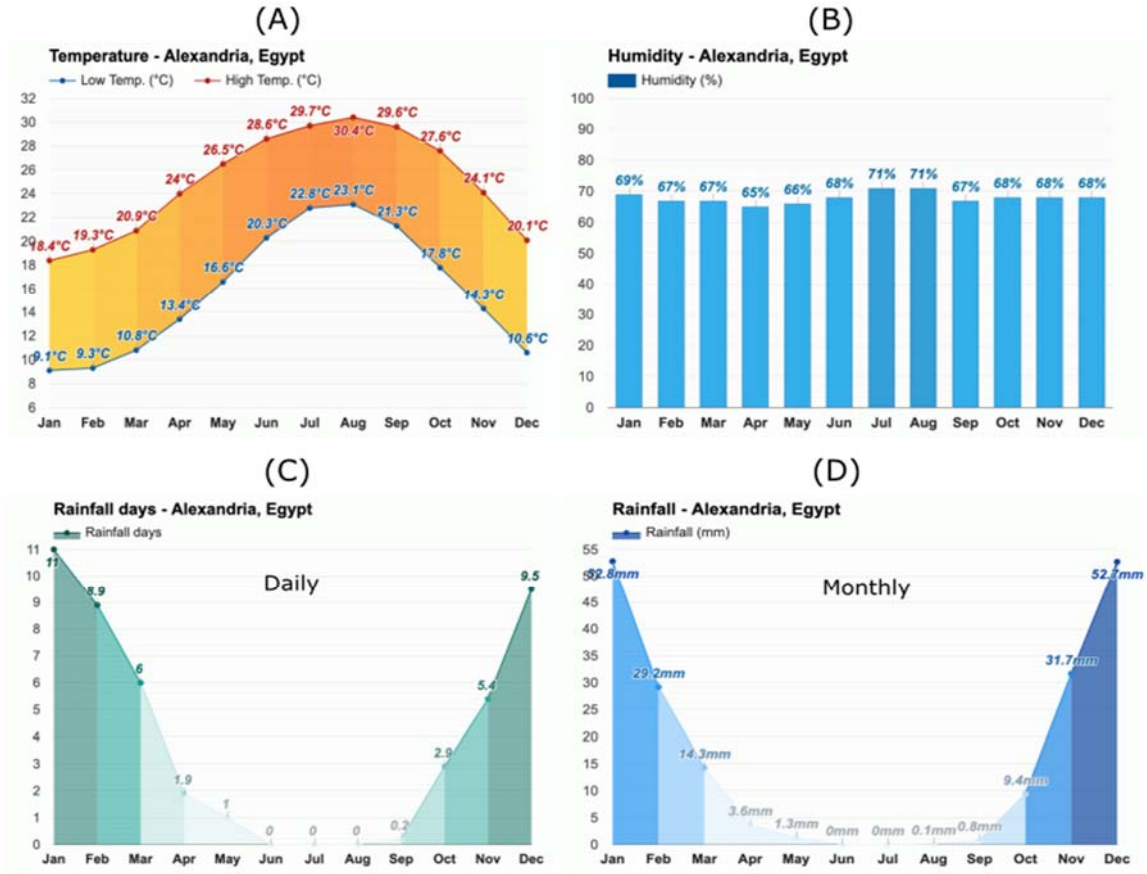


Fig. 3.1.9. Hyetographs for the meteorological data in Alexandria 2021. After https://www.weather-atlas.com/en/egypt/alexandria-climate (Accessed 19 May 2022).

Table 3.1.2. Wind dynamics in Alexandria, monthly in 2021 (after https://www.timeanddate.com/weather/egypt/alexandria/historic?month=12&year=2021).

Wind speed (km/h).	Jan	Feb	Mar	Apr	May	Jun	Jul	Aug	Sep	Oct	Nov	Dec
Max	26	26	31	**40**	39	37	36	**44**	36	34	30	23
Min	**7**	8	10	9	16	18	24	22	18	19	13	**7**



Fig. 3.1.10. (A and B) Rare snow falls over Alexandria in December 2021.

4.4. Anthropogenic damage

In 1899, Guiseppe Batti noticed and informed that many archaeological structures had been destroyed due to mining, quarrying, and other infrastructure activities in the district of El-Mafrouza, a road between El Mex and Anfushi. Some Egyptianizing façade, cornices, a frieze with a winged solar disc, and an architrave had been damaged in one of the hypogea at El-Mafrouza. In addition, some of the funeral structures at Anfushi's Necropolis were damaged [**76**]. Currently, the lack of maintenance and the neglect of this important site are considered anthropogenic factors for damage as well.

5. Materials and methods

To evaluate the impact of environmental dynamics in Alexandria over Anfushi's Necropolis, in-situ visits were carried out to take photographs the architectural and structural defects and degradation. In addition, deskwork was performed to sketch and map the decay and durability problems of the construction materials through engineering drawing. Satellite images were collected to monitor the sea level rise problem and its impact on Anfushi's Necropolis.

Highly weathered fallen archaeological samples were collected from the different parts of Anfushi's Necropolis (construction materials + rendering mortars) to carry out the assessment study of the decay through analysis and microscopic examination from the construction. The samples of the construction materials are divided into samples from the

casing stone and the bedrock with light colour and crust over the surface (**Fig. 3.1.11 A** and **B**). The rendering mortar samples are coarse and fine mortars for the first and second layers with blackish and yellowish colours, respectively (**Fig. 3.1.11- C**). The samples ranged from 3 cm to 7 cm^3 in size. In addition, some of the samples had been ground to be ready for analysis purposes (**Fig. 3.1.11- D**), and other samples were in a solid-state for microscopic examination.

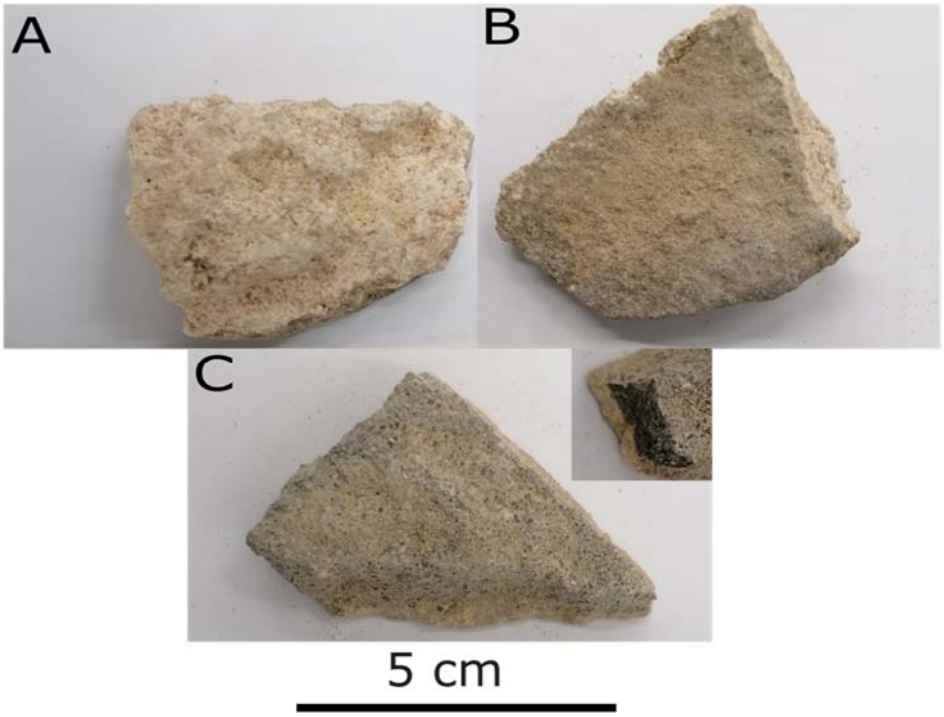


Fig. 3.1.11. (A-B) Construction stones (casing + bedrock). (C) Coarse and fine rendering mortars.

To detect the morphological features of the construction materials, a digital microscope was used, and thin sections were prepared and studied using an Olympus BH-2 polarized optical microscope to identify the different minerals, altered phases and textures of the samples. Small fragments were used to detect the durability problems and alterations through the textural features of the samples under high resolution using a scanning electron microscope (TESCAN-performance at 20.00 kV, WD: 17.73 mm and Vac: HiVac). In addition, EDS detector (EDAX 60 mm2 Octane Super) was utilized for salts phases detection,

degradation patterns, and elemental analysis for the detected salts. X-ray diffraction was utilized to identify the mineralogy of the stones and mortars. For this, a Bruker D-8 Advance ECO diffractometer equipped with a Lynxeye high-speed measurement detector was used under the following conditions: CuKα radiation filtered by Ni, graphite monochromator, and fixed slots, 2theta 5° to 60° scanning angle; diffractograms were interpreted with the software EVA (Bruker-AXS). A Bruker AXS M-4 Tornado sequential dispersive wave X-ray spectrometer with a Rh tube operating at 4000 W (XRF) was used to recognize the major and trace elements.

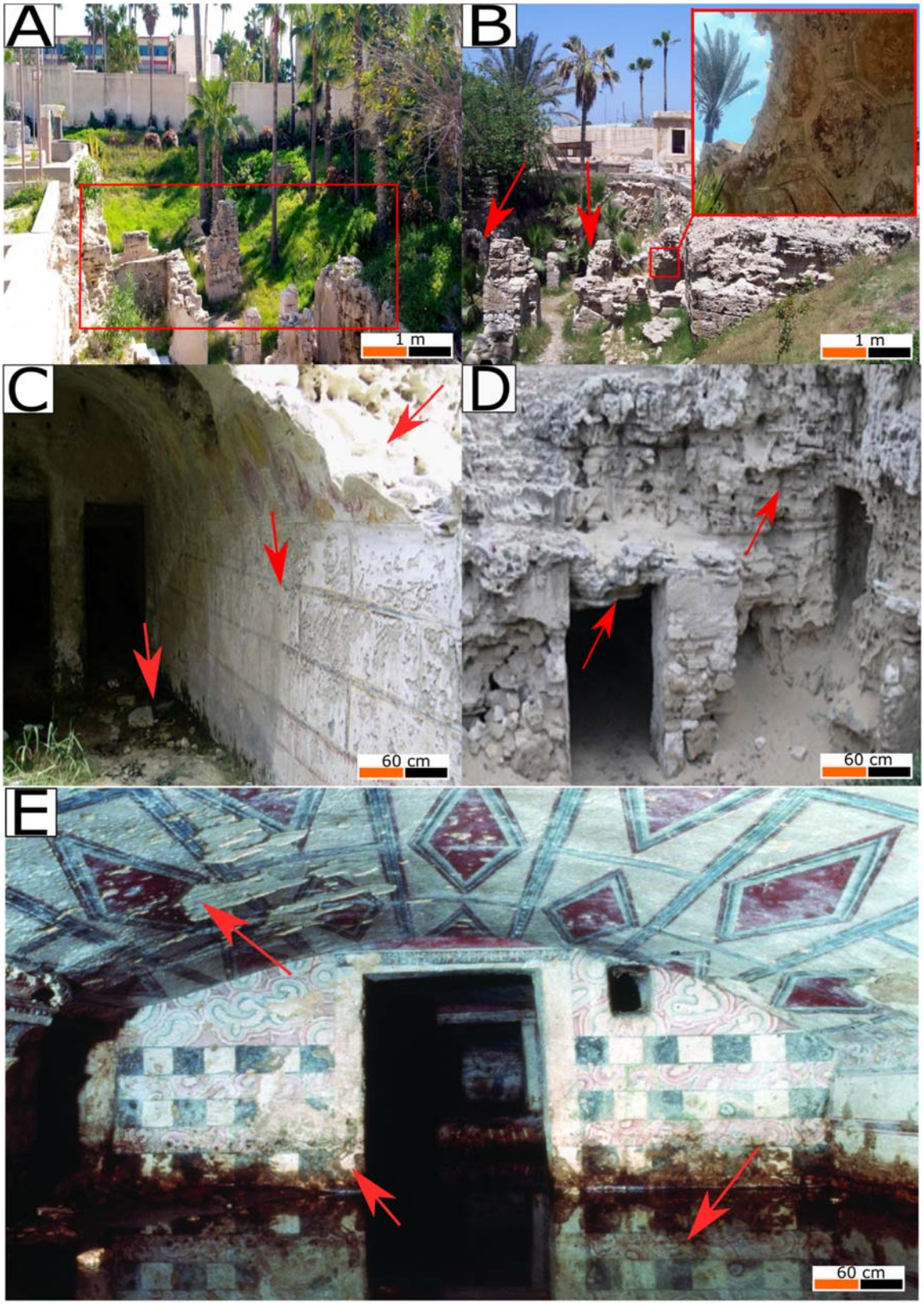
6. Results

6.1. In-situ recordings

Over the years, earthquakes in Alexandria have affected the archaeological site of Anfushi's Necropolis and its structural stability. During the ground motion, the accelerations of the earthquake go through the foundation and bedrock to the building structures. Accordingly, earthquake-induced damages are recorded and monitored, such as 1) horizontal displacement of some blocks; 2) vertical and horizontal wall displacements; 3) cracks and fractures (approximately from 2 to 4 mm of space); 4) collapsed ashlars and walls; 5) opened joints between blocks; and 6) chippings in most of the built structures (**Fig. 3.1.12 A** and **B**). The bedrock has its own geotechnical problems because the unconsolidated limestone presents many cavities, which affect the durability of the tombs and accelerate the ground motion of the earthquakes to be transmitted rapidly from the bedrock to the tomb structures (**Fig. 3.1.12 C-D**). Moreover, water reaching the ground level of the Necropolis was monitored, which is considered a damaging factor for the Necropolis as well. In that case, water could cause cavities in the bedrock and be responsible for the deterioration of the architectural and structural elements of the Necropolis (red arrows, **Fig. 3.1.12 C** and **D**). In general, it is observed that trees and vegetation around the necropolis and near the tomb structures could be an additional factor as a mechanical force (**Fig. 3.1.12 A-C**), and salt weathering, biological attack, discolouration, cracking, loss of material, and flaking are the main decay patterns for the walls and ceilings with their decorative motives due to the

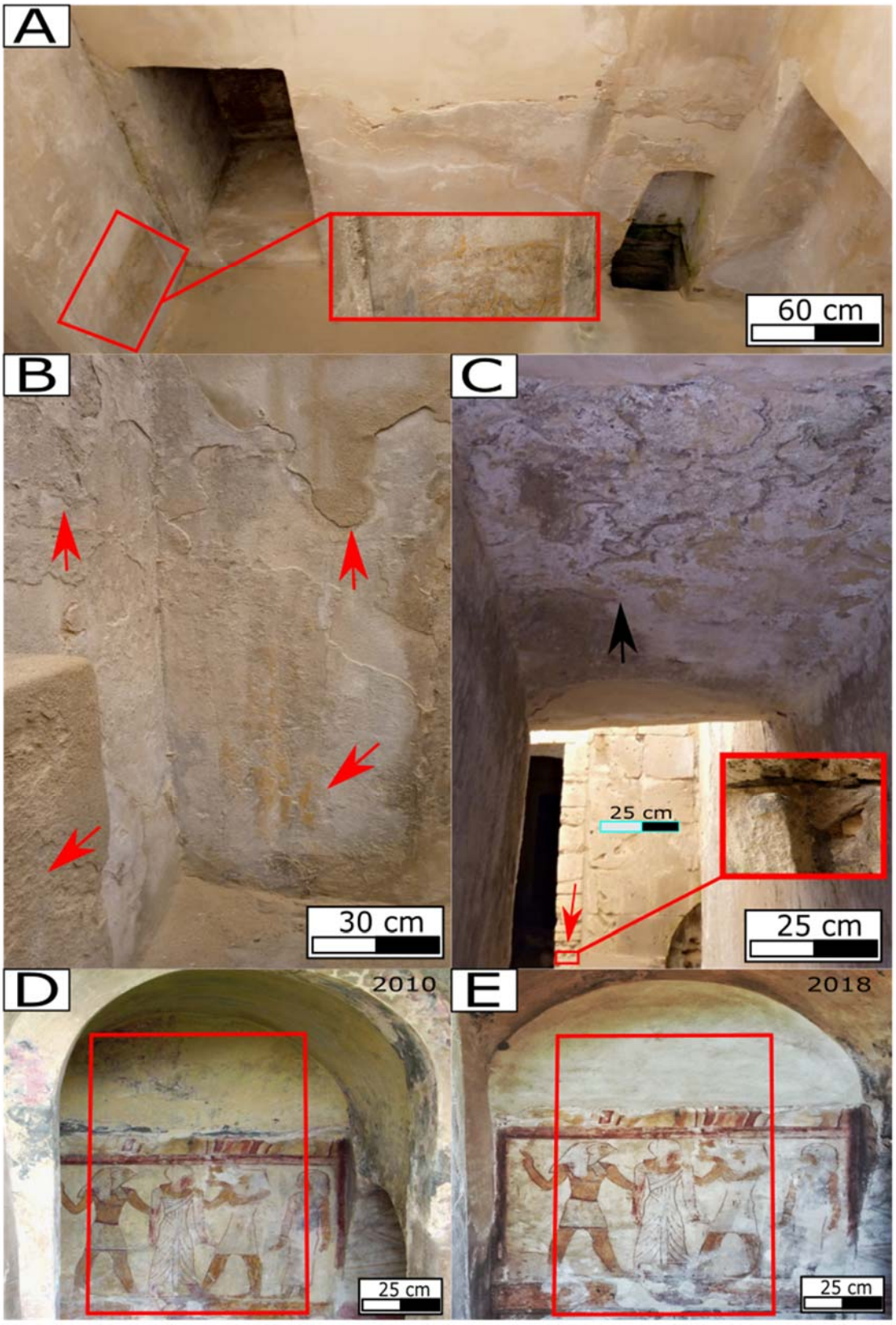
dampness. Finally, **Fig. 3.1.12** (**E**) shows the accumulation of water inside room number four of tomb number five. It is observed that the level of water rise reached to more than 50 cm over the painted walls. In the supplementary materials, there are more figures for the noticed decay and alterations in the construction materials of Anfushi's Necropolis (**SM1. Fig. 1-5**).

Moreover, many aspects of decay were recorded, such as alveolarization, exfoliation, flaking, salt erosion (efflorescence and subflorescence), discolouration, blistering, spalling and cracking. In this sense, **Fig. 3.1.13** (**A**) shows the severe state of preservation due to the degradation that occurs in the side room for one of the tombs of Anfushi's Necropolis. In that room, the degradation aspects are efflorescence and subflorescence, discolouration, blistering, eroded edges, chipping, paint layer removal, and cracking. In addition, we can see the horizontal displacement and crack for the front wall with approximately from 2 to 5mm. In **Fig. 3.1.13** (**B**)**,** the main degradation aspects include exfoliation, flaking, peeling, spalling, blistering, pitting, rising damps, subflorescence, discolouration and loss of the painting layer. In addition, **Fig. 3.1.13** (**C**) shows the alveolarization, chipping, and pitting decay forms in the front of the wall, but on the ceiling, the main degradation patterns are efflorescence and subflorescence, discolouration, and paint layer removal. **Fig. 3.1.13** (**D and E**) shows two historical photos that date back to 2010 and 2018 for the same area, respectively, where photo (**D**) shows a complete ritual scene with its painting layer in a good state. On the other hand, photo (**E**) shows the same scene after the loss of most of the painting layers and salt attachment due to marine conditions. In both photos (D and E), it can be observed a displacement of the wall (out of plane) above the Egyptian-style scene which estimated by 10 mm approximately. Finally, after taking different photographs, digital recordings were performed to monitor and evaluate the deterioration patterns in different areas for different architectural elements of Anfushi's Necropolis, showing that salt erosion, loss of materials, loss of painting layer, flaking and cracks are the most dominant decay aspects over the surfaces (**Fig. 3.1.14 A-C**).



(Caption is in next page)

Fig. 3.1.12. (A and B) Structural damage aspects due to earthquakes. (A) The red rectangle refers to the deformations in the structures. (B) The red arrows refer to the collapse, displacement for the blocks and opened joints, and the red square refers to the damage to walls with chipping. (C) Water intrusion impact on the architectural and structural elements Anfushi's Necropolis. Red arrows refer to biological growth, salt accumulation, and degradation of the stone and painting layers. (D) Geotechnical problems, unconsolidated bedrock with many cavities as shown by the red arrows. (E) Dampness impact over the structural and decorative elements of Tomb No 5(burial unit) at Anfushi's Necropolis. Red arrows refer to flaking, salt erosion and biological attack on the tomb construction materials [**77**].



(Caption is in the next page)

Fig. 3.1.13. (A-C) Different kinds of decay patterns due to the marine environment for the walls. (A) The red rectangle refers to areas with efflorescence, subflorescence, edge eroding, flaking and loss of the painting layer in the courtyard of Tomb No 4. (B) The red arrows refer to flaking, exfoliation, salt erosion, surface disintegration and loss of the painting layer in the courtyard of Tomb No 4. (C) Red squares refer to honeycomb and loss of material decay patterns, and black arrows refer to salt precipitation and loss of the painting layer in the corridor to the burial units of Tomb No 4. (D) A ritual scene in the necropolis and its state of preservation state in 2010from Tomb No. 2 (back wall of the burial chamber) (from https://mapsus.net/EG/necropolis-of-anfushi-5577). (E) The same ritual scene after 8 years, with a worsened state of preservation, where a large loss of the painting layer and renderings occurred due to the salt attack (from https://www.meretsegerbooks.com/gallery/581/anfushi-necropolis).

6.2. Sea level rise impact (SRL) and future scenarios

Currently, SLR is considered the main hazard for the archaeological sites in Alexandria. Accordingly, probabilistic analysis and assessment of the future impacts of SLR were carried out through satellite image observations from the accessible Climatic Central Analysis (CCA) (http://sealevel.climatecentral.org). Different topographical scenarios with an SLR ranging between 0.5 and 3 m were evaluated. The results showed that the morphological scenario of 0.5 m SLR would not cover Anfushi's Necropolis with water (**Fig. 3.1.15- A**), but the 1 to 3 m SLR scenarios would submerge it completely (**Fig. 3.1.15 B-F**).

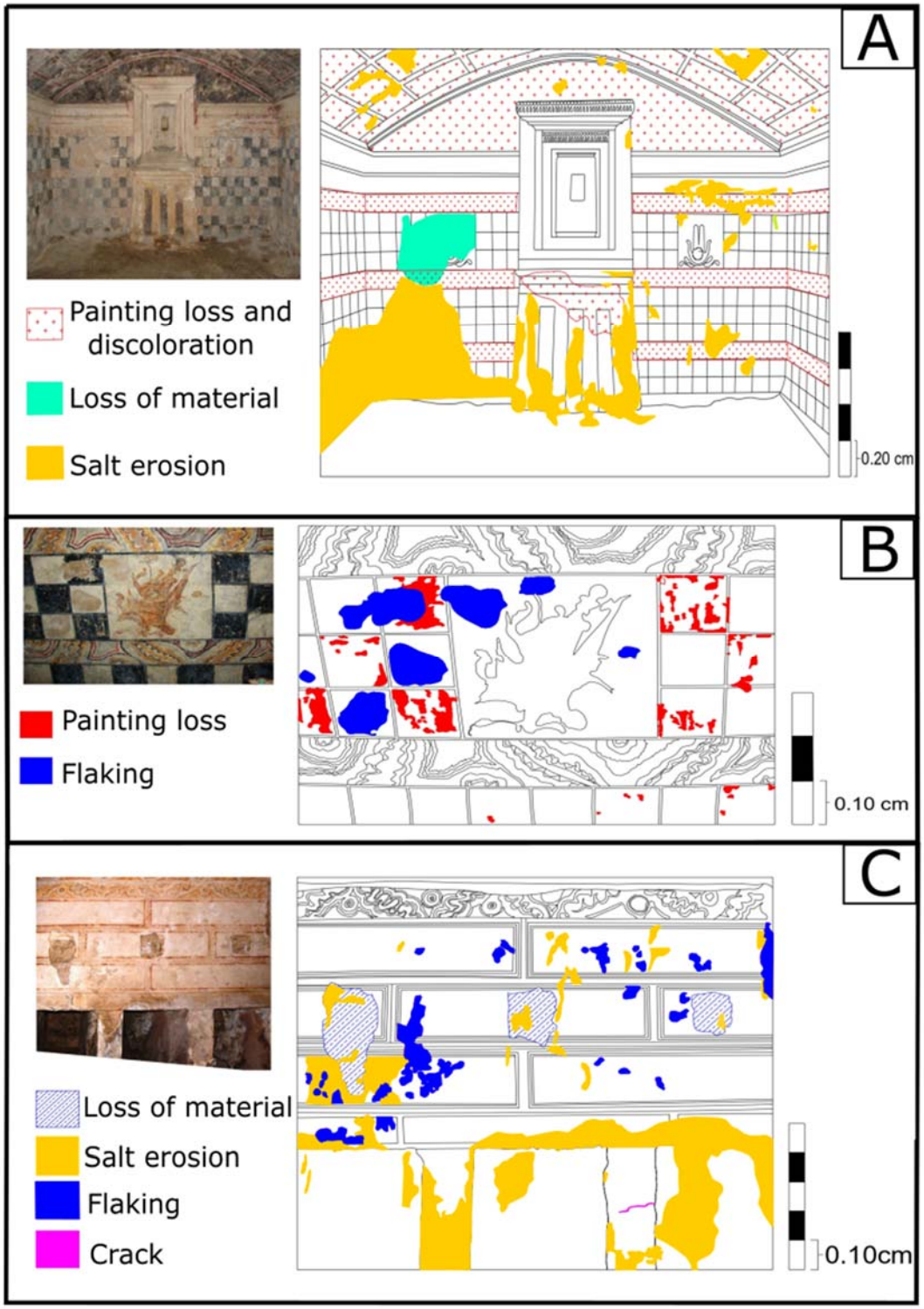


Fig. 3.1.14. (A-C) Different decay patterns for various architectural elements of Anfushi's Necropolis, where salt erosion is the main decay pattern on the surfaces in the Tomb No 2 rooms 1 and 2.

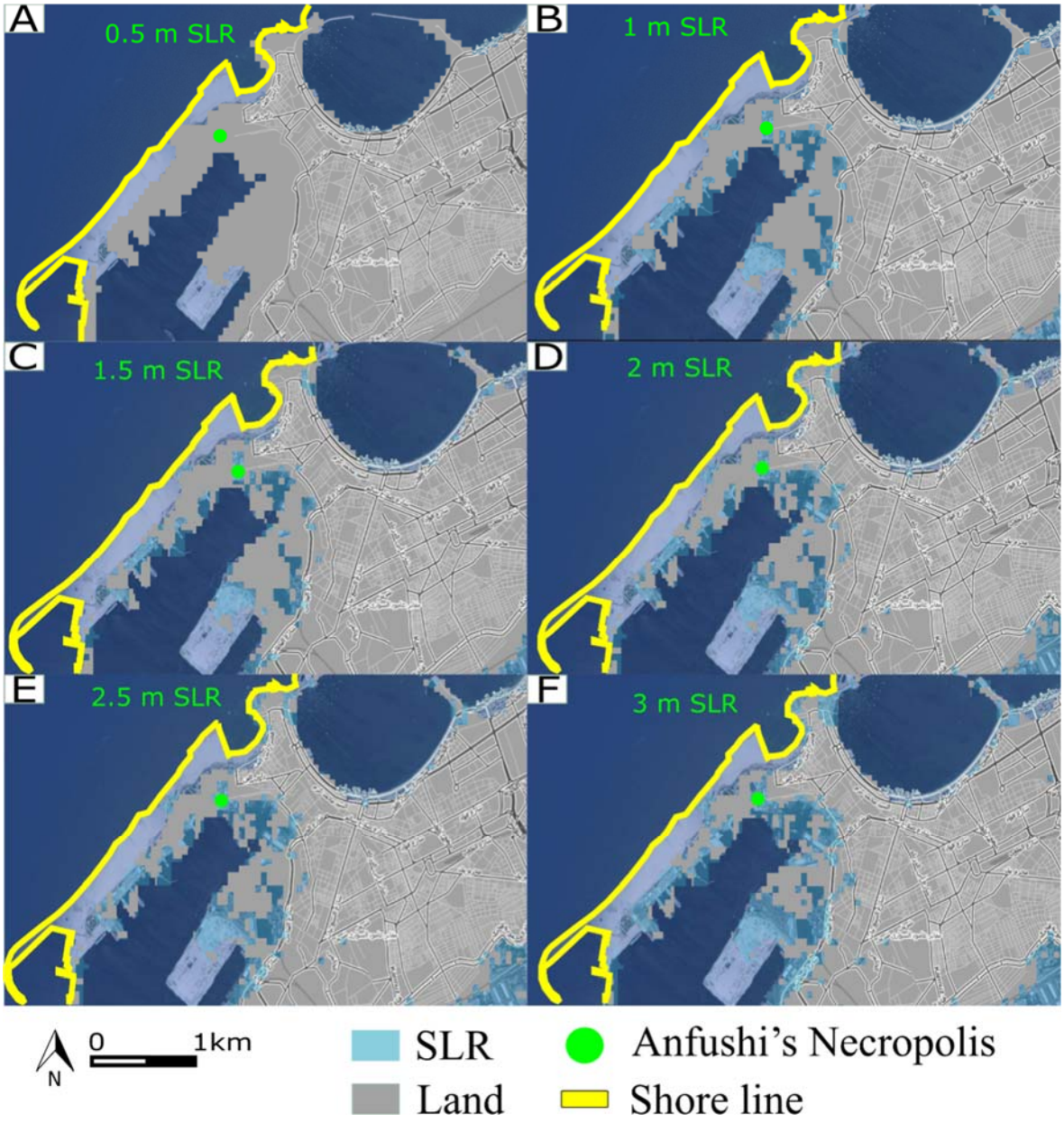


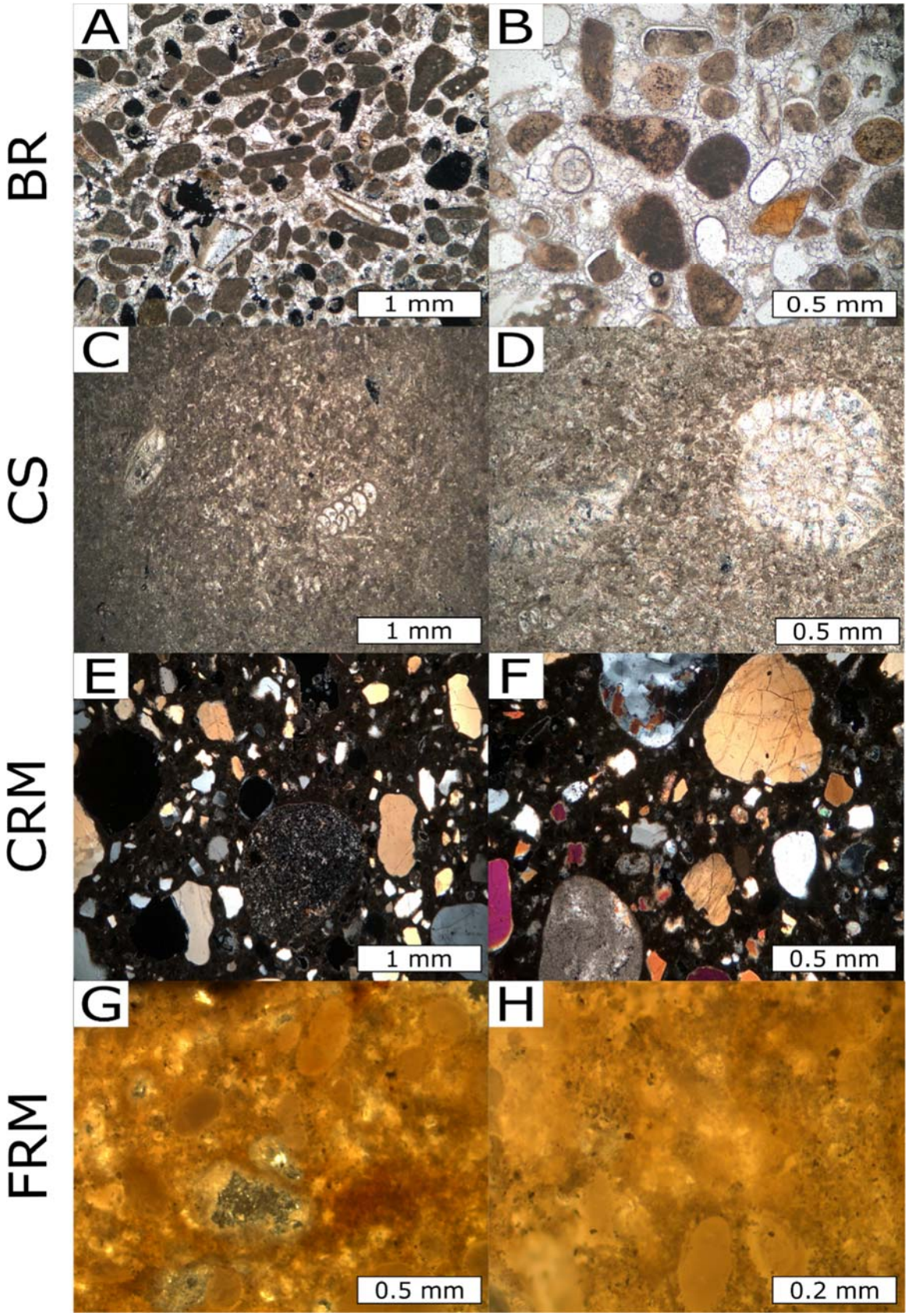
Fig. 3.1.15. (A-F) Various scenarios for SLR influence on Anfushi's Necropolis.

6.3. Construction materials characterization

6.3.1. Petrographic description

The thin section of the bedrock sample (BR, **Fig. 3.1.16 A** and **B**) shows a creamy oolitic limestone with recrystallized sparitic cement (early gravitational cement) and late geopetal micritic infills. Significant pores with rhombohedral calcite crystals exist due to their

formation in the absence of coccolithophorids. In addition, this kind of stone is made up of large intraclasts and sand-sized spheres (ooids/oosparite) of calcium carbonate. Fossil allochemical fragments of echinoderms, corals, red algae, bryozoans, gastropods, and foraminifera are present and distributed in the matrix with carbonate in peloid and pellet shapes. Rare subangular to rounded quartz grains are presented. Casing stone (CS, **Fig. 3.1.16 C** and **D**) is considered a creamy fossiliferous micritic limestone. Calcite embedded in micrite matrix rich in benthic foraminifera (*PseudochrtsalidinaConica*), nummulites, bivalves, molluscs, ostracods, sponge spicules, and other bioclasts. Rare subangular to angular quartz grains are also present. Coarse-grained rendering mortar after the stone casing layer (CRM, **Fig 3.1.16 E** and **F**), from morphological features, the main constituent of the mortar is quartz, which is poorly sorted, polycrystalline and angular to subangular. In addition, some quartz grains have undulatory extinction, and others are monocrystalline with normal extinction and a maximum diameter of 2 mm. Quartz grains are embedded in a micritic matrix with rock fragments, chert, plagioclase, and opaque minerals (iron oxides). **Fig. 3.1.16** (**G** and **H**) represent the fine-grained rendering mortar (FRM) before painting layer application. Subangular to rounded quartz grains are well-sorted, and the maximum grain size is 0.5 mm in diameter and embedded in a micritic matrix.



(Caption is in the next page)

Fig. 3.1.16. Photomicrographs of the geological and archaeological prepared thin sections. (A and B) Bedrock (BR) oolitic limestone with recrystallized sparitic calcite cement and sand-sized spheres (ooids/oosparite). (C and D) Casing stone (CS), creamy fossiliferous micritic limestone and calcite embedded in a micrite matrix rich in benthic foraminifera. (E and F) Coarse-grained rendering mortar (CRM) with quartz grains poorly sorted, polycrystalline, and angular to subangular, grains embedded in a micritic matrix with rock fragments. (G and H) Fine-grained rendering mortar (FRM) has well-sorted quartz grains, subangular to rounded, and these grains are embedded in a micritic matrix.

6.3.2. Mineralogical and chemical characterization

Semiquantitative mineralogical analysis using XRD (**Table 3.1.3**) revealed that the BR consists of calcite (very abundant), aragonite (abundant) and halite (rare) (degradation compound). CS is composed of calcite (very abundant), halite (abundant), and gypsum (rare), where halite and gypsum are considered degradation compounds. Regarding the mortar samples, CRM is composed of quartz (very abundant), calcite (abundant), and halite (rare), while FRM consists of calcite (very abundant) with minimum amounts of quartz, gypsum, and aragonite.

Elemental analysis by XRF and EDX was carried out to confirm the results of the mineralogical interpretation (**Table 3.1.4**). The results responded well to the XRD results. BR is mainly composed of calcium (93%) and chloride, silica, potassium, sulfates, and strontium as scarce elements. CS is mainly composed of calcium (83%), and sodium, chloride, sulfates, iron, magnesium, potassium, and strontium are detected as rare. CRM is mainly composed of silica (54%) and calcium (36%), with sulfates, chloride, aluminium, potassium, magnesium, and iron as scarce elements. Finally, FRM is composed of calcium (70%) and silica (18%), plus sulfates, chloride, iron, sodium, potassium and strontium. Chloride is detected in all samples as a degradation element. In addition, strontium is considered a significant trace element that is a signature of the coastal environment's impact on buildings because seawater contains approximately 8 mg/L strontium [**52**].

Moreover, halite and gypsum were detected in all samples with different ratios. For this, the content of halite and gypsum salts was calculated by dividing the total molecular weight of each salt on the molecular weight of the Cl and SO_3 on for all samples. In BR sample, the content of halite is 3.5% and gypsum is 0.6%. In CS sample, halite content is 5% and gypsum is 3%. In CRM sample, halite is 1.8% and gypsum 2.3%. Finally, in FRM sample, halite is 3.5 and gypsum is 2.3%. In this sense, it is clear that the two main decay salts are halite and gypsum and they detected with high content in CS and FRM samples. In FRM, gypsum could be an additive component to the preparation layer of paintings.

Table 3.1.3. Mineralogical analysis of Anfushi's Necropolis samples. BR: bedrock; CS casting stone; CRM: coarse-grained rendering mortar; FRM: fine-grained rendering mortar; Cal: calcite; Qz: quartz; Gp: gypsum; Ar: aragonite and Hal: halite (+++ Very Abundant; ++ Abundant; + Rare).

	Cal	Qz	Gp	Ar	Hal
BR	+++	-	-	++	+
CS	+++	-	+	+	++
CRM	++	+++	-	-	+
FRM	+++	+	+	+	+

6.3.3. Macroscopic and microscopic investigation

Binocular microscopy was used to examine the textural and morphological features, detecting the alterations and weathering aspects on the surfaces due to the marine environment impact. **Fig. 3.1.17** (**A**) represents the BR sample, where salt attack (efflorescence) is well observed on the surface and disintegration of the stone surface is seen. **Fig. 3.1.17** (**B**) shows the morphological texture of the CS, and salt erosion is considered the main feature of decay for the stone surface. Furthermore, **Fig. 3.1.17** (**C**) represents the coarse-grained rendering mortar, where quartz grains are clealry seen with

different sizes in the lime matrix. Disintegrated quartz grains and some gaps are detected. **Fig. 3.1.17** (**D**) shows a homogenous surface of the fine-grained rendering mortar and yellowish colour due to the high amount of lime with a minor amount of gypsum. In addition, there are a few quartz grains in the matrix. From textural observations, salt exists covering most of the mortar surface.

Table 3.1.4. Elemental analysis of major and minor elements, expressed in oxides (*wt.* %), for the Anfushi's Necropolis samples. BR: bedrock; CS casting stone; CRM: coarse-grained rendering mortar; FRM: fine-grained rendering mortar.

	CaO	SiO_2	Cl	Fe_2O_3	MgO	Na_2O	K_2O	Al_2O_3	SO_3	Sr
BR	93	1	2	-	-	-	1	-	1	2
CS	83	-	3	1	1	4	1	-	5	1
CRM	36	54	1	2	1	-	1	1	4	-
FRM	70	18	2	1	-	3	1	-	4	1

On the other hand, microscopically, the building materials were examined under a scanning electron microscope (SEM) with high resolution to evaluate the impact of marine dynamics on the building materials and their alterations/byproducts. For BR, **Fig. 3.1.18** (**A**) shows the morphological texture of the BR with a wide-large angle view for the bedrock sample. Euhedral to anhedral halite crystals with changeable habits and different growth phases are present due to the inhomogeneous absorption of the aqueous solution (**Fig. 3.1.18-B**). The initial state of gypsum nucleation formed in needle-like crystals along with halite crystals and gaps are observed as well (**Fig. 3.1.18-B**). **Fig. 3.1.18** (**C** and **D**) represents the morphological features and decay of the casing stone, where **Fig. 3.1.18** (**C**) shows the surface filled with pores and gaps, and **Fig. 18** (**D**) shows the distribution of the mesostructured halite, which is integrated with the stone surface. Microfissures and pores are present on the surface. **Fig. 3.1.18** (**E-H**) displays the decayed surface of the coarse-grained rendering mortar. In **Fig. 3.1.18** (**E** and **D**), the textural features exhibit the disintegration of the mortar, with many gaps and pores and the precipitation of the salt enveloping the quartz grains and filling the pores intensively. Furthermore, in **Fig. 3.1.18**

(**G**), quartz grains are distributed with different sizes in the white lime matrix. **Fig. 3.1.18** (**H**) shows the textural features of the mortar mixed with the precipitation of halite crystals (cubic and amorphous phases) and gypsum (needle habit). Finally, for FRM, **Fig. 3.1.18** (**I**) shows the lime-gypsum matrix with many pores and pitting in between. In **Fig. 3.1.18** (**J**), the precipitation of halite crystals is observed, and the needle habit of gypsum is present as an additive to the rendering mortar before the painting layer. Finally, EDS detector was utilized to detect and carry out elemental analysis for the salts on the surface for one of the selected samples of bedrock (BR) (**Fig. 3.1.19 A-C**).

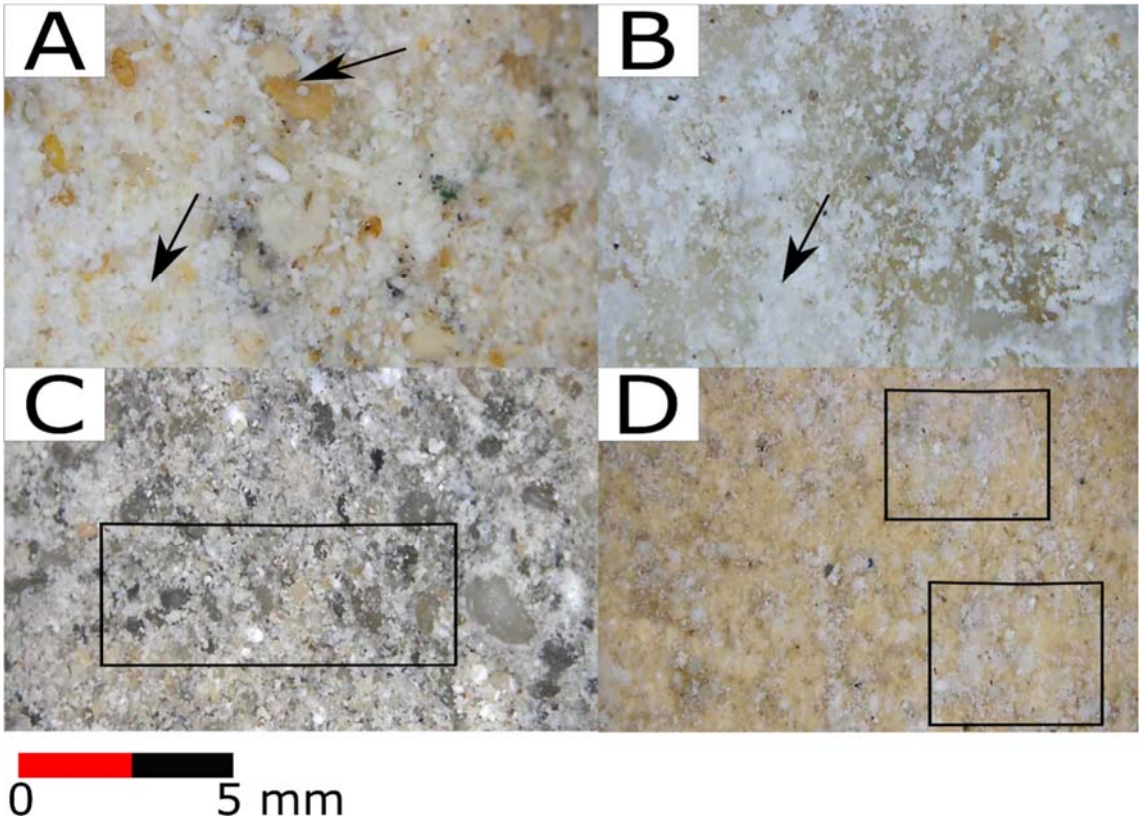
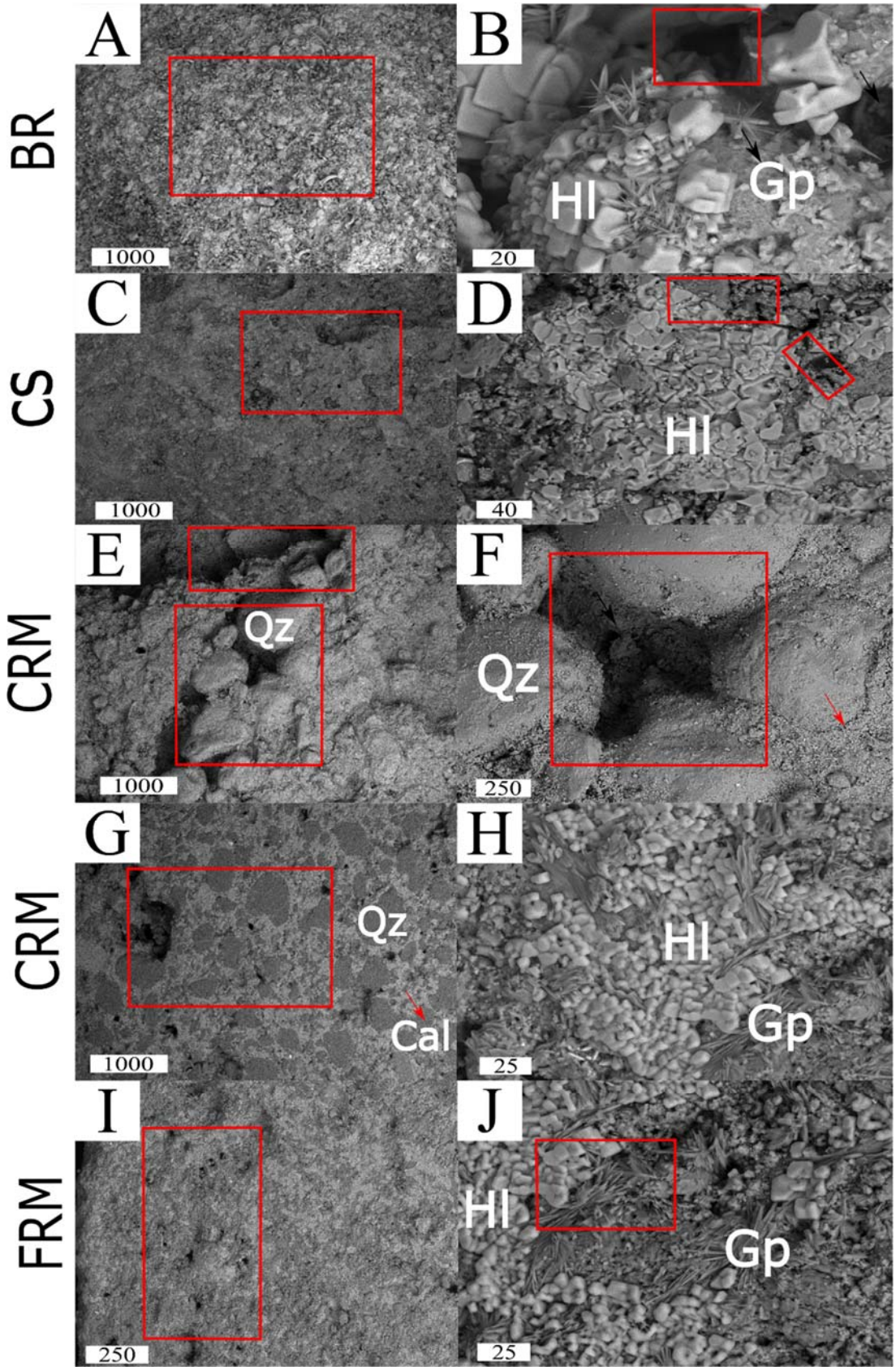


Fig. 3.1.17. (A-D) Photomicrographs under a binocular microscope for the bedrock (BR), casting stone (CS), coarse-grained rendering mortar (CRM) and fine-grained rendering mortar (FRM). Black arrows and rectangles show the ooids, quartz grains, disintegration and salt crusts on different samples. Apparently, salt erosion is the main feature of deterioration for all samples.



(Caption is in the next page)

Fig. 3.1.18. Micromorphological features of the construction building materials of Anfushi's Necropolis. (A and B) The oolitic limestone (BR, bedrock) surface texture with halite cubic crystals and needle-like gypsum. (C and D) The fossiliferous micritic limestone (CS, casing stone) morphological texture with halite crystal perceptions, pores and microfissures. (E - H) The coarse-grained rendering mortar (CRM) textural features with disintegrated grains, precipitation of halite (cubes), gypsum (needles), and detection of gaps and pitting. (I and J) Fine-grained rendering mortar (FRM) textural aspects with depositing halite mixed with needle-like crystals of gypsum, in addition to gaps and pitting. Red squares and rectangles refer to the disintegration feature of the samples due to salt weathering impact. Scales are expressed in microns.BR: bedrock; CS casting stone; CRM: coarse-grained rendering mortar; FRM: fine-grained rendering mortar; Hl: halite; Cal: calcite; Qz: quartz; Gp: gypsum.

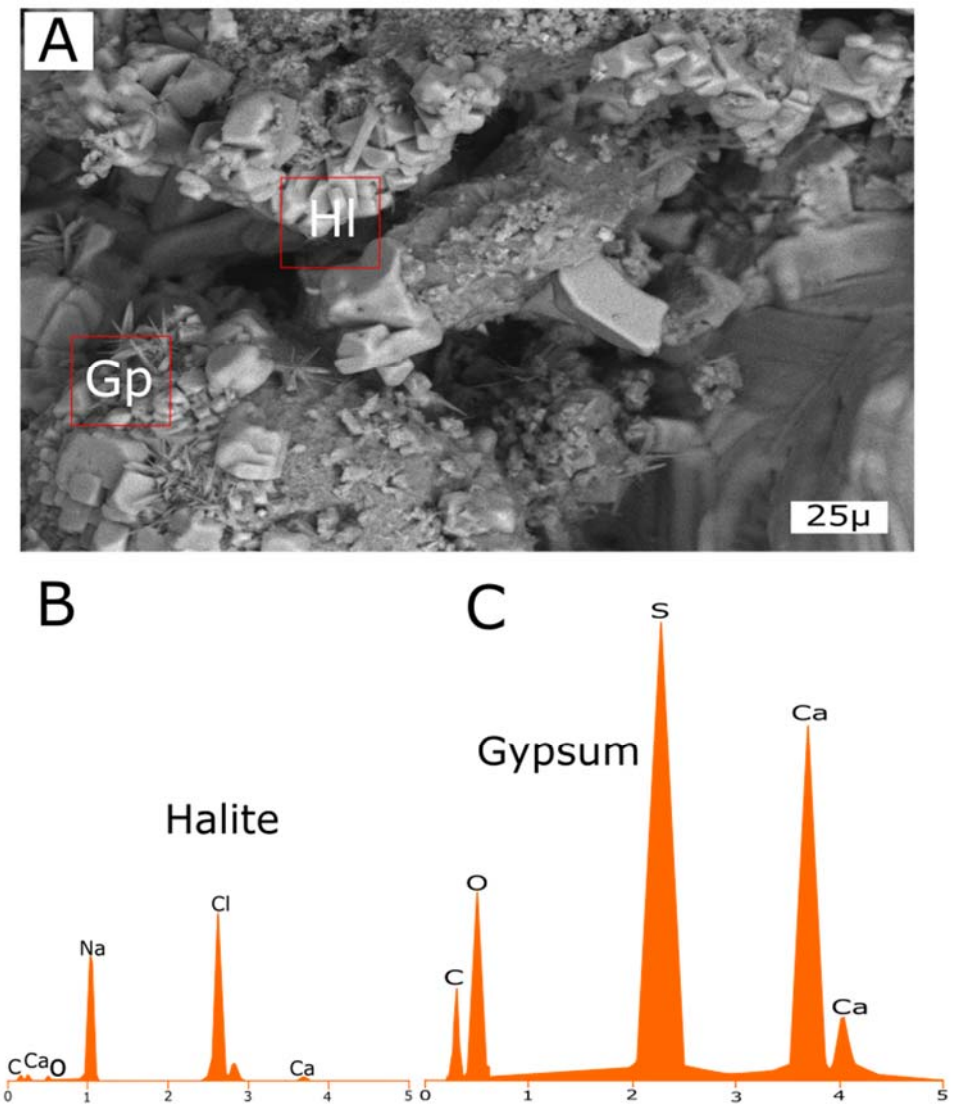


Fig. 3.1.19. (A) Micromorphological feature of (BR, bedrock) with halite cubic crystals and needle-like gypsum and the red squares were analyzed elementally using EDS . (B and C) EDS, elemental anylsis results for halite and gypusm salts for one of selected samples from bedrock of the necropolis.

6.4. Digital mapping

The heritage digitalization approach is considered a reproduction of physical interactions and interventions. Remote recontextualization and interactive models for heritage are

necessary since the world of conservation and restoration should follow up all advanced technologies to help protect world heritage. Indeed, the virtual recording and mapping of the monuments will decrease the physical interventions to the monuments and increase their authenticity and values [**78**]. In addition, using computer-mapping methods can reduce the mistakes of intervention by restorers, which will help save money for the budgets of restoration projects [**79**]. In this regard, a mapping the architectural and structural elements were carried out to preserve the archaeological site of Anfushi's Necropolis using AutoCad 2020. The process is important for virtual archiving to protect our heritage for the next generation, and some maps were carried out for the virtual retouching with original tones of colors for the paintings of the significant motives of Anfushi's Necropolis and this will help the future work of restoration. Geometrical surveys, documentation, data processing, interpretation, the creation of 2D models/maps, editing, and rendering were taken into consideration in the work during the digital restoration, as shown in **Fig. 3.1.20** (**A-D**). Find more drawings and sketches for reconstruction and retouching in the supplementary materials (**SM1. Fig. 6**)

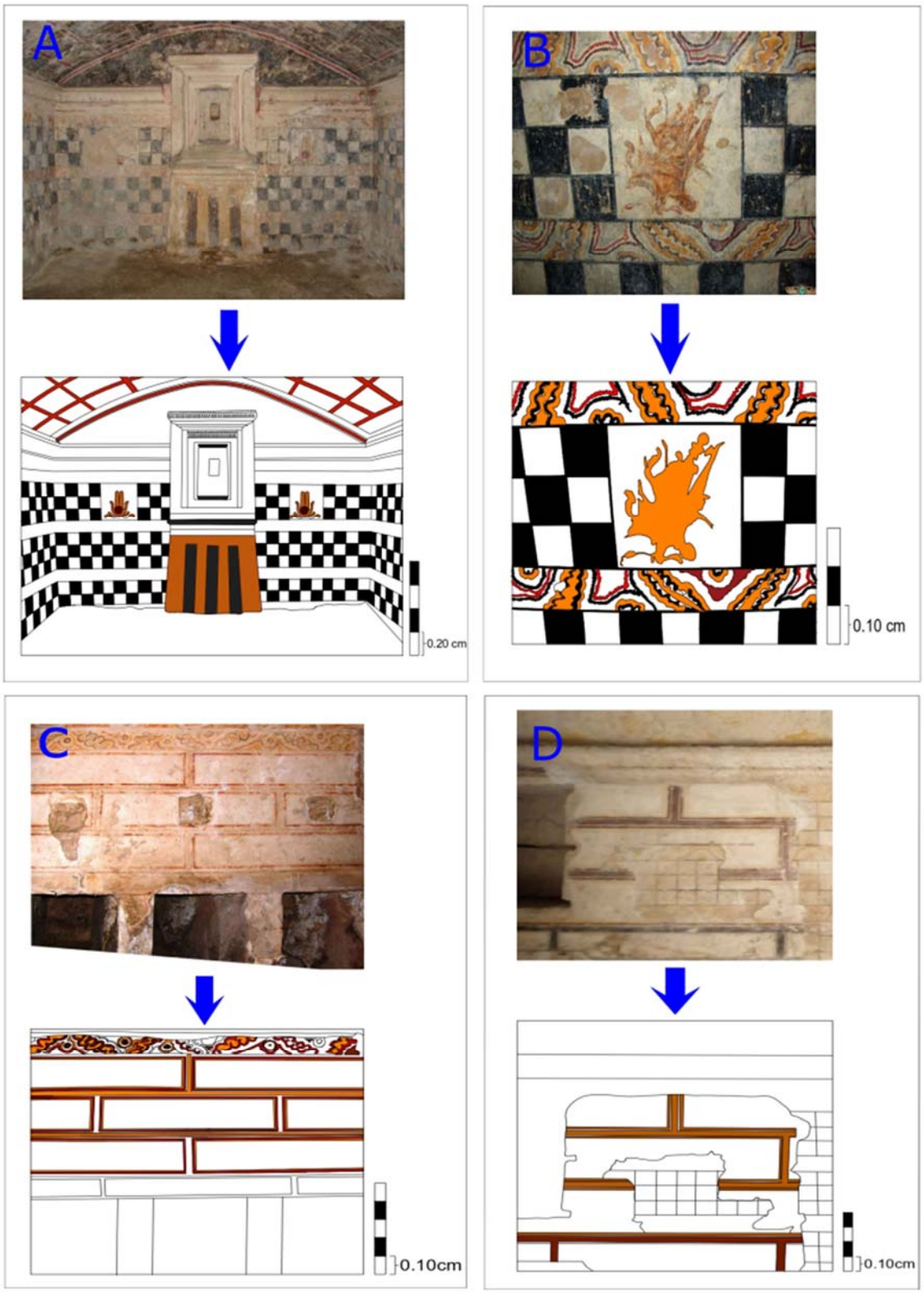


Fig. 3.1.20. (A-D) Digital restoration for some selected structural and architectural elements in Anfushi's Necropolis (Walls of Tomb No 2, rooms 1 and 2) using AutoCAD 2020.

7. Discussion

Anfushi's Necropolis is considered a rock cut in oolitic limestone as bedrock and is placed near the shore. Different aspects of marine dynamics have affected Anfushi's Necropolis, such as SLR, coastal and flash flooding, storminess, earthquakes, and various climate factors (temperature variations, rainfall, humidity, and wind), in addition to all anthropogenic factors that can affect historical buildings. The consequences of the marine dynamics led to the resilience/durability weakness of the Necropolis construction elements.

Historical pieces of evidence confirmed the sudden increasing rate of SLR. In this sense, the research depended on some historical satellite images that managed us to monitor the SLR rate through submergence phenomena. **Fig. 3.1.21** (**A** and **B**) shows two historical satellite images (2012 and 2013) that display the submergence of an ancient structure (old breakwater) in the eastern harbor (Island of Pharos). **Fig. 3.1. 21** (**C**) displays an old photo of the same area before submergence in 1916. **Fig. 3.1.21** (**D**) shows a recent Google Earth image (2022) with anthropogenic intervention by artificial nourishment using sands. Accordingly, Stanley et al. [**80**] confirmed that many ancient port structures and old coastal structures were submerged due to SLR. For these reasons, this research presented different SLR scenarios (**Fig. 3.1.15**) on Anfushi's Necropolis through satellite image observations from climatic central analysis (CCA), and the results assured that a rise of more than 1 m would submerge Anfushi's Necropolis completely. In this regard, Bekheet et al. [**28**] put the Anfushi area in the risk zone of the 1.5 m SLR scenario, and Shaltout et al. [**81**] confirmed that Alexandria was subjected to an observable SLR of 0.5 cm yearly before building a High Dam and after building it has become subject to 0.2 cm SLR yearly. Moreover, the World Bank [**82**] informed in their report about climate change that the SLR will reach +0.20 m by 2030, and regardless of the scenario of SLR, the SLR will increase during the next decades and a century more than the observed rates currently. This yearly increase in SLR has had a negative impact on the durability of Anfushi's Necropolis. For this, water reached to 30 cm on the ground of the necropolis because of water infiltration inside the tombs and caused salt weathering and deformations for the most of the walls and their valuable paintings.

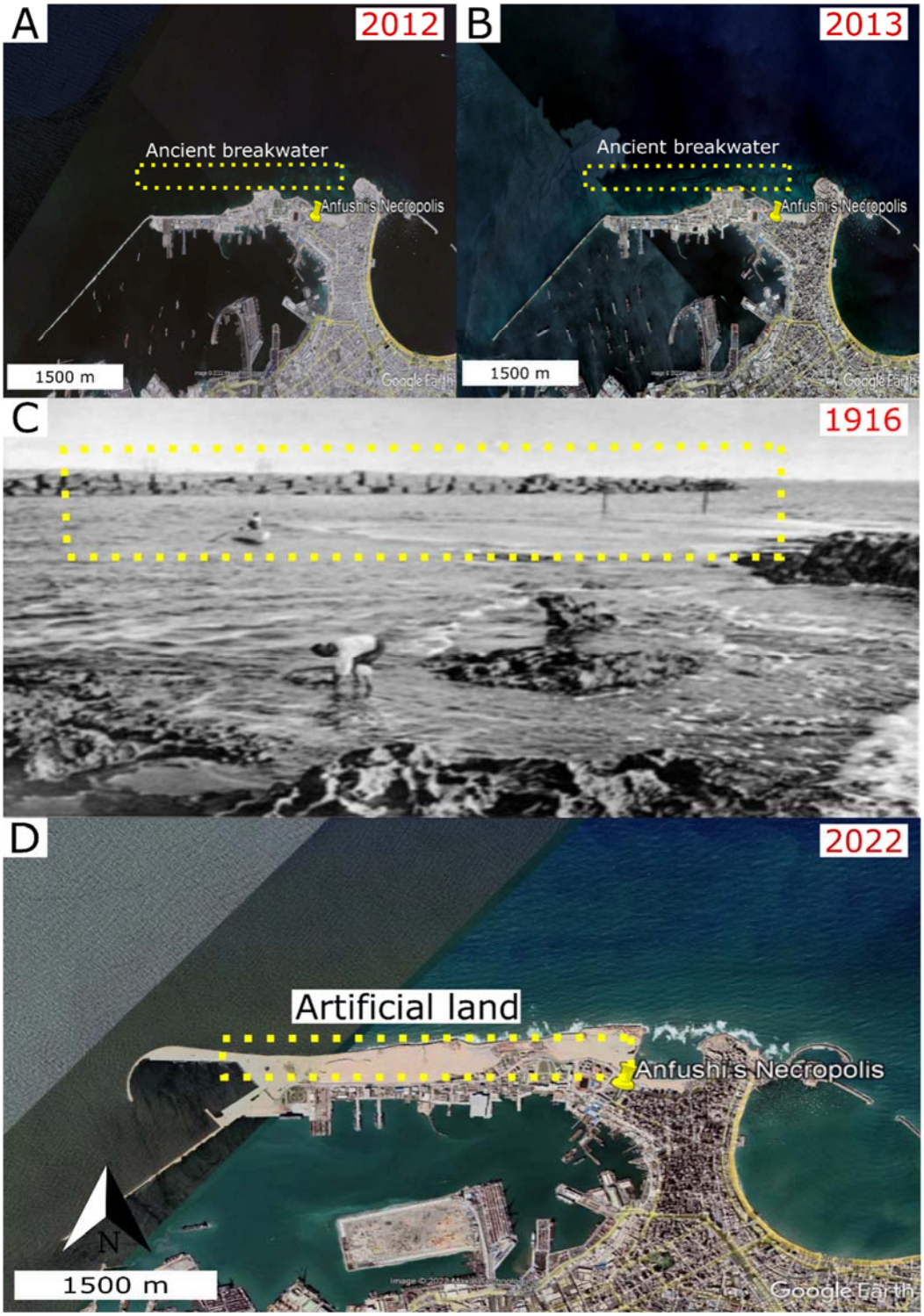


Fig. 3.1.21. (A and B) show two satellite images (2012 and 2013) confirming the submergence of the ancient structures. (C) Old photo (1916) of the same area before the submergence of the ancient structures, from [**83**], and a recent Google Earth image (D) for the same area with nourishment interventions.

Structural deficiencies were photographed and recorded due to the historical earthquakes' effect on Anfushi's Necropolis. These structural deformations are chipping off the blocks, collapsing, and horizontal displacements. Kázmér [**84**] explained these earthquake-induced damages to ancient structures as well. In addition, the geotechnical problems and the unconsolidated limestone of the bedrock of the tombs accelerated the impact of earthquakes in damaging the necropolis because the low-quality bedrock could amplify the ground motions during the earthquakes, which made the structure of the tomb more vulnerable to earthquake damage. In this sense, Hemeda et al. [**33**] observed that the tombs of the necropolis of Mustafa Kamil in Alexandria are not structurally safe for PGA (peak ground acceleration) values greater than 0.07-0.08 g. Furthermore, Mohamed et al. [**43**] confirmed that 25 strong earthquakes hit Alexandria from 320 to 2000 AD. These earthquakes definitely affected the structural states of the buildings, and the response at some sites was strong and damaging due to the site effect and unconsolidated deposits (soil problems/geotechnical problems). In this sense, Hamouda et al. [**64**] established that the ancient royal port of Alexandria approximately 1 km from Anfushi's Necropolis was influenced by land subsidence due to SLR, earthquakes, tsunamis, and sediment mass failure, where all these environmental actions caused land subsidence in Alexandria from the Ptolemaic era until now.

Alexandria is vulnerable to both flooding by rains and SLR, especially in the last two years in the winter season, due to the high dynamics of the coastal environment of Alexandria and rapid climate change. Alexandria is subjected to approximately 16 storms yearly during the winter season accompanied by strong winds, high waves, and heavy rains [**65, 67**]. Accordingly, the in-situ observation confirmed the gathering of water in the chambers due to flash flooding and storminess with high waves of the sea (**Fig. 3.1.12 - E**). The water inside Anfushi's Necropolis reached 30 cm over the ground, causing dampness for the architectural and structural elements through capillary actions. For this, the main observed deterioration aspects are salt erosion, spalling, layering, disintegration, and structural deformations.

The chemical analysis showed that halite is the main alteration compound and appeared in all compositional and elemental analyses. Halite is a soluble salt that comes to buildings

mainly from sea spray precipitation. Additionally, it could come from gathered water from flooding in the ground, saline rainwater, or even condensed atmospheric humidity. Efflorescence and subflorescence are considered the main decay patterns of salt erosion in most architectural and structural elements. Examination using a scanning electron microscope for the building materials (stones and mortars) showed the interaction between the stones and mortar surfaces with halite crystals, which nucleated heterogeneously and severely eroded the surfaces in their crystalline form or in the brine inside the pores or on the surface. The crystallization and recrystallization process of the halite salt led to the bleeding of the stone with many pores and pitting (disintegration)as shown in the microscopic results. In this regard, Benavente et al. [**85**] reported that salt crystallization in porous stones mainly occurs on the surface of the porous stone (efflorescence) and within the porous media of stone (subflorescence) and they confirmed that the halite salt source is mainly attached to sea spray. In addition, halite crystallization could be existed as result of humidity fluctuations under and above 75% RH. In this sense, Sato and Hattanji [**86**] said that halite is deliquescence salt and has affinity to absorb the moisture from the surrounding environment causing severe salt weathering for the stones. Finally, the calculations of halite content from elemental chemical analysis revealed that the casing stone (CS) contains highest content from all the samples with 5% but in the bedrock (BR) and fine rendering layer with 3.5%. For this, it is clear to find the degradation features such as spalling, flaking and powdering in many parts of the necropolis as a result of salt weathering along with climatic factors.

Gypsum is detected in the fine-grained rendering mortar as an additive to the mortar constituents with lime and quartz. In addition, gypsum is present in the casing stones behind the rendering layers with 3% as decay salt from the elemental chemical analysis result. In this case, gypsum could be delivered to the stone by immigration from the rendering mortar, causing salt attack on the stone [**25**]. The examination by SEM confirmed the existence of needle-like gypsum salt along with the crystals of halite. Charola et al. [**87**] mentioned that gypsum has low solubility and is less aggressive, but damage due to gypsum occurs in the case of dehydration–hydration reactions causing internal forces and cracks. In addition, strontium is detected in most of the samples as a significant trace element that is

a signature of the marine environment's impact on buildings because seawater contains approximately 8 mg/L strontium [**52**].

Furthermore, the content ratio of the existing salts is considered reasonable values for salt weathering for the stone surfaces and the paintings, especially with halite that it has been estimated as 5% in the casing stone sample. Comparing with previous study of [**86**], they confirmed the erosive role of 0.5, 5.3 and 7.7 of halite content (gram weights of salt in a 100 g salt-free rock specimen) in stone degradation.

The dynamics of climate, such as variations in temperatures, wind, humidity and rainfall, have affected the building materials of Anfushi's Necropolis. Fluctuations in temperature degrees daily and seasonally led to expansions and shrinkages in the building materials [**88**]. This thermal differentiation could lead to the cracking of surfaces and rendering layers' separations due to the various thermal coefficients between the minerals (calcite, quartz, gypsum, and halite) in the construction materials and their alterations. Mart et al. [**89**] explained the destructive impact of the mismatched thermal expansion values between salt (halite) and stone (calcite), where halite thermal stress is 35 GPa and could cause tensile strength of the stone with daily and seasonal changes in temperature degrees. When the stone hosts a high amount of halite, the higher thermal stresses will lead to cracks and flaking decay patterns, as observed in this necropolis. In addition, the changes of temperatures could cause a severe damage because of phase change for the salts and microclimate. In this context, Grossi et al. [**90**] said that halite salt can crystallize at a fixed humidity regardless the temperature and gypsum can be susceptible for crystallization to the changes between humidity and temperature. Moreover, wind power is considered one of the movers of the necropolis building materials decay, especially the wind speed in Alexandria, which reaches 44 km/h (strong), and wind power is considered 70% of the total dynamic in both sea level and current [**75**]. The wind is considered a way to transfer halite salt (marine spray) from the sea to construction materials. In addition, the wind is responsible for the formation of alveolar weathering (honeycomb) in the stones because of washing away the filled hollows with salts by the wind [**91**]. As an exceptional and recent case, very low temperatures could be considered a new and future environmental phenomenon in Alexandria. Last year Alexandria practiced rare snowfalls that could affect

the construction materials of Anfushi's Necropolis (**Fig. 3.1.10**). Snow can deteriorate the construction materials by soaking the water inside the pores of building materials, followed by cooling, which causes delamination and spalling as decay patterns. Moreover, probable subsequent and repeated freezing events in the following years could deteriorate the material if the water content from rainfall or a high-humidity environment is higher than the critical degree of saturation for the material at the time of freezing [**92**].

Anthropogenic actions are considered one of the damage factors to the structures of Anfushi's Necropolis due to ancient mining, quarrying, and other infrastructure activities around the necropolis in 1899 [**76**]. Recently, neglecting the archaeological site without any intervention for preservation has also been regarded as an anthropogenic factor. From field observations, trees and shrubs around the tombs of the necropolis affected the tombs mechanically and biologically, especially the trees, which can cause mechanical damage to the structures by the roots during growth. In this sense, Loperte et al. [**93**] mentioned that the roots of trees could cause direct and indirect damage to the structures of the historic buildings in case of direct contact between tree roots and the building or through the shrinkable soil indirectly, as is happening in this site.

From all of the above and field observations, the various marine dynamics factors (Coastal surrounding environment and salt decay) resulted in much structural and architectural decay for Anfushi's Necropolis, such as displacement of the wall, cracking, collapsing, block chipping, salt erosion (fluorescence and subflorescence), flacking, spalling, loss of material, alveolar, layering, disintegration, pitting, and loss of the paining layer.

Finally, this study presented a digital reconstruction and restoration of the architectural and structural elements of Anfushi's Necropolis through engineering drawing. In this regard, this part of digitalization is considered a significant contribution to safeguarding this important necropolis for the next generation as part of world heritage, especially with the new world of digitalization. We believe this virtual restoration and reconstruction is essential to work for any upcoming restoration project for this site. In addition, these maps and models will participate to achieve low-cost restoration projects with minimum physical interventions. Urgently, this archaeological site of Anfushi's Necropolis is needed for a project for restoration, conservation, and site management.

8. Conclusions

The research presented the durability problems of construction materials of Anfushi's Necropolis and the impact of environmental dynamics in Alexandria on the necropolis tombs. The tombs were excavated in the oolitic limestone ridge and covered by fossiliferous limestone. This necropolis was painted on two different preparation mortars. The first preparation mortar is coarse-grained, and the second preparation layer is fine-grained. These construction materials have been subjected to different factors of damage and decay, such as SLR, coastal and flash flooding, storminess, earthquakes, and various climate factors (temperature variations, rainfall, humidity, and wind).

The main decay patterns are structural cracks, horizontal displacement for the walls, chippings for the blocks, and collapsing. In addition to flaking, spalling, salt erosion, loss of materials, delimitations, alveolarization, and discolouration of the painting layer due to marine dynamics (earthquakes, flooding, windstorms, sea spray and climatic conditions). Moreover, SLR is considered a future risk for the necropolis that will lead to full submergence for the necropolis at 1m SLR during the next decades. Halite, as an aggressive soluble salt, is considered the main decay factor for architectural elements and their surfaces. Efflorescence and subflorescence precipitation of halite and gypsum are observed on all surfaces of Anfushi's Necropolis and detected by analytical and microscope investigation in all samples. The water level inside Anfushi's Necropolis reached 30 cm over the ground because of flooding and heavy rains, causing dampness for the architectural and structural elements through capillary actions. For this, the main observed deterioration aspects are salt erosion, spalling, layering, disintegration, and structural deformations. The responsibility for the destruction and poor state of preservation of the necropolis, not only the marine dynamics and environmental conditions but also the anthropogenic interventions, played a role in the destruction of some structural elements along with the recent failure to give due care to this important heritage site. Finally, this paper participated in mapping and recording of some selected architectural and structural elements of the Anfushi's necropolis through vector sketches with retouching of original tones of colours for the paintings to help in the retouching and restoration works in the future.

Acknowledgements A. Fahmy acknowledges SCiCYT and UGEA-PHAM at Cadiz of University for carrying out the main part of the archaeometrical analysis. E. Molina Piernas acknowledges co-funding from the European Social Fund (D1113102E3) and Junta de Andalucía. We acknowledge Professor Philip Machev from the Faculty of Geology and Geography at Sofia University (Bulgaria) for carrying out scanning electron microscope images and preparing the thin sections. We acknowledge Francois Olivier for providing us some photographs for Anfushi's Necropolis in figure 3.1.1C, figure 3.1.2B, and figure 3.1.12 C and D.

9. References

[1] Sullivan S, Mackay R. *Archaeological Sites: Conservation and Management*. J. Paul Getty Trust. 2012. Available from: https://www.getty.edu/publications/resources/virtuallibrary/9781606061244.pdf

[2] Vousdoukas M I, Clarke J, Ranasinghe R, Reimann L, Khalaf N, Duong T M, Ouweneel B, Sabour S, Iles C E, Trisos C H, Feyen L, Mentaschi L, Simpson N P. *African heritage sites threatened as sea-level rise accelerates*. 2022, *12*(March). https://doi.org/10.1038/s41558-022-01280-1

[3] Cassar M, Pender R. The impact of climate change on cultural heritage: evidence and response. 14th Triennial Meeting. 2001, 12-16 September 2005 on CD-ROM;610–6. Available from: https://discovery.ucl.ac.uk/id/eprint/5059/

[4] Gehrels R, Garrett E. Rising sea levels as an indicator of global change. Clim Change. Elsevier B.V. 2021, 205–217 p. Available from: http://dx.doi.org/10.1016/B978-0-12-821575-3.00011-6

[5] Nicholls RJ. Adapting to Sea-Level Rise. Resilience. Elsevier Inc. 2018, 13–30 p. Available from: http://dx.doi.org/10.1016/B978-0-12-811891-7.00002-5

[6] Marzeion B, Levermann A. *Loss of cultural world heritage and currently inhabited places to sea-level rise*. Environ. Res. Lett.2014, 9, 034001 https://doi.org/10.1088/1748-9326/9/3/034001

[7] Li Y, Jia X, Liu Z, Zhao L, Sheng P. *The potential impact of rising sea levels on China's coastal cultural heritage: a GIS risk assessment*. 2022, 406–421. https://doi.org/10.15184/aqy.2022.1

[8] Lewis R. Sea-Level Rise and Subsidence Effects on Gulf Coast Archaeological Site Distributions. American Antiquity. 2000, 65(3), 525-541. https://doi.org/10.2307/2694534

[9] Daly C. Climate Change and the Conservation of Archaeological Sites: A Review of Impacts Theory Climate Change and the Conservation of Archaeological Sites: a review of Dublin Institute of Technology. 2011, 0–20. https://doi.org/10.1179/175355212X13315728646058

[10] Dawson T, Hambly J, Kelley A, Lees W, Miller S. *Coastal heritage, global climate change, public engagement, and citizen science*. 2020, *117*(15). https://doi.org/10.1073/pnas.1912246117

[11] Fluck H, Dawson M. The Historic Environment: Policy & Practice Climate Change and the Historic Environment. *The Historic Environment: Policy & Practice*. 2021, *12*(3–4), 263–270. https://doi.org/10.1080/17567505.2021.1990492

[12] Bickler S, Clough R, Macready S. *The impact of climate change on the archaeology of New Zealand's coastline A case study from the Whangarei District*. Publishing Team. Department of Conservation, New Zealand. 2013. Available from: https://www.doc.govt.nz/documents/science-and-technical/sfc322high_res.pdf

[13] Westley K, Mcneary R. Assessing the Impact of Coastal Erosion on Archaeological Sites: A Case Study from Northern Ireland Assessing the Impact of Coastal Erosion on Archaeological Sites: A Case Study from Northern Ireland. Conserv. Manag. Archaeol. Sites. 2015, 5033. https://doi.org/10.1179/1350503315Z.00000000082

[14] Anderson D G, Bissett T G, Yerka S J, Wells J J, Kansa C, Kansa S W, Myers K N, Demuth R C, White D A. *Sea-level rise and archaeological site destruction: An example from the southeastern United States using DINAA (Digital Index of North American Archaeology)*. 2017, 1–25. https://doi.org/10.1371/journal.pone.0188142

[15] Harkin D, Davies M, Hyslop E, Fluck H, Wiggins M, Merritt O. *Impacts of climate change on cultural heritage*. 2020, 616–641. https://doi.org/10.14465/2020.arc26.che

[16] Andreou G M. Monitoring the impact of coastal erosion on archaeological sites: The Cyprus Ancient Shoreline Project. Cambridge University Press. 2018, 92(361), e4. https://doi.org/10.15184/aqy.2018.1

[17] Andreou G, Blue L, Breen C, Safadi C, El Huigens H O, Nikolaus J, Ortiz-Vazquez R, Westley K. *Maritime endangered archaeology of the Middle East and North Africa: The MarEA project*. 2020, *94* (January), 1–7.

[18] Bolton J. An Assessment of the Vulnerability of Coastal Stone Monuments in Ireland. Doctoral thesis. 2009. Available from: https://arrow.tudublin.ie/builtdoc/9/

[19] Morillas H, França F, Filho D M, Derluyn H, Maguregui M, Grégoire D, Manuel J. Decay processes in buildings close to the sea induced by marine aerosol: Salt depositions inside

construction materials. Science of the Total Environment. 2020, 721. https://doi.org/10.1016/j.scitotenv.2020.137687

[20] Morillas H, Mendonça Filho FF, Hannelore D, Maguregui M, David G. Decay processes in buildings close to the sea induced by marine aerosol: Salt depositions inside construction materials. Science of the Total Environment, Elsevier. 2020, 721, pp.137687. ⟨10.1016/j.scitotenv.2020.137687⟩. ⟨hal-02502454⟩

[21] Chameides W L, Stelson A W, Chameides AW. Aqueous-phase chemical processes in deliquescent sea salt aerosols: a mechanism that couples the atmospheric cycles of S and sea salts J. Geophys. Res.-Atmos. 1992, 97. https://doi.org/10.1029/92JD01923

[22] Hossain K M A, Easa S M, Lachemi M. Evaluation of the effect of marine salts on urban built infrastructure. *Building and Environment*.2009, *44*(4), 713–722. https://doi.org/10.1016/j.buildenv.2008.06.004

[23] Silva A, Neves L C, Gaspar P L, Brito J.*Probabilistic transition of condition: render facades Probabilistic transition of condition : render facades*.2016, *3218*. https://doi.org/10.1080/09613218.2015.1023645

[24] Cardell C, Delalieux F, Roumpopoulos K, Moropoulou A, Auger F, Van Grieken R. Salt-induced decay in calcareous stone monuments and buildings in a marine environment in SW France. *Construction and Building Materials*, 2003, *17*(3), 165–179. https://doi.org/10.1016/S0950-0618(02)00104-6

[25] Fahmy A, Molina-Piernas E, Martínez-López J, Domínguez-Bella S. Salt weathering impact on Nero/Ramses II Temple at El -Ashmonein archaeological site (Hermopolis Magna), Egypt. August 2022. https://doi.org/10.1186/s40494-022-00759-6

[26] El-Raey M. Vulnerability assessment of the coastal zone of the Nile delta of Egypt, to the impacts of sea level rise. 1998, 37(1), 29–40. https://doi.org/10.1016/S0964-5691(97)00056-2

[27] Elsharkawy H, Rashed H, Rached I. *Climate Change: The Impacts of Sea Level Rise on Egypt*. 2009, 1–11. Available from: https://www.isocarp.net/data/case_studies/1456.pdf Accessed 03 May 2022.

[28] Bekheet R A, Raey M, Yassin A. The crest line approach for assessing the development of coastal flooding due to sea level rise. *Mitigation and Adaptation Strategies for Global Change*. *October* 2017. https://doi.org/10.1007/s11027-016-9717-9

[29] El-Raey M, Regional Center for Disaster Risk Reduction (RCDRR). Impact of sea level rise on the Arab Region. UNDP Regional Bureau for the Arab States (UNDP-RBAS), Cairo, Egypt. 2010. Available from: https://research.fit.edu/media/site-specific/researchfitedu/coast-climate-adaptation-library/africa/morocco-algeria-tunisia/El-Raey.-2010.-SLR-Impacts-on-Arab-Region.pdf Accessed 05 May 2022.

[30] Belov A. *Navigational aspects of calling to the Great Harbour of Alexandria*. 2014. Available from: https://halshs.archives-ouvertes.fr/halshs00845524/file/Belov.A._forthcoming_Navigational_aspects_of_calling_to_the_Great_Harbour_of_Alexandria.pdf

[31] Ivanov S V. Russian underwater archaeological mission to Alexandria. General report (2003–2015). January 2019. https://doi.org/10.24411/2686-9276-2019-00005

[32] Abdelnaby A E, Elnashai A S. Integrity assessment of the Pharos of Alexandria during the AD 1303 earthquake Integrity assessment of the Pharos of Alexandria during the AD 1303 earthquake. *Engineering Failure Analysis*. 2013, *33*(October 2017), 119–138. https://doi.org/10.1016/j.engfailanal.2013.04.013

[33] Hemeda S, Pitilakis K, Bandis S. Geotechnical, geophysical investigations and seismic response analysis of the underground tombs in Mustafa Kamil Necropolis, Alexandria, Egypt. 2015, 15(1), 191–207.

[34] Hemeda S. Geotechnical modelling of the climate change impact on world heritage properties in Alexandria, Egypt. *Heritage Science*, 2021, 1–33. https://doi.org/10.1186/s40494-021-00547-8

[35] Kamal I, Fekri M, Abou I. *Mapping the impacts of projected sea-level rise on Cultural heritage sites in Egypt: Case study (Alexandria)*. 2021, *5*, 1–20. Available from: https://mfth.journals.ekb.eg/article_190350_9dbe1272982c21ec55d603fe0787213f.pdf

[36] Sousa R, Céu Fialho M, Haggag M., Rodrigues N. Alexandrea ad Aegyptvm the legacy of multiculturalism in antiquity. 2013. Available from: https://ler.letras.up.pt/uploads/ficheiros/16940.pdf Accessed 09 May 2022.

[37] Kyriakos S. Alexandrea in Aegyptvm. The Role of the Egyptian Tradition in the Hellenistic and Roman Periods: Ideology, Culture, Identity, and Public Lif. Doctoral thesis, Faculty of Archaeology, Universiteit Leiden. 2011. Available from: https://scholarlypublications.universiteitleiden.nl/handle/1887/16395 Accessed 10 May 2022.

[38] Kyriakos S. The Polyvalent Nature of the Alexandrian Elite Hypogea: a case study in the Greco-Egyptian Cultural Interaction in the Hellenistic and Roman Periods. Porto. 2013. Available from: https://digitalis-dsp.uc.pt/handle/10316.2/36162 Accessed 09 May 2022.

[39] Hosny A, Ali S M, Abed A. Study of the 26 December 2011 Aswan earthquake, Aswan area, South of Egypt. *Arabian Journal of Geosciences*. 2014, *7*(11), 4553–4562. https://doi.org/10.1007/s12517-013-1098-8

[40] El-Sharkawi M, Hamimi Z, El-Barkooky A, Martínez Frías J, Fritz H, Abd El-Rahman Y. The Geology of Egypt. Regional Geology Reviews. Springer, Cham. 2020. https://doi.org/10.1007/978-3-030-15265-9_1

[41] Ibrahim M I A, Mansour A M S. Biostratigraphy and palaeoecological interpretation of the Miocene–Pleistocene sequence at El-Dabaa, north-western Egypt. *Journal of Micropalaeontology*. 2002. *21*(1), 51–65. https://doi.org/10.1144/jm.21.1.51

[42] Stanley J D, Jorstad T F, Goddio F. Human impact on sediment mass movement and submergence of ancient sites in the two harbours of Alexandria, Egypt. *Norsk Geologisk Tidsskrift*. 2006, *86*(3), 337–350.

[43] Mohamed A A, Helal A M A, Mohamed A M E, Shokry M M F, Ezzelarab M. Effects of surface geology on the ground-motion at New Borg El-Arab City, Alexandria, Northern Egypt. *NRIAG Journal of Astronomy and Geophysics*. 2016, *5*(1), 55–64. https://doi.org/10.1016/j.nrjag.2015.11.005

[44] Torab M M. Paleo-geomorphological map of Alexandria site, Egypt by using submerged archaeological and other evidence. *International Conference on Agriculture, Science and Engineering*.2013. Available from: http://www.damanhour.edu.eg/pdf/artsfac/PALEO-GEOMORPHOLOGICAL%20MAP%20OF%20ALEXANDRIA%20SITE,%20EGYPT%20BY%20USING%20SUBMERGED%20ARCHAEOLOGICAL%20AND%20OTHER%20EVIDENCE2.pdf

[45] Evelpidou N, Repapis C, Zerefos C, Tzalas H, Synolakis C. Geophysical Phenomena and the Alexandrian Littoral. Archaeopress, 2019. https://doi.org/10.2307/j.ctvndv8sc.

[46] Arthur D G. The four harbours of Alexandria. The journal of the institution of civil engineers. 1940, 1. Available from: https://www.ancientportsantiques.com/wp-content/uploads/Documents/PLACES/Egypt-Libya/Alexandria/Alexandria-Tyr-Savile1940.pdfAccessed 10 May 2022.

[47] Fahmy A, Molina-Piernas E, Domínguez-Bella S, Martínez-López J, Helmi F. Geoenvironmental investigation of Sahure's pyramid, Abusir archaeological site, Giza, Egypt. *Heritage Science*.2022, 1–20. https://doi.org/10.1186/s40494-022-00699-1

[48] Hemeda S, Fahmy A, Sonbol A. Geo-Environmental and Structural Problems of the First Successful True Pyramid, (Snefru Northern Pyramid) in Dahshur, Egypt. *Geotechnical and Geological Engineering*.2019, *37*(4), 2463–2484. https://doi.org/10.1007/s10706-018-00769-x

[49] Hemeda S, Fahmy A, Moustafa A, Abd Hafez M E. The Early Basilica Church, El-Ashmonein Archaeological Site, Minia, Egypt: Geo-Environmental Analysis and Engineering Characterization of the Building Materials. 2019, 157–186. https://doi.org/10.4236/ojg.2019.93011

[50] Harrell J A, Storemyr P. *Ancient Egyptian quarries – an illustrated overview*. In Abu-Jaber N, Bloxam EG, Degryse P, Heldal T. Quarry Scapes: ancient stone quarry landscapes in the Eastern Mediterranean, Geological Survey of Norway Special Publication. 2009, 12, pp. 7–50. Available from: https://www.ngu.no/upload/Publikasjoner/Special%20publication/SP12_s7-50.pdf

[51] Akarish A, Dessandier D. Characterization and Source of Sedimentary Rocks of the Alexandria Lighthouse Archaeological Objects, Egypt. *Journal of Applied Sciences. 2011, 11: 2513-2524.https://dx.doi.org/10.3923/jas.2011.2513.2524*

[52] Dessandier D, Akarish A, Antonelli F, Lazzarini L, Leroux A. *Atlas of the stones of Alexandria Light House (Egypt)*. Final report BRGM/RP-56218-FR. 2008. Available from: https://www.lrmh.fr/Default/doc/SYRACUSE/50575/atlas-of-the-stones-of-alexandria-lighthouse-egypt-final-report?_lg=fr-FR

[53] https://climate.nasa.gov/vital-signs/sea-level/ Accessed 13 May 2022.

[54] Dawod G, Resrach W, Mohamed H F, Haggag G G. *Mean Sea Level and Tides Variations at Alexandria, Egypt over 1906-2020*. 2022. https://doi.org/10.21608/JESAUN.2022.114295.1105

[55] Eldeberky Y. Coastal adaptation to sea level rise along the Nile delta, Egypt. 1996, 149, 41–52. https://doi.org/10.2495/CP11

[56] Fitzgerald D M, Fenster M S, Argow B A, Buynevich I V. *Coastal Impacts Due to Sea-Level Rise*. *2008*. https://doi.org/10.1146/annurev.earth.35.031306.140139

[57] Agrawala S, Moehner A, Raey M El, Conway D, Aalst M, Van Hagenstad M, Smith J. Development and climate change in Egypt: focus on coastal resources and the Nile. 2004, 1–68. http://www.oecd.org/env/cc/33330510.pdf

[58] Sawires R, Peláez J, Fat-Helbary R, Ibrahim H, García Hernández M. An Updated Seismic Source Model for Egypt. In (Ed.), Earthquake Engineering - From Engineering Seismology to Optimal Seismic Design of Engineering Structures. Intech Open. 2015. https://doi.org/10.5772/58971

[59] El-Sayed A, Korrat I, Hussein HM. *Pure and Applied Geophysics Seismicity and Seismic Hazard in Alexandria (Egypt) and its Surroundings*. 2004, 161, 1003–1019. https://doi.org/10.1007/s00024-003-2488-8

[60] Badawy A, Gaber H, Ibrahim H. *Earthquake risk assessment of Alexandria, Egypt*. 2015, 159–170. https://doi.org/10.1007/s10950-014-9456-x

[61] Fergany E, Omar K, Mohammed G A, Fergany E, Omar K, Mohammed G A. Evolution in seismic monitoring system and updating seismic zones of Egypt. *NRIAG Journal of Astronomy and Geophysics*.2020, *9*(1), 548–557. https://doi.org/10.1080/20909977.2020.1803661

[62] Darwish N, Kaiser M, Koch M. Assessing the Accuracy of ALOS/PALSAR-2 and Sentinel-1 Radar Images in Estimating the Land Subsidence of Coastal Areas: A Case Study in Alexandria City, Egypt.2021. https://doi.org/10.3390/rs13091838

[63] Wöppelmann G, Cozannet G Le, Michele M De, Raucoules D, Cazenave A, Garcin M, Hanson S, Marcos M. *Is land subsidence increasing the exposure to sea level rise in Alexandria, Egypt? 2013,40*, 2953–2957. https://doi.org/10.1002/grl.50568

[64] Hamouda A Z, El-gharabawy S M, Fekry A, Nassar M A, Salah M. Subsidence model of the ancient Alexandria Royal port linked to sea-level rise and natural hazards using integrated geophysical methods. *The Egyptian Journal of Aquatic Research*.2021, *47*(3), 283–292. https://doi.org/10.1016/j.ejar.2021.07.003

[65] Zaghloul E. A. Physical geology and historical settlement in North Western Nile delta Region, Egypt. 2016. Available from: https://www.researchgate.net/publication/305950323_PHYSICAL_geology_and_historical_settlement_in_North_Western_Nile_delta_Region_Egypt Accessed 11 August 2022.

[66] Frihy O E, Deabes E A, Gindy A A E. Wave Climate and Nearshore Processes on the Mediterranean Coast of Egypt. *Journal of Coastal Research*.2010, *26*(1), 103–112. http://www.jstor.org/stable/27752790

[67] https://earth.org/data_visualization/sea-level-rise-by-the-end-of-the-century-alexandria/ Accessed 16 August 2022.

[68] Zevenbergen C, Bhattacharya B, Wahaab R A, Elbarki W A I, Busker T, Rodriguez C N A S. In the aftermath of the October 2015 Alexandria Flood Challenges of an Arab city to deal with extreme rainfall storms. *Natural Hazards*.2017. https://doi.org/10.1007/s11069-016-2724-z

[69] Bhattacharya B, Zevenbergen C, Wahaab R A W R A, Elbarki W A. *Characterization of flooding in Alexandria in October 2015 and suggested mitigating measures*. 2017, *19*, 14230. Available from: https://ui.adsabs.harvard.edu/abs/2017EGUGA.1914230B/abstract

[70] Young A. A rainfall threshold-based approach to early warnings in urban data-scarce regions: A case study of pluvial flooding in Alexandria, Egypt. 2021. https://doi.org/10.1111/jfr3.12702

[71] Ali N. A. Alexandria drowns: A philosophical reading of flood management in Post-revolution Egypt. 2015. https://doi.org/10.13140/RG.2.1.2635.9129

[72] Hafez M E. *Assessment of Climate Change Impact on Urban Heavy Rainfall Extremes Alexandria, Egypt Case Study*. 2017. Available from: https://journals.ekb.eg/article_154964_3faef7daa2e9bac56a7a241cb0586400.pdf Accessed 12/05/2022

[73] Mohamed B, Navy T E, Osman A, Saber S A, Allah H. M. *Assessment of weather and climate variability over Western Harbor of the climate.2020*. https://doi.org/10.21608/ejabf.2020.105861

[74] El-Geziry T M. Analysis of long-term rainfall and air temperature patterns in Alexandria (Egypt).2021. https://doi.org/10.1007/s12517-021-07589-z

[75] Khedr A M, Abdelrahman S M, El-din K A A. Currents and Sea Level Variability of Alexandria Coast in Association with Wind Forcing. 2018. https://doi.org/10.4197/Mar.28-2.3

[76] Amr A. *Alexandria in Antiquity A Topographical Reconstruction*. *I*. Doctoral thesis. 1996. Available from:https://www.tesisenred.net/bitstream/handle/10803/670088/amab1de5.pdf?sequence=1&isAllowed=y Accessed 17 May 2022.

[77] Venit M. Egypt as Metaphor: Visual Bilingualism in the Monumental Tombs of Ancient Alexandria. In Visualizing the Afterlife in the Tombs of Graeco-Roman Egypt (pp. 50-86). Cambridge: Cambridge University Press. 2015. doi:10.1017/CBO9781107256576.003

[78] Ioannides M, Fink E, Cantoni L, Champion E, Goos G. Progress in Cultural Heritage: 2020. (eBook) https://doi.org/10.1007/978-3-030-73043-7

[79] Jozef L, Oostwegel N, Jaud Š, Muhič S, Rebec KM. Digitalization of culturally significant buildings: ensuring high - quality data exchanges in the heritage domain using Open BIM. Heritage Science [Internet]. 2022; 1–14. Available from: https://doi.org/10.1186/s40494-021-00640-y

[80] Stanley J D, Carslon R W, Van Beek G, Jorstad T F, Landau E. A. Alexandria, Egypt, before Alexander the Great: A multidisciplinary approach yields rich discoveries. *GSA Today*.2007, *17*(8), 4–10. https://doi.org/10.1130/GSAT01708A.1

[81] Shaltout M, Tonbol K, Omstedt A. Sea-level change and projected future flooding along the Egyptian Mediterranean coast. *Oceanologia*.2015, *57*(4), 293–307. https://doi.org/10.1016/j.oceano.2015.06.004

[82] The World Bank. Climate Change Adaptation and Natural Disasters Preparedness in the Coastal Cities of North Africa Phase 1: Risk Assessment for the Present Situation and Horizon

2030 – Alexandria Area. 2011. Available from: http://web.worldbank.org/archive/website01418/WEB/IMAGES/ALEXANDR.PDF

[83] Jondet G. Les portssubmergés de l'ancienneîle de Pharos. Le Caire. 1916. Available from: https://www.ancientportsantiques.com/wp-content/uploads/Documents/PLACES/Egypt-Libya/AlexPharos-Jondet1916/JONDET-Texteintegral.pdf Accessed 10 May 2022.

[84] Kázmér M. Typology of Earthquake-Induced Damages in Ancient Buildings Damage Affecting a Single Wall. 2014, 1–7. https://doi.org/10.1007/978-3-642-36197-5

[85] Benavente D, García del Cura MA, García- Guinea J, Sanchez-Moral S, Ordonez S. Role of pore structure in salt crystallization in unsatured porous stone. 2004. https://doi.org/10.1016/j.jcrysgro.2003.09.004

[86] Sato M, Hattanji T. A laboratory experiment on salt weathering by humidity change: salt damage induced by deliquescence and hydration. Prog Earth Planet Sci. 2018, 5, 84. https://doi.org/10.1186/s40645-018-0241-2

[87] Charola AE, Puhringer J, Steiger M. *Gypsum: a review of its role in the deterioration of building materials*. 2007, 339–352. https://doi.org/10.1007/s00254-006-0566-9

[88] Zurbriggen R, Herwegh M. Daily and seasonal thermal stresses in tilings: a field survey combined with numeric modeling. Mater Struct. 2016. 49, 1917–1933. https://doi.org/10.1617/s11527-015-0623-5

[89] Mart J, Arizzi A, Benavente D. The Role of Calcite Dissolution and Halite Thermal Expansion as Secondary Salt Weathering Mechanisms of Calcite-Bearing Rocks in Marine Environments. 2021. https://doi.org/10.3390/min11080911

[90] Grossi C M, Brimblecombe P, Menéndez B, Benavente D, Harris I, Déqué M. Science of the Total Environment Climatology of salt transitions and implications for stone weathering. *Science of the Total Environment. 2011, 409*(13), 2577–2585. https://doi.org/10.1016/j.scitotenv.2011.03.029

[91] Doehne E, Price C A. *Stone Conservation: An Overview of Current Research*. 2010. https://doi.org/10.2307/3179804

[92] Robert K, Kvande T, Olav H, Vincent J, Harstveit K. *A frost decay exposure index for porous, mineral building materials*. 2007, *42*, 3547–3555. https://doi.org/10.1016/j.buildenv.2006.10.022

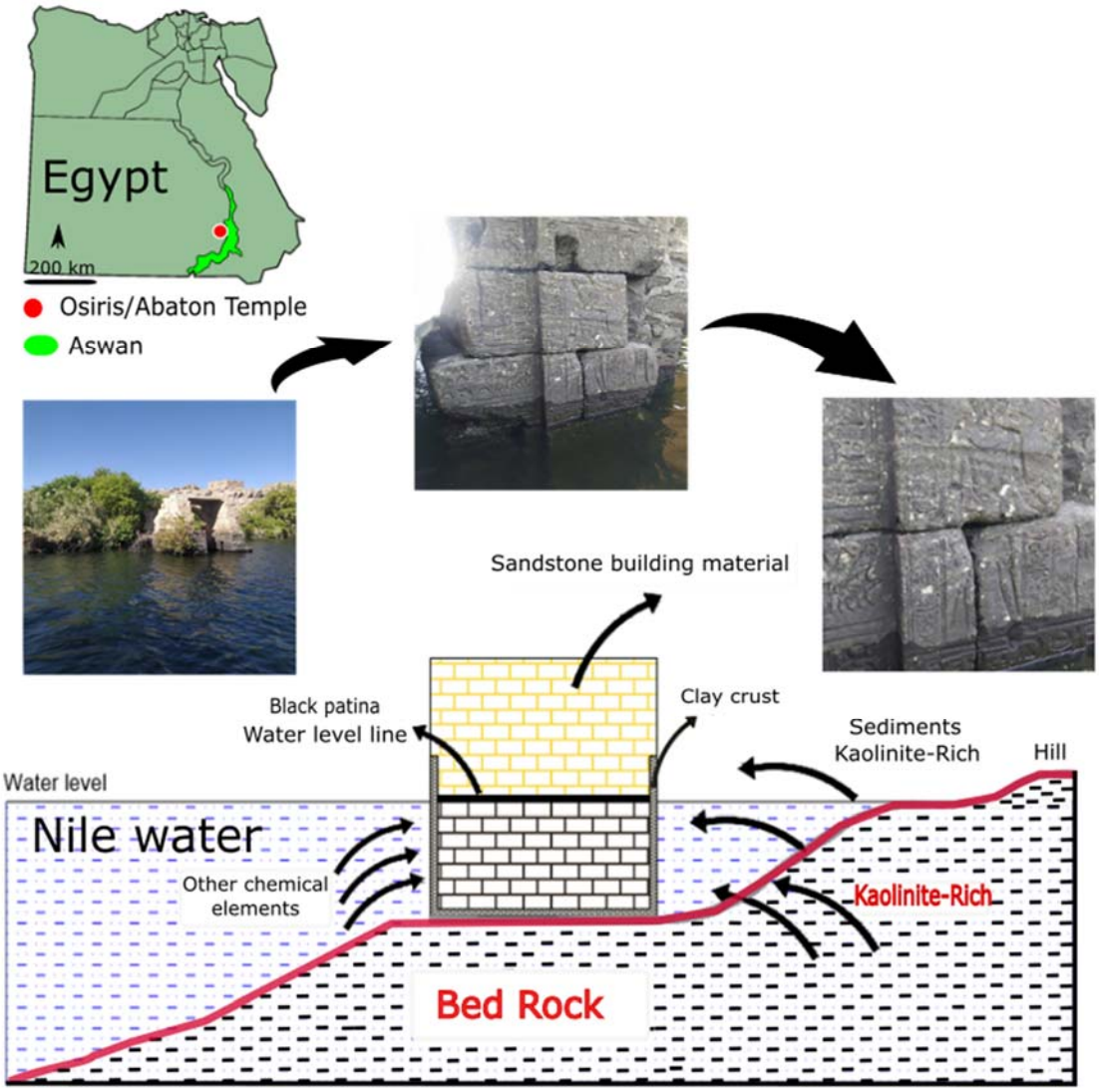
[93] Loperte A, National I, Proto M, National I, Bavusi M. *Geosciences Building damage caused by tree roots: laboratory experiments of GPR and ERT surveys*. *2010*. https://doi.org/10.5194/adgeo-24-133-2010

3.2. Multianalytical diagnostic approaches for the assessment of materials and decay of the archaeological sandstone of Osiris Temple (The Abaton) in Bigeh Island, Philae (Aswan, Egypt)

Highlights:

- Osiris Temple was not rescued during UNESCO saving campaign of Aswan temples.
- Yellowish and pinkish sandstones are the building materials of the temple.
- Fluctuations of Nile water level decayed the temple building materials severely.
- Main intrinsic decay factors are the clayed matrix of sandstones.

Graphical abstract



Abstract

The ancient Osiris Temple at Philae/Aswan, also known as Abaton, was considered one of the most sacred and mysterious temples in Egypt. In 1960, UNESCO rescued Philae temples because the rise of the water level after the construction of the Old and New Dam of Aswan caused the submergence of all temples underwater. Rescue camping was performed to protect all Aswan temples. Unfortunately, Osiris Temple was not rescued and was forgotten in its original place on Bigeh Island. Currently, this temple is subjected to Nile water effects and is partially submerged underwater due to Nile water level changes. This study aims to unravel and assess the conservation state of the temple sandstone-building material through multianalytical and examination techniques (X-ray diffraction, X-ray fluorescence, Raman spectroscopy, polarizing microscopy, binocular microscopy, and scanning electron microscopy). Furthermore, in situ records were obtained, and degradation maps were drawn to establish the patterns of damage and decay of the building material of the Osiris temple. The results showed that blackening, soiling, and disintegration are the dominant decay patterns in the building material of the temple. In addition, the Nile water as an extrinsic factor severely affected the conservation state of the temple due to the continuous exposure to water force. The mineralogical composition of sandstone played an important role in its degradation as an intrinsic decay factor due to mainly dispersion of clayed and/or carbonate matrix dissolution, quartz hydrolysis, and feldspar alteration.

Keywords: Osiris Temple, Abaton, Nile River, sandstone, water effect, decay.

1. Introduction

Ancient Egyptians used sandstones for their workability, accessibility, and affordability in construction as structural and architectural elements in their buildings, such as tombs and temples [1-3]. Many of the buildings of the Egyptians were erected in the vicinity of the course of the Nile River, so the flooding of the land caused by the construction of reservoirs threatens their preservation. For this reason, in March 1960, UNESCO called for a rescue campaign from financial and research points of view to protect Aswan temples from damage due to the building of the New Dam of Aswan (111 m above the Nile bed level) impounding water in a lake extending three hundred miles south of the first waterfall with a storage capacity of 164 billion cubic meters [4, 5]. To preserve the Aswan temples from permeant submergence, the campaign performed extensive geological and geotechnical studies on the construction materials of the Aswan temples. Moreover, determination of the internal stresses and places of cracks and fissures in the sandstone blocks and rocks, tests on cutting of sandstones, tests on physical and mechanical properties of sandstone, and hydrology studies were performed [6, 7]. Unfortunately, Osiris Temple was the only temple not rescued during the saving campaign of Aswan temples. In this regard, the motive behind leaving Osiris Temple without rescuing could be because the level of the Osiris Temple was higher than the opposite Temples of Philae and the water impact was not as significant as today's condition. However, the real motive behind ignoring Osiris Temple is not generally known. According to Willcock's report [8], during the building of the Aswan dam, taking up the Philae temples stone by stone and reconstructing them on the island of Bigeh, this suggestion was not welcomed because this action would cause damage to the Osiris Temple, and finally, Willcock had to recommend abandoning the construction of the Aswan Dam completely.

Osiris Temple is mainly built from sandstone and the lower part of the temple, and its foundation was always saturated under Nile water many years ago. Accordingly, the direct exposure to Nile water and its level fluctuations affected the durability and structural stability of the temple building materials. Scientists in the field of cultural heritage have tried to understand the susceptibility and conservation problems of sandstones as building

materials due to water impacts in different environments. For example, water can chemically interact with the internal composition of sandstones, releasing other byproducts of degradation compounds, such as soluble and insoluble salts [**9, 10**]. Water has a powerful action as a solvent and erosive agent in the disintegration of sandstone, and incidental chemical decomposition is likely to occur during abrasive actions. Furthermore, the damaging action of frozen water is especially illustrated in the expansive force of water during the conversion from a liquid to a solid phase that is graphically described as equal to the weight of a mile height column of ice, which means approximately 150 t/m^2 [**11, 12**]. On the other hand, the permeability of sandstone can be affected by high fluid velocity and salinity, and in-situ clay particles can be dispersed in the pores of the sandstone and cause many chemical and mechanical interactions [**13**]. In addition, clay content in sandstones plays an important role in strength reduction in water conditions since the decay actions depend on the clay, stone matrix mineralogy, and pore size distribution [**14**]. Sandstones cannot be highly decayed when they are without clay bonding material, but drying and wetting cycles could cause a notable reduction in sandstone strength by approximately 30% [**15-17**]. The magnitude of strength reduction after water saturation is very different among sandstone types, ranging from no appreciable effect on compressive strength in sandstones without clay to a marked reduction (55%) in compressive strength in sandstones with clay [**18**]. Water can enter and exit the stone pore network by diffusion, water vapour condensation, capillary action, and evaporation of water according to the porosity and permeability of the stone [**19**]. Salt crystallization pressure is increasing in sandstones with a high number of expandable clays, which leads to sanding decay problems for the construction materials due to loss of cohesion between the clasts of the sandstone [**20**]. Experimentally, the disintegration rate of sandstones that are subjected to salt crystallization is higher than that of sandstones that are subjected to wetting and heating cycles, although sandstones under wetting and heating cycles have different thermal behaviors that affect the durability of sandstones as construction materials [**21**]. In this sense, decayed sandstone building material has different kinds of degradation patterns, such as crumbling, flaking, scaling, fissures, and disintegration [**22**]. Sequentially,

exfoliation, granular disintegration, contour scaling, blackening and greening until the loss of material can be noticed as decay forms because of the water effect [**23, 24**].

The previous literature explains the influence of water in different environments on diverse types of sandstones using multianalytical and physical tests for their evaluation [**9-20**]. However, in Egypt, only few researches had been addressed to study the impact of groundwater and flooding on archaeological sites in southern Egypt [**25, 27**], and there have been no studies assessing the effects of Nile water and its level changes on submerged or semi submerged monuments since 1974. To solve this lack of knowledge this article addresses the following aim.

2. Aim of the paper

This paper presents the conservation problems such as mineralogical alterations, organic film and decay processes of the semi submerged Osiris Temple (Aswan, Egypt) due to the Nile water impact. Multianalytical (X-ray diffraction, X-ray fluorescence, Raman spectroscopy) and microscopic (polarizing, binocular, and scanning electron microscope) techniques are used to identify and assess the sandstone building material and its alterations. These techniques are recognized as the most suitable for the mineralogical and chemical characterization of samples and for the study of the alterations suffered because of weathering processes. To find answers, sandstone fragments were analyzed and checked paying attention to this valued heritage monument to be rescued and restored.

3. Geomorphological and geological context of the quarries and Temple

Osiris Temple is situated at a short distance upstream from the first waterfall of the Nile and is approximately 9 km to the south of Aswan town. In addition, it is located between Aswan's Old and New Dams (**Fig. 3.2.1-A,** red circles **1** and **3**, respectively). It was built on a massive granite basement [**28**]. Geomorphologically, the study area is surrounded by many hills, and Osiris Temple is adjacent to one of the islands in the middle of the Nile River called Bigeh Island (**Fig. 3.2.1-A**, red circle **2**). The water level of the Nile River in Aswan is approximately 87 m above sea level [**29, 30**]**.**

The geological setting of the study area is composed of a sedimentary succession from the Cretaceous to Quaternary approximately 500 m thick, and it is composed of igneous and metamorphic basement outcrops (**Fig. 3.2.1-B**) [**31**]. The basement rocks are overlain by sandstones of the Nubian Formation (Upper Cretaceous). This Nubian sandstone is divided into three groups (lower, middle, and upper) with total thicknesses ranging between 20 and 85 m (**Fig. 3.2.1**) [**4, 28** and **32-34**]**.** See the supplementary materials to see the formations through digital elevation model for the study area (**SM2. Fig.1**).

Ancient Egyptians used sandstone blocks for their high workability, variable colour, and absence of clear bedding planes, and they were extracted from different places in Aswan outcropping in the Nubian Formation (**Fig. 3.2.1-B**). On the one hand, quarries Gebel El Silsila extended from both banks of the Nile River and approximately 40 km south of Edfu, 18 km north of Kom Ombo, and 68 km north of Aswan (black squares in **Fig. 3.2.1-B**). They were used from the Middle Kingdom, extensively used in the New Kingdom, and until Roman times mostly used as building material in Karnak and Thebes cities. On the other hand, the quarries of Girtass are located approximately 40 km south of Aswan and were the source of all sandstone blocks used in the Philae area (green squares in **Fig. 3.2.1-B**). Moreover, on the eastern bank of the Nile River, massive quarries dated back mostly to Ptolemaic and Roman times. On the western bank of the Nile River, there were small quarries with so much archaeological evidence cut out into the rock that is kept until now (**Fig. 3.2.1-C**) [**1** and **35-37**]**.**

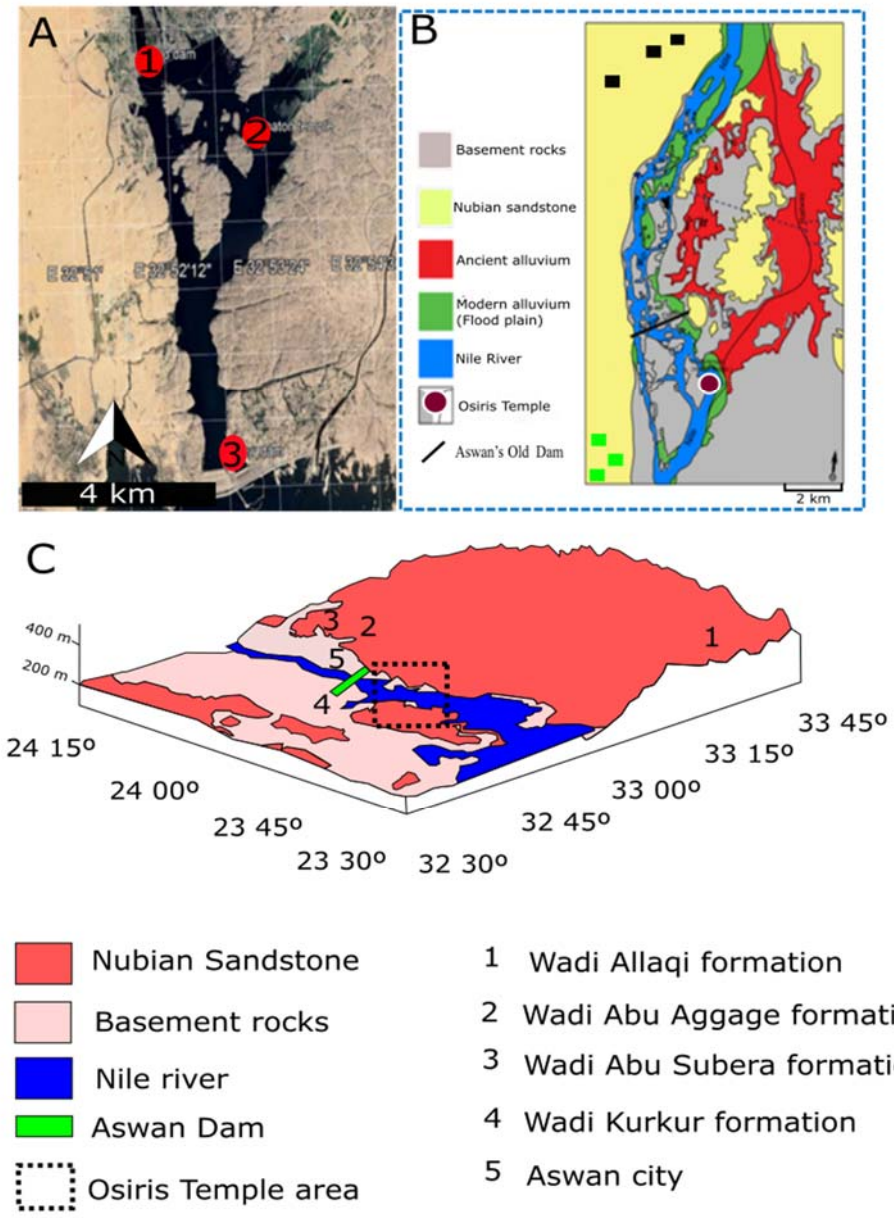


Fig. 3.2.1. (A) General map of the study area and the position of Aswan's Old and New Dam (red circles 1 and 3, respectively) and Osiris Temple (red circle 2). (B) Geological features of the area surrounding Osiris Temple, where black squares are the quarries Gebel El Silsila and green squares are quarries of Girtass in Aswan. (C) Digital elevation model and geomorphological features for Aswan, as well as showing Nubian sandstone formations such as the Kurkur Formation. The black dotted rectangle represents the area surrounding the Osiris temple. From [**38**].

4. Historical and architectural description

Bigeh Island is located opposite the original place of the Philae complex, south of most of the islands of the first waterfall and located south of Agilkia Island (**Fig. 3.2.2-A**). In this important area, the oldest buildings still exist, dating back to Nectanebo I 370 BC and Nectanebo II 359 BC. Most of the temples date back to the 25th dynasty. The importance of this site backs to its sacred role as an important cultic center of Isis and Osiris (**Fig. 3.2.2-B**) [**40**-**41**]. In Osiris Temple, the remaining façade of the outer hall consists of four columns decorated with floral capitals and combined with half of the column heights from the Ptolemaic-Roman periods. The ruins of the exterior walls date back to Ptolemy XIII**,** but the pylon gateway reliefs were inscribed in the era of Augustus, especially his cartouches appearing above the head of the officiating king in all the scenes and the dedicatory inscriptions [**42**]. The ground plan of the temple (**Fig. 3.2.2-B**) consisted of the interior space of the pylon, which was built by Augustus and led into the temple, where there isa modern granite slab that dates back to Ptolemy III. There is also an inclined approach or terrace, the foundation of an apse of a Christian church followed by a step, a preserved ancient pavement, and a cement pavement that dates back to 1910 due to restoration work. Finally, the stairs were built close to the bank of the Nile and led to the temple. See the supplementary materials showing a plan for the current ruins for the temple (**SM2. Fig.2**) and see (**SM2. Fig.3**) as well.

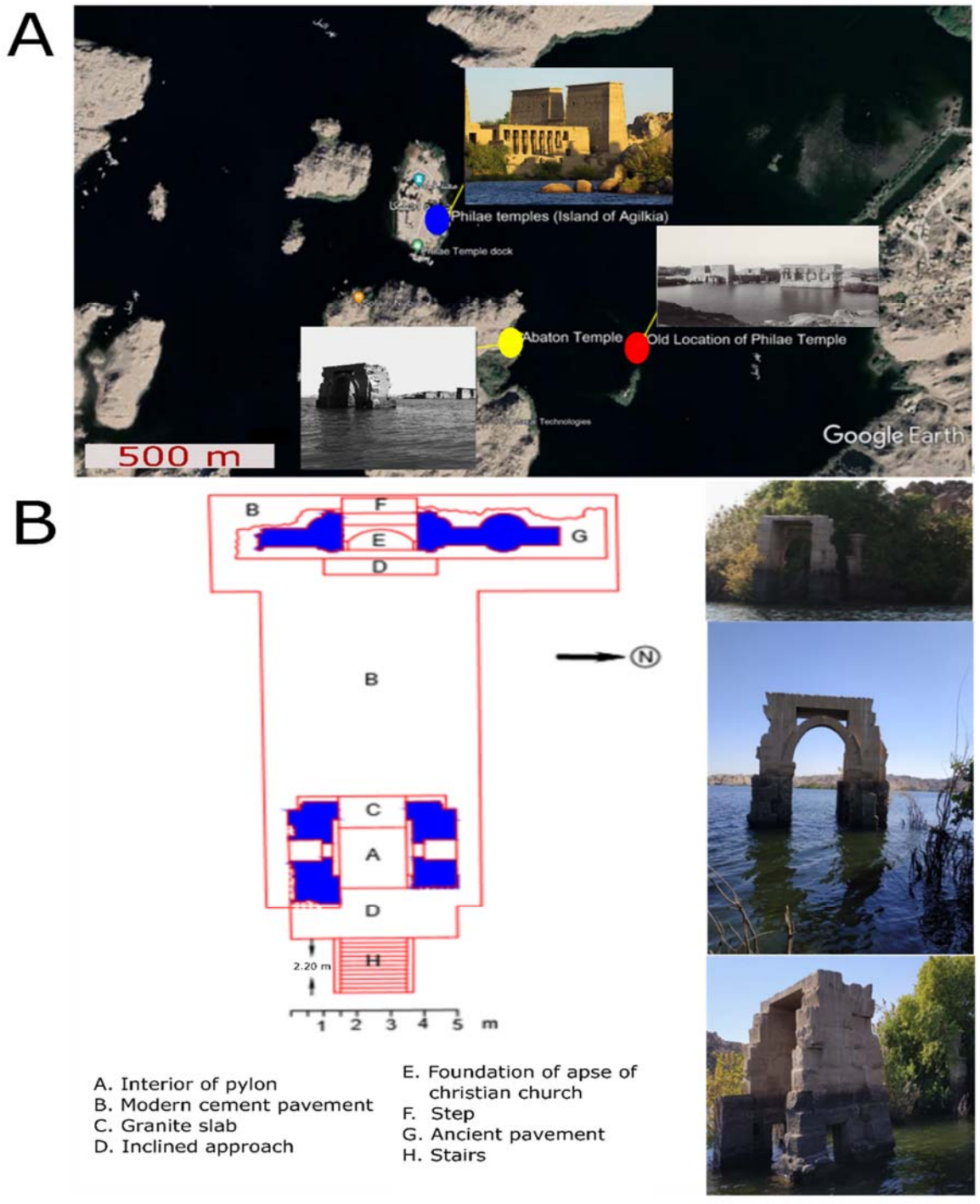


Fig. 3.2.2. (A) General map of Philae monuments, where circles represent the original location of Philae temples (in red), recent place of transferred temples from the original location to the Island of Agilkia (in blue) and Osiris Temple (Abaton Temple, in yellow). (B) The current state of the temple and its plan section. Modified after [**42**].

5. Materials and methods

5.1. Materials

The main building materials observed in this temple are sandstones, and two main groups could be chromatically differentiated: one yellowish to brown–yellow colour and the other represented by a pinkish colour. All samples were representative of the building materials used in the temple. They were taken from archaeological fallen and highly weathered fragments and parts for analysis, examination, and physical testing. The collected fragments were coded with S from 1 to 4, where 1 and 2 represented yellowish sandstone (**Fig. 3.2.3-A**), and 3 and 4 represented pinkish sandstone (**Fig. 3.2.3-B**). Three cubes of 3×3×3 cm in size were also prepared for both sandstone groups to measure the physical properties.

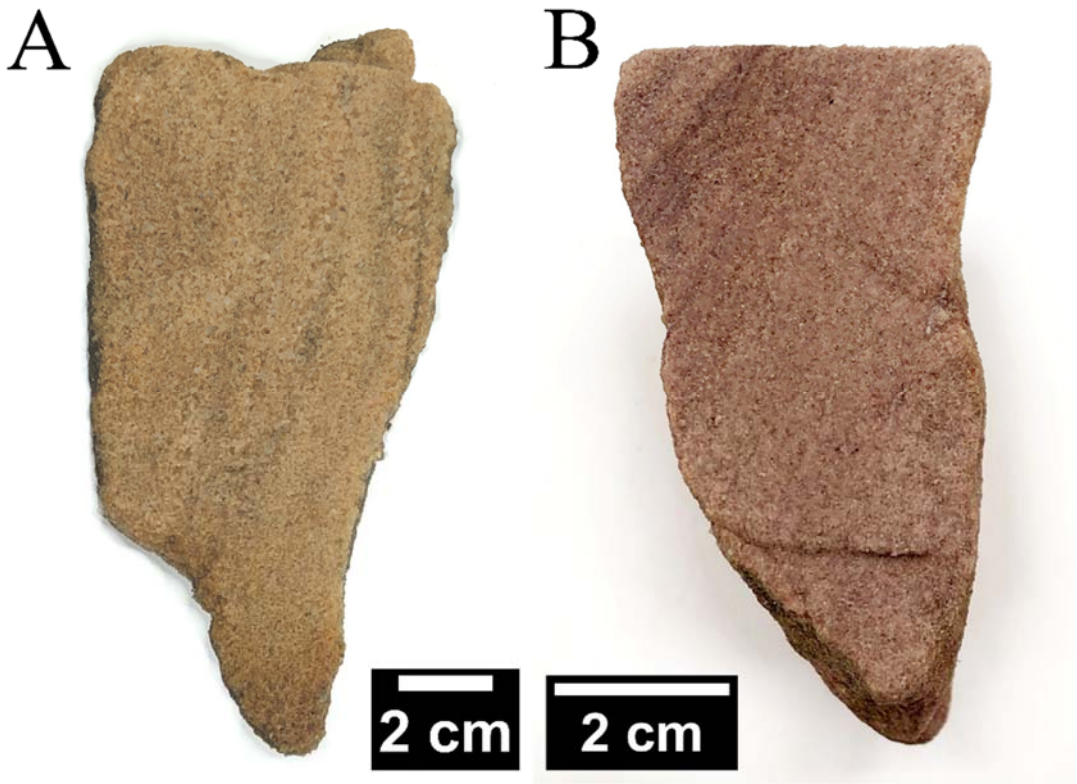


Fig. 3.2.3. Hand-samples of the yellow (A) and pink (B) sandstones.

5.2. Methdology

In situ observations were carried out to record all decay patterns and take photographs of the temple. A dgital microscope (DM) was used to detect the surface conditions of the temple building materials. Thin sections were prepared and studied using an Olympus BH-2 polarized optical microscope (POM) to identify the different minerals and altered phases of the samples. Small fragments were used to detect the decay through the textural features of the samples under high resolution, as well as to identify different kinds of altered materials after water reaction with the building materials, using a scanning electron microscope (TESCAN-performance at 20.00 KV, WD: 17.73 mm and Vac: HiVac). For mineralogical characterization, X-ray diffraction (XRD) was used both for the raw sample of sandstone building material and for its clay fraction after separation by centrifugation. In the case of clay mineralogy, diffractograms of untreated oriented aggregates and aggregates treated with dimethyl-sulfoxide and heated at 550 °C were carried out [**43**].For this purpose, a Bruker D-8 Advance ECO diffractometer equipped with a Lynx-Eye high-speed measurement detector was used under the following conditions: CuKα radiation filtered by Ni, graphite monocromator and fixed slots, 2theta 5° to 60° scanning angle; diffractograms were interpreted with the software EVA (Bruker-AXS). A portable Raman spectroscopy (i-Raman Pro, BW TEK) BW475-532S model equipped with a 785 nm laser was used to detect the main components of the building material and its by-products. Additionally, for the X-ray fluorescence (XRF) was used a Bruker AXS M-4 Tornado sequential dispersive wave X-ray spectrometer with a Rh tube operating at 4000 W was also used to recognize the major and trace elements.

Finally, some physical properties were calculated according to IS: 2386 (Part III) and ASTM C97 [**44, 45**]. The density of the stone indicates the unit weight of the stone and is calculated by dividing mass up by the total volume of the stone according to the formula D = m/v. Porosity is a measure of void spaces inside stones and is measured according to the formula Po = V_V/V_T. Water absorption is expressed as the percent weight change due to absorbed water and calculated according to the formula WA=$(M_{wet}-M_{dry})/M_{dry}$×100%. All cubes

prepared for testing are 3 cm in dimension instead of 5 cm for the limitations of sampling in the fluvial environment around the temple.

6. Results

6.1. Decay patterns of the construction material

Generally, Osiris Temple was and still is subjected to the effect of water level fluctuations daily and yearly as well as bank river erosion. As shown in **Fig. 3.2.4** (**A**), the temple is almost submerged and subjected to severe changes in the water level of the Nile River. It is clear that some building blocks are exposed to environmental impacts and that the second half of these building blocks are submerged directly underwater (**Fig. 3.2.4-A**). In addition, a black area can be observed in some others after undergoing the effect of rising and falling water.

In situ and visual inspections were performed to document all features of decay for the sandstone building materials. Many patterns of deterioration and deformation are observed, such as cracks (micro and macro), fractures, flaking, discoloration, pitting, crusting, and blackening. Man-made deterioration patterns have also been documented, such as scratches, spalling (flaking) and holes (**Fig. 3.2.4-B**). Moreover, the presence of plants was observed around the temples, which played a mechanical role in the destruction of blocks and caused many structural cracks in the building materials as shown in the general view (**Fig. 3.2.4-A**). Due to the water environment, biological matter adhered to the surface and integrated with other constituents, such as clay, to form black patina with variable thicknesses (**Fig. 3.2.4-B**). See more figures for the building materials decay and destruction in the supplementary materials (**SM2. Fig. 4** and **5**). Moreover, for more deterioration maps see (**SM2. Fig. 6** and **7**).

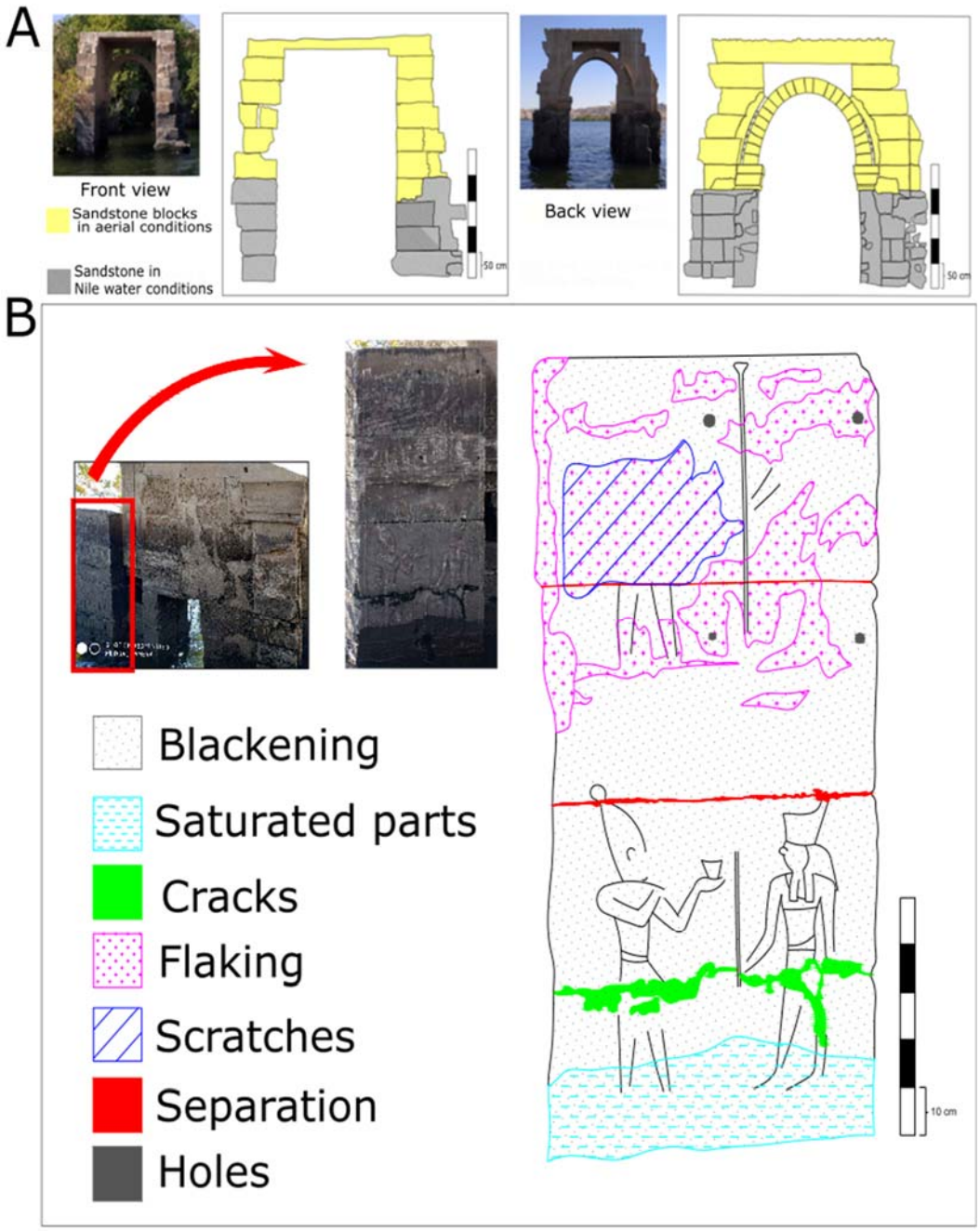


Fig. 3.2.4. (A) Front and back views of Osiris Temple and their current preservation state and (B) degradation patterns for building materials of the temple**.**

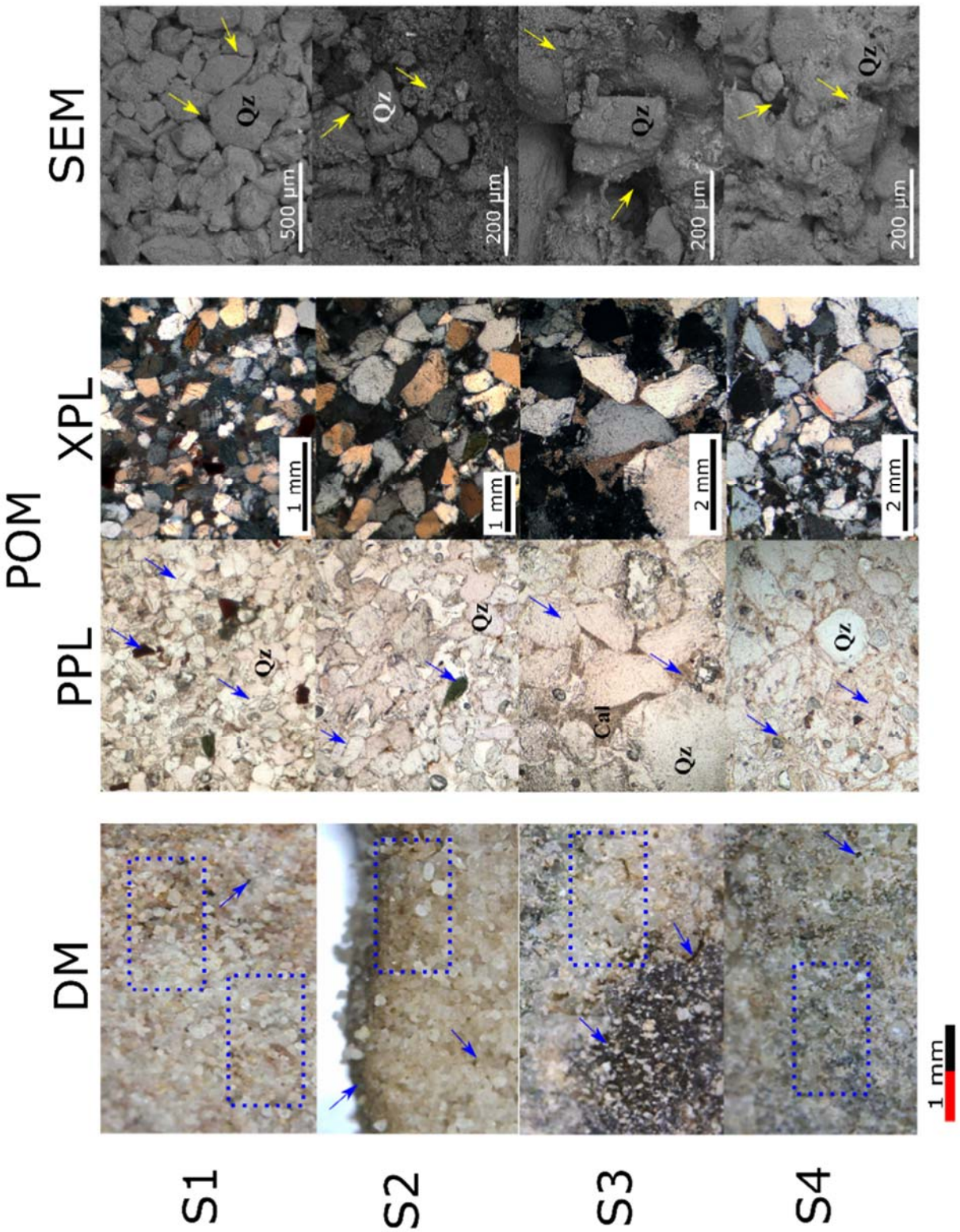
6.2. Macroscopic and microscopic investigation

Macroscopic examination presents decayed textural/morphological properties of the construction material of Osiris Temple, as shown in Fig. 5 (**S1-S4, DM** row). In S1 and S2, disintegrated and loose granules were detected as well as discoloration. In S3 and S4, blackening of the stone surface is strongly detected with a large thick layer. In Fig 6, the cross-section of one of the sandstone samples shows a thick black patina with an estimated thickness of 1 mm. Mostly all down parts of the temple show this black patinathat covered the valuable inscriptions (**Fig. 3.2.4-B**), which could be formed due to physical and chemical reactions between the stone surface and Nile water, and biological colonization.

Fig. 3.2.5 (**POM**) and **Table 3.2.1** show the main petrographical and textural results taken under plane-polarized light and crossed-polarized light. S1 (***Fig. 3.2.5*-S1, POM**) is *considered medium- to coarse-grained siliceous sandstone,* poorly sorted. The composition is mainly characterized by monocrystalline to polycrystalline, anhedral, and subrounded to subangular grains of quartz with sizes from 0.06 mm to 2 mm in diameter. Feldspars are detected with their cross-hatched pattern as characteristic twins, and some of them are altered by chemical weathering to kaolinite, which is seen in the worm shape due to the chemical alteration of alkali feldspar. Phyllosilicate aggregates (mainly muscovite) are observed. Furthermore, there are some tourmaline crystals, with green color and moderate relief and opaque iron oxide (hematite). Many microfractures in the quartz grains are detected due to the hydrolysis process of quartz, and pores between the grains are observed. S2 (***Fig. 3.2.5*-S2, POM**) is considered coarse- to fine-grained, very poorly sorted, monocrystalline to polycrystalline quartz grains with undulatory extinction, anhedral, and subrounded to subangular grains. The grain sizes of quartz were estimated to be between 0.25 mm and 2 mm in diameter. Some garnet crystals are observed as isotropic and monocolored. Some calcite crystals are detected as cement filling the pores between the framework of quartz grains. Furthermore, hematite is detected as an opaque mineral and fills the pores between the boundaries of quartz grains. Finally, some pores and microfractures in the grains of quartz are due to dissolution and hydrolysis processes. S3 (***Fig. 3.2.5*-S3, POM**) is coarse- to fine-grained and is mostly the same as the sandstones of

S1 and S2. Quartz grains are heterogeneously distributed and poorly sorted. It is characterized as subangular and twinned. The grain sizes are estimated from 0.4 mm to 1 mm. Some micritic calcite is observed as a matrix that fills the pores between the quartz grains. Moreover, greenish tourmaline is detected. Besides calcite, in some parts of the rocks, clay also acts as a binding constituent. Pores exist, and microfractures are detected in some of the quartz grains. Finally, S4 (***Fig. 3.2.5*-S4, POM**) is fine-coarse *quartz***,** poorly sorted, heterogeneous, subrounded to subangular, and monocrystalline to polycrystalline with an average grain size of 0.5 mm in diameter. Micas (muscovite) are detected with their laminate habits. It is observed that one of the muscovite grains framed one of the quartz grains and rare greenish tourmaline and prismatic zircons with flashy colors and high relief are detected. A clear alteration of K-feldspar (orthoclase) to kaolinite due to the hydrolysis process is detected. Some micritic calcite is detected as a cement component that fills the pores between some quartz grains.

The scanning electron microscope study (***Fig. 3.2.5-SEM***) allowed a microtextural/structural characterization to detect and specify the morphological properties of Osiris Temple's sandstones. The assessment of the vulnerability and durability went through checking the general morphological reading, grain size, shape, altered compounds, salts, and heterogeneity. In ***Fig.3.2.5*** *(***S1**), sandstone is full of pores between grains and microfractures because of the disintegration process due to the water effect. Originally, quartz grains are very poorly sorted, reflecting the heterogeneity of the natural stone, which accelerated the negative reaction between water and sandstone. Some quartz grains are fractured and characterized by high fatigue due to hydrolysis and the water force effect. In **Fig. 3.2.5-**(***S1-S3**),* the morphological texture shows the soiling layer and the solid crust on and between the quartz grains, as well as the clay matrix.



(Caption is in the next page)

Fig. 3.2.5. Samples of yellow (S1 and S2) and pink (S3 and S4) sandstones under a digital microscope (DM, left row), polarized optical microscope (POM, two rows in the middle under plane and cross-polarized light, respectively), and scanning electron microscope (SEM, right row) for macro-and microtextural investigation. Dotted blue rectangles refer to the disintegration areas of the sandstone. The blue and yellow arrows show the disintegration, soiling layer, black patina, pores and microfractures and fissures as decay patterns for the sandstones. Legends: (Qz) Quartz; (Cal) Calcite. The mineral legend according to [46].

Table 3.2.1. Summary table with the main characteristics observed by polarizing microscopy in the studied sample. According to [47]. Legends: (Qz) Quartz; (Or) Orthoclase; (Ms) Muscovite; (Tur) Tourmaline; (Hem) Hematite; (Grt) Garnet; (Cal) Calcite; (Kln) Kaolinite; (Zrn) Zircon, according to [46]**.**

Sample	Origin	Observed minerals	Grain type	Grain size (mm)	Grain texture	Sorting	Grain fabric
S1	Quartz arenite	Qz, Or, Ms, Tur, Hem	monocrystalline to polycrystalline	0.06 - 2	subrounded to subangular	poorly sorted	Concavo-convex contacts
S2	Quartz arenite	Qz, Grt, Cal, Hem	monocrystalline to polycrystalline	0.25 - 2	subrounded to subangular	very poorly sorted	Concavo-convex contacts
S3	Quartz arenite	Qz, Cal, clay minerals	monocrystalline	0.4 - 1	subangular	poorly sorted	Point contact
S4	Quartz arenite	Qz, Cal, Kln, Ms, Or, Tur, Zrn	monocrystalline to polycrystalline	0.5	Subrounded to subangular	poorly sorted	grain - supported

The black patina (**Fig. 3.2.6-A** and **B**) detected in several of the samples, in detail, is composed mainly of a thin film of amorphous organic matter (**Fig. 3.2.6-C**), with the presence of filaments, possibly of algae (red arrows in **Fig. 3.2.6-C** and **D**) and fragments of different species of fluvial diatoms (**Fig. 3.2.6-E** and **H**). In this patina, practically no crystals of secondary minerals have been observed, therefore, this patina could not be defined as a black crust.

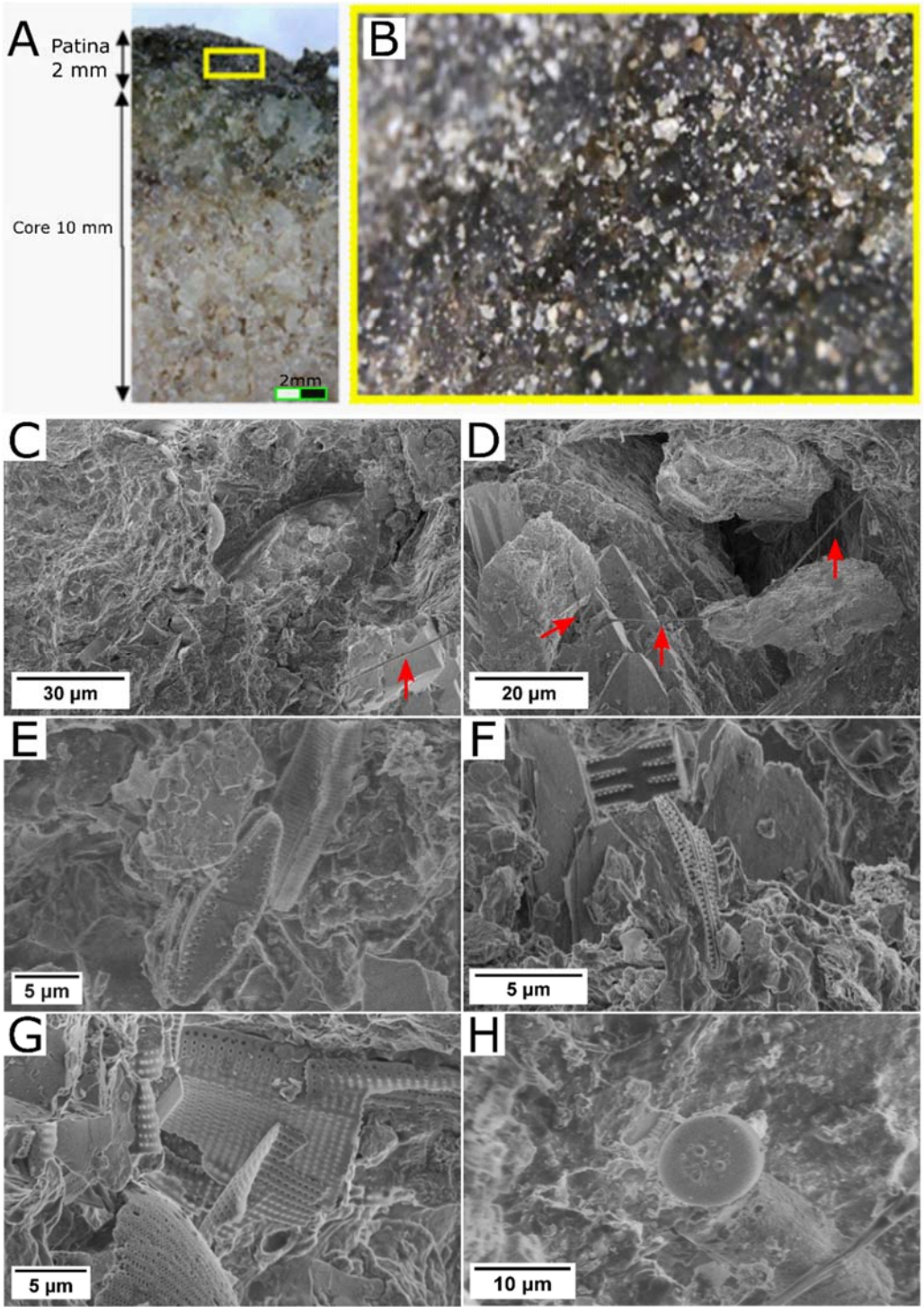


Fig. 3.2.6. (A) Cross-section of the sandstone (S3) and (B) a detail photography of the black patina by means of digital microscope. SEM photomicrographs of the black patina, where (C) shows a homogeneous distribution of the organic matter, (D) algae filaments (red arrows), and (E-H) different species of fluvial diatoms.

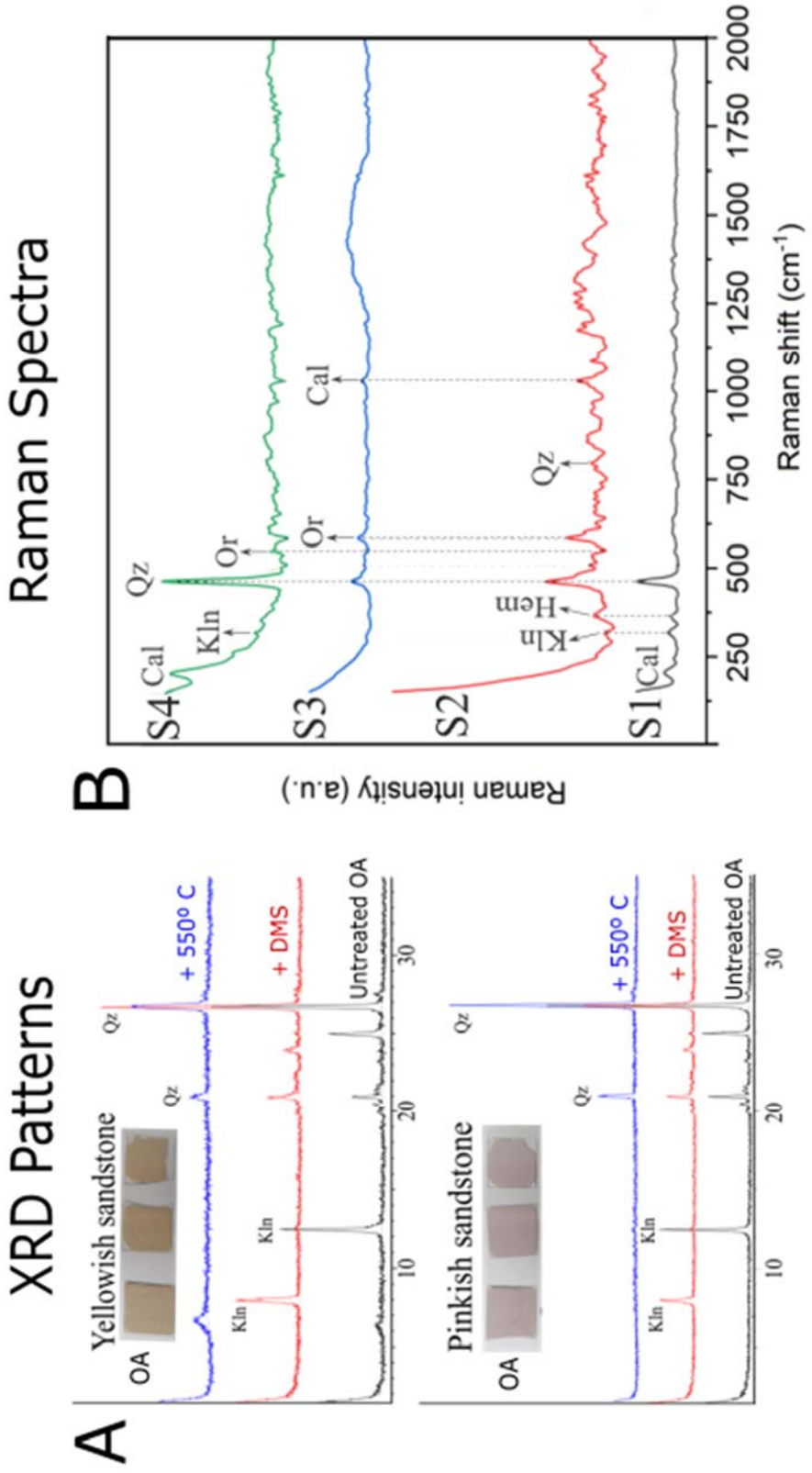
6.3. Chemical and mineralogical analysis

A semiquantitative analysis of the mineralogy of each sample was performed by X-ray diffraction using the relative intensities of each mineral. Quartz, calcite, kaolinite, orthoclase, and hematite were detected in samples S1 to S4 (**Table 3.2.2**). Quartz is very abundant in all samples, calcite is low in S2 and traces in S3 and S4, kaolinite is high in S1, low in S4, and traces in S2 and S3; orthoclase is low in S2, and hematite is low in S1. Nitratine and apatite appear in traces (**Table 3.2.2, S3**). On the other hand, after the separation process of the fraction below 2 microns, the clay mineralogy of the yellowish and pinkish sandstones has been determined, and the results showed that kaolinite only exists as a clay mineral in both sandstones (**Fig. 3.2.7-A**).

Table 3.2.2. Mineralogical content of Osiris Temple construction material samples (S1-S4). Legends: (Qz) Quartz; (Cal) Calcite; (Kln) Kaolinite; (Hem) Hematite; (Or) Orthoclase; (Apt) Apatite; (Nit) Nitratine; +++ = high; + = low; tr = traces. Mineral legend according to [**46**]**.**

	Qz	Cal	Kln	Hem	Or	Apt	Nit
S1	+++	-	++	+	-	-	-
S2	+++	+	tr	-	+	-	-
S3	+++	tr	tr	-	-	+	tr
S4	+++	tr	+	-	-	-	-

Under portable Raman spectroscopy (**Fig. 3.2.7-B**), the characteristic quartz peaks appear at 467cm^{-1} (S1-S4), 520, and 834 cm^{-1}[**48**]. Calcite peaks are assigned at 153cm^{-1} (S1 and S4) and at 1085cm^{-1} (S2 and S3) [**49**], kaolinite band is at 394 cm^{-1}(S1, S2 and S4) [**50**], and the characteristic spectral feature of orthoclase is at peak positions at 583 and 513 cm^{-1}[**51**]. According to the RRUFF database [**52**], the main hematite band for the 785 nm laser occurs at 300 cm^{-1}.



(Caption in the next page)

Fig. 3.2.7. (A) Diffraction patterns for clay minerals after separation and oriented aggregate (OA) preparation of the clay fraction for yellowish and pinkish sandstones. In the black line (untreated OA), red line (OA treated with dimethyl-sulfoxide, +DMS, note the displacement of the kaolinite peak from 7.18 to 11.1 Å), and blue line (OA heating at 550 °C). (B) Raman spectrum for the four construction sandstones (S1-S4). Legend: Kln: kaolinite; Qz: quartz; Cal: calcite; Hem: hematite; Or: orthoclase. The mineral legend according to [**46**]**.**

X-ray fluorescence was used to identify the chemical elements to confirm the results of X-ray diffraction and Raman spectroscopy. The results agree with the mineralogical analysis. Si, Al, Ca, Fe, K, and Ti ions are present, as shown in **Table 3.2.3**. Silica reaches between 65 and91% as a major ion with a notable amount of aluminum and few amounts of iron and potassium (**Table 3.2.3. S1-S2**), while calcium and magnesium are absent in S1. In **S2**, aluminum as a major element, and calcium, iron, and potassium exist as minor elements. On the other hand**,** in S3 and S4, calcium, magnesium, potassium, and iron are considered minor elements. Finally, titanium is observed in all samples as a trace.

Table 3.2.3. Results of elemental analysis of sandstone construction material. Major and minor elements are expressed in oxides (wt. %).

Sample	Al_2O_3	SiO_2	K_2O	CaO	TiO_2	Fe_2O_3	MgO
S1	12	84	1	-	2	1	-
S2	12	65	3	11	1	5	3
S3	3	91	-	4	1	1	-
S4	16	78	-	5	1	1	-

6.4. Physical properties of sandstone

Density, porosity, and water absorption have been tested on six cubes of yellow and pinkish sandstones to assess the effect of water on the temple construction materials. It is observed that the average value of density is 2 g/cm^3, porosity is 21.5% and water absorption by total immersion is 10.15% (**Table 3.2.4**).

Table 3.2.4. Physical properties testing for Osiris Temple building material. Legend:ρ is density (in g/cm^3), Po is open porosity (in %), and A_w is the water absorption coefficient (in %).

Sample	Yellowish sandstones			Average	Pinkish sandstones			Average	Total Average
	1	**2**	**3**	**1-3**	**4**	**5**	**6**	**4-6**	**1-6**
ρ	2.2	2.3	2.3	**2.2**	1.8	2.0	1.9	**1.9**	**2**
P_o	20.2	25.2	24.0	**23.1**	18.8	21.2	19.6	**19.9**	**21.5**
A_w	9.0	10.9	10.3	**10.0**	10.0	10.5	10.2	**10.2**	**10.15**

7. Discussion and conclusions

This study focused on investigating and analysing the sandstone of the Osiris Temple to evaluate its durability problems in water conditions. The sandstone-building material was extracted from Nubian sandstone quarries in two different colors (yellow and pink), and they were preferred in the construction at that time because they were soft, workable, accessible, and esthetic natural building materials. Nubian sandstone contains kaolinite minerals and titanium elements as fingerprints. Additionally, it contains tourmaline and zircon as ultrastable heavy minerals [**53**, **54**]. In this regard, the sandstone of the Osiris Temple contains kaolinite that was identified under X-ray diffraction and polarizing microscopy. Titanium was found in the elemental analysis in all samples and could be an indication of the presence of anatase (or rutile, perhaps also as an ultrastable heavy mineral). In addition, tourmaline and zircon were identified in small quantities in the study with polarizing microscopy, especially in S1 and S2.

This research focused on the interaction processes between water and the sandstone-building materialof Osiris Temple throughout the field and laboratory work. In this regard, old photos were collected to confirm the preservation state of the temple in different years. For instance, an old painting in 1838 by David Roberts showed the temple structure

without submergence in the water (**Fig. 3.2.8-A,** left) [**55**]. Meanwhile, in 1909, the photo showed that Osiris Temple was out of the Nile water reach (**Fig. 3.2.7-A,** middle). Finally, in 1970, the photo showed the temple before starting the safeguarding project to protect Philae temples and after finishing the construction of the New Dam in Aswan, where all temples were partly submerged and severely subjected to water levels rising up and down, as shown in the orange dotted rectangles (**Fig. 3.2.8-A,** right). In this sense, several anthropical and environmental factors caused the destruction of the temple; among them, we can cite the following: 1) coverage of the temple by reaching up of water (+121 m) in the season of flooding after building the Old Dam (**Fig. 3.2.8-B**); 2) the lowering of the water level in Lake Aswan after the construction of the New Dam (Sadd el Aali), leaving the water level at the middle of the temple construction (110 m) with daily fluctuations of three meters that continue to the present day (**Fig. 3.2.8-B**) [**7,39,56,57**]; 3) environmental impacts, such as earthquakes occurring, ancient flooding, changes in water salinity, sedimentation in the river and Lake Nasser, erosion of the river banks, beds and delta and resettlement issues [**58**,**59**]; and 4) conversion of the temple into a Christian church, as well as the removal of some blocks to reuse them in the construction of houses [**60**].

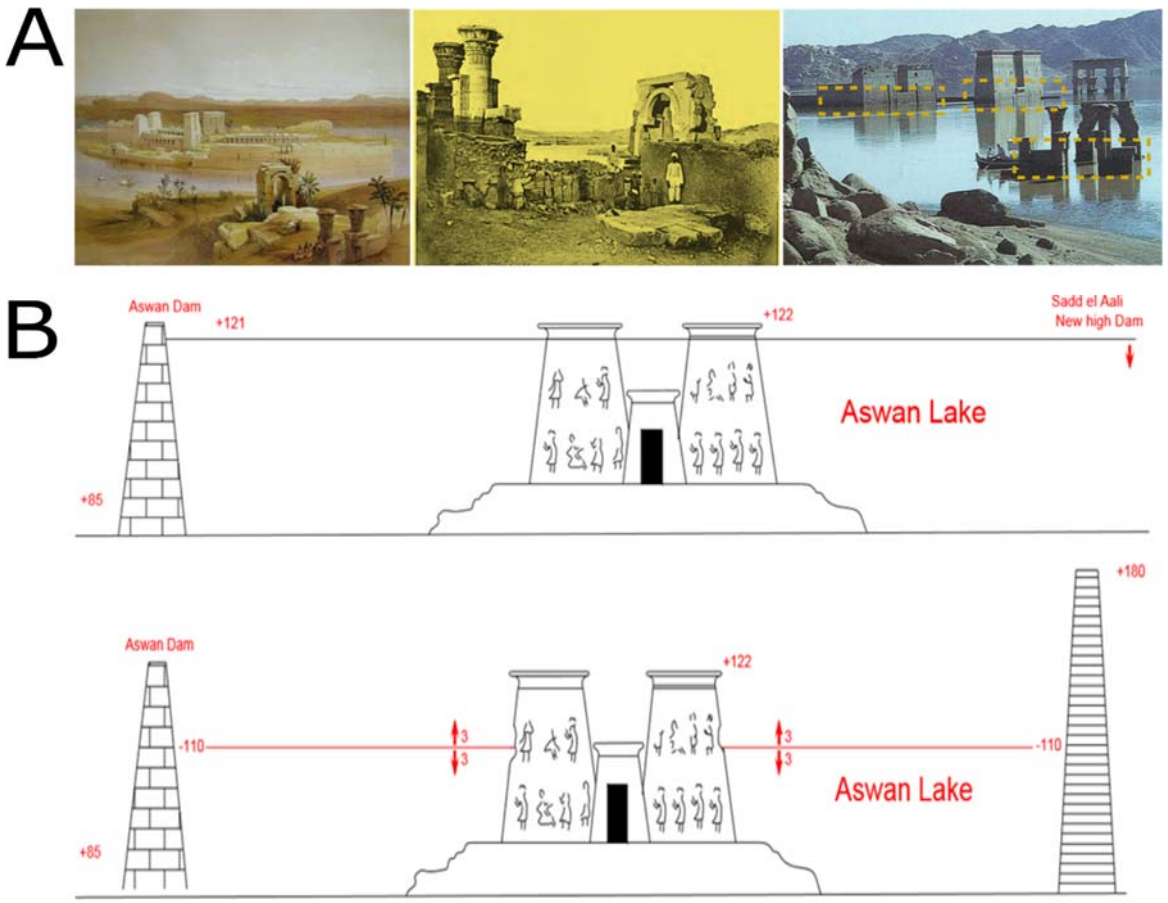


Fig. 3.2.8. (A) Old paintings and photos showing the preservation state of the temple in 1838, 1909, and 1970 from left to right, respectively. (B)Water level around the Philae temples and Osiris Temple after building Aswan's Old and New Dams. Modified after [**39**].

Many decay forms, such as blackening, disintegration, flaking, soiling, fractures, discoloration, and micro- and macrocracks, were recorded in the temple building materials due to the continuous reaction between water and building materials and the internal problems of the sandstones. Blackening and disintegration are the dominant degradation patterns. For decades, sandstone-building materials have been saturated under Nile water. In this regard, water still plays a corrosive role through the dispersion, dissolution, and hydrolysis of the mineral composition of sandstone. The blackening of the sandstone is one of the main patterns of decomposition. This thick black patina is formed mainly by the

organic material (amorphous organic matter, filaments of algae, and diatoms) (Fig. 6), left behind after the movement of water up and down over the temple. Discoloration of sandstones appeared because of the reaction of the iron content of the building materials with water [**23**]. Chemical and mineralogical analysis showed a reasonable amount of kaolinite as a matrix in all yellowish and pinkish sandstone samples. The presence of kaolinite can be considered an intrinsic problem in building materials, as it plays an important role in increasing water absorption due to its high-water absorption capacity. In addition, kaolinite can be dispersed in the water, leaving spaces between quartz grains and causing disintegration [**61, 62**]. In addition, pores and spaces between quartz grains were detected due to the alteration of feldspars to kaolinite during the hydrolysis process. The hydrolysis of quartz in sandstones has been noted as an internal decay factor. Water and quartz react chemically through the replacement of weaker hydrogen bonds −Si−OH−HO−Si− instead of strong silica bonds −Si−O−Si− [**63**]. Consequently, severe physiochemical decay for the sandstone building materials was seen by growing the subcritical cracks because of the hydrolysis process of quartz. These cracks were detected under a polarizing microscope, which confirmed the decomposition of sandstone building materials under the effect of Nile water. Moreover, after long exposure to the hydrolysis process, the strength of sandstone decreased remarkably, which is why many structural cracks appeared in the walls and ceiling. Moreover, nitrate (Nitratine) and phosphates (Apatite)(traces)were found as salts because of contaminated water around the temple. In this sense, Sharaky et al. [**64**] mentioned that the pollution of Nile water is due to agriculture, forestry, and septic tank activities in Aswan, while nitrate concentration values in Nile waters range from <0.003–0.01 mg/l, and the phosphate concentration is approximately 0.02 mg/l. Moreover, bird's waste drops were noticed and could cause chemical etching on the stone surfaces of the temple [**65**].

The water reaches more than 120 cm to sandstone building materials over Osiris Temple due to capillary force. Sandstones showed different sizes of grains that could behave differently concerning water absorption through capillary forces [**66, 67**], which could cause differential weathering for the sandstone building material. Petrophysically, the porosity of

sandstone can be classified into three types: low (<10%), medium (10–20%), and high (>20%) [**68**]. Furthermore, Salvatici et al. [**23**] confirmed that water could remove the clay and matrix, leaving the stone entirely disintegrated and increasing its inner porosity. Accordingly, the porosity of the temple building material is medium-high to very high due to the disintegration and dispersion of the kaolinite matrix in water and the dissolution of calcite. The explained intrinsic and extrinsic problems between sandstone and water led to severe decay in the natural stone of the temple. Consequently, engineering and structural defects in the building were observed.

Finally, an urgent safeguarding project for this semisubmerged temple is needed similar to what had been done previously with all Aswan temples to be saved. This paper characterized the building material of the temple and its decay processes. In this sense, this research could help in future planning for the conservation and restoration of this temple. The conservation project in our case requires cleaning, consolidation, and replacement of stone blocks to protect and strengthen stone building materials. In addition, accurate engineering and geological studies are needed to guarantee safe transportation and establishment of this temple into a stable hill around this area.

Acknowledgement

Fahmy acknowledges SCiCYT and UGEA-PHAM at Cadiz University for carrying out the main part of the archaeometric analysis. E. Molina Piernas acknowledges co-funding from the European Social Fund (D1113102E3) and Junta de Andalucía, and the Project CEIJ-004 financed by CEI MAR through the axis of scientific improvement of the CEI MAR 2021 Own Plan: “research projects of Young Researchers CEI MAR 2021”. We acknowledge Professor Philip Machev from the Faculty of Geology and Geography at Sofia University (Bulgaria) for carrying out scanning electron microscope images of figure 3.2.5.

8. References

[1] Harrell J, Storemyr P. Limestone and sandstone quarrying in ancient Egypt: tools, methods, and analogues. Marmora.2013; 9(9), 19–44. https://doi.org/10.1400/231999

[2] Hemeda S, Fahmy A, Sonbol A. Geo-Environmental and Structural Problems of the First Successful True Pyramid, (Snefru Northern Pyramid) in Dahshur, Egypt. Geotechnical and Geological Engineering. 2019; 37(4), 2463–2484. https://doi.org/10.1007/s10706-018-00769-x

[3] Fahmy A, Molina-Piernas E, Domínguez-Bella S, Martínez-López J, Helmi F. Geoenvironmental investigation of Sahure's pyramid, Abusirarcheological site, Giza, Egypt. Heritage Science. 2022; 10(61), 1–20. https://doi.org/10.1186/s40494-022-00699-1

[4] Wilson JA. The Nubian Campaign: An Exercise in International Archaeology. Proceedings of the American Philosophical Society. 1967; 111(5), 268–271. http://www.jstor.org/stable/986044

[5] Hassan F A. The Aswan High Dam and the International Rescue Nubia Campaign. AfrArchaeol .2007; Rev24**,** 73–94 https://doi.org/10.1007/s10437-007-9018-5

[6] Voûte C. Some geological aspects of the conservation project for the Philae Temples in the Aswan Area. GeologischeRundschau. 1963; 52(2), 665–675. https://doi.org/10.1007/BF01821149

[7] Berg L. The salvage of the Abu Simbel temples. Monumentum. 1974; 17, 25–56. Available from: https://www.icomos.org/monumentum/vol17/vol17_2.pdf

[8] Willcocks W. Report on Perennial Irrigation and Flood Protection for Egypt. Cairo: National Printing Office. 1894. Available from: https://www.forgottenbooks.com/en/download/ReportonPerennialIrrigationandFloodProtectionforEgypt_10693485.pdf

[9] Billard TC, Burns G, Wilson-Yang KM. Salinization in the Nile Valley: The Karnak Area. Journal of the American Research Center in Egypt. 1982; 19, 111. https://doi.org/10.2307/40000436

[10] Alves C, Figueiredo C A M, Sanjurjo-Sánchez J, Hernández A C. Effects of water on natural stone in the built environment - a review. Geosciences (Switzerland). 2021;11(11), 1–13. https://doi.org/10.3390/geosciences11110459

[11] George P. The Principles of Rock Weathering. Published by: The University of Chicago Press Stable. 1896. https://www.jstor.org/stable/30054908

[12] Afifi AA, Bricker OP. Weathering reactions, water chemistry and denudation rates in drainage basins of different bedrock types: I - sandstone and shale. Dissolved Loads of Rivers and Surface Water Quantity/Quality Relationships. Proc. Hamburg Symposium, 1983; 141, 193–203.

[13] Tchistiakov AA. Effect of flow rate and salinity on sandstone permeability. Proceedings of Geothermal Conference Basel, Switzerland. 1999; 28-30 Sept 1999, 2.

[14] Wu B, Tan CP. Effect of water-cut on sandstone strength and implications in sand production prediction. In DC Rocks. 2001; the 38th U.S. Symposium on Rock Mechanics (USRMS) (p. ARMA-01-0027).

[15] Winkler EM. Natural Deformation of Rock and Stone. In: Stone: Properties Durability in Man's Environment. Applied Mineralogy/TechnischeMineralogie. 1973; vol 4. Springer, Vienna. https://doi.org/10.1007/978-3-7091-4120-5_3

[16] Baud P, Zhu W, Wong T. Failure mode and weakening effect of water on sandstone. Journal of Geophysical Research. 2000; 105, 371–389. Available from: https://agupubs.onlinelibrary.wiley.com/doi/pdf/10.1029/2000JB900087

[17] Özarslan A, Köken E. Effect of Water on the mechanical properties of sandstone and siltstone rocks. New Glass. 2015; 21(3), 41–46. Conference: 5th Aachen International Mining Symposium- Mineral Resources and Mine Development, AIMS 2015 At: Aachen. Available from: https://www.aims.rwth-aachen.de/wp-content/uploads/2015/05/Abstractvolume.pdf

[18] Duda M, Renner J. The weakening effect of water on the brittle failure strength of sandstone. Geophysical Journal International. 2013; 192(3), 1091–1108. https://doi.org/10.1093/gji/ggs090

[19] Watsantachad N. Scholarly Commons Theses (Historic Preservation) Graduate Program in Historic Preservation an Investigation of Sandstone Consolidation Method for the Northern Gopura of the Phimai Sanctuary, a Khmer Monument in Thailand. 2001. http://repository.upenn.edu/hp_theses/521

[20] Molina E, Benavente D, Sebastian E, Cultrone G. The influence of rock fabric in the durability of two sandstones used in the Andalusian Architectural Heritage (Montoro and Ronda, Spain). In Engineering Geology 2015; vol. 197, pp. 67–81. https://doi.org/10.1016/j.enggeo.2015.08.009

[21] Ghobadi M H, Babazadeh R. Experimental Studies on the Effects of Cyclic Freezing–Thawing, Salt Crystallization, and Thermal Shock on the Physical and Mechanical Characteristics of Selected Sandstones. In Rock Mechanics and Rock Engineering 2015; vol. 48, Issue 3, pp. 1001–1016. https://doi.org/10.1007/s00603-014-0609-6

[22] Sebastián E, Cultrone G, Benavente D, Linares Fernandez L, Elert K, Rodriguez-Navarro C. Swelling damage in clay-rich sandstones used in the church of San Mateo in Tarifa (Spain). In Journal of Cultural Heritage. 2008, vol. 9, Issue 1, pp. 66–76. https://doi.org/10.1016/j.culher.2007.09.002

[23] Salvatici T, Calandra S, Centauro I, Pecchioni E, Intrieri E, Garzonio C A. Monitoring and evaluation of sandstone decay adopting nondestructive techniques: On-site application on building stones. Heritage. 2020; 3(4), 1287–1301. https://doi.org/10.3390/heritage3040071

[24] Smith B J, Gomez-Heras M, McCabe S. Understanding the decay of stone-built cultural heritage. Progress in Physical Geography. 2008; 32(4), 439–461. https://doi.org/10.1177/0309133308098119

[25] Ahmed A A, Fogg G E. Journal of African Earth Sciences The impact of groundwater and agricultural expansion on the archaeological sites at Luxor, Egypt. Journal of African Earth Science. 2014; 95, 93–104. https://doi.org/10.1016/j.jafrearsci.2014.02.007

[26] Hemeda S, Fahmy A, Moustafa A, Abd Hafez M E. The Early Basilica Church, El-Ashmonein Archaeological Site, Minia, Egypt: Geo-Environmental Analysis and Engineering Characterization of the Building Materials. 2019; 157–186. https://doi.org/10.4236/ojg.2019.93011

[27] Ahmed EA. Investigation of environmental impacts on sandstone blocks at Luxor temple and concepts for conservation. 2016; 1 (1), 23–45. https://dx.doi.org/10.21608/jguaa2.2016.3893

[28] Hosny A, Ali S M, Abed A. Study of the 26 December 2011 Aswan earthquake, Aswan area, South of Egypt. Arabian Journal of Geosciences.2014; 7(11), 4553–4562. https://doi.org/10.1007/s12517-013-1098-8

[29] Khamies A A, El-Tarras M M. Surface and subsurface structures of Kalabsha area, southern Egypt, from remote sensing, aeromagnetic and gravity data. Egyptian Journal of Remote Sensing and Space Science. 2010; 13(1), 43–52. https://doi.org/10.1016/j.ejrs.2010.07.006

[30] Hamdan A M, Sensoy M M, Mansour MS. Evaluating the effectiveness of bank infiltration process in new Aswan City, Egypt. Arabian Journal of Geosciences, 2013; 6(11), 4155–4165. https://doi.org/10.1007/s12517-012-0682-7

[31] Elshazly E M, Abdel-Hady M A, El Ghawaby M A, El Kassas A. Geologic interpretation of ERTS-1 satellite images for West Aswan Area, Egypt, NASA. Goddard Space Flight Center, Work of the US Gov. Public Use Permitted. 1974. https://ntrs.nasa.gov/citations/19740022657

[32] Noweir AM, EL Ela AM, Abu Sewifi BM. New contributions to the geology, geochemistry and tectonic setting of the Aswan granites, southern Egypt. Qatar Uni. Sci. 1990; Bull. 10:395-419.

[33] Hamdan A M A, Rady A R A. Vulnerability of the groundwater in the quaternary aquifer at El Shalal-Kema area, Aswan, Egypt. Arabian Journal of Geosciences. 2013; 6(2), 337–358. https://doi.org/10.1007/s12517-011-0363-y

[34] Hamdan M A, Hassan F A. Quaternary of Egypt. 2020. https://doi.org/10.1007/978-3-030-15265-9_12

[35] Kucharek A. Gebel El-Silsila. UCLA Encyclopedia of Egyptology, Los Angeles. 2012. http://digital2.library.ucla.edu/viewItem.do?ark=21198/zz002c2fj3

[36] Nilsson M. Gebel El-Silsila: Field report from the Main Quarry. Journal of Intercultural and Interdisciplinary Archaeology. 2015; 0(02), 147–191. https://doi.org/10.11588/jiia.2015.02.29460

[37] Heldal T, Bloxam E, Storemyr P. Geology and Archaeology of the Ancient Silicified Sandstone Quarries at Gebel Gulab and Gebel Tingar, Aswan, Egypt. 2020. Available from: https://www.researchgate.net/publication/32894154_Geology_and_Archaeology_of_the_Ancient_Silicified_Sandstone_Quarries_at_Gebel_Gulab_and_Gebel_Tingar_Aswan_Egypt

[38] Khedr E S, Yousef A A E, AbouElmagd K, Khozyem H M. Tectono-stratigraphic subdivision of the clastic sequence of Aswan area, southern Egypt. Fifth International Conference on the Geology of the Tethys Realm, South Valley University, January2010; 197–216.

[39] UNESCO. Report on the safeguarding of the Philae monuments. Netherland Government. Netherlands Engineerings consultants Nedeco. Geological bureau vote. November. Netherland. 1960. Available from: http://link.library.missouri.edu/portal/Report-on-the-safeguarding-of-the-Philae/r8WLcAu2RHw/

[40]Paul GPM. The geography of the temple and tomb of Osiris in relation to the Rituals 1994; Ch. IV, n. 128. https://doi.org/10.1163/9789004283831_018

[41] Kamel S, Sabry Ghada H, Hassan F, Refat M, Abeer Abd A S, Doaa E, Hassan K, Rashed R. Architecture and Urbanism: A Smart Outlook Proceedings of the 3rd International Conference on Architecture and Urban Planning, Cairo, Egypt. 2020. https://link.springer.com/book/10.1007%2F978-3-030-52584-2

[42] Hall H R, Blackman A M. The Temple of Bigeh. The Journal of Egyptian Archaeology. 1916; 3(1), 63. https://doi.org/10.2307/3853598

[43] González G S, Sánchez C M. Differentiation of kaolinite from chlorite by treatment with dimethyl-sulfoxide. Clay Minerals. 1968; 7(4), 447-450. https://doi.org/10.1180/claymin.1968.007.4.08

[44] Bureau of Indian Standards. Method of Test for aggregate for concrete. IS 2386- Part III - Specific gravity, density, voids, absorption and bulking. 1963; New Delhi, (Reaffirmed 2002). Available from: https://law.resource.org/pub/in/bis/S03/is.2386.1.1963.pdf

[45] ASTM. C97/C97 M-18 Standard Test Methods for Absorption and Bulk Specific Gravity of Dimension Stone, ASTM International, West Conshohocken, PA,2018. www.astm.org

[46] Whitney D L, Evans B W. Abbreviations for names of rock-forming minerals. American Mineralogist, 2010; 95(1), 185–187. https://doi.org/10.2138/am.2010.3371

[47] Tucker M E. Sedimentary petrology: An Introduction to the Origin of Sedimentary Rocks. Oxford. Blackwell scientific publications. 1994. Available from: https://archive.org/details/sedimentarypetro0000tuck

[48] Krishnan R. Raman Spectrum of Quartz. Nature. 1945; 155, 452. https://doi.org/10.1038/155452a0

[49] Donnelly F C, Framont V, Cleary O, Dunne P W, Gun Y K. Synthesis of CaCO3 nano- and microparticles by dry ice carbonation. Chemical Communications. 2017; 53, 6657–6660. https://doi.org/10.1039/C7CC01420A

[50] Michaelian K H. The Raman spectrum of kaolinite #9 at 21C. Can. J. Chem. 1986. Available from: https://cdnsciencepub.com/doi/pdf/10.1139/v86-048

[51] Freeman J J, Wang A, Kuebler K E, Jolliff B. Characterization of natural feldspars by Raman spectroscopy for future planetary exploration. 2008. https://doi.org/10.3749/canmin.46.6.1477

[52] Lafuente B, Downs R T, Yang H, Stone N. The power of databases: the RRUFF project. In: Highlights in Mineralogical Crystallography, T. Armbruster and R. M. Danisi, eds. Berlin, Germany, W. De Gruyter, 2015;pp 1-30.

[53] Sherbiny E, Eng J M S, Sherbiny S A El, Amin S K. Journal of Material Sciences & Engineering Characterization and Use of Egyptian Nubian Sandstone in the Ceramic Tile Industry. 2012;1(2), 1–6. https://doi.org/10.4172/2169-0022.1000112

[54] Knox R W O B, Stadelmann R, Harrell J A, Heldal T. Mineral fingerprinting of Egyptian siliceous sandstones and the quarry source of the Colossi of Memnon. 2009; 77–85. Available from: http://www.ngu.no/upload/Publikasjoner/Special%20publication/SP12_s77-85.pdf

[55] Pope J. Figural Graffiti from the Meroitic Era on Philae Island. Edited by Geoff Emberling and Suzanne Davis Along the Nile and Beyond Kelsey Museum Publication 16 Kelsey Museum of Archaeology University of Michigan. 2019. August. Available from: http://exhibitions.kelsey.lsa.umich.edu/graffiti-el-kurru

[56] Stephenson J. People and Place. Planning Theory and Practice. 2010; 11(1), 9–21. https://doi.org/10.1080/14649350903549878

[57] Ozden C. The pontifex minimus: William Willcocks and engineering British colonialism. Annals of Science. 2014; 71(2), 183–205. https://doi.org/10.1080/00033790.2013.808378

[58] Biswas AK, Tortajada C. Impacts of the High Aswan Dam. Water Resources Development and Management. 2012; 379–395. https://doi.org/10.1007/978-3-642-23571-9_17

[59] Elsayed SM. Comparative study of different scenarios for the morphological evolution in a river stream. Masterthesis, Politecnico Di Milano, October 2013. http://hdl.handle.net/10589/82763

[60] Dijkstra J H F. Religious encounters on the southern Egyptian frontier in Late Antiquity (AD 298- 642). University of Groningen. 2005. Available from:https://research.rug.nl/en/publications/religious-encounters-on-the-southern-egyptian-frontier-in-late-an

[61] Liu X, Wu L, Zhang Y. Frequency properties of acoustic emissions from dry and saturated rock. Environ Earth Sci. 2019; 78**,** 67. https://doi.org/10.1007/s12665-019-8058-x

[62] Chen X, Feng W, Zhang G, Gao Y. Raman spectra of quartz and Pb4+-Doped SiO_2 crystals at different temperature and pressure. Crystals, 2019; 9(11), 1–9. https://doi.org/10.3390/cryst9110569

[63] Cai X, Zilong Z, Kewei L, Xueming D, Haizhi Z. Water-Weakening Effects on the Mechanical Behavior of Different Rock Types: Phenomena and Mechanisms. *Applied Sciences. 2019;* 9, 20: 4450. https://doi.org/10.3390/app9204450

[64] Sharaky A, Salem T, Aal A A. Assessment of Water Quality and Bed Sediments of the Nile River from Aswan to Assiut, Egypt. In A. M. Negm (Ed.), The Nile River (pp. 207–238). Springer International Publishing. 2017. https://doi.org/10.1007/698_2016_118

[65] Gomez-Heras M, Benavente D, Buergo M A De. The decay of stone based Cultural Heritage Soluble salt minerals from pigeon droppings as potential contributors to the decay of stone based Cultural Heritage. June 2004. https://doi.org/10.1127/0935-1221/2004/0016/0505

[66] Bläuer C. Weathering of Bernese sandstones. 5th International Congress on Deterioration and Conservation of Stone, Lausanne. 1985; 381-390. Available from:https://www.researchgate.net/publication/235330837_Weathering_of_Bernese_sandstones

[67] Fahmy A, Piernas E M, López J M, Bella S D. Salt weathering impact on Nero / Ramses II Temple at El -Ashmonein archaeological site (Hermopolis Magna), Egypt. *Heritage Science*.2022; 1–21. https://doi.org/10.1186/s40494-022-00759-6

[68] Ruedrich J, Bartelsen T, Dohrmann R, Siegesmund S. Moisture expansion as a deterioration factor for sandstone used in buildings. Environ Earth Sci. 2011; 63: 1545–64. https://doi.org/10.1007/s12665-010-0767-0.

Part II: Characterization of construction building materials in subaerial environments

3.3. Geoenvironmental investigation of Sahure's pyramid, Abusir Archeological site, Giza, Egypt

Abdelrhman Fahmy, Eduardo Molina-Piernas, Salvador Domínguez-Bella, Javier Martínez-López, and Fatma Helmi. 2022. "Geoenvironmental Investigation of Sahure's Pyramid, Abusir Archeological Site, Giza, Egypt". Heritage Science 10 (1). https://doi.org/10.1186/s40494-022-00699-1

3.4. Salt weathering impact on Nero/Ramses II Temple at El-Ashmonein archaeological site (Hermopolis Magna), Egypt

Abdelrhman Fahmy, Eduardo Molina-Piernas, Javier Martínez-López, and Salvador Domínguez-Bella. 2022. "Salt Weathering Impact on Nero/Ramses II Temple at El-Ashmonein Archaeological Site (Hermopolis Magna), Egypt". Heritage Science 10 (1). https://doi.org/10.1186/s40494-022-00759-6

3.5. Sand dunes movement and flooding risk analysis for the pyramids of Meroe, Al Bagrawiya archaeological site, Sudan

Abdelrhman Fahmy, Eduardo Molina-Piernas, Javier Martínez-López, and Salvador Domínguez-Bella. Sand dunes movement and flooding risk analysis for the pyramids of Meroe, Al Bagrawiya archaeological site, Sudan. (Under revision, submitted to International Journal of Architectural Heritage).

3.3. Geoenvironmental investigation of Sahure's pyramid, Abusir Archeological site, Giza, Egypt

Highlights

- Sahure’s pyramid casing stone is from limestone and the inner core is from sandy limestone.
- Geoenvironmental conditions affected on the pyramid's architectural, structural, and engineering stability.
- Mineralogical content in the construction materials was an intrinsic problem.
- Basaltic mortar as first trial for green concrete manufacturing in the Egyptian Old Kingdom, Fifth Dynasty was revealed

Abstract

Abusir is the name of an elaborate burial area in Egypt, dotted with 19 pyramids and other temples, stretching on the western side of the Nile from the south of the Giza Plateau to the northern rim of Saqqara. It seems to have been created as the resting site for the Pharaohs dated from 2494 to 2345 BC. The name Abusir, originally spoken as Busiri, means “Temple of Osiris”. Over time, the name has become so popular because more than 60 villages now carry this name, but only one is the archaeological site. This paper focused on one of its most important pyramids from the Abusir archaeological area, Sahure's pyramid, since it is one of Egypt’s little-known but heavily damaged treasures. Field and laboratory studies have been carried out to investigate and understand the durability problems and construction materials of this pyramid, leading to results that confirmed the impact of the geoenvironmental conditions on the pyramid's architectural, structural, and engineering stability. Moreover, the results showed that mineralogical content in the construction materials was an intrinsic problem due to the presence of swellable (expansive) clays, which are considered responsible for pyramid decay and damage. In addition to external factors such as the effect of temperature variations, rain, pollutants, wind, and earthquakes and their interactions with intrinsic building material defects. Finally, this paper revealed a new discovery for basaltic mortar as the first trial for green concrete manufacturing in the Egyptian Old Kingdom, Fifth Dynasty.

Keywords: Abusir archaeological site, Sahure's pyramid, geoenvironmental factors, petrological characterization, petrophysical properties, geochemistry, stone decay, sandy limestone, mortar.

1. Introduction

Studies on the impact of geoenvironmental conditions and how external agents affect construction materials are a recurring topic in new construction but are especially important in the materials of historical and archaeological heritage since its understanding will allow better preservation of this cultural heritage [1]. There are several previous studies on stone weathering; for example, Charola et al. [2] explained salt weathering for porous building materials and showed some related deterioration patterns on archaeological stone masonry because of environmental conditions such as fissures, granular disintegration, splitting in building materials, and salt efflorescence. Fitzner and Heinrichs [3] presented a study about weathering impacts on monumental stones and their forms and rates. In addition, they showed the nonvisible/nanoscale deterioration patterns of archaeological stones, visible deterioration in micro- and meso/macroscale-like mass loss, and structural stability. Grossi et al. [4] studied the effect of air pollution, salt weathering, and climate change on the durability of archaeological stones, showing that the blackening of the stones returned to high levels of sulfate deposition, diesel soot, and nitrogen deposition from vehicular sources around the archaeological buildings. Additionally, Figueiredo et al. [5] studied the degradation factors that affected some Roman archaeological buildings due to the effect of lichen exudates that led to observed physical and chemical alterations in granite. Sandrolini et al. [6] studied the environmental aggressiveness on historical stonework and the weathering patterns and rates using the material identification method and structural finite element modelling to identify the decay causes and outline the efficient restoration procedures. Khanlari et al. [7] showed the influence of freeze–thaw cycles on the mechanical and physical properties of archaeological sandstone and concluded that the pore size distribution plays an essential role in the resistance of sandstones during freeze–thaw cycles. Derluyn et al. [8] explained the damage of salt weathering on building materials and compared the damage of thenardite and halite salts. Additionally, they used high-resolution neutron radiography simultaneously to monitor the crystallization process and deformations. Their results showed that cracking occurred during the drying for the limestone samples due to halite, and no damage was observed during drying due to

thenardite. Hemeda [9] explained and studied the climate change risks on archaeological sites in Alexandria and their impacts on building materials and concluded that. In addition, Risdonne et al. [10] used analytical techniques to identify plaster surfaces and evaluate weathering byproducts. Moreover, Villacreses et al. [11] interpreted the impacts of environmental conditions on the mechanical stability and behavior of masonries, especially earth walls. Finally, Hatır et al. [12] determined very specific deterioration maps to identify and qualify the weathering forms in the archaeological sites.

Specifically, in Egypt, several studies have been carried out to study the effect of environmental conditions and climate changes on archaeological sites. For instance, in the Giza pyramid area, Emery [13] studied the weathering conditions on the Great Pyramid and revealed four types of limestone used to build it, such as gray hard dense limestone, soft gray limestone, gray shaly limestone, and yellow limy shaly sandstone. Furthermore, Hanafy and Holail [14] presented a diagnosis study of the middle Eocene "nummulite bank" of the Giza Pyramid Plateau and explained that the early diagenetic alteration of the rock matrix was followed by partial to complete dolomitization of the limestone matrix and nummulite grain. Reader [15] studied the weathering problems and erosion on Sphinx and presented a geomorphological study for Giza Necropolis. USAID of Egypt [16] presented an assessment report to study the environmental impacts on the Giza plateau and suggested a methodology for groundwater lowering. In addition, Gandah [17] studied and discussed the environmental impacts of rain, wind, and salts on the pyramid of Khufu and presented hypotheses for restoration and conservation. Zalewski [18] studied and gave us the opportunity to see the construction materials of the Great pyramid in his study through the petrography observations of the building stones. Finally, Hemeda and Sombol [19] studied and discussed the durability problems of the Great pyramids and the effect of subsurface and underground water on the stability of the pyramid.

In Saqqara necropolis, Madkour and Khallaf [20] explained the degrading process of the faience inside the step pyramid, and the results showed that salt crystallization from the wall support (Bedrock) was the main problem that generally affected the faience and the substructure of the pyramid. Kukela [21] studied the degradation patterns for the step

pyramid of Saqqara and showed isometric deterioration maps for the pyramid. Furthermore, Khalil et al. [22] showed the effects of strong ground shaking on the stability of the step pyramid and showed that there are many earthquakes in Greater Cairo with low magnitudes but with accumulative effects for the long term on the pyramid. Additionally, Rossi [23] utilized the advanced digital documentation method to monitor the area of the New Kingdom in Saqqara and showed the effect of wind, humidity, and temperature on the archaeological building. Finally, Ahmed [24] described the deterioration patterns for all faces of the step pyramid and showed the geoenvironmental challenges, such as earthquakes, over the step pyramid. In Dahshour necropolis, Hemeda et al. [25] studied the geoenvironmental impacts and structural problems on the northern pyramid of Snefru at the archaeological site. Often, there are no more studies that investigate the geoenvironmental problems and material characterizations at the Dahshour and Abusir archaeological sites. Accordingly, the present study is a significant study to investigate the durability and environmental problems of the construction materials of Sahure's pyramid at the Abusir archaeological site.

Of the sixty villages named Abusir in Egypt, only one is an archaeological site of first-class importance. It is located in the southern direction of the Giza Plateau and north of the Saqqara archaeological site and is considered one of the most enriched archaeological sites of the Memphis necropolis [26]. The ancient name of Abusir is called Busiri "the house or temple of the Osiris". It has a cemetery of the Fifth Dynasty kings, but its actual history is much older than the Fifth Dynasty because in the Early Dynastic Period (c. 3150 - c. 2613 BCE), it became a rapidly growing cemetery. In the south, close to the Early Dynastic cemetery in northern Saqqara, a rich upper-middle-class cemetery dating from the First and Second Dynasties was discovered at the beginning of the twentieth century by a German archaeological expedition directed by Hans Bonnet [27]. At the beginning of the 1960s, two Italian scholars, Vito Maragioglio and Celeste Rinaldi, contributed to the research on Abusir to make a survey for the site and provided us with rich information on the Abusir pyramids and development plans of the monuments [28]. At the same time, a Czech archaeological expedition started to work in this area, and in the mid-1970s, the Czech team transferred

its research to the not yet investigated southern area of the necropolis, and this institute is carrying out excavations at Abusir until now led by Miroslav Bárta [**29**]. Abusir was the only short-lived cemetery with pyramid complexes of three kings of the Fifth Dynasty: 1) Sahure; 2) NeferirKare; and 3) Niuserre [**30**] (**Fig. 3.3.1-a** and **b**). In 2015, Abusir was scanned and modelled by the Czech Institute of Egyptology and the Japanese team to document the NeferirKare pyramid with a 3D scanning laser and gave us 3D images for the pyramid to provide both qualitative and quantitative information for the pyramid and its preservation state [**31**].

Abusir is a sophisticated archaeological site with different kinds of building materials and pyramids. The preservation state of this site is extremely poor and forgotten. Sahure's pyramid has been affected by damage from various geoenvironmental impacts. In this sense, the durability and resistance of the pyramid decreased physically and mechanically (**Fig. 3.3.1-c** and **1-d**). For all these motives, the main aims of this paper are 1) to identify the geological and meteorological conditions related to this site; 2) to characterize the construction materials of Sahure's pyramid by means of geochemical, petrographical, and petrophysical approaches; 3) to evaluate the durability and vulnerability of the ancient construction materials of the pyramid; and 4) to present a proposal for scientific conservation and protection of the pyramid. To achieve all these aims, this study has carried out a hazard analysis for the construction materials of the pyramid utilizing different analytical and examination techniques of X-ray diffraction, X-ray fluorescence, and optical microscopy. In addition, the physical properties of the core building material of the pyramid are determined to confirm the environmental impacts on the physical properties of the construction materials used.

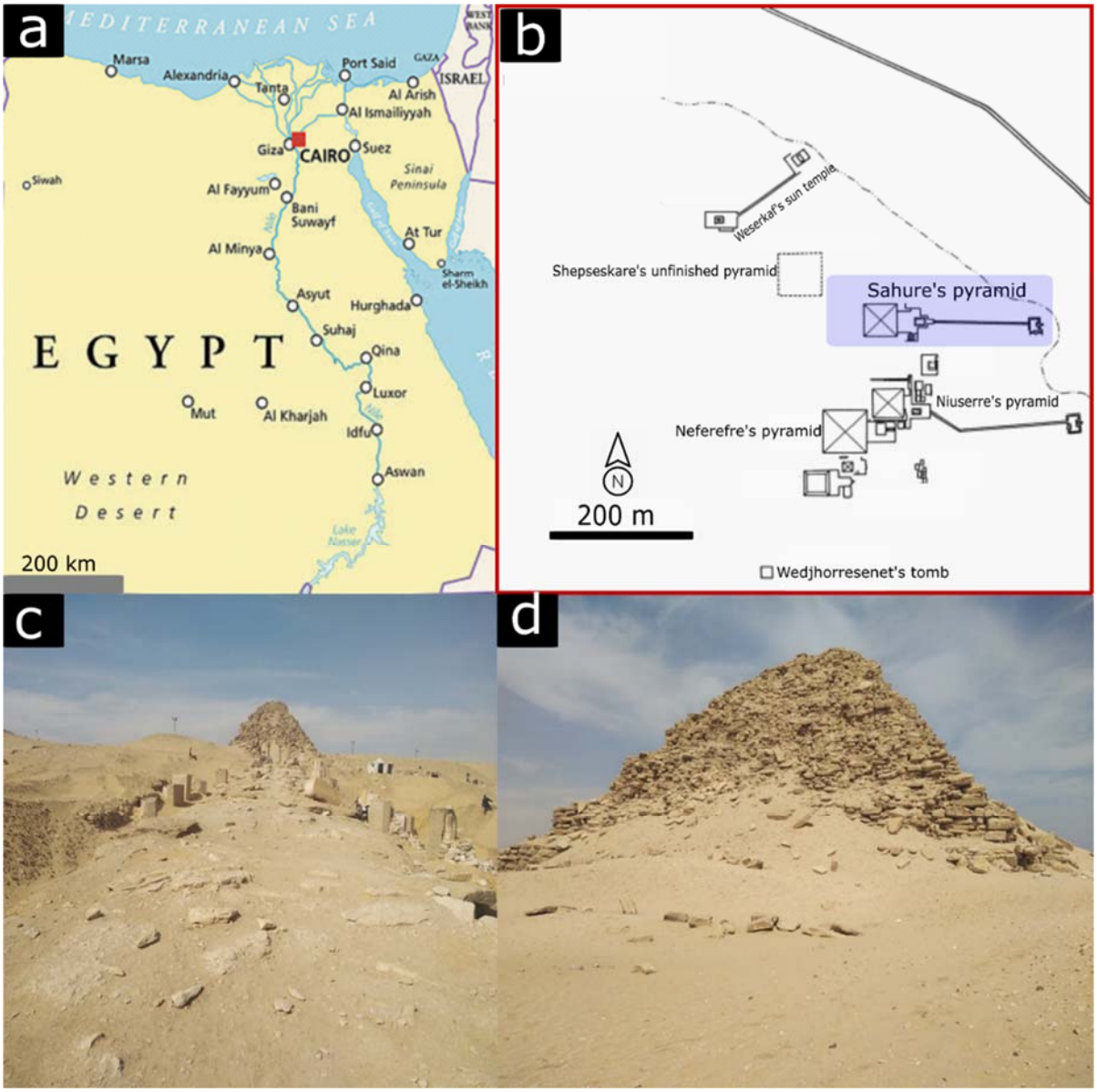


Fig. 3.3.1. (a) General map of Egypt and location of the Abusir archaeological site in Giza. (b) Pyramids at the Abusir archaeological site and specifically the Sahure's pyramid (edited after http://www.narmer.pl/map/abusir_en.htm). (c) General view of Sahure's pyramid from the causeway of the pyramid. (d) The preservation state of the pyramid.

2. Sahure's pyramid Context

2.1. Description of Sahure's pyramid

Sahure's pyramid is located on a hill, and the elevation from the valley temple adjacent to the Nile is approximately 20 m. It is relatively small because it has a base of approximately seventy-eight meters and rises to a height of forty-seven meters (**Fig. 3.3.2-a** and **b**). According to Verner [**32**], this pyramid was built using better quality stone and more diverse types than the pyramids of the Fourth Dynasty. For example, the base presents at least two layers of limestone, but it has not been excavated until now. Additionally, the core of the pyramid was composed of six steps of limestone jointed with mud mortar, and the entrance located to the north was cased in fine white limestone from Massara (**Fig. 3.3.2-a**). On the other hand, casing stone was built from massive limestone blocks with dimensions of 5×5.5×1 m, which were prepared and brought from the Tura and Massara quarries [**33**]. The same materials and quarries were the sources of the casing stones at Neferefre's (unfinished pyramid) and the Great Pyramid [**32**]. Meanwhile, the inner chambers of Sahure's pyramid were cased by using smaller blocks [**33**]. The core of the pyramid was packed with a rubble fill of limestone chips, pottery shards, sand, and clay mortaring [**33, 32, 34**]. This construction technique was performed to reduce the cost, effort, and time for pyramid construction. Additionally, the architects made a notable error in planning the base, causing the southeast corner of the pyramid to extend 1.58 m to the east [**32**] (**Fig. 3.3.2-b**).

Architecturally, the pyramid is surrounded by limestone, which is used for paving, but the mortuary temple is paved by basalt and is accessed from the temple's north and south sides with a tall courtyard and rounded enclosure wall 3.15 m thick [**35**]. On the other hand, the pyramid substructure access is found slightly above ground on the pyramid's north face [**32**]. A short descending corridor lined with granite leads into a vestibule [**34**]. In addition, the route and its walls are cased and guarded by a pink granite portcullis (**Fig. 3.3.2-a)** [**32, 36**]. The descending corridor is 4.25 m long with a slope of 24°48’ and has a passage 1.27 m wide and 1.87 m high [**34, 37**]. The corridor following is lined with limestone begins with a

slight ascent before becoming horizontal land lined with granite [34]. The ascending portion is 22.3 m long with a slope of 5°, while the horizontal section is 3.1 m long [37]. Finally, the burial chamber is a single chamber measured to be 12.6 m east–west and 3.15 m north–south [32, 34, 36].

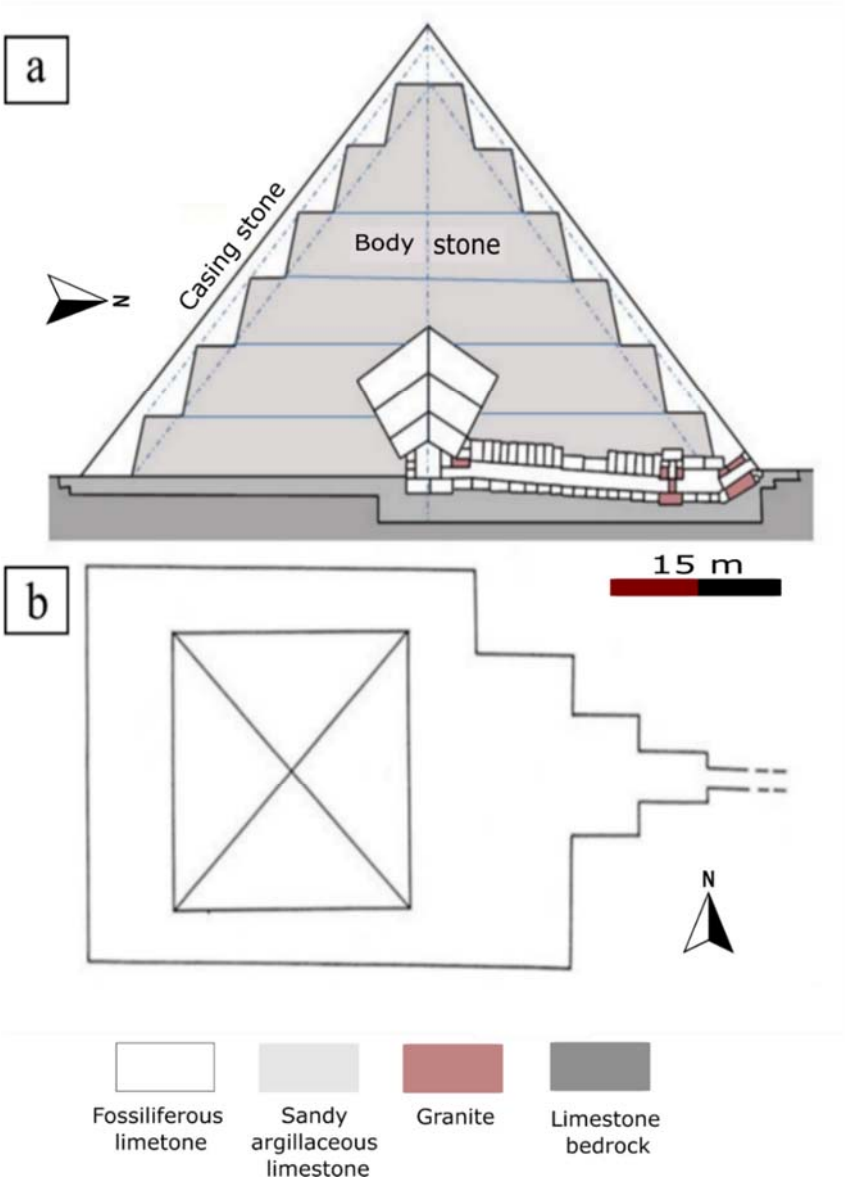
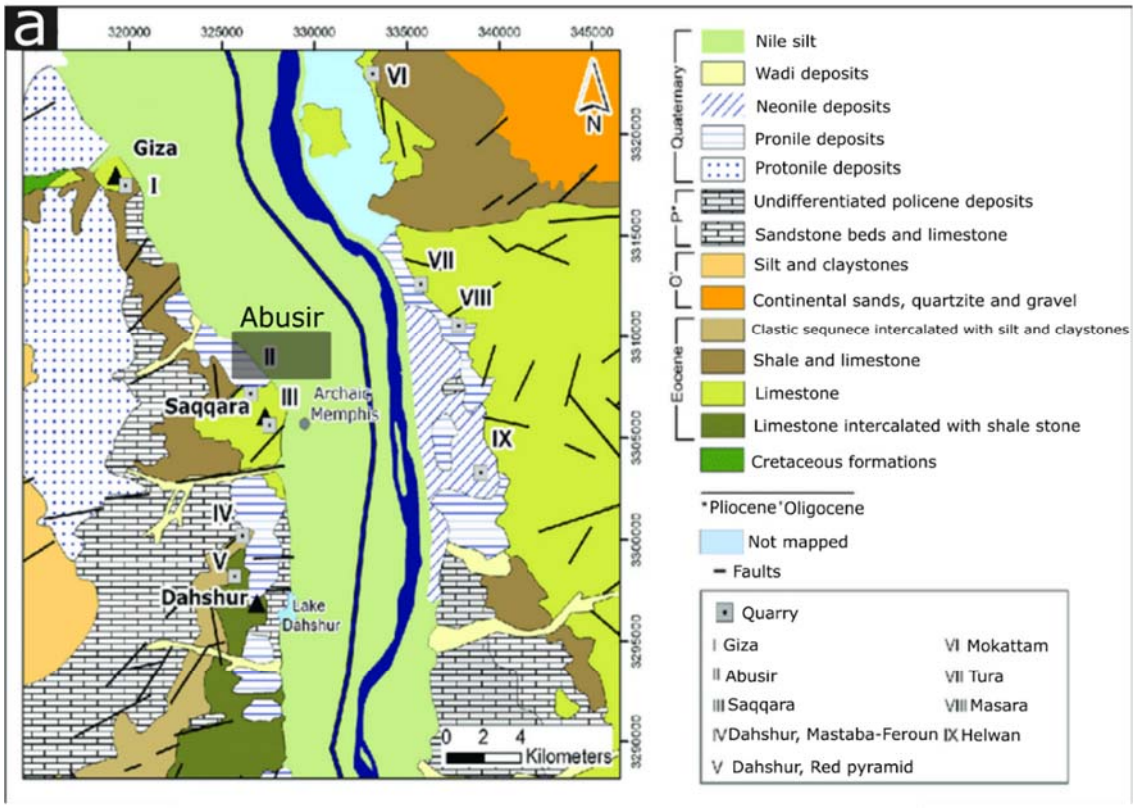
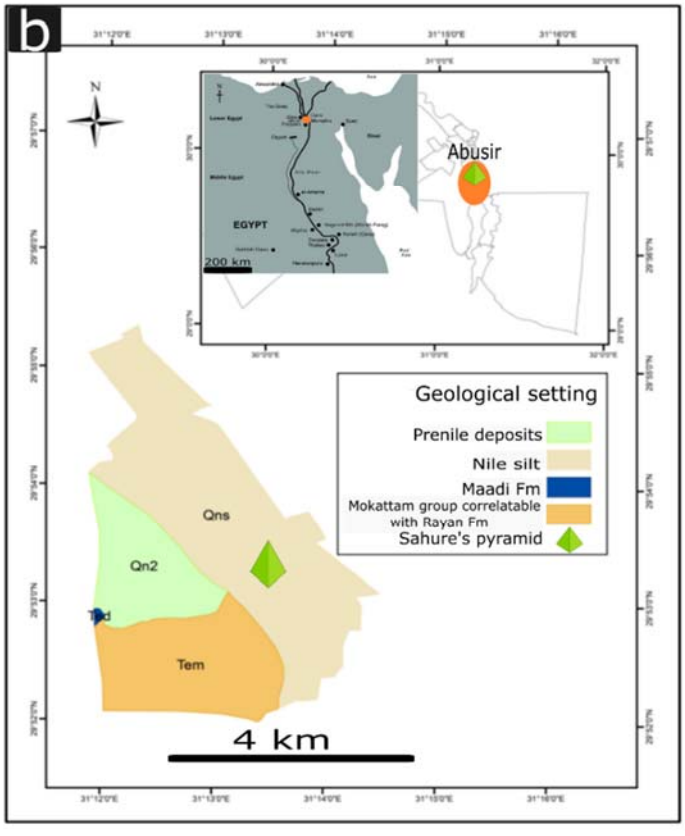


Fig. 3.3.2. (a) Cross section and (b) Plan of the Sahure's pyramid. The colors in cross-section represent the white fossiliferous limestone from the Tura quarry (casing stone, in white); the body of the pyramid made by laminated sandy argillaceous limestone (marl, in white gray); granite (casing for entrance and some parts in the corridor, in red); and bedrock from limestone (in dark gray). Edited after [35].

2.2. Geological context

Generally, the Memphis area consists of different geological features, such as Nile silts, which are located on the eastern and western sides of the Nile River and adjacent to the archaeological sites in Memphis, Wadi (Valley). In addition, deposits include neonile deposits, pronile deposits, undifferentiated pronile deposits, limestone intercalated with shale stones, and Cretaceous formations [**38**] (**Fig. 3.3.3-a**). Specifically, Abusir geological formations are considered from the Late Eocene, and Maadi limestone, clay-limestone, and marls crop out (tafla) (**Fig. 3.3.3-a** and **b**). The upper member of the Maadi Formation (blue legend, **Fig. 3.3.3-b**), which is connected to the Abusir area, is developed mostly as porous brown sandy limestone in-tempestite facies [**38**]. According to Bebermeier et al. [**39**], ancient settlements are covered by more than 7 meters of alluvial and aeolian deposits. These formations of Mokattam (**Qn2, Fig. 3.3.3-b**) and Maadi are repeatedly intercalated with fossils such as oysters, nummulites, and shale or sandy shale. Moreover, Bebermeier et al. [**39**] said that the fluvial sediments belonging to a former river system called prenile deposits (**Qns, Fig. 3.3.3-b**) occupied the present-day Nile basin in the early Pleistocene. In the middle Pleistocene, the prenile deposited fluvial sediments (**Qn2**, **Fig. 3.3.3-b**) east of the (Qns) deposits, closer to the present-day floodplain of the river Nile. These sediments (Qns and Qn2) were deposited directly on top of Eocene bedrock. Sahure's pyramid is located on the Nile silts (Qns), which reflects the geotechnical problems of the pyramid from the beginning of the construction due to the clay to claystone base (**Fig. 3.3.3-b**).





(Caption in the next page)

Fig. 3.3.3. (a) General geological map of the Memphis area and (b) a simplified geological map of the Abusir area. As shown in the legend, the pyramid is connected to the Mokattam formation and Maddi formation. Sahure's pyramid is located on Nile deposits/silt that was deposited directly to cover the Eocene bedrock. Edited after [**39**].

2.3. Stone quarries and pyramids construction materials

Generally, ancient Egyptians exploited approximately 200 quarries (**Fig. 4**) as sources of different kinds of stones, which were used as architectural, ornamental, and structural elements to build their temples, tombs, and pyramids from the predynastic era to the late Roman period, but limestone and sandstone were the dominant building materials for their buildings [**40, 41**]. In fact, most of the limestone blocks used by ancient Egyptians were brought from Tertiary formations, mainly Eocene, Paleocene, and Pliocene. In addition, some limestone building materials were from the Quaternary age. On the other hand, most of the sandstone blocks were prepared from Cretaceous Nubian formations [**40-42**]. Specifically, the stones and joint materials (mortars) of the pyramids are important and interesting to reveal much information related to ancient technology and their sustainability [**25**]. Pyramids were built from different kinds of stones, such as limestone, sandstone, sandy limestone, basalt, and granite. Cutting and preparation of stones from different quarries were an important process as the primary step for preparations of blocks of pyramids using different kinds of tools and techniques, such as using dolerite and crushed quartzite with sands in polishing of the stone surfaces [**43**] (**Fig. 3.3.4**).

Ancient Egyptian architects depended on different kinds of stones based on their quality, and they exploited dozens of quarries to extract different materials (**Fig. 3.3.4,** gray squares). For that, they used high-quality limestone in the pyramid's casing and its internal chambers [**44**]. Additionally, they used granite in the casing of the internal chambers, corridors, and bases. In addition, they used basalt in the pavements for mortuary temples for the pyramids, which represents approximately 20% of the pyramid construction. On the other hand, the remaining 80% approximately corresponds to the core part of the pyramids

and was brought from local quarries, such as those placed in the Giza Plateau, Abusir, Saqqara, and Dahshour [**25, 45, 44**]. Tura and Massara quarries (**Fig. 4**, red circle) were the main places to extract high-quality limestone types that had been used as casing stones for the pyramids and their elements. In addition to the tombs and temples. Both quarries are located near Cairo on the eastern bank of the Nile from pyramids [**46**]. The Widan El-Faras quarry (**Fig. 4**, yellow circle), in the northern Fayoum, was the source of the basalt stones for the pavements of mortuary temples from the Old Kingdom. This stone was used on the floor of the mortuary temple of the pyramid with a height of 0.4 m, width of 25 m, and length of 15 m [**47**]. The local quarry of Abusir and the surrounding area was the source of the core building material of Sahure's pyramid that is adjacent to the local quarry of Saqqara and Dahshour archaeological site as sources of their pyramid core stones (**Fig. 4**, blue circle). Additionally, to reduce the huge mining work to extract the stone blocks from the local quarry, they used the geomorphological structures and beds to be part of Sahure's pyramid, such as the causeway that connects the valley temple and mortuary temple of the pyramid [**39**].

2.4. Geoenvironmental context

Egypt is a country susceptible to climate change and geoenvironmental hazards such as sea-level rise, in addition to an increase in the intensity and frequency of temperature, wind (with sand and dust storms), heavy rains, and flash floods [**48, 49**]. Many geoenvironmental conditions affect the area of Abusir, especially temperature fluctuations, strong winds, and humidity. These environmental factors lead to physiochemical and mechanical damage to the structural materials and result in partial or total decay and collapse in some parts of the pyramids.

Recent analyses of the current climatic tendency reveal a warming trend in recent decades in Egypt, with average temperature increases of 1.4 °C and 2.5 °C projected by 2050 and 2100, respectively [**50**]. In this sense, climate change has been notable for the last ten years and has had a risky impact on archaeological building materials, such as the thermal stress effect that leads to accelerated decay in stone construction materials. Moreover, the

variation in temperature causes changes in material volume, especially when material deformations occur heterogeneously, which leads to differential strains in the stone body [51].

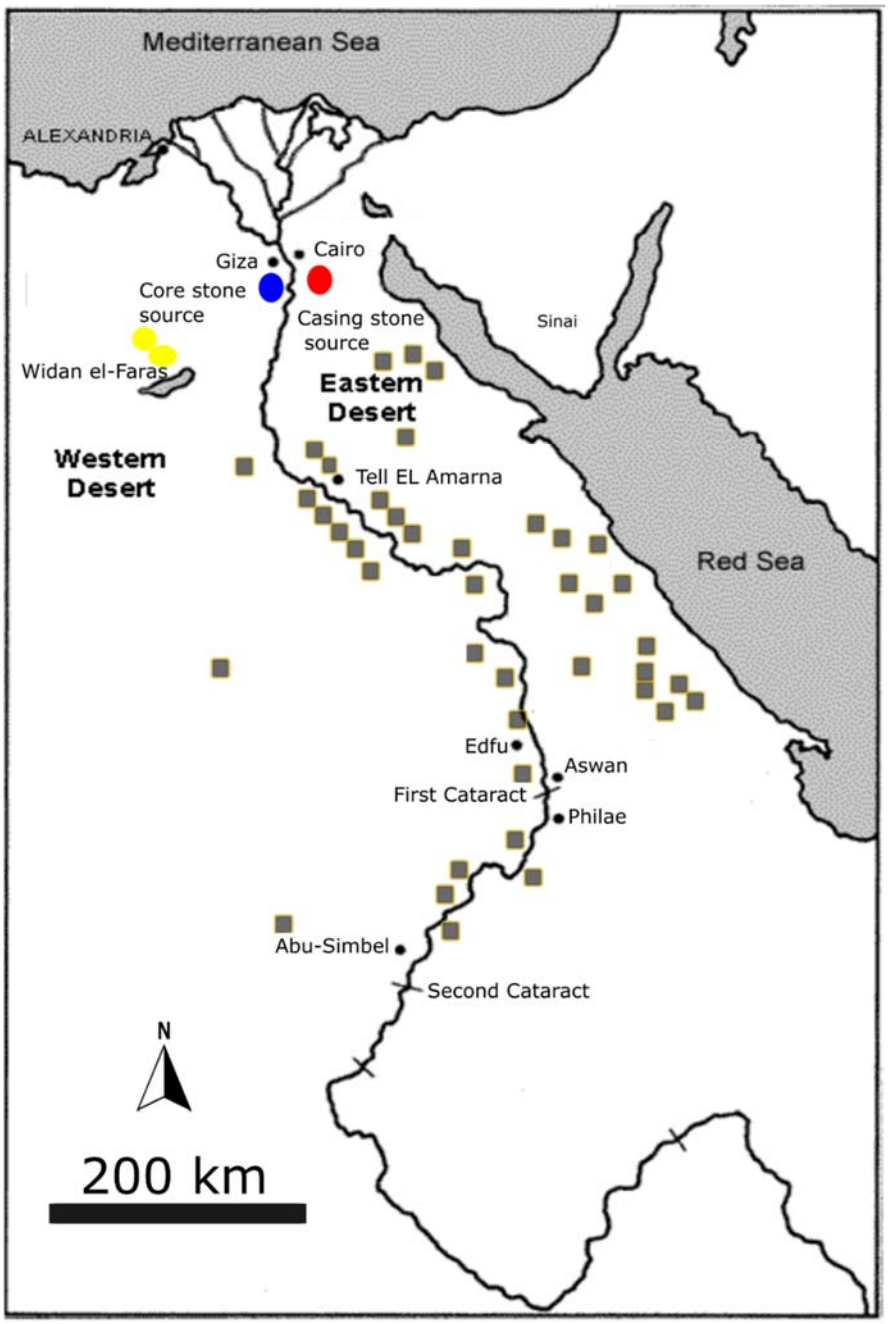


Fig. 3.3.4. Map of ancient Egyptian quarries (gray squares). The yellow circle refers to the Widan El-Faras quarry, the red circle refers to the Tura and Massara quarries as the source for casting blocks, and the blue circle is the local quarry of the Abusir site as the source for core blocks.

From the readings and recordings for meteorological data in Giza, meteorological Station ID: EGE00147729, it is noticed that the warmest month of the year is July, with an average temperature of 27.5 °C and an average annual temperature of 14.5 °C. On the other hand, the driest month is May with 0 mm, and the wettest month is January (4 mm) (https://en.climate-data.org). Moreover, rainfall is considered rare, with an annual average of 12 mm. However, rainwater, as concentrated in the northern part of the country, is between 150 and 200 mm and decreases gradually to the south, reaching approximately 24 mm. Meanwhile, rainfall on the Mediterranean coastal strip decreases eastward from 200 mm/year at Alexandria to 75 mm/year at Port Said. It also declines inland to approximately 25 mm/year near Cairo and 1 mm/year at Aswan. Moreover, significant intensities of rainfall are recorded on parts of the Red Sea coast. In addition, humidity ranges between 70 and 72% in the northern part of Egypt during the summer months and reaches 13% in the southern part of the Nile valley at Aswan [**52**].

Additionally, Egypt experiences dust storms in spring and early summer, with dry and windstorms usually arriving in April but occasionally occurring in March and May. The winds flow in low-pressure areas in the Isthmus of Suez and sweep across the northern coast of Africa, reaching high velocities. In addition, they carry large quantities of sand and dust from deserts that extend strongly from the red sea and Nile River to the Mediterranean Sea and from the north-northeast to south-southwest with large amounts of sand and dust (**Fig. 3.3.5-a-d**). These sandstorms, often accompanied by winds of up to 140 km, can cause temperatures to rise as much as 20°C in two hours and may blow continuously for three or four days at a time, followed by an inflow of much cooler air [**53**].

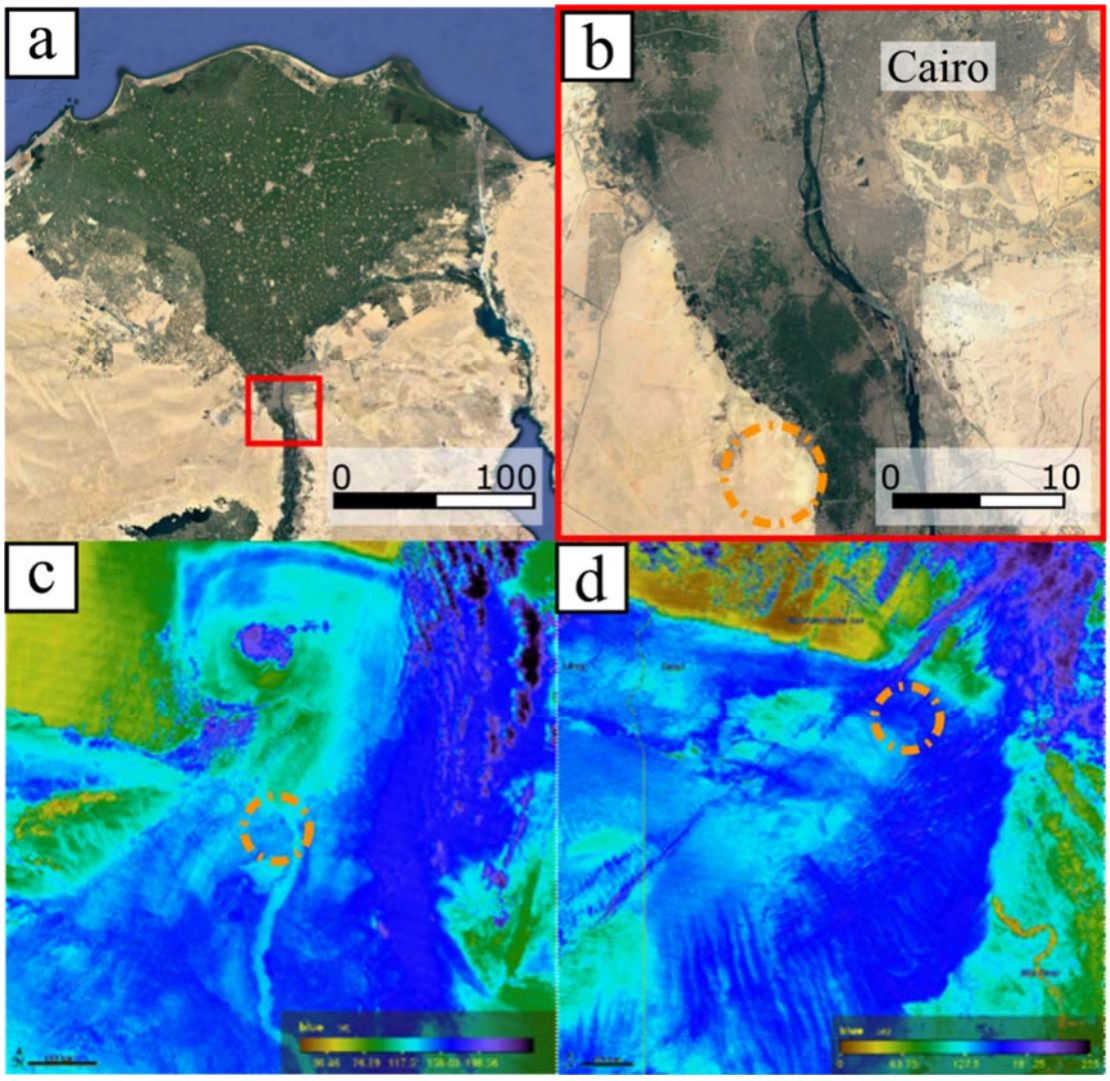


Fig. 3.3.5. (a) General map of Egypt, where the red square marks the Abusir zone, referring to the Abusir archaeological site in an orange circle (b). (c) The treated satellite image on the NASA Terra satellite (May 2010) explains the dust and sandstorms over Egypt spirally in blue, which extends strongly from the red sea and Nile River to the Mediterranean Sea. The amount of sand and dust thickly exists and results in the total hiding of the land surface below (edited after https://earthobservatory.nasa.gov/images). (d) The treated satellite image from the NASA Terra satellite (April 2012) explains the dust and sandstorms in blue, which extends strongly from north-northeast to south-southwest. The amount of sand and dust is high, resulting in the total hiding of the land surface below (edited after https://earthobservatory.nasa.gov/images).

Air pollution is considered one of the environmental factors and challenges that affects the stones of Sahure's pyramid because it causes chemical weathering of the construction materials and thick black crust over the stone surfaces [**54**]. In Giza, it is noticed that from September to November, the number of pollutants decreases. On the other hand, in the season of wind, when the sky is strongly dark and strongly dark from March to May, the number of pollutants increases, such as carbon monoxide, nitrogen oxides, ozone, and sulfur dioxide [**55**].

2.5. Intrinsic factors

Intrinsic factors are defined as the internal problems of the construction materials, which are related to the chemical, physical and mechanical properties of the stones, and intrinsic problems are also related to the interaction between the environmental conditions and the intrinsic properties of the pyramid construction materials. Both intrinsic agents and geoenvironmental agents work together in pyramid stone decay. For example, gypsum salt is detected by means of chemical analysis in the weathered casing limestone of the pyramid due to the reaction between sulfate pollutants and carbonate to produce gypsum [**56**]. In this sense, and from in situ visual and macroscopic examinations, it is noticed that the fabric of stone is full of impurities and stained areas with yellowish spots, which reflects the weakness of the construction materials of the pyramid.

The main composition of the pyramid construction is yellowish sandy limestone as a core building material and white limestone as casing building material. Therefore, calcite is a common mineral in construction materials and is always exposed to variable and severe environmental conditions, such as humidity, pollutants, and heavy rains; accordingly, calcite is dissolved in water and reacts with outdoor pollutants [**57**]. Additionally, the decay of the pyramid stones occurred due to the incompatibility in physical and mechanical properties between the casing and core stones, especially during their differential reaction with environmental conditions [**57**]. Core stones were quarried from the Abusir local quarry, and the natural beds are characterized by high porosity and inhomogeneity. On the other hand, the casing stones are characterized by very low porosity and homogeneity [**44**], which reflects the extent of the difference in the physical properties between these two kinds of

construction stones. Therefore, the environmental interactions will affect them differently and accelerate the rate of construction material decay.

2.6. Geodynamic factors

Egypt was exposed to many historical earthquakes that were recorded and reported from 2200 BCE to 1899 AD. Most of the earthquake epicenters were located in Cairo, and the damage from earthquakes affected Cairo, the Nile Delta, and the Nile valley. For example, in 520 AD, a large one happened, and many cities and villages were swallowed up [**58**] (**Table 3.3.1**). In 1992, Memphis pyramids were affected by the Dahshour earthquake with an estimated magnitude of 5.3 and depth of 30 km. Thus, geotechnical problems were observed, such as soil settlement and the settlement estimated in some villages at 1.75 km. Accordingly, the most common damage patterns for the buildings were the complete collapse, separations of the buildings, and diagonal cracks [**59, 60, 61**]. Other important examples of earthquake damage can be found in the northern pyramid of Snefru, where structural damage appeared, such as longitudinal structural cracks in the internal chamber [**25**]. In addition, both the Dahshour and Aqaba earthquakes caused partial collapse of the pyramid step [**22**]. Finally, earthquakes also affected the Abusir archaeological site and its pyramids because it is very near the Dahshour site. Accordingly, limestone enclosure walls of the shaft tomb of Udjahorresnet at Abusir were damaged and crumbled [**62**]. In addition, Sahure's pyramid was damaged, and many features of structural damage that resulted from the earthquakes were monitored.

Table 3.3.1. Examples of historical earthquakes with their approximate latitudes and intensities. Edited after [**58**].

Date	Lat. E	Intensity (MMI)
2200 BC	30.75 (Tell Basta)	VII (destructive)
39 AD	30.20 (Northern Egypt)	VI (very strong)
520 AD	31.00 (Northern Egypt)	VII (destructive)
885 AD	30.10 (Northern Egypt)	VII (destructive)
1847 AD	29.50 (Northern Egypt)	VIII (very destructive)

3. Materials and methods

3.1. Materials

Some fragments of limestone (casing stone) and sandy limestone (core stone) (**Fig. 3.3.6-b**) were collected for analysis from the original quarries (**Fig. 3.3.6-a**, red circle) to use in the analysis and identification of physical properties. Highly weathered fallen parts were collected for analysis and examination purposes (**Fig. 3.3.6-a**, blue circle). In this sense, samples taken from the quarry are referred to in the text as "unweathered", while those taken from the fallen blocks of the pyramid are called "weathered". Finally, a fragment of mortar was taken from highly weathered fallen parts for its analysis and investigation (**Fig. 3.3.6-c**).

3.2. Methods

3.2.1. Visual and morphological description

Visual examination was carried out to collect information about the construction materials to identify the specific problems of the different construction materials of the pyramid. Additionally, the morphological examination was performed by using a digital microscope (USB digital microscope with stand), magnification between 20-400x, and equipped with a digital camera 1.3 Mpx. In addition, some in situ visits and field work were made to record all problems of the pyramid, structural deficiencies, documentation, and geoenvironmental analysis.

3.2.2. Mineralogical characterization

A polarized light microscope (PLM) was carried out in the central lab of the Egyptian General Authority of Mineral Resources as a mineralogical and petrological analysis for stone samples. It has been used to identify the minerals and to specify the alteration processes of these minerals because of the geo-environmental effects on the building materials of the pyramid. X-ray diffraction (XRD) was utilized to identify the mineralogical content of the core stone, unweathered and weathered casing stone, and basaltic mortar. For that, a few grams of the samples were ground in an agate mortar, and the powders were analyzed using

an PW-1480 X-beam diffractometer with the following conditions: CuK_{α} radiation, goniometer speed 2θ = 1 degree/min at a steady voltage 40 kV and 30 mA.

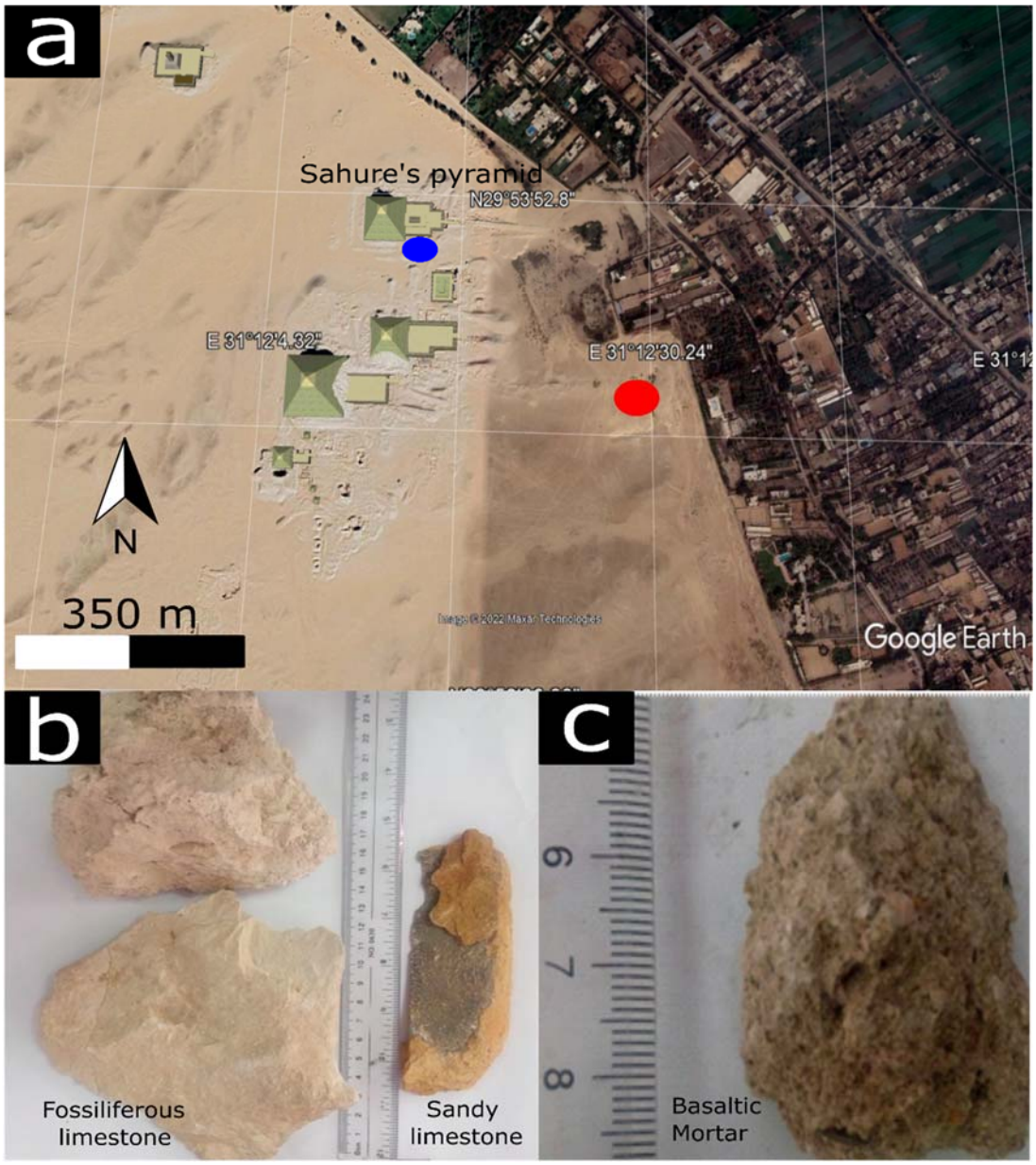


Fig. 3.3.6. (a) Image from Google Earth map showing the representative sampling areas for the construction material of the pyramid near Abusir village. The red circle refers to the local quarry from which the core blocks of the pyramid were extracted, and in the blue circle, the place where some fragments were collected from fallen and highly weathered fragments/samples. These fragments represent the fossiliferous limestone as casing stone and sandy limestone as core building material (b) and the mortar fragment (c).

On the other hand, the clay fraction was carried out throughout the separation process for clay minerals from core stone. Accordingly, a few grams of core stone powder were prepared and admixed in a solution with 1000 ml of distilled water and 100 ml of acetic acid, followed by stirring the mixture for 20 minutes every day until no reaction was observed. The clay fraction was collected on three glass slides for analysis. The first slide was considered an oriented untreated aggregate, the second slide was treated using dimethyl sulfoxide, and the third slide was thermally treated at 550 °C for 2 hours.

Chemical characterization was carried out by means of X-ray fluorescence (XRF) in the Central Laboratory of Egyptian General Authority of Mineral Resources as an elemental analysis for the stone samples to identify the major and minor elements. Elemental analysis was carried out using an X-ray fluorescence spectrometer on pressed powder pellets to determine the bulk chemistry.

3.2.3. Physical properties

To determine the petrophysical properties, such as specific gravity, apparent density, water absorption, moisture content, and porosity, nine cubic samples were prepared from local sandy limestone at the Abusir archaeological site at 5x5x5 cm. The samples were weighed naturally after drying at 105 °C, and then the samples were saturated in water to determine the natural weight, dried weight, and saturated weight.

Petrophysical testing was measured and calculated according to IS: 2386 (Part III) [**63**] and ASTM C97 [**64**]. The moisture content (MC) of the stone was expressed as a percentage by subtracting the dried weight of the stone from the natural weight and then dividing them by the dried weight according to the formula MC = ($weight_{wet}$–$weight_{dry}$)/$weight_{dry}$×100) [**65**]. In addition, water absorption (WA) is expressed as the percent weight change due to absorbed water and calculated according to the formula WA = ((M_{wet}–M_{dry}) /M_{dry}×100%). Moreover, the density (D) of the stone indicates the unit weight of the stone and is calculated by dividing the mass up the total volume of the stone according to the formula D = m/v [**66**]. Furthermore, unit weight (UW) was calculated by the gravitational force on a mass and is represented by the formula UW = m×g, where weight can be g×mm/s^2. In addition, Specific Gravity (SG) is the ratio of the density of the stone to the density of water,

and the specific gravity of natural stones ranges from 2 to 3 and is expressed as SG = ($\rho_{substance}/\rho_{H2O}$). Finally, the porosity (Po) is a measure of void spaces inside stones and was measured according to the formula Po = V_V/V_T [**67**].

4. Results

4.1. In situ investigation

Field observations were carried out to evaluate the current state of preservation, photographing, and recording for all deterioration patterns due to the effect of both geoenvironmental and internal (stone properties) deterioration factors. Remarkable structural deformations and damage have been observed, and they were recorded, such as total separation and collapse of casing stones, wall crumbling, and structural damage. The damage has occurred because of the accumulative effects of historical and recent earthquakes with wind stresses (**Fig. 3.3.7-a** and **b**). Visually, the main forms of decay are exfoliation, delamination, scaling, powdering and alveolarization due to wind, wet-dry cycling, rain, and pollution conditions (**Fig. 3.3.7-c, d, e,** and **f**, respectively). Moreover, the degradation form of detachment/layering on construction materials is due to daily exposure to thermal and cooling cycling, which causes the expansion or contraction/shrinkage of minerals of the stone and finally leads to laminations and layering patterns [**68**].

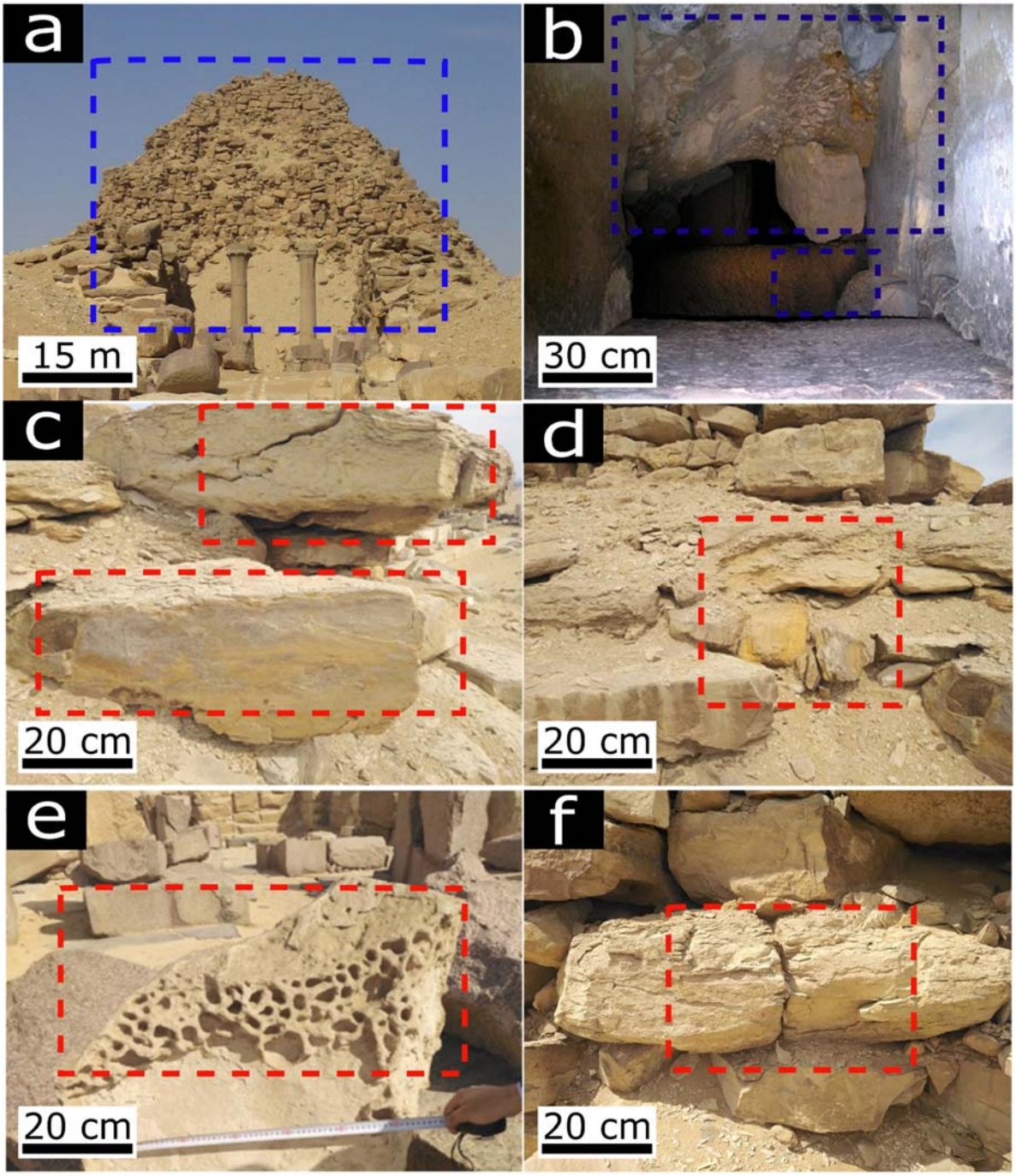


Fig. 3.3.7. Features of damage and degradation of Sahure's pyramid building materials. (a) Collapsed blocks from core and casing stones due to earthquakes and environmental impacts (blue rectangle). (b) Structural cracks and crumbling of stone blocks due to earthquakes (blue rectangle). (c) Exfoliation and detachments of the stone blocks (red rectangle). (d) Scaling, powdering, and differential weathering of sandy limestone blocks (red rectangle). (e) Alveolar weathering. (f) Weakening and splitting of stone blocks.

4.2. Macro and microscopic description

A digital microscope was used for the morphological description of the core and casing building stones, as well as the mortar, to study their morphological and textural features, as well as to identify and reveal the deterioration sources and patterns.

The core stone (sandy limestone, **Fig. 3.3.8-a** and **b**) texture of the pyramids is very fine to fine-grained. The stone is laminated due to relative variation in mineral composition and grain sizes and orientations, which reflects the differential behavior towards the geoenvironmental impacts, and this is considered one of the intrinsic problems of the stone body. Some irregular pore spaces and microcracks were detected with a considerable amount of sand grains inside the fractures. Black crusts were observed on the surfaces of stone, and some salts (possibly gypsum) partially fill the pores of the stones as well as cover some areas on the surfaces.

The unweathered casing stone (fossiliferous limestone) of the pyramid is a very white stone (**Fig. 3.3.8-c**), with microveinlets filled by calcite and quartz, and comb texture is observed in some of the microveinlets (**Fig. 3.3.8-d**). On the other hand, the surface of the weathered casing limestone presented a honeycomb texture due to the dissolution of the carbonate matrix and the production of pores over the surface (**Fig. 3.3.8-e** and **f**).

The mortar sample was examined and showed a fine- to coarse-grained texture, composed of numerous mineral grains, mainly quartz, and rock fragments spread in a very fine-grained matrix (**Fig. 3.3.8-g**). Regarding the rock fragments used as sand (grains), apart from quartz and some limestone fragments, others were observed with a very dark color, black to greenish. This color and the crystalline appearance suggest that these fragments may be basaltic rocks (**Fig. 3.3.8-h**)**.** Finally, significant irregular interparticle pores were detected in the sample.

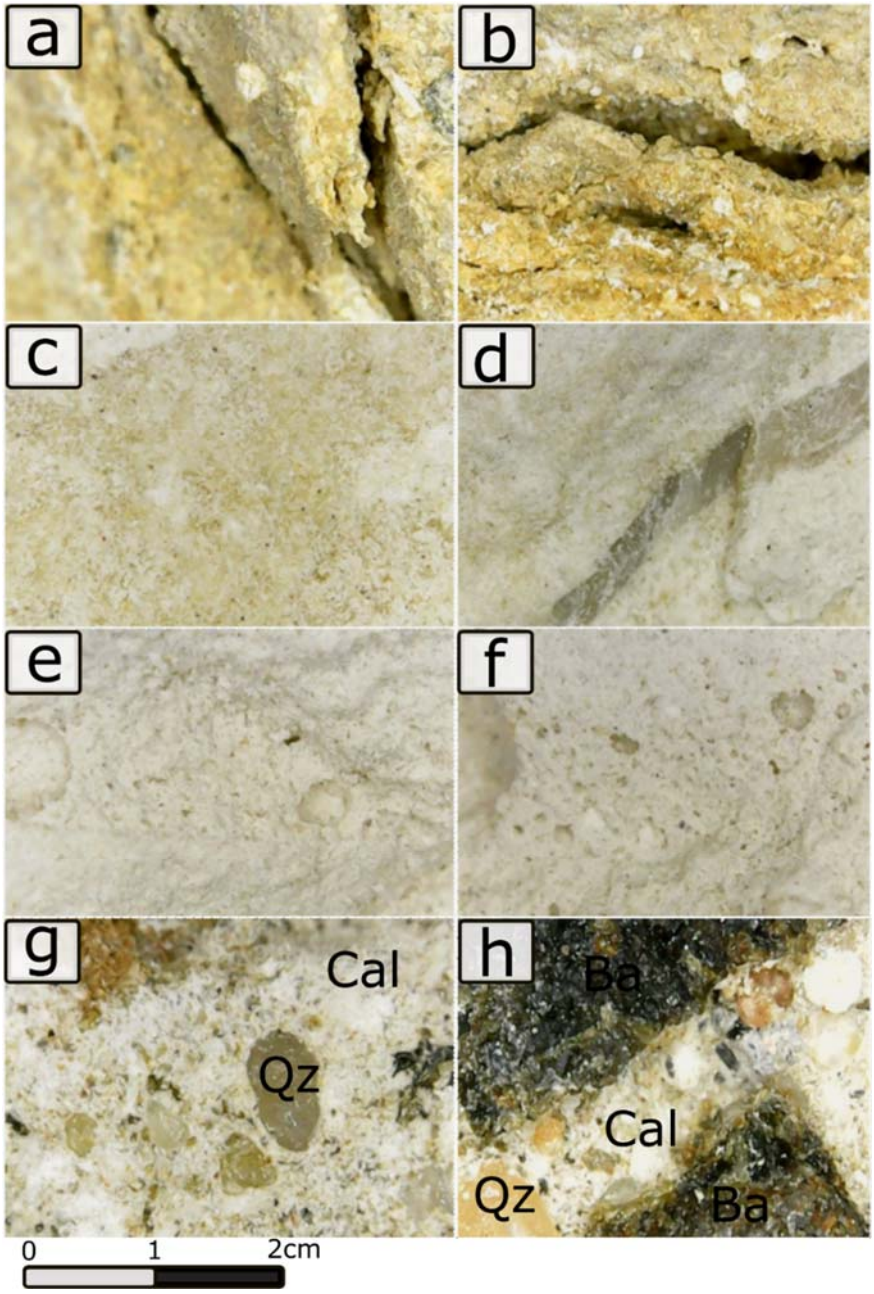


Fig. 3.3.8. Microphotographs under the digital microscope for the construction materials of Sahure's pyramid. (a and b) Core stone, grains of quartz admixed with calcite, fractures, laminations, and microcracks are detected. (c and d) Unweathered casing limestone is a very white stone, microveinlets filled with calcite and quartz are observed, and comb texture is observed in some microveinlets. (e and f) Weathered casing limestone of the pyramid with clear irregular pore spaces present in the carbonate matrix of the stone and comb texture is observed. (g and h) Sample of mortar with a significant number of

microfossils and fossil fragments are observed in the carbonate samples and in the groundmass, and several irregular interparticle pores are detected in the mortar. Legend: Cal (calcite), Qz (quartz), and Ba (basalt rock fragments).

Under the polarizing microscope, the core stone (**Fig. 3.3.9-a**) is very fine- to fine-grained, essentially composed of calcite and, as secondary mineralogy, dolomite, clay minerals, and quartz, associated with iron oxides, opaque minerals, and rare amounts of feldspar, glauconite and phosphatic minerals. Carbonates occur as very fine-grained, anhedral to subhedral crystals that represent the matrix of the stone. Clay minerals occur as very fine-grained anhedral aggregates admixed with carbonates. Quartz is present as very fine-to-fine grain crystals scattered in the matrix, and the average grain size of fine quartz is 3 mm**.** Iron oxides are present in minor amounts and related to the clay minerals, as well as disseminated in the stone to be responsible for the reddish or/and yellowish colors. A significant number of microfossils and fossil fragments are observed, and some microfossils are filled with secondary calcite and quartz. Some irregular pores and fractures are detected in the sample, and microveinlets are filled by secondary calcite, quartz, and iron oxides cut across the sample. Dolomite may be present as mineral alternation after calcite (dolomitization process).

For the casing stone, unweathered and weathered samples have been observed. In the first case, the unweathered sample (**Fig. 3.3.9-b**) is mainly composed of micritic minerals as the essential component associated with minor amounts of dolomite, rare iron oxides, quartz, phosphate minerals, and opaque minerals. Iron oxides are observed as staining over some parts of the sample due to their dissemination, especially in the presence of humidity or water source, which causes discolouration and disintegration of the stone. Quartz is detected as very fine-grained crystals scattered in the matrix. Phosphate occurs as very fine bone fragments scattered in the stone. Some pores with irregular shapes and various sizes are observed scattered in the rock. Microveinlets are filled with calcite, and quartz is observed cutting through the sample. On the other hand, the weathered sample (**Fig. 3.3.9-c**) is composed mainly of micrite and dolomite as the essential components associated with quartz and rare amounts of feldspars, gypsum, opaque minerals, iron oxides, and clay

minerals. Quartz occurs as very fine- to fine-grained, anhedral grains scattered in the matrix. Significant amounts of microfossils of different sizes and shapes are scattered in the matrix of the sample, where some of them are filled by secondary sparite. Some parts of the stone are stained by traces of iron oxides. Secondary quartz replaces calcite both in the matrix and in some microfossils. Secondary gypsum replaces calcite and partially fills cavities and pore spaces.

Finally, the mortar is mainly composed of aggregate particles by rock fragments, quartz, and feldspar associated with minor amounts of iron oxides, opaque minerals, and clay minerals cemented by calcite. The matrix appears admixed with gypsum. The observed stone fragments are of sedimentary (limestone, gypsum, or feldspathic graywacke) and igneous (porphyritic basalt and rhyolite) origin. Rock fragments are coarse- to medium-grained and have rounded to subangular shapes. Limestone fragments are the most abundant constituent. They comprise very fine- to fine-grained, subhedral to anhedral-interlocked calcite crystals. Most of the limestone fragments are microfossils of different sizes and shapes (**Fig. 3.3.9-d**). Some of the limestone fragments are cut by fine microveinlets filled by secondary calcite. Gypsum rock fragments are composed of a network of very fine-grained irregular gypsum crystals, and the identification of this texture is characteristic of secondary gypsum after anhydrite, which is created where the precursor of anhydrite rehydrated to gypsum [**69**] (**Fig. 3.3.9-e**). Some gypsum fragments are dissolved, leaving relics on the inner border of the secondary pores. Porphyritic basalt fragments in the archaeological sample are generally composed of very fine- to fine-grained plagioclase (anorthite) associated with olivine and/or pyroxene. Plagioclase in these fragments is slightly altered to sericite, while olivine is high to completely altered to iddingsite, which is partially altered to limonite as well. Pyroxene is slightly altered to chlorite and iron oxides (**Fig. 3.3.9-f**). Mafic minerals (pyroxene and altered olivine) present as very fine- to fine-grained crystals that are observed in the matrix that reflect strong alterations of the rock fragments and the whole sample. Feldspathic greywacke fragments comprise very fine-to-fine grains of poorly sorted quartz (sand grains) associated with major feldspars and rare mica embedded in a very fine matrix of clay minerals and iron oxides. Ironstone fragments

are composed of very fine- to fine-grained quartz and minor calcite embedded in the cement of iron oxides and opaque minerals. Ironstone fragments are generally porous. Rhyolite fragments are the least abundant and are composed of very fine- to fine-grained quartz and potash feldspars (mainly microcline). K-feldspars are slightly altered to clay minerals. Free quartz grains occur as very fine to fine-grained grains with rounded to subangular outlines, and some grains are polycrystalline. Feldspar (anorthite) occurs as fine-grained euhedral to subhedral crystals scattered in the matrix of the sample (**Fig. 3.3.9-f**). Calcite occurs as very fine-grained (micrite) aggregates that represent the majority of the matrix of the rock. Iron oxides and opaque minerals occur as very fine- to medium-grained scattered minerals in the sample. Gypsum occurs as very fine-grained, fibrous aggregates to needle-like crystals scattered in the matrix of the sample. Clay minerals occur as very fine-grained admixed with all the matrix components. Some irregular pores and fine fractures are detected in the sample (**Fig. 3.3.9-f**).

4.3. Minerological and chemical studies

The mineralogical results of the pyramid construction materials using XRD showed that the core stone sample is composed of calcite (79%), quartz (3%), and dolomite (18%) (**Fig. 3.3.10, CS**) (**Table 3.3.2, CS**). In addition, swellable clay minerals have been detected in the core stone after carrying out the separation process of clay minerals from the core stone powder of the pyramid. We observed that the main peak (with a spacing ≈13 Å) moved towards greater spacing when dimethylsulfoxide (≈18.6 Å) was applied. In addition, heat treatment was applied and caused the collapse of the structures of these swelling clays, where their spacing decreased to ≈9 Å (**Fig. 3.3.11**). Moreover, the unweathered casing stone is composed of calcite (93%) and dolomite (7%) (**Fig. 3.3.10, UWsC**) (**Table 3.3.2, UWsC**), while the weathered casing stone is composed of calcite (80%), dolomite (3%) and quartz (15%) (**Fig. 3.3.10, WsC**) (**Table 3.3.2, WsC**). Finally, the mortar is composed of calcite (40%), gypsum (30%), quartz (10%), and anorthite (20%) (**Fig. 3.3.10, BM**) (**Table 3.3.2, BM**).

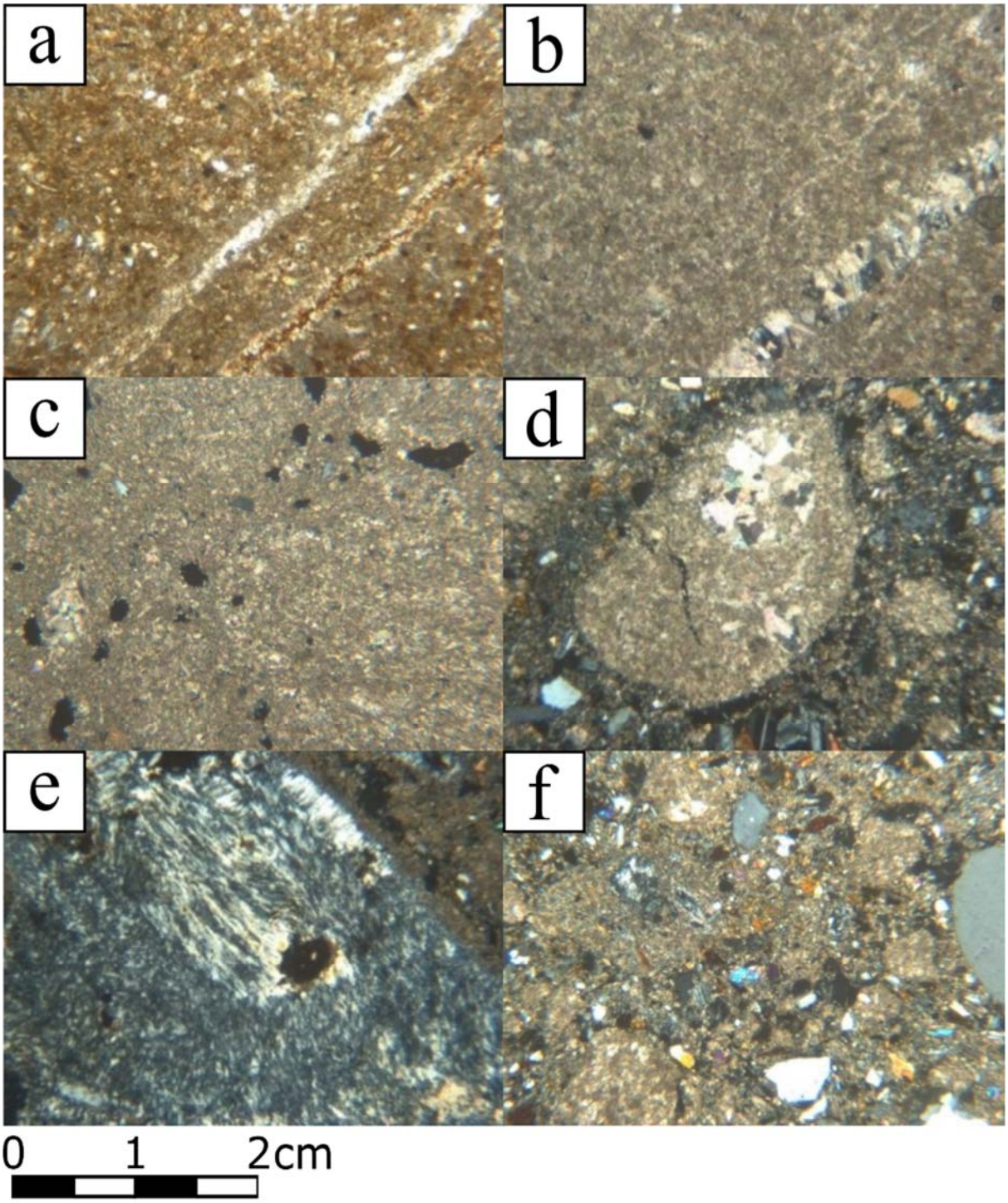


Fig. 3.3.9. (a) Thin section for the core stone investigated under the polarizing microscope. The sample shows the pore spaces, channels (microcracks), and dolomite presented as alteration minerals after calcite (dolomitization process). (b) The casing stone under a polarizing microscope. The stone is cut by microveinlets filled with secondary calcite and traces of quartz. Quartz presents as a secondary replacement mineral over carbonates,

especially microfossils. (c) The decayed casing stone under a polarizing microscope. Secondary quartz replaces calcite both in the matrix and in some microfossils. Secondary gypsum replaces calcite and partially fills cavities and pore spaces. (d) Observed stone fragments are of sedimentary (fossiliferous limestone, gypsum (chemical alteration byproduct), feldspathic graywacke, and ironstone) and igneous (porphyritic basalt and rhyolite) origin (e) in basaltic mortar. Gypsum rock fragments are composed of a network of very fine-grained irregular gypsum crystals, and this texture is characteristic of secondary gypsum after anhydrite. (f) Some grains of quartz are polycrystalline, feldspar (anorthite) occurs as fine-grained euhedral to subhedral crystals scattered in the matrix, calcite occurs as very fine-grained (micrite), iron oxides and opaque minerals occur as very fine to medium-grained, gypsum occurs as fibrous aggregates to needle-like crystals, and some irregular pore spaces and fine channels are detected.

Table 3.3.2. XRD results of the core, casing, and basaltic mortar/concrete of the pyramid. Legend: CS, core stone; UWsC, unweathered casing stone; WcS, weathered casing stone; BM, basaltic mortar; "-", a mineral phase not registered; Cal, calcite; Dol, dolomite; Qz, quartz; Gyp, gypsum; An, anorthite (according to [**70**]).

	Cal	**Dol**	**Qz**	**Gyp**	**An**
CS	79	18	3	-	-
UWsC	93	7	-	-	-
WsC	80	3	15	2	-
BM	40	-	10	30	20

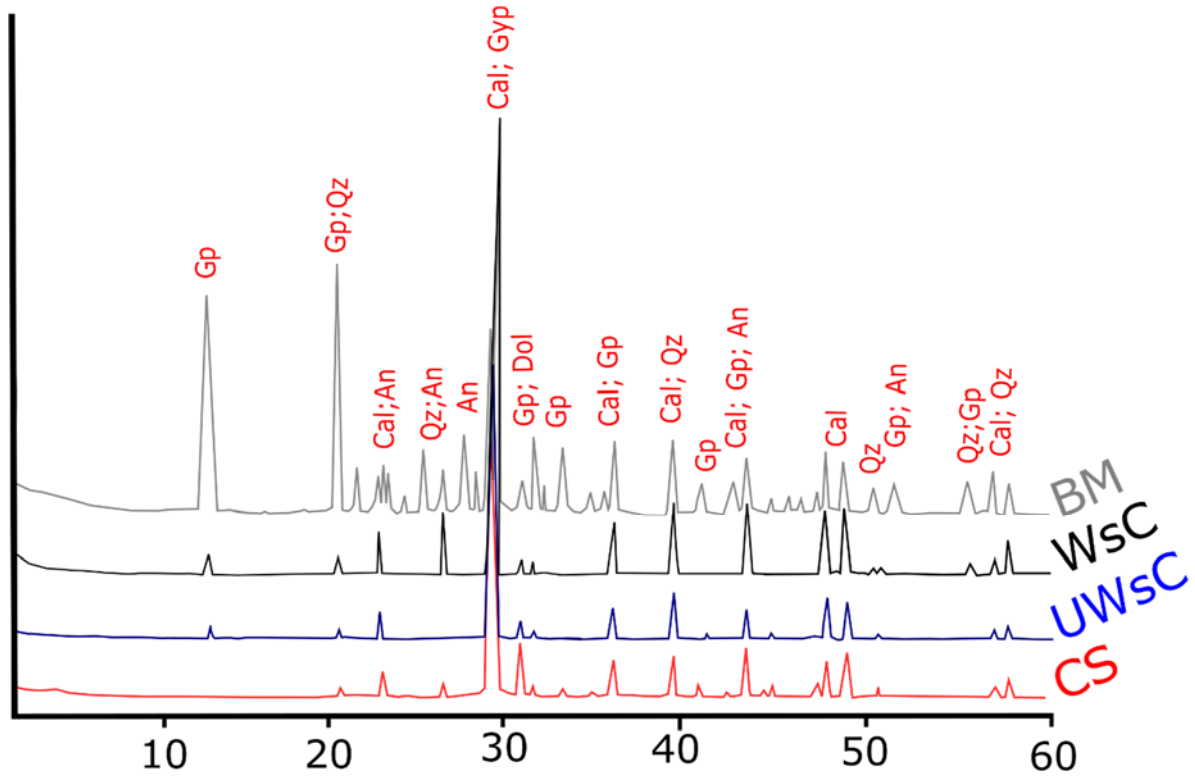


Fig. 3.3.10. X-ray diffraction patterns of the construction materials of Sahure's pyramid. Legend: CS, core stone; UWsC, unweathered casing stone; WcS, weathered casing stone; BM, basaltic mortar; Gyp, gypsum; Qz, quartz; Cal, calcite; An, anorthite; Dol, dolomite (according to [**70**]).

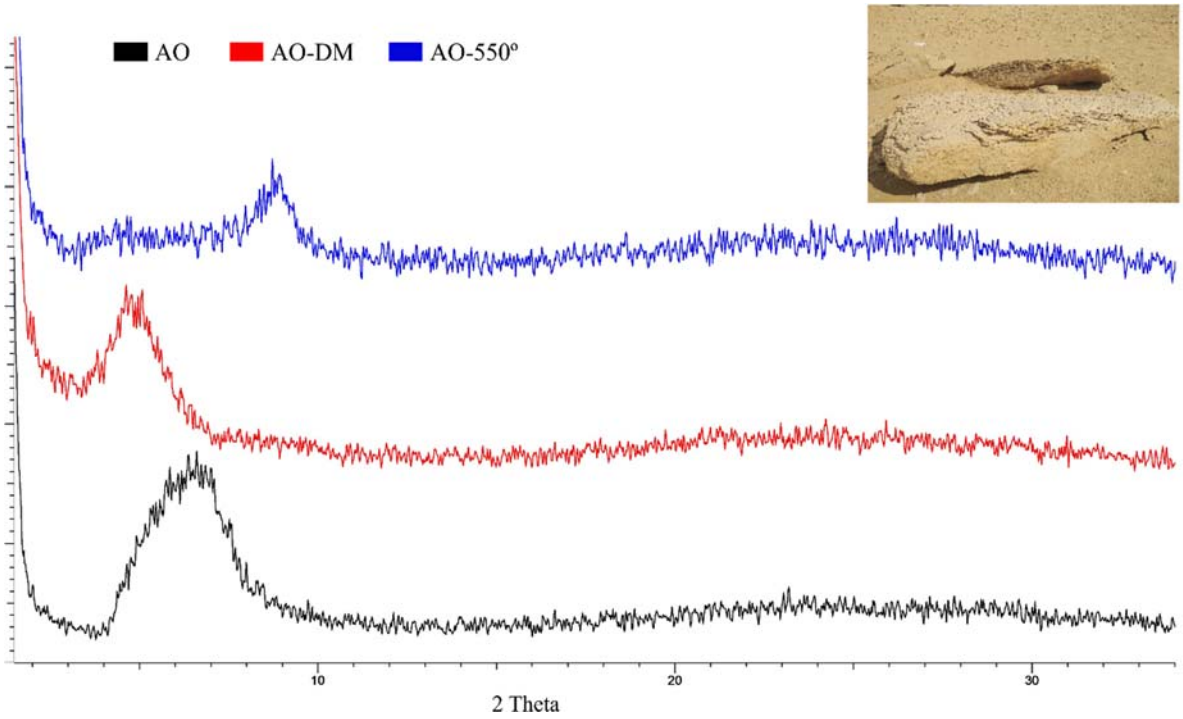


Fig. 3.3.11. X-ray diffraction patterns of the clay fraction from the core stone sample, where the main peak observed corresponds to swellable clays. The AO sample (black line) corresponds to oriented aggregates without treatment, AO-DM (red line) after treatment with dimethyl sulfoxide, and finally, AO-550° (blue line) treated thermally at 550 °C.

Furthermore, all samples were analyzed elementally using X-ray fluorescence, and the identified elements were Ca, Fe, Si, Mg, Al, Na, K, Cl, and Ti (**Table 3.3.3**). The percentage of each element is clearly related to the mineralogy identified by XRD, observing that Ca has similar values. On the other hand, Si and Mg quantities vary more significantly, which is related to the quantities of quartz and dolomite in these rocks. In CS, there is also a contribution of elements related to silicates, such as Al. Likewise, the amount of Fe detected would be linked to the natural variability that these samples present with respect to the Fe oxides described previously. Last, the mortar sample is very different from the rocks. It has much less Ca, but instead the values of Si, Al, Mg, Fe, and K due to the presence of basaltic and rhyolitic rock fragments. Additionally, elements such as P, Cl, and S are present in greater quantities than in rocks, where the presence of P and Cl could be due to the

presence of secondary salts and S could be due to the addition of gypsum to the mortar with lime.

Table 3.3.3. Chemical composition of the core stone, unweathered and weathered casing stones, and basaltic mortar from Sahure's pyramid. Major and minor elements are expressed in wt. %. Legend: CS, core stone; WCS, weathered casing stone; UWCS, unweathered casing stone; BM, basaltic mortar.

	CaO	SiO_2	TiO_2	Al_2O_3	Fe_2O_3	MnO	MgO	Na_2O	K_2O	P_2O_5	Cl	SO_3	LOI
CS	47.90	4.80	0.10	0.40	5.10	0.09	2.40	0.09	0.06	0.02	0.23	0.69	37.90
WCS	53.22	1.90	0.10	0.11	0.50	0.03	1.18	0.07	0.06	0.08	0.18	0.66	41.80
UWCS	52.74	3.54	0.12	0.18	0.52	0.01	1.10	0.04	0.01	0.01	0.19	0.69	40.50
BM	31.19	18.80	0.80	3.79	7.93	0.10	0.97	0.12	0.90	0.14	0.40	16.9	17.50

4.4. Physical properties

Physical properties were measured for the core stone to identify the moisture content (MC), water absorption (WA), density (D), unit weight (UW), specific gravity (SG), and open porosity (Po). To evaluate the durability problems and the geoenvironmental effects on probable changes in stone physical properties.

The results of the physical properties are summarized in **Table 3.3.4**, where the moisture content ranges from 26 to 31.6%, the water absorption ranges from 29.2 to 31.9%, the density is 2.7 g/cm^3, the unit weight is 27 g.mm.s^2, the specific gravity is 2.7 g/cm^3 and the open porosity ranges from 0.7 to 1.6%.

Table 3.3.4. Results of the petrophysical properties for the core stone (sandy limestone) of the pyramid. Legend: L, length (in cm); W, width (in cm); H, height (in cm); V, volume (in cm^3); M, mass (in g); NW, natural weight (in g); DW, dry weight (in g); SW, saturated weight (in g); MC, moisture content (in %); WA, water absorption (in %); D, density (g/cm^3); UW, unit weight ($g.mm.s^2$); SG, specific gravity (g/cm^3); Po, open porosity (in %).

Sample	1	2	3	4	5	6	7	8	9
L	5.0	5.0	4.7	5.0	4.9	4.7	5.0	5.0	5.0
W	5.0	4.8	5.0	5.0	5.0	5.0	5.0	4.8	5.0
H	4.8	5.0	4.7	5.0	5.0	5.0	5.0	5.0	5.0
V	120.0	120.0	110.5	125.0	122.5	117.5	125.0	120.0	125.0
M	324.0	324.0	298.3	337.5	330.8	317.2	337.5	324.0	337.5
NW	291.8	307.3	306.3	319.7	315.2	297.05	300.3	302.2	317.3
DW	292	306	306	318.5	314.3	296	299	301	316
SW	293	307	307.2	319.4	315.2	297	300	303	317.4
MC	26	30.6	30.5	31.9	31.4	29.6	30	30.1	31.6
WA	29.2	30.6	31.6	30.9	31.5	29.6	30	30.2	31.7
D	2.7	2.7	2.6	2.7	2.7	2.6	2.7	2.7	2.7
UW	27	27	26	27	27	26	27	27	27
SG	2.7	2.7	2.6	2.7	2.7	2.6	2.7	2.7	2.7
Po	0.8	0.8	1.0	0.7	0.7	0.8	0.8	1.6	1.1

5. Discussion

The main purpose of this research is to study the effects of geoenvironmental impacts on the sustainability and durability of Sahure's pyramid, as well as to study the interaction process between both intrinsic properties/defects of the construction materials and surrounding geoenvironmental conditions. Additionally, this research presents a new finding of the oldest trial in the world for mortar/concrete manufacturing, and it is called basaltic mortar/concrete, which is used as joint mortar in pyramid building.

The natural heterogeneity of the sandy limestone that is used in the core construction of the pyramid back to its mineralogical content, such as iron oxides, reflected the reddish or/and yellowish color of the stone and played a role in the accelerating rate of stone decay against environmental conditions. Aggregates of sands admixed with carbonates and clay minerals existed in minor amounts and disseminated in the stone. Additionally, the core building materials have their own internal defects that lead to the weakness of their durability and resiliency towards aggressive and cyclic environmental and weathering impacts, which could be due to thermal stresses, wind, and rain. Petrographical and analytical results showed that the core stone is composed of calcite, dolomite, gypsum, clay minerals, and quartz, associated with minor amounts of iron oxides and opaque minerals and rare amounts of feldspar, glauconite, and phosphate minerals. Among all the mineralogy, the presence and content of phyllosilicates, glauconite, and especially swellable clays suppose a serious risk to the integrity of this natural stone. According to Mahrous [**71**], both phyllosilicates (smectite and glauconite) are present in the limestone from different quarries in Egypt, and their proportions vary according to the quarry, such as Helwan (1.10%), Qena (0.78%), Minia (0.61%), Assiut (0.60%), Aswan (0.20%), Sinai (0.13%), Sohag (0.55%) and Suez (0.43%). Smectite was detected after the separation process of clay minerals from the core stone powder, and it commonly exists in sandstones and is characterized by specific physicochemical properties, such as a highly active surface with high cation exchange properties due to its structure, chemical composition, and small crystal sizes [**72, 73, 74**]. Consequently, smectite has a large affinity for absorbing water from the surrounding environment, especially montmorillonite, which causes severe decay for the pyramid building material due to its shrinkage and swelling characteristics [**75**]. In this sense, Tiennot et al. [**76**] studied and confirmed the influence of smectite and glauconite on stone monuments and found that low moisture content has a high impact on swelling action to smectite and glauconite, and they assured that under normal environmental conditions, those clay minerals could cause clear weakness planes in the stones. Accordingly, the core stone of the pyramid with its content of swellable clays showed its weakness against changeable environmental conditions, especially in the fluctuation between temperature and humidity conditions. In addition to the heavy rains

and wind loads that led to detachments, layering, and delamination, partial and total structural collapse occurred with dynamic actions. These previous deterioration patterns are considered the main decay patterns in the building materials of the pyramid (see **Fig. 3.3.7**). Furthermore, iron oxides were detected as minor impurities in the chemical composition of the core stone, and in correlation with previous studies, clay minerals rich in iron oxides existed in the composition of the samples of limestone from Al-Zahir Baybars Mosque in Old Cairo. In fact, they were the reason for the reddish color of the stones, and iron oxides dissolved in the water source of sewage caused many patterns of decay, such as powdering and disintegration of stone blocks [**77**]. Accordingly, the color of the core stone is strongly reddish, and because of the dissolution process, the stones are full of pores, microcracks, and laminations.

Moreover, in Giza, many pollutants are observed with increasing rates from September to November, such as carbon monoxide, nitrogen oxides, ozone, and sulfur dioxide [**55**]. Accordingly, gypsum byproducts appear in core stone with 2% because of the reaction of calcium carbonate with sulfuric acid as an environmental pollutant [**78**]. In the same context, gypsum salt is formed inside the porous building materials due to the accumulative reaction between sulfuric acid and calcium carbonate that leads to irreversible damage to the stones, and the internal fabric of the stone is replaced with gypsum [**79, 80**]. In addition, the presence of dolomite might have occurred because of the dolomitization process originally, where the limestone was altered into dolomite when the stone was in contact with water rich in magnesium, and this transformation was accompanied by an increase in porosity [**81**].

Since the two components of calcite and quartz have existed, it is expected that the differential thermal expansion rates will be different, which could cause many internal stresses leading to microcracks, fissures, and disintegration for the stones. In particular, the thermal coefficient volumetric expansion of quartz is 0.36 between 20 and 100 °C; calcite shows anisotropic thermal strain behavior due to its positive and negative linear thermal expansion coefficients. These different coefficients generate high tensile stresses along crystal boundaries, significantly influencing the disintegration of stones in the high

frequency of fluctuations of the temperature daily and monthly. Similar to calcite, dolomite is present in the core stone, and they have different thermal expansion coefficients [**82, 83**]. Accordingly, many deterioration patterns, such as layering and cracking, could be noticed because of the various thermal expansion coefficients of different minerals in the core building materials.

On the other hand, ancient Egyptians utilized limestone from ancient quarries (Tura and Massra quarries) that were typically light gray on unweathered surfaces but were also nearly white or pale yellowish to pinkish [**84**]. Accordingly, the unweathered casing stone of Sahure's pyramid is mainly calcite (93%) with some dolomite that was extracted from the Tura and Massra quarries in Helwan. This casing stone is relatively soft due to its abundance of calcite and relatively porous due to some impurities, such as iron oxides, quartz, a phosphate mineral, and opaque minerals. Limestone owes its own hardness to either more coarsely crystalline calcite or the presence of secondary dolomite as the casing stone of the pyramid [**85**]. Tura and Massra stones consist mainly of calcite. In addition, they contain fossils (molluscs, and especially echinoids and globigerinid, nummulite foraminifera, *Ostreaelegans*, *Pectens. p*, *Lucina mokattamensis*) plus one or more of the following impurities: dolomite, quartz (as detrital sand silt grains or diagenetic chert nodules); iron oxides (hematite or goethite) and various clay minerals (aluminosilicates). In contrast, the weathered samples of casing stone are composed mainly of calcite and dolomite as the essential components associated with a few amounts of quartz and traces of feldspars, gypsum, biotite, opaque minerals, iron oxides, and clay minerals. Secondary quartz replaces calcite, and some parts of the stone are stained by traces of iron oxides. Additionally, secondary gypsum is also replacing calcite because of a chemical weathering reaction between pollutants and calcium carbonate leading to partial cavities and pore spaces.

For the mortar and after petrographical and analytical studies, the results showed that it is affected by a slight alteration over essential mineral constituents. Some microfossils are filled by secondary calcite, and limestone fragments are occasionally cut by fine microveinlets filled by recrystallized secondary calcite. Gypsum fragments are generally secondary after anhydrite because of acidic rains. In this context, Sievert et al. [**86**]

confirmed the conversion of anhydrite into gypsum during hydration when anhydrite is exposed to a water source and water molecules enter through the cracks of the anhydrite surface. In addition, when there are sufficient Ca^{2+} and SO_4^{2-} ions and water molecules at the surface, nuclei of gypsum are formed. Finally, a large amount of gypsum is formed, and the remaining anhydrite is left behind. Furthermore, some gypsum fragments are dissolved, leaving relics on the inner border of the secondary pores in the mortar. In this sense, gypsum can be soluble and dissolved in the presence of an unsaturated aqueous solution releasing Ca^{2+} and SO_4^{2-} ions due to the chemical characteristics of gypsum [**87**]. Moreover, sericite was detected as an alteration of plagioclase (in fragments and free crystals), and sericite is a common alteration mineral of orthoclase or plagioclase feldspars in regions that are subject to thermal alteration; this process is called sericitization [**88**]. However, olivine (in fragments and free crystals) is high to completely decomposed to iddingsite and then partially altered to limonite. In this regard, Smith et al. [**89**] confirmed that olivine is the most reactive mineral under both thermal and weathering conditions. The formation of the iddingsite by oxidative weathering and olivine begins with a solution of Mg from planar fissures, and the oxidation of Fe within the remaining olivine provides nuclei for the growth of goethite. In addition, pyroxene (in fragments and free crystals) is slightly altered to chlorite and iron oxides.

From petrophysical measurements for the core stones, the water absorption coefficient ranged from 29.2% to 31.7%, the average density was 2.7 g/cm3, the average specific gravity (GS) was 2.7 (g/cm^3) and the open porosity ranged from 0.8 to 1.1% (**Table 3.3.4**). Water absorption of stones is categorized into low-absorbing stone (1 to 10%), moderate-absorbing stone (10 to 50%), and high-absorbing stone (50 to 100%) [**90**]. According to the physical properties, core stones of the pyramid are categorized as moderately absorbed stones [**90**]. Water absorption is considered the most important physical property that has relationships with density and porosity due to the reaction of water with the internal composition of stones leaving pores and spaces because of the alterations and dissolution processes. Finally, when the degree of water saturation and absorption increase, the durability of stones decreases [**90,91**].

Furthermore, and according to the recordings of historical seismological data, shear forces due to previous earthquakes have affected the pyramid structure. The most important factor that effectively caused major deterioration and structural problems of the red pyramid near the Abusir archaeological site was the impact of the accumulative earthquakes [**25**]. Specifically, in 1992, an earthquake occurred at Dahshur with an estimated local magnitude of 5.3 M on the Richter scale [**25**]. This earthquake caused notable crumbling, casing and body stone collapsing, and structural cracks in Sahure's pyramid. The previous environmental weathering and bleeding of the construction materials helped the damaging impact of the earthquake on the pyramid.

Finally, this study revealed that the first trial for mortar/concrete manufacturing in the world dates back to 2494 to 2345 BCE. In this sense and according to previous studies, the oldest mortar was made from mud and clay back to the 10^{th} millennia BCE. On the other hand, concrete manufacturing dates back to 1400-1200 BCE in the royal palace of Tiryns (Greece). This concrete was composed of lime and pebbles, and small usages of it have been recorded in some structures in the ancient Nabataea culture as well [**92**]. The name of our study mortar is called basaltic mortar/concrete, and the main precursors of this concrete are basalt and limestone fragments with lime and gypsum. The source area of basalt fragments is the Widanel-Faras quarry, which was referred to in part of the ancient Egyptian quarries (**Fig. 3.3.4,** yellow circle). This kind of mortar/concrete gives more attention to the impressive mentality of ancient Egyptians in the technology of building materials for their pyramids.

6. Preservation proposal for the pyramid

Sahure's pyramid has been affected by many factors of deterioration (physical, mechanical, and chemical). Many fallen stone blocks and loss of cohesion of construction materials are well observed. Therefore, urgent restoration and conservation are needed to safeguard this important pyramid. The preservation plan should include the fine restoration, structural interventions, preventive conservation, and management of the archaeological site of Abusir. For protection, the dust over the whole body of the pyramid is cleaned, salts are removed from the stone surfaces, stone blocks are consolidated, the gaps are filled, and

grouting is performed by using improved traditional mortars such as lime mortar. Finally, a replacement for highly weathered blocks with new blocks is highly needed in most of the pyramid parts.

For structural intervention, the authors suggest carrying out geotechnical studies to investigate structural problems and assessment for the soil problems as well using finite element modelling to specify the areas of deficiencies. In this sense, urgent design for steel or wooden supports for the structural stability of inner chambers is recommended to prevent structural collapse.

Last, the site management plan for the Abusir archaeological site should be carried out for sustainability and preventive conservation purposes. Abusir is listed as a world heritage site with all of Memphis, but very few tourists and researchers go there due to the lack of infrastructure, services, and maintenance. After the development plan for the site, it will be strongly a significant and competitive destination for the tourism industry and researchers in Egypt.

7. Conclusions

Intrinsic problems related to the mineralogical composition of the construction materials of Sahure's pyramid played an important role in the decay and degradation of these building stones. Clay minerals in core stones, such as smectite and glauconite, affected the durability of the stones due to the swelling force of these clay minerals. Moreover, the paper showed that one of the internal defects of the pyramid construction materials is the original pores in the stone resulting from the dolomitization process of calcite. In addition, pores and spaces are present due to weathering agents and environmental interactions with construction materials. Additionally, gypsum salt replaced calcite and partially filled pore spaces inside stones to form crusts over the stone surfaces and weaken the resiliency of the stones. On the other hand, the presence of anhydrite has been detected because of the high thermal impact of the surrounding environment. The secondary phase of gypsum from

anhydrite has been detected due to the chemical decay of construction materials. Moreover, disseminated iron oxides with humidity caused the staining that made the stones visible as reddish or/and yellowish. In addition, the dissemination of the iron oxides caused pores and spaces because of their dispersion in water. Different thermal behaviors of calcite, quartz, and dolomite affected the durability of the stones, causing disintegrations and layering degradation patterns for the building blocks of the pyramid. Meanwhile, the wind and wet-drying cycle's effects caused the honeycomb decay pattern in some blocks. Petrophysically, the stones have been affected by environmental conditions and categorized as moderate water-absorbing, which makes stones so susceptible to future environmental impacts. Dynamically, the research discussed that the environmental impacts and intrinsic problems were not only the factors of decay and damage but also the accumulative effect of historical earthquakes. Dahshour earthquake (1992), which is adjacent to the Abusir archaeological site, and the Aqaba earthquake (1995) both led to a partial collapse and structural damage of the Sahure's pyramid. Additionally, the paper investigated and confirmed that the core stone of the pyramid is from a local quarry and that the casing stones were extracted from the Tura and Massara quarries. Finally, this work revealed a new discovery related to basaltic mortar/concrete that was the first trial of concrete fabrication in the Old Kingdom in Egypt.

Acknowledgments

A. Fahmy acknowledges SCiCYT and UGEA-PHAM at Cadiz University for carrying out the main part of the archaeometrical analysis. E. Molina Piernas acknowledges co-funding from the European Social Fund (D1113102E3) and Junta de Andalucía.

8. References

[1] Camuffo D, Fernicola V, Bertolin C. Basic Environmental Mechanisms Affecting Cultural Heritage: Understanding deteriorations mechanisms for conservation purposes. 1st ed. Brussels: Nardini editore; 2010. Available from: https://www.cost.eu/publication/basic-environmental-mechanisms-affecting-cultural-heritage-understanding-deterioration-mechanisms-for-conservation-purposes/

[2] Charola AE, Pühringer J, Steiger M. Gypsum: A review of its role in the deterioration of building materials. Environ Geol. 2007; 52 (2):207–20. https://doi.org/10.1007/s00254-006-0566-9

[3] Fitzner B, Heinrichs K. Damage diagnosis at stone monuments - Weathering forms, damage categories and damage indices. Acta Universitatis Carolinae, Geologica. 2001; 45(1), 12–13.

[4] Grossi CM, Brimblecombe P. Effect of long-term changes in air pollution and climate on the decay and blackening of European stone buildings. Geol. Soc. Spec. Publ. 2007; 271(1): 117–30.https://doi.org/10.1144/GSL.SP.2007.271.01.13

[5] Figueiredo MO, Silva TP, Veiga JP. Analysis of degradation phenomena in ancient, traditional and improved building materials of historical monuments. Appl. Phys. A Mater. Sci. Process. 2008; 92(1): 151–4. https://doi.org/10.1007/s00339-008-4466-6.

[6] Sandrolini F, Franzoni E, Sassoni E, Diotallevi PP. The contribution of urban-scale environmental monitoring to materials diagnostics: A study on the Cathedral of Modena (Italy). J. Cult. Herit. 2011; 12(4): 441–450. https://doi.org/10.1016/j.culher.2011.04.005

[7] Khanlari G, Sahamieh RZ, Abdilor Y. The effect of freeze–thaw cycles on physical and mechanical properties of Upper Red Formation sandstones, central part of Iran. Arab. J. Geosci. 2014; 8(8): 5991–6001.https://doi.org/10.1007/s12517-014-1653-y

[8] Derluyn H, Vontobel P, Mannes D, Derome D, Lehmann E, Carmeliet J. Saline Water Evaporation and Crystallization-Induced Deformations in Building Stone: Insights from High-

Resolution Neutron Radiography. Transp. Porous Media. 2018; 128(3): 895–913.https://doi.org/10.1007/s11242-018-1151-x

[9] Hemeda S. Geotechnical modelling of the climate change impact on world heritage properties in Alexandria, Egypt. Herit. Sci. 2021; 9(1). https://doi.org/10.1186/s40494-021-00547-8

[10] Risdonne V, Hubbard C, Puisto J, Theodorakopoulos C. A multianalytical study of historical coated plaster surfaces: the examination of a nineteenth-century V & A cast of a tombstone. Herit. Sci. 2021; 9(1).https://doi.org/10.1186/s40494-021-00533-0

[11] Villacreses JP, Granados J, Caicedo B, Torres-Rodas P, Yépez F. Seismic and hydromechanical performance of rammed earth walls under changing environmental conditions. Constr. Build. Mater. 2021; 300: 124331. https://doi.org/10.1016/j.conbuildmat.2021.124331

[12] Hatır E, Korkanç M, Schachner A, İnce İ. The deep learning method applied to the detection and mapping of stone deterioration in open-air sanctuaries of the Hittite period in Anatolia. J. Cult. Herit. 2021; 51: 37–49. https://doi.org/10.1016/j.culher.2021.07.004

[13] Emery KO. Weathering of the Great Pyramid. J. Sediment. Res.1960; 30(1):140–143. https://doi.org/10.1306/74D709DE-2B21-11D7-8648000102C1865D

[14] Hanafy, Holail M. Diagenesis of the middle Eocene "nummulite bank" of The Giza pyramids plateau, Egypt: petrologic and 18°/16° evidence, Qatar Univ. Sci. J. 1994; 14 (I): 146-152.

[15] Reader CD. A Geomorphological Study of the Giza Necropolis, with Implications for the Development of the Site. Archaeometry. 2001; 43(1):149–65.https://doi.org/10.1111/1475-4754.00009

[16] Pyramids Plateau Groundwater Lowering Activity. Environmental Assessment Report, United States Agency for International Development. USAID Egypt, 2010. https://pdf.usaid.gov/pdf_docs/PA00HS7G.pdf Accessed 25 Feb 2022.

[17] Gandah AF. The Conservation Status of the Pyramid of Khufu. Hist.R.L. 2015; 26:12–22. https://www.iiste.org/Journals/index.php/HRL/article/viewFile/26963/27646

[18] Franc Z. Petrographic Observations of the Building Stones of the Great Pyramid of Giza. J. Eng. Geol. 2017; 28; 5(4). 10.17265/2328-2193/2017.04.002

[19] Hemeda S. Geotechnical modelling of the climate change impact on world heritage properties in Alexandria, Egypt. Herit Sci. 2021; 9(1):1–32. https://doi.org/10.1186/s40494-021-00547-8

[20] Madkour FS, Khallaf MK. Degradation Processes of Egyptian Faience Tiles in the Step Pyramid at Saqqara. Procedia Soc. 2012; 68:63–76. https://doi.org/10.1016/j.sbspro.2012.12.207

[21] Kukela A. Assessment of Stone Material Deterioration of the Exposed Surfaces of the Step Pyramid in Saqqara. Earth Sci. Eng. 2013; 3:238-244.

[22] Khalil AE, Abdel Hafiez HE, Girgis M, Taha MA. Earthquake ground motion simulation at Zoser pyramid using the stochastic method: A step toward the preservation of an ancient Egyptian heritage. NRIAG J. Astron. 2017; 6(1):52–9. https://doi.org/10.1016/j.nrjag.2016.11.003

[23] Rossi C. Aristotle's mirror: Combining digital and material culture. ISPRS - Int. Arch. Photogramm. Remote Sens. Spat. Inf. Sci. 2019; 42(2/W11):1025–9. https://doi.org/10.5194/isprs-Archives-XLII-2-W11-1025-2019

[24] Ahmed G. Using smart technology in conservation of the ancient Egyptian monuments from environmental impacts. Artic. J. Urban Res. 2021; 5 (40):78-97. 10.21608/JUR.2021.31603.1003

[25] Hemeda S, Fahmy A, Sonbol A. Geo-Environmental and Structural Problems of the First Successful True Pyramid, (Snefru Northern Pyramid) in Dahshur, Egypt. Geotech. Geol. Eng. 2018: 37(4):2463–84. https://doi.org/10.1007/s10706-018-00769-x

[26] Hawass Z. The treasures of the pyramids. In: Accomazzo L, Fabianis VM, editors. White Star.S.R.L.Vercelli.2003.https://gizamedia.rc.fas.harvard.edu/documents/hawass_treasures_282-285.pdf Accessed 21 Jan 2022.

[27] New Discoveries in the Abusir Pyramid Field. https://egypte.xsbb.nl/viewtopic.php?t=786663 Accessed 21 Jan 2022.

[28] Verner M. Abusir. L'annuaire du Collège de France. 2012; 1; (111): 897–900. https://doi.org/10.4000/annuaire-cdf.1799

[29] Bárta M, Coppens F, Krejčí J. Abusir and Saqqara in the year 2020. Proceedings of the conference held in Prague. Czech Institute of Egyptology, Faculty of Arts, Charles University in June 22-26. 2021. https://cegu.ff.cuni.cz/wp-content/uploads/sites/50/2022/01/2021_Abusir_Saqara_2020.pdf Accessed 25 Jan 2022.

[30] Verner M. Abusir.The Necropolis of the sons of the sun. 2nd ed. Cairo: AUCPress; 2017.

[31] Kawae Y, Yasumuro Y, Kanaya I, Dan H, Chiba F. Abusir 3D survey Univerzita Karlova, Filozofická fakulta. https://core.ac.uk/display/156980921 Accessed 26 Jan 2022.

[32] Verner M. the pyramids. Their archaeology and history. 1th ed. London: Grove Atlantic Ltd; 2002. Available from: https://www.meretsegerbooks.com/pages/books/M4134/verner-miroslav/the-pyramids-their-archaeology-and-history

[33] Verner M. Forgotten pharaohs. Lost pyramids: Abusir. 1st ed. Prague: Škodaexport Academy; 1994. Available from: https://www.meretsegerbooks.com/pages/books/M1683/verner-miroslav/abusir-forgotten-pharaohs-lost-pyramids

[34] Lehner M. The Complete Pyramids: Solving the ancient mysteries. 1th ed. New York: Thames & Hudson; 2008. Available from: https://www.pdfdrive.com/the-complete-pyramids-solving-the-ancient-mysteries-d187727359.html

[35] Borchardt L. Das Grabdenkmal des Königs Sáḥu-re‘ (Ausgrabungen der Deutschen Orient-Gesellschaft in Abusir 1902-1908). Univ. Bibl. Leipzig: Hinrichs; 1982. https://doi.org/10.11588/diglit.3364

[36] Wilson JA. The pyramids of Egypt. I.E.S Edwards. J. Near East. Stud. 1948; 2(7). https://doi.org/10.1086/370872

[37] Rainer S. Die Ägyptischen Pyramiden: vom Ziegelbau zum Weltwunder. 3rd ed. Zabern: Mainz am Rhein; 1997. Available from: http://www.gizapyramids.org/pdf_library/stadelmann_pyramiden_80-158.pdf

[38] Bárta M. Abusir in the Third Millennium BC. https://cegu2.ff.cuni.cz/en/research/projects/field-projects/abusir/abusir-in-the-third-millennium-bc/ (2015). Accessed 08 Mar 2022.

[39] Bebermeier W, Alexanian N, Blaschta D, Ramisch A, Schütt B, Seidlmayer SJ. Analysis of Past and Present Landscapes Surrounding the Necropolis of Dahshur. GfE Berlin. 2011; 142(3):325-52. https://www.die-erde.org/index.php/die-erde/article/view/38

[40] Heldal T, Bloxam E, Storemyr P, Kelany A. The Geology and Archaeology of the Ancient Silicified Sandstone Quarries at Gebel Gulab and Gebel Tingar. Marmora an Int J Archaeol Hist Archaeom Marbles Stones. 2005; 1:11–35. https://www.torrossa.com/en/catalog/preview/2242664

[41] Harrell JA, Storemyr P. Ancient Egyptian quarries – an illustrated overview. Geol. Soc. Spec. Publ. 2009; 12: 7–50. Available from: https://www.ngu.no/upload/Publikasjoner/Special%20publication/SP12_s7-50.pdf

[42] Bloxam E. Quarries and mining (stone). http://digital2.library.ucla.edu/viewItem.do?ark=21198/zz0026jkd5 (2010). Accessed 12 Mar 2022.

[43] Laukamp LC. The Pyramids of Egypt. *Hispanic Baroque Ekphrasis*. 2020; 157–184. https://doi.org/10.2307/j.ctv16km07k.12

[44] Klemm DD. The stones of the pyramids: provenance of the building stones of the Old Kingdom pyramids of Egypt - University of Missouri Libraries. http://link.library.missouri.edu/portal/The-stones-of-the-pyramids--provenance-of-the/2y73ukLuBH4/ Accessed 21 Jan 2022.

[45] Jana D. Evidence from detailed petrographic examinations of casing stones from the great pyramid of Khufu, a natural limestone from Tura, and a man-made (Geopolymeric) limestone. International Cement Microscopy Association - 29th International Conference on Cement Microscopy. 2007:206–265. Available from:https://anarkia333data.center/livre/evidence-detailed-petrographic-examinations-casing-stones-great-pyramid-khufu-natural

[46] Harrell JA. Mapping the Tura-Masara Limestone Quarries. Journal of the American Research Center in Egypt [Internet]. 2016 [cited 2022 Jan 21]; 52:199–214. Available from: https://lockwoodonlinejournals.com/index.php/jarce/article/view/76

[47] Bloxam E, Storemyr P. Old Kingdom Basalt Quarrying Activities at Widan El-Faras, Northern Faiyum Desert. JEA. 2002; 88(1): 23–36. https://journals.sagepub.com/doi/10.1177/030751330208800103

[48] World Bank Group. *Climate Risk Profile: Egypt*. 1818 H Street NW, Washington, DC 20433, 2020. Available from: https://climateknowledgeportal.worldbank.org/sites/default/files/2021-01/15723WB_Egypt%20Country%20Profile-WEB.pdf

[49] Egyptian Environmental Affairs Agency. Egypt Third National Communication under the United Nations Framework Convention on Climate Change. 2016. Available from: https://unfccc.int/sites/default/files/resource/TNC%20report.pdf

[50] Masria A. Climate Change at Egypt. SciFed Journal of Global Warming. 2017; 5;1(2). https://doi.org/10.23959/sfjgw-1000009

[51] Ito WH, Scussiato T, Vagnon F, Ferrero AM, Migliazza MR, Ramis J, et al. On the Thermal Stresses Due to Weathering in Natural Stones. Appl. Sci. 2021; 28; 11(3): 1188. https://doi.org/10.3390/app11031188

[52] Abdel-Shafy HI, El-Saharty AA, Regelsber M, Platzer C. Rainwater in Egypt: quantity, distribution and harvesting. Mediterranean Marine Science. 2010; 1; 11(2): 245. https://doi.org/10.12681/mms.75

[53] Climate change Profile in Egypt https://www.government.nl/documents/publications/2019/02/05/climate-change-profiles (2019). Accessed 11 Mar 2022.

[54] Charola AE. Stone deterioration characterization for its conservation. Geonomos. 2017; 24(2), 16-20. https://doi.org/10.18285/geonomos.v24i2.836

[55] Aboel Fetouh Y, El Askary H, El Raey M, Allali M, Sprigg WA, Kafatos M. Annual Patterns of Atmospheric Pollutions and Episodes over Cairo Egypt. Satheesh SK, editor. Adv. Meteorol. 2013; ID: 984853. https://doi.org/10.1155/2013/984853

[56] Graue B. Stone deterioration and replacement of natural building stones at the Cologne cathedral - A contribution to the preservation of cultural heritage. Doctoral thesis [Internet]. 2013 [cited 2022 Jan 24]; Available from: http://dx.doi.org/10.53846/goediss-4185

[57] Angeli M. Multiscale study of stone decay by salt crystallization in porous networks. Doctoral thesis [Internet]. 2007 [cited 2022 Jan 21]. Available from: https://tel.archives-ouvertes.fr/tel-00239456

[58] Badawy A. Historical seismicity of Egypt. Acta Geodaetica et GeophysicaHungarica, 1999;34(1–2), 119–135. https://doi.org/10.1007/BF03325564

[59] Soliman M M. The Dahshour (Egypt) Earthquake of 12th of October 1992. October, 1992. International Conferences on Recent Advances in Geotechnical Earthquake Engineering and Soil Dynamics. 1995; 14. https://scholarsmine.mst.edu/icrageesd/03icrageesd/session07/14

[60] Mossaad M. Liquefaction during the October 12, 1992Dahshour, Egypt, Earthquake and Its Potential in the Nile Valley and Delta. *Soils and Foundations*. 1996; *36*(2), 13–27. https://doi.org/10.3208/sandf.36.2_13

[61] Moustafa SSR, Takenaka H. Stochastic ground motion simulation of the 12 October 1992 Dahshour earthquake. Acta Geophys. 2009; 57(3): 636–56.https://doi.org/10.2478/s11600-009-0012-y

[62] Bares L. Foundation Deposits in the Tomb of Udjahorresnet at Abusir. ZÄS; Z. ägypt. 1996; 123(1):1–9. https://doi.org/10.1524/zaes.1996.123.1.1

[63] Bureau of Indian Standards. Method of Test for aggregate for concrete. IS 2386- Part III - Specific gravity, density, voids, absorption and bulking. 1963; New Delhi, (Reaffirmed 2002). https://law.resource.org/pub/in/bis/S03/is.2386.1.1963.pdf. Accessed 13 Mar 2022.

[64] ASTM. C97/C97 M-18 Standard Test Methods for Absorption and Bulk Specific Gravity of Dimension Stone, ASTM International, West Conshohocken, PA, 2018. www.astm.org. Accessed 13 Mar 2022.

[65] Standard Test Methods for Laboratory Determination of Water (Moisture) Content of Soil and Rock by Mass [Internet]. www.astm.org. [Cited 2022 Jan 21]. Available from: https://www.astm.org/d2216-19.html

[66] Pereira D. Stone testing. Natural Stone and World Heritage. 1th ed. CRC Press: 2019;22;37–89.https://doi.org/10.1201/9781351013352-6

[67] Datta D, Thakur N, Ghosh S, Poddar R, Sengupta S. Determination of Porosity of Rock Samples from Photomicrographs Using Image Analysis. 2016 IEEE 6th International Conference on Advanced Computing (IACC). 2016. https://doi.org/10.1109/IACC.2016.67

[68] Siegesmund S, Snethlage R. Stone in Architecture. Berlin, Heidelberg: Springer Berlin Heidelberg. 2011. https://link.springer.com/book/10.1007%2F978-3-642-14475-2 Accessed 8 Mar 2022.

[69] Rafiei, B., Rahmani, S. Textural pattern of secondary gypsum in the Basal Anhydrite of the Asmari Formation, SW Iran. *Geopersia*, 2017; 7(2): 267-278. https://dx.doi.org/10.22059/geope.2017.229055.648305

[70] Whitney DL, Evans BW. Abbreviations for names of rock-forming minerals. American Mineralogist. 2009; 95(1): 185–7.https://doi.org/10.2138/am.2010.3371

[71] Mahrous AM, Tantawi MM, El-Sageer H. Evaluation of the engineering properties of some Egyptian limestones as construction materials for highway pavements. Construction and Building Materials. 2010; 24(12): 2598–603. https://doi.org/10.1016/j.conbuildmat.2010.05.016.

[72] Odom IE. Smectite clay minerals: properties and uses. Math. Phys. Eng. Sci.1984; 14; 311(1517): 391–409. https://doi.org/10.1098/rsta.1984.0036

[73] McKinley JM, Worden RH, Ruffell AH. Smectite in Sandstones: A Review of the Controls on Occurrence and Behaviour during Diagenesis. Clay Mineral Cements in Sandstones.1999; 109–28. https://doi.org/10.1002/9781444304336.ch5

[74] Hemeda S, Fahmy A, Moustafa A, Hafez MAE. The Early Basilica Church, El-Ashmonein Archaeological Site, Minia, Egypt: Geo-Environmental Analysis and Engineering Characterization of the Building Materials. ojg. 2019; 09(03): 157–86. https://doi.org/10.4236/ojg.2019.93011

[75] Sparks DL. Inorganic Soil Components. Environmental Soil Chemistry. 2003; 43–73. https://doi.org/10.1016/B978-012656446-4/50002-5

[76] Tiennot M, Mertz J-D, Bourgès A. Influence of Clay Minerals Nature on the Hydromechanical and Fracture Behaviour of Stones. Rock Mechanics and Rock Engineering. 2019; 22; 52(6):1599–611. https://doi.org/10.1007/s00603-018-1672-1

[77] Aldoasri M, Darwish S, Adam M, Elmarzugi N, Ahmed S. Enhancing the Durability of Calcareous Stone Monuments of Ancient Egypt Using CaCO3 Nanoparticles. Sustainability. 2017; 10; 9(8): 1392. https://doi.org/10.3390/su9081392

[78] Kumar A. Industrial Pollution & Management. 1th ed. Delhi: APH publishing cooperation Google Books. APH Publishing; 2004. Available from: https://books.google.com/books?id=xk9SX3heeRkC&pgis=1

[79] Charola AE. Salts in the Deterioration of Porous Materials: An Overview. J. Am. Inst. 2000; 39(3): 327–43. https://doi.org/10.1179/019713600806113176

[80] Alves C, Figueiredo CAM, Sanjurjo-Sánchez J, Hernández AC. Salt Weathering of Natural Stone: A Review of Comparative Laboratory Studies. Heritage. 2021; 4(3): 1554–65. https://doi.org/10.3390/heritage4030086

[81] Wang G, Li P, Hao F, Zou H, Yu X. Dolomitization process and its implications for porosity development in dolostones: A case study from the Lower Triassic Feixianguan Formation, Jiannan area, Eastern Sichuan Basin, China. J. Pet. Sci. Eng. 2015; 131: 184–99. https://doi.org/10.1016/j.petrol.2015.04.011

[82] Turkington AV, Paradise TR. Sandstone weathering a century of research and innovation. Geomorphology. 2005; 67(1-2): 229–53. https://doi.org/10.1016/j.geomorph.2004.09.028

[83] Zhang Z, Liu J, Li B, Yang X. Thermally induced deterioration behaviour of two dolomitic marbles under heating–cooling cycles. R. Soc. Open Sci. 2018; 5(10): 180779. https://doi.org/10.1098/rsos.180779

[84] Sweeny D. UCLA Encyclopedia of Egyptology. UCLA Encycl Egyptol. 2011; http://digital2.library.ucla.edu/viewItem.do?ark=21198/zz0027fc04 Accessed 9 Mar 2022.

[85] Ahmed HT. Physical and Mechanical Characteristics of Helwan Limestone: For Conservation Treatment of Ancient Egyptian Limestone Monuments. J Am Sci. 2015; 11(2).

[86] Sievert T, Wolter A, Singh NB. Hydration of anhydrite of gypsum (CaSO4.II) in a ball mill. Cem Concr Res. 2005; 35(4): 623–30. https://doi.org/10.1016/j.cemconres.2004.02.010

[87] Hong D, Fan M, Yu L. *An experimental study simulating the dissolution of gypsum rock*. Energy Explor. Exploit.2018; 36(4): 942–954. https://doi.org/10.1177/0144598717751927

[88] Kumral M, Abdelnasser A, Budakoglu M. Geochemistry of hydrothermal alteration associated with cenozoic intrusion-hosted Cu-Pb-Zn mineralization at tavşanlı area, Kütahya, NW Turkey. Minerals. 2016; 6(1). https://doi.org/10.3390/min6010013

[89] Smith KL, Milnes AR, Eggleton RA. Weathering of basalt: formation of iddingsite. Clays Clay Miner. 1987; 35(6):418–28. https://doi.org/10.1346/CCMN.1987.0350602

[90] Ünal M, Altunok E. Determination of Water Absorption Properties of Natural Building Stones and Their Relation to Porosity. E-journal New World Sci Acad. 2019; 14(1): 39–45. https://doi.org/10.12739/nwsa.2019.14.1.1a0429

[91] Ozcelik Y, Ozguven A. Water absorption and drying features of different natural building stones. Constr. Build. Mater. 2014; 63: 257–70. http://dx.doi.org/10.1016/j.conbuildmat.2014.04.030

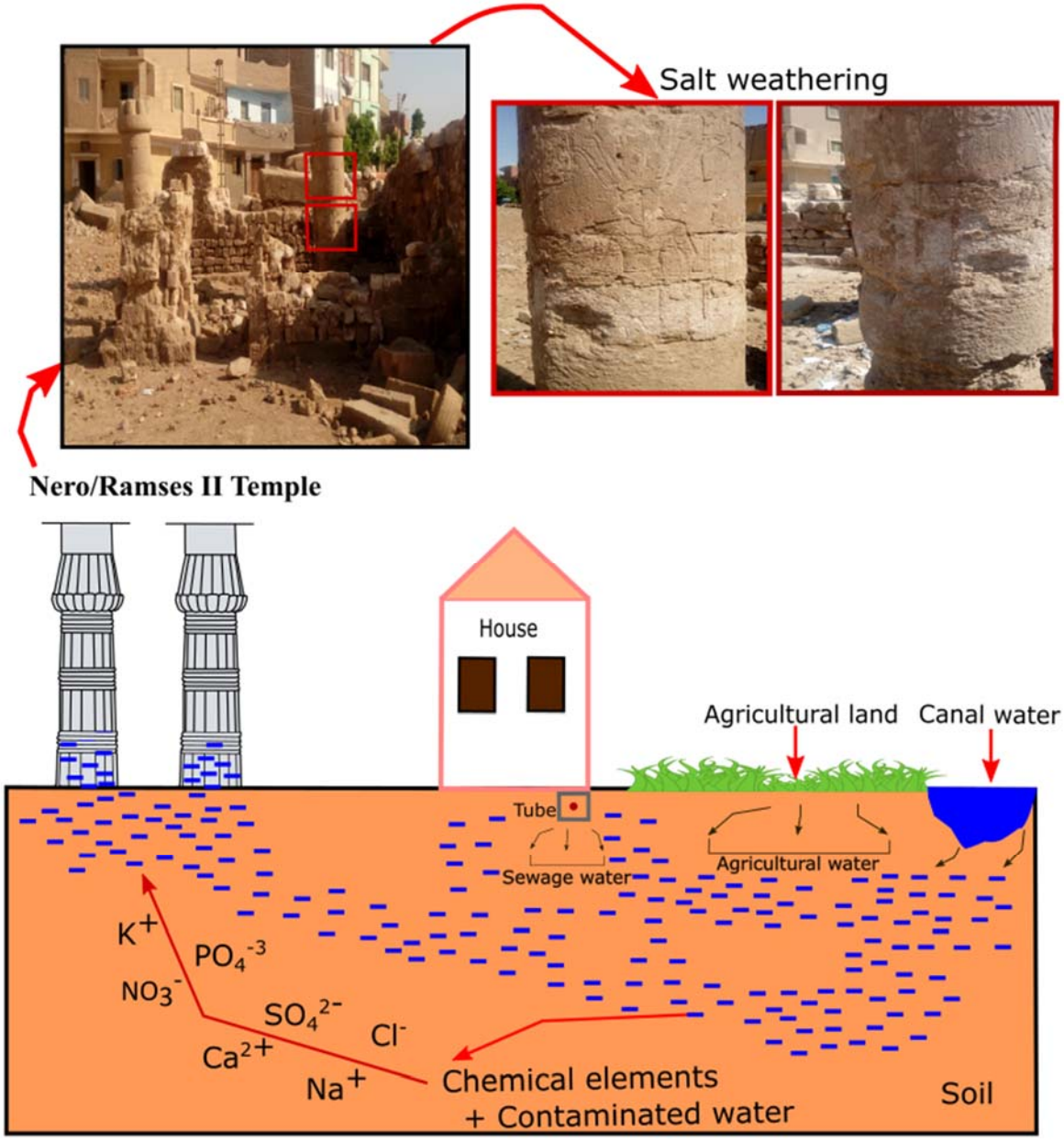
[92] Li Z. Introduction to Concrete. Adv Concr Technol. 2011; 1–22. https://doi.org/10.1002/9780470950067.ch1

3.4. Salt weathering impact on Nero/Ramses II Temple at El-Ashmonein archaeological site (Hermopolis Magna), Egypt

Highlights

- The sources of the contaminated water around Nero's Temple are canals, houses, and agriculture.
- A series of analyses found salt to be the main factor in the decay of Nero's temple.
- Sulphates and chlorides were identified as the main damaging components of the salts in Nero's Temple.
- Conservation plan is needed considering the prevention of saline water flowing in Nero's Temple.

Graphical abstract



Abstract

Nero's Temple at El-Ashmonein archaeological site, in Minia (middle of Egypt), is considered one of the most important of all temples of Nero. This temple dates back to 1520 BC-1075 BC in the New Kingdom and was reused in the era of Nero (the Fifth Emperor of Rome). The temple construction materials are severely decayed from surrounding environmental impacts, especially contaminated water sources. The main objective of this paper is to identify the construction materials of Nero's Temple and their decay by-products. To achieve them, X-ray diffraction, micro-X-ray fluorescence spectrometry, and portable Raman spectroscopy were utilized to identify the compositions and alteration by-products/degradation compounds (mainly saline efflorescence and crusts) from the construction materials, such as limestone walls, and structural mortars of the temple. In addition, a polarizing microscope was used to identify the minerals inside the construction materials and reveal the alteration of the minerals because of decay. Digital microscopy and scanning electron microscopy with EDS were used to detect decayed materials' morphological features. Finally, results showed that the main decay factor is salt attack (chlorides, sulfates, phosphates, nitrates, carbonates, and bicarbonates) for all architectural and structural elements of the temple, which have been carried to the construction materials from various sources of contaminated water (canal, sewage, and agricultural water).

Keywords: Nero's Temple, El-Ashmonein archaeological site, salt attack, contaminated water, building stone, mortar, decay, weathering.

1. Introduction

Salt weathering can be considered one of the main problems of ancient construction materials decay in Egypt. Chlorides, nitrates, and sulfates are the most common salts that attack Egyptian stone building materials [**1-3**]. Many scientists specializing in geoenvironmental science, earth sciences, and heritage conservation science have made great efforts to understand and study the effects of different kinds of salt and their formation mechanisms on built heritage [**4-11**]. Bradley and Middleton [**12**] studied the soluble salt's effect on ancient Egyptian limestone due to the changes in relative humidity that decreased the durability of the stones. Tombs and ancient Egyptian monuments in Thebes were affected by salt efflorescence because of natural weathering, and human impacts [**13, 14**]. Aboushook et al. [**15**] evaluated the surrounding local environment's impact on the Egyptian stone monuments, and the quantification of the deterioration process was carried out through digital image processing. They explained that black crusts in the middle and upper parts of stone walls were formed mainly by gypsum salt and soot from vehicles and the whitish crusts in the lower parts of stone walls were formed mainly by halite. Navarro et al. [**16**] studied calcium and magnesium sulfate formation in situ and explained that these salts were the main decay factor of the main façade of the sixteenth-century Royal Chancery due to humidity and acidic atmosphere in the city of Granada (Spain). Erić et al. **[17]** said that the epsomite and hexahydrate formed as an efflorescence of limestone of Holy Virgin church walls, and they showed that the origin of sulfate in the soil solution could be related to the presence of sulfides in the surrounding serpentinites, whose decomposition leads to the formation of sulfuric acid. They also explained that the potassium and nitrate ions required for the formation of niter most likely originate from the soil solution. Menéndez [**18**] studied the damage of salt and its volume variations with changing environmental conditions with a thermodynamic model (ECOS-RUNSALT). Finally, calcium sulfate or mixtures of chlorides, sulfates, and nitrates of sodium, calcium, magnesium, and potassium have been studied and estimated in salt weathering on archaeological buildings to determine the sources of degradation and their effects [**19**].

Hygroscopic salts have an affinity to absorb water from different sources and cause a damp rise for water to all structural elements of the building, producing severe damage [**20**].

Crystallization pressure is the main factor in salt weathering for heritage masonry [**21**]. Sodium and magnesium sulfate salts had been studied to observe their extreme effects on limestone because they are responsible for successive stone layers and crack formation and propagation inside stone samples, respectively [**22-24**]. Sodium chloride is considered a soluble salt with less aggressiveness for stone damage, but sodium sulfate with wet and drying cycles produces surface submicron crystals with high capillary action [**25**]. Lopez-Arce et al. [**26**] carried out an experimental study for aging on limestone samples using single magnesium sulfate and a mixture of magnesium and calcium sulfates, and sodium chloride to evaluate the damage of those salts to limestone masonry. Therefore, magnesium sulfate as a single salt increased the decay process of the stone walls of Lady of Succour Basilica in Spain with dissolution and dehydration actions (high pressure of crystallization). Then, salt crystals are forming in heterogeneous shapes inside the wall's pores, but double salts imply a lower pressure of crystallization since the double salt crystals are forming in a homogeneous shape inside the pores of the walls [**27]**. Fitzner [**28**] proposed a quantitative assessment of salt weathering carried out using monument mapping to categorize the damage into six categories: 1) no visible damage, 2) very slight damage, 3) slight damage, 4) moderate damage, 5) extreme damage and 6) very extreme damage. On the other hand, the salt susceptibility index/classification (SSI) had been used to categorize the damage resulting from salt attack as exceptionally salt-resistant, salt-resistant, salt-prone, and exceptionally salt-prone [**29**]. Doehne et al. [**30**] used an environmental scanning electron microscope to predict and assess the salt weathering of sodium chloride and sodium nitrate to monitor the grain size of the salt crystals during the crystallization process. Finally, the weathering forms of salt attack are taffoni, honeycombs, exfoliation, flaking, blistering, scaling, micro-and macro-cracking, uniform expansion, granular disintegration (loss of compact), and delamination [**31-33**].

The case study (Nero/Ramses II Temple) located at El-Ashmonein archaeological site (Minia, Egypt) is considered an example of an archaeological site affected by agricultural, urban, and subsurface water. This archaeological site is located near agricultural areas and human activities, and for this reason, some of the buildings show significant signs of deterioration due to the presence of salts. Therefore, the gathering of contaminated water in and around

the construction materials of Nero's Temple is permanent. Consequently, the construction materials are currently bleeding due to severe salt weathering impacts, which led to chemical and physical alterations. For these reasons, the present paper aims to study and understand the construction materials and decay effects due to the presence of salts, and to determine the current factors that cause extreme physical and chemical decay of the architectural and structural elements of Nero's Temple. To achieve this goal, both petrographical and geochemical studies were carried out using scanning electron microscopy with EDS, digital microscopy, polarizing microscopy, X-ray diffraction, micro-X-ray fluorescence spectrometry, and portable Raman spectroscopy. Finally, the salt weathering rate was categorized through alteration pattern mapping.

2. Location, archaeological, and site context

Nero's Temple is located at coordinates 27°46'55"N, 30°48'11"E at El-Ashmonein archaeological site, Mellawy center, Minia Governorate. The distance between Nero's Temple and the Nile River is approximately 10.5 km, and the distance to nearby water canals (El-Ibrahimia canal and Bahr Yousef canal) is approximately 2.5 km (**Fig. 3.4.1. A, B,** and **C**). Nero's Temple is considered a small temple built on top of the ruins of the temple of Ramses II in the New Kingdom (1520 BC-1075 BC) and decorated with many inscriptions and cartouches dating back to the period of Ramses II. Additionally, in the era of Emperor Nero, the stone blocks from the temple of Ramses II were reused in his temple construction [**34, 35**]. Nero's Temple was mainly constructed using the Minia limestone from the local limestone quarry with rectangular shapes. Additionally, some of these blocks were brought from different temples, such as the temple of Ramses II, where some blocks carry the name of king Ramses II. These blocks appear in the foundations and the rest of the temple [**35**]. The quarries in Minia were distributed from El-Bahnasa to Tell el Amarna and Mallay city and they had been utilized in different dynasties in ancient Egypt [**36, 37**] (**Fig. 3.4.1. B**). For example, at Zawyet el-Amwat the limestone was prepared from this area from the New Kingdom to Roman and at Beni Hassan from the Old Kingdom to Roman [**36**].

Architecturally, figure 3.4.1. (**D**) shows different architectural elements of Nero's Temple such as the main entrance of the temple in the north direction, the open courtyard, the

front hall, and the columns hall in the south direction. The main entrance of the temple located in the northern direction is damaged totally. Then, after the main gate, there is an open courtyard that is destroyed with dimensions of 8.50 m from south to north and 11 m from east to west. From the open courtyard, there is a front hall with some remaining walls with dimensions of 3.25 m from south to north and 10.20 m from east to west. Finally, the column hall has dimensions of 10.20 m from east to the west and 6 m from south to north; this hall partially exists with architectural elements such as two walls and three columns [**38**] (**Fig. 3.4.1. D**). Furthermore, there is a mud-brick enclosure wall around the temple. The stone blocks were settled in horizontal and vertical systems of the wall construction, flooring, and foundations (**Fig. 3.4.1. E**). Near Nero's Temple, there is a red brick wall from the Roman era, which confirms the reuse of stone blocks from Ramses II. (**Fig. 3.4.1. F**) [**38**].

The soil of the archaeological site is formed by the annual deposition of river sediments (mud and silt) during flooding events between August and October. This type of soil represents most of the territory of Minia governorate and its villages near the border of the eastern highlands and western desert, while the calcareous soil covers the land available for eastern highlands, near Maghagha and Bani Mazar cities (**Fig. 3.4.2**) [**39**]. The chemical analysis of well water used in irrigation in Minia showed that the high range of total dissolved salts varied between 1477 and 2497 mg L^{-1} and the electrical conductivity varied between 2.24 and 3.86 dSm^{-1}. Additionally, after irrigation, total soluble cations (Ca^{2+}, Mg^{2+}, Na^{+}, and K^{+}) and soluble anions (Cl^{-}, SO_4^{2-}, CO_3^{2}, and HCO_3^{-}) remain behind in irrigated soils as water wipes out rapidly [**40, 41**]. Meteorologically, the average annual temperatures of the surrounding area are 36.9 °C (maximum) in June and 20.4 °C (minimum) in January. The driest months are January, February, April, May, June, July, and August. On the other hand, October is considered the wettest month with 2 mm of precipitation. January and December are the most humid months. May is the least humid month, and the average annual percentage of humidity is 38.0% [**42**].

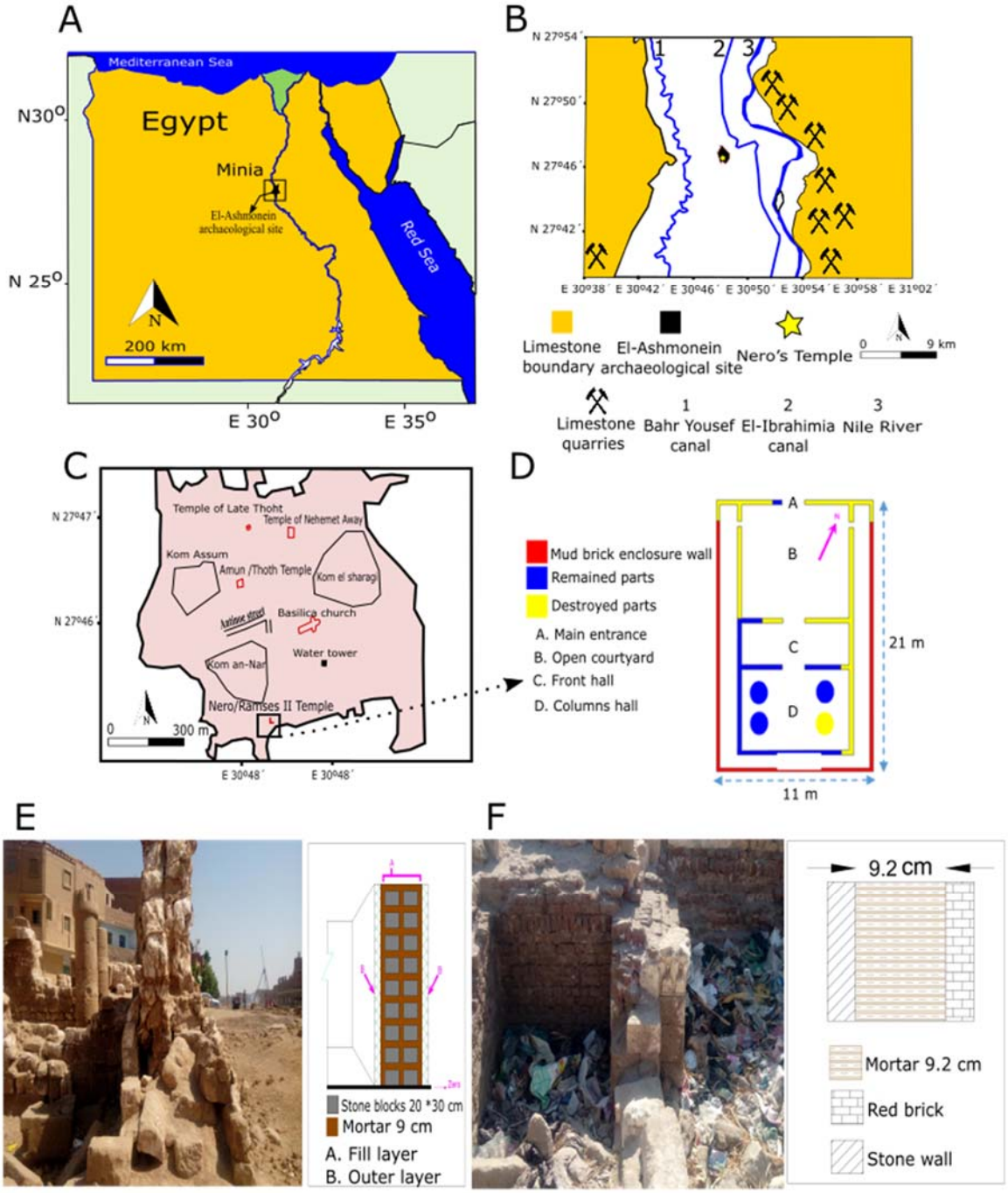


Fig. 3.4.1. (A) General map of Egypt. Black square refers to Minia and the black star refers to El-Ashmonein archaeological site. (B) El-Ashmonein archaeological site and its location regarding the Minia limestone quarries and water sources. (C) El-Ashmonein archaeological site and its monuments; the black square refers to Nero's Temple. (D) Plan of the Nero's Temple. (E) Cross-section and the system of construction for the walls, indicating the

architectural elements with dimensions of the stone blocks. (F) The cross-section for the construction materials confirms the reuse of stone blocks from Ramses II and using Roman red bricks and Roman mortar admixed together in one construction building near Nero's Temple.

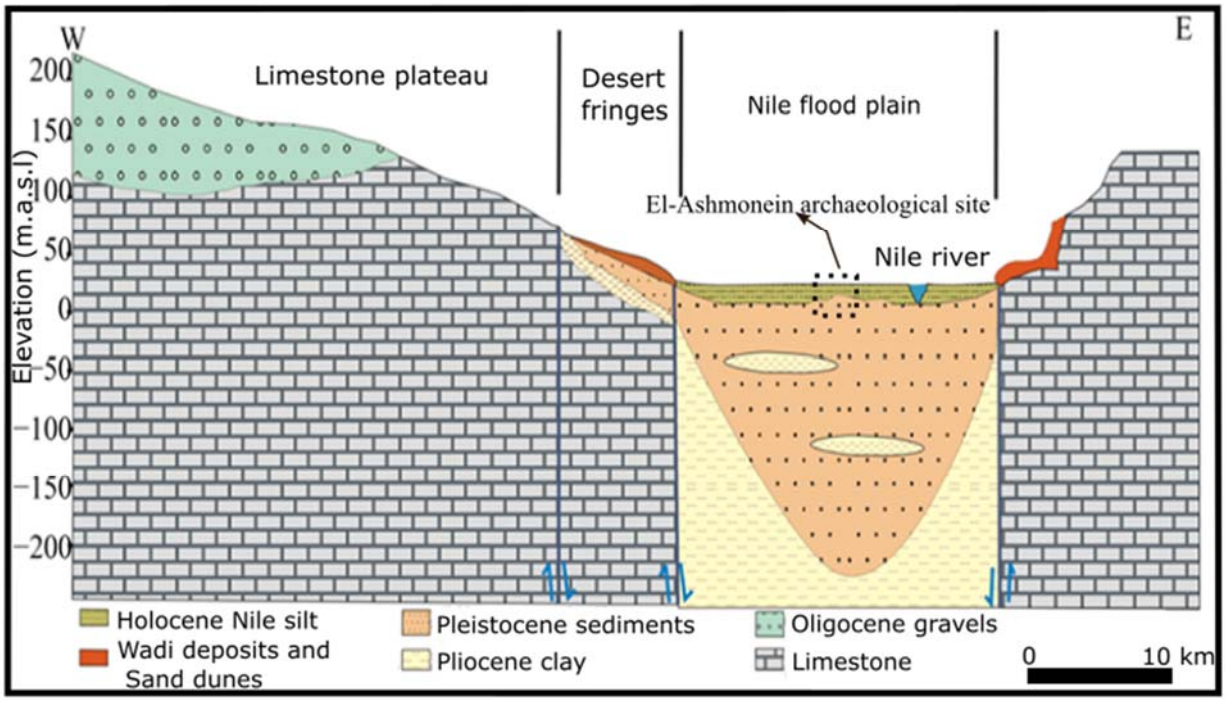


Fig. 3.4.2. Cross-section of the geological and geohydrological features of Minia, including the study area (dotted black square referrers to Al-Ashmonein archaeological site). Edited after [**39**].

3. Materials and methods

3.1 Materials

The collected samples carry six codes in Nero's Temple (NT), where NT1 (crust) was taken from a fallen highly weathered part that represents the crust. NT2 (stone) was collected from fallen parts on the ground that represents the altered stone. NT3 (crust) was taken from fallen highly weathered parts in different locations that represent the crust. NT4 (mortar) was collected from the fallen parts on the ground and represents the joint mortar

of the temple. Finally, NT5 (mortar) and NT6 (mortar) were taken from the fallen parts on the ground that represent the Roman mortar. The samples were about 10 cm^2 and thickness of 4 cm. The samples were prepared in a solid and powered state for analysis and examination purposes (**Fig. 3.4.3. A** and **B**).

3.2 Methods

3.2.1 In-situ and desk investigation

The in-situ investigation was performed for photographing and documentation of the current conditions of Nero's Temple during various visits to the archaeological site. A visual inspection of the temple was done to assess and record the deterioration causes and decay pathology. The surrounding environmental features were also observed to identify the sources of the contaminated water. The recording of the degradation aspects of the building materials and data collection for the architectural and structural elements for engineering drawing purposes were done using AutoCAD software 2021. Finally, salt decay identification, classification, and categorization were recorded from degradation maps.

3.2.2 Analytical study

Multi-analytical and examination techniques were carried out for the qualitative and quantitative assessment of salt decay of Nero's Temple construction materials using polarizing optical microscopy (POM), X-ray diffraction (XRD), micro-X-ray fluorescence spectrometry (μXRF), portable Raman spectroscopy (PRS), digital microscopy (DGM), scanning electron microscopy (SEM) with EDS. These techniques let us identify the construction materials of Nero's Temple (stones + mortars) and their by-products. All these types of equipment have been hosted in the Department of Earth Sciences (UGEA-PHAM service) and Central Services of Scientific, and Technological Research (SC-ICYT) at the University of Cadiz (Spain). All the techniques described below were applied to the six selected samples.

1. Thin sections were prepared for study under an Olympus BH-2 polarizing optical microscope to identify the different minerals and altered phases of the construction materials.
2. XRD analysis was carried out to recognize the components of the samples and detect the by-products of minerals resulting from alterations and reactions between the substrate (construction materials) and geoenvironmental conditions. A Bruker D-8 Advance ECO diffractometer was used, equipped with a high-speed measurement Lynxeye detector, using the following specifications: CuKα radiation filtered by Ni, graphite monochromator, and fixed slots, 2theta 5° to 60° scanning angle; diffractograms were interpreted with the software EVA (Bruker-AXS).
3. Portable Raman spectroscopy (i-Raman Pro, BW TEK) BW475-532S model, equipped with a 785 nm laser, is a powerful non-destructive technique (NDT) to identify the components of the construction materials and detect the sources of the decay of the building materials of Nero's Temple.
4. A Bruker AXS M-4 Tornado sequential dispersive wave X-ray spectrometer with a Rh tube operating at 4000 W was used to identify the elemental composition of the samples and to confirm the results of X-ray diffraction.
5. A binocular microscope (USB digital microscope with stand), magnification between 20 and 400×, and equipped with a digital camera of 1.3 Mpx was used to survey the morphological characteristics of the samples and to detect different kinds of degradation aspects.
6. A scanning electron microscope (Quanta 200), voltage between 200 V to 30 kV, resolution 3.0 nm at 30 kV and 10 nm at 3 kV, and supplied with EDAX 60 mm 2 Octane Super EDS detector was utilized for salts phases detection, degradation patterns, and elemental analysis for the detected salts.

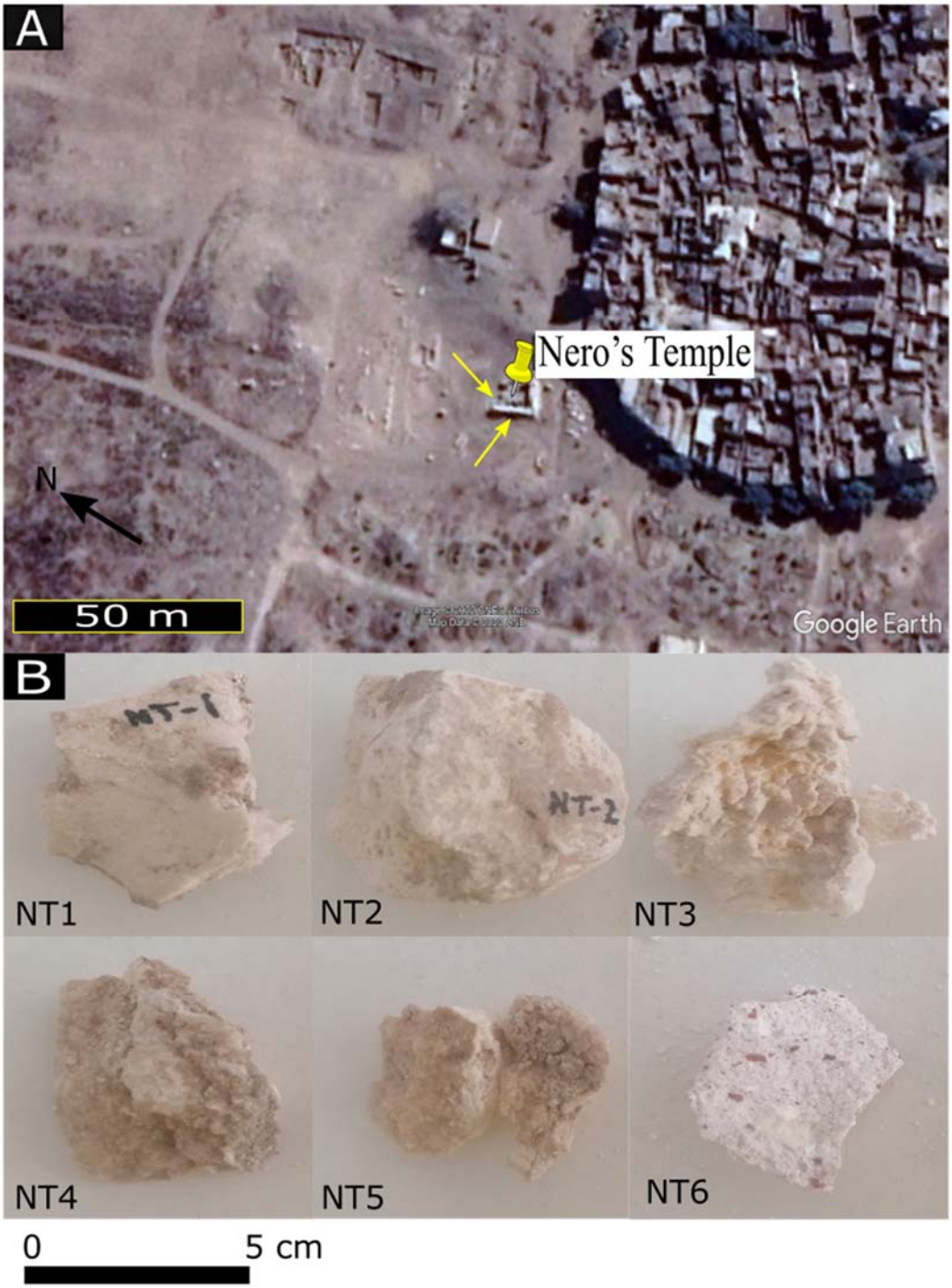


Fig. 3.4.3. (A) Google Earth view, Nero's Temple in yellow pin and yellow arrows represent the sampling places. (B) The samples of the study temple, where NT1 and NT3 represent the surface crust, NT2 altered construction stone, NT4, and NT5 represent the structural mortar and NT6 represents the structural roman mortar.

4. Results

4.1 In-situ observation

The current preservation state of Nero's Temple is extremely decayed due to the salt erosion effects on the structural and architectural elements of the temple. From field inspections, the contaminated water from canals, agricultural lands, and sewage systems of the houses around the archaeological site, even from flooding events for several decades led to extreme chemical weathering (salt erosion) for the construction materials of the temple (**Fig. 3.4.4**). The distance between the temple and houses, canals, and agricultural lands are 50, 300, and 500 m, respectively (**Fig. 3.4.4 A**). **Fig. 3.4.4** (**B**) presents the conservation problems of the temple since 1983 due to the contaminated water around the temple. The structural elements of the temple were in direct contact with water and the water level reached up to 1 m that affecting the durability of the construction materials. Figure 3.4.4 (**C-E**) show the recent maintenance situation of the temple. It has been observed that most of the building materials have been degraded and damaged severely due to the accumulative impact of the contaminated water that resulted in high salt weathering. Moreover, the degradation maps were drawn to record the decay aspects of the structural and architectural elements (**Fig. 3.4.5**). It has been noticed that flaking, scaling, fracturing, efflorescence, sub-florescence, loss of material, blistering, and layering are the deterioration patterns in the construction materials of Nero's Temple due to the effect of salt weathering. In addition, soiled patinas, cracks, and microbial growth have been also observed (**Fig. 3.4.5. A, B,** and **C**). Efflorescence and sub-florescence are the dominant decay forms in the whole stones and semi qualitatively they are estimated as about 90% of the total decay patterns in the building stones.

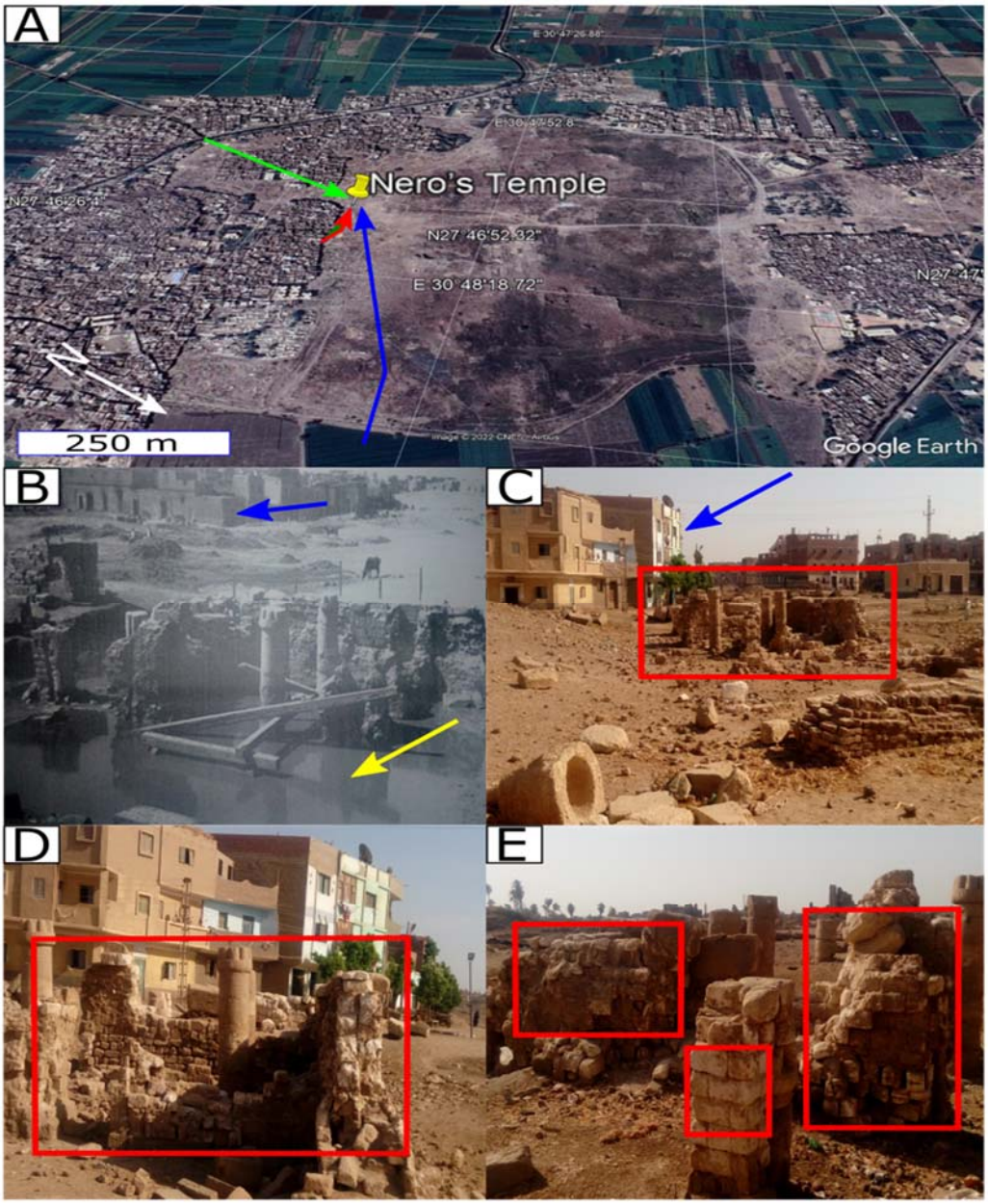


Fig. 3.4.4. (A) Nero's Temple and the contaminated water sources. Green, red and blue arrows refer to canal water, houses, and agricultural lands, respectively. (B) The preservation state of the temple in 1983. The Blue arrow refers to the near houses and the yellow arrow indicates the gathered water, from [**43**]. (C-E) The current state of preservation in 2022 for Nero's Temple with its decayed and damaged elements due to salt weathering. Red rectangles refer to the degradation and deformation of the temple's architectural and structural elements. The blue arrow refers to the houses near the temple.

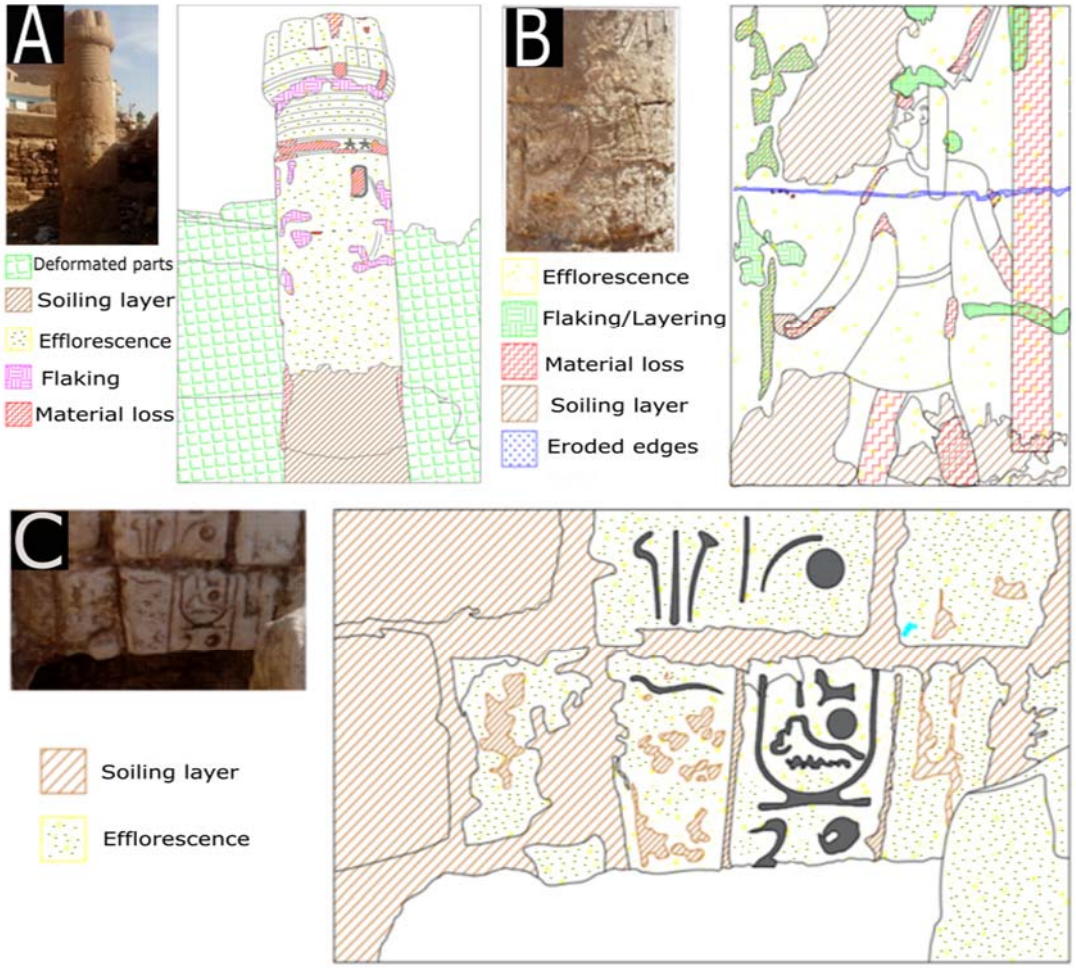


Fig. 3.4.5. Deterioration maps for the remaining parts of Nero's Temple. (A) Refers to the general deterioration aspects (soiling layer, salt erosion, and loss of material) of the remaining column. (B) Refers to the focused deteriorated part with a high rate of decay in the column that shows the figure of Emperor Nero. (C) Refers to the severe decay of the important cartouche of Ramses II king.

4.2 Petrological study

Thin sections were prepared to investigate the composition of the archaeological samples and identify their components, mineral alterations, and by-products because of the chemical and physical deterioration of the temple construction materials (**Fig. 6**). The construction material (**Fig. 3.4.6. NT1** (crust) and **NT2** (stone)) is a biomicritic limestone with peloids, and the appearance reflects the natural texture of the rock is well preserved. Therefore, the building material is mainly composed of calcite with rare amounts of

dolomite, gypsum, quartz, halite, iron oxides, and opaque minerals. Anhydrite is partially replaced by gypsum (**Fig. 3.4.6. NT1**).

On the other hand, **NT2** is a recrystallized limestone with bioclasts such as nummulitic remains. Calcite occurs as fine- to medium-grained, anhedral, sutured interlocked crystals showing mosaic textures. Calcite is partly fragmented (granulated and crushed) and deformed into very fine-grained crystals and surrounded by the original crystals. Carbonate minerals are slightly stained and outlined by thin films of iron oxides. Additionally, some carbonate minerals are partly replaced or invaded by microcrystalline quartz or gypsum at their boundaries and interstices of grains. Dolomite occurs in rare amounts as fine-grained, subhedral to euhedral crystals in the finer matrix of the rock. Halite occurs as fine- to very fine-grained anhedral aggregates and partially fills some pore space. Moreover, **NT2** shows a cataclastic effect (deformation), where coarser-grained carbonate minerals (calcite) are crushed and granulated to form a finer matrix of calcite. Pore spaces are present in significant amounts due to the dissolution of original carbonate minerals. The rock was also affected by alteration due to secondary alteration of gypsum and quartz (microcrystalline silica) replacement over carbonate. In **NT 3** (crust), considerable amounts of pores are detected in the stone due to weathering.

The structural mortars (**Fig. 3.4.6. NT4** and **NT5**) are very fine- to coarse-grained, showing porphyritic texture (coarse-grained quartz and rock fragments enclosed in a fine-grained matrix). Several irregular pores and cavities were detected in the sample. The mortar is very fine-grained to coarse and composed of rock fragments, quartz cemented by a very fine-grained matrix of carbonate (main calcite) admixed with gypsum, and minor amounts of iron oxides associated with rare amounts of halite, feldspars (plagioclase) with a lamellar appearance and biotite, muscovite, epidote, opaque minerals. Rock fragments are represented by main limestone (calcite), chert and flint and occur as coarse- to medium-grained rounded to subangular outlines and scattered in the very fine-grained sample matrix. Few microfossils are observed scattered in the rock fragment of calcite and a rare amount of clay (**Fig. 6. NT4** and **NT5**). Quartz and feldspars occur as medium- to fine-grained subrounded to subangular outlines and cemented by a mixture of a very fine-grained

matrix. Iron oxides and opaque minerals occur as fine- to medium-grained scattered in the sample. Halite is represented by traces enclosed in some pore spaces. Mafic minerals are fine-grained and observed in the matrix of the sample. A significant number of irregular pores with different shapes and sizes are scattered in the sample. **Fig. 3.4.6** (**NT6**) represents different kind of mortar (Roman mortar used in the period of Emperor Nero) mainly composed of pottery fragments, sand (quartz) and lime (calcite), and single grains of quartz are clearly observed.

The essential components for mortars (**Fig. 3.4.6. NT4, NT5,** and **NT6**) are affected by deformations, showing microcracks in quartz, rock fragments, and corroded boundaries and edges. Several pore spaces and cavities (vugs) are present due to the alteration and dissolution of the essential components such as calcite and calcium sulfates. Biotite and mafic minerals are partly to highly affected by alteration.

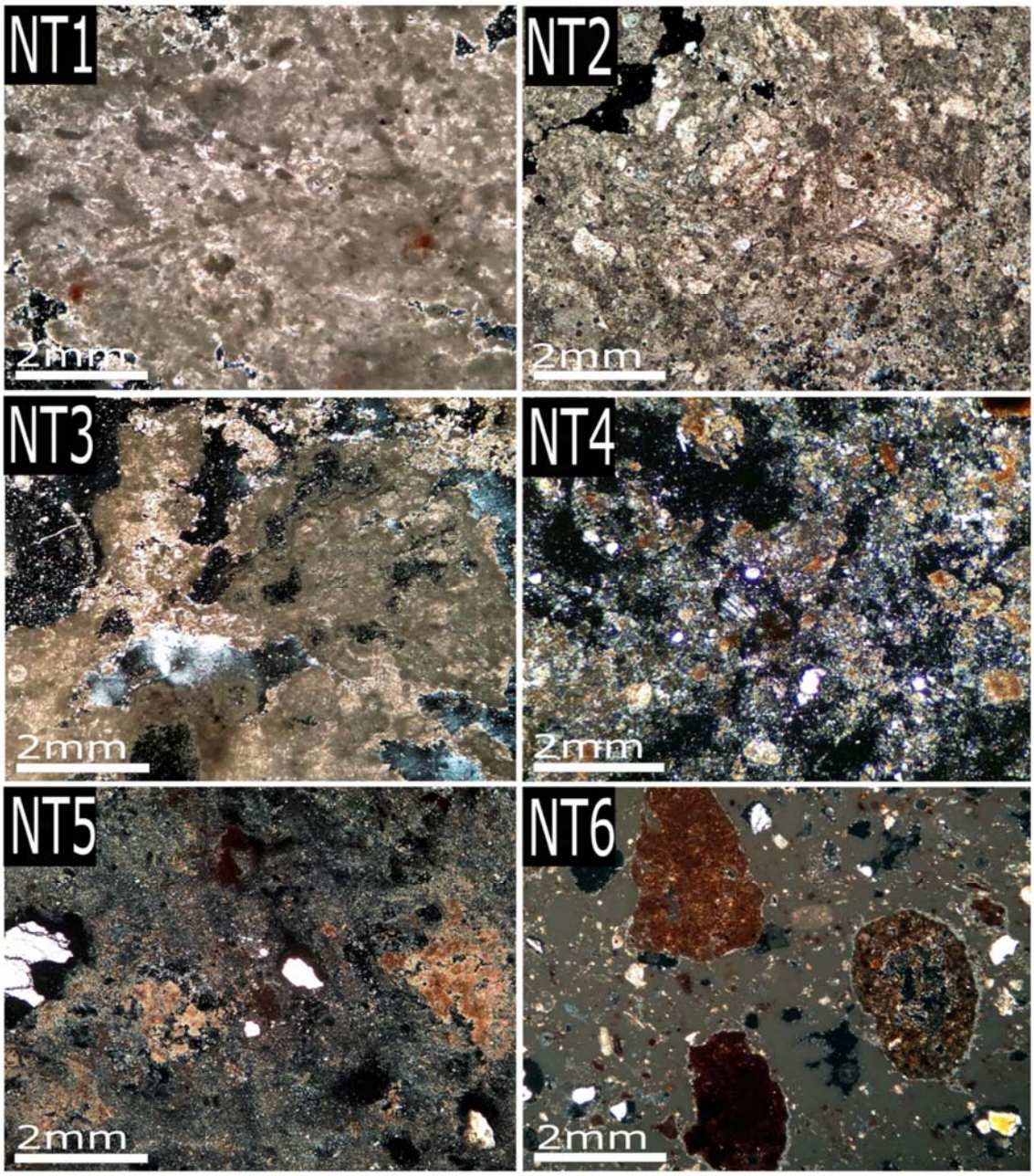


Fig. 3.4.6. Thin section photomicrographs of limestone and mortars of Nero's Temple. (NT1, NT3) crust sections with significant amounts of pores are existed due to the dissolution and weathering processes of original carbonate minerals. (NT2) Altered biomicrite limestone as fine- to medium-grained; anhedral, sutured interlocked crystals. (NT4, NT5) Structural mortar with very fine to coarse grains and mainly composed of sand, lime, and gypsum. (NT6) Roman mortar is composed of sand with angular single grains of quartz, pottery fragments, and crushed limestone.

4.3 Mineralogical and elemental analysis of the construction materials

4.3.1 Mineralogical analysis

X-ray diffraction was used to identify the mineral composition of the construction building materials and the structural mortar semi-quantitatively (**Table 3.4.1**). Salts and the alteration by-products on the surfaces of the stones were analyzed. Sixteen minerals were detected that were composed of mainly hydrated and anhydrous sulfates, nitrates, carbonate, phosphates, and chlorides. For crusts (**Table 3.4.1. NT1**), calcite is the main constituent. In addition to the degradation compounds, they are classified as chlorides (halite and sylvite) and bicarbonates (nahcolite, $NaHCO_3$). Calcite and halite existed as very abundant, while nahcolite and sylvite existed as scarce. In Table 3.4.1 (**NT3**), calcite was detected as a common mineral. Degradation compounds were detected and classified as chloride (halite), nitrate (humberstonite, $Na_7K_3Mg_2(SO_4)_6(NO_3)_2.6H_2O$, and ungemachite, $K_3Na_8Fe\ (SO_4)_6(NO_3)_2.6H_2O$)), and anhydrous sulfate (anhydrite). Halite appeared as very abundant, calcite and humberstonite appeared as abundant, and ungemachite and anhydrite appeared as scarce. For stone blocks (core) (**Table 3.4.1. NT2**), calcite was detected as the main constituent of stone blocks, while halite was detected as an abundant alteration compound.

For structural mortar (**Table 3.4.1. NT4**), calcite, quartz, and gypsum are the main constituents, which were composed mainly of lime, gypsum, and sand. Additionally, the alteration by-products were detected and classified as hydrated sulfate minerals (gypsum, bassanite, and starkeyite ($MgCaSO_4.4H_2O$), anhydrous sulfate (anhydrite), chloride (halite), phosphates (brushite), carbonates (natron), and silicates (illite). Halite appeared very abundant, and the rest of the compounds appeared as scarce. On the other hand, in Table 1 (**NT5**) calcite, quartz, and gypsum are the main constituents of the mortar, which was also composed mainly of lime, gypsum, and sand. Additionally, the alteration by-products were detected and classified as anhydrous sulfate (anhydrite) and chloride (halite). Gypsum appeared abundant, and the rest of the compounds appeared as scarce.

Structural Roman mortar (**Table 3.4.1. NT6**) is composed of calcite, quartz, microcline, and sepiolite. As compounds of degradation, hydrated sulfate (gypsum and basanite), anhydrous sulfate (anhydrite), and phosphates (strengite $FePO_4.2H_2O$) were detected. Calcite is present as very abundant, and the rest of the compounds are present as scarce.

Furthermore, the samples were analyzed using Raman spectroscopy with an extended wavelength range from 100 to 2000 cm^{-1}. The results of the analysis responded well to XRD results. The majority of the minerals and salts detected by XRD were found in the Raman analysis such as calcite, quartz, halite, gypsum, anhydrite and brushite. Calcite is a common mineral in all samples and is identified at 156, 284, 711, and 1086 cm^{-1} (**Fig. 3.4.7**). In this regard, [**45**] confirmed that the carbonate minerals show four prominent absorption bands in the regions 890-870, 720-700, 1000-1100, and 1450-1420 cm^{-1}, and calcite and dolomite groups are characterized by the presence of peaks at 288 and 309 cm^{-1}. The anhydrite phase, which is completely altered from gypsum, is identified at 417, 500, 611, 629, 676, 1018, 1130, 1160, 1582, and 1610 cm^{-1} (**Fig. 3.4.7**). Salt of brushite signed at 1000 cm^{-1}. Finally, halite as common salt in all samples is identified between 100 and 430 cm^{-1}, as shown in NT2, NT4, and NT6 (**Fig. 3.4.7**).

Table 3.4.1 presents semi-quantitative mineralogical analysis of the samples, where NT1 and NT3 represent the surface crust, NT2 altered construction stone, NT4, and NT5 represent the structural mortar and NT6 represents the structural roman mortar. Legends: (Cal) calcite; (Hl) halite; (It) illite; (Hbe) humberstonite; (Ugm) ungemachite; (Gp) gypsum; (Anh) anhydrite; (Bas) bassanite; (Brt) brushite; (Qz) quartz; (Na) natron; (Mc) microcline; (Sep) sepiolite; (Nah) nahcolite; (Stk) starkeyite; (Stg) strengite; (Syl) sylvite; x, scarce; xx, abundant; xxx, very abundant. Minerals symbols after [44] except for (It) illite; (Hbe) humberstonite; (Bas) bassanite; (Brt) brushite; (Na) natron; (Nah) nahcolite; (Stk) starkeyite; (Stg) strengite; (Syl) sylvite.

	NT1	NT2	NT3	NT4	NT5	NT6
	Crust	Stone	Crust	Mortar	Mortar	Mortar
Cal	+++	+++	++	+	+	+
Hl	+++	++	+++	+++	+	
It				+		
Hbe			++			
Ugm			+			
Gp				+	++	
Anh			+	+	+	+
Bas				+		+
Brt				+		
Qz				+	+	+
Na				+		
Mc						+
Sep						+
Nah	+					
Stk				+		
Stg						+
Syl	+					+

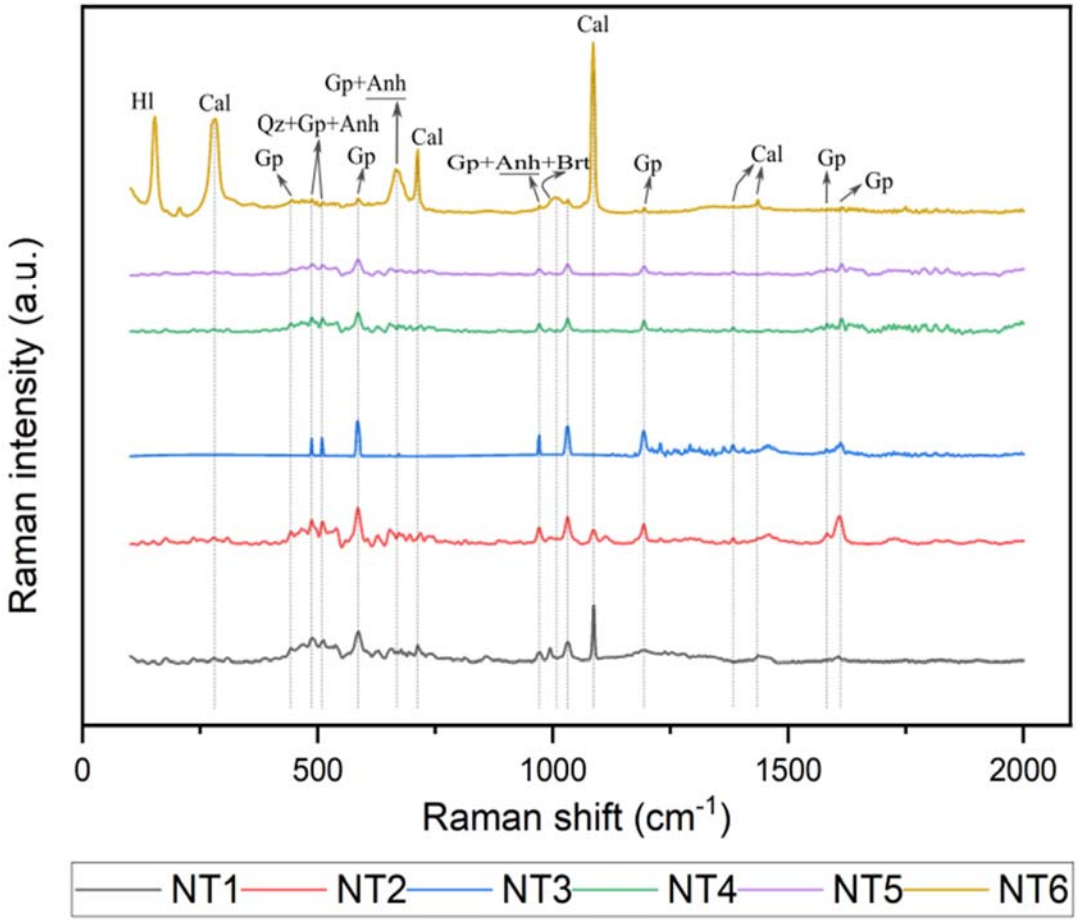


Fig. 3.4.7. Raman spectra for NT1 and NT3 (Crust) NT2 (altered stone), NT4 and NT5 (structural mortar), and NT6 (structural roman mortar). Legend: Anh (anhydrite); Hl (halite); Cal (Calcite); Gp (gypsum); Brt (brushite); Qz (quartz). Minerals symbols after [**44**] except for Brt (brushite).

4.3.2 Elemental analysis

Micro X-ray fluorescence was carried out to identify the elements for each sample of construction materials and to confirm the results of X-ray diffraction (**Table 3.4.2**). The results responded well to the mineralogical analysis results, where the analysis showed the existence of salt ions (Ca^{2+}, Mg^{2+}, K^{+}, Na^{+}, Al^{+}, SO_4^{2-}, NO_3^{-}, and Cl^{-}), and the most dominant ions were sulfate, chloride, sodium, and calcium. Chloride, sodium, and sulfate ions were significant in NT1, NT2, NT3, and NT4. In NT5 and NT6, the most predominant ions were

silicate, chloride, and sulfate. Magnesium appeared significantly in NT3. Iron and aluminium ions appeared clearly in NT5 and NT6.

Table 3.4.2. Chemical composition of the six construction materials. Major and minor elements are expressed in wt. % oxides.

	NT1	NT2	NT3	NT4	NT5	NT6
	Crust	Stone	Crust	Mortar	Mortar	Mortar
CuO	0.003	-	0.007	-	0.002	-
Al_2O_3	0.795	-	0.725	0.662	1.009	4.039
SiO_2	1.957	0.250	2.134	8.100	12.174	40.458
K_2O	8.629	2.809	17.833	3.073	1.908	0.589
CaO	26.059	37.729	11.768	29.403	44.942	49.997
Cl	16.506	13.374	7.111	8.419	1.246	-
TiO_2	0.046	-	0.086	0.119	0.342	0.528
Fe_2O_3	0.185	0.015	0.422	0.509	1.042	2.914
MgO	1.615	0.291	3.853	1.680	1.187	0.298
SO_3	15.259	6.509	30.738	32.255	33.755	0.625
Na_2O	28.903	39.000	25.241	15.546	2.130	0.625
ZrO	0.008	0.004	0.012	0.012	0.021	0.025
Cr_2O_3	0.033	0.009	0.010	-	0.010	-
SrO	-	0.009	0.002	0.048	0.212	0.021
P_2O_5	-	-	0.052	0.150	-	0.461
MnO	-	-	0.005	0.012	0.016	0.044
V_2O_5	-	-		0.009	-	-

4.4 Microscopic investigation

4.4.1 Digital microscope

Textural aspects from digital microscopy were made to examine and investigate the decay and salt weathering of the Nero temple building materials, such as limestone, crusts, and mortars (**Fig. 3.4.8**). Efflorescence and sub-florescence exist in the building materials

because of salt weathering, where there is a loose salt deposit on the surface mixed with the soiling layer and a loose salt deposit below the surface of the construction materials, as well as pores, layering, and disaggregation are observed (**Fig. 3.4.8. NT1** and **NT2**). In Fig. 3.4.8 (**NT3**), the morphological feature indicates the disintegrated texture of the stone. The precipitation of the salt is observed and the flaking decay pattern of the stone surface is detected due to the salt erosion. In Fig. 3.4.8 (**NT4**), micro-fissures, soiling, and surface crust are noticed as degradation patterns for the structural mortar. Salt precipitation on the surface is seen as well. In Fig. 3.4.8 (**NT5**), the surface texture shows an extreme disintegration for the structural mortar with many pores**.** Efflorescence and sub-florescence are observed on and below the surface. Fig. 3.4.8 (**NT6**) presents the textural properties of the Roman Mortar. The various grain sizes of the quartz and Calcite fragments are observed. Moreover, calcite is found as a matrix, and pottery fragments are observed as well. Pores and salt deposits are detected. Finally, pores are seen on the surface and below the surface of the construction materials as intrinsic component and their size can be increased due to dissolution processes for the stone minerals because of water existing and its fluctuations. Salt erosion is considered the most dominant degradation pattern in all samples.

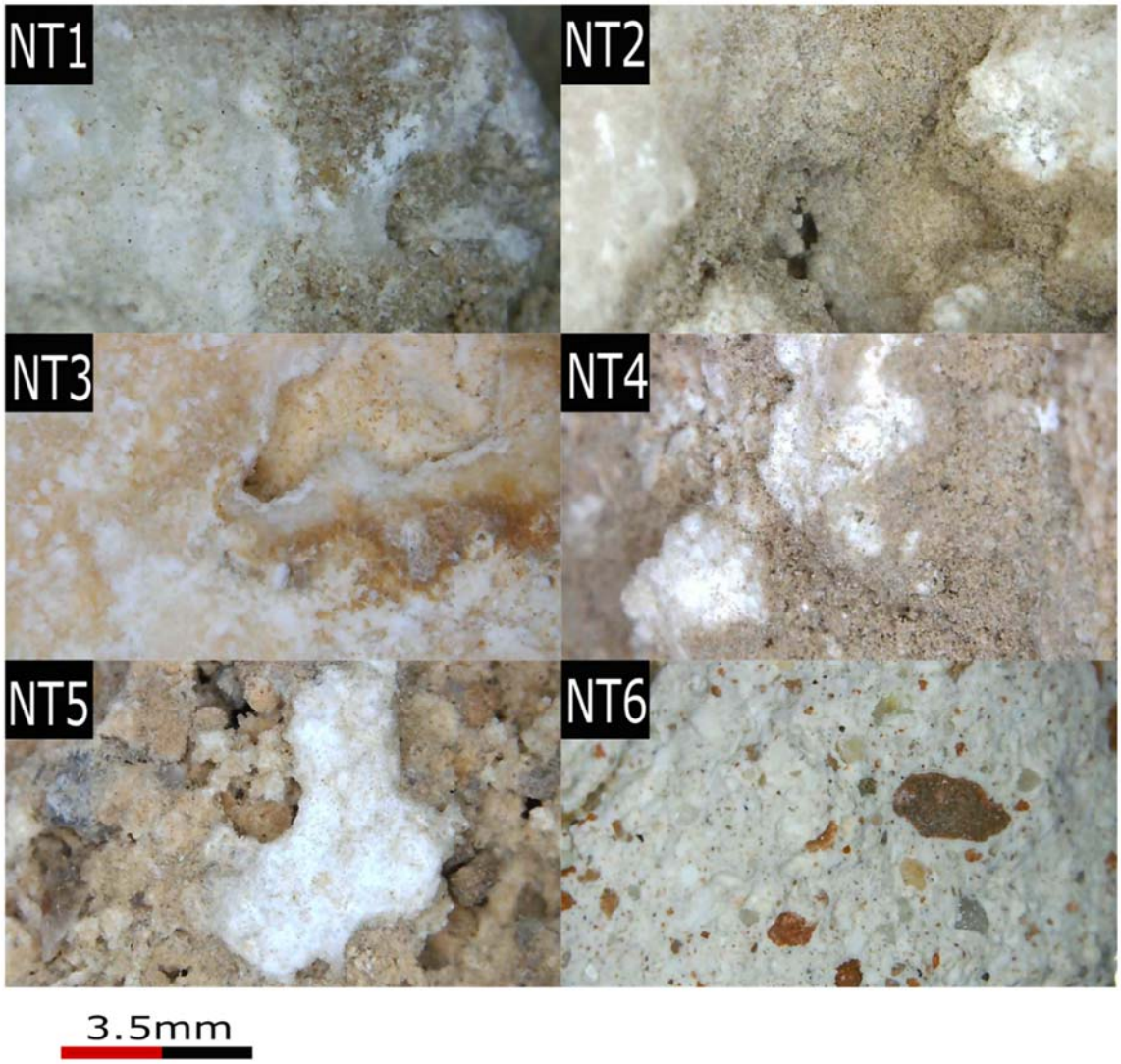


Fig. 3.4.8. Microphotographs for the construction elements to detect the texture features of decayed stones and mortars. NT1 (crust), NT2 (altered stone), NT3 (crust), NT4 (mortar), NT5 (mortar) and NT6 (mortar). Salts precipitation and disintegration are dominant decay patterns for all samples.

4.4.2 Scanning electron microscope investigation (SEM)-EDS

The microstructural and morphological features reflected the severe decay conditions of the construction elements; the disintegration and salt weathering were clear and detected. Halite was detected as the most dominant salt in cubic shapes and existed in euhedral, subhedral, and anhedral forms, as halite crystals are unstable due to their high solubility.

Halite is present in the liquid phase and integrated with the crystallized crystals in all samples. This halite has a massive texture and covered the grains, as well as interacts with the stone surfaces, as shown in NT1, NT2, NT3, NT4, and NT5 (**Fig. 3.4.9**). Gypsum existed in layers, nodules, and flower shapes between and around the grains, and gypsum crystals were thin and looked like needles with smooth surfaces, as shown in NT4 and NT5 (**Fig. 3.4.9**). Bassanite was detected in different shapes between square rods and massive shapes, as shown in NT4 and NT6 (**Fig. 3.4.9**). Moreover, anhydrite was detected in euhedral shapes and massive amounts in clear nodule shapes, as shown in NT3, NT5, and NT6 (**Fig. 3.4.9**). In NT3 (**Fig. 3.4.9**), double salt crystals of humberstonite and ungemachite exist in isometric shapes and integrate with other sulfate salts and halite. Finally, microcracks and cavities were detected in the mortar and stone blocks, which reflect the chemical and physical weathering of the construction materials.

Elemental analysis (EDS) was carried out to prove the existence of different kinds of salts (sulfates, chlorides, phosphates, nitrates, carbonates, and bicarbonates) that caused high salt decay for the temple construction materials. The EDS results responded well to the XRD, Raman analysis, and μXRF results. Sodium, chlorine, calcium, sulfur, magnesium, phosphorous, and potassium were detected as the most common ions. Chlorine and sodium were the dominant elements in all samples, as shown in NT1, NT2, NT3, NT4, and NT6 (**Fig. 3.4.10**). Phosphorous was detected clearly in samples NT1 and NT6, as it is shown in **Fig. 3.4.10** (**NT1-A** and **NT6-H**) confirming the presence of phosphate salts.

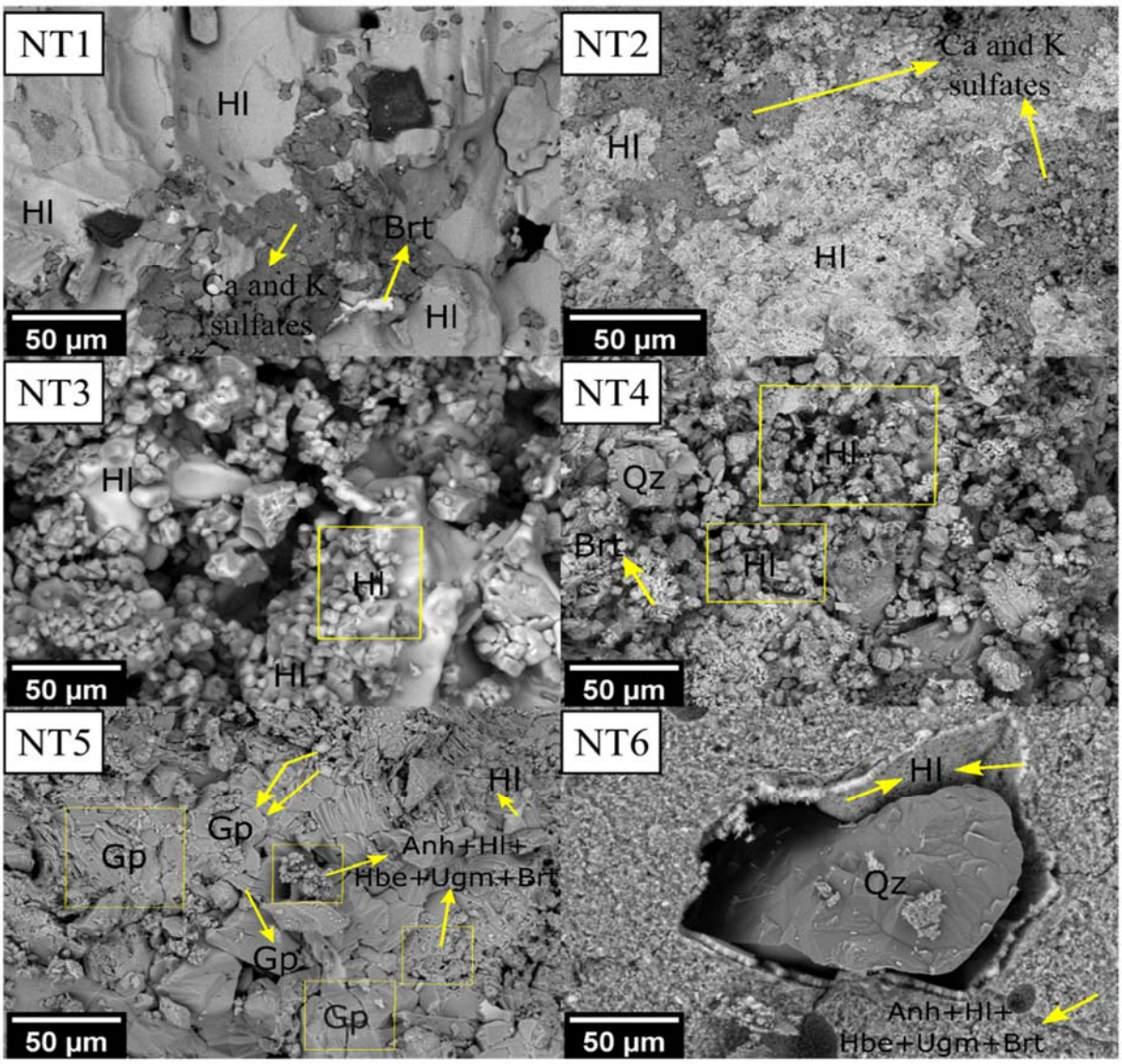
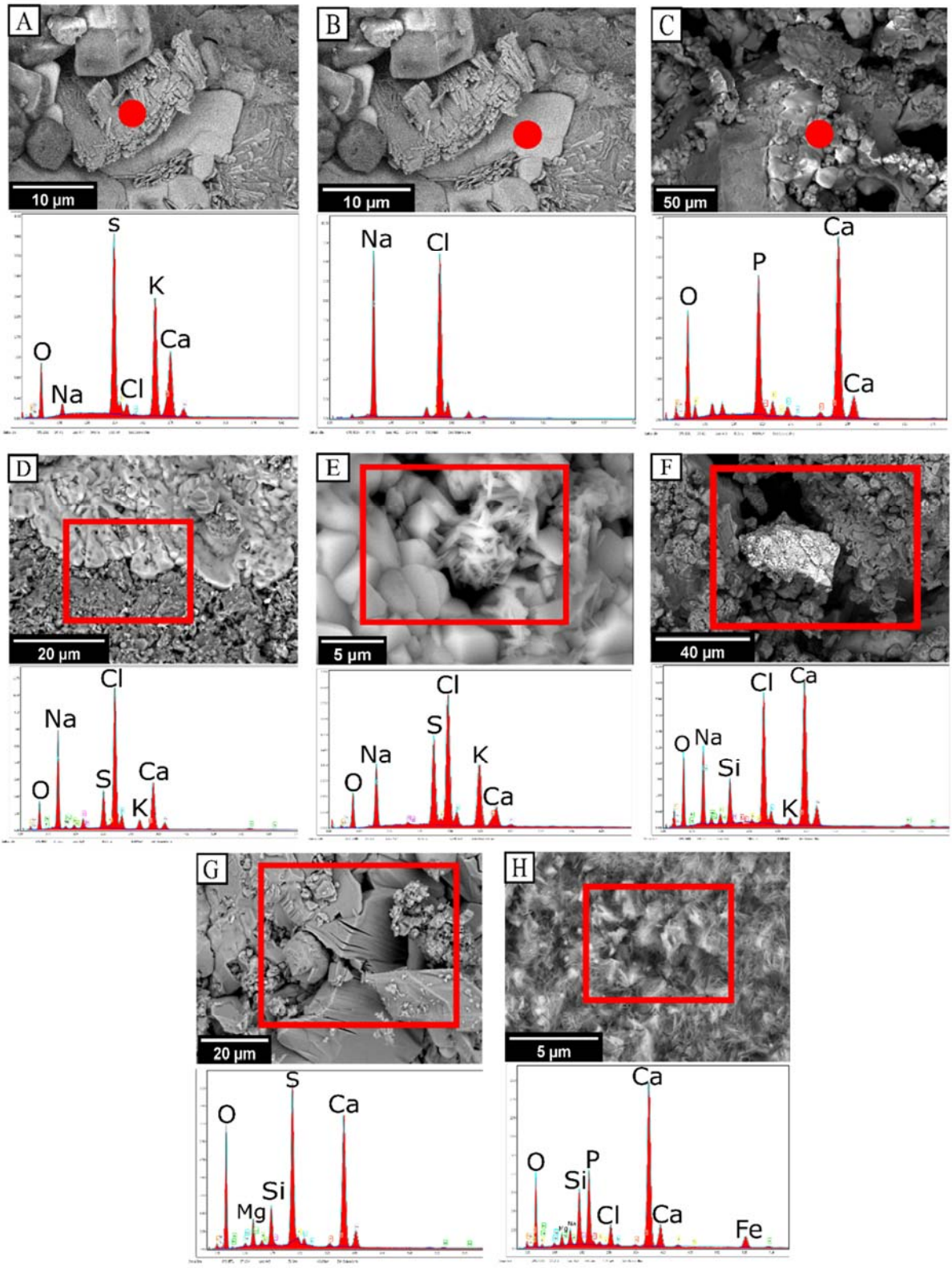


Fig. 3.4.9. General morphological view of the six samples (NT1-NT6). In NT1 to NT4, the halite (light gray) and Ca and K sulfates (dark grey) crusts are shown, with some calcium-phosphate crystals (in white) and black organic particles. NT5 shows a crust composed mainly of layered and mesostructured gypsum with traces of Na and Cl (halite) and sulfates. In NT6, there is a pore with a quartz grain with signs of corrosion and a film with acicular-planar halite crystals, and a matrix composed of calcite and a mixture of calcium silicates, halite, sulfates, and calcium-phosphate. Legends: Legend: Hl (halite); Gp (gypsum); Anh (anhydrite); Brt (brushite); Qz (quartz); Hbe (humberstonite); Ugm (ungemachite). Minerals symbols after [**44**] except for Brt (brushite).



(Caption is in the next page)

Fig. 3.4.10. EDS results of detailed points and areas (dots and rectangles areas, respectively) for the temple construction materials. In sample NT1, (A) refers to sulfates, (B) refers to chlorides, and (C) refers to phosphates. In NT2 (D) and NT3 (E), the red rectangles refer to two types of salt attack (sulfates and chlorides). In NT4 (F), quartz grains of the mortar surrounded by halite can be distinguished. NT5 (G) shows an example of a salt attack of sulfates of structural mortar and NT6 (H) shows a different kind of salt attack (phosphates and chlorides) over the Roman mortar.

5. Discussion

Results revealed that limestone (biomicritic) is the main building material of Nero's Temple, which was quarried from Minia formations. Significant lime gypsum mortar appeared in the results and was confirmed by the polarizing microscope, micro-X-ray fluorescence, Raman spectroscopy, and scanning electron microscope with EDS for the samples (NT 4 and NT 5). This mortar consists of lime, gypsum, and sand, dating back to the Ramses II era (Egyptian New kingdom 1540 – 1075 BC). In this regard, gypsum was used in the horizontal and vertical structural joints of construction materials. Gypsum was added to the lime to have a mixture of so-called gypsum concretes, and this technology was also found in tell Amarana in Minia [**46**]. Roman hydraulic lime mortar from the era of Emperor Nero (50 – 54 CE) was detected in NT 6, which consists of lime, quartz, pottery fragments, and clay additions. Pottery fragments, microcline and sepiolite (pozzolans) were detected by analytical techniques as a source of silica and alumina in the mortar combination to strengthen the hydraulicity of the mortar. Accordingly, Caro [**47**] confirmed that Romans added ceramics to the lime mortars to improve their durability and hydraulicity properties.

These previous construction materials have been subjected to the accumulated impact of salt weathering. In this sense, chlorides, hydrated Ca-Mg-Na-Al-K sulfates, nitrates, phosphates, carbonates, and bicarbonates were detected as precipitated salts. From the site investigation, different sources of water (canals, sewage, and agricultural) near the temple are the clearest proposals as sources of the decay salts. In this sense, the mechanism of salt weathering for the temple was due to the rising up of the contaminated water from

the soil solution under the temple by capillary action/suction through the fine pores. Then, the capillaries draw water from the soil beneath the temple to the whole building structures against the force of gravity, leading first to the damp, which carries up the salts to the base of the temple walls, and then to the whole masonry materials. When the water evaporates from the walls, the salts are left behind. Repeated wetting and drying cycles with daily and seasonal changes led to the cyclic precipitation of salts and resulted in severe salt attacks on the structural and architectural elements of the temple (**Fig. 3.4.11**). In this regard, Young [**48**] confirmed this mechanism of salt attack and explained that the quality of the building materials and of construction and subsequent maintenance, climate, and soil conditions are strong drivers of the severity of salt-damp problems. Moreover, Abdel-Mageed et al. [**40**] confirmed that the water source used for irrigation in Minia contains sodium, chlorides, and calcium and magnesium ions, and they indicated a high concentration of total soluble salts (TSS) (ranging from 1477 to 2497 mg L^{-1}), chloride and bicarbonate concentrations, with a water electrical conductivity ranging from 2.24 to 3.86 dS m^{-1}.

Halite (NaCl) is present in all analyzed samples as abundant to very abundant, and sylvite (KCl) is only present in NT1 as scarce (cruts). Halite is considered the main decay anhydrous salt for construction materials and structural mortars. In this sense, Derluyn et al. [**49**] explained that halite plays a serious role in the salt crystallization decay of the construction elements because it can dissolve in water or in humid environments and precipitates as cubic crystals, but the solubility of sodium chloride is only slightly temperature-dependent. The precipitation of halite crystals accumulates on the stone surfaces and causes efflorescence (on the surface) and sub-florescence (beneath the surface). After forming halite crystals on the surfaces, the crystals with drying cycles lose the water and cause blistering, layering, micro-cracking, granular disintegration, flaking, horizontal cracking, and scaling for building stones. Furthermore, chloride and sodium ions in the irrigation and contaminated water react with limestone (carbonates) as the main building material to produce a soluble salt called calcium chloride and other soluble salts such as sodium carbonate, calcium chloride, and sodium carbonate. These phases react with each other to

produce calcium carbonate (insoluble salt) and sodium chloride (soluble salt) as a crust. Consequently, many cycles of dissolution and crystallization led to weakness and decreased the strength and bearing capacity of the temple construction materials.

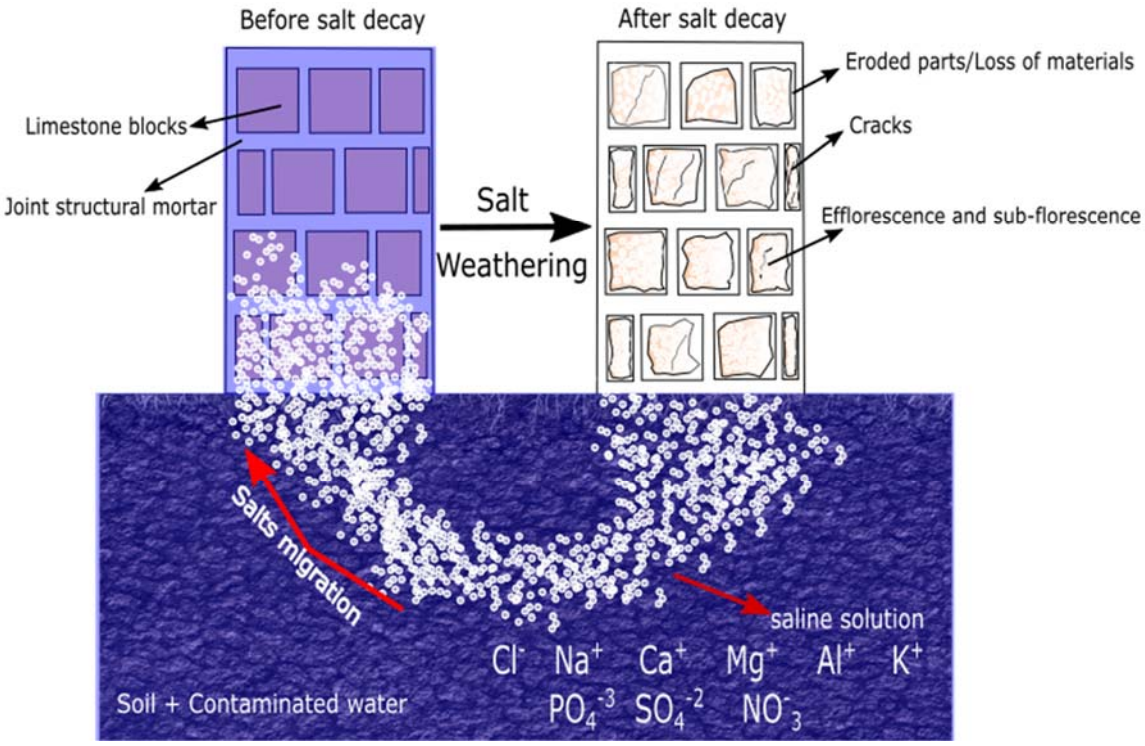


Fig. 3.4.11. Salt decay mechanism and salts migration to the construction materials of Nero's Temple.

Gypsum ($CaSO_4 \cdot 2H_2O$), bassanite ($2CaSO_4 \cdot H_2O$), and anhydrite ($CaSO_4$) were detected in some samples as alteration by-products in NT1, NT4, NT5, and NT6, but in NT4 and NT5, gypsum existed as a secondary adding to the lime gypsum mortar. The construction materials deteriorated by gypsum, and it transformed into the bassanite phase (most likely by dissolution–precipitation, starting from the surface in contact with the fluid or humidity). This phase represents a secondary stage, as it is unstable with respect to anhydrite. Additionally, Vaniman et al. [**50**] mentioned that the situation might also be complicated by groundwater dynamics, wherein static batch systems only gypsum precipitates, but in flowing systems, gypsum plus anhydrite precipitates. Cation exchange reactions can occur between clay minerals and Mg-sulfates in the absence of free liquid (H_2O), accompanied by

the formation of gypsum or bassanite. The dehydration and hydration processes of gypsum are considered a critical point in stone decay, as when dehydration occurs, the stone surfaces are converted to powder form and lose their cohesiveness. The dehydration of gypsum occurs at temperatures above 42 °C or where highly saline water exists and the temperature at the archaeological site of Nero's Temple could reach 44 °C, especially in the summer months. For this, Vaniman et al. [**50**] confirmed that in diluted solution, anhydrite forms at somewhat generally above ~40 to 60 °C. However, the activity of water has a significant effect, and in concentrated solutions, anhydrite can form at temperatures as low as 18 °C, with a water activity of 0.75. Gypsum exists as white surface crusts that are common in arid environments and produces silt-sized crystals several centimeters in length. Anhydrite exists as an alteration mineral and reflects the severe bleeding of the stone blocks, where it is existed as abundant to very abundant in most of the temple samples.

Hydrated magnesium sulfate (starkeyite, $MgSO_4 \cdot 4H_2O$) was detected in the NT4 sample (Mortar). In this context, Balboni et al. [**51**] explained that the hydration and dehydration of magnesium sulfate salts ($MgSO_4 + H_2O$) in many examples were due to their presence in contaminated water sources and they can cause damage in the drying and during condensation or uptake of rain and groundwater. Additionally, Gázquez et al. [**52**] confirmed that the precipitation of hydrated Mg sulfates plays a severe role in the decay rate of the architectural elements of buildings.

On the other hand, humberstonite ($Na_7K_3Mg_2(SO_4)_6(NO_3)_2 \cdot 6H_2O$) was detected as abundant salt and ungematchite ($K_3Na_8Fe(SO_4)_6(NO_3)_2 \cdot 6H_2O$) was detected as scarce salt in the NT3 sample (crust). These salts are considered composite because they are composed of sodium, calcium, magnesium, iron sulfate, and nitrate ions together. Benavente et al. [**27**] confirmed that pigeon droppings lead to crust formation and deposits, and their lixiviated water produces efflorescence, therefore these kinds of salts could be present due to the continuous pigeon droppings. Balboni et al. [**51**] also reported that sodium sulfate causes slower damage during the rewetting process than magnesium sulfate and depends on the viscosity of the solution. However, it could cause extreme damage to the building materials, as it expands over 300% concerning another mineral conversion, especially from anhydrite

[53]. Rodriguez-Navarro et al. [54] concluded that sodium sulfate is damaging mainly because it undergoes a high degree of volume change when hydrated. Moreover, nitrate salts accumulate anywhere where nitrogen compounds and Na, K, Mg, and Fe ions exist [55]. The source of nitrogen and Na, K, Mg, and Fe in the present study is from the soil solution around Nero's Temple. In this sense, Erić et al. [17] confirmed as an example that the potassium and nitrate ions required for the formation of nitrogen most likely originate from the soil solution.

Alkali-bicarbonate and carbonate salts (nahcolite, $NaHCO_3$, and natron, $Na_2CO_3 \times 10H_2O$) exist in the samples of NT1 (crust) and NT4 (mortar), respectively. Their presence was probably due to the condensation process and saline soil solution, and these alkali sodium carbonate salts could contribute to salt efflorescence, layering, cracking, and blistering for the building materials. In this sense, [56, 57] confirmed that efflorescence is mainly composed of alkali sodium salts due to rising dampness and the possible accumulation of water from flood events and saline soil.

Additionally, brushite ($CaHPO_4 \times 2H_2O$) and strengite ($FePO_4 \times 2H_2O$), as phosphate minerals, were found as scarce in samples NT4 (mortar) and NT6 (mortar). The deposition of phosphates could be associated with the presence of fresh or desiccated bats/birds [58, 59]. Besides phosphates may come from irrigation water and wastewaters. Brushite and strengite salt affected the durability of Nero's Temple during the rising up of water from the ground to the structural elements of the temple. Water carries phosphate (PO_4^{3-}) ions, which are released from irrigation water or wastewaters to react with the calcium (Ca^{2+}) ions of limestone in building materials.

The various mentioned salts could cause a high mechanical salt load for the building materials, as each salt has its own pressure parameter during crystallization, hydration, dehydration, hygroscopic expansion, thermal expansion, and capillary [60]. For example, Fernandez [61] said that magnesium and sodium sulfate salts have the ability to absorb water into their structure, which changes the lattice parameters to form a new crystal. The addition of water to crystallization often causes an increase in the molar volume of the salt

and a change in the crystal structure, and this process is called hydration pressure. Accordingly, in the present study, the dehydration of gypsum into bassanite and anhydrite could be accompanied by thermal expansion pressure during the dehydration process [62]. In addition, anhydrous and hydrated sulfates exist, and according to Stambolov and Van Asperen De Boer [63] anhydrous sulfates are precipitated in the pores from their oversaturated solutions as hydrates, and as the evaporation of water proceeds, the deposits of these hydrates drain out. The anhydrous salts formed are thus microcrystalline aggregates due to their fine porous structure. They promote the flow of more solutions from the interior of the pore to the surface. An increase in the relative humidity of the air (during cooling, mist, fog, or rain) will hydrate the dried-out anhydrous salt, which will lead to volume expansion and therefore pressure on the walls of the pores (pressure of hydration). Last, the differential behavior of the hydration expansion pressure of gypsum, basanite, and anhydrite and between hydrous and anhydrous sulfates leads to various degradation patterns in the building materials (cracking, flaking, and powdering).

Finally, all kinds of salts could react with climatic changes and environmental conditions to add more cycles of dissolution and crystallization processes. For instance, efflorescence on the temple walls could be formed by rainwater or water vapor, and these salts can be dissolved and recrystallized into the porous system and cause more decay for the building materials.

6. Conclusions

For the determination of the construction materials and their alterations, a series of multi-analytical, microscopic examinations and site investigation was carried out. The main construction material of the temple is limestone from Minia quarries. Lime gypsum joint mortar from Ramses II eras and hydraulic lime mortar from Emperor Nero were used as structural joint materials. Significantly, the research found that gypsum was added to lime as a second additive to enhance the mechanical and physical strength of the mortar. Furthermore, microcline and sepiolite were added as pozzolans to improve the resistance and durability of the Roman structural mortar, especially against water.

Salt weathering mainly causes the damage and decay of Nero's Temple. Different water sources (agricultural, wastewaters, and canals water) carried different kinds of soluble salts (chlorides, sulfates, carbonates, bicarbonates, phosphates, and nitrates), which were detected by mineralogical and elemental analysis. These salts led to the reduction of the durability and resilience of the temple building materials. Halite is considered the main decay salt that played an important role in the chemical weathering of the building materials and led to efflorescence and sub-florescence as the most dominant decay patterns in the temple construction materials. The scanning electron microscope with EDS revealed cubic and massive phases of sodium chlorides that covered the stone surfaces and created a very thick crust layer. Double Ca, Mg, and K sulfates salts (humberstonite and ungematchite) are considered the second key to salt weathering after chlorides. SEM images showed these double salt phases were in a grey dark crust over the surfaces.

Moreover, three phases of calcium sulfates (gypsum, bassanite, and anhydrite) were found in most of the samples. These salts contributed to the salt weathering of the temple construction materials as well. The dehydration of gypsum to bassanite and anhydrite is considered the critical point for the degradation of stone and mortar surfaces. SEM images presented a significant amount of gypsum and anhydrite nodules over the construction surfaces of the temple. Phosphate salts (brushite and strengite) were detected and probably they came from irrigation water and wastewaters as precipitated on and behind the construction materials. Accordingly, materials deformations, pores, flaking, granular disintegration, loss of material, and erosions were observed by scanning electron microscope and digital microscope as a result of salt weathering and repeated cycles of dissolution and precipitation for the salts on construction materials.

Finally, the research was conducted on the salt decay for the construction materials of Nero's Temple and an assessment of the current state of preservation of this important monument. However, future studies will be needed to carry out soil studies for Nero's Temple. In addition, an urgent restoration plan should be executed to restore and preserve the remaining structural and architectural elements starting from fine (surface cleaning, salt

removal, and consolidation) to geostructural (soil enhancement, columns repairs, blocks re-joining, and replacement) restoration to be kept as a world heritage monument.

Acknowledgments

A. Fahmy acknowledges UGEA-PHAM at University of Cadiz for carrying out the main part of the archaeometrical analysis. XRD, mXRF and SEM-EDX analysis were carrying in the SCICYT of the University of Cadiz. E. Molina Piernas acknowledges co-funding from the European Social Fund (D1113102E3) and Junta de Andalucía.

7. References

[1] Ahmed AA, Fogg GE. Journal of African Earth Sciences The impact of groundwater and agricultural expansion on the archaeological sites at Luxor, Egypt. J. African Earth Sci. 2014; 93–104. https://doi.org/10.1016/j.jafrearsci.2014.02.007

[2] Aly N, Heras MG, Hamed A, Buergo M.A, Soliman F. *The influence of temperature in a capillary imbibition salt weathering simulation test on Mokattam limestone*.2015; 65(317). Available from: https://materconstrucc.revistas.csic.es/index.php/materconstrucc/article/view/1682

[3] Aly N, Hamed A. The impact of salt crystallization on the building stones of Al-Azhar Mosque. 2020; 11(4):895–904. Available from: https://ijcs.ro/public/IJCS-20-65_Aly.pdf Accessed 10 April 2022.

[4] Fitzner B. Porosity properties of naturally or artificially weathered sandstones – Proc VIth International Congress on Deterioration and Conservation of Stone, Torun, 12-14 Sept 1988; 236-245.

[5] Winkler M. Moisture and Salts in Stone. In: Stone in Architecture. Springer, Berlin, Heidelberg 1997. https://doi.org/10.1007/978-3-662-10070-7_6

[6] Benavente D, García del Cura MA, García-Guinea J, Sánchez-Moral S, Ordóñez S. Role of pore structure in salt crystallization in unsaturated porous stone. J Cryst Growth. 2004; 260: 532–44. https://doi.org/10.1016/j.jcrysgro.2003.09.004.

[7] Moropoulou A, Labropoulos K, Konstanti A, Bakolas A. Fracture and Failure of Natural Building Stones. *Fracture and Failure of Natural Building Stones*, *January* 2008; vol. 53https://doi.org/10.1007/978-1-4020-5077-0

[8] Cardell C, Benavente D, Rodríguez-Gordillo J. Weathering of limestone building material by mixed sulfate solutions. Characterization of stone microstructure, reaction products and decay forms. Mater Charact 2008; 59: 1371–85. https://doi.org/10.1016/j.matchar.2007.12.003.

[9] Brimblecombe P. Weathering of Building Materials. In: Urban pollution and changes to materials and building surfaces, Book Series: Air Pollution Reviews 2016; Vol. 5: 19-64, Imperial College Press, London

[10] Oguchi CT, Yu S. A review of theoretical salt weathering studies for stone heritage. Prog Earth Planet Sci 2021; 8. https://doi.org/10.1186/s40645-021-00414-x.

[11] Fahmy A, Molina Piernas E, Domínguez-Bella S, López JM, Helmi F. Geoenvironmental investigation Sahure's pyramid Abusir archeological site, Giza, Egypt. Herit. Sci [Internet]. 2022; 1–20. Available from: https://doi.org/10.1186/s40494-022-00699-1

[12] Bradley SM, Middleton AP. A Study of the Deterioration of Egyptian Limestone Sculpture. *J. Am. Inst. Conserv.*1988; *27*(2): 64–86. https://doi.org/10.2307/3179403

[13] Wu RAJ, Schlu C. *The Origin of Soluble Salts in Rocks of the Thebes Mountains, Egypt: The Damage Potential to Ancient Egyptian Wall Art*. 2000; 1161–1172. https://doi.org/10.1006/jasc.1999.0550

[14] Mahmoud HM, Kantiranis N, Stratis JA. *Salt Damage on the Wall Paintings of the Festival Temple of Thutmosis III, Karnak Temples Complex, Upper Egypt*. *Int. J. Environ. Sci.* 2010; 1(3): 133-142.

[15] Aboushook M, Park HD, Gouda M, Mazen O, El-Sohby M. Determination of durability of some Egyptian monument stones using digital image analysis, Proceedings of the 10th IAEG Congress – Engineering Geology for Tomorrow's Cities, Nottingham, UK, The Geological Society of London, 2006, Paper Number: 80, pp.1-10. Available from: https://kau.edu.sa/Files/135/Researches/59046_29391.PDF Accessed 18 April 2022.

[16] Navarro R, Pereira D, Fernández de Arévalo E, Sebastián-Pardo EM, Rodriguez-Navarro C. Weathering of serpentinite stone due to in situ generation of calcium and magnesium sulfates. Constr Build Mater. 2021; 280:122402. https://doi.org/10.1016/j.conbuildmat.2021.122402.

[17] Erić S, Matović V, Kremenović A, Colomban P, Batoćanin DS, Nešković M, et al. The origin of Mg sulfate and other salts formed on pure calcium carbonate substrate - Tufa stone

blocks built into the Gradac Monastery, Serbia. Constr Build Mater. 2015; 98:25–34. https://doi.org/10.1016/j.conbuildmat.2015.08.101.

[18] Menéndez B. Estimation of salt mixture damage on built cultural heritage from environmental conditions using ECOS-RUNSALT model. J Cult Herit. 2017; 24:22–30. https://doi.org/10.1016/j.culher.2016.11.006.

[19] Menéndez B. Estimators of the impact of climate change in salt weathering of cultural heritage. Geosci. 2018; 8. https://doi.org/10.3390/geosciences8110401.

[20] Franzoni E. Rising damp removal from historical masonries: A still open challenge. Constr Build Mater. 2014; 54:123–36. https://doi.org/10.1016/j.conbuildmat.2013.12.054.

[21] Rodriguez-Navarro C, Doehne E. Salt weathering: Influence of evaporation rate, supersaturation and crystallization pattern. Earth Surf Process Landforms. 1999; 24:191–209. https://doi.org/10.1002/(sici)1096-9837(199903)24:3<191::aid-esp942>3.0.co;2-g

[22] Ruiz-Agudo E, Mees F, Jacobs P, Rodriguez-Navarro C. The role of saline solution properties on porous limestone salt weathering by magnesium and sodium sulfates. EnvironGeol. 2007; 52,269-281. https://doi.org/10.1007/s00254-006-0476-x

[23] Caruso F, Maria A, Sanchez A, Scherer GW, Flatt R J. *Chemomechanics of salt damage in stone*. 2014; 1–5. https://doi.org/10.1038/ncomms5823

[24] Scrivano S, Gaggero L. An experimental investigation into the salt - weathering susceptibility of building limestones. *Rock Mech Rock Eng*. 2020; *53*(12), 5329–5343. https://doi.org/10.1007/s00603-020-02208-x

[25] Doehne E, Selwitz C, Carson D, DeTagle A. Prevention of Salt Damage to Monuments: Esem and Time-Lapse Studies. *Microscopy and Microanalysis.* 2001; *7*(S2), 466-467. https://doi.org/10.1017/s1431927600028403

[26] Lopez-Arce P, Doehne E, Martin W, Pinchin S. Sales de sulfato magnésico y materiales de edificios históricos: Simulación experimental de laminaciones en calizas mediante ciclos de humedad relativa y cristalización de sales. Mater Constr. 2008; 58: 125–42. https://doi.org/10.3989/mc.2008.v58.i289-290.77.

[27] Benavente D, de Jongh M, Cañaveras JC. Weathering processes and mechanisms caused by capillary waters and pigeon droppings on porous limestones. Minerals. 2021; 11: 1–16. https://doi.org/10.3390/min11010018.

[28] Fitzner BJ. Investigation of Weathering Damage on Stone Monuments. *Geonomos. 2016*; 21–28. https://doi.org/10.18285/geonomos.v24i2.835

[29] Kamh GME, Koltuk S, Ismael H. Refinement of categorization and scaling of weathering-related damage to natural stone: case study on oolitic limestone from El-Shatbi Tombs (Egypt). Bull Eng Geol Environ 2017; 76:39–57. https://doi.org/10.1007/s10064-016-0946-7.

[30] Doehne E, Selwitz C, Carson D, DeTagle A. Damage to monuments from the crystallization of mirabilite, thenardite and halite: mechanisms, environment, and preventive possibilities. Elev Annu V M Goldschmidt Conf. 2001; 1:3212.

[31] Doehne E. Salt weathering: A selective review. Geol Soc Spec Publ 2002; 205:51–64. https://doi.org/10.1144/GSL.SP.2002.205.01.05.

[32] Heinrichs K, Fitzner B. Stone monuments of the Nemrud Dag sanctuary/Turkey petrographical investigation and diagnosis of weathering damage. Zeitschrift Der Dtsch Gesellschaft Für Geowissenschaften. 2007; 158: 519–48. https://doi.org/10.1127/1860-1804/2007/0158-0519.

[33] Hemeda S, Fahmy A, Sonbol A. Geo-Environmental and Structural Problems of the First Successful True Pyramid, (Snefru Northern Pyramid) in Dahshur, Egypt. *Geotech. Geol. Eng*. 2019; *37*(4), 2463–2484. https://doi.org/10.1007/s10706-018-00769-x

[34] Leclant J. Revue Archéologique.1962. [Internet]. 2022 Jun 25; 1: 115–20. Available from: http://www.jstor.org/stable/41754847.

[35] Bailey DM, Davies WV, Spencer AJ. British Museum expedition to Middle Egypt: Ashmunein (1980), British Museum Occasional Paper. 1998;2; 37, London.

[36] Harrell JA, Storemyr P. *Ancient Egyptian quarries – an illustrated overview*. *2009*; 7–50. Available from:

https://www.ngu.no/upload/Publikasjoner/Special%20publication/SP12_s7-50.pdf . Accessed 22 April 2022.

[37] Hemeda S, Fahmy A, Moustafa A, Hafez MA El. The Early Basilica Church, El-Ashmonein Archaeological Site, Minia, Egypt: Geo-Environmental Analysis and Engineering Characterization of the Building Materials. Open J Geol 2019; 09: 157–86. https://doi.org/10.4236/ojg.2019.93011.

[38] Fakhry M. Temples of Minia in Nero era 54-68AD, Doctoral thesis. Department of Archaeology (Greco-roman), Faculty of Arts, Minia University. 2015.

[39] Moneim AAA, Fernández-Álvarez JP, Abu El Ella EM, Masoud AM. Groundwater Management at West El-Minia Desert Area, Egypt Using Numerical Modelling. J Geosci Environ Prot. 2016;04:66–76. https://doi.org/10.4236/gep.2016.47008.

[40] Abdel-Mageed Y, Hassan H, Abdel-Rahim A, Abd EL- Azeim M, Matouk M. Evaluation of Groundwater Quality for Irrigation and its Effects on some Soil Chemical Properties in the Western Desert of El-Minia Governorate, Egypt. J Soil Sci Agric Eng 2018;9:283–94. https://doi.org/10.21608/jssae.2018.35872.

[41] El-Deeb, H and El Rawy, M and Habib E. Water Resources Management: Case Study of El Minia Governorate, Egypt. Int J Sci Eng Res. 2015;6.

[42]https://weather-and-climate.com/average-monthly-Rainfall-Temperature-Sunshine,al-minya-eg,Egypt Access 12 April 2022.

[43] Spencer AJ, Bailey DM. *Excavations at El-Ashmunein*. Published for the Trustees of the British Museum by British Museum Publications.1983; London.

[44] Whitney DL, Evans BW. Abbreviations for names of rock-forming minerals. Am Mineral. 2010;95:185–7. https://doi.org/10.2138/am.2010.3371.

[45] Gunasekaran S, Anbalagan G, Pandi S. Raman and infrared spectra of carbonates of calcite structure. J Raman Spectrosc. 2006;37:892–9. https://doi.org/10.1002/jrs.1518.

[46] Vitti P. Mortars and masonry — structural lime and gypsum mortars in Antiquity and Middle Ages. Archaeol Anthropol Sci [Internet]. 2021; Available from: https://doi.org/10.1007/s12520-021-01408-y

[47] Caro S. An investigation of Roman mortar technology through the petrographic analysis of archaeological material. Constr Build Mater. 2008; 22:1807–11. https://doi.org/10.1016/j.conbuildmat.2007.05.003

[48] Young D. Salt attack and rising damp: A guide to salt damp in historic and older buildings. Heritage council of NSW. Heritage Victoria. South Australian Department for environment and heritage. Adelaide city council. November 2008; P. 4. ISBN 978-0-9805126-5-6 Available from: https://cdn.environment.sa.gov.au/environment/docs/saltdamp_techguide.pdf Accessed 07 April 2022.

[49] Derluyn H, Dewanckele J, Boone MN, Cnudde V, Derome D, Carmeliet J. Crystallization of hydrated and anhydrous salts in porous limestone resolved by synchrotron X-ray microtomography. Nucl Instruments Methods Phys Res Sect B Beam Interact with Mater Atoms. 2014; 324: 102–12. https://doi.org/10.1016/j.nimb.2013.08.065.

[50] Vaniman DT, Martínez GM, Rampe EB, Bristow TF, Blake DF, Yen AS, et al. Gypsum, bassanite, and anhydrite at Gale crater, Mars. Am Mineral. 2018; 103: 1011–20. https://doi.org/10.2138/am-2018-6346.

[51] Balboni E, Espinosa-Marzal RM, Doehne E, Scherer GW. Can drying and rewetting of magnesium sulfate salts lead to damage of stone? Environ Earth Sci. 2011; 63: 1463–73. https://doi.org/10.1007/s12665-010-0774-1.

[52] Gázquez F, Rull F, Medina J, Sanz-Arranz A, Sanz C. Linking groundwater pollution to the decay of 15th-century sculptures in Burgos Cathedral (northern Spain). Environ Sci Pollut Res. 2015; 22:15677–89. https://doi.org/10.1007/s11356-015-4754-6.

[53] Thickett D, Stanley B. *Management of sodium sulfate damage to polychrome stone and buildings*. 4th International Conference on Salt Weathering of Buildings and Stone Sculptures Management. 2017; 135–142. Available from:

https://www.englishheritage.org.uk/siteassets/home/learn/conservation/collections-advice--guidance/management-of-sodium-sulphate-damage-to-polychrome-stone-and-buildings.pdf. Accessed 08 April 2022.

[54] Rodriguez-Navarro C, Doehne E, Sebastian E. How does sodium sulfate crystallize? Implications for the decay and testing of building materials. Cem. Concr. Res.2000; 30(10): 1527–1534. https://doi.org/10.1016/S0008-8846(00)00381-1

[55] Steiger M, Charola AE, Sterflinger K. Weathering and Deterioration. In: Siegesmund S., Snethlage R. Stone in Architecture. Springer 2014; Berlin, Heidelberg. https://doi.org/10.1007/978-3-642-45155-3_4

[56] Gonçalves TD, Rodrigues J D, Abreu M M, Esteves AM, Silva A S. Causes of salt decay and repair of plasters and renders of five historic buildings in Portugal. *Proceedings of the International Conference on Heritage, Weathering and Conservation, 2006*; *1*: 273–284.

[57] Shahid SA. Developments in Soil Salinity Assessment, Modeling, Mapping, and Monitoring from Regional to Submicroscopic Scales. In: Shahid S, Abdelfattah M, Taha F. (eds) Developments in Soil Salinity Assessment and Reclamation. Springer, Dordrecht. 2013. https://doi.org/10.1007/978-94-007-5684-7_1

[58] Onac BP, Sumrall J, Mylroie JE, Kearns JB. Cave Minerals of San Salvador Island, Bahamas Cave Minerals of San Salvador Island, Bahamas. 2009. Available from: https://www.researchgate.net/publication/241834538_Cave_Minerals_of_San_Salvador_Island_Bahamas Accessed 08 April 2022.

[59] Valsami-jones E. Mineralogical controls on phosphorus recovery from wastewaters Mineralogical controls on phosphorus recovery from wastewaters. 2014. https://doi.org/10.1180/002646101317018433

[60] Siedel H, Plehwe EV, Leisen H. Salt Load and Deterioration of Sandstone at the Temple of Angkor Wat, Cambodia. *11th International Congress on Deterioration and Conservation of Stone, Torun, Poland 2008. Proceedings Volume 1, 267-274*, *I*(August), 267-274.

[61] Fernandez SP. *Factors influencing salt-induced weathering of building sandstone*. P44. RobertGordon University. 1999; [online], PhD thesis. Available from: https://openair.rgu.ac.uk Accessed 16 May 2022.

[62] Ballirano P, Melis E. Thermal behaviour and kinetics of dehydration of gypsum in air from in situ real-time laboratory parallel-beam X-ray powder diffraction. Phys Chem Miner. 2009; 36: 391–402. https://doi.org/10.1007/s00269-008-0285-8.

[63] Stambolov T, Van Asperen De Boer JRJ. *The deterioration and conservation of porous building materials in monuments. A preliminary review*. International centre for the study of the preservation and restoration of cultural property 1967, Stampatopresso it laboratoriotipo-litograficodella DAPCO s.r.l. Via Dandolo, 8 - 00153 ROMA, Second enlarged edition. Available from: https://www.iccrom.org/sites/default/files/2018-02/1976_stambolov_deterioration_eng_21362_light.pdf.Accessed 10 May 2022.

3.5. Sand dunes movement and flooding risk analysis for the pyramids of Meroe, Al Bagrawiya archaeological site, Sudan.

Submitted to International Journal of Architectural Heritage

Authors: Abdelrhman Fahmy, Salvador Domínguez-Bella, Javier Martínez-López and Eduardo Molina-Piernas.

Highlights:

- Nubian sandstone is the main building materials of the pyramids of Meroe.
- Wind is considered the main catalytic force for the damage of the pyramids of Meroe.
- Satellite images showed that the sand dunes are Barchan type around the pyramids of Meroe.
- Sand dunes along with heavy rains and flooding are the main decay factors for the pyramids of Meroe.

Abstract

The pyramids of Meroe are a significant archaeological placeat Al Bagrawiya archaeological site (Sudan) with hundreds of pyramids dating back to the kingdom of Kush (1070 BC –550 AD). In this area, winds, heavy rains, and flooding events are the main geohazards that need assessments and solutions because pyramids are subjected to an accumulation of sand dunes around them and also the risk of flooding, affecting their durability. The research aims to assess the impacts of sand dunes on the stability of pyramids structures in addition to assessing for risk of flooding using satellite image observations and the damage and decay assessment of the pyramids' building materials was carried out through digital mapping. The results from satellite image analysis and monitoring showed that sand dunes along with heavy rains and flooding are the main decay factors, causing the collapse, disintegration, crumbling, alveolarization, loss of materials, and cracking of the sandstone ashlars, detecting an increase in deterioration, even considering only the last three decades.

Keywords: Pyramids of Meroe, Al Bagrawiya archaeological site, sand dunes, wind, flooding, construction materials, stone decay.

1. Introduction

Several studies had been carried out about geoenvironmental and geohazards' impacts on archeological sites and buildings. For instance, Stambolvo [1] explained the role of wind and rains in the deterioration of porous building materials, where water can penetrate the stones by wind power and capillary suction to cause the decay of the stone. Fitzner et al. [2] studied the conservation state of the construction materials in the temples of Karnak and Luxor, and they categorized the damage as no visible, very slight, slight, moderate, severe, and very severe damage. They concluded that disintegration, detachments, and flaking degradation are degradation aspects due to salt weathering. Sandrolini et al. [3] used the available long record urban scale environmental data, and finite element analysis to identify the decay sources and problems of the cathedral of Modena (Italy). They concluded thatwind blowing to the facades resulted in tensile stresses and loads to the façade plane. Hemeda et al. [4] studied various environmental factors that affected the pyramid of Snefru structurally. Weathering, geotechnical, and seismic loads were the main damage factors for the pyramid. In addition, in the middle of Egypt, the geoenvironmental and geotechnical assessment for damage at the archaeological site of El-Ashmounein archaeological sites was applied where stone columns were broken due to flooding and seismic loads [5,6]. Fahmy et al. [7] studied the impact of the external environmental factors and intrinsic defects on the sustainability of Sahure's pyramid and showed that external factors such as earthquakes and climatic conditions are the main factor of damage as external factors, while the clay content of the stone played a damaged role as an intrinsic factor.

In fact, the challenges in relation to protecting the cultural heritage need to be better understood if we are all to avoid further destruction of the cultural heritage landscape [8]. Arid or semi-arid climates can be considered a potential environmental problem for the cultural heritage [9], causing partial or total collapse and sliding of the archaeological buildings and findings in the coast and desert systems [10]. In this sense, sand dunes show considerable morphological diversity with active and inactive movements [11]. In this context, wind could be an extra load on the dunes covering the buildings for a short or long time depending on wind power [12], and especially with windblown sand action, causing

sand erosions [13]. On the other hand, floods are an unusual environmental hazard to the preservation of archaeological sites [14] and river floods are the most common type of natural disaster [15]. Flood events can also cause irreversible destruction to the archaeological sites and their built heritage [16]. Fahmy [17] studied the effect of flooding on the Basilica Church at El-Ashmounein archaeological site (Egypt), and found that flash flooding reached 3 meters above caused the collapse of the granite columns and shifted some structural elements to other places (displacement). Fernandes [18] studied the impact of heavy rains on built heritage on Madeira Island, concluding that the trails near the canals were damaged by heavy rains and the tourism activities were affected. Petra's afforestation, terracing, and construction of check and storage dams are considered solutions to protect the archaeological site from flooding by 70% [19].

In Sudan, Sweek et al. [20] carried out a conservation project for the Amun Temple because the architectural elements of the temple were affected by different kinds of decay mechanisms due to the poor quality of sandstone and heavy rains. Osman et al. [21] studied several properties of the Nubian formations and their geotechnical problems, because these formations were the sources of construction materials in different archaeological buildings in Sudan. The governmental report of Sudan in March 2021 [22] mentioned different vulnerabilities that threaten the archaeological sites in Sudan. Among these vulnerabilities are natural encroachments such as strong winds, earthquakes, flash flooding, and Nile flooding. They explained that wind power could transport the sand particles and weaken the sandstone building materials of the archaeological buildings. In addition, the floods affected many archaeological sites, especially the Island of Meroe. Onderka and Vrtal [23] showed the damage to the red brick and mud-brick structures in Wad Ben Naga's archaeological site is due to the seasonal heavy rains. Fahmi et al. [24] studied the challenges of Sudanese heritage and mentioned that around 150 pyramids near to Nile River were affected during the recent flooding. Boozer [25] said the Meroe pyramids were well preserved in the early 18th, 19^{th,} and 20th but subsequently were damaged. In addition, discussed that Hinkel and Yellin (scholars)observed unrecorded damage to many offering chapels and displacement of pyramid and chapel blocks at Meroe.

Remote sensing and satellite imaging observation have been used in archaeology for management and monitoring purposes. For example, Hadjimitsis et al. [**26**] said that satellite remote sensing and GIS analysis are tools for archaeological site observations and multi-analysis of risk assessment. These tools are preserving time and effort instead of in situ observation. Tapete [**27**] explained that remote sensing observation is extremely important in climate change issues, especially probable floods, drought, and other consequences in the relations with water. In addition, he added that very high-resolution satellite images could help for damage mapping and assessment in the archaeological sites. Angeli and Battistin [**28**] carried out a monitoring and assessment project for soil erosion and its impact on the buried archaeological heritage of Antonine Wall and Falerii Novi, in Italy. Hu and Li [**29**] used GeoEye images and CORONA images with high resolution in order to reveal some archaeological ruins that were covered by sand dunes. In addition to the assessment of other ruins affected by wind erosion and surrounded by sand dunes and nebkhas.

From the above literature review, very few studies are referred to problems of flooding and sand dunes on Sudan archeological sites. For this motive, the present study is focusing on sand dunes and flooding risk assessment upon the pyramids of Meroe. To achieve it, treated and untreated satellite images were used to monitor and assess the geohazards' problems of sand dunes and flooding over the pyramids. Moreover, mapping of the different decay forms of the pyramids of Meroe and damage rate had been performed to assess the durability conditions of the pyramids.

2. Al Bagrawiya Pyramids'studied area.

The pyramids of Meroe at the Al Bagrawiya archaeological site were built about 200km North of Khartoum, between the Nile River and the Atabrah River (**Fig.3.5.1-A**) with coordinates latitude N 16°56.111', longitude E 33°42.852' [**30**].

Al Bagrawiya archaeological site is a World Heritage Site with significant pyramid-shaped structures of the Meroe kingdom. Meroe was an ancient city in Sudan, and it was the seat of the government and the royal palace [**31**]. The pyramids of Meroe back to the kingdom

of Kush, between the 8th century BC and 4th century AD and were devoted as a necropolis site for the kings and queens of Meroe (**Fig.3.5.1-B**). In addition, it contains more than 100 pyramids in the north, south, and west of Al Bagrawiya (**Fig.3.5.2-A**) [**32**]. In comparison between the Egyptian and Meroitic pyramids, the inclination angle of the Meroe pyramids ranges between 68 to 81 degrees, while the Egyptian pyramid's inclination angle is lower than 52 degrees. Furthermore, the pyramids of Meroe are not enormous as the Egyptian ones because the height of the Meroitic pyramids ranges between 10 to 30m, and the base range from 4.5 to 17.5m. Some pyramids were constructed with sandstone blocks with a rubble-filled core in the earlier periods (**Fig. 3.5.2-B**) but some other pyramids were covered by brick or coursed rubble and rendered by a lime or gypsum mortar for painting [**33**,**30**]. Additionally, pyramid number 10 contains different architectural elements such as temenos walls, chapel, inclined passage, and burial chamber as shown in the plan and cross-section (**Fig. 3.5.2-B**).

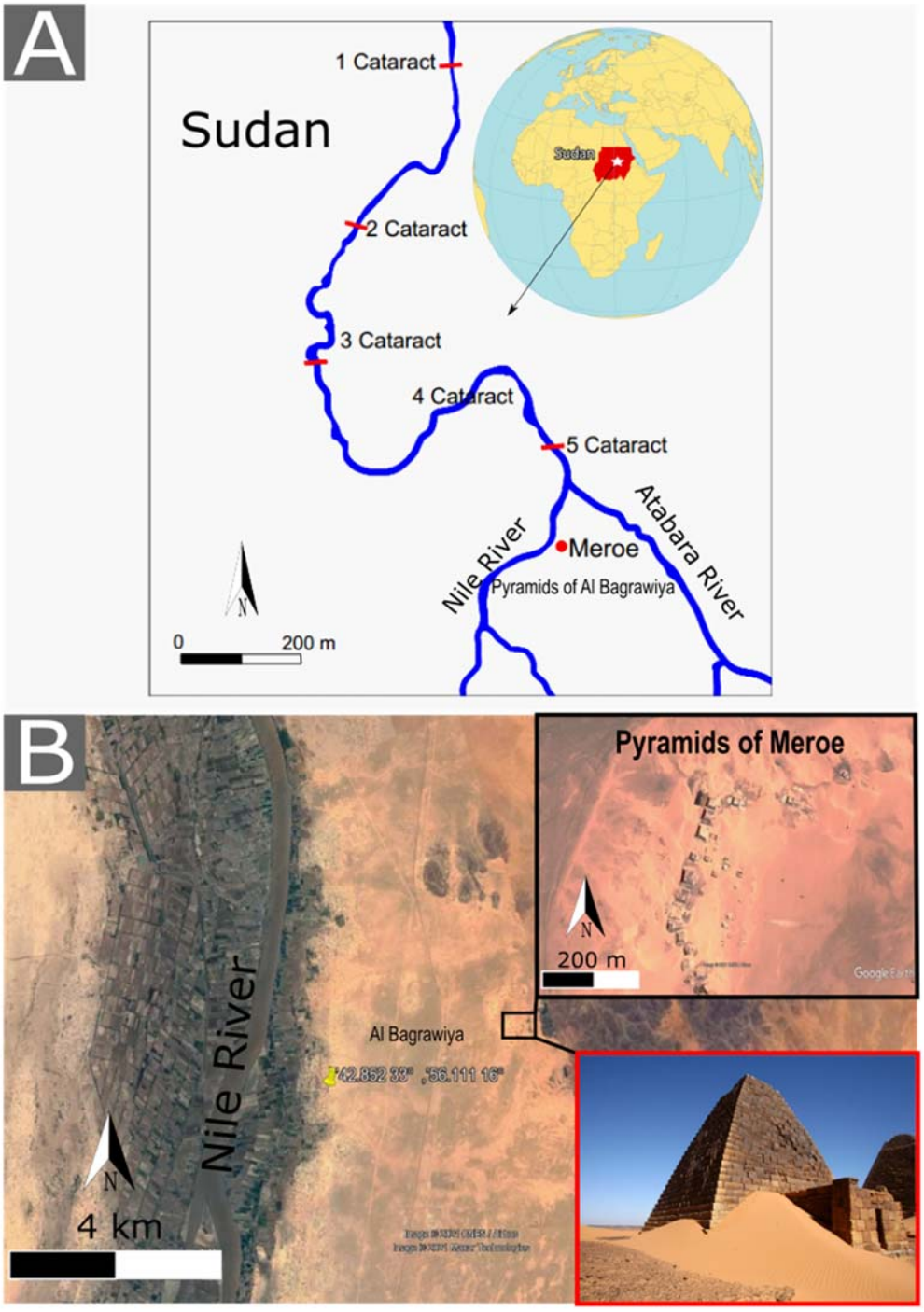


Fig. 3.5.1. (A) Map of Sudan and location of the pyramids of Meroe at Al Bagrawiya (red point). (B) The pyramids of Meroe at Al Bagrawiya and their general view.

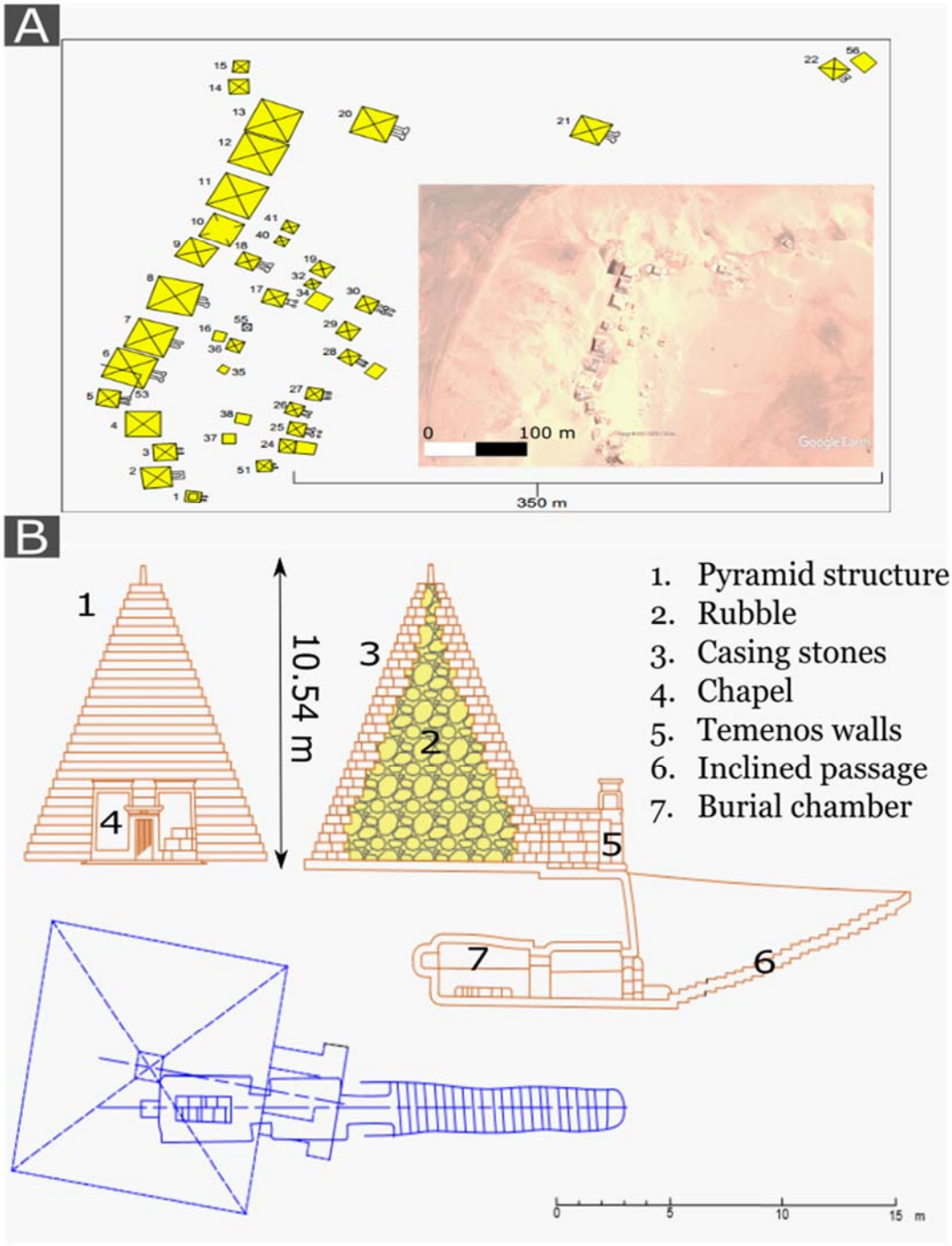


Fig. 3.5.2. (A) General map with plans for the pyramids at Al Bagrawiya (edited after [**31**]). (B) Elevation and plan view of the Pyramid number 10 and its architectural and structural elements (edited after [**30**]).

3. Geological and climate context

The geomorphological and geological features of Sudan vary from desert lands, hills, plutonic/volcanic formations, and valleys from various eras [**34**]. The Sudan plain consists of dark clays and red-brown sands [**35**]. The general geological column of Sudan is composed of coastal plain deposits, Nubian formations, Paleozoic sandstone formations, and a basement complex (mainly Precambrian) [**36**]. Deposition of the fluvial and marine sediments overlying the amalgamated terranes, from the Cambrian onwards was because of the erosion of the Trans- Gondwanan Mountain belt and subsequent recycling of the eroded detritus during later inversion tectonics (**Fig. 3.5.3-A**) [**37**]. In addition, continued actions of erosion and continental deposition result in a widespread formation of sandstones such as the Mesozoic Nubian Sandstone Formation [**38**]. The Nubian series (different kinds of sandstones) is the main geological and geomorphological feature of the Meroe area. In addition, the basement rocks present unconformably (**Fig. 3.5.3-A**). Nubian sandstone is a cretaceous formation similar to sandstone in Upper Egypt. It is characterized by a general absence of basal conglomerates. Consequently, it is poorly cemented and fragile except for the sandstone that occurred over the basement complex. Finally, basement rocks include igneous, metamorphic and sedimentary rocks. In the sixth cataract, the basement rocks existed largely (large outcrop) [**30**, **34**, **38**, **39**].

Many quarries had been used in the kingdom of Kush; those ferruginous sandstone quarries (Nubian Formations) were used as raw materials to prepare the stone blocks for pyramids construction [**40**]. Brigitte Cech [**41**] classified Meroitic quarries into five sectors (**Fig.3.5.3-B**) as 1) Northwest Sector: Q01 to Q25; 2) Northeast Sector: Q26 to Q34; 3) Central Sector West: Q35 to Q80; 4) Central Sector East: Q81 to Q91; and 5) South Sector: Q92.

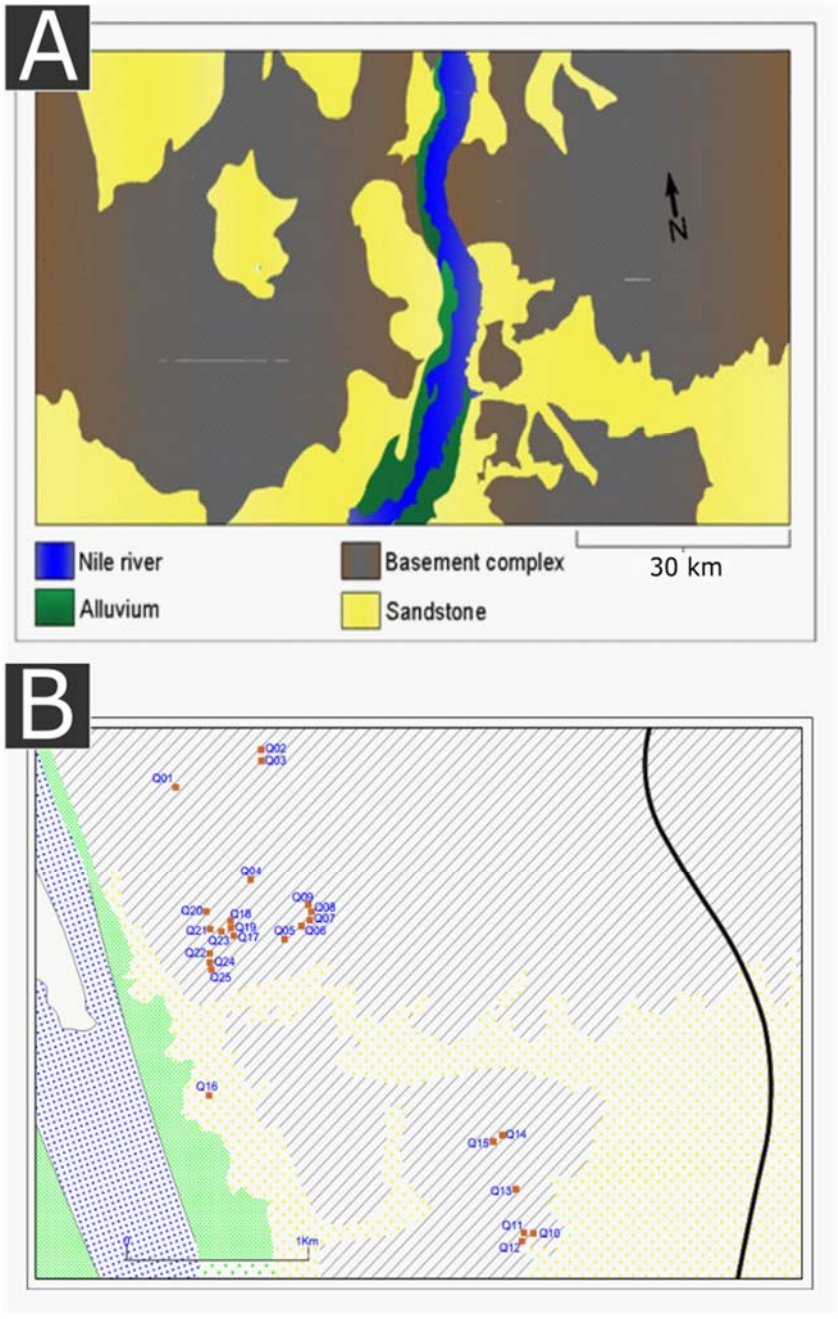


Fig. 3.5.3. (A) Lithological map of the study area. (B) Ancient Meroitic quarries in the northwest sector.

Meteorologically, this region lies within the zone of tropical continental climate with fluctuations in rainfall and temperature from south to north. Generally, the season of rains lasts five to eight months in the southern and heavy rains for one to three months in the northern part of Sudan. The annual rainfall ranges from 100 to 600mm and temperatures

can rise up to 43 ˚C [**42**]. The temperature in Sudan ranges from 26 ˚C to 32 ˚C annually and since 1960; the temperature is increasing from 0.2 ˚C to 0.4 ˚C per decade (**Fig.3.5.4**) (https://climateknowledgeportal.worldbank.org). Rainfall patterns divide Sudan into five zones from North to South: 1) desert with 0–75 mm of precipitation annually; 2) semi-desert with 75-300mm; 3) low rainfall savannah on clay and sand with 300-800mm; 4) high rainfall savannah with 800-1500mm; 5) mountain vegetation with 300-1000mm of precipitation [**43**]. The archaeological site of Al Bagrawiya is situated in the zone of semi-desert with 75-300mm as shown in the rainfall and flooding map of Sudan (**Fig.3.5.5**).In this context, Salih et al. [**44**] mentioned that rainfall could be classified into five classes: 1) Weak (W) is defined as 0.1 to 1.0 mm/day; 2) Moderate (M) is >1.0 to 10.0 mm/day; 3) Moderately strong (MS) >10.0 to 20.0 mm/day; 4) Strong (S) >20.0 to 30.0 mm/day; 5) very strong (VS) >30.0 mm/day.

Sand/dust storms are one of the main environmental events in Sudan [**45**]. They are related to arid and semi-arid areas but can happen as long as there are dry sediments. The process of sandstorms involves three steps: 1) entrainment or emission of surface material; 2) transportation through the atmosphere; and 3) deposition [**46**]. Sherif [**47**] collected some sand particles from Atbara, which is adjacent to a recent study area of Al Bagrawiya in order to characterize the sand particles. In general, Khartoum and Atabra particle sizes are less than 0.3mm but Atbara's dust size contains a high percentage of larger particles. In addition, the majority of particles transported more than 100 km from the source are <0.02 mm in diameter [**46**].

Furthermore, Sudan practices a potential wind power and the wind speed in Sudan at 50 m height varies between 5.1 – 7.1 m/s. According to the wind power analysis that had been carried out for 25 towns in Sudan, the wind speed at 90m height varies between 8.96–8.73 m/s [**48**]. Most regions of Sudan are not subjected to hurricanes though some thunderstorms with relatively high speeds for a short duration cover some areas in the centre of Sudan during the rainy season [**49**].

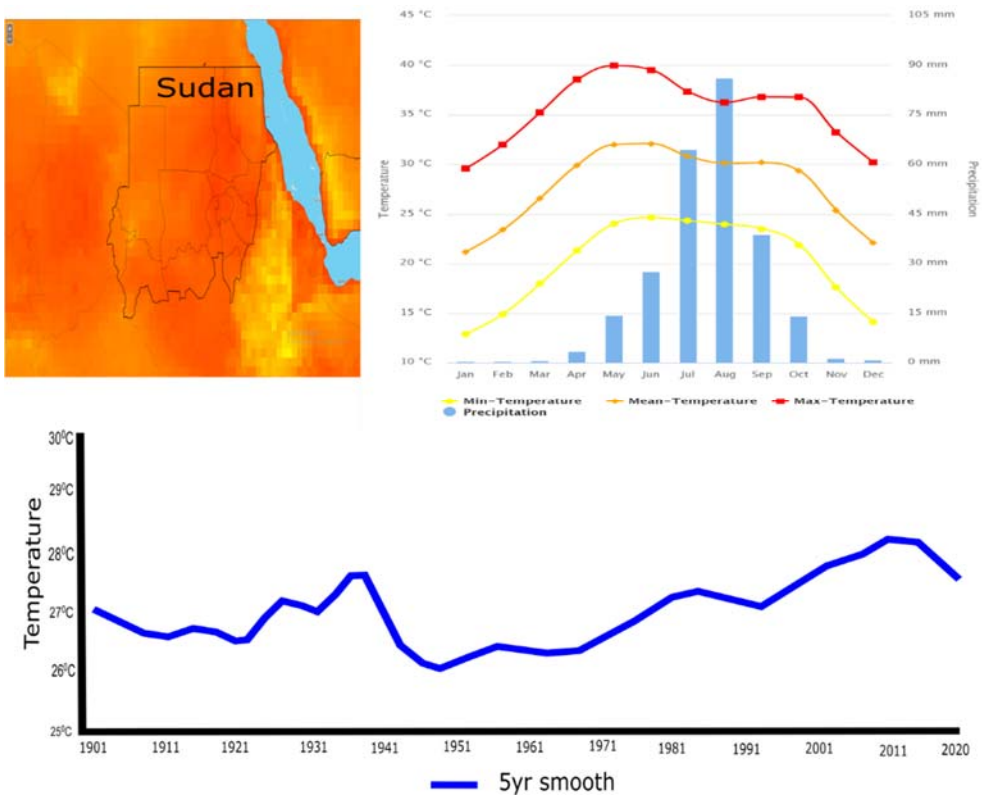


Fig. 3.5.4. Thermal map (up-left) and chart of temperature(up-right) over Sudan monthly. (Down) Historical temperature records from 1901 to 2020. Edited after: https://climateknowledgeportal.worldbank.org/country/sudan/climate-data-historical

4. Methodology

The scientific methodology depends on archaeological mapping for the monitoring and risk assessment using Google Earth images and Satellite images from Spectro radiometer MODIS on NASA's Aqua satellite (NASA). SeaDAS had been used as a remote sensing tool to treat Earth images and Satellite images. These treated satellite images were used to manage and monitor the sands dune's movement through high-resolution and detailed images during the years 2004, 2010, 2014, and 2021 according to available data in these years. Moreover, sandstorms, heavy rains, and flooding risks were observed and assessed through Spectro radiometer MODIS on NASA's Aqua satellite images. Finally, decay deterioration mapping had been carried out using digital engineering drawing to assess the actual preservation state and geohazard impacts on the pyramids of Al Bagrawiya and their building materials.

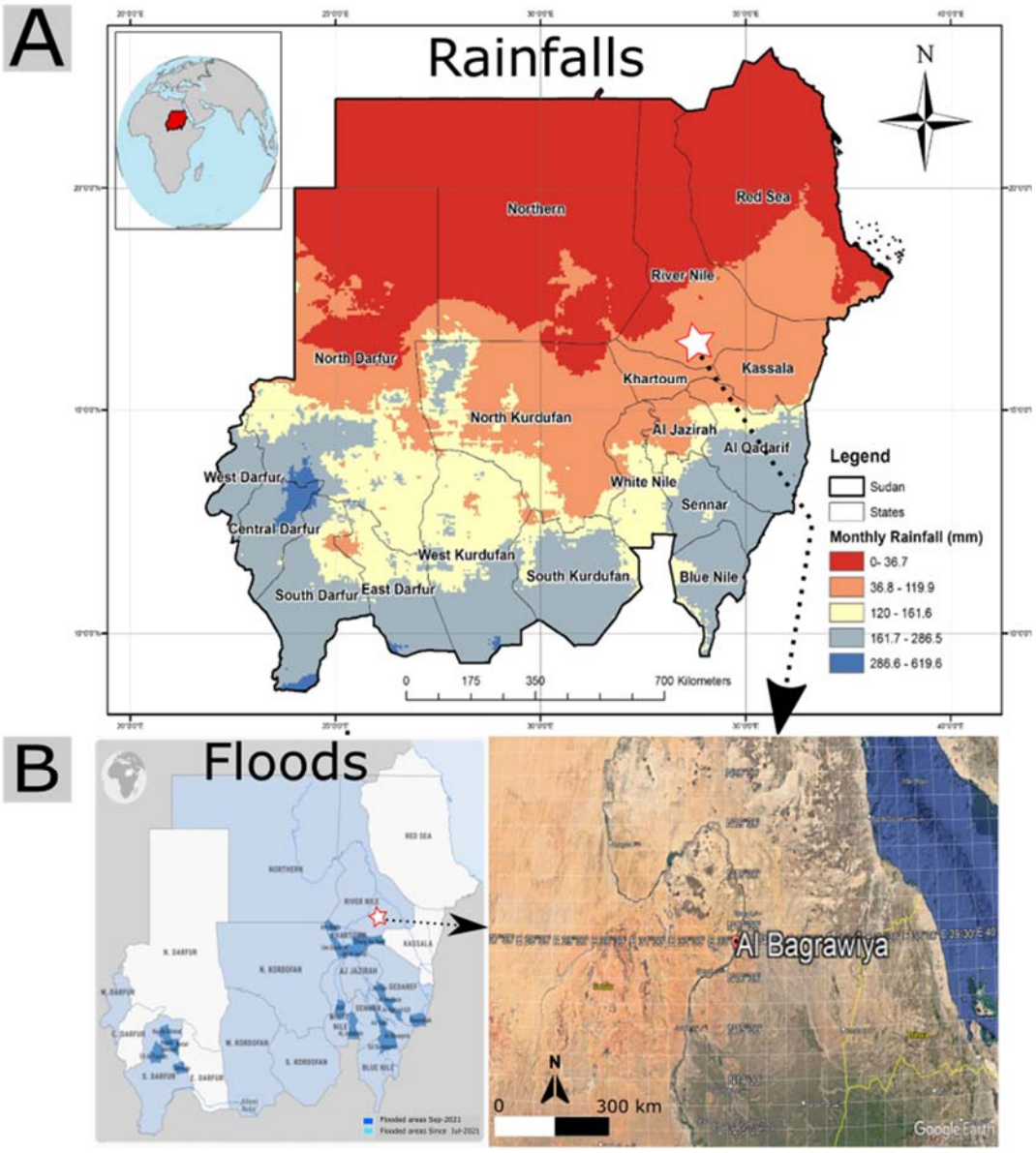


Fig. 3.5.5. (A) Map of Sudan's rainfalls (after [**43**]). (B) Map of affected areas by flooding in Sudan (after [**50**]). White stars present the case study.

5. Results and discussion

5.1. Destruction of the pyramids

The pyramids of Meroe were made of Nubian sandstones prepared from various quarries from the Nubian formation. The sandstone building materials of the pyramids are subjected to different kinds of damaging hazards and risks, probably as the main, sand dunes

formation around the pyramids causing mechanical stresses and instability for the construction elements of the pyramids. Heavy rains and sandstorms are considered the main damaging factors for the pyramids' construction materials as well. Finally, flooding is a risk that threatens the archaeological sites and the pyramids in Sudan.

5.2. Sand dunes and wind impacts

A sand dune can be considered a loose sand hill formed in different sizes and shapes (barchans, longitudinal, transverse, parabolic, barchanoid, and star) due to wind flows and the morphological feature of the sand dunes formed around the pyramids is barchans shape (**Fig. 3.5.6-A**) [**51**]. In Sudan, sand flows have been estimated over 100m (width) in one month and at the peak of the season may reach up to 50,000 kg, focusing more on the northwest of Sudan and they could be movable or fixed. In this sense, sand dunes are the most serious and dangerous environmental problem in the northern part of Sudan which affected the archeological sites in Sudan. Generally, the strongest wind in Sudan is from December to April and the calm wind is from June to October (**Fig.3.5.7**). Google earth images were collected and treated by software (SEADAS) to monitor the movements of the dunes around the pyramids from June 2004 until July 2021. It is noticed that during the last 15 years the dunes increased from one year to another and covered parts of the pyramids from one to three meters (**Fig.3.5.8**).

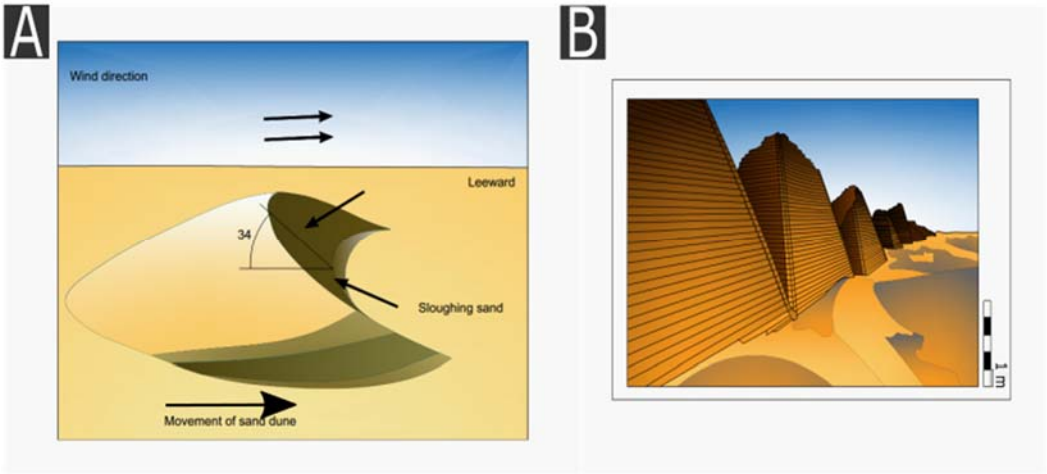


Fig. 3.5.6. (A) Barchan sand dunes components and movement. (B) Schematic formation of barchan sand dunes around pyramids.

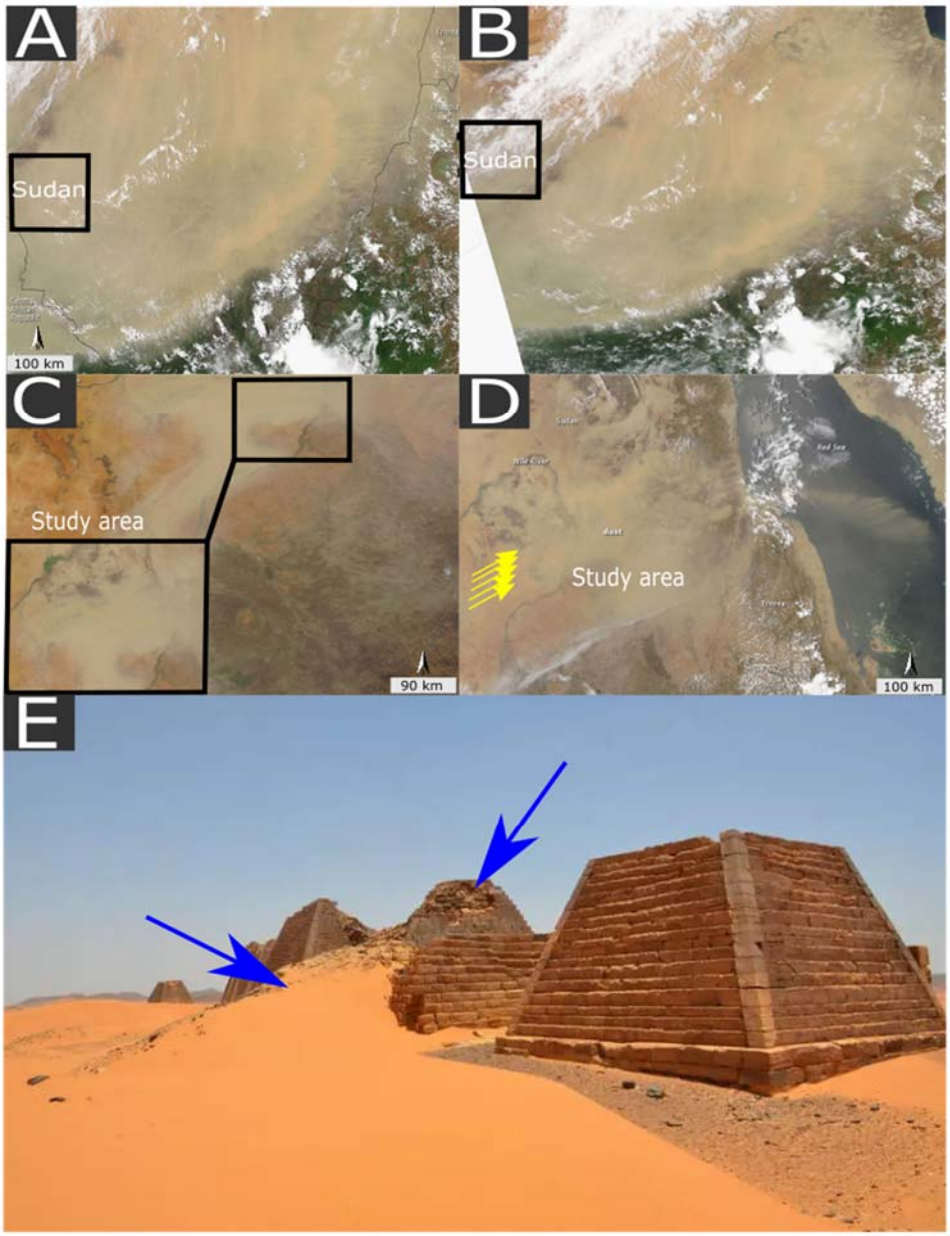


Fig. 3.5.7. (A and B) Captured satellite images for sandstorm over Sudan in 9 May 2009 (from https://earthobservatory.nasa.gov/images/38459/dust-storm-over-sudan). (C and D) A sandstorm over the archaeological site of Al Bagrawiya in 14 May 2013 (from https://earthobservatory.nasa.gov/images/81127/dust-storm-in-sudan). Yellow arrows in (D) refer to the wind directions. (E) General view of the pyramids of Meroe and the impact of the sand dunes over the building materials of the pyramids. Taken by Martchan/Shutterstock(https://www.theafricandream.net/sudan-forgotten-pyramids-are-more-than-egypt/).

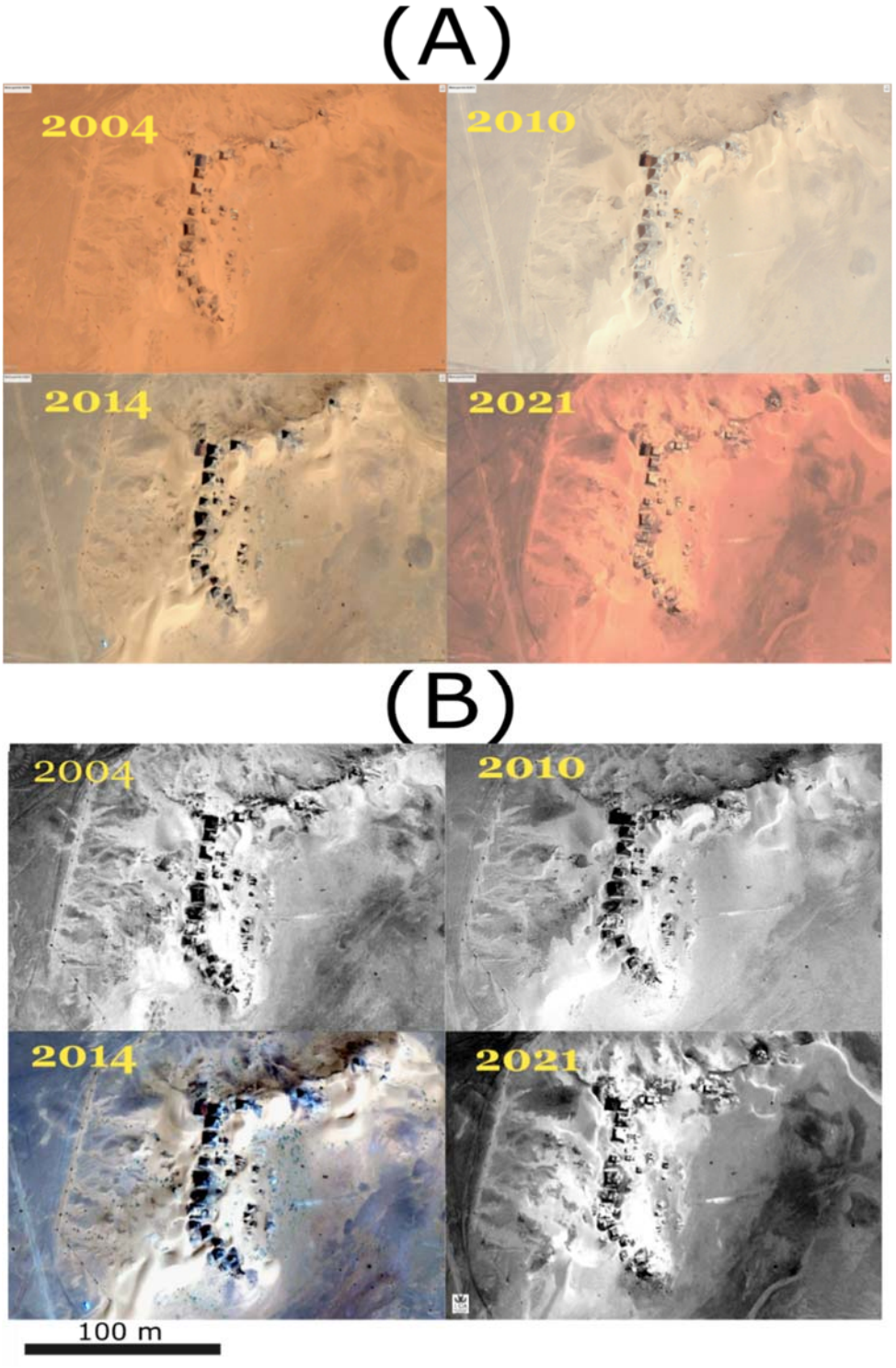


Fig. 3.5.8 (A) Images for monitoring the movement of sand dunes around the pyramids from Google Earth. (B) Treated images to clearly see this movement around the pyramids. Images of 2004 to 2021 are in grey colour, except for 2014 is in RGB colour.

Fig. 3.5.9 presents the risk analysis mapping for sand dunes coverage around the pyramids. It is noticed that the rate of coverage from 2004 to 2021 increased, especially in the years 2010, 2014, and 2021. The covered area by sands around the pyramids is around 15400 m^2 with volumes of 15400, 30800, and 46200 m^3, and an estimated thickness of 1, 2, and 3 m, respectively. In this sense, **Fig. 3.5.10** shows the rate of coverage for the sand dunes over the pyramids and was carried out to assess to what extent the pyramids have been covered by sands. The classification of coverage rate has been divided into three categories as uncover, partially covered, and totally covered. In 2004, one pyramid was uncovered, 12 pyramids were partially covered, and 6 pyramids were totally covered by sand. In 2010, 3 pyramids were uncovered, 8 pyramids were partially covered and 7 pyramids were totally covered. In 2014, one pyramid was uncovered, 14 pyramids were partially covered and 4 pyramids are totally covered. Finally, in 2021, 7 pyramids were partially covered, 12 pyramids were totally covered and there were no uncovered pyramids. From the previous observations, in 2021 the coverage of sands over the pyramids was higher than in other compared years and the coverage rate of the sands over the pyramids depended on the wind power and its direction.

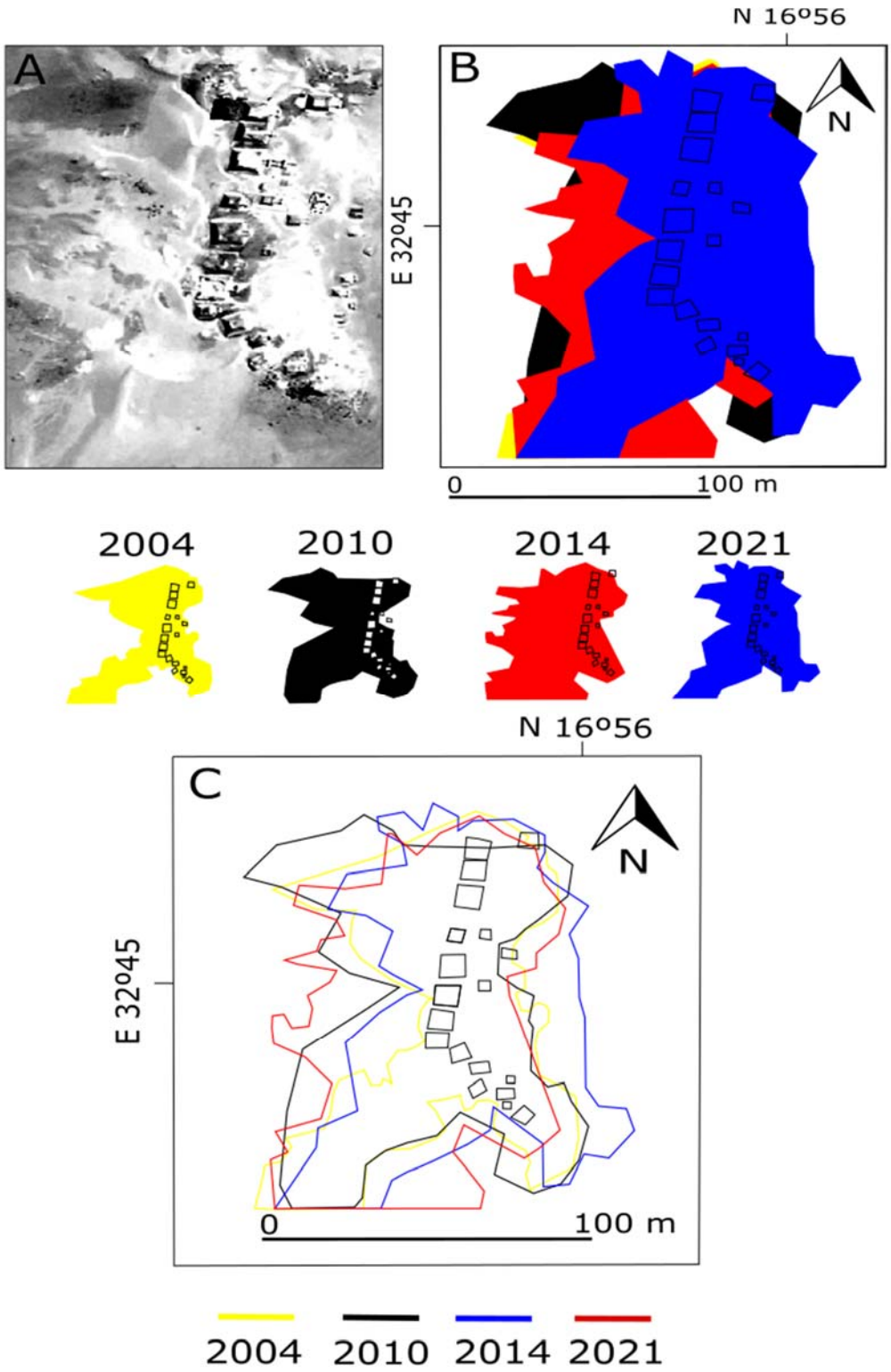


Fig. 3.5.9. (A) Base map for the studied area. (B) Coloured estimation for the sand dunes coverage around the pyramids and their variations from 2004 to 2021. (C) Linear outlines for the variations of sand dunes coverage from 2004 to 2021.

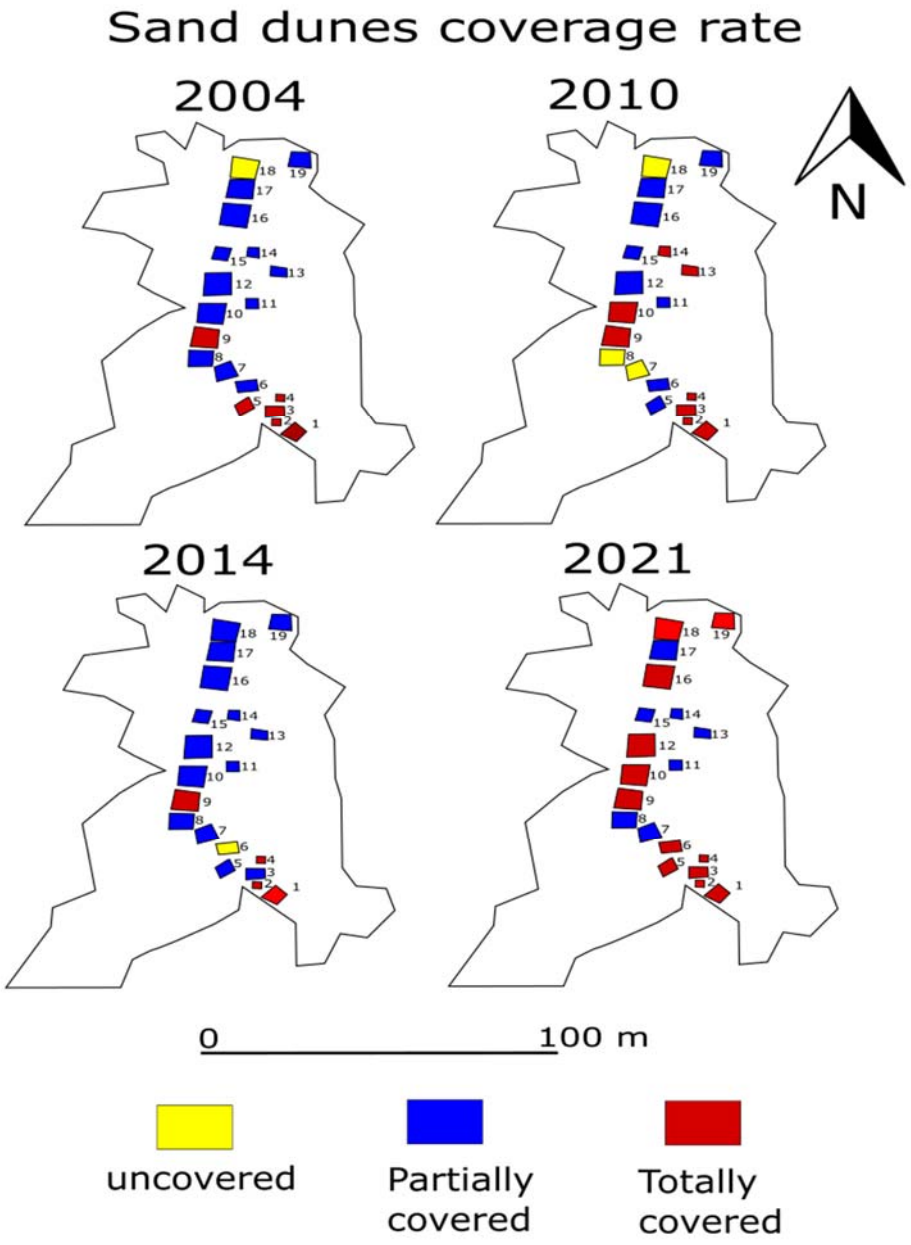


Fig. 3.5.10. The coverage rates of the accumulated sands over the studied pyramids in the years of 2004, 2010, 2014 to 2021.

Moreover, there are different processes and mechanisms for sand dune impacts over the pyramids, especially during wind movement towards the pyramids. In the action on movements of sands there are three processes of saltation, suspension, and sandblasting are happening, which have a vital role in pyramids damage. Saltation/bombardment is when wind transports particles, mainly quartz, between 0.063 and 0.5 mm and usually at a

height less than 1.5 m above ground level. Suspension is the transportation of the particles for a long time and the particles' diameters are less than 0.063mm. Sandblasting is a process whereby saltation particles bombard soil aggregates, causing aggregate fragmentation and release of fine particles [**46**]. **Fig. 3.5.11** (**A**) explains the mechanism of saltation, transportation, suspension, and sandblasting of particles around the pyramids of Meroe. On the other hand, macroprocesses, such as the accumulation of sands around the pyramids can represent an external force over the structure of the walls causing structural deformations, especially when the sands are mixed with water to be more compact with a high load (**Fig. 3.5.11-B**).In this regard, wind erosion (encroachment) is the most dangerous geoenvironmental factor in Sudan that causes the degrading not only of archaeological buildings but also of causes the soil degradation (dissertation) in arid and semi-arid areas [**52**]. Likewise, wind speed is the main key in the decay of the building materials of the pyramid, especially when the potential energy of wind is more than 5 m/sec. In this context, recent studies in Sudan confirmed that the potential of wind energy exists in many areas with an average annual wind speed of more than 5 m/sec [**53**].

In addition, wind can transfer the heat and moisture inside the construction materials of the pyramids increasing decay. According to Masaru et al. [**54**], they mentioned that wind-driven rain loads might lead to moisture flow into the interior surfaces of the buildings increasing the humidity and heat transmission to the walls. The interaction of climatic factors such as variations of temperatures and humidity along with wind could cause acceleration and more damage to the construction materials of the pyramids. In this sense, Moncmanová [**55**] confirmed that decreasing and increasing temperatures could cause differential thermal conductivity between the outer layer and inner core of the stones which will lead to fine cracks, spalling, and lack of strength.

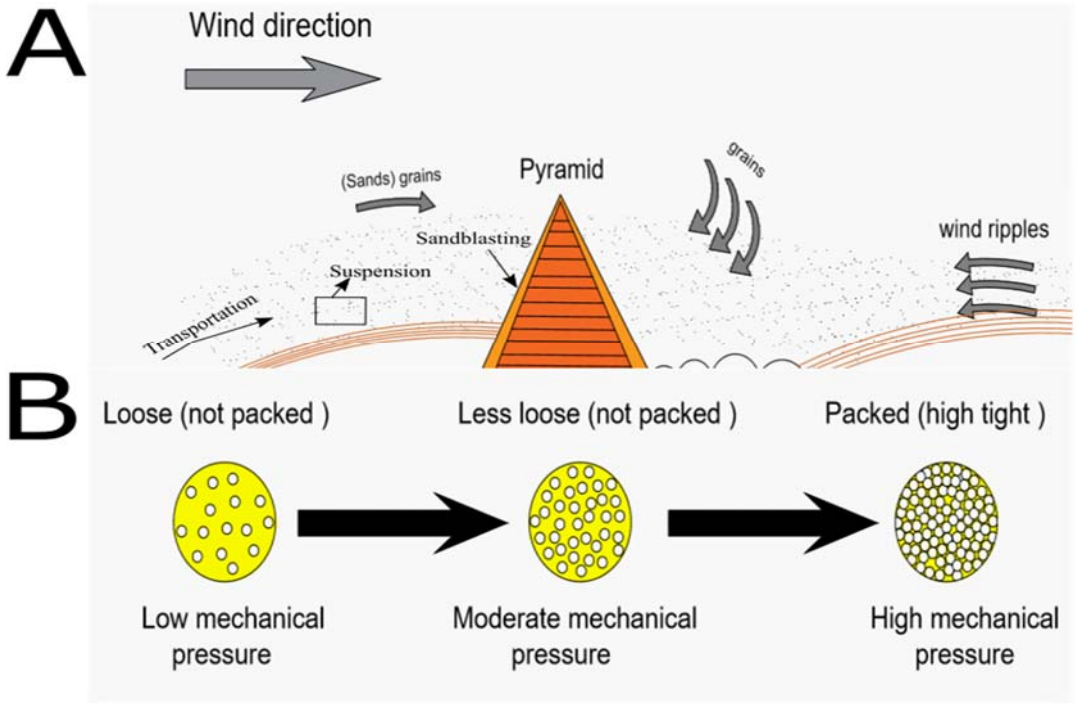


Fig. 3.5.11. (A) Mechanism of sands accumulation around the pyramids. (B) Three possible phases for the sands as external forces on pyramids structures.

5.3. Heavy rains and flash flooding risks

Sudan is subjected to flash floods and heavy rains yearly from July to September. Many destructions are happening to houses, people, and infrastructures. In 2007, during the season of flooding, Sudan was subjected to the worst heavy/intense rains, which affected so much of the infrastructure and the archaeological sites in Sudan (**Fig. 3.5.12**). According to the Sudanese report on 12 August 2021, heavy rains and flooding affected so much six locations in River Nile state such as Atbara, Shendi, Al Matama, Barbar, Abu Hamad, and Ad Damar from 7th to10th August 2021. The floods led to vast destruction for the new houses and built heritagewhere the flood rate passed the risk level. (**Fig. 3.5.13-A** and **B**) [**50**]. In this regard, [**23**] displayed the damage to the red brick and mud-brick structures in Wad Ben Naga's archaeological site due to the seasonal heavy rains and flooding. The Sudanese report on 16 September 2021, confirmed that the floods affected many archaeological sites, especially the Island of Meroe. In addition, they mentioned that water levels of the Nile

River have risen above flooding risk levels in Khartoum, Atbara, Shendi, and Ed Diem stations. Water levels reached 17 m, which was 50 cm above the flooding risk level [**50**].

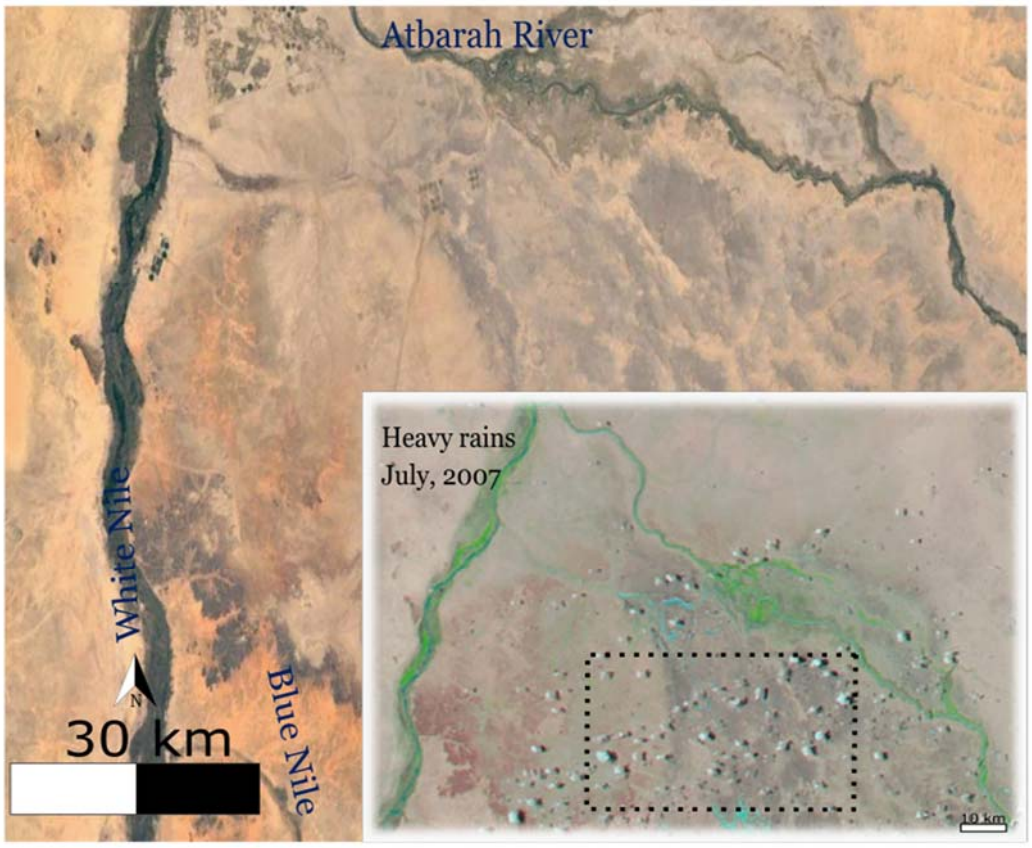


Fig. 3.5.12. Aerial satellite image to show the heavy rains over the case study in July 2007. From https://earthobservatory.nasa.gov/images

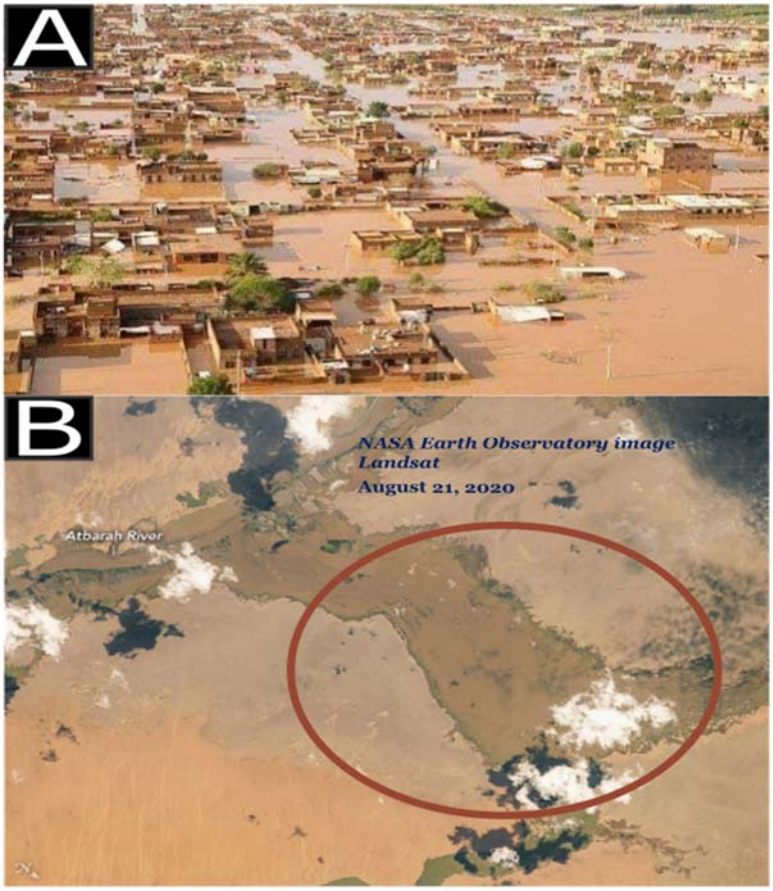


Fig. 3.5.13. (A) The impact of flooding in Sudan. From: https://dailynewsegypt.com/2020/09/06/egypt-dispatches-urgent-aid-to-flood-hit-sudan/. (B) Satellite image for the flooding over Atbara and near to Al Bagrawiya archaeological site. From: https://earthobservatory.nasa.gov/images/147288/record-flooding-in-sudan.

5.4. Damage rate and decay patterns of the pyramids

Risk analysis for the damage rate over the pyramids was carried out in order to identify the state of conservation for each pyramid in the study area. The damage is classified into three categories slightly, moderately, and severely damaged. **Fig. 3.5.14** presents the damage rate of the pyramids throughout several years. In 2004, there were 3 pyramids slightly damaged, 7 pyramids were moderately damaged and 9 pyramids were severely damaged. In 2010, there were 2 pyramids slightly damaged, 5 pyramids were moderately damaged and 12 pyramids were severely damaged. In 2014, there was one pyramid slightly damaged, 6

pyramids were moderately damaged and 12 pyramids were severely damaged. In 2021, there were 4 pyramids moderately damaged and 15 pyramids were severely damaged. From the previous observation, in the last two periods in 2014 and 2021, the damage rate increased due to the increasing activity of wind powers and climate changes.

In **Fig. 3.5.15** (**A-F**) are shown the most dominant deterioration patterns over the construction material of the pyramids of Meroe at the Al Bagrawiya archaeological site, such as collapsing, crumbling, buckling, disintegration, alveolarization, loss of materials, and cracking. In this sense, Fratini and Rescic [**56**] confirmed that the abrasive effect of wind is an important factor that causes the alveolarization of ancient building materials. In this arid area, wind has a significant potential for causing failures for the blocks of the pyramid and can cause wall collapse and detachment of the casing stones; in addition to out-of-plane buckling [**57**]. Cracks and disintegration could be caused by the expansion and contraction of the construction materials in accordance with the heating and cooling effect of temperature and wind power [**58**].

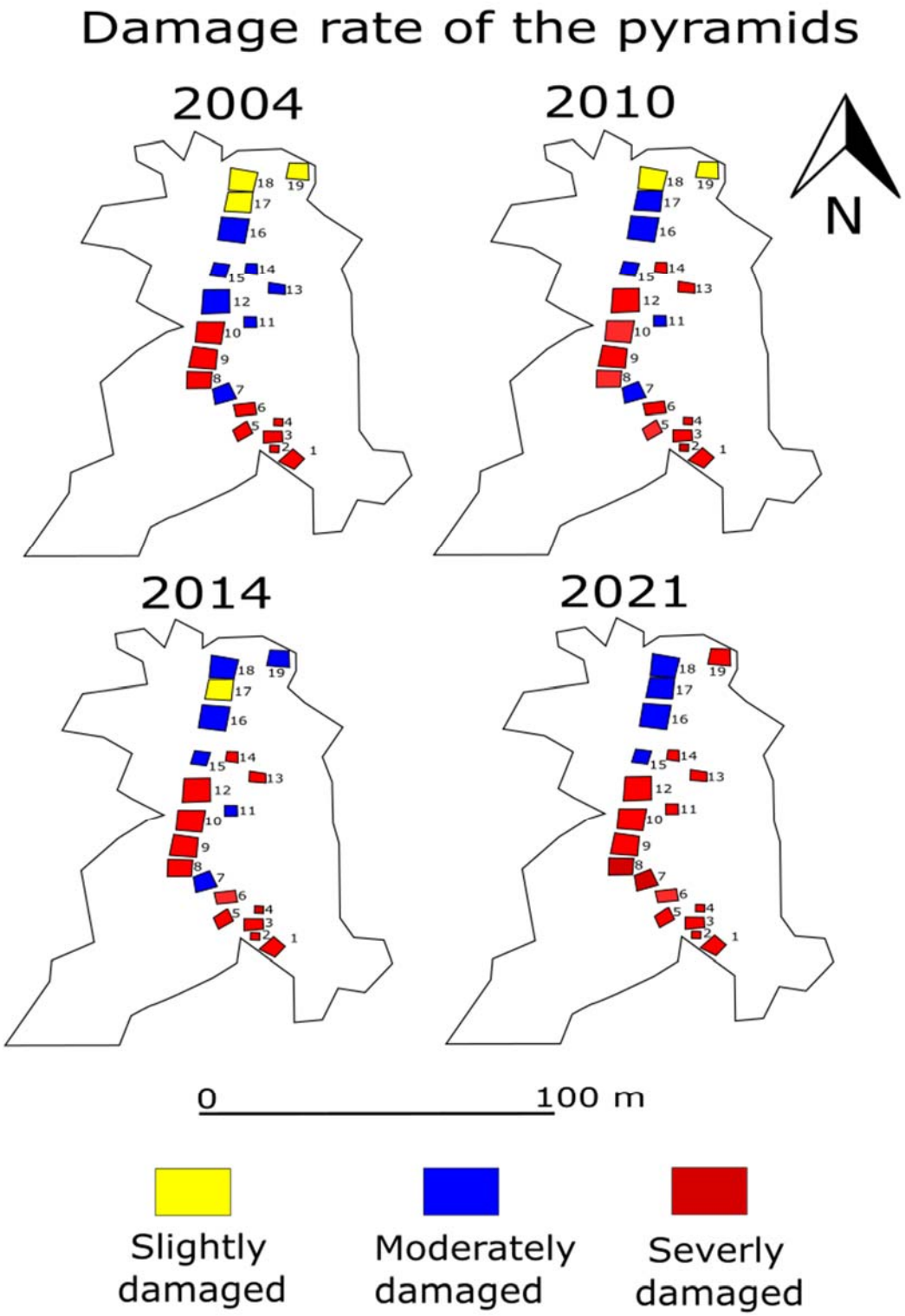


Fig. 3.4.14. Damage rate for the pyramids in 2004, 2010, 2014 and 2021.

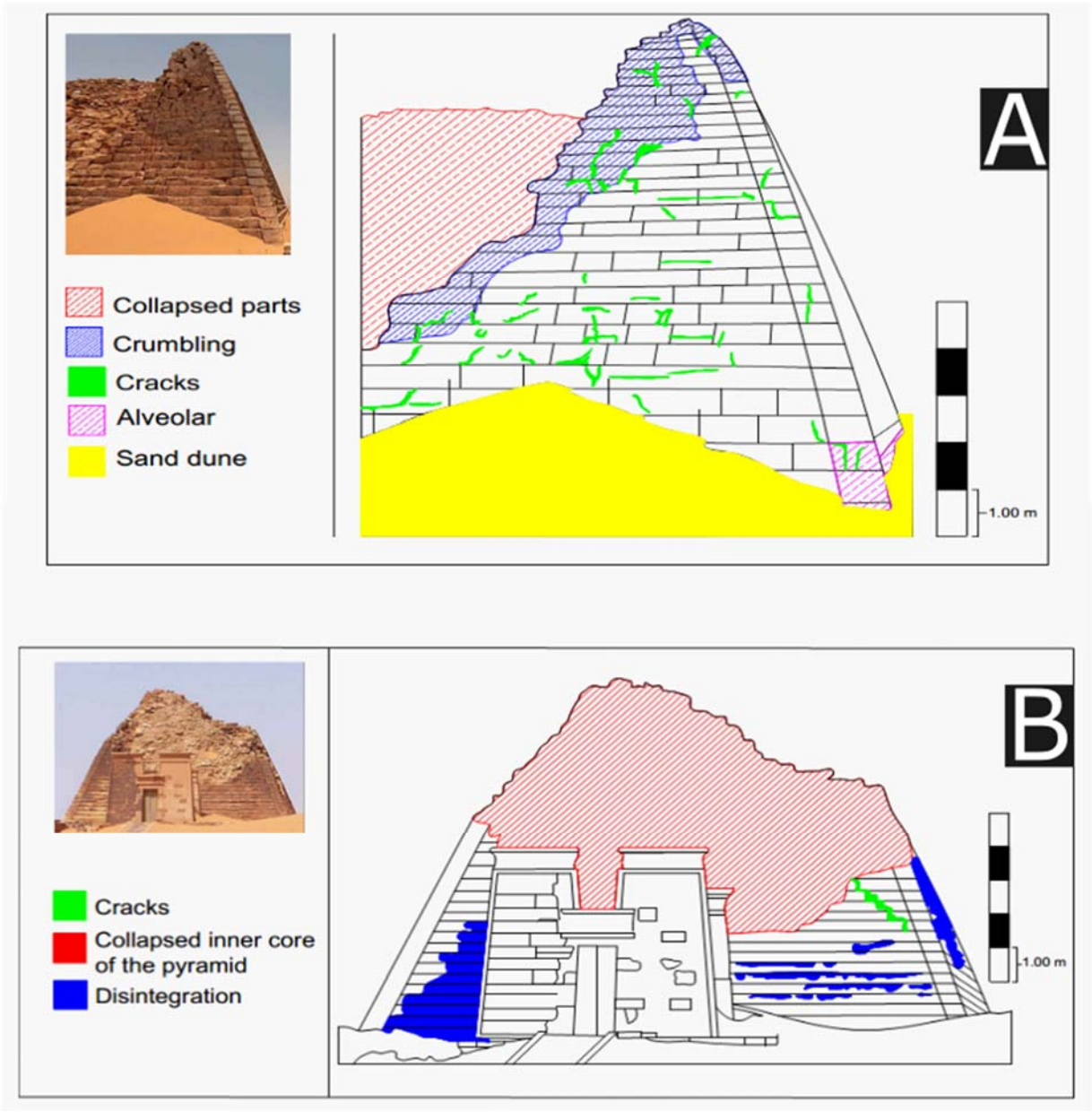


Fig. 3.5.15. (A-F) Degradation maps for the construction materials for the pyramids of Meroe.

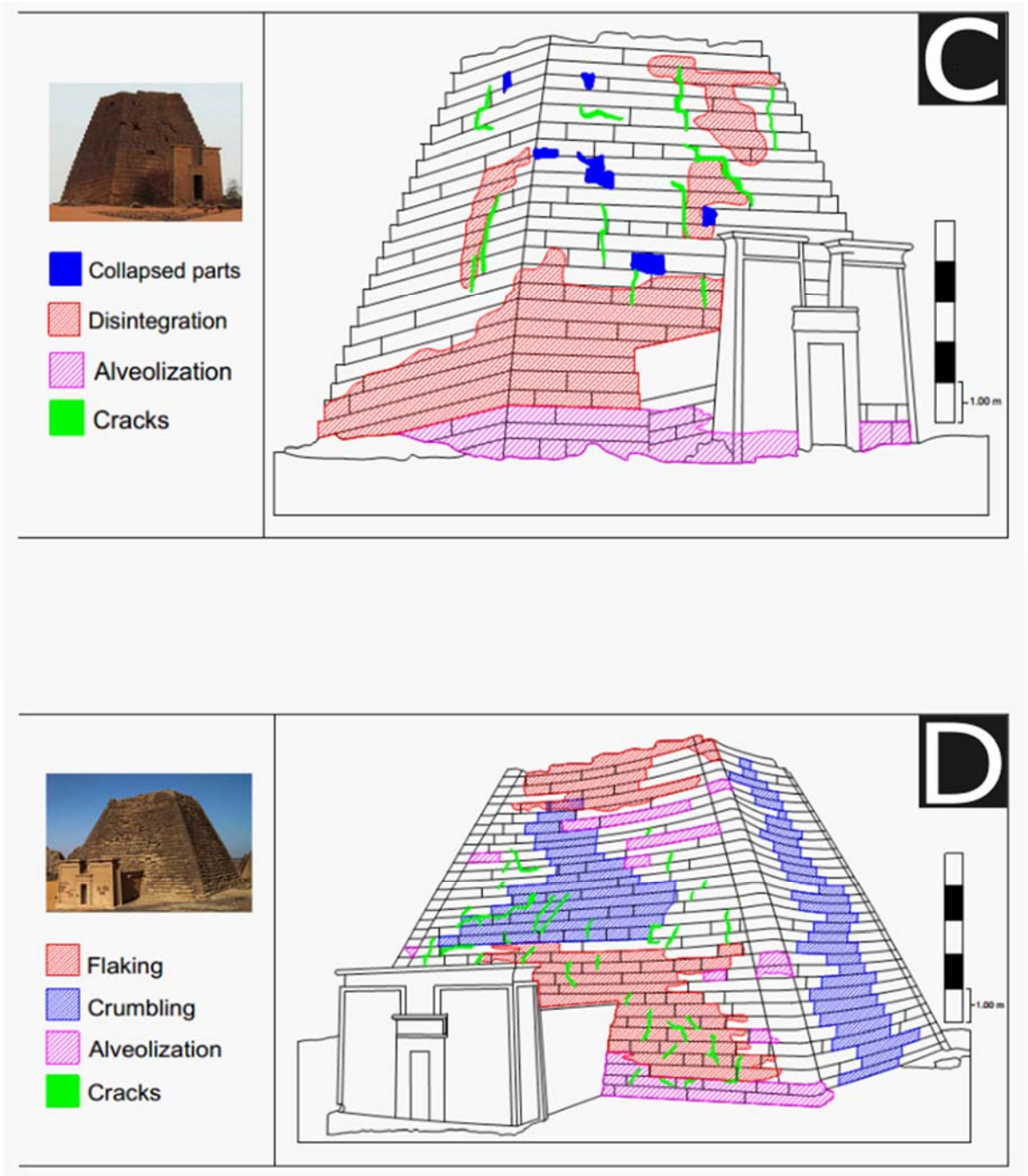


Fig. 3.5.15. (C and D) cont.

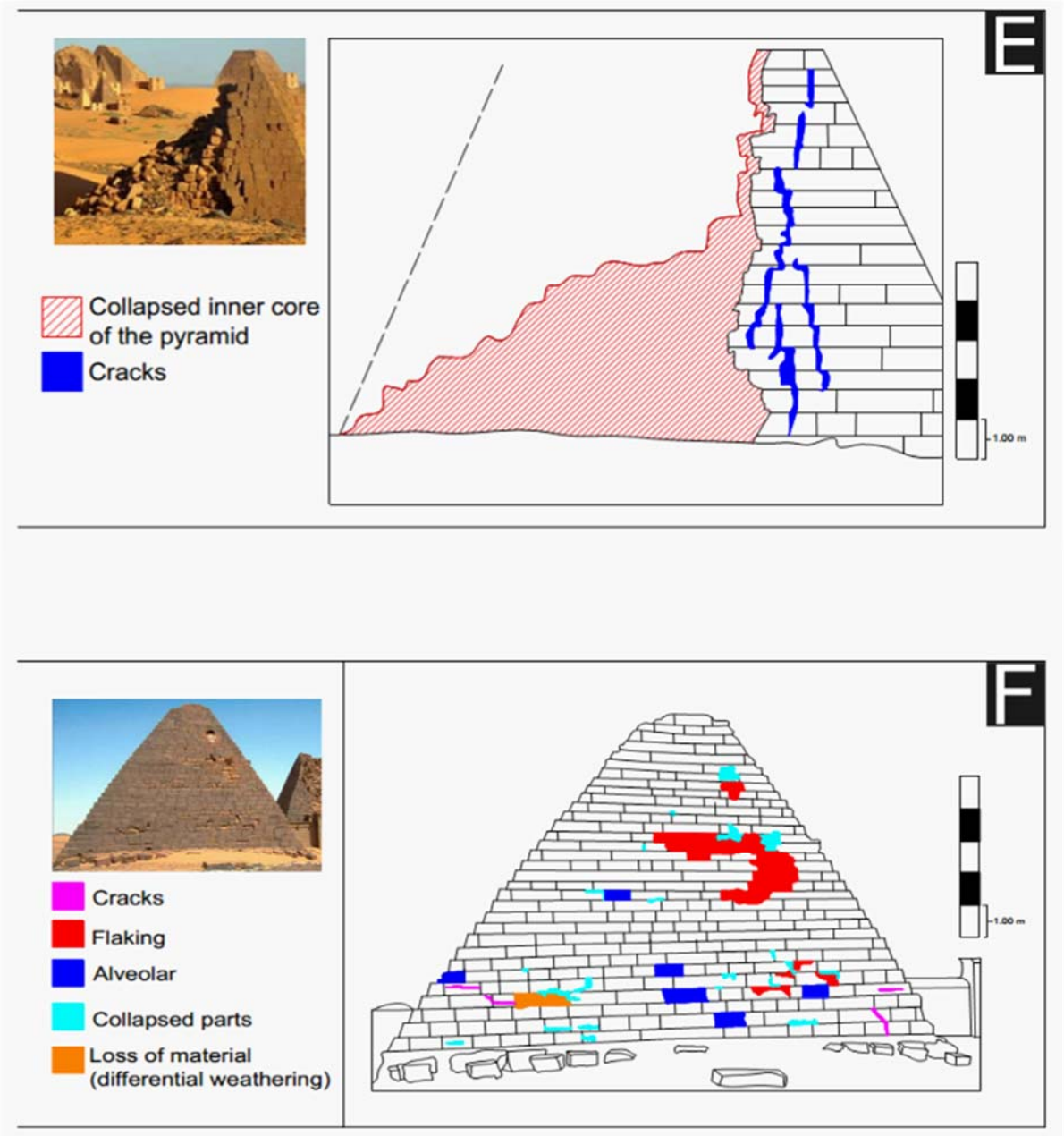


Fig. 3.5.15. (E and F) cont.

6. Conclusion

Sand dunes played a significant role in the destruction and degradation of the building materials of the pyramids of Meroe. Satellite images showed that the sand dunes areBarchan type that increased each year due to the accumulation of sands during the strong wind and sandstorms that cause damage and degradations to the pyramids. Wind is considered a deterioration key at Al Bagrawiya the archeological site that led to sand dunes formations and abrasion for the building materials for the pyramids.

Sand dunes and wind loads resulted in decay and destruction patterns of the building materials of the pyramids such as total collapse, disintegration, loss of materials, crumbling, cracks and buckling. Flooding from heavy rains and rising Nile River water is considered a potential threat at Al Bagrawiya archeological site and its pyramids. In 2020 and 2021, the water levels reached 17 meters beyond the safe flooding rate, which gives us a red alarm to take all precautions to carry out preventive protection for the archaeological sites from probable damage of flooding.

Aknowledegement

A. Fahmy acknowledges UGEA-PHAM at University of Cadiz for carrying out the main part of the archaeometrical analysis. XRD, mXRF and SEM-EDX analysis were carrying in the SCICYT of the University of Cadiz. E. Molina Piernas acknowledges co-funding from the European Social Fund (D1113102E3) and Junta de Andalucía.

References

[1] Stambolov T. The Deterioration and Conservation of Porous Building Materials in Monuments. 1976. Available from: https://www.iccrom.org/sites/default/files/2018-02/1976_stambolov_deterioration_eng_21362_light.pdf

[2] Fitzner B, Heinrichs K, Bouchardiere D L. Weathering damage on Pharaonic sandstone monuments in Luxor - Egypt. 2003; 38, 1089–1103. https://doi.org/10.1016/S0360-1323(03)00086-6

[3] Sandrolini F, Franzoni E, Sassoni E, Paolo P. The contribution of urban-scale environmental monitoring to materials diagnostics: A study on the Cathedral of Modena (Italy). 2011; 12:441–50.

[4] Hemeda S, Fahmy A. Sonbol A. Geo-Environmental and Structural Problems of the First Successful True Pyramid, (Snefru Northern Pyramid) in Dahshur, Egypt. Geotechnical and Geological Engineering, 2019;37(4), pp. 2463–2484. DOI: 10.1007/s10706-018-00769-x.

[5] Hemeda S, Fahmy A, Moustafa A, Hafez MA El. The Early Basilica Church, El-Ashmonein Archaeological Site, Minia, Egypt: Geo-Environmental Analysis and Engineering Characterization of the Building Materials. Open J Geol 2019; 09: 157–86. https://doi.org/10.4236/ojg.2019.93011.

[6] Fahmy A, Molina-Piernas E, Martinez-López J, Domínguez-Bella S. Salt weathering impact on Nero / Ramses II Temple at El - Ashmonein archaeological site (Hermopolis Magna), Egypt. Heritage Science [Internet]. 2022; 1–21. Available from: https://doi.org/10.1186/s40494-022-00759-6

[7] Fahmy A, Molina-Piernas E, Domínguez-Bella S, Martínez-López J, Helmi F. Geoenvironmental investigation of Sahure's pyramid, Abusirarcheologicalsite,Giza, Egypt. 2022;1–20. https://doi.org/10.1186/s40494-022-00699-1

[8] Delaney A, Devaney FM, Martin JM, Barron SJ. Monitoring survey of Annex I sand dune habitats in Ireland. Irish Wildlife Manuals, No. 75. National Parks and Wildlife Service, Department of Arts, Heritage and the Gaeltacht, Dublin, Ireland.2013.

[9] Stancheva, M. Sand Dune Destruction Due to Increased Human Impacts along the Bulgarian Black Sea and Estonian Baltic Sea Coasts. 2011; (64), pp. 324–328.

[10] Barbaro G, Foti G. Chiara G. Beach and Dune Erosion: Causes and Interventions, Case Study: Kaulon Archaeological Site.2022.

[11] Wilson P. Sand dunes and archaeology. 2015. Available from: https://www.researchgate.net/publication/277328144_Sand_dunes_and_archaeology

[12] Tsoar H. Cohenzada A L. The conflict between urban planning and the preservation of sand dunes – The case of the Big Dune in the city of Ashdod, Israel.City and Environment Interactions. 2020;5, p. 100034. DOI: 10.1016/j.cacint.2020.100034.

[13] Ra L. Bruno L. Windblown sand action on civil structures: Definition and probabilistic modelling. 2019; 178(June 2018), pp. 88–101. DOI: 10.1016/j.engstruct.2018.10.017.

[14] Ortiz R, Ortiz P, María J, Auxiliadora M. A new approach to the assessment of flooding and dampness hazards in cultural heritage , applied to the historic centre of Seville (Spain). Science of the Total Environment, The [Internet]. Science of the Total Environment. 2016;551–552:546–55. Available from: http://dx.doi.org/10.1016/j.scitotenv.2016.01.207

[15] Drdácký MF, Eng D, Ph D, Asce M. Impact of Floods on Heritage Structures. 2010;24(October):430–1. https://ascelibrary.org/doi/full/10.1061/%28ASCE%29CF.1943-5509.0000152

[16] Iosub M, Enea A, Minea A. Flash flood impacts on the cultural heritage in Moldova region, Romania. Case study: Jijia valley.19th International Multidisciplinary Scientific GeoConference SGEM. 2019; 30 June - 6 July, pp.839-846. DOI:10.5593/sgem2019/2.2/S11.103.

[17] Fahmy A. Geo-environmental and seismic response analysis of free-standing stone columns at El-Ashmonein archaeological site- Minia- Egypt. With practical applications for restoration and preservation. Master thesis. 2019. Available from: http://research.asu.edu.eg/handle/123456789/177612

[18] Fernandes F.Built heritage and flash floods: hiking trails and tourism on Madeira Island. 2016;6631. DOI: 10.1080/1743873X.2015.1082574.

[19] Al-Weshah R A, El-Khoury F. Flood Analysis and Mitigation for Petra Area in Jordan. 1999; 125, Issue 3 (May). DOI: 10.1061/(ASCE)0733-9496(1999)125:3(170).

[20] Sweek T, Anderson J R, Tanimoto S. Architectural Conservation of an Amun Temple in Sudan. 2012;10(2), 8–16. http://doi.org/10.5334/jcms.1021202

[21] Osman M A, Ali E M, Elhaj O B. A Study on Geotechnical Properties of Weak Rocks in Sudan Abstract. 2014;17, 13–27. https://doi.org/10.53332/jbrr.v17i.597

[22] Government of Sudan (2021) Report: Sudan Rapid Post Disaster Needs and Recovery Assessment (Rapid PDNRA). Available from: https://www.gfdrr.org/sites/default/files/Sudan_RPDNRA-English_HighRes.pdf

[23] Onderka P, Vrtal V. Preliminary report on the nineteenth excavation season of the archaeological expedition. 2021;145–163. https://doi.org/10.37520/anpm.2021.012

[24] Fahmi M M, Ahmad Y, Hashim H. The Challenges for Preserving Glorious Heritage of Sudan: Status and Solutions. 2022; 9(2), 25–38. Available from: https://www.informaticsstudies.org/index.php/informatics/article/download/334/434

[25] Boozer AL. A historiography of archaeological research at Meroë, Sudan. 2017;16, 209–248. https://doi.org/10.2143/AWE.16.0.3214940

[26] Hadjimitsis D G, Agapiou A, Themistocleous K, Alexakis D D, Sarris A. Remote Sensing for Archaeological Applications: Management, Documentation and Monitoring. In (Ed.), Remote Sensing of Environment - Integrated Approaches. IntechOpen. 2013.https://doi.org/10.5772/39306

[27] Tapete D. Remote Sensing and Geosciences for Archaeology. 2018.https://doi.org/10.3390/books978-3-03842-764-3

[28] Angeli S De, Battistin F. Archaeological site monitoring and risk assessment using remote sensing technologies and GIS. 2021; 145–154. https://doi.org/10.4337/9781788974639.00024

[29] Hu N K, Li X. Sand dunes, mobility, and cultural heritage. 2017;1–125. https://iopscience.iop.org/article/10.1088/1755-1315/57/1/012028

[30] Ahmed SM, Welspy D. The Archaeological Sites of the Island of Meroe. Nomination File: World Heritage Centre. 2019. Available from: https://whc.unesco.org/document/168998

[31] Yellin J. Meroitic royal chronology: the conflict with Rome and its aftermath', Sudan & Nubia. 2015;19, 2-15.Available from: https://issuu.com/sudarchrs/docs/s_n19_yellin/1

[32] Riedel A, Bashir M S. Mohamed MB. The Qatari Mission for the Pyramids of Sudan – Archaeological Investigation, Conservation and Site Management at Meroe. 2016. Available from: http://www.sudarchrs.org.uk/wp-content/uploads/2019/07/SARS_SN20_Riedel-et-al.pdf

[33] Hinkel F W. The Royal Pyramids of Meroe. Architecture, Construction and Reconstruction of a Sacred Landscape, Sudan & Nubia. 2000;4, 11-26.Available from: https://issuu.com/sudarchrs/docs/s_n04-hinkel

[34] Ahmed A H. Mineral Deposits. 2022. DOI: 10.1007/978-3-030-96443-6.

[35] Worrall G A. A simple introduction to the geology of the Sudan. Sudan Notes and Records. 1957; 38, 2–9. http://www.jstor.org/stable/41710729

[36] Whiteman A J. Geology and scenery of Sudan. Sudan Notes and Records, vol. 47. 1966; pp. 137–44. http://www.jstor.org/stable/44947310. Accessed 25 Apr. 2022.

[37] Fielding L, NajmanY, Millar I, Butterworth P, Ando S, Padoan M, Barfod D, Kneller B. A detrital record of the Nile River and its catchment. Journal of the Geological Society. 2016; 174(2), 301–317. https://doi.org/10.1144/jgs2016-075

[38] Williams M. Geology and Soils. In The Nile Basin: Quaternary Geology, Geomorphology and Prehistoric Environments (pp. 33-58). Cambridge: Cambridge University Press. 2019. https://doi.org/10.1017/9781316831885.005

[39] Abujaball MM.Sedimentary Facies & Depositional Environment of Shendi Formation, Al-Musauwarat/Umm Ali Area, Sudan. Master thesis. 2019. Available from: http://dspace.iua.edu.sd/bitstream/123456789/5235/1/introd.pdf

[40]Humphris J, Bussert R, Alshishani F, Scheibner T, Humphris J, Bussert R. Azania : Archaeological Research in Africa The ancient iron mines of Meroe The ancient iron mines of Meroe. 2018;5534. Available from: https://doi.org/10.1080/0067270X.2018.1515922.

[41] Cech B.The Quarries of Meroe, Sudan. The Quarries of Meroe, Sudan. 2018.https://doi.org/10.5339/uclq.2018.9789927118883

[42] World Bank. Sudan. 2021;pp. 1–9. Available from: https://www.climatecentre.org/wp-content/uploads/RCCC-ICRC-Country-profiles-Sudan.pdf

[43] Siddig K, Stepanyan D, Wiebelt M, Grethe H, Zhu T, Berlin H. Climate change and agriculture in the Sudan : Impact pathways beyond changes in mean rainfall and temperature. Ecological Economics [Internet]. 2020;169(October 2018):106566. Available from: https://doi.org/10.1016/j.ecolecon.2019.106566

[44] Salih AAM, Ahmed N, Tjernström M, Zhang Q. Characterization of the Sahelian-Sudan rainfall based on observations and regional climate models. Atmospheric Research [Internet]. 2018;202(November 2017):205–18. Available from: https://doi.org/10.1016/j.atmosres.2017.12.001

[45] UNEP. More action needed on sand and dust storms. 2017. Available from: https://www.unep.org/es/node/331

[46] UNEP, WMO, UNCCD. Global Assessment of Sand and Dust Storms. United Nations Environment Programme, Nairobi. 2016. Available from: https://wesr.unep.org/redesign/media/docs/assessments/global_assessment_of_sand_and_dust_storms.pdf

[47] Sharif S M.Dust Storms in Sudan: Intensity and Particles; Characteristics.2014;pp. 26–29. Available from: https://www.researchgate.net/publication/262602280_Dust_Storms_in_Sudan_Intensity_and_Particles_Characteristics

[48] Khadam A M A, Hamouda E A, Doud K R. Wind Power Harnessing in Sudan, Opportunities and Challenges Wind Power Harnessing in Sudan, Opportunities and Challenges. 2016. DOI: 10.13140/RG.2.2.22530.68802.

[49] Wahab. Probability distribution of extreme wind speeds in Sudan. Sudan Engineering Society Journal. 2001; 47.No.39. Available from: https://pdfcoffee.com/wind-in-sudanpdf-3-pdf-free.html

[50] OCHA. Sudan. Situation Report. 2021; 13(13), pp. 1–21. Available from: https://reliefweb.int/sites/reliefweb.int/files/resources/Situation%20Report%20-%20Sudan%20-%2019%20Sep%202021.pdf

[51] Ghrefat H A.The geology of sand dunes.2021. Available from: https://www.researchgate.net/publication/287244680_The_geology_of_sand_dunes

[52] Ayoub A T. Extent, severity and causative factors of land degradation in the Sudan. 1998; pp. 397–409.

[53] Gamri T El. Sand Dunes: Mechanisms, Impacts and Control Measures in the Sudan Sand Dunes: Mechanisms, Impacts and Control Measures in the Sudan. 2021. Available from: https://www.researchgate.net/publication/349378038_Sand_Dunes_Mechanisms_Impacts_and_Control_Measures_in_the_Sudan

[54] Masaru A, Janssen H, Roels S. Impact of wind-driven rain on historic brick wall buildings in a moderately cold and humid climate: Numerical analyses of mould growth risk, indoor climate and energy consumption'. Energy and Buildings. 2009;41(1), 101-110. DOI: 10.1016/j.enbuild.2008.07.011.

[55] Moncmanová A. CHAPTER 1 Environmental factors that influence the deterioration of materials. 2007; 28, 1–25. https://doi.org/10.2495/978-1-84564-032-3/01

[56] Fratini F, Rescic S .The stone materials of the historical architecture of Tuscany. Geological Society, London, Special Publications.2016. DOI: 10.1144/SP391.5.

[57] Maraveas C. Fasoulakis Z. Wind-Induced Failure Analysis and Retrofit of an Existing Steel Structure. 2018; pp. 271–291.DOI: 10.4236/ojce.2018.83021.

[58] Zanke A S. Building Cracks: Causes and Preventions. 2020; 5(8), pp. 165–169.

Part III: Consolidation

3.6. Multi-functional monodispersed SiO_2-TiO_2 NPs and TEOS in the consolidation of archaeological lime mortars surfaces.

Submitted to Journal of Construction and Building Materials.

Authors: Abdelrhman Fahmy[1,2]*, Anna Gołąbiewska[3], Wiktoria Wojnicz[4], Alicja Stanisławska[4], Jakub Kowalski[4], Justyna Łuczak[5], Adriana Zaleska-Medynska[3], Salvador Domínguez-Bella[1], Javier Martínez-López[1] and Eduardo Molina-Piernas[1]

[1]Department of Earth Sciences, Faculty of Sciences, University of Cadiz, Campus Río San Pedro, 11519, Puerto Real, Spain.

[2]Conservation Department, Faculty of Archaeology, Cairo University, 12613, Giza, Egypt.

[3]Department of Environmental Technology, Faculty of Chemistry, University of Gdansk, WitaStwosza 63, 80-308 Gdansk, Poland.

[4]Faculty of Mechanical Engineering and Ship Technology, Gdansk University of Technology, 11/12 Narutowicza Str. 80-233 Gdańsk, Poland.

[5]Department of Process Engineering and Chemical Technology, Faculty of Chemistry, Gdansk University of Technology, Gdansk, Poland.

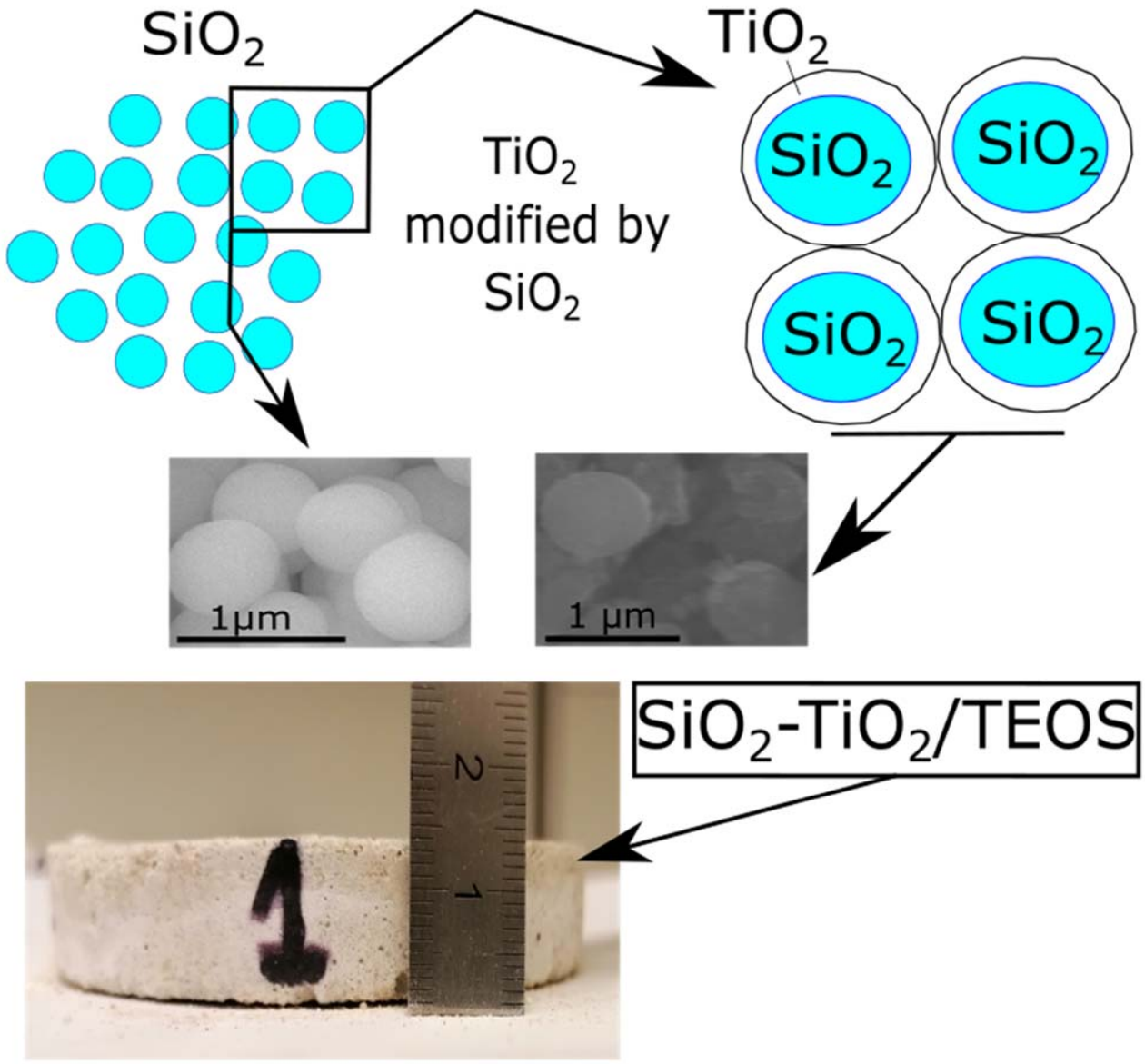
* Corresponding author: abdelrhman.fahmy@uca.es

3.6. Multi-functional monodispersed SiO_2-TiO_2 NPs and TEOS in the consolidation of archaeological lime mortars surfaces.

Highlights

- 3% and 5% SiO_2-TiO_2 NPs/TEOS enhanced the lime mortar surfaces multifunctionally.
- 3% and 5% are suitable consolidates for lime mortar surfaces without leaving chromatic changes.
- 7% SiO_2-TiO_2 NPs /TEOS did not enhance the lime mortars physically and mechanically.
- Low concentration and monolayer is an efficient application method for SiO_2-TiO_2 NPs /TEOS utilization.

Graphical abstract



Abstract

Archaeological traditional lime mortars are susceptible to many environmental conditions such as the impact of water (rains, humidity, groundwater, etc.), variation of temperatures' degrees, winds and/or pollution. Accordingly, this research aims to provide newly assessed multifunctional nano-coating for the purpose of archaeological lime mortar protection. For this, the study combined physicochemical and mechanical characterizations in performance assessment of 3%, 5%, and 7% of the synthesized SiO_2-TiO_2 nano-particles (NPs) and TEOS as consolidants on the surfaces of the experimental lime mortars. A series of techniques and tests were fulfilled for the evaluation. For analysis, X-ray diffraction and UV-Vis along with scanning electron microscopy were used to identify microstructure. Furthermore, wettability, colorimetric, self-cleaning, petrophysical, nano-indentation and uniaxial compressive strength tests were performed in order to select the most suitable consolidate between 3%, 5%, and 7% SiO_2-TiO_2 NPs/TEOS. Durability assessments were carried out through salt weathering, thermal and UV aging tests. The results showed that 3% and 5% of SiO_2-TiO_2 NPs/TEOS enhanced the physical and mechanical properties of the lime mortars. On the other hand, 7% SiO_2-TiO_2 NPs/TEOS proved their insufficient efficacy in improving the surfaces of lime mortars for the high amount of TiO_2 and its behavior for aggregation.

Keywords: photocatalytic, hydrophobic, self-cleaning, nano-SiO_2, nano-TiO_2, TEOS, nano-test, durability, lime mortar.

Abbreviations and symbols:

NPs: Nanoparticles

TEOS: Tetraethoxysilane

XRD: X-ray diffraction

UV-Vis: Ultraviolet-visible light

SEM: Scanning electron microscope

EDS: Energy dispersive spectrometry

UCS: Uniaxial compressive strength

CIE: Commission Internationale de l´Eclairage

ASTM: American standard of testing materials

NDT: Non-destructive technique

CA: Contact angle

MB: Methylene blue

L^*: brightness coordinate

a^*: red–green coordinate

b^*: yellow–blue coordinate

ΔE^*: Color change

GPa: Gigapascal

WA: water absorption

Po: porosity

V_V: volume of voids

V_T: Total voids

D: Density

m: mass

v: volume

ΔM: mass loss

H: Hardness

E_s: Young's Modulus

MPa: Megapascal

1. Introduction

Lime mortar and lime plasters were widely used in archeological sites at various times and cultures as structural and architectural elements in the buildings [1]. Regarding the conservation and restoration of ancient building materials, lime-based mortars without improvements have advantages (economic, eco-friendly, and compatible) and disadvantages (moderate mechanical resistance, high permeability, slow setting, high drying shrinkage, and unstable) [2]. In this sense, it is important in the field of archaeological conservation to keep paying attention to developing and improving the physical, chemical, and mechanical properties of traditional mortars using nano-based and compatible materials in restoration projects. For this, the improvement of the lime mortars incorporates some additives such as nano-metal oxides to obtain structure/coating with properties like superplasticizers, water repellents, and photocatalysts.

Recently, nano-SiO_2 was used in lime mortar combinations in the conservation field to enhance the durability of the archeological mortar by strengthening its mechanical and physical properties. In general, mortar-based materials containing SiO_2 nanoparticles are mechanically better than those containing SiO_2 fume because nano-SiO_2 strengthens the mortars [3]. Senff et al. [4] reported a piece of evidence related to the study of the enhanced properties of nano-SiO_2 and SiO_2 fume addition in different tests to define compressive strength, rheological properties, and water absorption. For example, nano-SiO_2 with 7% (wt.) presented a faster formation of structures during the rheological measurements and the compressive strength increased when compared to mortars without treatment. Calia et al. [5] used nano-SiO_2 in the enhancement of porous stones characteristics and concluded that nano-SiO_2 of 7% managed to improve the mechanical resistance and surface abrasion resistance for consolidation of carbonate porous stones. In addition, it manifested good penetration for more than 5mm and good preservation for the chromatic characteristics. Ferri et al. [6] applied alkoxysilanes and modified silica nanoparticles on stone surfaces (sandstone, marble, and granite) to characterize their performance in improving surface properties. They found that the hydrophobicity of the surfaces was enhanced, especially for granite. Al-Dosari et al. [7] tested the efficacy of nano-SiO_2 combined with ethyl silicates

tetraethoxysilane (TEOS) in the consolidation of sandstone. This silica/polymer nanocomposite led to strengthening the mechanical and physical properties of the historic sandstones. In addition, it manifested high durability against erosion, acids, and salts. Diaz et al. [**8**] mentioned that the addition of nano-SiO_2 to lime mortar up to 4% (wt.) improves its mechanical properties, i.e., it increased the strength to 50% for the air lime mortars and 150% for the hydraulic lime mortars. Zhang et al. [**9**] synthesized core–shell nano-SiO_2/fluoro acrylate composite in the consolidation of stone surfaces. They concluded that the content of 8.0% (wt.) of hexafluoro-butyl methacrylate (HFMA) and SiO_2 at 4.0% (wt.) played a protective role in the consolidation of carbonate stone surfaces with high compatibility. In modern applications, nano-SiO_2 is added to cement-based mortar in soil stabilization. This addition of nano-SiO_2 improved the mechanical strength of the mortar, as well as increased the pozzolanic catalytic activity of the mortar [**10**]. Moreover, Stucchi et al. [**11**] assumed that nano-SiO_2 consolidates have the potential in the protection of mortar and types of cement. For this, they synthesized two different dimensional ranges of particles of nano-SiO_2 in order to assess their efficacy in improving stone surfaces (sandstone and granite). They observed that the humidity caused aggregations for nanoparticles, leading to penetration prevention into the stone. Accordingly, nano- SiO_2 particles should be applied in a dried environment.

In addition, nano-TiO_2 is also widely used in the conservation field to protect the archeological surfaces biophysically. Nano-TiO_2 is considered a promising photocatalytic material because it has the efficacy to catalyze and degrade many contaminants. In this way, nano-TiO_2 is very useful as a coating material for contaminated surfaces of the cultural heritage, especially for substrates of building materials [**12**]. Nano-TiO_2 can improve the peeling and washing properties along with the photocatalytic performance of surfaces of the construction materials if it is embedded in carbon-dots-grafted [**13**]. In fact, nano-TiO_2 could show a decreased photocatalytic oxidation activity rate because of the increasing number of nano sheet layers which generate carriers and make it hard to be diffused in the surface layer. Therefore, the monolayer film of nano-TiO_2 exhibits high activity compared with well-investigated sol-gel derived anatase TiO_2 film [**14**]. According to Ferrari et al. [**15**],

nano-TiO_2 could last for ten years with high workability and activity. In this regard, when nano-TiO_2 emission occurs to air completely, the life cycle of nano-TiO_2 starts falling apart. Furthermore, nano-TiO_2 can be applied in a spray or in brush methods with one single-layer treatment or more than one layer. In particular, the low thickness and uniformity of nano-TiO_2 cannot adjust the visual appearance of the treated substrate [**16**]. In addition, the brushing method of application of nano-TiO_2 in the treatment of rendering layers is an effective way in order to guarantee a high amount of deposited titania nanoparticles on the surface [**17**]. During the redox reactions of nano-TiO_2 with treated surfaces, the reactions can be useful to define air purification of NO_x, SO_x, VOCs, self-cleaning, de-soiling, anti-fogging, anti-microbial and anti-biofouling properties [**17**]. Saeli et al. [**18**] mentioned that nano-TiO_2 is a preferred photocatalytic additive to lime-based mortars/construction material because it is considered economic, stable chemically, biocompatible, and widely material that is used in daily life and is treated as green and eco-friendly. In fact, TiO_2 has three crystal phases (anatase, brookite, and rutile forms) among which the anatase nanocrystals present the highest photocatalytic activity [**19**]. Moreover, nano-TiO_2 contributes to increasing the mechanical resistance of the treated architectural surfaces and enhances preventive conservation [**20**]. Nano-TiO_2 tends to aggregate, and this results in an enlargement of the average particle size of TiO_2 and affects its catalytic performance [**21**]. In addition, in practice, TiO_2 is combined with other materials such as Ag, Si, etc. Moreover, TiO_2-based nano coatings are extremely dependent on the porosity and roughness of the surfaces, the amount of TiO_2, and their compositions (single or combined for treatment) [**22**].

Therefore, the evidence on the composition of SiO_2-TiO_2 NPs material is still under investigation. Wang et al. [**23**] prepared SiO_2-TiO_2 and PDMS compound that was used as coating material. This compound demonstrated good performance as photocatalytic and superhydrophobic material. The SiO_2-TiO_2 compound presents significant workability to different substrates such as stone, mortars, glass, and wood as well as can be applied directly on the surfaces to add values of superhydrophilic and self-cleaning for the surfaces [**24**]. Additionally, Pinho et al. [**25, 26**] declared that SiO_2-TiO_2 with a non-ionic surfactant

(n-octylamine) could give additional values for non-reactive pure carbonate stones such as a crack-free surface layer, high mechanical strength, self-cleaning properties and high penetration inside the pores of the stones. Moreover, TiO_2 is homogeneously disseminated in the SiO_2-TiO_2 composite and plays a vital role in the photodegradation of methylene blue under UV relying on deposition cycles and heat treatment [**27**]. Furthermore, SiO_2 is considered a support for TiO_2 that prevents the formation of large clusters of TiO_2 and creates nano-TiO_2 colloidal with high catalytic activity for different applications [**28**]. Gemelli et al. [**29**] carried out an experimental study to evaluate SiO_2-TiO_2 nano-composite as an anti-fouling and anti-microbial applied on historic Roman mortar. They reported the efficient role of SiO_2-TiO_2 integration as a durable coating material for the preservation of the mortar surface. In addition, they concluded that after 4 years of application of SiO_2-TiO_2 nano-composite, led to 40% removal in organic crust and 61% prevention of biological growth. Nowadays, SiO_2-TiO_2 NPs could enhance cement mortar to add more functionalities such as aerial decontamination of pollutants. In that concern, the photo degradation rate reached 65% to 80% up to 1 h under solar light for NO_X, while orange II degradation reached 18% to 50% after 9 h under visible light [**30**].

Considering the results of cited studies, one can observe that the researchers focused mainly on the physiochemical characterizations of the SiO_2-TiO_2/TEOS NPs applications. Therefore, this research was addressed to characterize SiO_2-TiO_2 NPs/TEOS by using multi-techniques such as mechanical tests to identify the mechanical resistance of the synthesized SiO_2-TiO_2/TEOS NPs on the lime mortar surfaces along with physiochemical measurements. The aim of the work is to compose an appropriate consolidation product with multi-functional performances to preserve the lime mortar surfaces. To accomplish this, three SiO_2-TiO_2 mixtures were prepared and synthesized (at 3%, 5%, and 7%), and embedded in TEOS. Several analytical and microscopic techniques (X-ray diffraction, UV-Vis, and scanning electron microscope with EDS) were used in order to identify the synthesized nano-materials and to assess their efficacy, performance, and durability. Moreover, there had been conducted different tests to define water repellence properties, to specify the chromatic properties of treated and untreated samples, and to assess self-cleaning

behavior. In addition, a nano-indentation test was conducted to assess the nano-hardness (hardness) and Young's modulus of the treated and untreated samples. In addition, the uniaxial compressive test was performed to estimate compressive strength (UCS), and these results were used to assess the limitations of the treatment of the lime mortars. Finally, aging tests were conducted such as salt, thermal, and UV aging to assess the durability and resistance of the treated samples.

2. Ancient lime mortar decay

Lime mortars as architectural and structural elements of ancient buildings are continuously subjected to intrinsic and extrinsic degradations factors. In this context, Hees et al. [**31**] outlined that the most important factors affecting the degradation of mortars are connected to the environment, material, design, workmanship, construction procedures, and preventive conservation (maintenance). Rains and their frequencies are considered one of the most powerful environmental decay factors. The water of rains can enter firstly through the joint mortars to the whole building because mortars are observed to be the weak part of the structures for their low/moderate mechanical and physical strength than the building stone blocks. In this sense, water can cause damping and moisturizing for the joint structural mortar that initiates a change in chemical and physical properties and involves mechanical deformations [**32, 33**]. Pollutants can increase the degradation of mortars, especially in the presence of water and ozone. For instance, lime mortar is susceptible to SO_3 pollutants in presence of water and ozone. On the other hand, NO_2 pollutant has lower reactivity to lime mortar than NO pollutant gas [**34**]. Moreover, mechanical stresses are treated as deterioration factor that is the result of overloading, thermal expansion, differential thermal expansion, and /or fluctuations of moisture content [**35**]. Daily cycles between wetting and drying can cause granulation for the mortar composition. In addition, it is a driver for salt weathering by dissolution and crystallization of soluble salts causing differential pressures and texture change [**36-38**]. Moreover, scaling, disintegration, efflorescence, sub-fluorescence, cracking, and flaking are considered additional common forms of deterioration for lime mortars (**Fig. 3.6.1 A-D**) [**39**]. That is why the consolidation of the lime mortar surfaces with multi-functional and advanced nano-

based materials is considered the required treatment to increase the durability and sustainability of these ancient mortars.

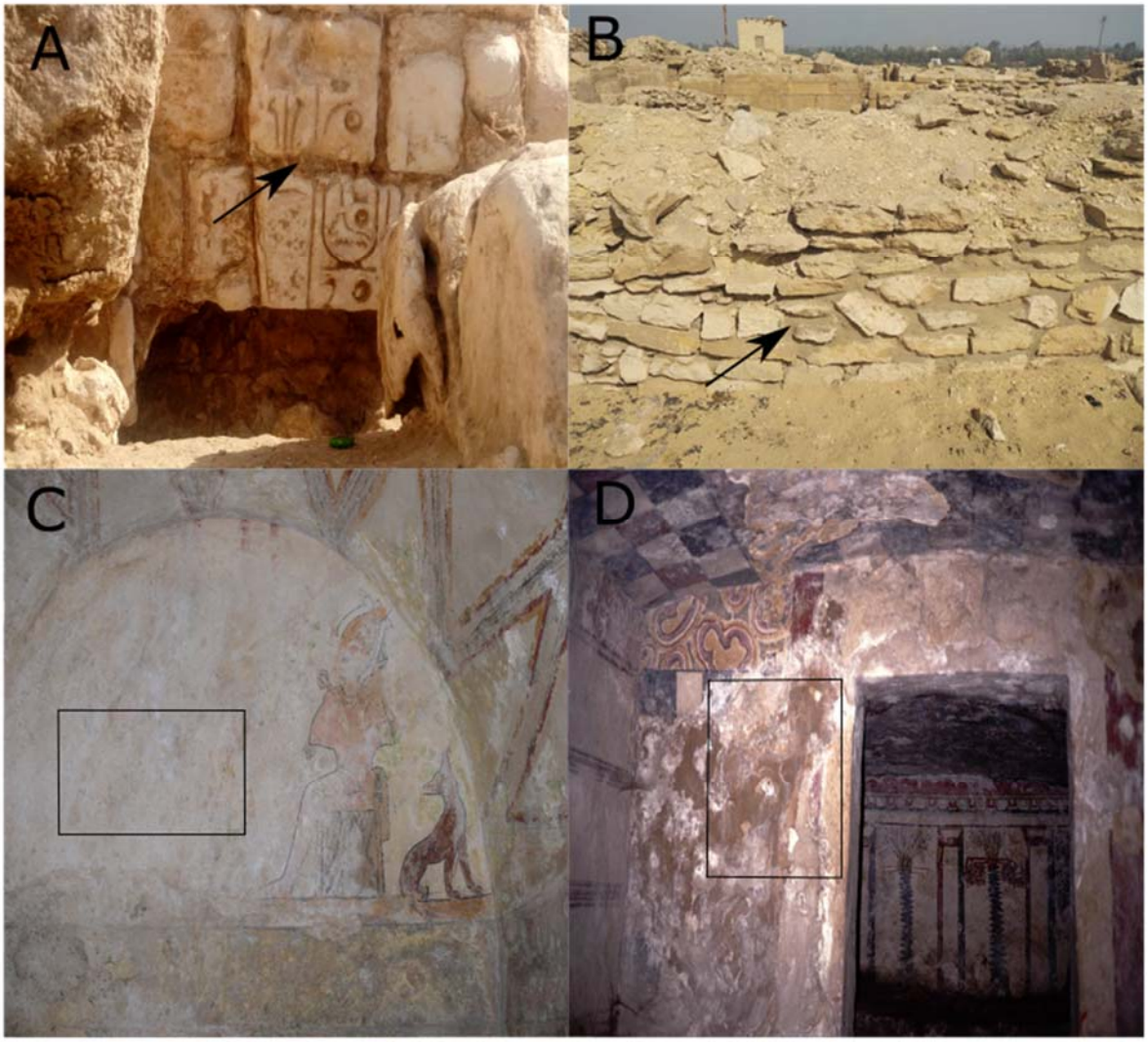


Fig.3.6.1. The degradations of the ancient lime mortar (structural joint material) and lime rendering from various archaeological sites in Egypt. (A) Temple of Ramses II, Al-Ashmounien archeological site, Egypt, where the joint mortar between blocks was disintegrated as shown in the black arrow. (B) Abusir archaeological site, Giza, Egypt, where the lime mortar between blocks was decomposed and disintegrated as referred to as the black arrow. (C and D) The salt weathering of lime rendering is shown in the rectangles, of Anfushi's necropolis, Alexandria, Egypt.

3. Materials and methods

3.1 Materials

3.1.1 Preparation of experimental mortars

To get well-mixed lime mortars in modern times, lime mortar should have a mix proportion of around 1:3 (lime: sand). Nevertheless, historic lime mortars often contain more lime with mixed proportions of 1:1 or 1:2 and historic mortars can contain more lime inclusions in the form of lumps of unmixed lime, under burnt material, or hard-burnt particles [**40**]. In this regard, fifty experimental lime-based mortar samples were prepared. The mortar consists of 1 lime, 2 sand, and 0.5 limestone aggregates according to Jeremy [**40**] and [**41**]. They were cast into plastic Petri dishes 1.5 cm in thickness and 8.5 cm in diameter **Fig. 3.6.2** (**A-D**). Experimental samples had been prepared in order to get casted samples that are similar to the traditional lime mortar.



Fig. 3.6.2. (A) The used proportion in preparation of lime mortar. (B) The preparation process of the mortar. (C and D) Presentation of experimental casted lime mortar samples.

3.1.2 Chemicals

Some chemicals had been prepared as raw materials and reagents for the synthesis of SiO_2 and SiO_2-TiO_2 NPs such as ammonia (NH_4OH), tetraethoxysilane (TEOS) (Si (C_2H_5)$_4$), tetrabutytitanate (TBOT)($CH_2CH_2CH_2CH_3$), acetylacetone ($C_5H_8O_2$), ethanol (C_2H_6O) and Distilled water.

3.1.2.1 Synthesis of SiO_2 NPs

To obtain microspheres of SiO_2, suspension (A) was prepared from 36 ml of ethanol, 10 ml of ammonia (NH_4OH) and 20 ml of distilled water. In addition, magnetic stirring was required for 20 minutes 300 r/minute. On the other hand, suspension (B) was also prepared by adding 15.7 ml of TEOS + 19.9 ml of ethanol and this suspension was added slowly to suspension (A). Then, the magnetic stirring for both suspensions was carried out for 2 hours at 300 r/minute. Additionally, washing and filtering were applied in the centrifuge for 15 minutes with 6000 r/minute. Finally, the centrifuged product was dried for 24 h at 60 °C according to Wang et al. [**23**].

3.1.2.2 Synthesis of SiO_2-TiO_2 NPs

Monodispersed SiO_2-TiO_2 NPs were chemically synthesized according to Wang et al. [**23**]. At first, suspension (A) had been prepared from 120 ml ethanol, 120 ml distilled water, and 4ml acetylacetone. Secondly, suspension (B) was prepared from 20 g of microspheres of SiO_2, 40 ml TBOT and 280 ml of ethanol. Then, suspension (B) was added to suspension (A) using the dropwise method. In addition, magnetic stirring for 24 h at 300 r/minute was carried out. Furthermore, the final suspension was centrifuged for 20 minutes at 6000 r/minute and then dried for 24 h at 60 °C.

3.1.2.3 Preparation of SiO_2-TiO_2 NPs/TEOS

In the assumption of the total beaker content of SiO_2-TiO_2 NPs, TEOS and ethanol is 50 g. Consequently, the needed grams of 3%, 5% and 7% of SiO_2-TiO_2 NPs were 1.5 g, 2.5 g and 3.5 g, respectively. Moreover, the required TEOS was 10.8 ml and 63.38 ml of Ethanol in all cases. Finally, different concentrations of SiO_2-TiO_2 NPs were added to 20% TEOS and

dispersed in Ethanol. These different proportions of 3%, 5% and 7% of SiO_2-TiO_2 NPs/TEOS was evaluated in their efficacy in the multifunctional consolidation of the lime mortar surfaces.

3.2.1 Mineralogical and textural techniques

To characterize the SiO_2-TiO_2 NPs and identify their crystalline structures, a Bruker (X-ray diffraction) D-8 Advance ECO diffractometer was used, equipped with a high-speed measurement Linxeye detector by using the following specifications: CuKα radiation filtered by Ni, graphite monochromator, and fixed slots, 2theta 5° to 60° scanning angle; diffractograms were interpreted with the software EVA (Bruker-AXS). In addition, UV-Vis spectroscopy (Shimadzu, UV-2600) within the wavelength range of 200 to 800 nm was utilized to recognize the reflectance and absorbance of the synthesized SiO_2-TiO_2 NPs. These analytical techniques were hosted by the Department of Environmental Technology, Faculty of Chemistry (University of Gdańsk, Poland).

A scanning electron microscope with EDS (Quanta 200) with a range of voltage [200; 30 000] and resolution 3.0 nm at 30 kV and 10 nm at 3 kV, and supplied with EDAX 60 mm 2 Octane Super EDS detector was utilized to recognize the particle size of the SiO_2-TiO_2 NPs and their distribution. In addition, SEM had been used to evaluate the textural features of the treated and untreated surfaces with 3%, 5%, and 7% of SiO_2-TiO_2 NPs/TEOS and to select the most efficient percentage for the consolidation of the archaeological lime mortar surfaces. Moreover, it managed to detect the penetration of the SiO_2-TiO_2 NPs/TEOS inside the lime mortars and their interparticle interaction with the treated samples' surfaces. Furthermore, it was used to detect changes in the treated samples after UV, thermal, and salt accelerating aging. The Department of Environmental Technology, Faculty of Chemistry (University of Gdańsk, Poland), SCiCYT, and UGEA-PHAM (University of Cadiz, Spain) hosted this examination.

3.2.2 Contact angle test

To measure the contact angle for the synthesized nanoparticles and their hydrophobicity properties, three different concentrations of 3%, 5% and 7% of SiO_2-TiO_2 NPs/TEOS were applied on the glass surfaces to be tested using the OCA 15EC package (**Fig. 3.6.3 A-C**). This package is supplied with a movable table for the samples, a 6x parfocal zoom lens, video measuring, led lighting, and the software module SCA 20-contact angle. The Faculty of Chemistry (Gdańsk University of Technology, Poland) hosted this test.

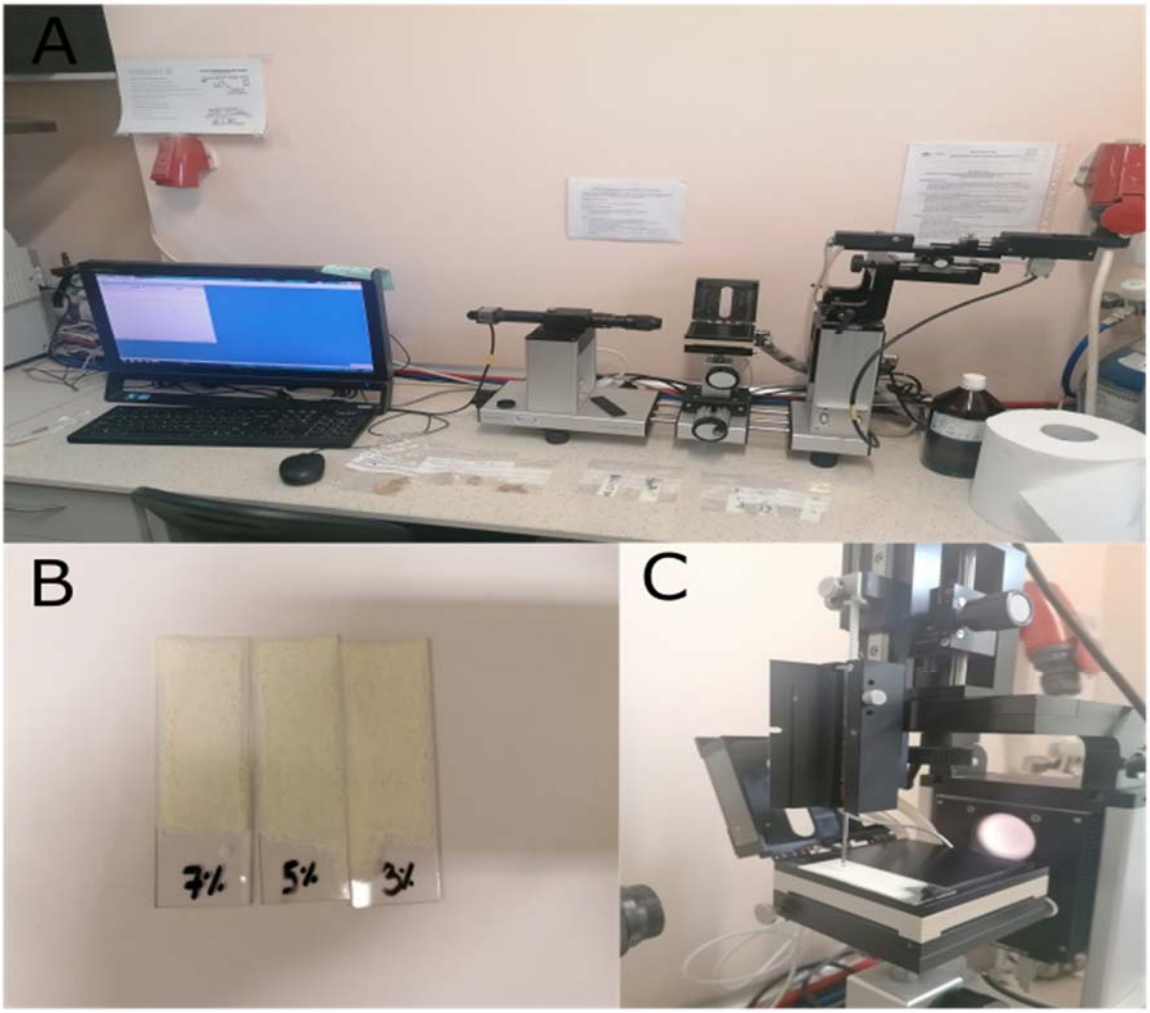


Fig. 3.6.3. (A) Contact angle test equipment**.** (B) Glass surfaces supplied with 3%, 5% and 7% of SiO_2-TiO_2 NPs/TEOS. (C) During test operation and droplets releasing.

3.2.3 Spectrophotometric measurements

o measure and detect chromatic values and changes in the treated and untreated surfaces, a double-beam Optimatch spectrophotometer and data color international Spectraflash SF450-UK were used. These CIE Lab values were carried out at the National Institute of Standards (NIS) (Cairo, Egypt). In this system, L*= brightness coordinate (100 = white, 0 = black), a*= red–green coordinate (positive sign = red, negative sign = green), and b*= yellow–blue coordinate (positive sign = yellow, negative sign = blue). It can be calculated as the Euclidean distance between two points in CIELAB color space and this measurement was agreed upon by the Commission Internationale de l' Éclairage (CIE) in 1976 according to the next equation according to UNE-EN 15886 [**42**] and Kim et al. [**43**]:

$$\Delta E = \sqrt{\Delta L^{*2} + \Delta a^{*2} + \Delta b^{*2}}$$

where ΔE^* is the color change, ΔL^* is the change of brightness coordinate, Δa^* is the change of red–green coordinate, and Δb^* is the change of yellow–blue coordinate.

3.2.4 Methyl blue test (self-cleaning test)

To perform self-cleaning tests for the treated and untreated samples with different concentrations of 3%, 5% and 7% SiO_2-TiO_2 NPs/TEOS the following components had been used: 100 µmol/L methylene blue (500 ml ethanol + methylene 0.0003899 ml). Then, samples were exposed to the ultraviolet light of 365 nm to irradiate the samples inside the prepared chamber for self-cleaning photodegradation analysis (**Fig. 3.6.4**). Moreover, after the application of methylene blue (pollutant), the samples were under UV exposure cycle/20 minutes (10 cycles) according to ISO 10678:2010(E) [**44**]. In addition, photos were taken and chromatic values were recorded after each measurement. The Department of Environmental Technology, Faculty of Chemistry, University of Gdansk, Poland hosted this test.

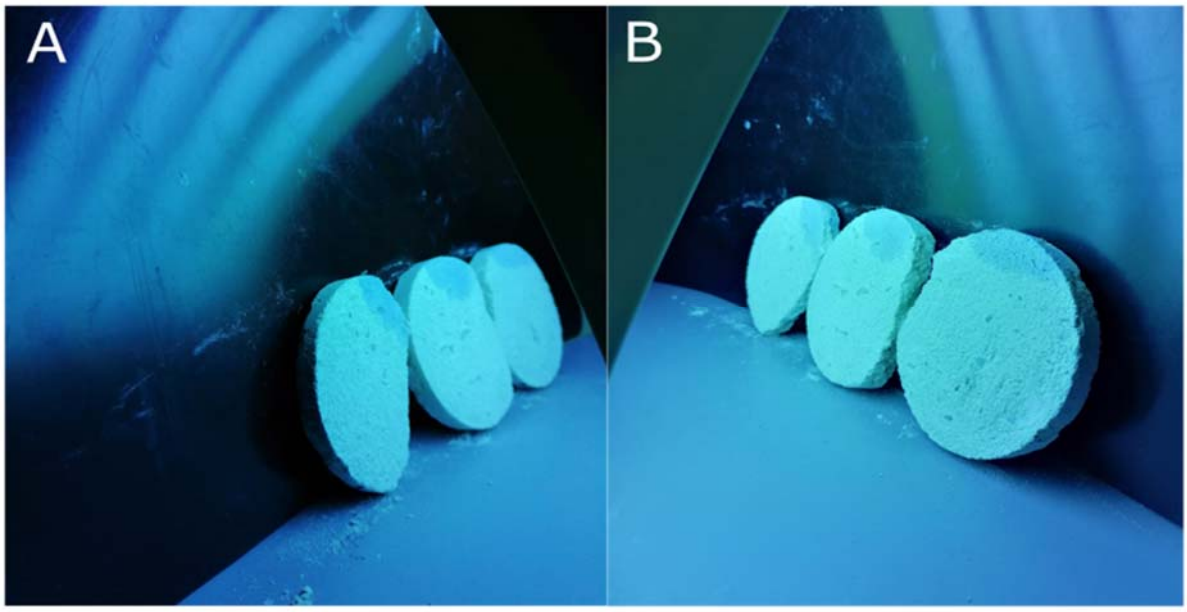


Fig. 3.6.4. (A and B) Prepared UV chamber for the self-cleaning test.

3.2.5 Mechanical properties

3.2.2.5.1. Nano-indentation test

Nano-indentation test (nano test) is conducted to carry out the mechanical properties of a material, coatings and thin films and can be classified as a non-destructive technique (NDT). This technique is appropriate for applications of physical samples that are rare and very small, especially in cultural heritage [**45**]. In general, the least value of pressure under the Berkovich indenter (which is a regular tetrahedron with a triangular base) produces an imprint (permanent set) at the center of the area of contact and is used to assess hardness according to the relation H (hardness) = P_{max} (maximum load) / A (contact indenter-material area) [**46, 47**]. In addition, Young's Modulus (E_s) is determined from the unloading curve and defined by the Olivier-Pharr method [**48**]. In practice, nano-indentation tests are applied to assess the hardness and Young's modulus of the surface and the surface adhesion to the substrate.

In this study, nano-indentation was carried out to identify the mechanical strength (nano-hardness (hardness) and Young's modulus) of the mortar samples (untreated and nano-treated samples). It is worth emphasizing that the results of a nano-indentation study

presented in this paper should be treated as a pioneer application for nano-materials assessment in the conservation field and archaeological science. In addition, it contributes to assessing the behaviors of nano-treatment in enhancing the mechanical properties of the lime. Each result of the nano-indentation consists of a minimum of ten successful indentations for each sample (**Fig. 3.6.5 A-C**). In this study, each sample for the nano-indentation test was included in a resin and tested on the nano-Test Vantage nano-indentation measurement system (Micro Materials, UK) at the temperature of 20^0C according to ISO 14577 [**49**] and ASTM 2546 [**50**]. The number of measurements for each sample was 10 indentations with 5s dwell at maximum load equaled 5 mN with 2 nN load resolution, 0.1 mN limit stop load, 0.002 nm displacement resolution, 50 s loading time, 50s unloading time, no more than 0.4 µm repositioning accuracy and 1 µN contact surface loading and 1 min of exchange time. The distance between the two following indentations was 15 µm (counted from the most distant points of the two indentations). The distance between the most distant points of the first indentation and the last (tenth) indentation was 1,35 mm. During each test, following parameters were measured: maximum depth [nm], plastic depth [nm], hardness [GPa], and Young's modulus [GPa]. Nano-indentation test was performed at the Faculty of Mechanical Engineering and Ship Technology, Gdansk University of Technology, Poland.

3.2.2.5.2. Uniaxial compressive test

The compressive load was applied to evaluate the compressive strength of the untreated and one-side treated samples. In addition, on the base of the results of this test, the most efficient percentage of the nano-treatments for consolidation of the lime mortars (3%, 5%, and 7% of SiO_2-TiO_2 NPs) was identified. To carry out this test, six samples were prepared with 8.5 cm (diameter) and 1.5 cm (height) (three untreated samples and three one surface treated samples (3%, 5%, 7%). Static tensile test was performed on testing machine INSTRON 8503 (500 kN) in temperature 20 ˚C by using equipment for compressive testing. The average speed of testing developed between the initial phase of testing and its end phase was 0.215 mm/s for untreated samples, and 0.467 mm/s for one surface treated samples (3%, 5%, 7%). Note that the end phase means rapid cracking development and it

was set as the point of estimation of compressive strength *Rc*. The UCS test was performed at the Faculty of Mechanical Engineering and Ship Technology (Gdansk University of Technology, Poland).

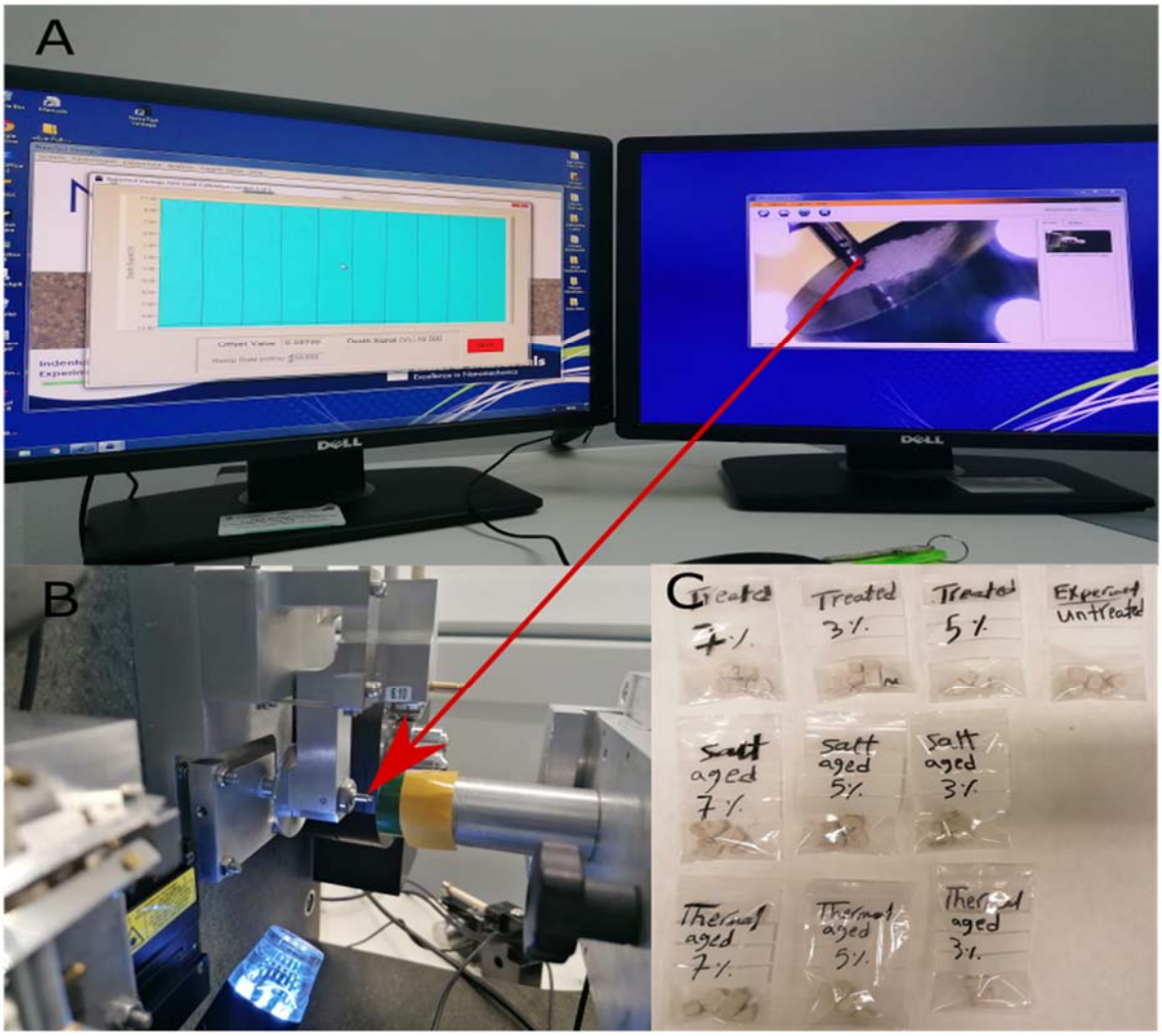


Fig. 3.6.5. (A-B) Indentations were taken by nano test equipment. (C) The prepared samples for the nano-test.

3.2.6 Physical properties

Porosity, water absorption, and density were measured as petrophysical properties in order to assess the petrophysical behavior of the samples before and after consolidation with 3%, 5%, and 7% of SiO_2-TiO_2 NPs/TEOS. Nine for each untreated and treated samples were prepared to carry out this test and the sample's dimensions were 8.5 cm (diameter) and 1.5

cm (height). The samples were divided into three groups, each group has three samples for a specific percentage of nano-materials (3%, 5%, and 7% of SiO_2-TiO_2 NPs/TEOS) for the treated samples. In addition, for the untreated samples, the samples were classified into three groups of three samples for each test. The samples were weighed naturally after drying at 105 °C, and then the samples were saturated in water to determine the natural weight, dried weight, and saturated weight. Petrophysical testing was performed and calculated according to IS: 2386 (Part III) [**51**] and ASTM C97 [**52**]. The water absorption (WA, in %) is expressed as the percent weight change due to absorbed water and calculated according to the formula WA= $(M_{wet}-M_{dry})\ /M_{dry}$×100, where M_{wet} means weight after saturation and M_{dry} means weight after drying. Moreover, porosity (Po) is a measure of the void of spaces inside stones and was measured according to the formula Po = V_V/V_T, where V_V means the volume of voids and V_T means total voids. Finally, the density (D) of the stone (indicating the unit weight of the stone) was calculated by dividing m the mass up by v the total volume of the stone according to the formula D = m/v.

3.2.7 Durability assessment

3.2.7.1. Salt crystallization aging

According to Schaffer [**53**] and the European standard, UNE-EN 12370 [**54**], salt of NaCl had been used in salt weathering with 25% concentration, and the experimental consolidated samples with three different concentrations of 3%, 5%, and 7% of SiO_2-TiO_2 NPs/TEOS had been exposed to the sodium chloride for 2 hours then subjecting to normal chamber conditions for 28 hours at 25 ºC and 40% RH. Finally, the samples were put in the oven for 16 hours at 105 ºC for repeated 15 cycles. Moreover, to calculate the salt resistance, the loss of mass was calculated according to the European standard [**55**] from the formula ΔM= (M_o-M_n/M_o) ×100%, where M_O means initial weight and M_n means Dried weight. This test was hosted at the laboratories of the Department of Environmental Technology, Faculty of Chemistry, University of Gdansk, Poland.

3.2.7.2. Thermal aging

In order to evaluate the efficacy and durability of the treated samples with SiO_2-TiO_2 NPs/TEOS against variations of the temperature degrees, the samples were subjected to 18 hours of total immersion in water and then 6 h in a temperature inside a controlled oven at 105 ˚C. In this study, 30 cycles of the subjection (variations of the temperature degrees) had been conducted according to UNE-EN 14066 [**56**]. This test was carried out at the laboratories of the Department of Environmental Chemistry, Faculty of Chemistry, University of Gdansk, Poland.

3.2.7.3. UV aging

UV accelerated aging test (weathering test) was performed to assess the durability and the performance against UV of the untreated and treated samples with SiO_2-TiO_2 NPs/TEOS. In this sense, a bench UV lamp with the ultraviolet light of 365 nm and 40W BLB Tubes 120 V was used at a distance of 20 cm from the samples according to the recommendation described in **[57]**.

4. Results and discussion

4.1 Characterizations of NPs

X-ray diffraction was used to identify the crystal structure of synthesized nanoparticles. In addition, it is a potential tool for recognizing the specific phase of the synthesized nano-SiO_2 and nano-TiO_2. Nano-TiO_2 peaks were identified at around 25.5° 2θ and 48° 2θ, which confirms the fingerprint of the anatase structure (**Fig. 3.6.6A**). The sharpness of the peaks reveals the good crystalline nature of TiO_2 nano-particles. This TiO_2 anatase structure is matched with JCPDS data (PDF No: 21-1272) [**58**] and the next literature results [**59, 60**]. In this sense, the anatase phase gives the highest photocatalytic activity [**28**]. For the synthesized nano-SiO_2, the diffraction peak appeared strongly at 23° 2θ (**Fig. 3.6.6A**) and this characteristic peak affirms its amorphous nature and matches with Sun et al. [**61**] results.

Furthermore, the synthesized nano-particles had been analyzed under UV-Vis spectroscopy to recognize the characteristic optical properties of nano-SiO_2 and nano-TiO_2. In this sense, pure nano-SiO_2 has light absorption between 200 to 400 nm (**Fig. 3.6.6B**), while SiO_2-TiO_2 NPs showed a serious absorption spectrum of under UV-Vis, with a strong absorbance in the ultraviolet region of 250–375 nm (**Fig. 3.6.6B**). In addition, SiO_2 microspheres were coated by nano-TiO_2 particles with similar light absorption properties to TiO_2 and SiO_2 increased the absorption of TiO_2 in the field of UV light. In this context, this result will take part in the good photocatalytic activity illuminated by UV light of SiO_2–TiO_2 on the treated lime mortars and this result responded well with the results presented in studies of Sun et al. [**62**] and Thongpool et al. [**63**] studies.

The synthesized nanoparticles were examined under the scanning electron microscope. In **Fig. 3.6.7** (**A**), the micrograph shows the whitish nano-spheres of SiO_2, and sphere diameters are around 500 nm sizes and the sizes are relatively close to each other with homogenous distribution of approximately and purity of 99.5%. On the other hand, **Fig. 3.6.7** (**B**) displays the composite of nano-SiO_2 and nano-TiO_2 in gray color and the size is kept approximately the same, but with more coherent features between the particles. The color change came because of nano-SiO_2 decoration by nano-TiO_2. In addition, the little-observed coherence/agglomeration of the particles back to the existence of some small-size of nano-particles after doping [**64**] or it could be due to the insufficient grinding of the composite particles or the poor dispersion effect of the powder in the preliminary experiment [**65**].

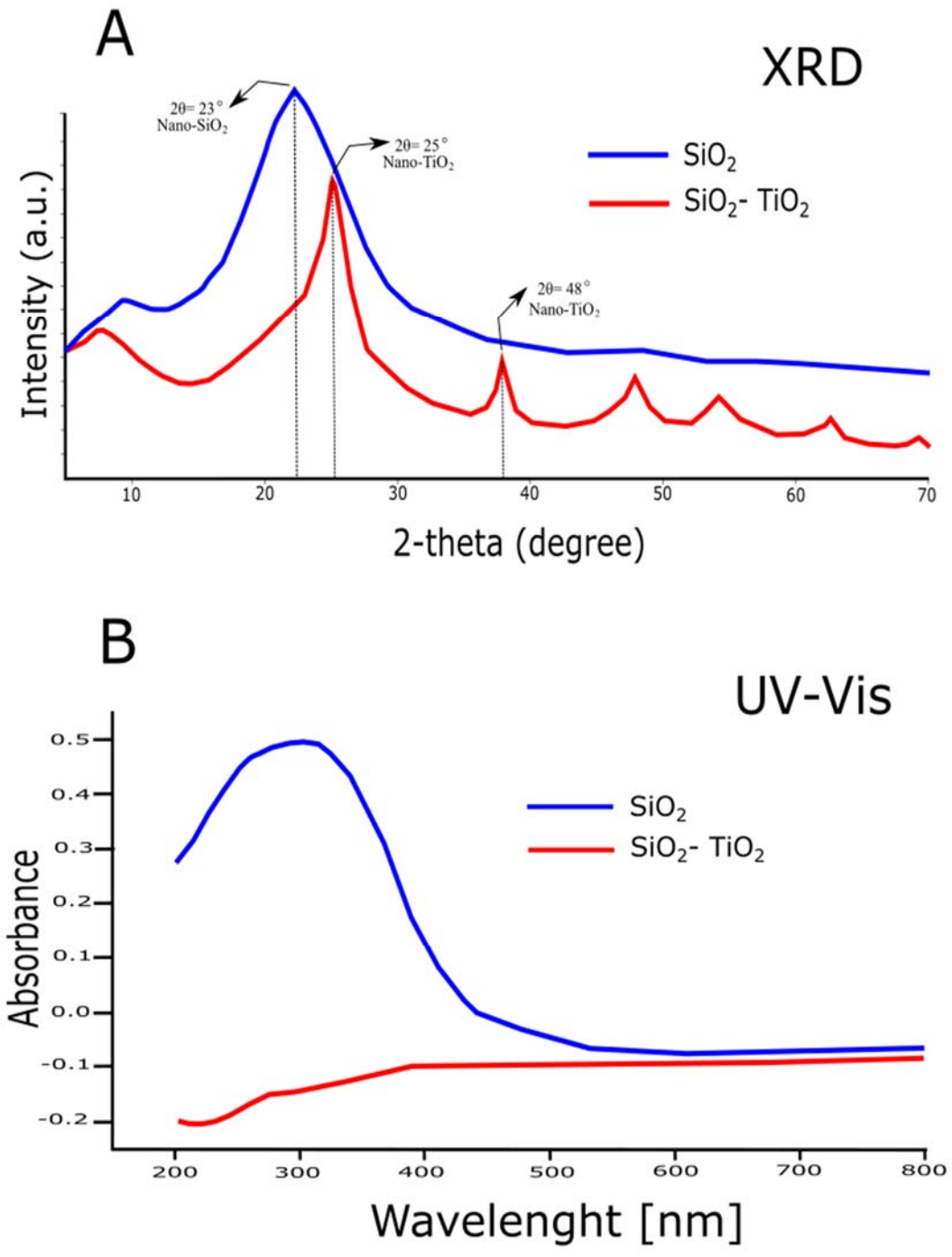


Fig. 3.6.6. (A) XRD patterns of nano-SiO_2 and SiO_2-TiO_2 NPs. (B) UV–Vis diffuse reflectance spectra of nano-SiO_2 and SiO_2-TiO_2NPs.

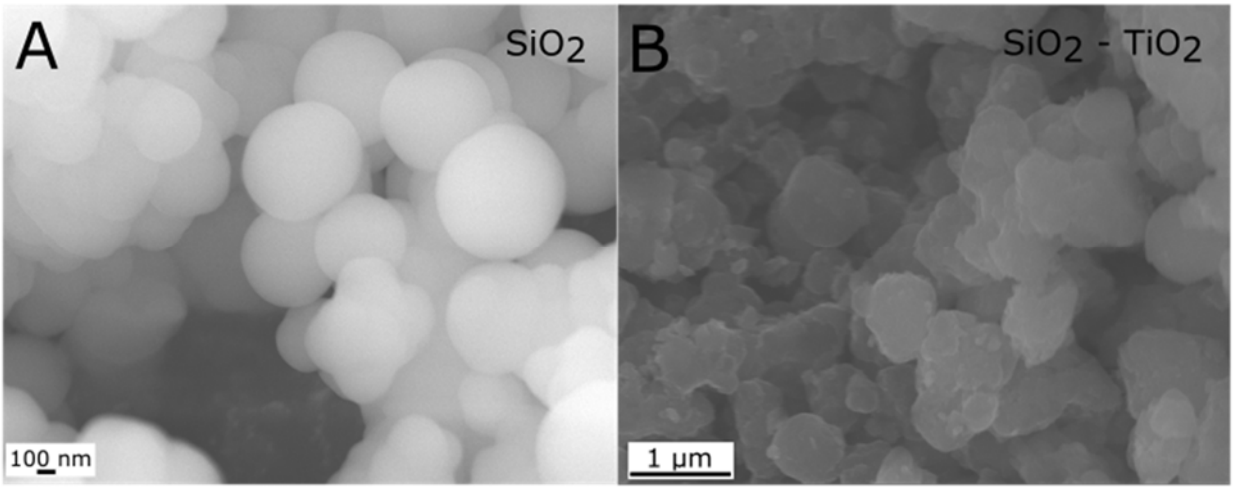


Fig. 3.6.7. Micrograph under SEM for the nano-SiO_2 particles with characteristic spherical shape (A) and SiO_2-TiO_2NPs (B).

Additionally, SEM-EDS was utilized in order to observe the mortar surfaces microstructure deeply. The observations were performed on untreated samples and treated samples with 3%, 5%, and 7% SiO_2-TiO_2 NPs/TEOS. The micrograph of the untreated sample of the lime mortar shows the heterogeneity of the mortar surface with pores and micro-cracks (**Fig. 3.6.8A**). A micrograph of the treated sample with 3% of SiO_2-TiO_2 NPs/TEOS displays the microstructure and textural features of lime mortar surface integrated with consolidation film (**Fig. 3.6.8B**). It is observed that the coating layer fused with the mortar surface aggregates in order to enhance the cohesion between the mortar grains. However, it is noticed that some micro-cracks also appear and it could be due to the consolidated shrinkage. In **Fig. 3.6.8** (**C**), a micrograph of 5% SiO_2-TiO_2 NPs/TEOS on the lime mortar surface was seen in a very homogenous pattern. The amalgamated feature between the consolidated and the mortar is clearly strong. In addition, there are no visible cracks or voids and this indicates high performance of consolidation and cohesion. In **Fig. 3.6.8** (**D**), a micrograph of 7% of SiO_2-TiO_2 NPs/TEOS covers and is combined with the mortar surfaces, which manifests complete coating and binding. Small layers are observed and it could be because of the high concentration of SiO_2-TiO_2 NPs/TEOS consolidate. Furthermore, there are no visible cracks or pores. One can notice very few free nano-SiO_2 that are not combined with nano-TiO_2 and this agrees with the evidence presented by Du et al. [**65**]. Finally, the

elemental chemical analysis was carried out in two different spots for the treated and untreated samples by using the attached unit of EDS. In **Fig. 3.6.8** (**E**), the elemental analysis results of the untreated mortar show that Ca is detected as the dominant element. Additionally, Si and Mg are observed as minors. **Fig. 3.6.8** (**F**) presents the elemental analysis results of the treated mortar with SiO_2-TiO_2 NPs/TEOS and one can identify that elements Si, Ti, and Ca are detected and considered the dominant elements.

4.2. Physical properties

Bulk density, porosity, and water absorption were measured in order to assess the physical behaviors of the casted lime mortars before and after the consolidation of 3%, 5%, and 7% SiO_2-TiO_2 NPs/TEOS. **Fig. 3.6.9** (**A**) shows the values of the porosity and can be noticed the improvement of the surface porosity after the application of the consolidates. In this context, the average values before and after the consolidation with 3%, 5% and 7% SiO_2-TiO_2 NPs/TEOS have been 21.0% – 19.7%, 27.7% – 19.5%, and 23.7% – 21.7%, respectively. **Fig. 3.6.9** (**B**) display the average values of water absorption before and after the consolidation of three concentration of 3%, 5% and 7% SiO_2-TiO_2 NPs/TEOS. The average value of the samples after consolidation with 3% SiO_2-TiO_2 NPs/TEOS is 10% and before consolidation, it was 11%. In addition, the values of the treated samples with 5% SiO_2-TiO_2 NPs/TEOS is 10% and before consolidation, it was 14%. On the other hand, the average value of the samples after consolidation with 7% SiO_2-TiO_2 NPs/TEOS is 11% and before consolidation, it was 12.3%. In this sense, it is observed that the water absorption of the samples has been improved especially with 5% SiO_2-TiO_2 NPs/TEOS. Moreover, the density of the lime mortars sample has been slightly improved after consolidation with a total average of 2 g/cm^3 (**Fig. 3.6.9C**). According to previous studies, the standard average range of traditional lime mortar porosity is between 26.9% and 27.4%. On the other hand, the water absorption average values are between 12.29% and 12.61%, and the average value for the density is 2.6 g/cm^3 [**66**]. Finally, the experimental samples before treatment responded well with the standard values and after the consolidation, the physical properties were improved for porosity, water absorption and density.

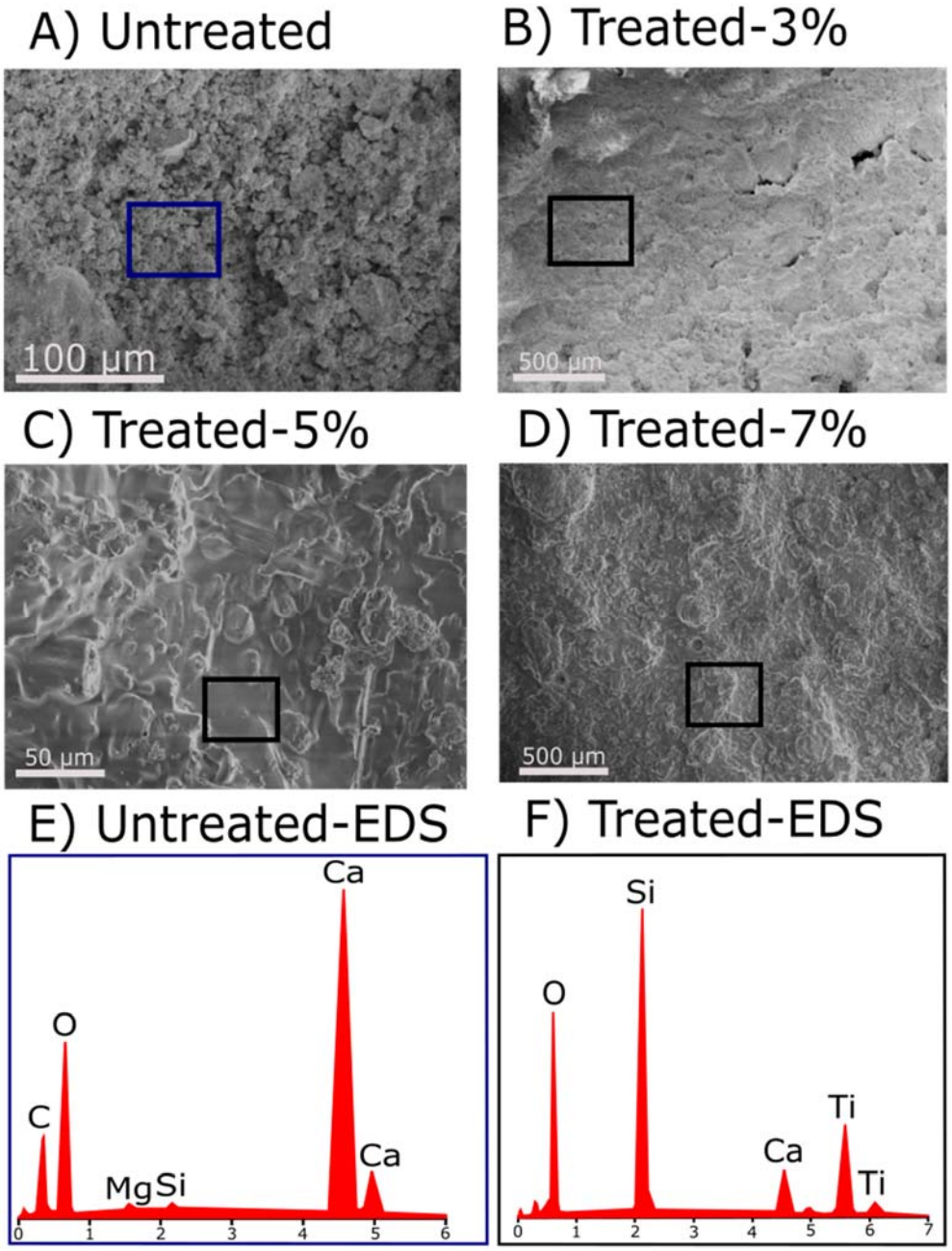


Fig. 3.6.8 (A) Untreated lime mortar sample with inhomogeneous textural details as shown in the blue square. (B) Surface consolidation of the lime mortar by 3% of SiO_2-TiO_2 NPs/TEOS. Black square presents the coating layer of consolidate. (C) Microstructure features of the consolidated surface by 5% of SiO_2-TiO_2 NPs/TEOS. The black square shows the homogenous texture and binding of the surface after consolidation. (D) The surface cohesion after consolidation by 7% of SiO_2-TiO_2 NPs/TEOS as seen in the black square. (E and F) Elemental analysis results by EDS for the treated (mainly Si and Ti) and untreated mortar (mainly Ca) surfaces.

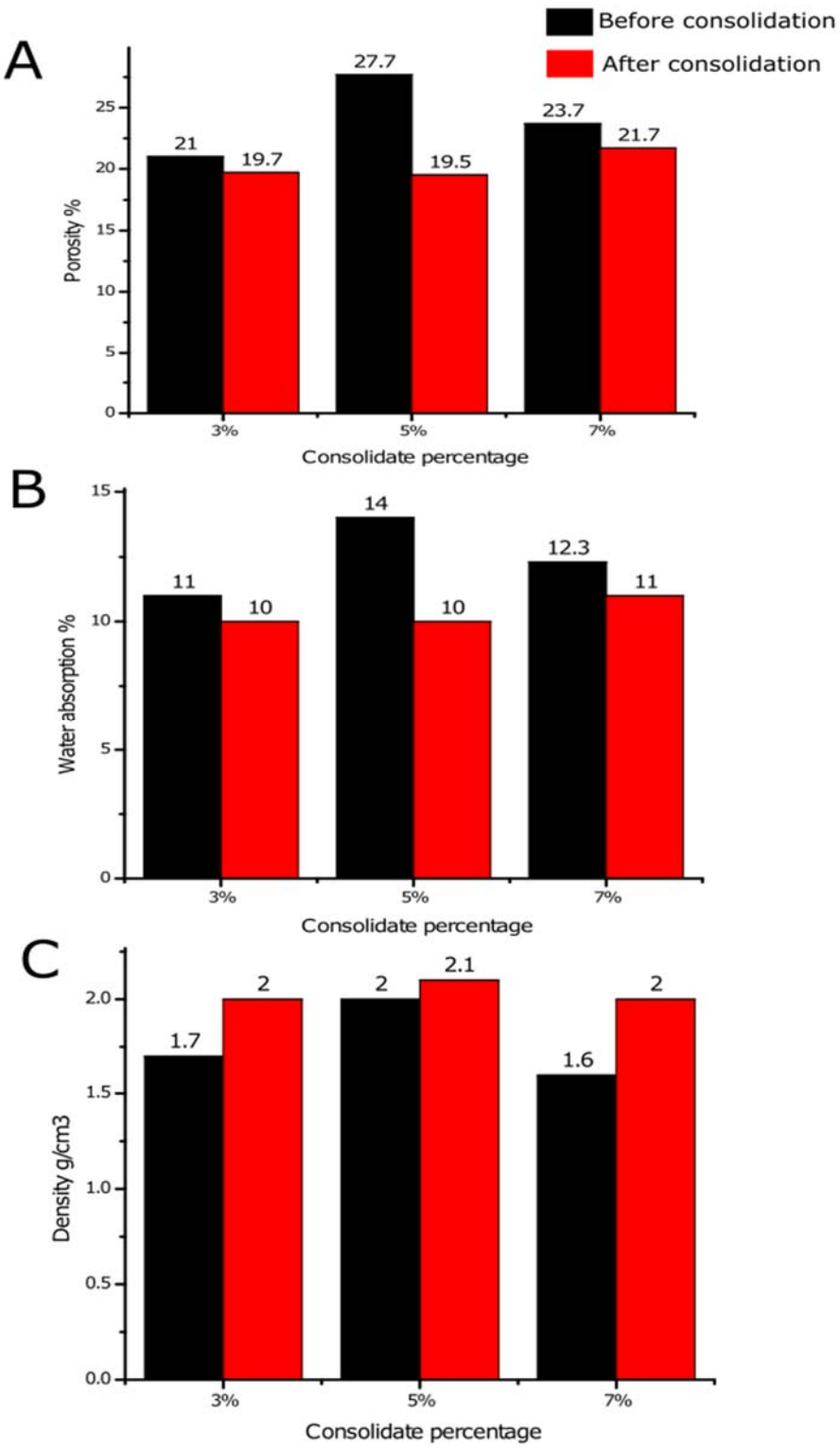


Fig. **3.6.9.** (A-C) Physical properties and average values of experimental lime mortars before and after consolidation (3%, 5% and 7% of SiO_2-TiO_2 NPs/TEOS) for assessment the porosity (A), water absorption (B), and density (C).

4.3. Spectrophotometric measurements

Colorimetric measurements were carried out for both treated and untreated lime mortars in order to guarantee that there are no visible changes in the surface chromatic properties. The untreated sample recorded ΔE* = 2.00, meanwhile, the color changes after treatment were ΔE* = 3.80, 4.32 and 4.08 for samples treated at 3%, 5%, and 7%, respectively (**Table 1**). For restoration and conservation purposes, the consolidation should not allow any visible change the original chromatic properties of the mortar's surfaces. In this sense and for aesthetic reasons, color change parameters for the used consolidate should not present ΔE* > 5, where ΔL*, Δa* and Δb* refer to the difference between the value of each chromatic coordinate in treated samples and untreated ones [**67, 68**]. Based on the obtained results, one can note that all the recorded values for the consolidates of 3%, 5% and 7% SiO_2-TiO_2 NPs/TEOS displayed ΔE* < 5 with no visible changes in color (**Table 3.6.1**). Especially, 3% SiO_2-TiO_2 NPs/TEOS gave the most efficient consolidate which did not present much difference from the original chromatic parameter.

Table 3.6.1. Colorimetric parameters for the lime mortars before and after consolidation at 3%, 5%, and 7% of SiO_2-TiO_2 NPs/TEOS.

Samples	L*	a*	b*	Δ E*
Untreated	79.704	0.004	-0.001	2.00
3%	75.754	1.479	-2.911	3.80
5%	78.369	2.595	-3.398	4.32
7%	77.369	2.028	-3.530	4.08

4.4. Hydrophobic properties

Hydrophobic characterization had been carried out on casted lime mortar to assess the performance of hydrophobic activity after the consolidation. In general, the application of SiO_2-TiO_2 NPs/TEOS on the surface comes up with low surface energy and tension leading to the characteristic property of hydrophobicity. Each nano-material has its own wettability parameter through the measurement of contact angle. In this sense, the contact angle has been divided into three types: 1) hydrophilic surface (CA< 90º), 2) hydrophobic surface (CA>

90º) and 3) super-hydrophobic surface (CA> 150º) [**69**]. The all-treated surfaces with SiO_2-TiO_2 NPs/TEOS showed hydrophobic surfaces. In this context, the contact angles for samples treated at 3% are 124.6º (left) and 124.7º (right), at 5% are 116º (left) and 116.3º (right), and at 7% are 110.6º (left) and 110.6º (right) (**Fig. 3.6.10A**). Accordingly, it is observed that 3% SiO_2-TiO_2 NPs/TEOS gave the highest performance as hydrophobic consolidate. Furthermore, after measurement of the contact angle, the treated surfaces were left for one hour to see the continuity and stability of water drops on the surfaces. It is noticed that the two consolidated concentrations of 3% and 5% SiO_2-TiO_2 NPs/TEOS kept their hydrophobic performance strongly (**Fig. 3.6.10B** and **C**). On the other hand, 7% SiO_2-TiO_2 NPs/TEOS consolidate changed from the hydrophobic phase to the hydrophilic phase (**Fig. 3.6.10B**).

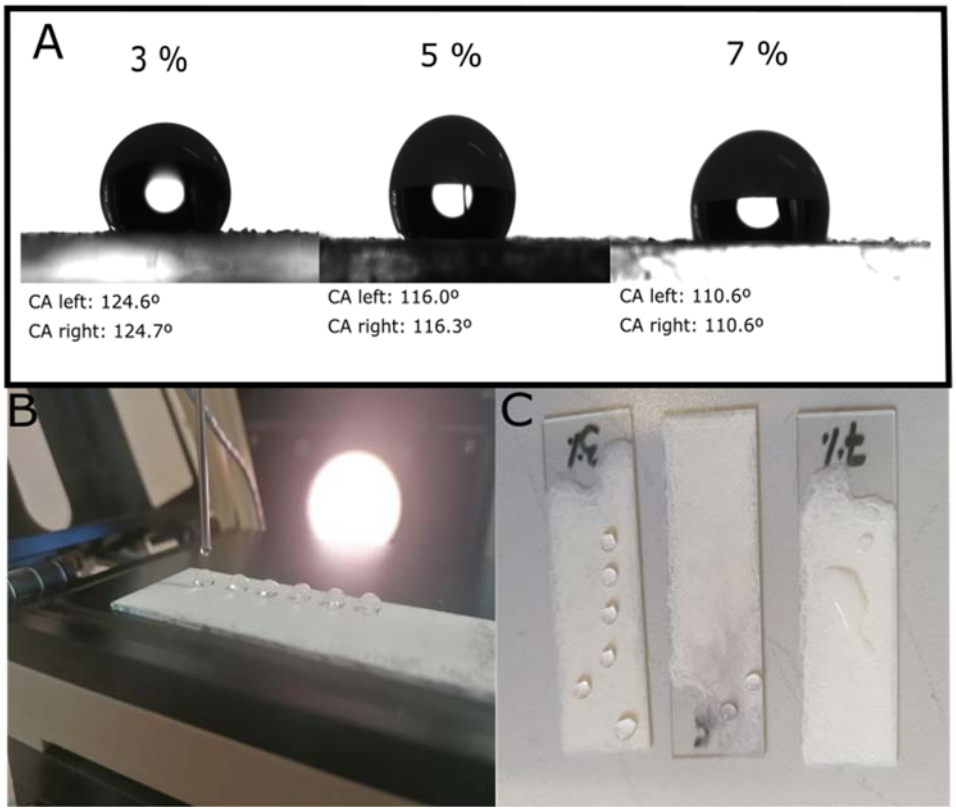


Fig. 3.6.10. (A) Static contact angle values for 3%, 5% and 7% SiO_2-TiO_2 NPs/TEOS over glass slides. (B and C) The monitoring of the consolidates behaviors and changes detection over the surfaces after one hour of droplets releasing. 3% and 5% SiO_2-TiO_2 NPs/TEOS maintained their hydrophobic activity, meanwhile, the 7% SiO_2-TiO_2 NPs/TEOS consolidate and converted into a hydrophilic phase.

4.5 Methylene Blue Test (self-cleaning and Photocatalytic test)

The self-cleaning test was measured using methylene blue (MB) as surface staining and irradiation with UV were applied. In fact, the photocatalytic properties are activated under irradiation with UV light depending on the band gap of the nano-materials [**69**]. The results showed a significant photodegradation behavior for the staining (MB) with all three parentages of 3%, 5%, and 7% SiO_2-TiO_2 NPs/TEOS (**Fig. 3.6.11 A-C**). In order to follow up on the photo degradation rate, colorimetric measurements were carried out. Accordingly, **Table 3.6.2** exhibits the color change ΔE values of each percentage of SiO_2-TiO_2 NPs/TEOS, especially after the application of MB and after each cycle/20 minutes of exposure. The color change (ΔE*) was recorded relying on the standard sample (zero/minutes) which has values of color change: a) ΔE* = 27.2115 for samples 3% SiO_2-TiO_2 NPs/TEOS; b) ΔE* = 30.6092 for samples 5% SiO_2-TiO_2 NPs/TEOS; and c) ΔE* = 29.1772 for samples 7% SiO_2-TiO_2 NPs/TEOS. These values have been changed after the photodegradation activity of SiO_2-TiO_2 NPs/TEOS. In this sense, the ΔE* values of the treated sample after 10 cycles were as follow: a) ΔE* = 7.7633 for samples 3% SiO_2-TiO_2 NPs/TEOS); b) ΔE* = 7.5145 for samples 5% SiO_2-TiO_2 NPs/TEOS; and c) ΔE* = 7.6697 for samples 7% SiO_2-TiO_2 NPs/TEOS. It is observed that the stained treated surfaces were self-cleaned by 3%, 5% and 7% SiO_2-TiO_2 NPs/TEOS effectively because of photocatalytic reaction under UV light.

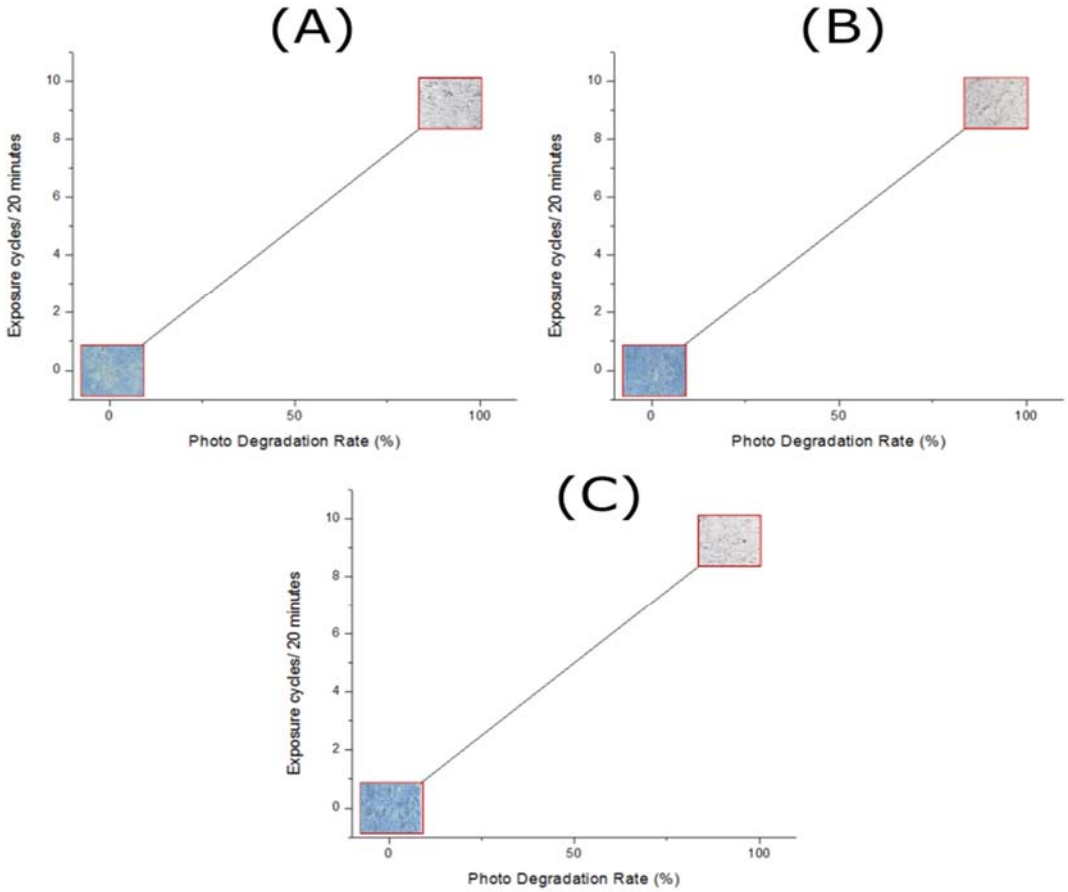


Fig. 3.6.11. Photocatalytic activity of 3% (A), 5% (B), and 7% (C) SiO_2-TiO_2 NPs/TEOS and their efficacy in pollutant degradation.

Table 3.6.2. Color change values ΔE* for 3%, 5% and 7% SiO_2-TiO_2 NPs/TEOS and their chromatic behaviors during the self-cleaning test.

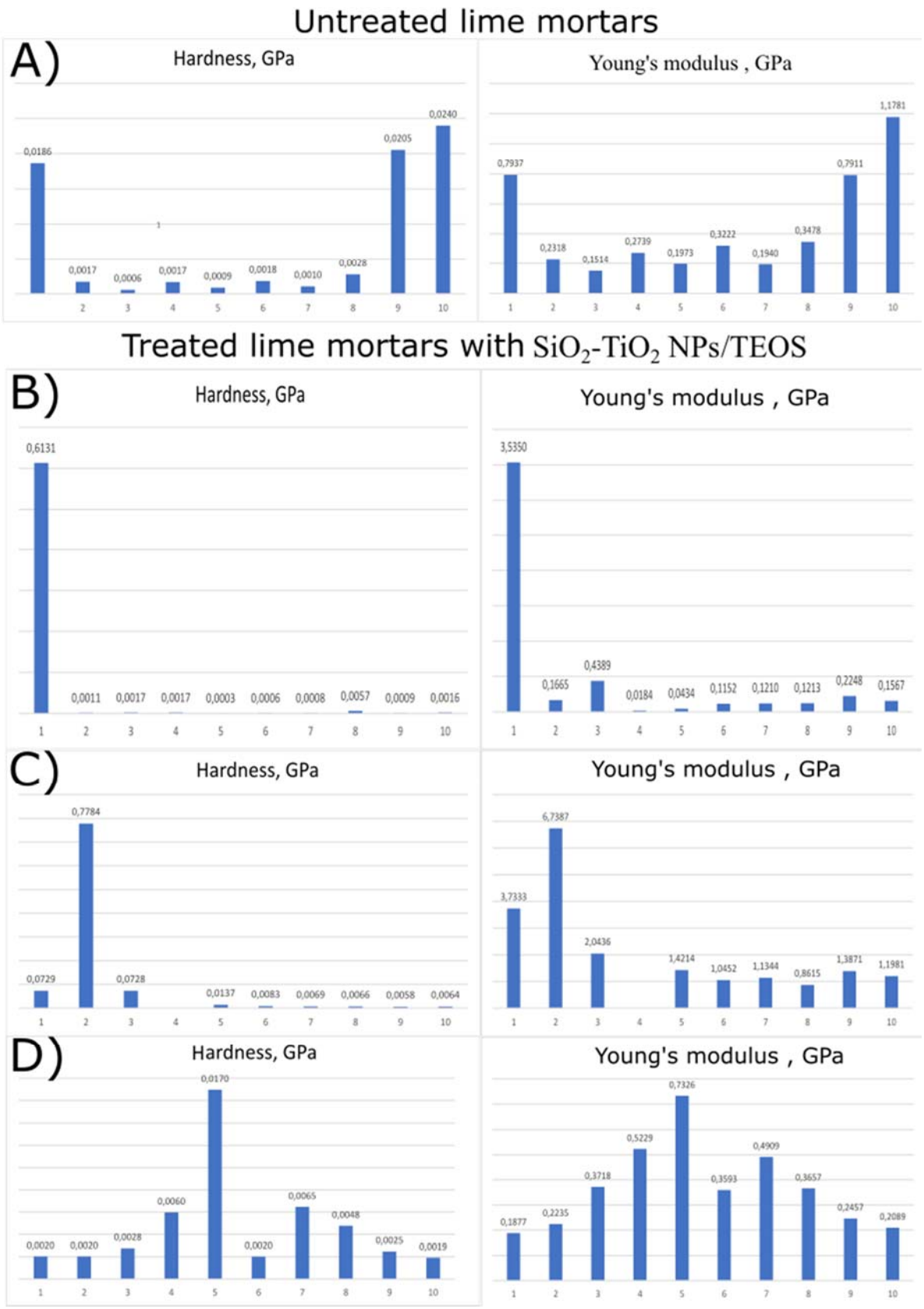
UV cycles / Methylene Blue	Percentage	L*	a*	b*	ΔE*
Zero/mins	3%	58.19	-7.26	-17.16	27.21
	5%	62.32	-2.16	-26.38	30.61
	7%	64.28	-3.89	-25.61	29.18
1-20/mins	3%	64.20	-4.90	-9.96	17.48
	5%	69.65	-5.74	-9.52	13.73
	7%	79.50	-5.77	-9.90	11.9
10-20/mins	3%	83.40	1.87	-4.95	7.76
	5%	74.25	4.87	-4.57	7.52
	7%	77.67	7.03	-6.53	7.67

4.6 Mechanical tests

4.6.1 Nano-indentation test

Fig. 3.6.12 shows the distribution of the results of nano-indentation hardness (H) and Young's modulus (E_s) for the untreated lime mortars (A) and treated lime mortars with SiO_2-TiO_2/TEOS NPs with concentration 3% (B), 5% (C), and 7% (D). Considering hardness results, one can notice that the untreated sample and 7% SiO_2-TiO_2 NPs/TEOS sample have fewer differential results with respect to the hardness distribution of 3% and 5% SiO_2-TiO_2 NPs/TEOS samples. The maximum hardness value of the untreated surface is 0.0240 GPa and the maximum value of E_s for the untreated surface is 1.1781 GPa (**Fig. 3.6.12A**). Moreover, the maximum hardness values for the treated surfaces with 3%, 5% and 7% SiO_2-TiO_2 NPs/TEOS are 0.6131 GPa, 0.7784 GPa and 0.0170 GPa, respectively (**Fig. 3.6.12B-D**).On the other hand, the results of Young's modulus of 3% SiO_2-TiO_2 NPs/TEOS present more differential results in comparison with untreated samples and 5% and 7% SiO_2-TiO_2 NPs/TEOS samples, where the maximum recorded values of E_s for the treated surfaces with 3%, 5% and 7% SiO_2-TiO_2 NPs/TEOS are 3.5350 GPa, 6.7387 GPa and 0.7326 GPa, respectively (**Fig. 3.6.12B-D**). Accordingly, it is noticed that the consolidates with 3% and 5% SiO_2-TiO_2 NPs/TEOS proved their efficacy in the improvement of mechanical properties of the treated lime mortar surfaces compared to the untreated surfaces.

Fig.3.6.12. *(In next page)* Distribution results of nano-indentation Hardness and Young Modulus for the untreated lime mortars (A) and treated lime mortars with SiO_2-TiO_2 NPs /TEOS with concentration 3% (B), 5% (C), and 7% (D).


Untreated lime mortars
A)
Hardness, GPa
0,0186
0,0017
0,0006
0,0017
0,0009
0,0018
0,0010
0,0028
0,0205
0,0240
Young's modulus , GPa
0,7937
0,2318
0,1514
0,2739
0,1973
0,3222
0,1940
0,3478
0,7911
1,1781
Treated lime mortars with SiO2-TiO2 NPs/TEOS
B)
Hardness, GPa
0,6131
0,0011
0,0017
0,0017
0,0003
0,0006
0,0008
0,0057
0,0009
0,0016
Young's modulus , GPa
3,5350
0,1665
0,4389
0,0184
0,0434
0,1152
0,1210
0,1213
0,2248
0,1567
C)
Hardness, GPa
0,0729
0,7784
0,0728
0,0137
0,0083
0,0069
0,0066
0,0058
0,0064
Young's modulus , GPa
3,7333
6,7387
2,0436
1,4214
1,0452
1,1344
0,8615
1,3871
1,1981
D)
Hardness, GPa
0,0020
0,0020
0,0028
0,0060
0,0170
0,0020
0,0065
0,0048
0,0025
0,0019
Young's modulus , GPa
0,1877
0,2235
0,3718
0,5229
0,7326
0,3593
0,4909
0,3657
0,2457
0,2089

4.6.2 Uniaxial compressive strength (UCS)

The static compressive test was conducted to define the compressive strength (Rc) of three untreated samples and three 3%, 5%, and 7% one-side treated samples. The average compressive strength of tested untreated samples equals 2.376 MPa (**Table 3.6.3**). On the other hand, the values of UCS for the treated surfaces with 3%, 5%, and 7% SiO_2-TiO_2 NPs /TEOS are 2. 2.310MPa, 2.829MPa, and 5.292MPa, respectively (**Table 3.6.3**). On the base of these results, one can deduce that the consolidates of 5% and 7% SiO_2-TiO_2/TEOS NPs achieved the enhancement of mechanical properties of lime mortars compared to the untreated samples. According to Sneff et al. [**70**], the compressive strength of mortars by adding SiO_2-TiO_2 NPs can be improved by adding nanoparticles with superior fineness and chemical nature.

Table 3.6.3. Average values for untreated lime mortars and for the treated lime mortars with 3%, 5%, and 7% SiO_2-TiO_2 NPs /TEOS under uniaxial compressive strength (Rc, in MPa).

Samples	Rc
Untreated	2.376
3%	2.310
5%	2.829
7%	5.292

4.7. Durability assessment

4.7.1. Salt crystallization test

For the salt weathering test, additional microscopic examinations using a scanning electron microscope were used to detect any changes in the morphological features of the untreated and treated surfaces with 3%, 5%, and 7% SiO_2-TiO_2 NPs/TEOS after salt crystallization. **Fig. 3.6.13** (**A**) presents the textural features of the untreated lime mortar surface after exposure to NaCl salt for 15 cycles. The surfaces showed insufficient resistance to salt attack. For this, the face side of the untreated sample displays the dendritic efflorescence of NaCl that was used in salt weathering/aging. On the other hand, **Fig. 3.6.13** (**B-D**) exhibits the microstructural aspects of the treated samples after salt artificial aging. In addition, the salt resistance test was carried out to assess the mass loss, especially for the treated

samples (**Table 3.6.4**). The consolidate of 3%, 5% and 7% SiO_2-TiO_2 NPs/TEOS showed total loss of 5.7%, 5.1% and 5.2%, respectively. On the other hand, the untreated sample showed a total loss of 6% due to salt crystallization. In fact, 3% and 5% 7% SiO_2-TiO_2 NPs proved their slight efficacy and durability against the salt attack and its nucleation compared to the untreated sample, but some pores and slight salt growth were detected (**Fig. 3.6.13B** and **C**). The consolidate of 7% SiO_2-TiO_2 NPs / TEOS (**Fig. 3.6.13D**) is affected by salt nucleation in some parts. In this regard, Spathis et al. [**70**] mentioned that the addition of TiO_2 in the surface protection could resist the salt attack and increase the hydrophobicity of the surfaces with various rates depending on the TiO_2 amount and surface nature.

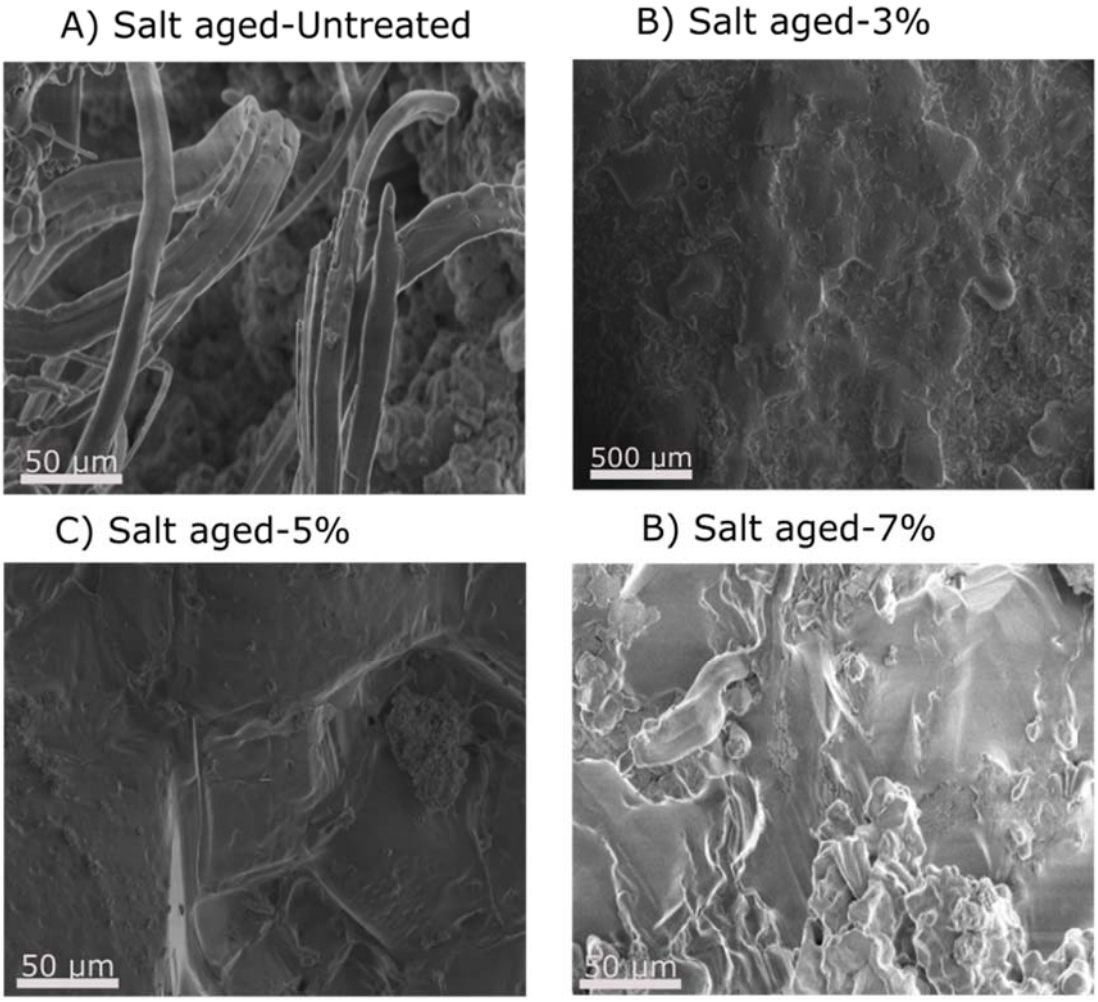


Fig. 3.6.13. Micrographs of the untreated (A) and treated surfaces after salt weathering (B-D).

Table 3.6.4. Measurement of the salt resistance (mass loss) of the treated samples. Legends: (M_0, in g) mass of the dried samples in grams, (M_n, in g) mass of the dried specimen after exposure cycles and (ΔM, in %) percentage of mass loss.

Sample	M_0	M_n	ΔM
Untreated	131	123.2	6
3%	110.7	104.5	5.7
5%	116.2	110.2	5.1
7%	125.6	119	5.2

4.7.2 Thermal aging

For efficacy assessment purposes, the treated samples were subjected to many cycles of temperature variations and after the final cycle were evaluated by using the scanning electron microscope. The results showed that the treated sample with 3% SiO_2-TiO_2 NPs/TEOS gave high resistance and there were no observed changes in the microstructures of the treated surface (**Fig. 3.6.14A**). In **Fig. 3.6.14** (**B**), the textural features of treated surfaces with 5% SiO_2-TiO_2 NPs/TEOS showed moderate durability against fluctuations of temperatures. For this, cracks and flaking are observed as the decay form on the treated surface. On the other hand, **Fig. 3.6.14** (**C**) showed the lowest resistance of 7% SiO_2-TiO_2 NPs/TEOS, where flaked and blistered surfaces were detected. In this regard, the moderate and low durability behavior against thermal aging for the consolidates of 5% and 7% SiO_2-TiO_2 NPs/TEOS is due to the potential difference in the coefficient of thermal expansion, especially with the existence of nano-TiO_2 which could cause variations in the coefficient of thermal expansion and lead to internal stresses and decays [**71**]. The consolidation with 3% SiO_2-TiO_2 NPs/TEOS proved its efficacy against thermal because of the harmonious combination of SiO_2-TiO_2 and low amount of nano-TiO_2.

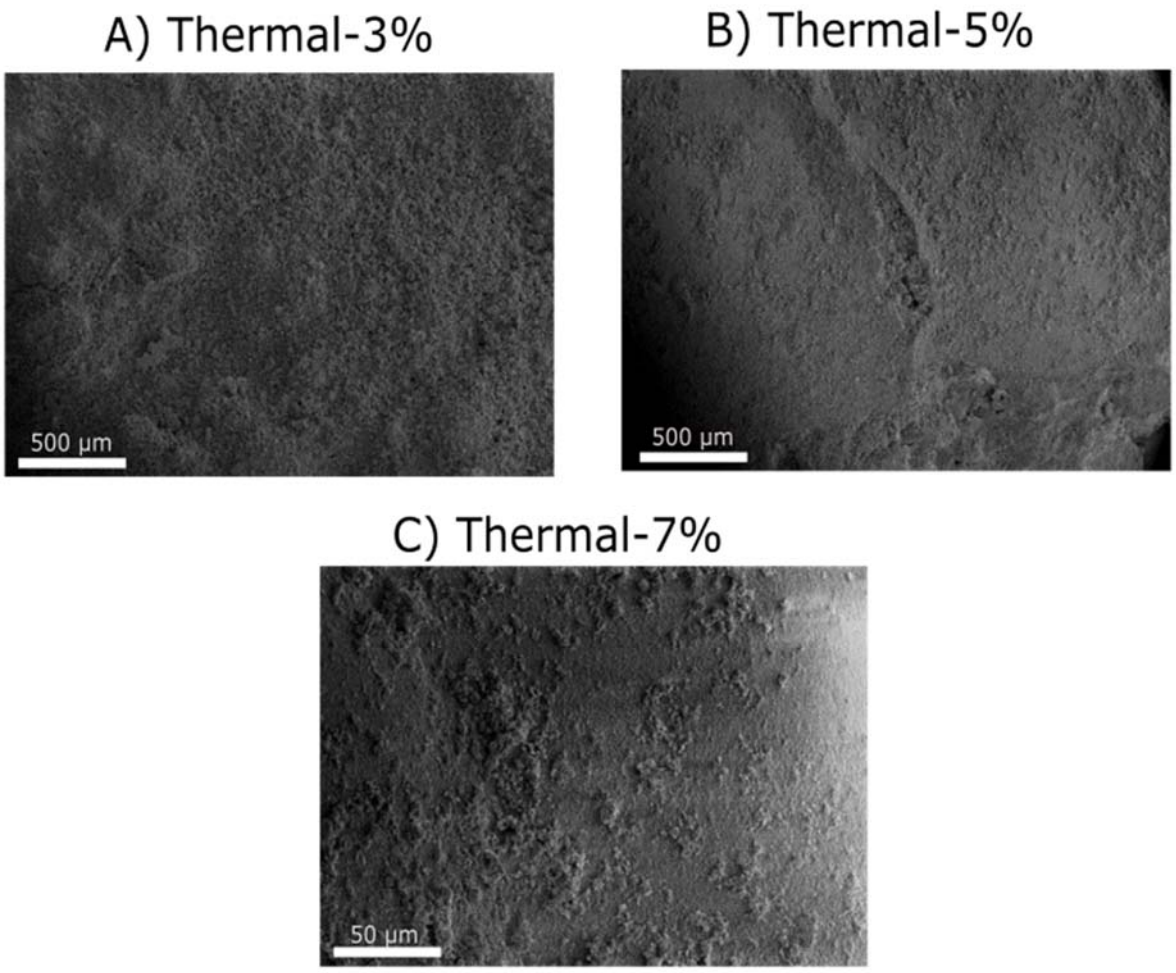


Fig. 3.6.14. (A) Micrograph of the treated surface with 3% SiO_2-TiO_2 NPs/TEOS after thermal aging without change detection. (B) Micrograph of the treated surface with 5% SiO_2-TiO_2 NPs/TEOS after thermal aging with moderate durability. (C) Micrograph of the treated surface with 7% SiO_2-TiO_2 NPs/TEOS after thermal aging with low resistance and noticed changes in the surface.

4.7.3. UV aging

Ultraviolet light of 365 nm was used in order to check out the resilience behavior of the treated and untreated surfaces against UV. After exposure, micrographs of each tested surface were taken by using the scanning electron microscope. **Fig. 3.6.15A** presents the morphological aspects of the untreated surface of lime mortar. Pores and micro-cracks were detected which could be because of the thermal part of the UV impact. **Figure 3.6.15** (**B** and

C) displays the treated surface with 3% and 5% SiO_2-TiO_2 NPs/TEOS after UV aging. The micrographs showed good resistance of the consolidates against UV aging without any observed changes in the textural features of the mortar surfaces. On the other hand, **Fig. 3.6.15** (**D**) exhibits insufficient durability behavior against UV aging because some pores and micro-cracks were observed.

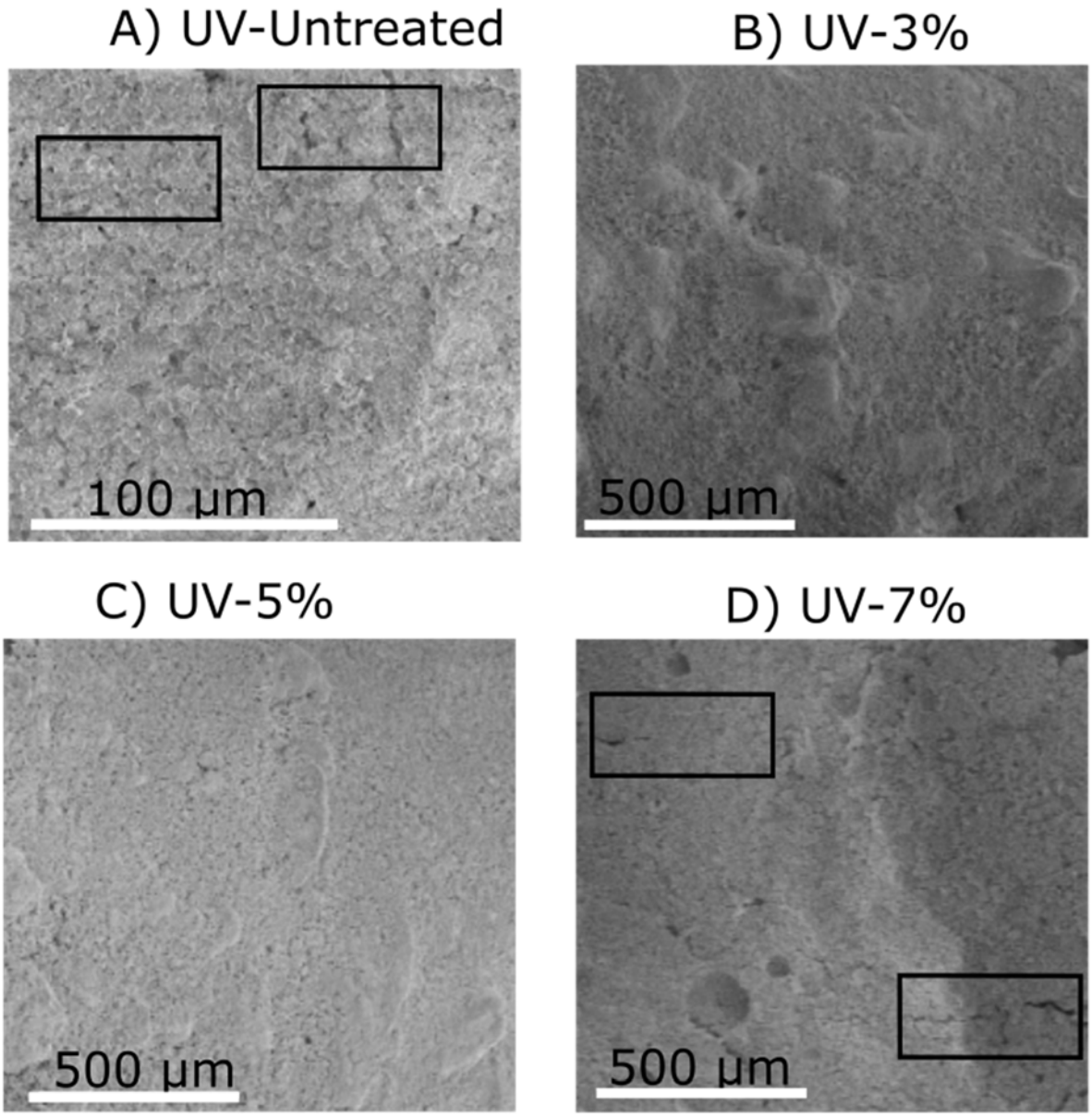


Fig. 3.6.15. Micrographs for the untreated (A) and treated lime mortar surfaces with 3% (B), 5% (C), and 7% (D) SiO_2-TiO_2 NPs /TEOS after UV aging. (A and D) Pores and micro-cracks were observed (black rectangles), which (B and C) no changes were detected.

5. Conclusions

In this current study, three different concentrations of SiO_2-TiO_2 NPs/TEOS consolidate were evaluated physically and mechanically on experimental lime mortar surfaces in order to achieve multifunctional surface consolidation. The comparison between the treated and untreated surfaces was applied through the paper using various tests and techniques.

Untreated lime mortar was characterized as porous surfaces and micro-cracks were observed micro-structurally. Physically, the untreated lime mortars were assessed to have high porosity (23.8%) and high-water absorption (12.5%) which could affect the durability of the lime mortar. Mechanically, the untreated lime mortars proved their low strength with very low hardness and young's modulus. In addition, salt aging and UV aging affected the untreated samples where salt nucleation was noticed along with pores and cracks because of thermal stresses from UV.

Accordingly, 3%, 5%, and 7% SiO_2-TiO_2 NPs/TEOS were synthesized and prepared to consolidate the lime mortar surfaces. 3% and 5% SiO_2-TiO_2 NPs/TEOS proved their high efficacy in improving the physical and mechanical properties of the lime mortar surfaces. Micrographs under SEM showed very good and harmonious coating for surfaces consolidation as follows:

1. Physically, these consolidates enhanced the petrophysical properties, especially by decreasing the values of porosity and water absorption by around 20% to 20.3% and 10.6% instead of 23.8% and 12.5%, respectively.
2. Mechanically, 3% and 5% SiO_2-TiO_2 NPs /TEOS strengthen the mechanical properties of lime mortar surfaces by more than 40% approximately. In this regard, the hardness of 3% and 5% SiO_2-TiO_2 NPs/TEOS increased by 0.6131(GPa) and 0.7784 (GPa) instead of 0.0240 (GPa) for the untreated sample. The young's modulus increased by more than 40% for 3% SiO_2-TiO_2 NPs/TEOS and more than 60% for 5% SiO_2-TiO_2 NPs/TEOS.
3. Both concentrations 3% and 5% did not show clearly visible color changes after consolidation and values are in the permitted standard for conservation purposes $\Delta E^* < 5$.

4. Both consolidates of 3% and 5% showed a good hydrophobic properties and self-cleaning where the methylene blue was removed by more than 60% during 3 hours of UV exposure.
5. the durability resistance tests exhibited sufficient resilience of 3% and 5% SiO_2-TiO_2 NPs/TEOS to salt, thermal and UV aging, where there were no detected changes in the microstructure of the surfaces, except for very slight nucleation of salt for 5% SiO_2-TiO_2 NPs/TEOS.

On the other hand, 7% SiO_2-TiO_2 NPs/TEOS displayed inefficient performance under many techniques of evaluation physically and mechanically. It showed low mechanical efficacy for the lime mortar surfaces, especially in hardness and Young's modulus of the surface. In addition, 7% SiO_2-TiO_2 NPs/TEOS presented hydrophilic performance with low surface tension CA<90º. The weathering tests proved the low resilience of this percentage after artificial weathering with salt, thermal, and UV. Many textural features were changed such as appearing pores, cracks, and nucleation of salt crystals on the mortar surface.

Finally, this study recommends using 3% and 5% SiO_2-TiO_2 NPs/TEOS consolidates in the protection of lime mortar using monolayer application in out and indoor lime mortar or plasters. Future studies for assessment of triple-doped nano-materials to see their efficacy in increasing the mechanical and physical properties of the lime mortar.

Aknowledegement

A. Fahmy acknowledges UGEA-PHAM at University of Cadiz for carrying out the main part of the archaeometrical analysis. XRD, mXRF and SEM-EDX analysis were carrying in the SCICYT of the University of Cadiz. E. Molina Piernas acknowledges co-funding from the European Social Fund (D1113102E3) and Junta de Andalucía. We would like to thank Anna Gołąbiewska, Wiktoria Wojnicz, Alicja Stanisławska, Jakub Kowalski, Justyna Łuczak, Adriana Zaleska-Medynska from Department of Environmental Technology, Faculty of Chemistry, University of Gdansk, Faculty of Mechanical Engineering and Ship Technology and Department of Process Engineering and Chemical Technology, Faculty of Chemistry, Gdansk University of Technology, Gdansk, Poland for their contributions.

6. References

[1] Daniele V, Rosatelli G, Macera L, Taglieri G. New aqueous nanolime formulations for fully compatible consolidation treatments of historical mortars for hypogeum environment. *Construction and Building Materials*. 2022 ;*356*, 129316. https://doi.org/https://doi.org/10.1016/j.conbuildmat.2022.129316

[2] Ergenç D, Sierra-Fernandez A, Barbero-Barrera M, Gomez-Villalba L S, Fort R. *Assessment on the performances of air lime-ceramic mortars with nano-Ca (OH)$_2$ and nano-SiO $_2$ additions*. 2020; *232*. https://doi.org/10.1016/j.conbuildmat.2019.117163

[3] Al-Rifaie W N, Ahmed W K. Effect of nanomaterials in cement mortar characteristics. 2016; *11*(9), 1321–1332. Available from: https://jestec.taylors.edu.my/Vol%2011%20issue%209%20September%202016/11_9_8.pdf

[4] Senff L, Hotza D, Repette W L, Ferreira V M, Labrincha J A. Mortars with nano-SiO_2 and micro-SiO_2 investigated by experimental design. *Construction and Building Materials*. 2010; *24*(8),1432–1437. https://doi.org/https://doi.org/10.1016/j.conbuildmat.2010.01.012

[5] Calia A, Masieri M, Baldi G. *The evaluation of nanosilica performance for consolidation*. *October*. 12th International Congress on the Deterioration and Conservation of Stone Columbia University, New York. 2012. Available from: https://www.researchgate.net/publication/270898434_THE_EVALUATION_OF_NANOSILICA_PERFORMANCE_FOR_CONSOLIDATION_TREATMENT_OF_AN_HIGHLY_POROUS_CALCARENITE

[6] Ferri L De, Paolo P, Lorenzi A, Montenero A, Salvioli-Mariani E. *Study of silica nanoparticles – polysiloxane hydrophobic treatments for stone-based monument protection*. 2011; *12*, 356–363. https://doi.org/10.1016/j.culher.2011.02.006

[7] Al-Dosari M A, Darwish S, El-Hafez M A, Elmarzugi N, Mansour S. *Effects of Adding Nanosilica on Performance of Ethylsilicat (TEOS) as Consolidation and Protection Materials for Highly Porous Artistic Stone*. 2016; *6*, 192–204. https://doi.org/10.17265/2161-6213/2016.7-8.002

[8] Diaz J, Ševčík R, Mácová P, Menéndez B, Frankeová D, Slížková Z. Impact of nanosilica on lime restoration mortars properties. *Journal of Cultural Heritage*, 2022; *55*, 210–220. https://doi.org/https://doi.org/10.1016/j.culher.2022.03.014

[9] Zhang X, Wen W, Yu H, Qiu F, Chen Q, Yang D. Preparation, characterization of nano-silica/fluoroacrylate material and the application in stone surface conservation. *Journal of Polymer Research*. 2016; *23*(4), 75. https://doi.org/10.1007/s10965-016-0967-8

[10] Zhang X, Gao J, Fan H, Li X, Gao Z, Xue L, Sun S. Study on the Mechanism of Nano-SiO_2 for Improving the Properties of Cement-Based Soil Stabilizer. Nanomaterials (Basel). 2020; 25; 10(3):405. DOI: 10.3390/nano10030405. PMID: 32106519; PMCID: PMC7152852.

[11] Stucchi N M E, Tesser E, Antonelli F, Benedetti A. *Synthesis and characterization of nanosilica products for the consolidation of stones.* 2019; 299–304. IMEKO TC-4 International Conference on Metrology for Archaeology and Cultural Heritage Florence, Italy. Available from: https://www.imeko.org/publications/tc4-Archaeo-2019/IMEKO-TC4-METROARCHAEO-2019-55.pdf

[12] La Russa M F, Ruffolo S A, Rovella N, Belfiore C M, Palermo A M, Guzzi M T, Crisci G M. Multifunctional TiO_2 coatings for Cultural Heritage. *Progress in Organic Coatings*. 2012; *74*(1), 186–191. https://doi.org/https://doi.org/10.1016/j.porgcoat.2011.12.008

[13] Zhang X, Lin G, Ma S, Liu M, Jiang W, Wu C. Efficiency and durability of carbon dots grafted TiO_2-based coatings applied on concrete under peeling and washing trials. *Diamond and Related Materials*. 2022 ;*129*, 109333. https://doi.org/https://doi.org/10.1016/j.diamond.2022.109333

[14] Shibata T, Sakai N, Fukuda K, Ebina Y, Sasaki T. Photocatalytic properties of titania nanostructured films fabricated from Titania nanosheets. *Physical Chemistry Chemical Physics: PCCP*. 2007;*9*(19), 2413–2420. https://doi.org/10.1039/b618448k

[15] Ferrari A M, Pini M, Neri P, Bondioli F. *Nano-TiO_2 Coatings for Limestone: Which Sustainability for Cultural Heritage?.* 2015; 232–245. https://doi.org/10.3390/coatings5030232

[16] Quagliarinia E, Bondioli F,Goffredo GE, Licciulli A, Munafò P. *photo-induced hydrophilicity of TiO 2 coatings on stone surfaces*. 2012;2–8. https://doi.org/10.1016/j.culher.2012.02.006

[17] Franzoni E, Fregni A, Gabrielli R, Graziani G, Sassoni E. Compatibility of photocatalytic TiO_2-based finishing for renders in architectural restoration: a preliminary study, Building and Environment. 2014; 80, 125-135, DOI: 10.1016/j.buildenv.2014.05.027.

[18] Saeli M, Tobaldi D M, Rozman N, Sever A, Labrincha J A, Pullar R C. *Photocatalytic nano-composite architectural lime mortar for degradation of urban pollutants under solar and visible (interior) light*. 2017; *152*, 206–213. https://doi.org/10.1016/j.conbuildmat.2017.06.167

[19] Kim D, Noh W, Jo S, Lee T S. Electrospun mesoporous silica nanofibers decorated with titanium dioxide nanoparticles for a repeatable photocatalysis. *Molecular Crystals and Liquid Crystals*. 2021; *730*(1), 85–100. https://doi.org/10.1080/15421406.2021.1956761

[20] Munafò P, Goffredo G B, Quagliarini E. TiO_2-based nanocoatings for preserving architectural stone surfaces: An overview. *Construction and Building Materials*. 2015;*84*, 201–218. https://doi.org/https://doi.org/10.1016/j.conbuildmat.2015.02.083

[21] Kroftová K, Šmidtová M, Kuřitka I. *Nanotechnology in the cultural heritage - influence of nanospensions adopted by nanoparticles of TiO_2 for cleaning the surface*. 2017; *19*, 216–221. https://doi.org/10.14311/CEJ.2017.03.0019

[22] Quagliarini E, Graziani L, Diso D, Licciulli A, &D'Orazio M. Is nano-TiO_2 alone an effective strategy for the maintenance of stones in Cultural Heritage? *Journal of Cultural Heritage*. 2018;*30*, 81–91. https://doi.org/https://doi.org/10.1016/j.culher.2017.09.016

[23] Wang X, Ding H, Sun S, Zhang H, Zhou R, Li Y, Liang Y, Wang J. Preparation of a temperature-sensitive superhydrophobic self-cleaning SiO2-TiO2@PDMS coating with photocatalytic activity. *Surface and Coatings Technology*. 2021; *408*, 126853. https://doi.org/10.1016/j.surfcoat.2021.126853

[24] Adachi T, Latthe S S, Gosavi S W, Roy N, Suzuki N, Ikari H, Kato K, Katsumata K, Nakata K, Furudate M. Applied Surface Science weight, flexible polycarbonate substrates. *Applied Surface Science*. 2018; *458*(July), 917–923. https://doi.org/10.1016/j.apsusc.2018.07.172

[25] Pinho L, Elhaddad F, Facio D S, Mosquera M J. A novel TiO_2-SiO_2 nanocomposite converts a very friable stone into a self-cleaning building material. Applied Surface Science. 2013;275, 389-396. https://doi.org/10.1016/j.apsusc.2012.10.142

[26] Pinho L, Mosquera M J.Titania-Silica Nanocomposite Photocatalysts with Application in Stone Self-Cleaning. *J. Phys. Chem. C*. 2011; *115*, 22851–22862. https://doi.org/10.1021/jp2074623

[27] Zu G, Shen J, Wang W, Zou L, Lian Y, Zhang Z. Silica–Titania Composite Aerogel Photocatalysts by Chemical Liquid Deposition of Titania onto Nanoporous Silica Scaffolds. ACS Publications. Collection. 2016. https://doi.org/10.1021/am5089132

[28] Kim D, Noh W, Jo S, Lee T S. Electrospun mesoporous silica nanofibers decorated with titanium dioxide nanoparticles for a repeatable photocatalysis. *Molecular Crystals and Liquid Crystals*. 2021; *730*(1), 85–100. https://doi.org/10.1080/15421406.2021.1956761

[29] Gemelli G M C, Luna M, Zarzuela R, Gil Montero M L A, Carbú M, Moreno-Garrido I, Mosquera, M J. 4-Year in-situ assessment of a photocatalytic TiO_2/SiO_2 antifouling treatment for historic mortar in a coastal city. *Building and Environment*. 2022;*225*, 109627. https://doi.org/https://doi.org/10.1016/j.buildenv.2022.109627

[30] Senff L, Tobaldi D M, Lucas S, Hotza D, Ferreira V M, Labrincha J A. *Composites: Part B of pollutants in buildings*. 2013; *44*, 40–47.

[31] Hees P R P J, Van Binda L, Papayianni I, Toumbakari E. *Characterisation and damage analysis of old mortars*. 2004;*37* (November), 644–648. https://doi.org/10.1007/BF02483293

[32] Fahmy A, Molina-Piernas E, Martínez-López J, Machev P, Domínguez-Bella S. (). Coastal Environment Impact on the Construction Materials of Anfushi's Necropolis (Pharos's Island) in Alexandria, Egypt. In *Minerals.* 2022; 12, Issue 10. https://doi.org/10.3390/min12101235

[33] Fusade L, Orr S A, Wood C, O'Dowd M, Viles H. Drying response of lime-mortar joints in granite masonry after an intense rainfall and after repointing. *Heritage Science*. 2019;*7*(1), 38. https://doi.org/10.1186/s40494-019-0277-7

[34] Martínez-Ramírez S, Puertas F, Blanco-Varela M T, Thompson G E. Studies on degradation of lime mortars in atmospheric simulation chambers. *Cement and Concrete*

Research. 1997; *27*(5), 777–784. https://doi.org/https://doi.org/10.1016/S0008-8846(97)00065-3

[35] Zacharopoulou G. *The renascence of lime based mortar technology. An appraisal of a bibliographic study.* 2015. Available from: https://www.researchgate.net/publication/265591139_The_renascence_of_lime_based_mortar_technology_An_appraisal_of_a_bibliographic_study

[36] La Russa M F, Ruffolo S A. Mortars and plasters - How to characterize mortar and plaster degradation. *Archaeological and Anthropological Sciences*. 2021 ;*13*(10), 165. https://doi.org/10.1007/s12520-021-01405-1

[37] Fahmy A, Molina-Piernas E, Domínguez-Bella S, Martínez-López J, Helmi F. Geoenvironmental investigation of Sahure's pyramid, Abusir archeological site, Giza, Egypt. *Heritage Science*. 2022; *10*(1), 61. https://doi.org/10.1186/s40494-022-00699-1

[38] Fahmy A, Molina-Piernas E, Martínez-López J, Domínguez-Bella S. Salt weathering impact on Nero/Ramses II Temple at El-Ashmonein archaeological site (Hermopolis Magna), Egypt. *Heritage Science*, 2022; *10*(1), 125. https://doi.org/10.1186/s40494-022-00759-6

[39] Hemeda S, Fahmy A, Sonbol A. Geo-Environmental and Structural Problems of the First Successful True Pyramid, (Snefru Northern Pyramid) in Dahshur, Egypt. *Geotechnical and Geological Engineering*. 2019; *37*(4), 2463–2484. https://doi.org/10.1007/s10706-018-00769-x

[40] Jeremy P. Mortar, plaster, and render, Editor(s): Jeremy P. Ingham, Geomaterials Under the Microscope, Academic Press, 2013; 137-162, ISBN 9780124072305, https://doi.org/10.1016/B978-0-12-407230-5.50016-9

[41] https://www.buildingconservation.com/articles/mythmix/mythmix.htm accessed on 13 October 2022.

[42] UNE-EN 15886. Conservation of cultural property - Test methods - Colour measurement of surfaces.2010.

https://cdn.standards.iteh.ai/samples/28486/bf9d5f31b80548ab9416eea7d8d4d617/SIST-EN-15886-2010.pdf

[43] Kim A, Kim H, Park S. *Measuring of the Perceptibility and Acceptability in Various Color Quality Measures*. 2011; *15*(3), 310–317. http://dx.doi.org/10.3807/JOSK.2011.15.3.310

[44] International Standard. ISO 10678:2010(E). 2010. Available from: https://cdn.standards.iteh.ai/samples/46019/391027c6de86443b9c8412f3973d4bd8/ISO-10678-2010.pdf

[45] Freeman A, Łukomski M, Beltran V. *Mechanical characterization of a cross-sectional TiO_2 acrylic-based paint by nano-indentation*. 2020.https://doi.org/10.1080/01971360.2019.1603062

[46] Gyurkó Z, Nemes R. *Static Hardness Testing of Cement Mortars Containing Different Types of Recycled Construction Waste Powders*. Solids. 2021; 2, 331–340. https://doi.org/10.3390/solids2040021

[47] Oliver W C. *Measurement of hardness and elastic modulus by instrumented indentation: Advances in understanding and refinements to methodology*. Journal of Materials Research. 2004; 19, 3. https://doi.org/10.1557/jmr.2004.19.1.3

[48] Oliver WC, Pharr GM. An improved technique for determining hardness and elastic modulus using load and displacement sensing indentation experiments. Journal of Materials Research. 1992; 7, 1564–1583. https://doi.org/10.1557/JMR.1992.1564

[49] ISO 14577-3. Metallic materials — Instrumented indentation test for hardness and materials parameters — Part 3: Calibration of reference blocks. 2015.https://www.iso.org/obp/ui/#iso:std:56626:en

[50] ASTM 2546. Standard Practice for Instrumented Indentation Testing. 2018.https://www.astm.org/e2546-15.html

[51] Bureau of Indian Standards. Method of Test for aggregate for concrete. IS 2386- Part III - Specific gravity, density, voids, absorption and bulking.1963; New Delhi, (Reaffirmed 2002). https://law.resource.org/pub/in/bis/S03/is.2386.1.1963.pdf . Accessed 12July 2022.

[52] ASTM. C97/C97 M-18 Standard Test Methods for Absorption and Bulk Specific Gravity of Dimension Stone, ASTM International, West Conshohocken, PA, 2018. www.astm.org.Accessed 15July 2022.

[53] Schaffer R J. The Weathering of Natural Building Stones. Building Research Special Report No18. Originally published by HMSO. Reprinted by Donhead Publishing Ltd, 2004.

[54] DIN EN 12370. Natural Stone Test Methods - Determination of Resistance to Salt Crystallization; German Version EN 12370.2020

[55] SIST EN 14147. Natural stone test methods - Determination of resistance to ageing by salt mist. 2004.https://standards.iteh.ai/catalog/standards/sist/86198a90-18a3-47df-8df5-27c8261edff0/sist-en-14147-2004

[56] UNE- EN 14066. Natural stone test methods - Determination of resistance to ageing by thermal shock. 2014. https://www.en-standard.eu/une-en-14066-2014-natural-stone-test-methods-determination-of-resistance-to-ageing-by-thermal-shock/

[57] https://www.micromaterials.co.uk/wp-content/uploads/2019/02/NanoTest-Vantage-Datasheet.pdf accessed on 15 October 2022

[58] He J, Du Y, Bai Y, An J, Cai X, Chen Y, Wang P. *Nanocomposites with Enhanced Photocatalytic Activity*. Molecules. 2019; 24, 1–14, 2996; doi:10.3390/molecules24162996.

[59] Thirugnanasambandan T, Alagar M. *Titanium dioxide (TiO_2) Nanoparticles - XRD Analyses – An Insight*. *2013*. Available from: https://www.researchgate.net/publication/244990066_Titanium_dioxide_TiO2_Nanoparticles_XRD_Analyses_An_Insight

[60] Pratheepa M I, Lawrence M. *X-Ray Diffraction Analyses of Titanium Dioxide Nanoparticles International Journal of Scientific Research in Science and Technology (IJSRST) X-Ray Diffraction Analyses of Titanium Dioxide Nanoparticles*. *December 2017*. IJSRST. International Conference on Advanced Materials Held on 14, 15 December 2017, Organized by Department of Physics, St. Joseph's College, Trichy, Tamilnadu, India. 2019. Print ISSN: 2395-6011, Online ISSN: 2395-602X.

[61] Sun J, Xu Z, Li W, Shen X. *Effect of Nano-SiO_2 on the Early Hydration of Alite-Sulphoaluminate Cement*. 2017; 1–15. https://doi.org/10.3390/nano7050102

[62] Sun S, Deng T, Ding H, Chen Y, Chen W. Preparation of Nano-TiO_2-Coated SiO_2 Microsphere Composite Material and Evaluation of Its Self-Cleaning Property.

Nanomaterials (Basel, Switzerland). 2017;7(11), 367. https://doi.org/10.3390/nano7110367

[63] Thongpool V, Phunpueok A, Jaiyen S, Rojviroon T. *Synthesis, characterization and photocatalytic activity using SiO_2-TiO_2 nanocomposites under UV light. Mater. Res. Express.* 2020;8,015001. https://doi.org/10.1088/2053-1591/abd33d

[64] Zhou D, Jiang J Z, Dunphy X R, Brinker D R. Influence of Material Properties on TiO_2 Nanoparticle Agglomeration. *PLoS ONE*. 2013; *8*(11), 81239. https://doi.org/10.1371/journal.pone.0081239

[65] Du B, Chen F, Luo R, Zhou S, Wu Z. Synthesis and Characterization of Nano-TiO_2/SiO_2-Acrylic Composite Resin. *Advances in Materials Science and Engineering*. *2019*; 6318623. https://doi.org/10.1155/2019/6318623

[66] Chever L, Pavía S. Howard R. Physical properties of magnesian lime mortars. Mater Struct 2010; 43, 283–296. https://doi.org/10.1617/s11527-009-9488-9

[67] Ahmed S M, Darwish S S, Elmarzugi N A, Al-Dosari M A. *Evaluation of Photocatalysis TiO_2 Nano-particles as a Self-Cleaning to Calcareous Stone Monuments Surface*. 2016.

[68] Zuena M, Ruggiero L, Caneva G, Bartoli F, Ventura G D, Ricci M A, Sodo A. Assessment of Stone Protective Coatings with a Novel Eco-Friendly Encapsulated Biocide. In *Coatings.* 2021; 11, Issue 9. https://doi.org/10.3390/coatings11091109

[69] Rosales A, Esquivel K. SiO_2-TiO_2 Composite Synthesis and Its Hydrophobic Applications: A Review. 2020.https://doi.org/10.3390/catal10020171

[70] Senff L, Hotza D, Lucas S, Ferreira V M, Labrincha J A. Effect of nano-SiO_2 and nano-TiO_2 addition on the rheological behavior and the hardened properties of cement mortars. *Materials Science & Engineering A*. 2012; *532*, 354–361. https://doi.org/10.1016/j.msea.2011.10.10 2

[71] Spathis P, Karapanagiotis I, Manoudis P, Kantiranis N, Zacharopoulou A. Protection of Dolomite Marble against Salts Weathering with Titanium Dioxide Nanocomposite Coatings. J Mod Chem Sci. 2017; 1: 001.

[72] Moro C, Francioso V, Velay-Lizancos M. Nano-TiO_2 effects on high temperature resistance of recycled mortars. *Journal of Cleaner Production*. 2020; *263*, 121581. https://doi.org/https://doi.org/10.1016/j.jclepro.2020.121581

Chapter 4

General conclusions, original contributions and future prespectives

4.1. General conclusions

The current thesis presents several case studies from Egypt and Sudan in terms of studying the durability problems of the construction materials under different environmental conditions. The research carried out rigorous of analysis and examinations using X-ray diffraction, X-ray fluorescence, Raman spectroscopy, UV-Vis spectrometry, binocular microscope, polarizing microscope and scanning electron microscope with EDS. Mechanical (uniaxial compressive strength, hardness and young's modulus) and physical (porosity, water absorption and density) characterizations were addressed to the construction materials. Furthermore, mapping and satellite images for the damages and decay rate were conducted using AutoCAD, ArcMap 10.8, SeaDAS, QGIS. As well as to carry out geographical, geological and morphological maps. Moreover, experimental study was conducted in order to preserve the construction materials surfaces in different environmental conditions, especially for the lime mortars. The application of using nano consolidate of SiO_2-TiO_2 NPs/TEOS with different percentages was carried out to enhance the mechanical and physical properties of the lime mortar surfaces as selected construction material.

The main conclusions that have been obtained are:

1. Sahure's pyramid in Abusir (Giza, Egypt) is affected by many decay and damage factors physically, mechanically, and chemically. Many fallen stone blocks and loss of cohesion of construction materials are noticed. For this, urgent restoration and conservation are needed to safeguard this important pyramid. The mineralogical composition affected the construction materials, especially the swellable clays content in the stones. The surrounding environmental conditions such as temperature variations, rains and winds affected the pyramid as well. Lastly, earthquakes caused a mechanical damaged and dismantled most of the casing stone of the pyramids and caused fractures and structural cracks in the chambers of the pyramid.

2. The study about Nero's Temple at El-Ashmonein archaeological site (El-Ashmonein, Minia, Egypt) concluded that salt weathering mainly causes the damage and decay

of Nero's Temple. Different water sources (agricultural, wastewaters, and canals water) carried different kinds of soluble salts (chlorides, sulfates, carbonates, bicarbonates, phosphates, and nitrates). In addition, an urgent restoration plan should be executed to restore and preserve the remaining structural and architectural elements starting from fine (surface cleaning, salt removal, and consolidation) to geostructural (soil enhancement, columns repairs, blocks re-joining, and replacement) restoration to be kept as a world heritage monument.

3. Construction materials of Anfushi's Necropolis in Alexandria (Egypt) showed that the main decay patterns are structural cracks, horizontal displacement for the walls, chippings for the blocks, and collapsing. In addition to flaking, spalling, salt erosion, loss of materials, delimitations, alveolarization, and discolouration of the painting layer due to marine dynamics (earthquakes, flooding, windstorms, sea spray and climatic conditions). In addition, mapping and recording of some selected architectural and structural elements through vector sketches were carried out, with retouching of original tones of colours for the paintings to help in the retouching and restoration works in the future.

4. The impact of Nile water fluctuations of the sandstones of the Osiris Temple at Philae/Aswan (Egypt) shows many decay forms, such as blackening, disintegration, flaking, soiling, fractures, discoloration, and micro- and macrocracks. It is due to the continuous interaction between water and building materials and the internal problems of the sandstones. For decades, sandstone-building materials have been saturated under Nile water, playing a corrosive role through the dispersion, dissolution, and hydrolysis of the mineral composition of sandstone. In addition, pores and spaces between quartz grains were detected due to the alteration of feldspars to kaolinite during the hydrolysis process. The hydrolysis of quartz in sandstones has been noted as an internal decay factor. Finally, accurate engineering and geological studies are needed to guarantee safe transportation and establishment of this temple into a stable hill around this area.

5. The pyramids of Meroe at Al Bagrawiya archaeological site (Sudan) are strongly affected by sand dunes, which play a significant role in the destruction and degradation of the building materials of these pyramids. In this sense, wind is considered a deterioration key of the archeological site, that led to sand dunes formations and abrasion for the building materials for the pyramids. In addition, flooding from heavy rains and rising Nile River water is also considered a potential threat at Al Bagrawiya archeological site and its pyramids.

6. The elaboration and comparison of the behavior of different proportions of SiO_2-TiO_2 NPs in TEOS for the surface protection of the ancient lime mortars concluded that 3% and 5% SiO_2-TiO_2 NPs/TEOS proved their efficacy on in order to enhance the mechanical and physical properties of the lime mortar experimentally.

7. Each environment from the selected sites in Egypt and Sudan has its own aggressiveness or environmental chanllenges toward the construction materials resilience and durability. However, it is observed that the urban, coastal, and fluvial environments are more aggressive than the arid environments.

8. Urgent conservation and restoration plans are needed for the selected building of the Sahure's pyramid, Anfushi's Necropolis, Nero's Temple, Osiris Temple in Aswan, and the pyramids of Meroe by architectural and structural retrofitting. Nevertheless, the priority for the intervention should be for Anfushi's Necropolis, Nero's Temple and Osiris Temple in Aswan.

4.2. Original contributions

The current study is considered the first study to highlight on the risks and durability problems of the ancient construction materials in semisubmerged state in Nile River (Aswan) such as Temple of Abaton. This study compared and linked the environmental impacts on the construction building materials in the coastal environmental (Alexandria) and fluvial environment (Nile River). In addition, there are few studies had been addressed to study the ancient construction materials and their alterations in different kinds of environments. For this reason, the research presented an expended study to investigate and compare the conservation problems in aqueous (coastal and fluvial) and subaerial environments (urban, agricultural and desertic).

For the first time, the first ancient trial of the concrete manufacturing had been revealed in the study of durability problems and construction materials of Sahure's pyramids in Abusir, Giza, Egypt. Furthermore, this study called the attention to the environmental risks on the Pyramids of Meroe in Sudan. The factors that affected the pyramids are sand dunes movements, wind erosion, flooding and heavy rains. Satellite imaging and mapping were utilized for monitoring and change detection. The mean reason to address this part of study is the lackage of studies on the conservation problems of these pyramids.

This study investigated and analyzed wide range of construction building materials from different quarries and different archaeological sites such as (limestone, sandy limestone, sandstones, basaltic mortar, lime mortar, gypsum mortar). Their various degradation and alteration in different environmental conditions were studied utilizing multi-techniques for analysis, examination and testing.

Finally, this thesis put on view a novel multifunctional nano composite material in order to protect the archaeological lime mortars in different environment conditions. The study concluded that 3% and 5% SiO_2-TiO_2 NPs/TEOS enhanced multifunctionally the lime mortars surfaces. This is a new contribution in the field of archaeological conservation science by creating and characterizing new nano-martial can be used in the field for consolidation and coating the lime mortars in the archaeological sites.

4.3. Future perspectives

This study aimed to chacareras several construction building materials in many case studies in different archaeological sites Egypt and Sudan. Various building materials such as natural stones and mortars were assessed by identification them and understanding the mechanism of degradation and alterations in different environmental conditions (Coastal, fluvial, desert, agricultural and urban). More structural assessments for the archaeological sites in Egypt and Sudan are needed, especially for the mechanical durability of the archaeological construction materials in various environmental context. Flooding, wind and earthquake responses analysis are needed to study the impact of these geohazards on the archaeological sites and presenting solutions for interventions and preservation. In addition, the studied cases are urgently needed to be restored and preserved architecturally and structurally. New novel nano-materials are needed in order to protect the submerged monuments with reversible and superhydrophobic materials. Moreover, joint materials for the repairing the damaged and broken stone blocks are needed to be enhanced using nanotechnology. Finally, satellite images and space-archaeology are strongly recommended for characterizing the construction building materials, hazards assessment, degradation, damage, site management and presenting solutions in the endangered archaeological sites.

Appendixes

Annex 1: Supplementary materials for Chapter 3.1 titled "Coastal environment impact on the construction materials of Anfushi's Necropolis (Pharos's Island) in Alexandria, Egypt**".**

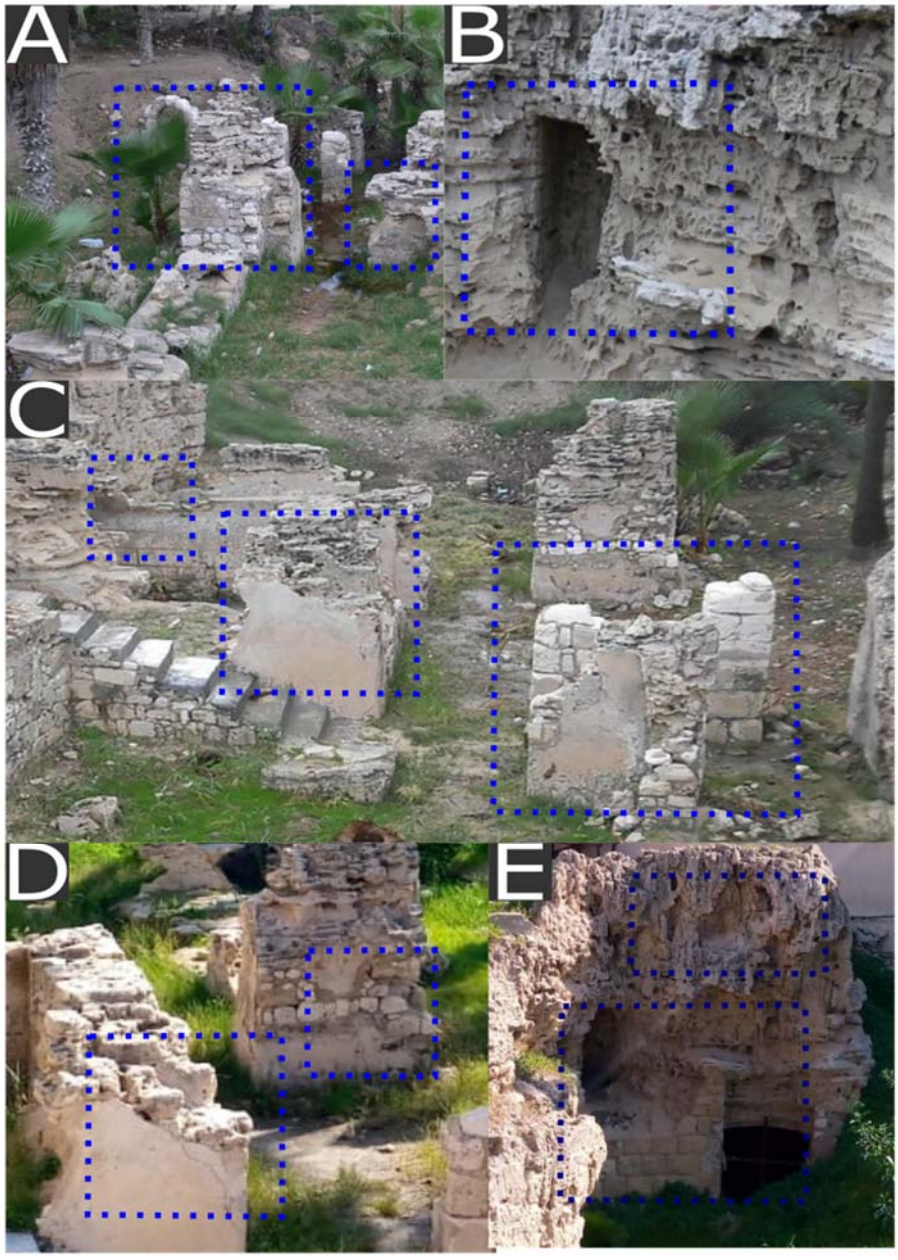
Annex 2: Supplementary materials for Chapter 3.2 titled "Multianalytical diagnostic approaches for the assessment of materials and decay of the archaeological sandstone of Osiris Temple (The Abaton) in Bigeh Island, Philae (Aswan, Egypt)".

Annex 3: Scientific activities (Publications, conferences, fieldwork, workshops, and courses).

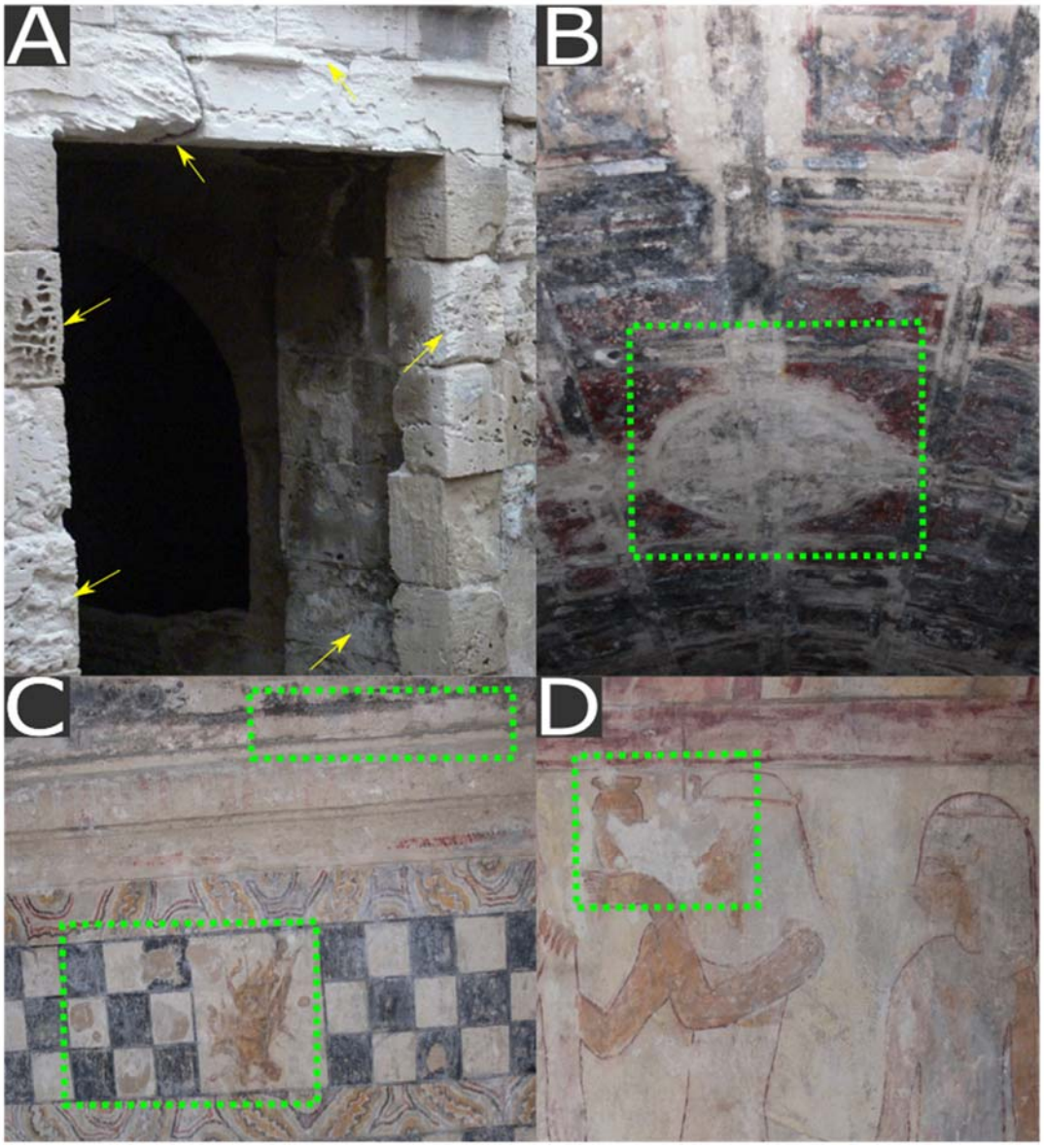
Annex 4: List of publications and contributions.

Annex 5: Plan of the Investigation.

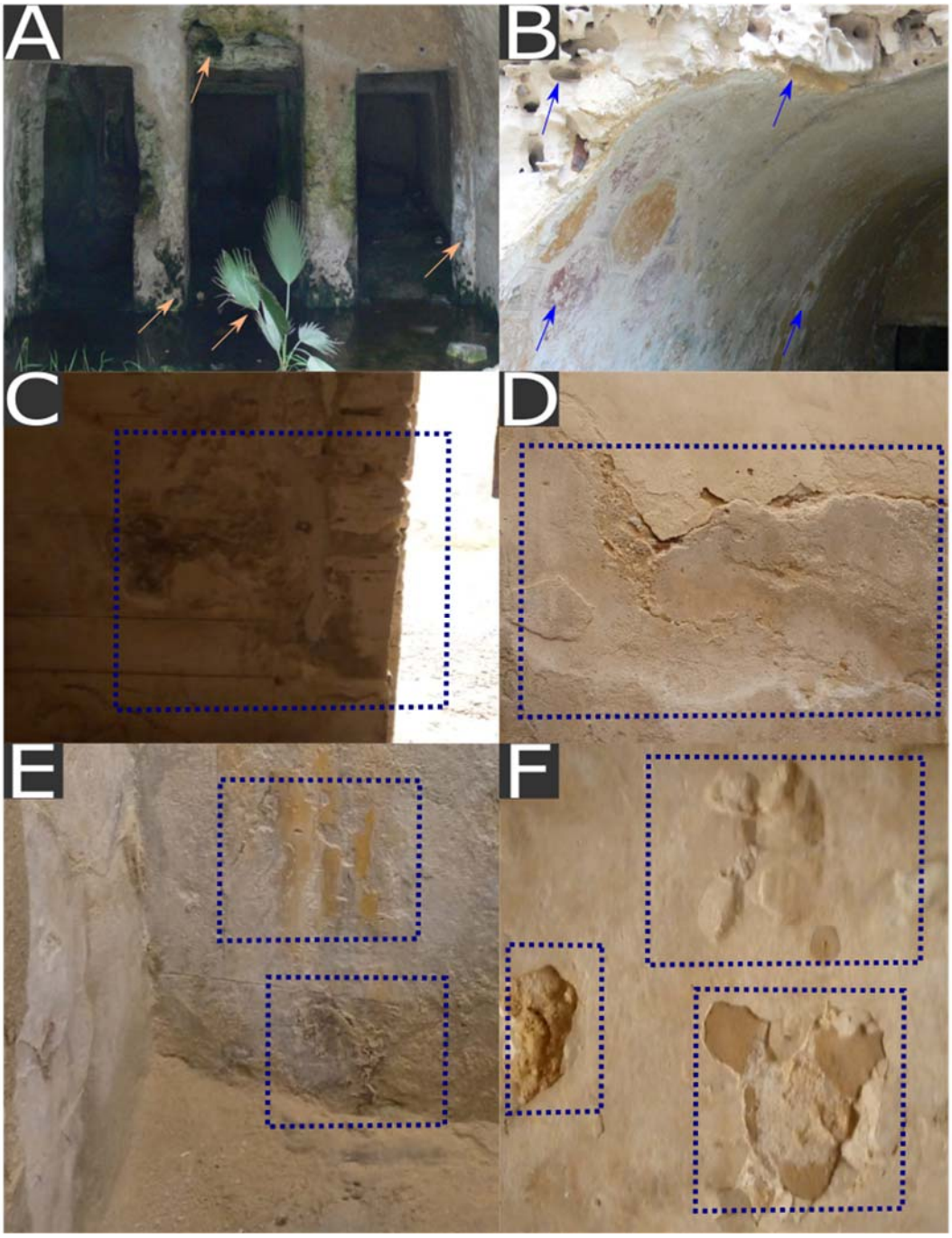
Annex 1: Supplementary materials for Chapter 3 titled "Coastal environment impact on the construction materials of Anfushi's Necropolis (Pharos's Island) in Alexandria, Egypt**"**



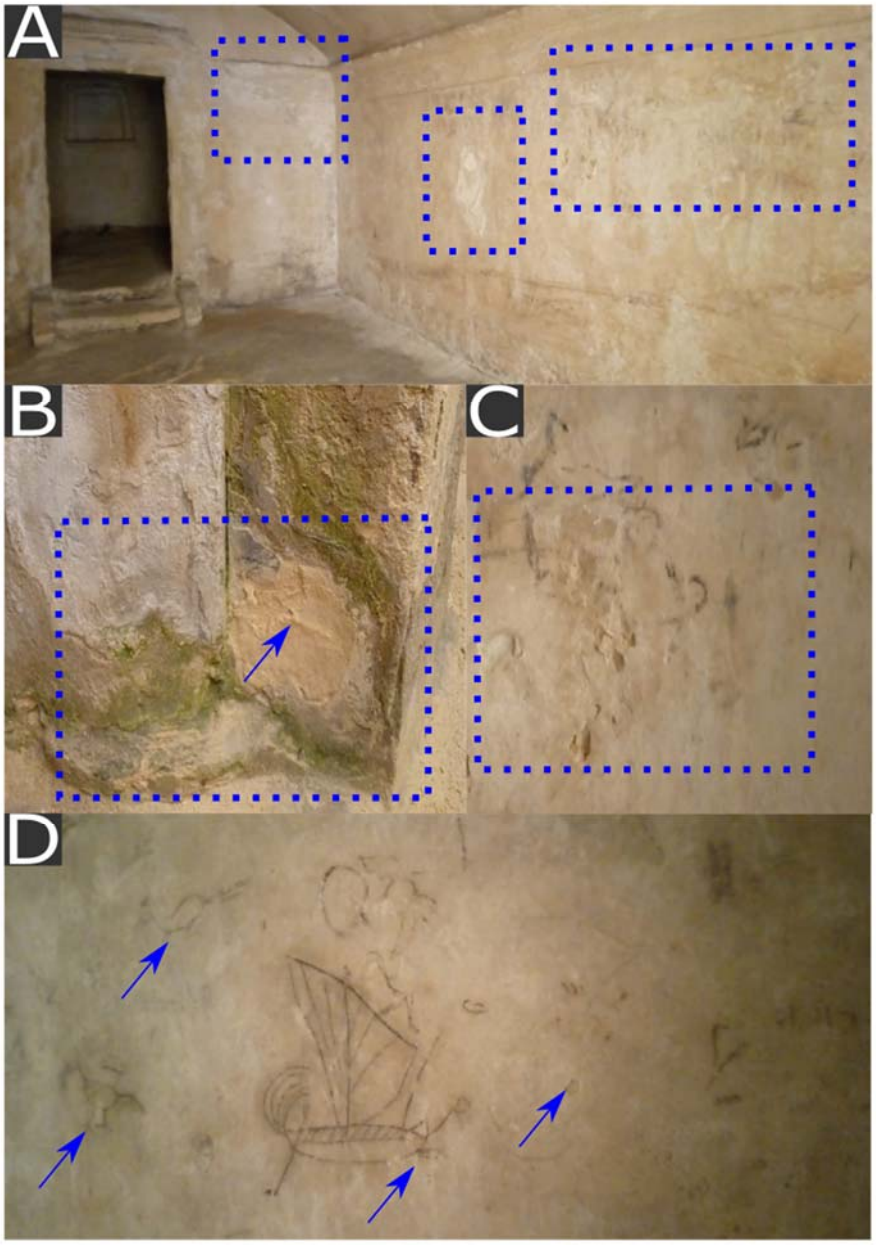
SM1. Fig. 1. (A) Ruins of collapsed structures and displacements. (B) Gaps in the bedrocks indicate the geotechnical problems of the Anfushi's Necropolis. (C) Crumbling and deformations in the walls and vaults. (D) Loss of materials and loss of rendering layers. (E) Collapsed parts from bedrock and chipped blocks.



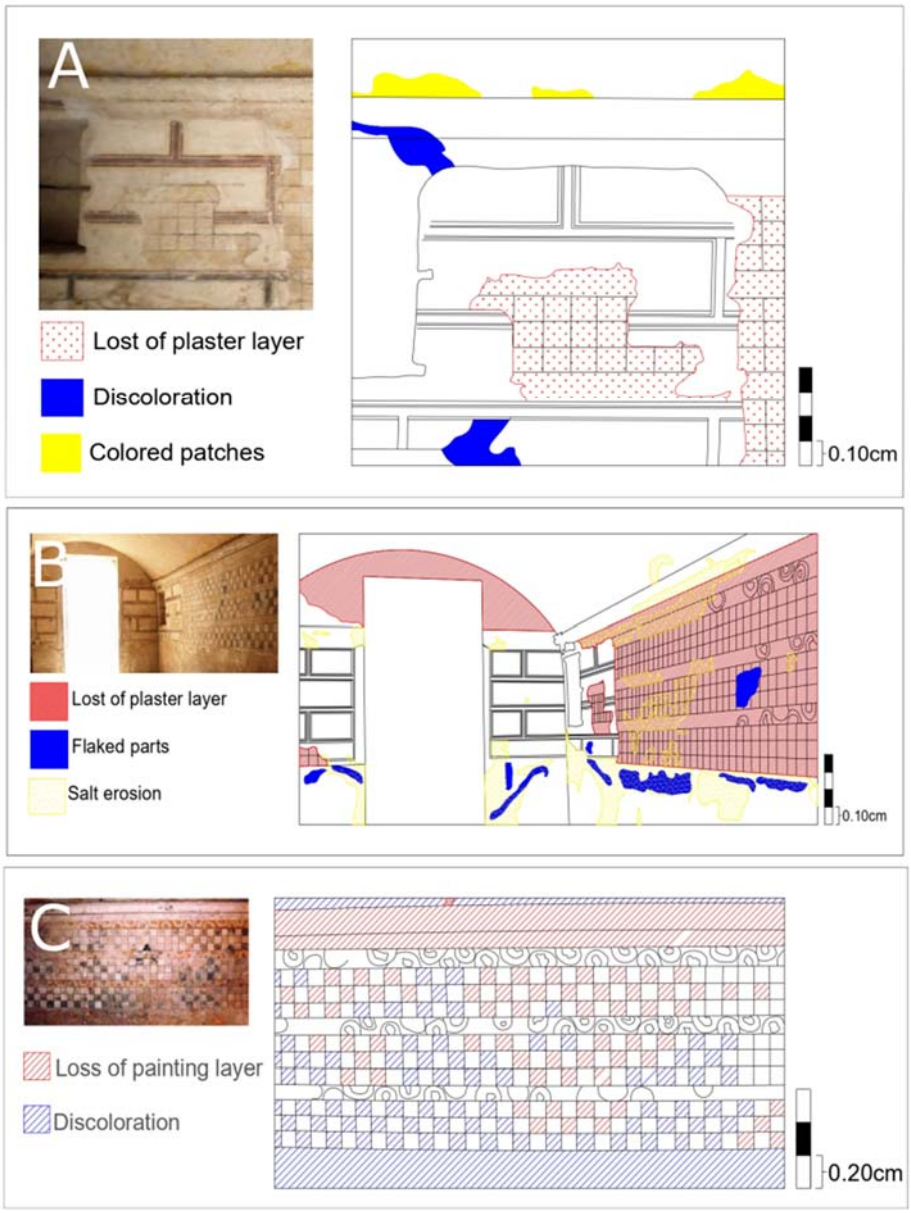
SM1. Fig. 2. (A) Alveolar weathering (honeycomb), crack in the blocks, chipped blocks, salt erosion, flaking, and pittings. (B) Loss of painting layer due to salt erosion. (C) Flaking, scaling, chipped blocks, and salt crystallization. (D) Salt erosion (efflorescence and sub fluorescence).



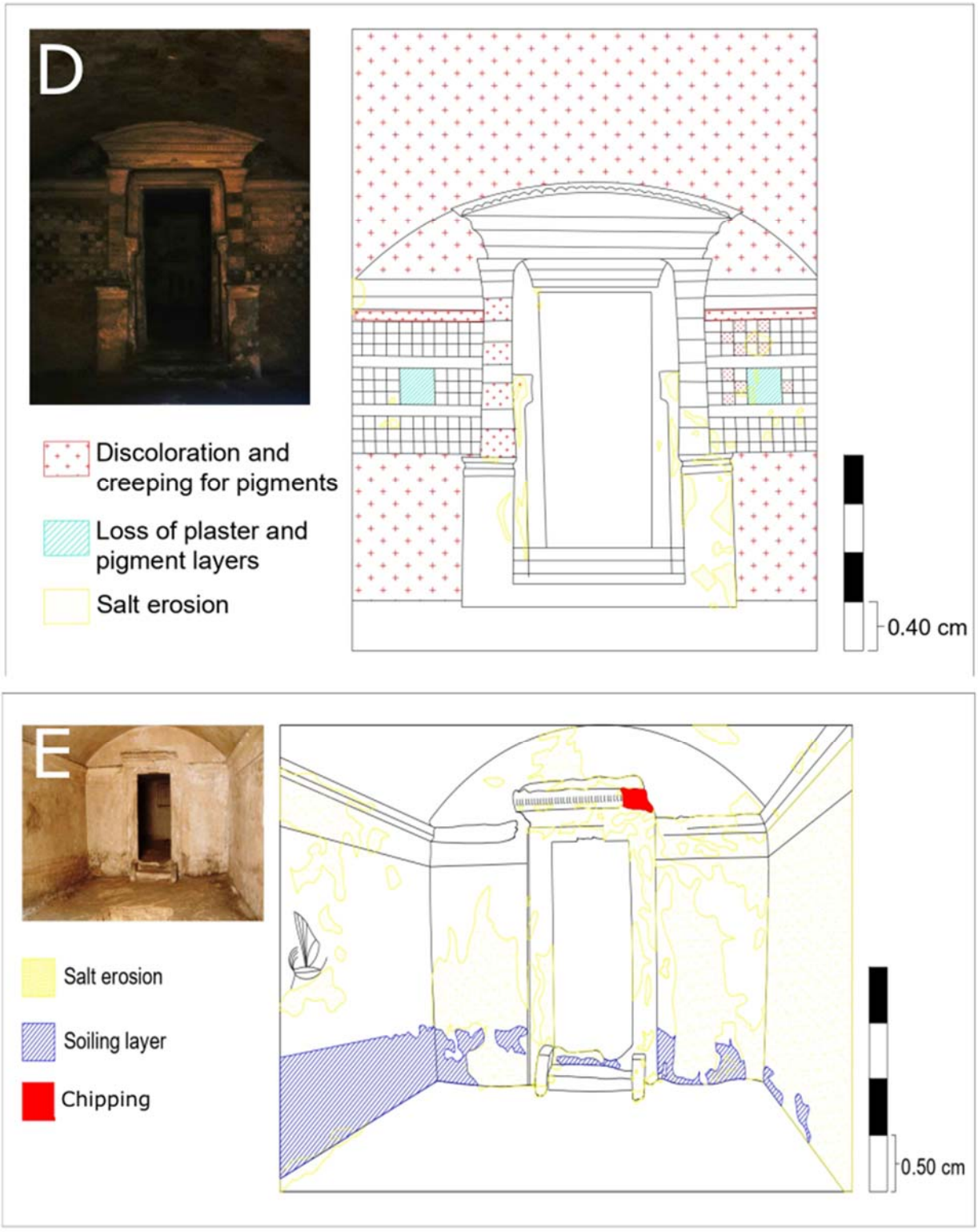
SM1. Fig. 3. (A) Green arrows refer to fallen parts from the bedrock, salt erosion, dampness due to water gathering, and plant growth. (B) Blue arrows show the gaps in the bedrock, chipping patterns, salt erosion, and eroded parts from the structure of the tomb. (C) Missing rendering layers. (D) Layering for the surface, bulking of the wall, and salt erosion. (E) Loss of painting layer and delamination. (F) blistering, flaking and loss of materials.



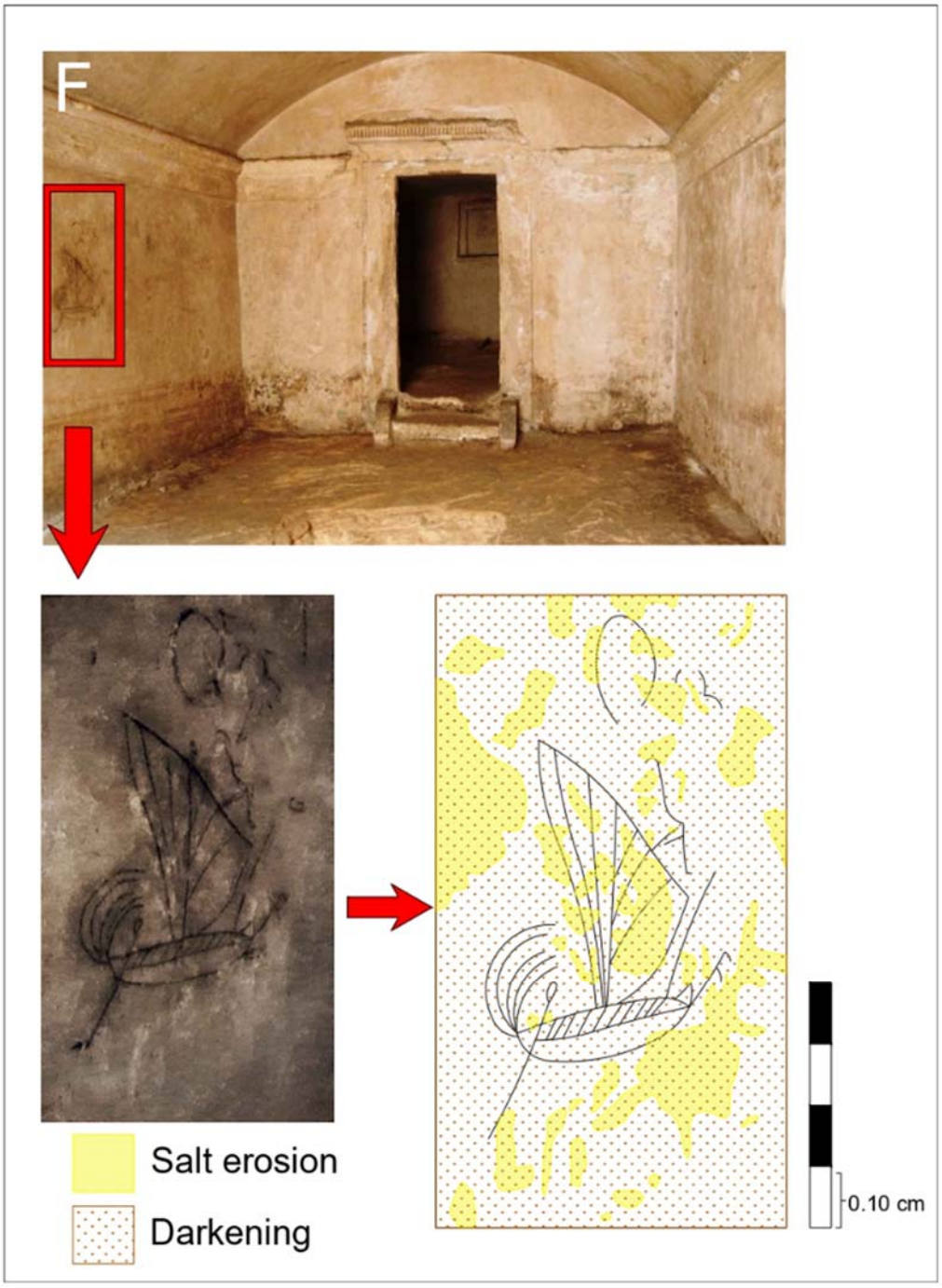
SM1. Fig. 4. (A) The dotted blue rectangular and squares refer to the salt erosion on the surfaces of Anfushi's Necropolis. (B and C) shows the flaking and layering patterns, blue arrow refers to recent restoration for filling a gap. (D) Significant graffiti and endangered with salt crystallization.



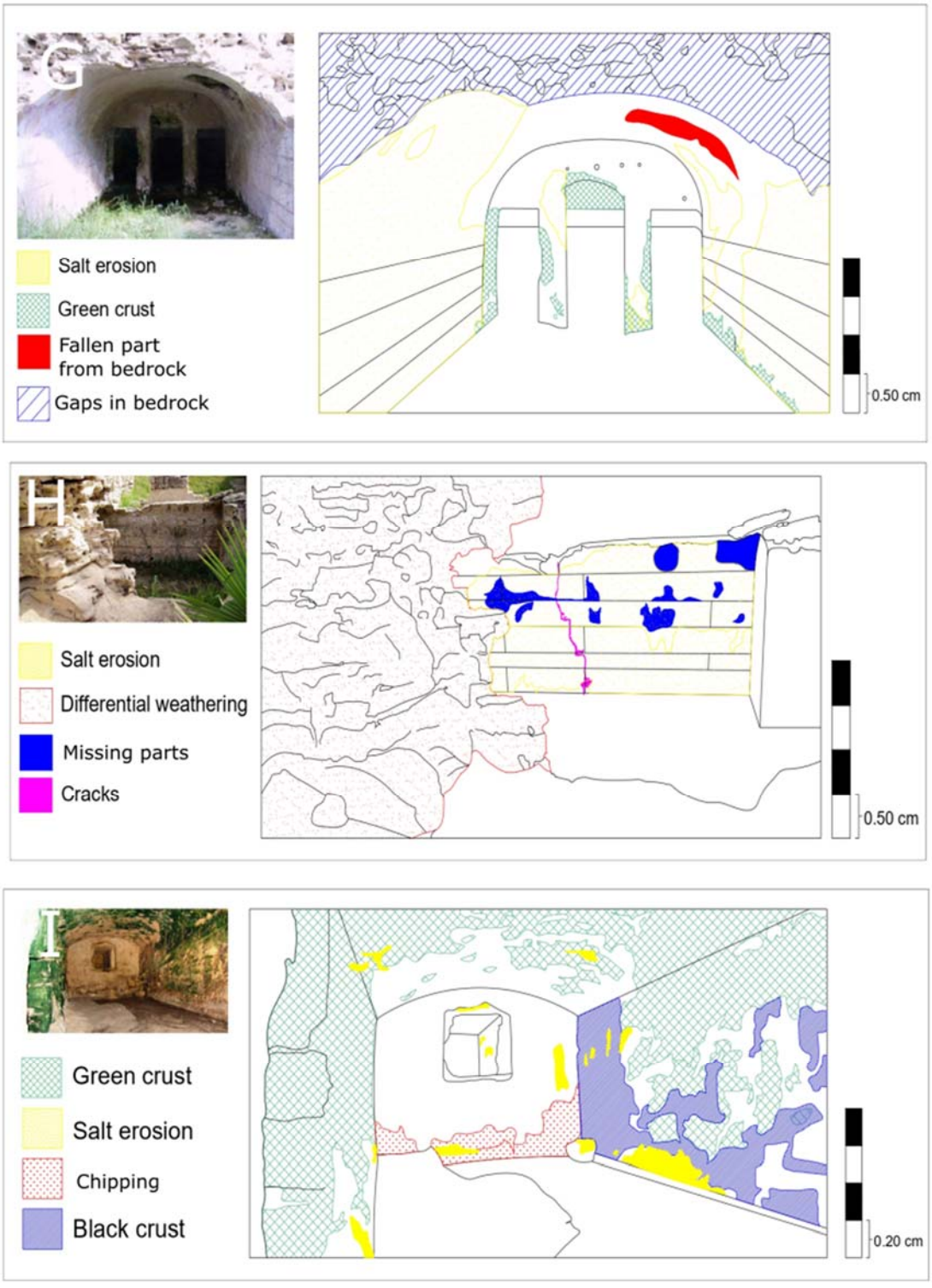
SM1. Fig. 5. (A-R) Various decay patterns for the building materials of the Anfushi's Necropolis due to the marine dynamic impact. The most dominant patterns are salt erosion, loss of materials, loss of rendering layers, discoloration, pittings, alveolar weathering, flaking, cracks and layering.



SM1. Fig. 5. (D and E) Cont.



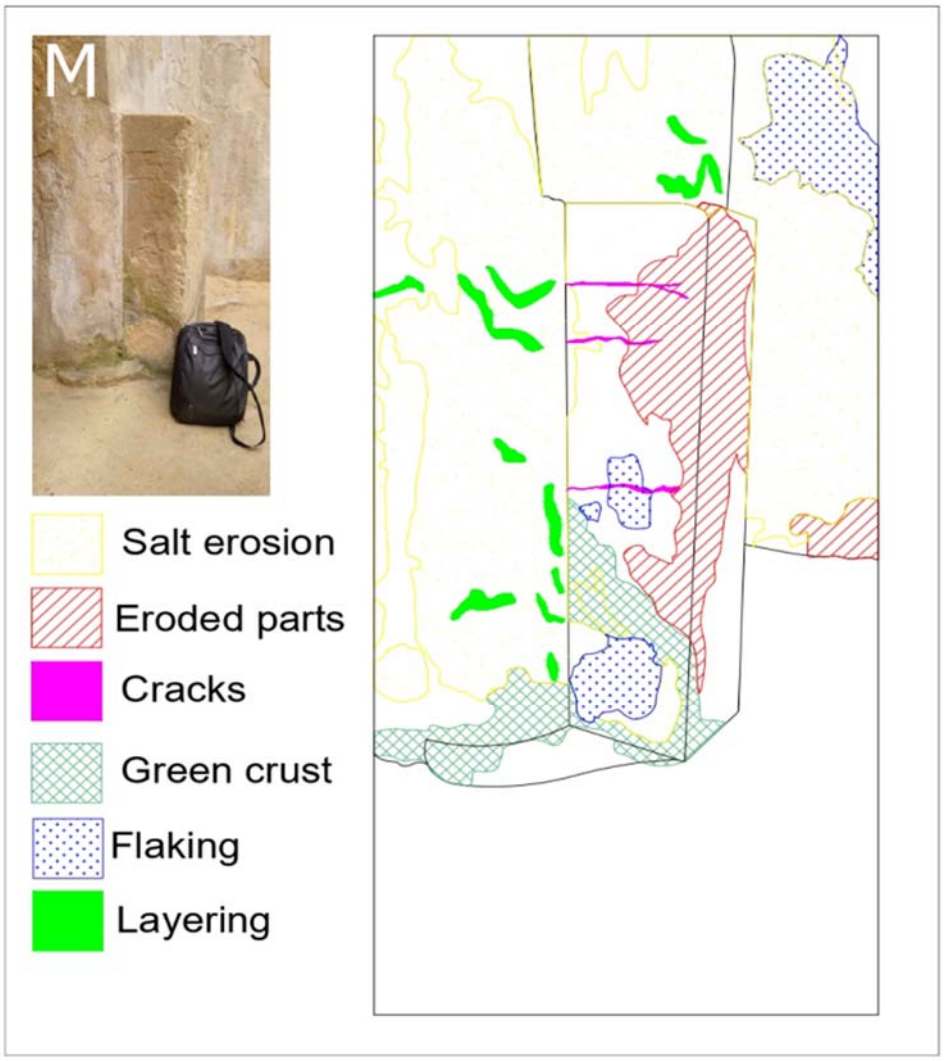
SM1. Fig. 5. (F) Cont.

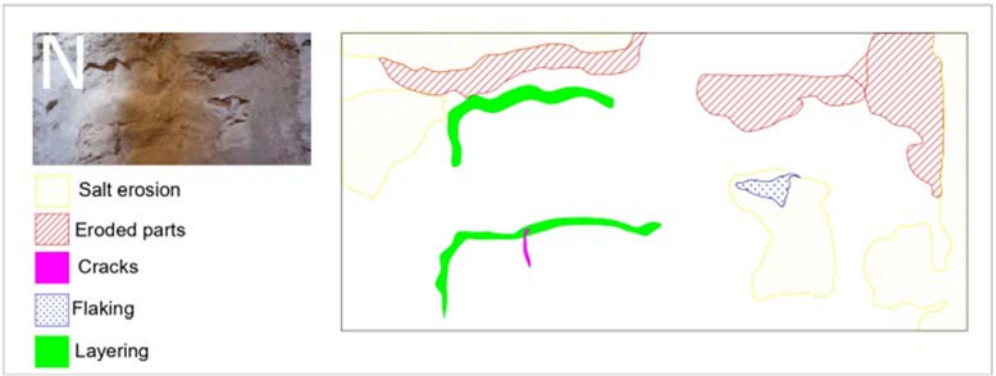


SM1. Fig. 5. (G-I) Cont.

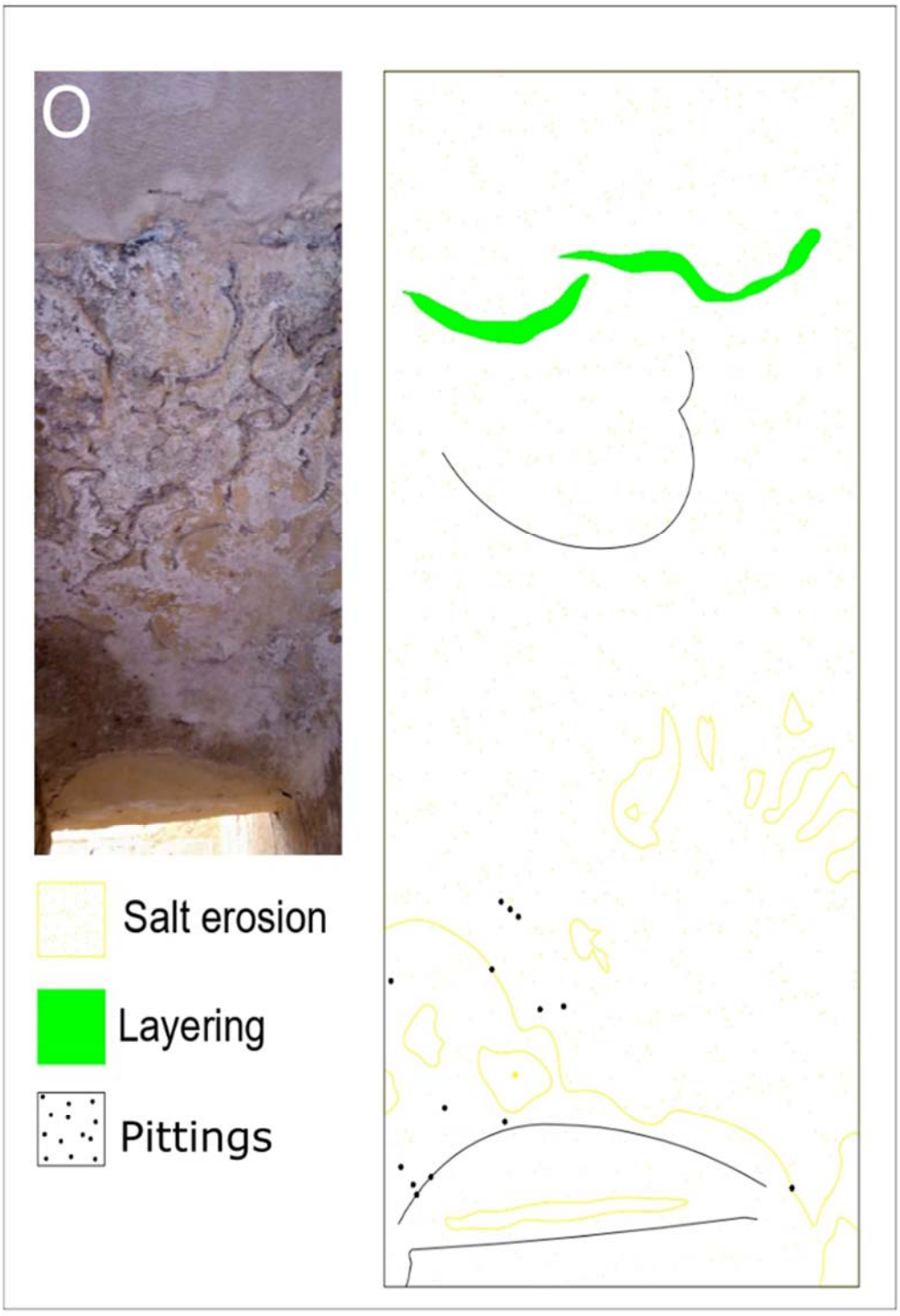


SM1. Fig. 5. (J-L) Cont.

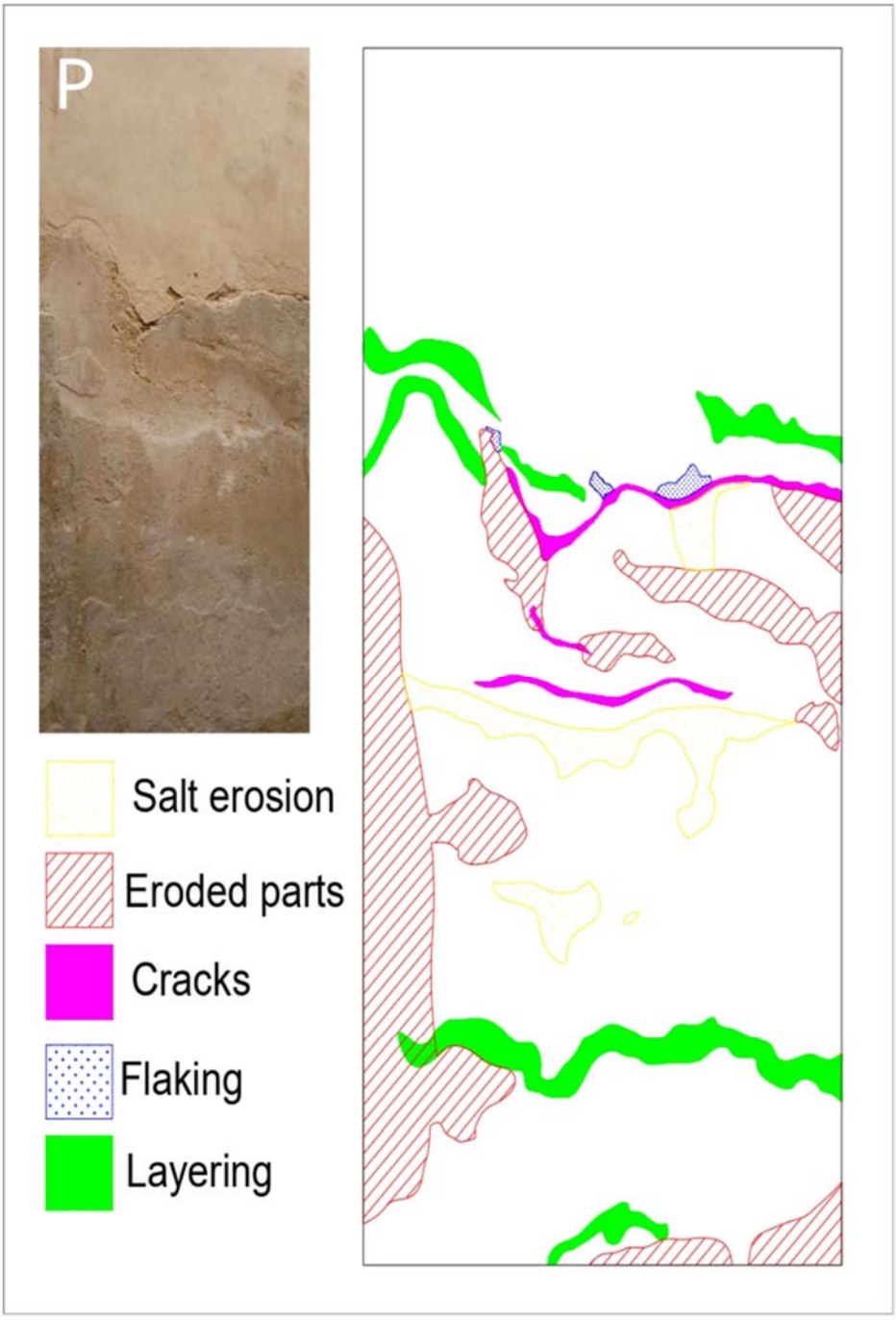




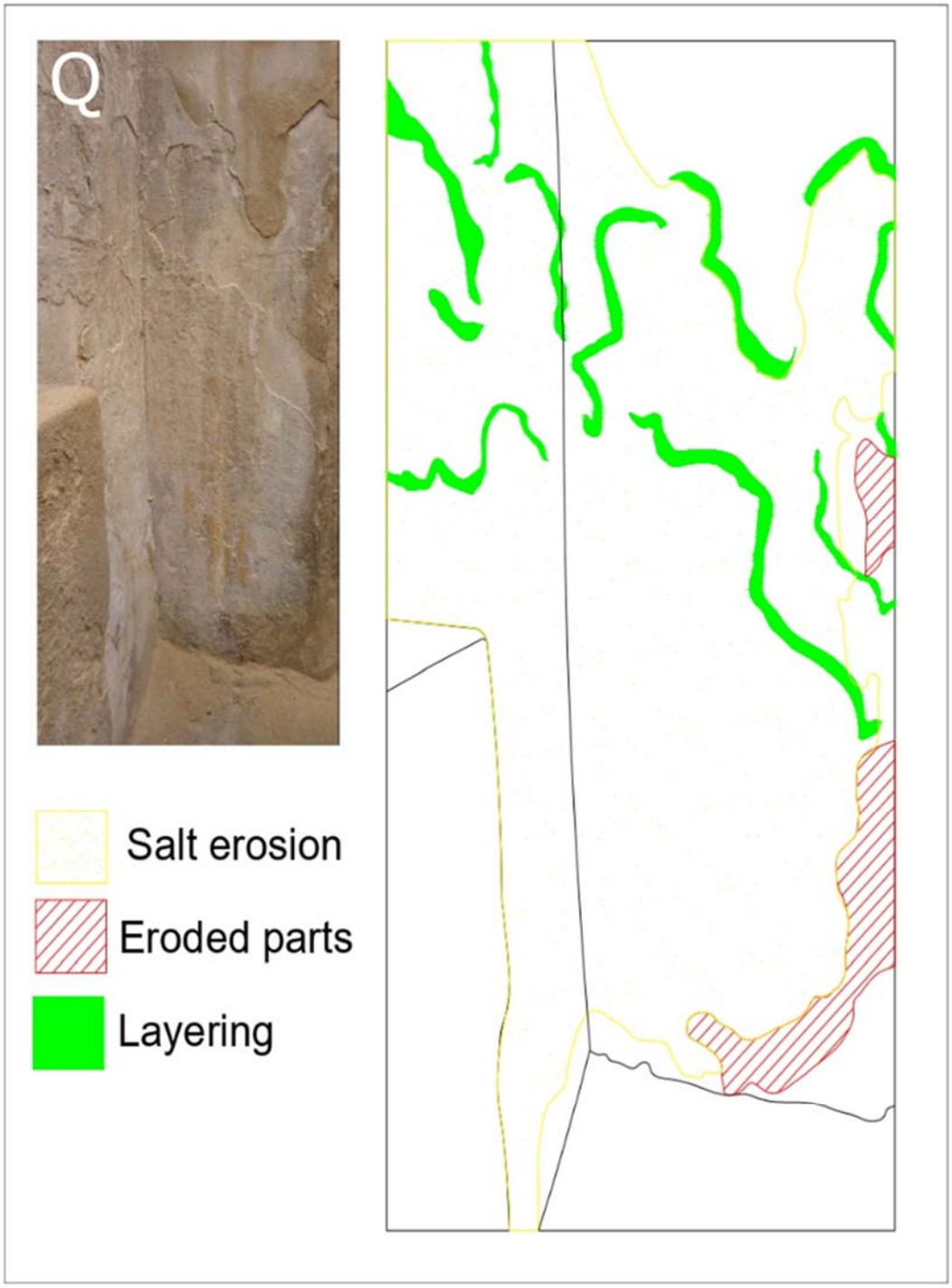
SM1. Fig. 5. (M-N) Cont.



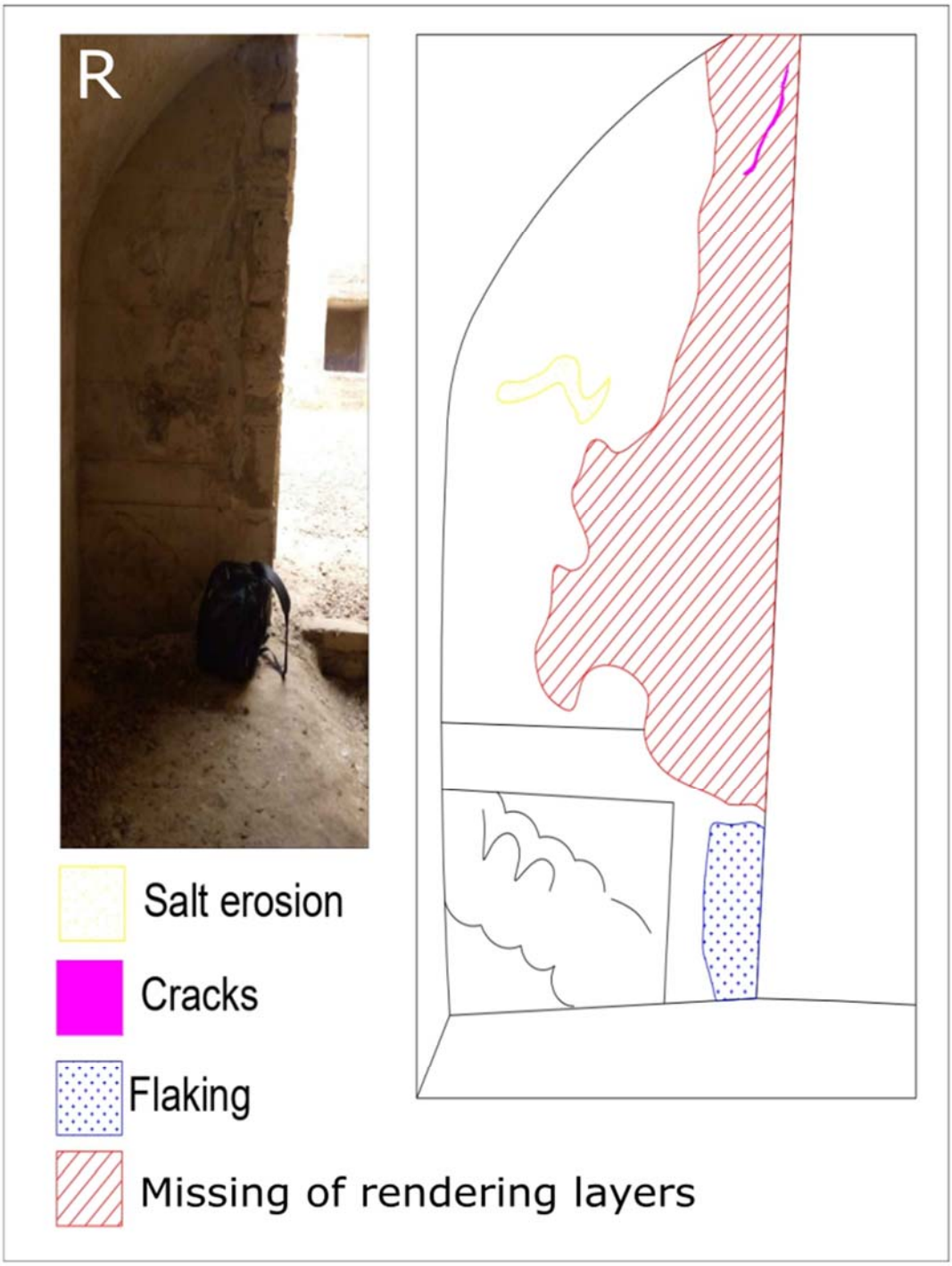
SM1. Fig. 5. (O) Cont.



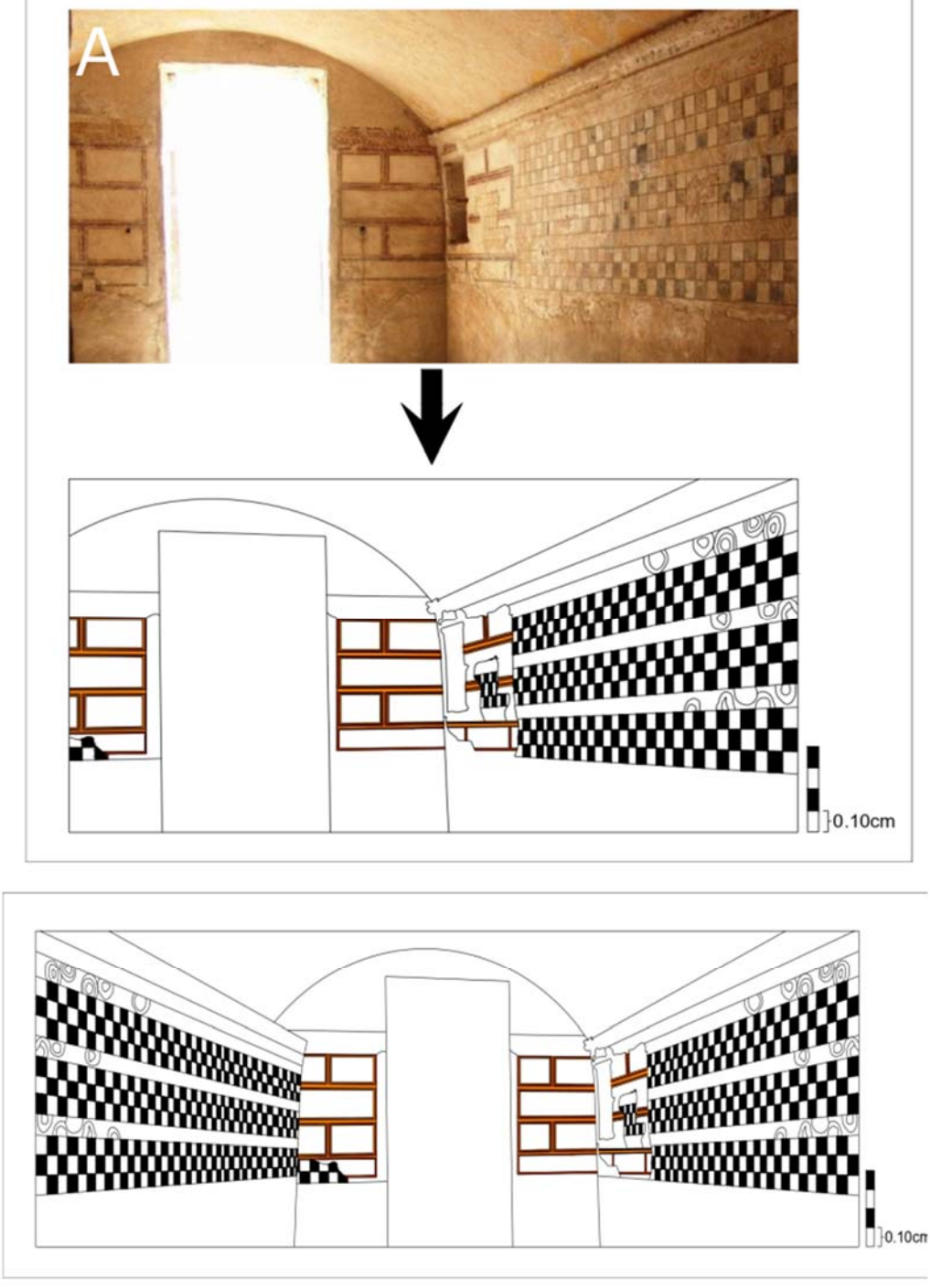
SM1. Fig. 5. (P) Cont.



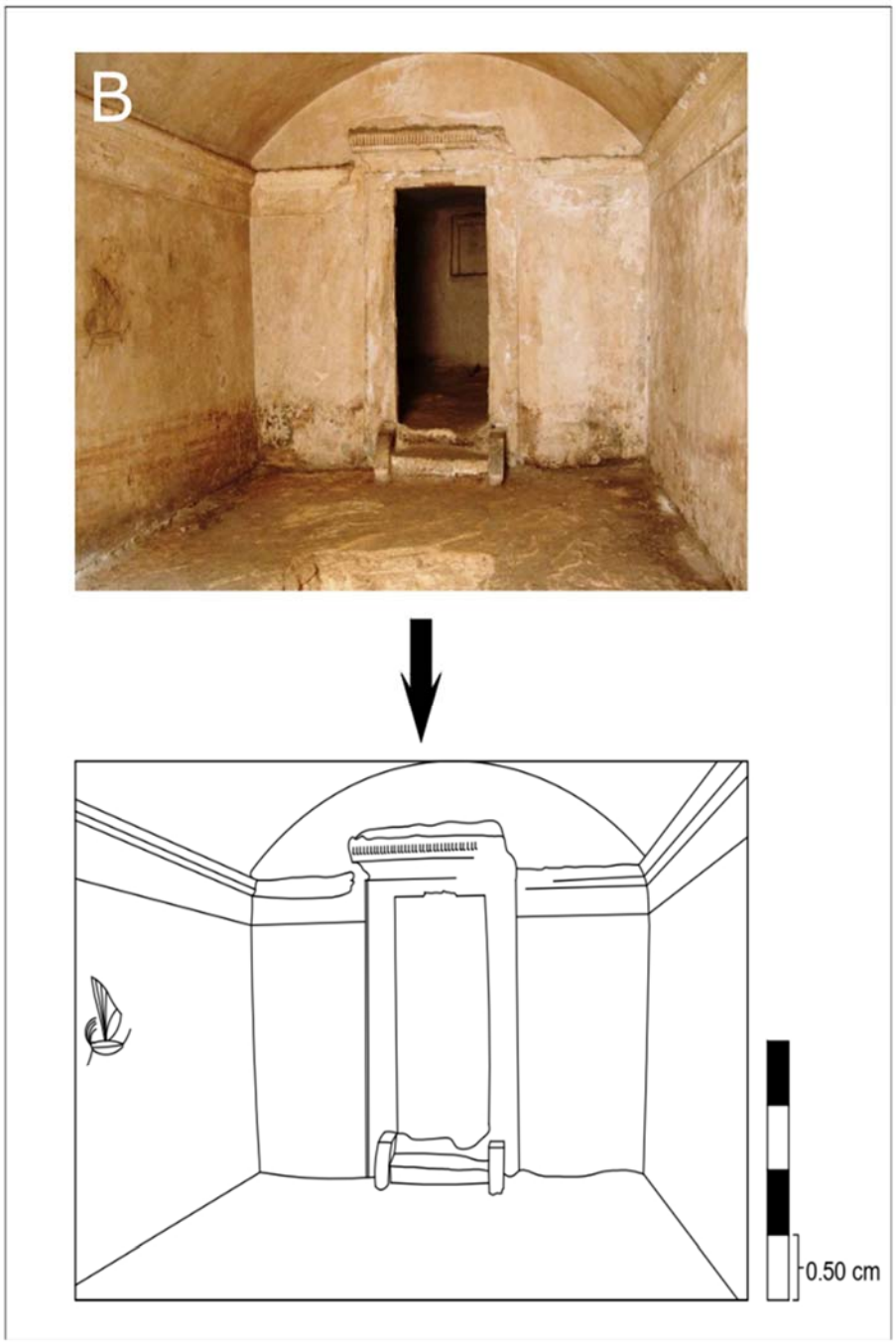
SM1. Fig. 5. (Q) Cont.



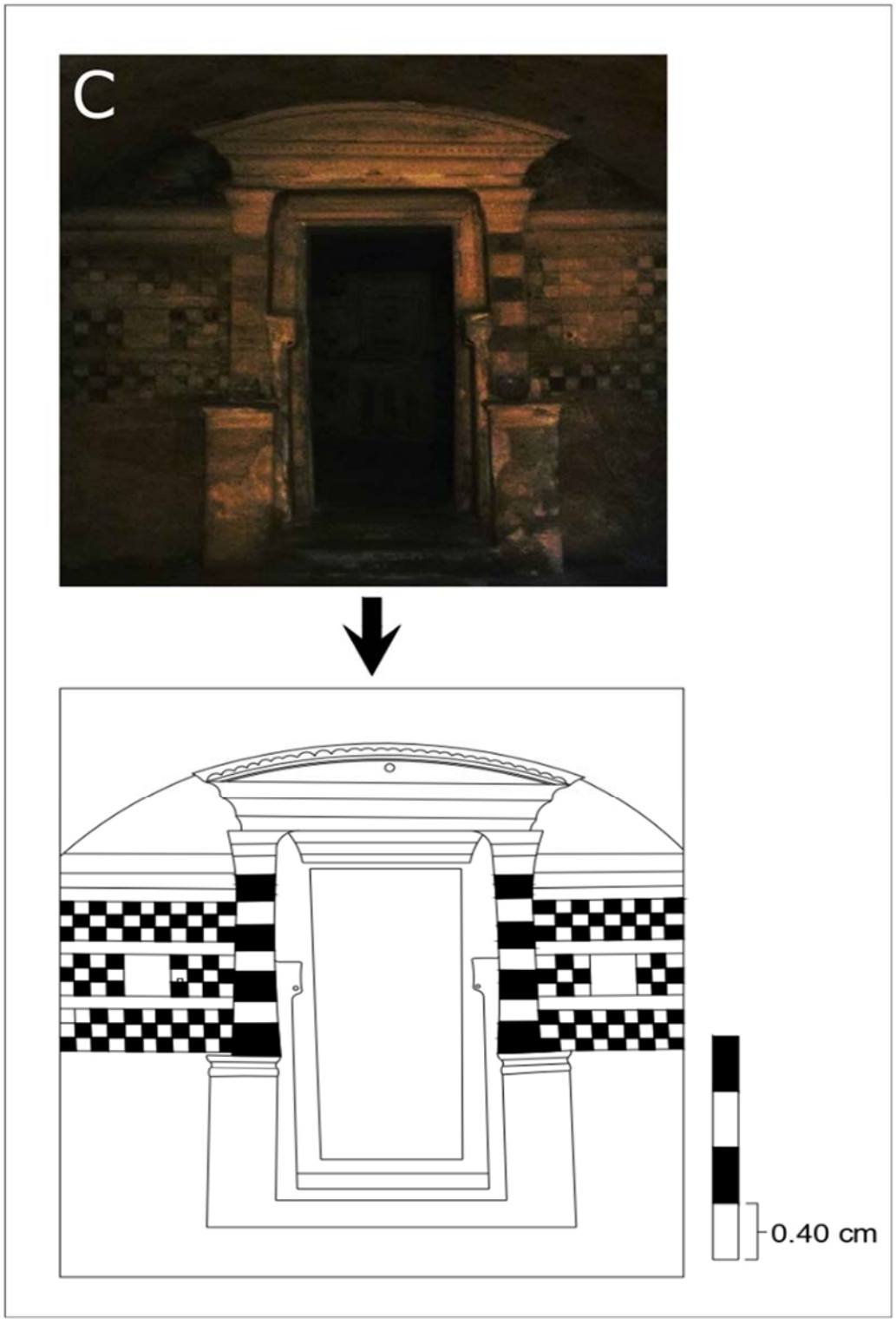
SM1. Fig. 5. (R) Cont.



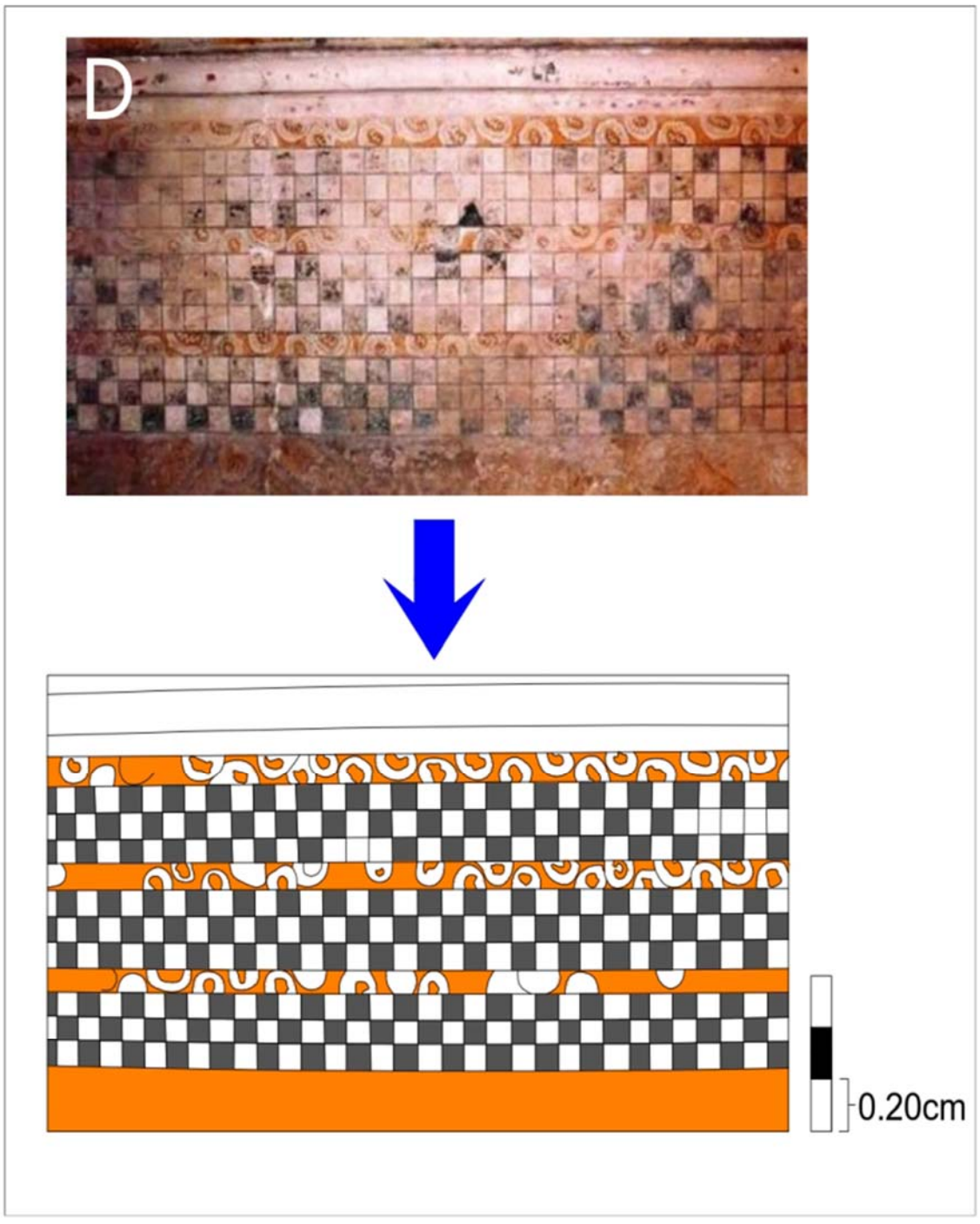
SM1. Fig.6. (A-E) Reconstruction and retouching for the architectural and structural elements of the Anfushi's Necropolis.



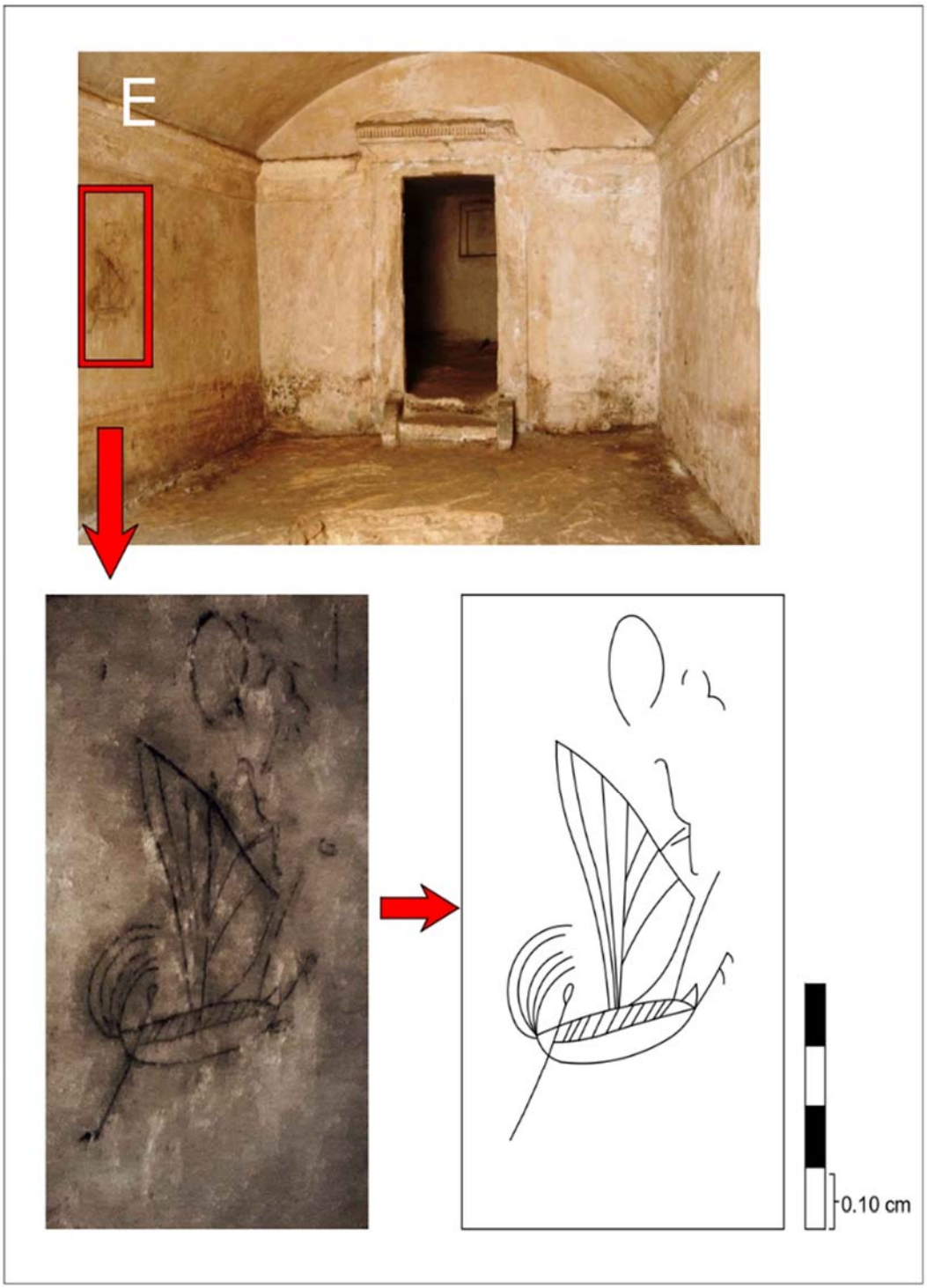
SM1. Fig. 6. (B) Cont.



SM1. Fig. 6. (C) Cont.

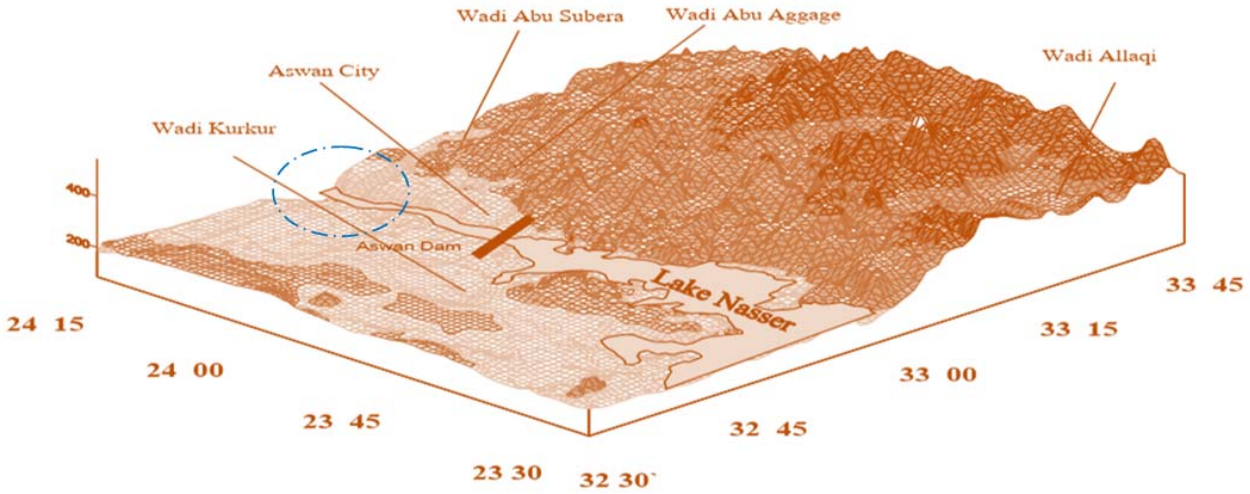


SM1. Fig. 6. (D) Cont.



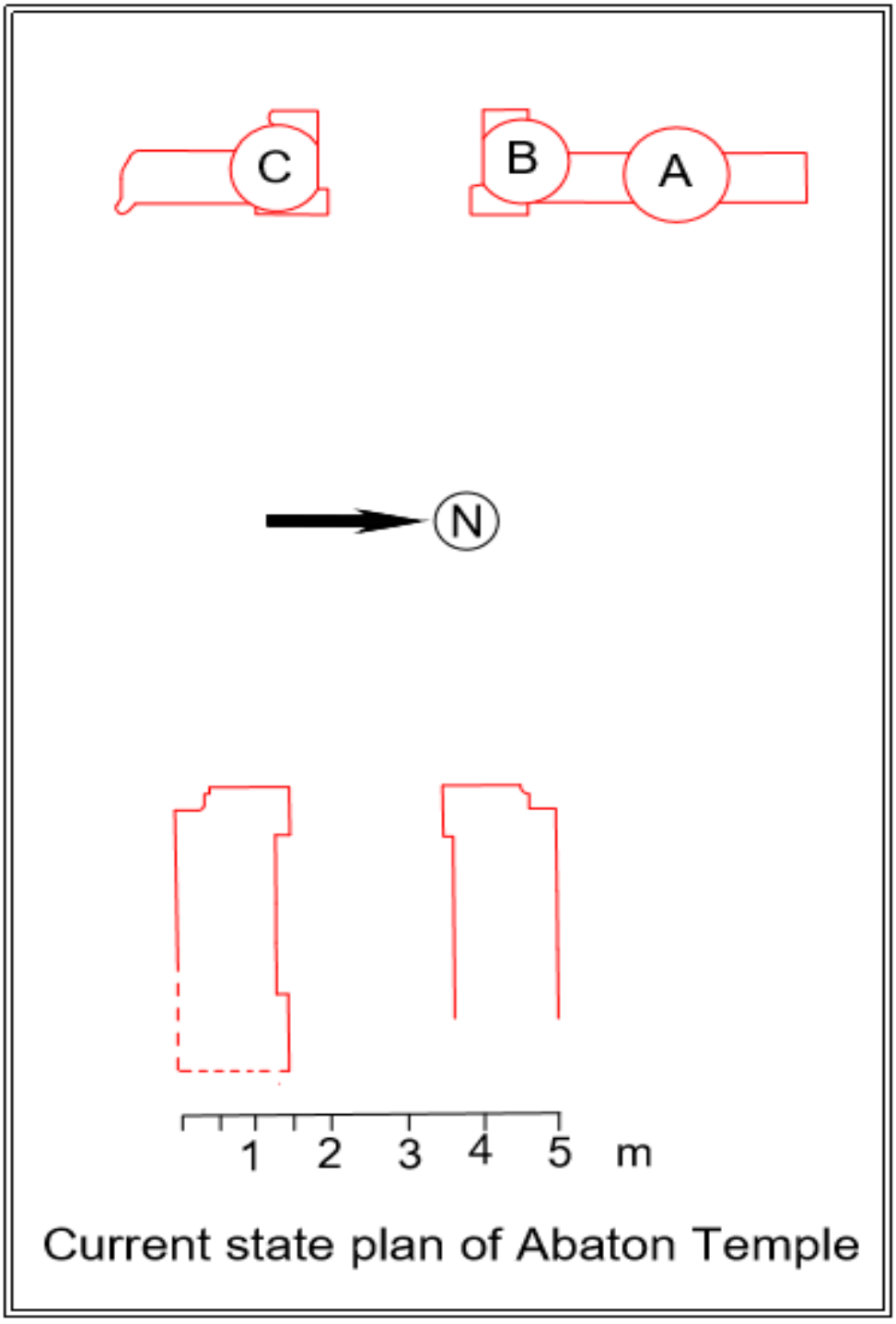
SM1. Fig. 6. (E) Cont.

Annex 2: Supplementary materials for Chapter 4 titled "Multianalytical diagnostic approaches for the assessment of materials and decay of the archaeological sandstone of Osiris Temple (The Abaton) in Bigeh Island, Philae (Aswan, Egypt)"

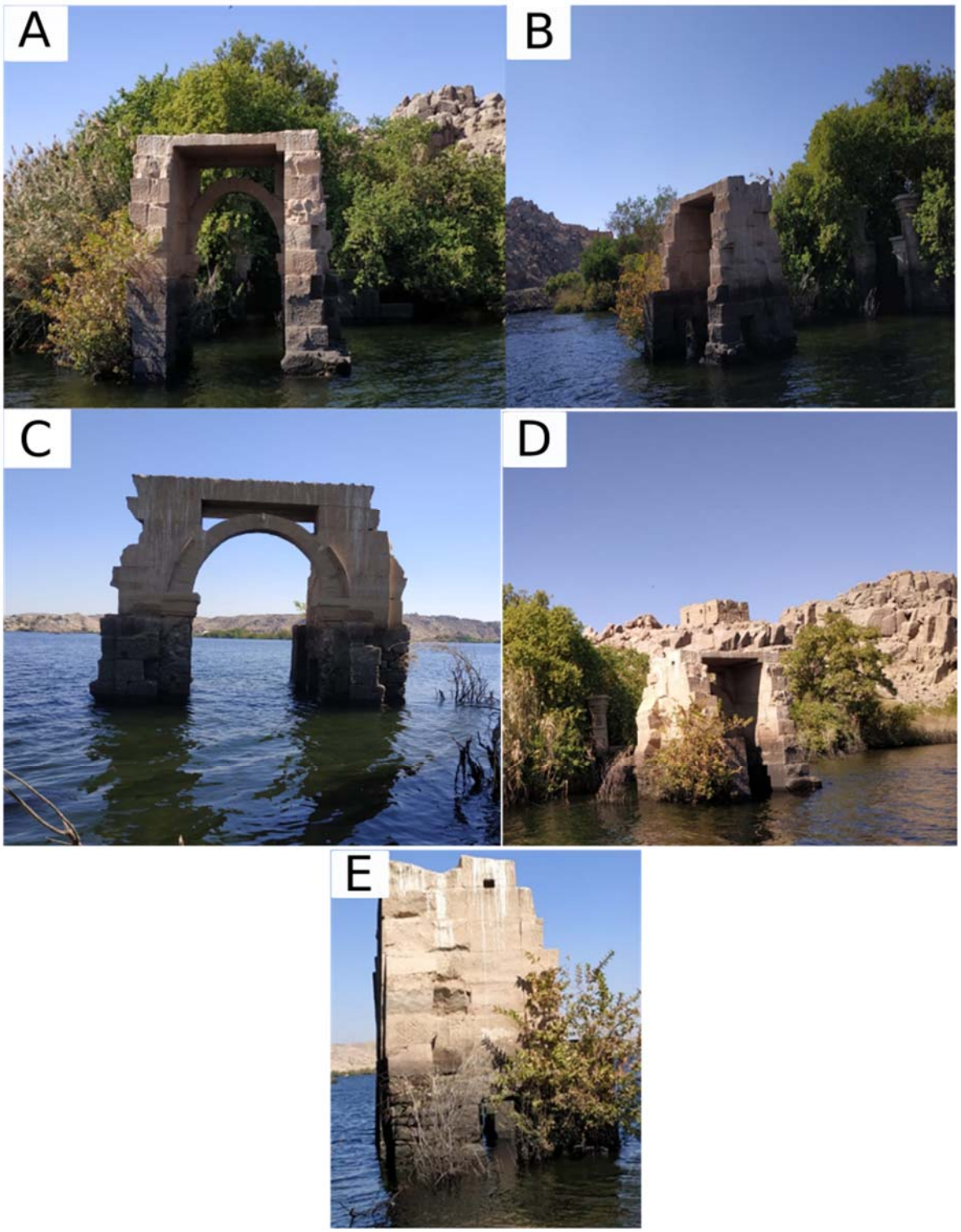


SM2. Fig. 1. Digital elevation model and geomorphological features for Aswan as well as it shows Nubian sandstone formations such as Kurkur formation, the blue dotted circle represents the surrounding area of Osiris temple. From Khedr et al**. (2010)**[1].

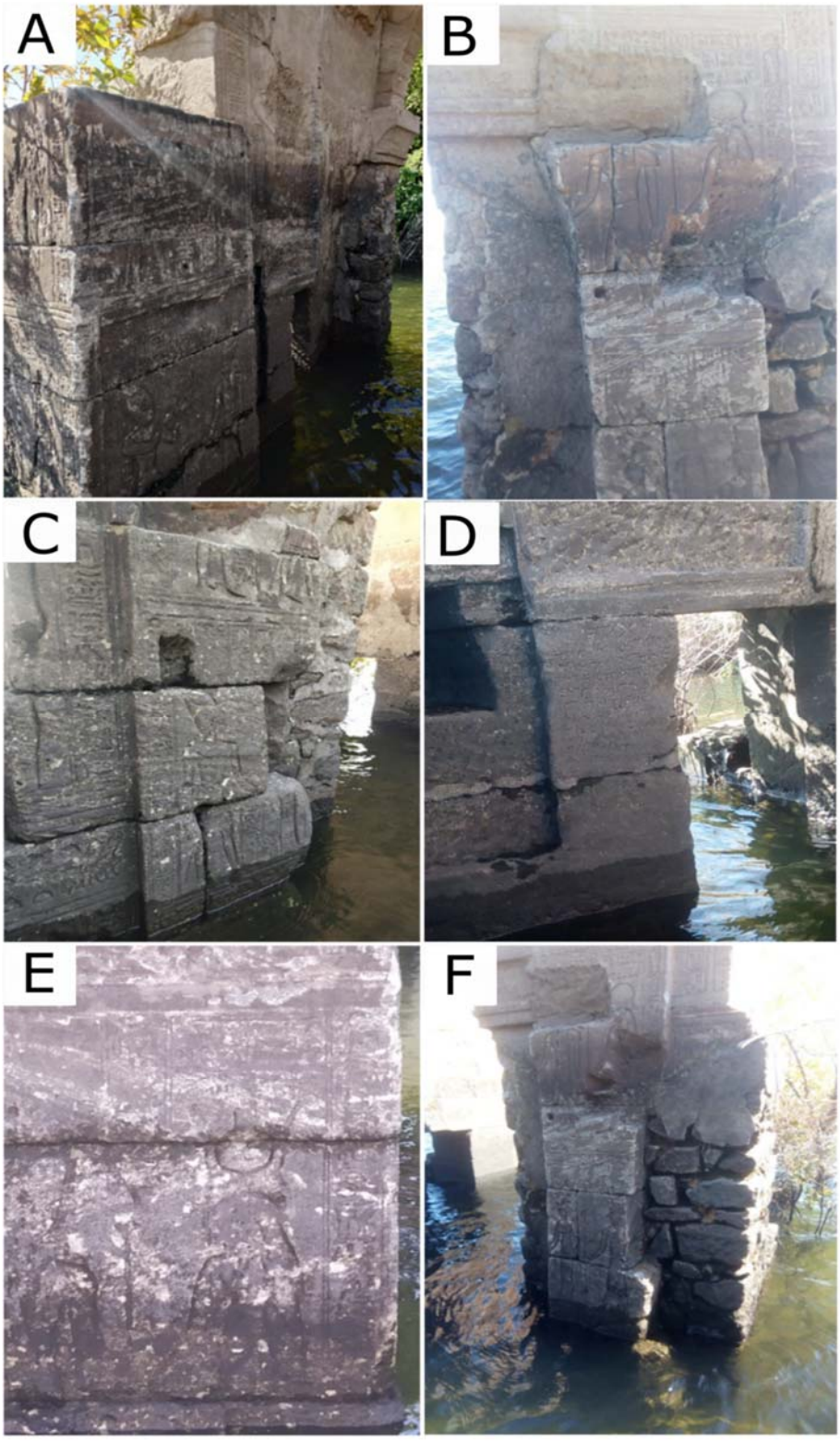
[1] Khedr, E. S., Yousef, A. A. E., Abou Elmagd, K., & Khozyem, H. M. (2010). Tectono-stratigraphic subdivision of the clastic sequence of Aswan area, southern Egypt. *Fifth International Conference on the Geology of the Tethys Realm, South Valley University*, *January*, 197–216.



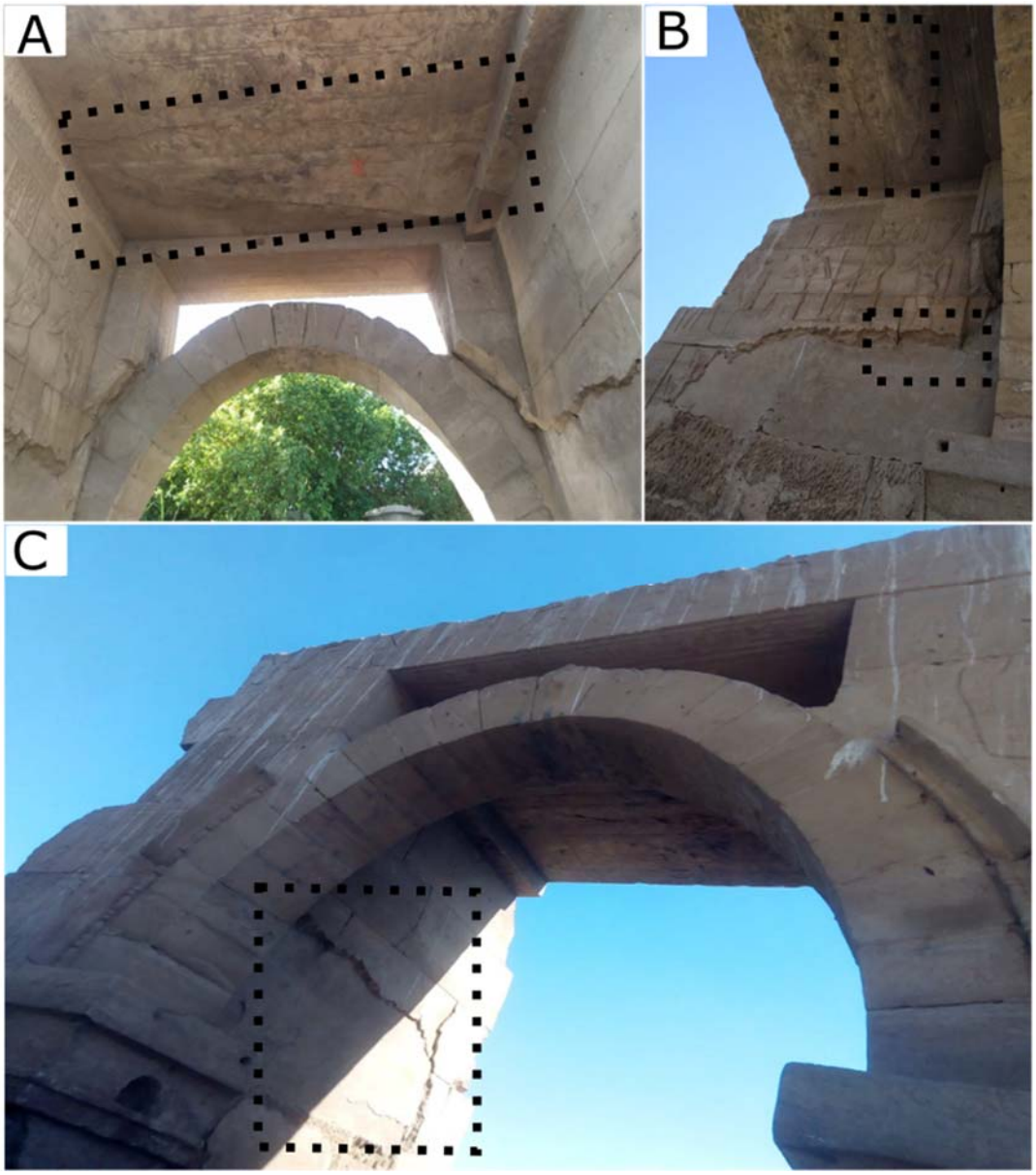
SM2. Fig. 2. Osiris Temple (the Abaton) current plan. Those drawn remains are underwater and some parts above the water. A, B and C represent columns.



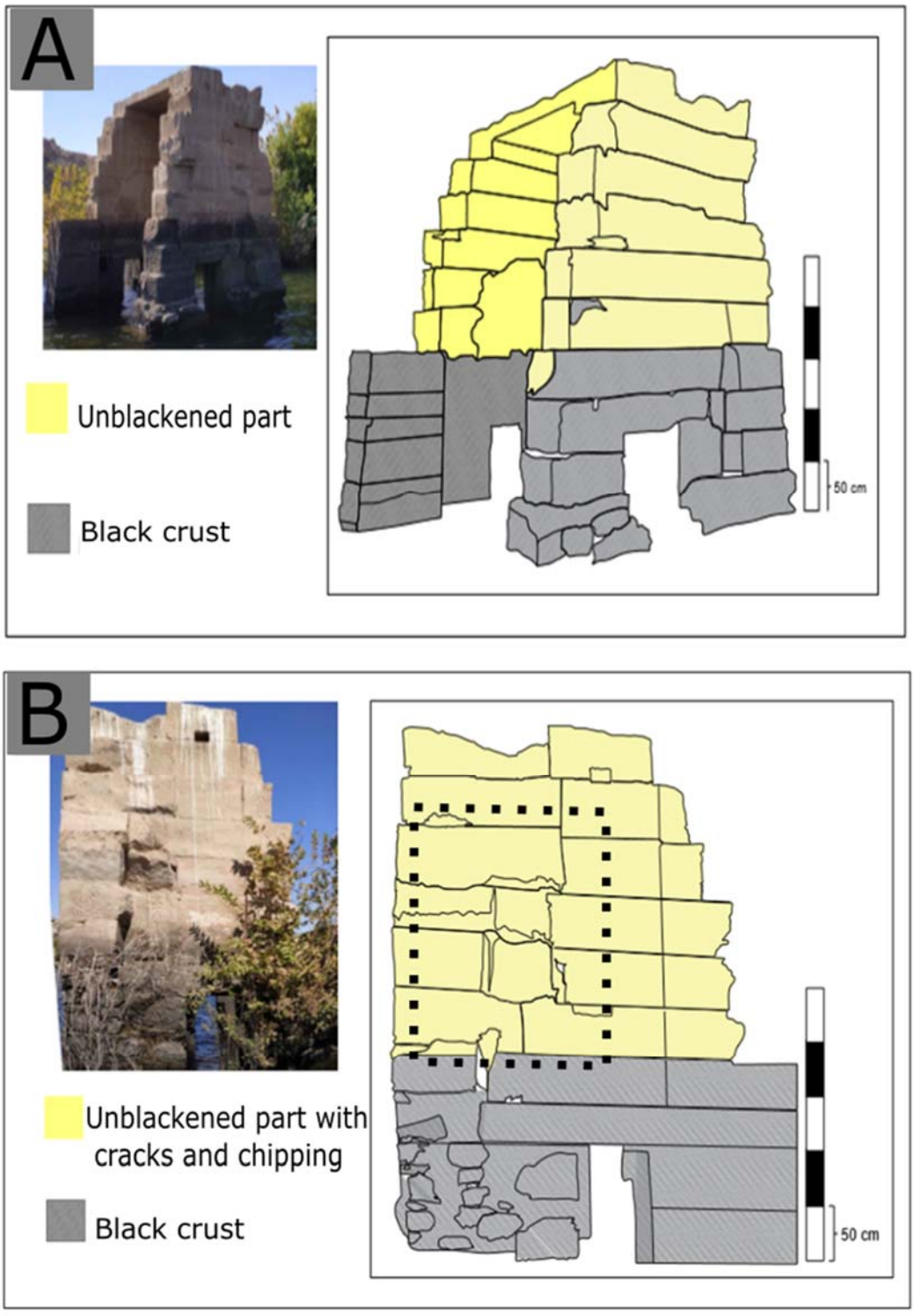
SM2. Fig. 3 (A-E) General views for the Osiris temple and surrounding environment.



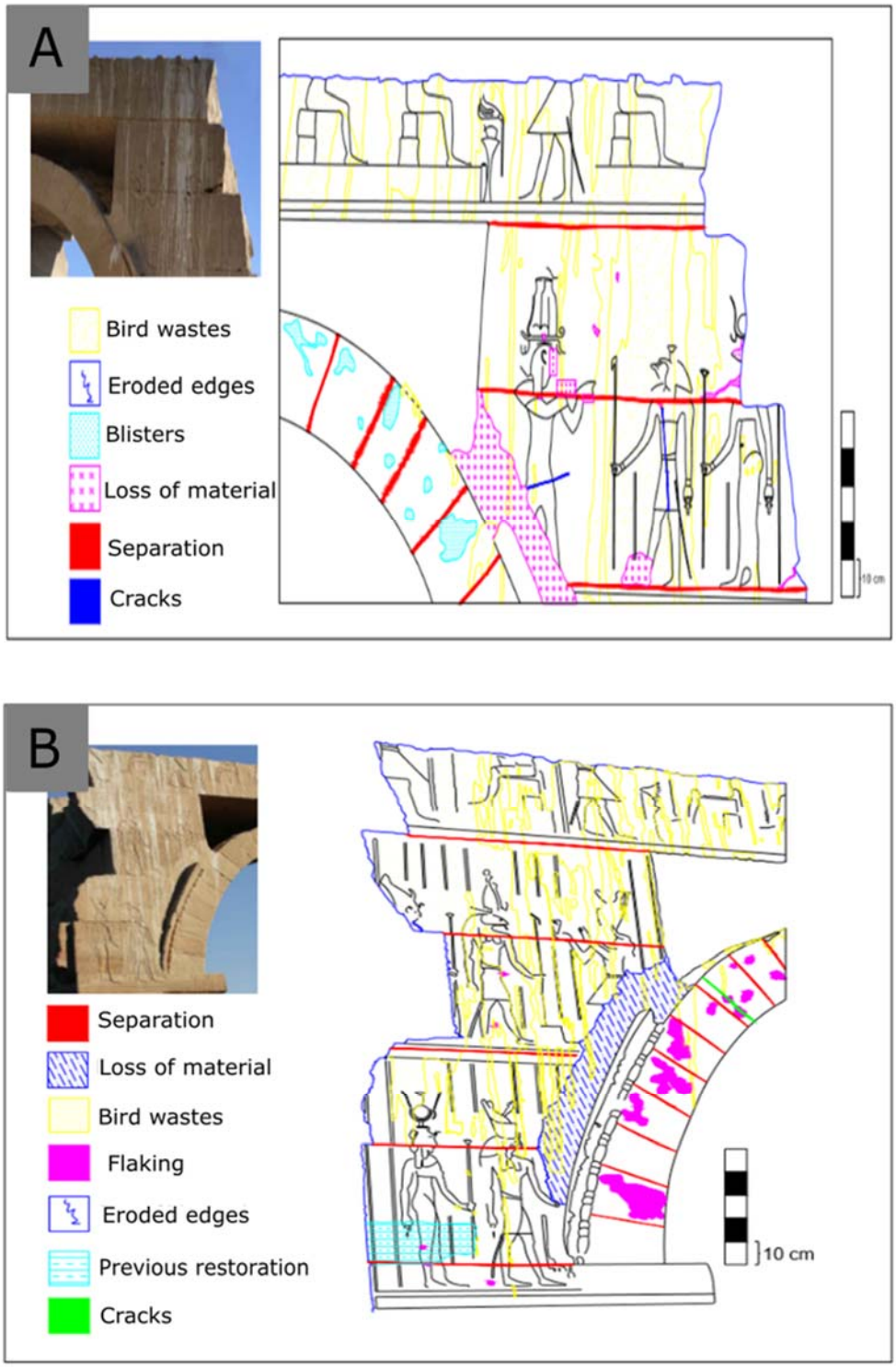
SM2. Fig. 4. Different photographs document the dominant black crust and general decay state of Osiris temple stone surfaces.



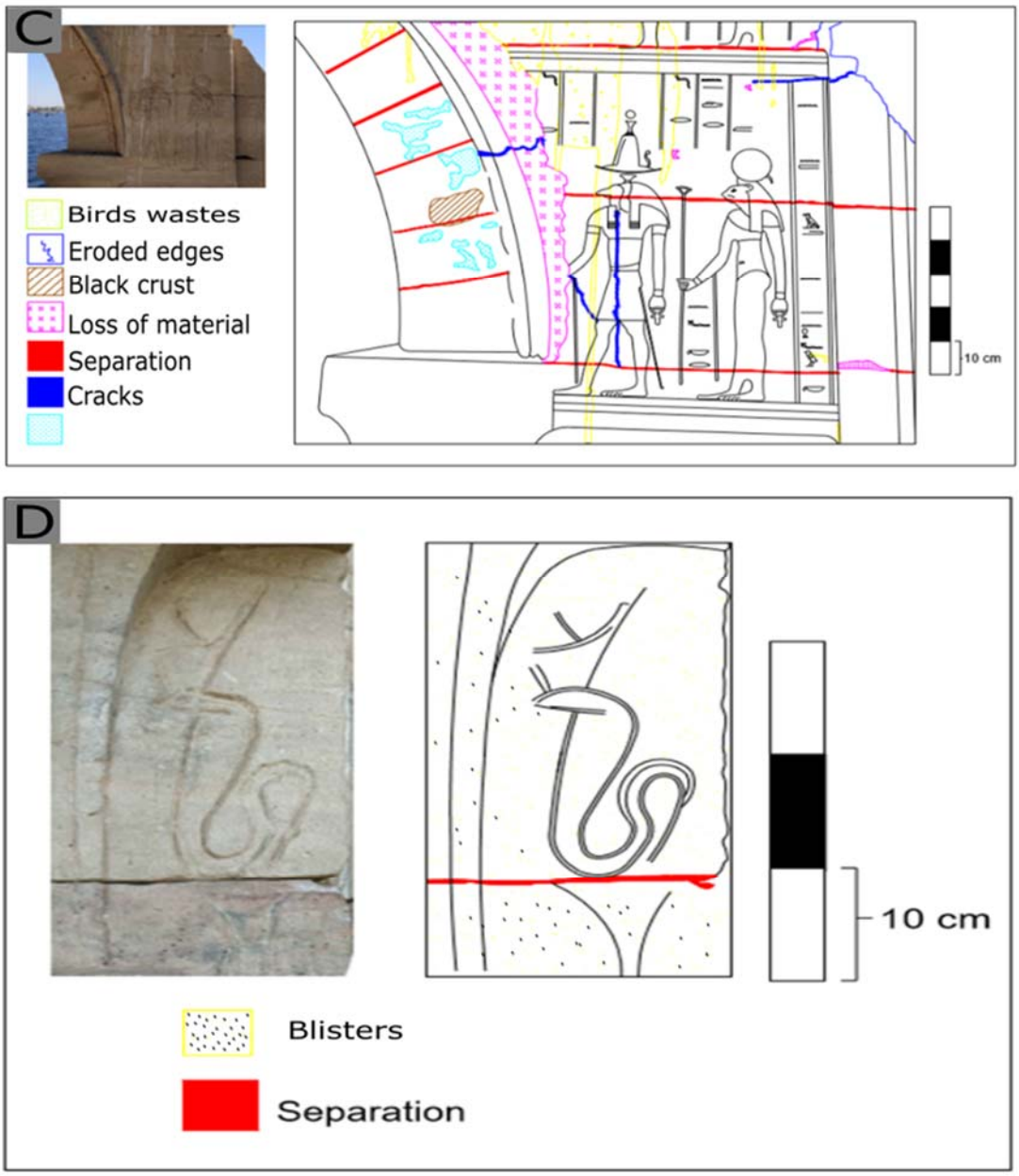
SM2. Fig. 5. Different photographs document the structural instability of the temple (Structural cracks in black rectangular patches).



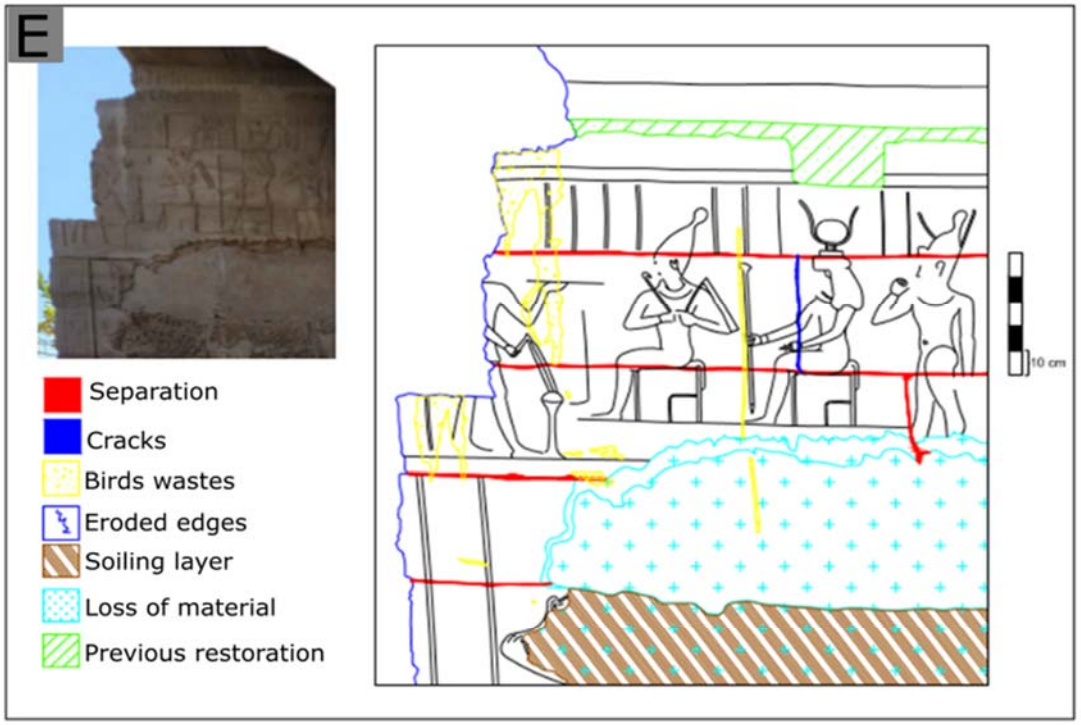
SM2. Fig. 6. (A and B) General sketches of preservation state for Osiris Temple.

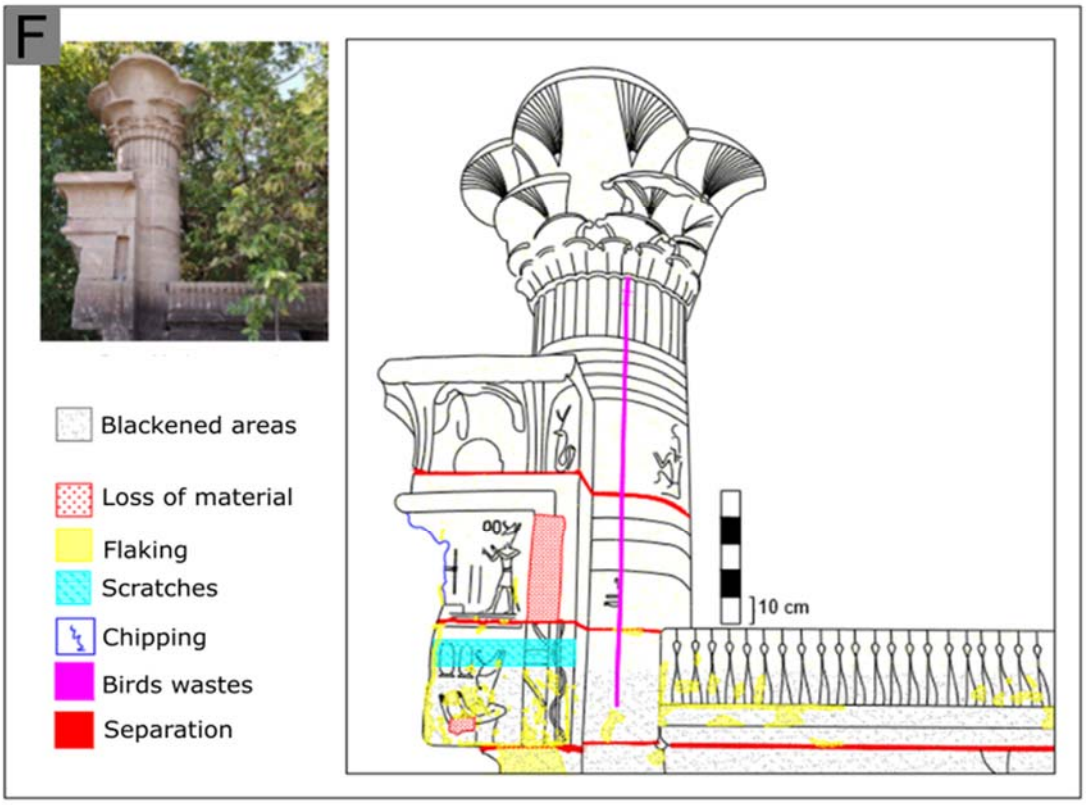


SM2. Fig. 7. (A-B) the detailed degradation patterns and problems for building materials of the Osiris temple. Each figure has its own scale and legend.

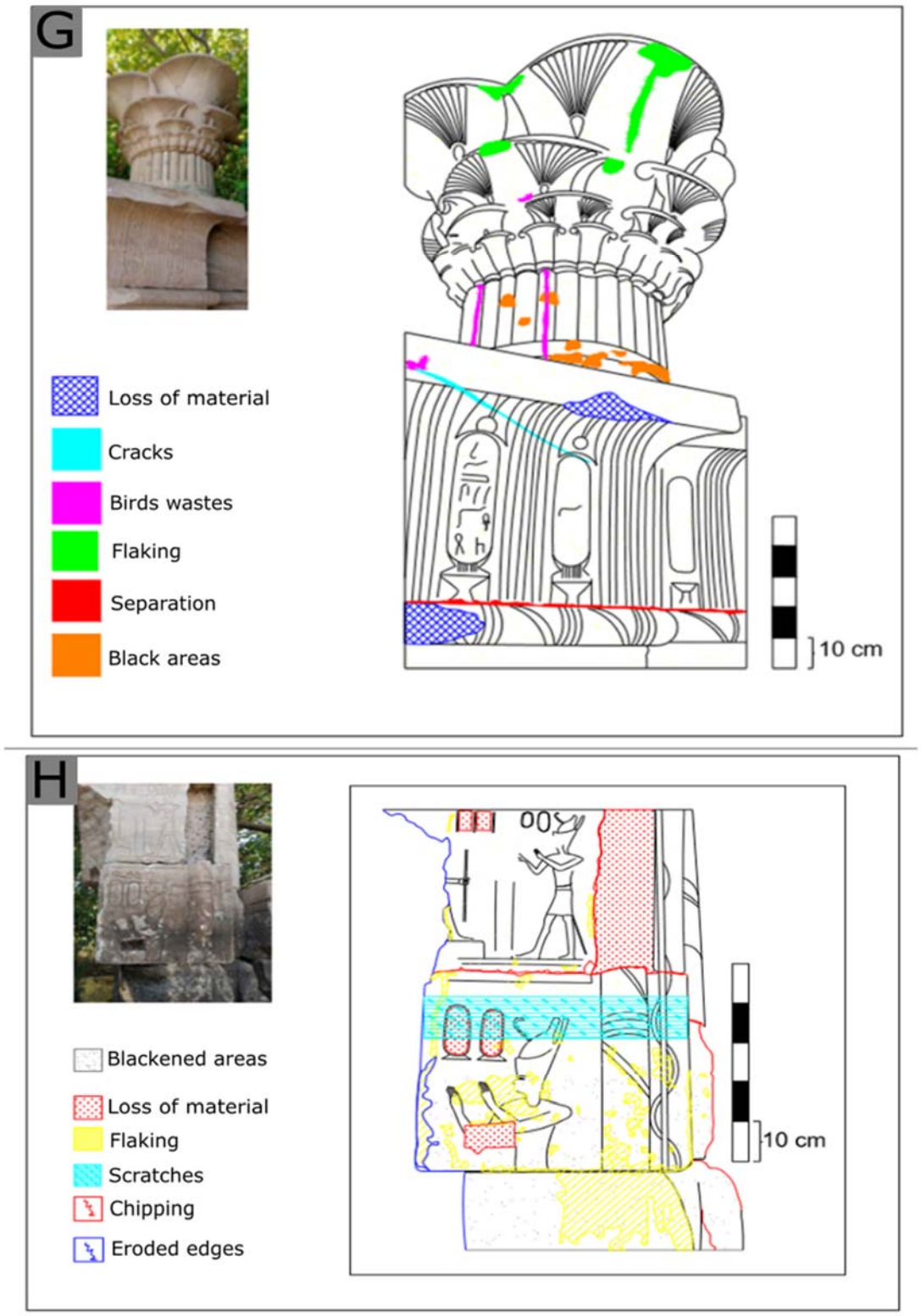


SM2. Fig. 7. (C and D) Cont.

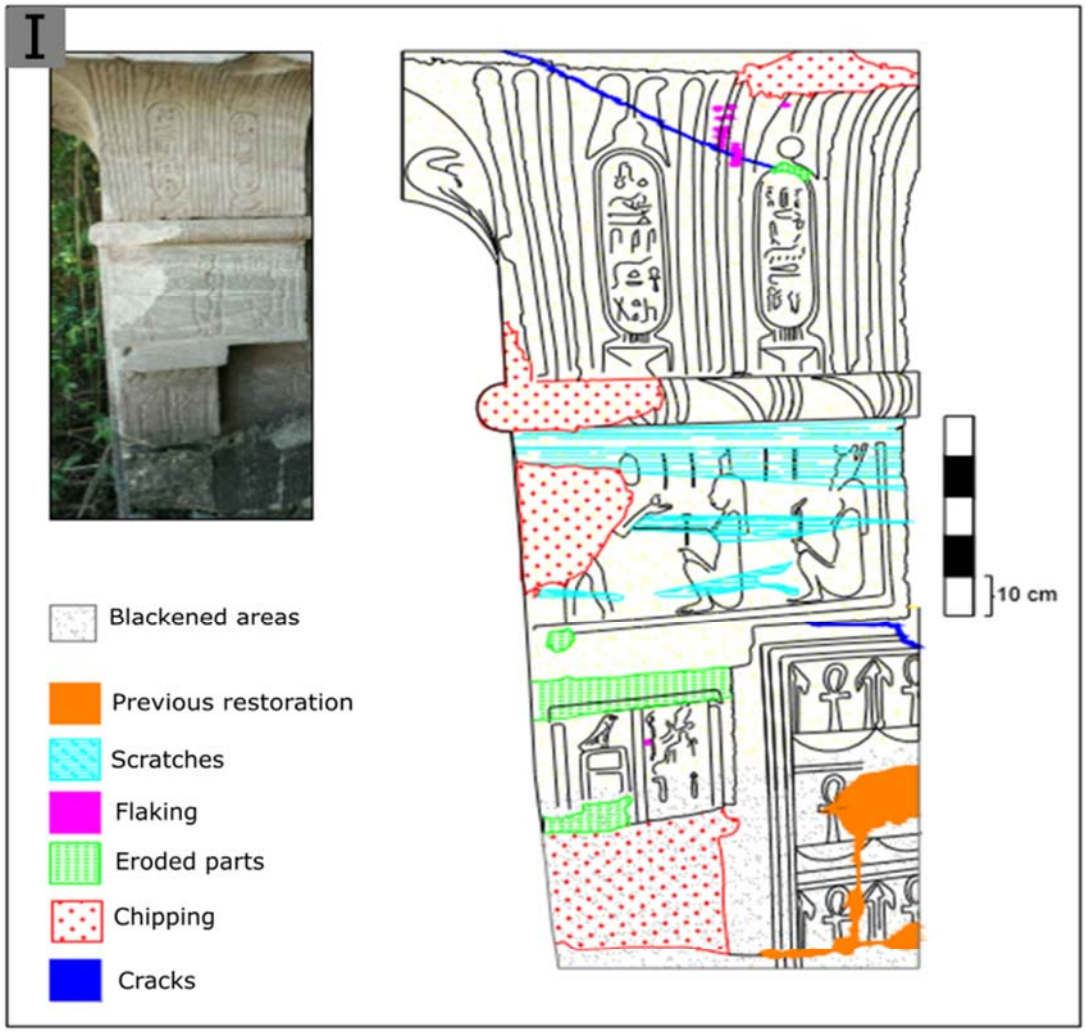


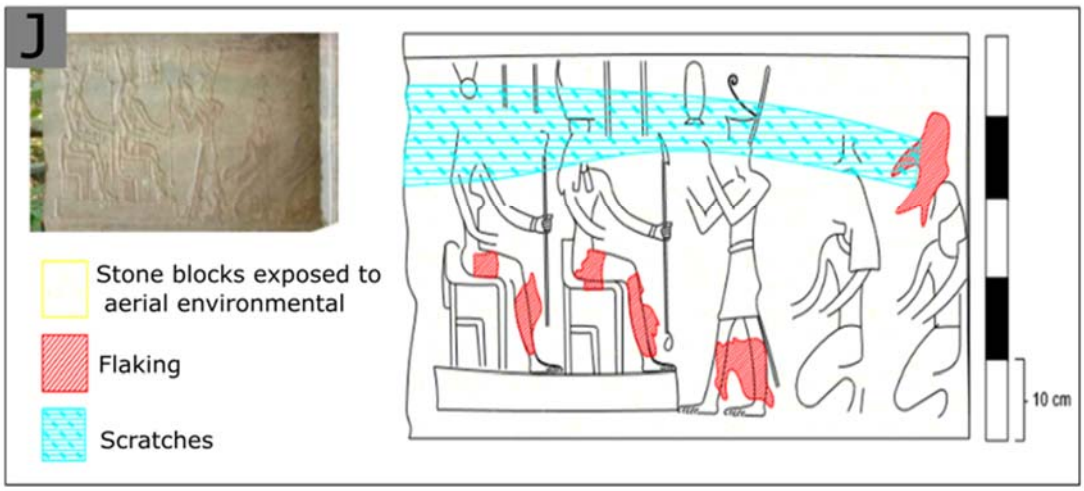


SM2. Fig. 7. (E and F) Cont.

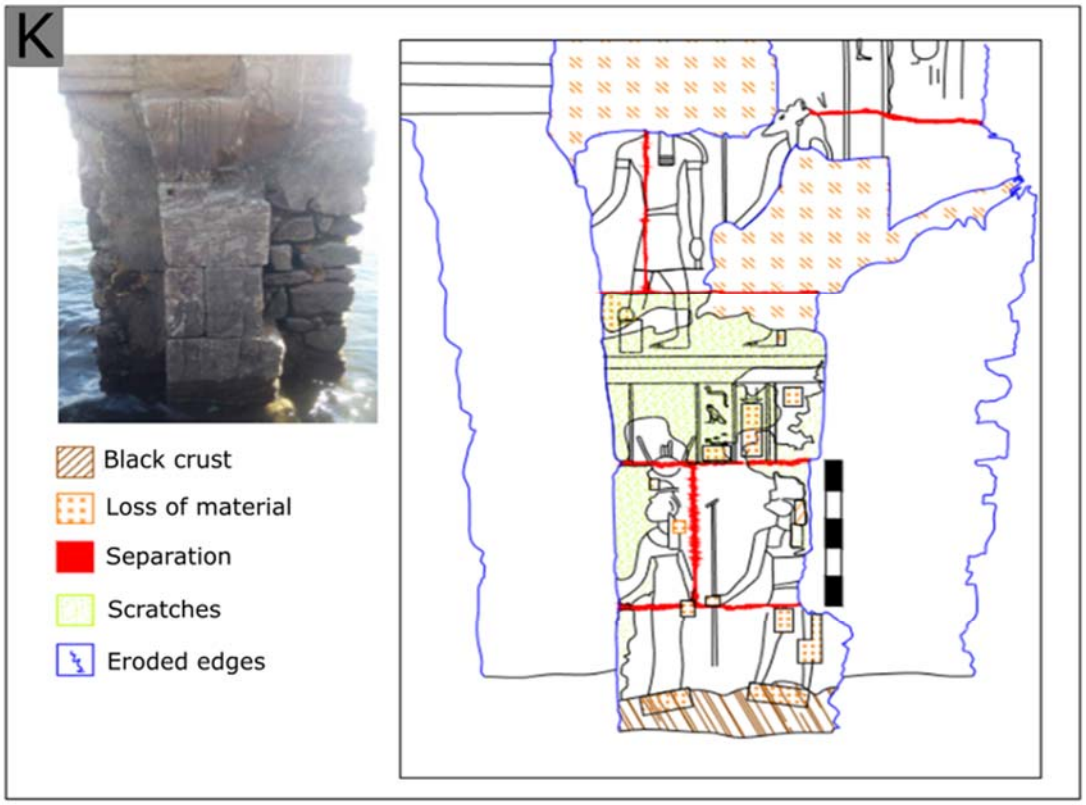


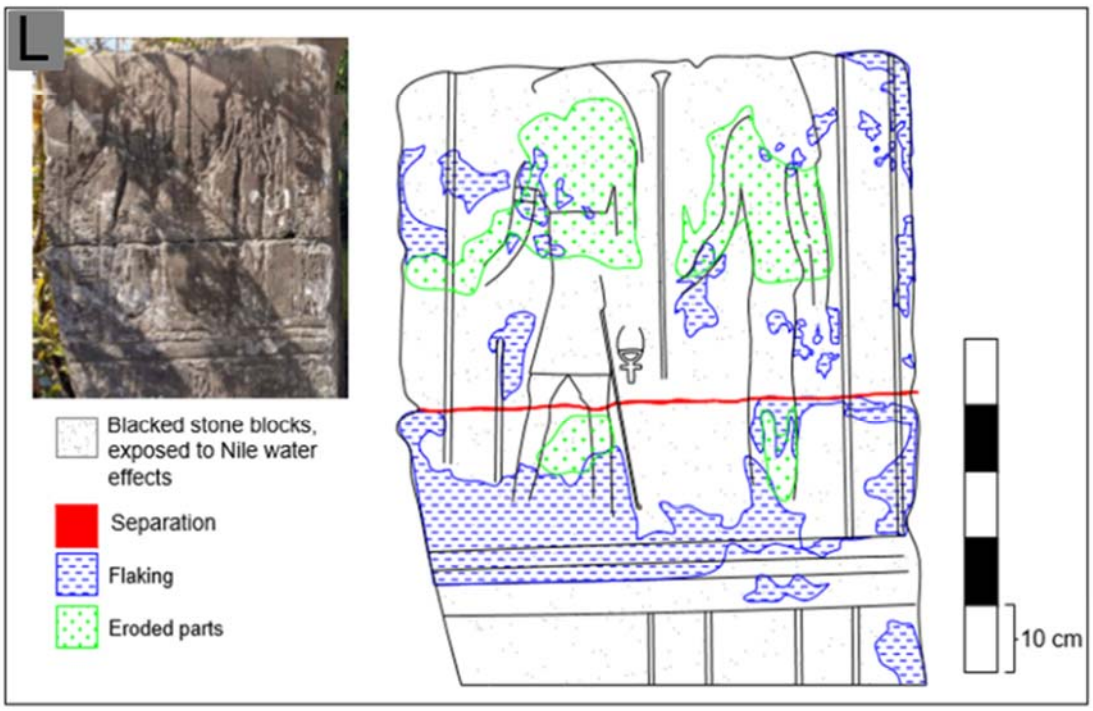
SM2. Fig. 7. (G and H) Cont.



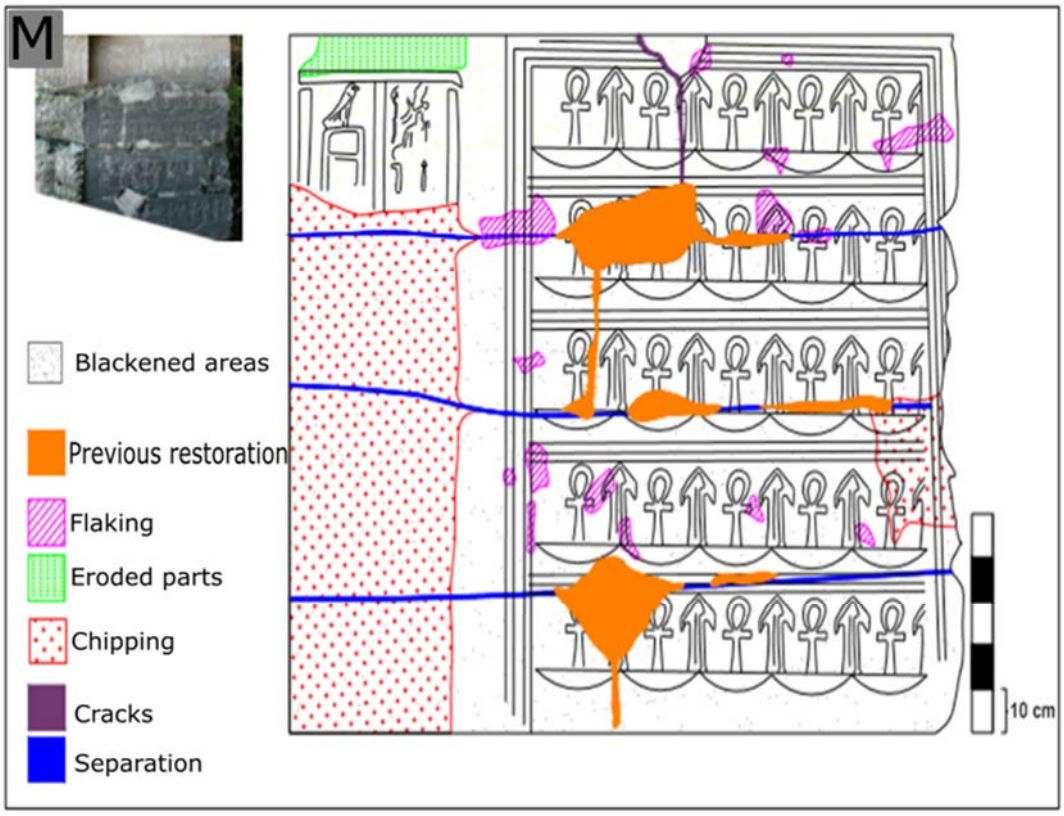


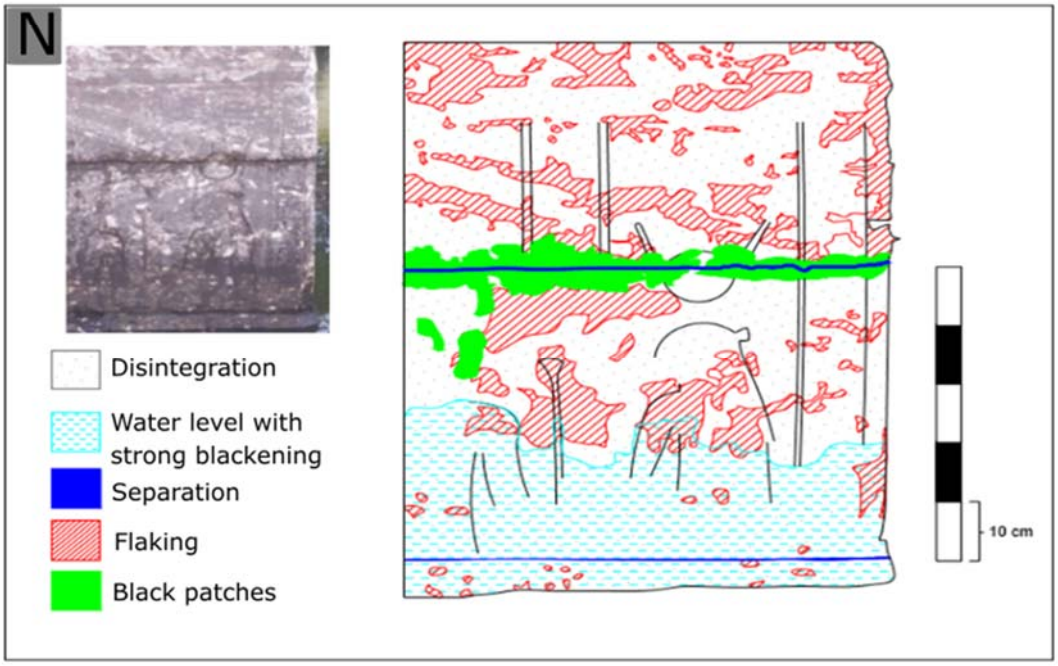
SM2. Fig. 7. (I and J) Cont.



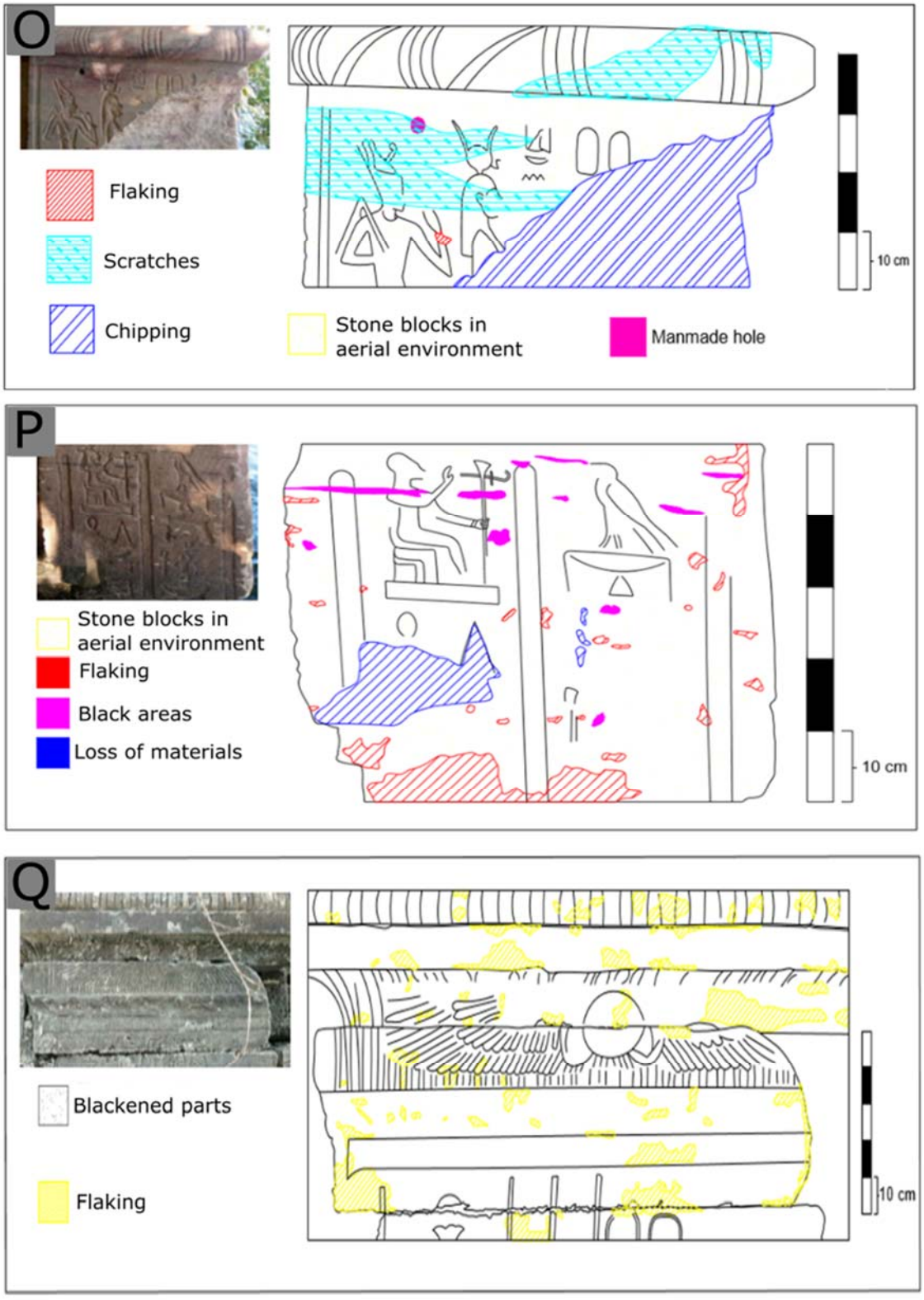


SM2. Fig. 7. (K and L) Cont.

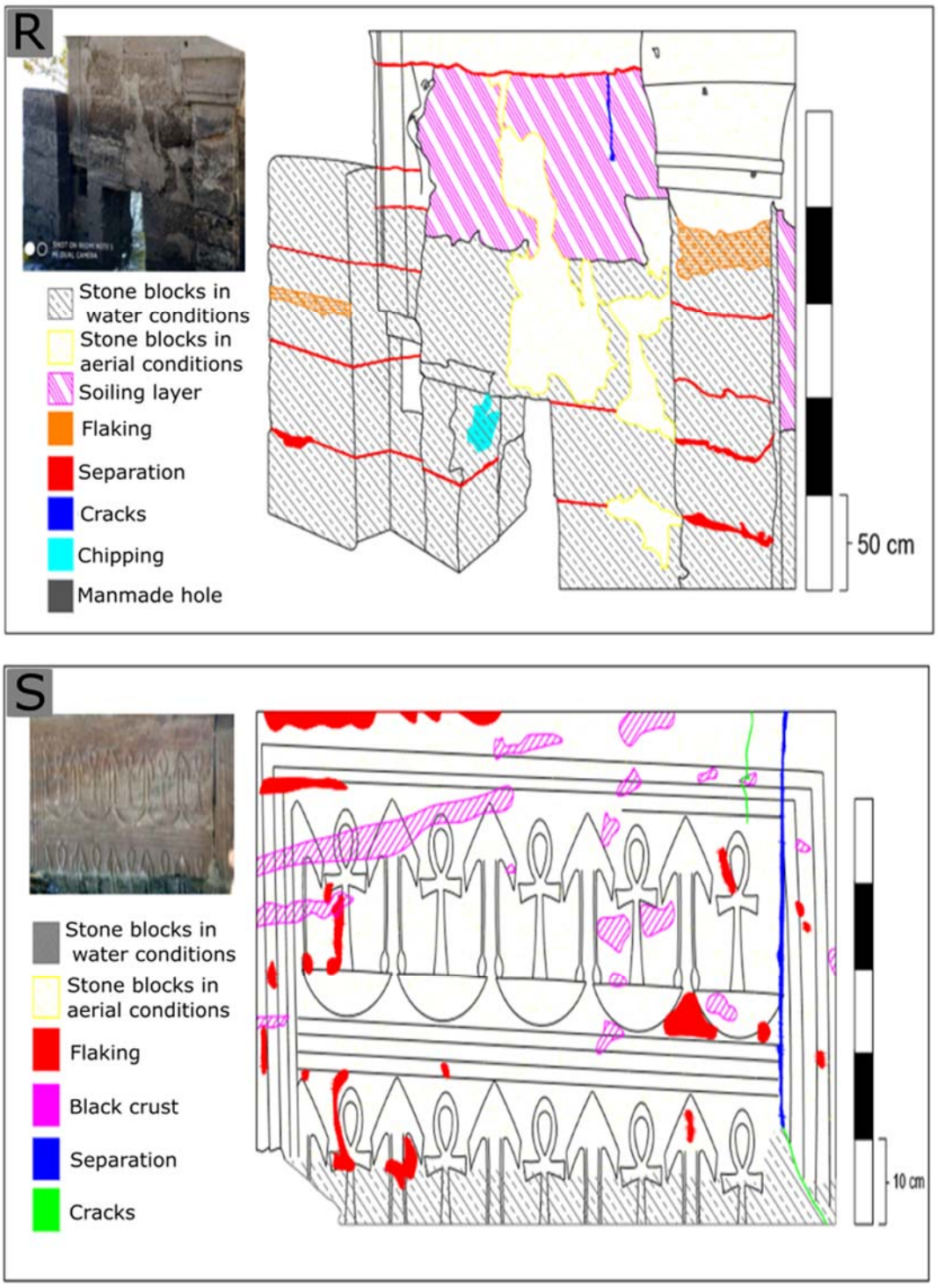




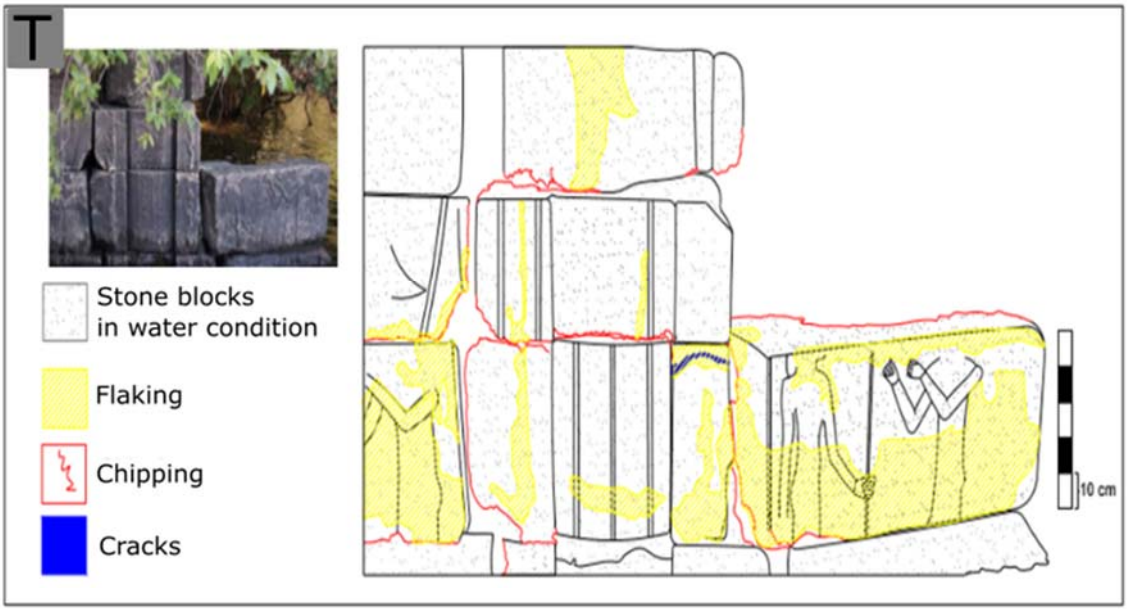
SM2. Fig. 7. (M and N) Cont.

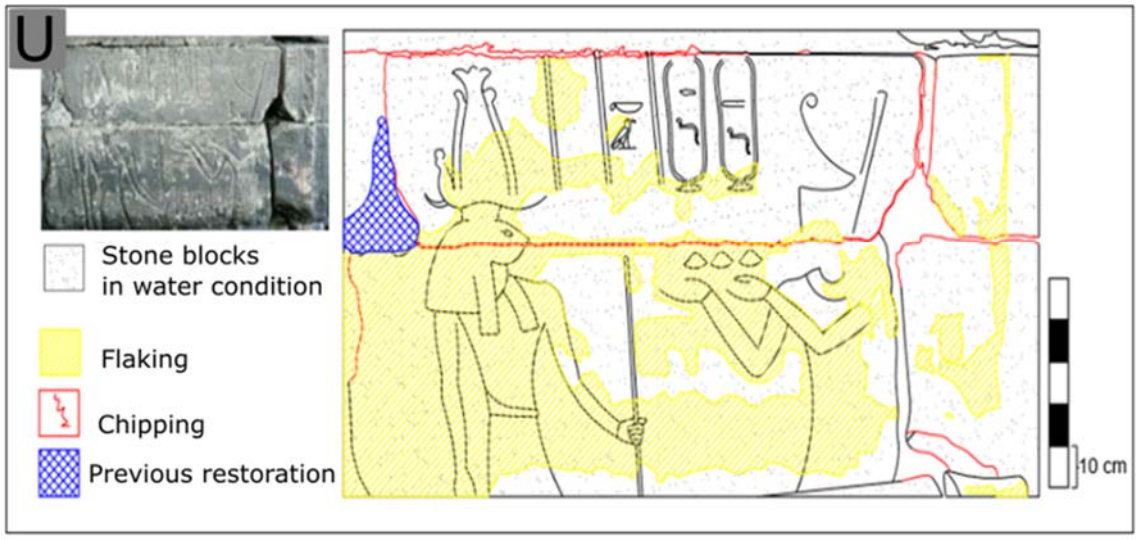


SM2. Fig. 7. (O-Q) Cont.



SM2. Fig. 7. (R and S) Cont.





SM2. Fig. 7. (T and U) Cont.

Annex 3: Scientific activities (Publications, conferences, fieldwork, workshops and courses)

DOCUMENTO DE ACTIVIDADES FORMATIVAS DE DOCTORADO
(Estudios regulados por R.D. 99/2011 de 28 de Enero)

EIDEMAR, Escuela Internacional de Doctorado en Estudios del Mar

Estudiante:	**A20325343 D. ABDELRHMAN MUHAMED FAHMY SAYED AHMED**
Programa de Doctorado:	**8207 - Historia y Arqueología Marítimas**
Título de la tesis:	**Durability problems of the archaeological construction materials in aqueous and subaerial environments, with applications for restoration and conservation in Egypt and Sudan // Problemas de durabilidad de los materiales de construcción arqueológicos en ambientes acuosos y subaéreos, con aplicaciones a la restauración y conservación en Egipto y Sudán**
Director(es):	**DOMINGUEZ BELLA, SALVADOR** **MOLINA PIERNAS, EDUARDO**

De conformidad con la instrucción UCA/ I04VP/2015, de 30 de abril de 2015, del Vicerrector de Planificación de la Universidad de Cádiz, por la que se desarrolla el procedimiento para el depósito y la defensa de la tesis doctoral en la Universidad de Cádiz, se pone a disposición de los miembros del tribunal el Documento de Actividades Formativas de D. ABDELRHMAN MUHAMED FAHMY SAYED AHMED para su conocimiento con carácter previo a la evaluación de su tesis doctoral.

Actividad formativa: 8207B01 Publicaciones o artículos científicos

Tipo: **Obligatoria (mínimo 200.00 h.)** Horas realizadas:**500.00 h.** **Actividad superada**

Curso	Descripción	Documento justificativo	Horas
2021/22	1. Article published in springer nature	s40494-022-00699-1.pdf	100.00
2021/22	2. Article published in springer nature 2022	s40494-022-00759-6_4_.pdf	100.00
2021/22	Attached cover of new book archaeological conservation science	cover_of_the_book.pdf	100.00
2022/23	New article published	minerals-12-01235.pdf	100.00
2022/23	New publication in elsevier	1- s2.0- S1296207422001741- main.pdf	100.00

Actividad formativa: 8207B02 Cursos de formación o especializados de investigación

Tipo: **Obligatoria (mínimo 100.00 h.)** Horas realizadas:**969.00 h.** **Actividad superada**

Curso	Descripción	Documento justificativo	Horas
2021/22	A2- ESPANOL LENGUA	A2- ESPANOL_LENGUA.pdf	180.00
2021/22	B2-1 ESPANOL LENGUA	Espanol_B2.1.pdf	90.00
2021/22	"Búsqueda, gestión y comunicación de la información científica"	A20325343_112918.pdf	35.00
2021/22	Caree development for doctoral students _ activity _SEA EU	Screenshot_20210614_170028.pdf	40.00
2021/22	Certificate of attendance, jornada de Egiptología, Sevilla	Abdelrahman.pdf	13.00
2021/22	Certificate of attendance - Paper Writing Academy	SEA- EU_certificate_PaperWritingAcademy_...pdf	90.00
2021/22	Course at Kiel University.. Slidewriting	Certificate_Slidewriting_Storylining_Fa...PDF	8.00
2021/22	Curso básico de SIG y Teledetección aplicados a la gestión de pr	A20325343_112460gis.pdf	40.00
2021/22	Curso intensivo: Estrategia y Responsabilidad Social Corporativa	CERTIFICADO_ABDELRHMAN_MUHAMED.pdf	3.00
2021/22	De Egipto a Gadir. Arte y rituales en el mundo antiguo	Muhamad_Fahmy_Sayed_Ahmed_Abdelrhman_RF...pdf	10.00
2021/22	El primer nivel del curso de español A1	WhatsApp_Image_2021-01-14_at_12.02.26.pdf	180.00
2021/22	"Iniciación a los Estudios de Doctorado (Modalidad no presencial	A20325343_114606.pdf	25.00
2021/22	"Jornada de Recepción para nuevos doctorandos UCA" (8200T009_vir	A20325343_112425_journada.pdf	5.00
2021/22	"Jornadas Doctorales específicas (Artes y Humanidades)" (8201P04	1.pdf	20.00
2021/22	La erosión costera: efectos en el litoral y modalidades de respu	A20325343_125060.pdf	25.00
2021/22	Neuvas tecnologías en arqueología... Curso	nuevas_tecnologA_as_.pdf	50.00
2021/22	Seminario de Metodología de la Investigación en Artes y Humanida	A20325343_113551.pdf	50.00
2021/22	"VI JORNADAS DOCTORALES EIDEMAR (CON SALIDA DE CAMPO)" (8200P004	2.20210118132116.pdf	15.00
2022/23	Nivel B2.2 ESPANOL	Spanish_lang_B2.2.pdf	90.00

DAF10919100230126d99118030.1/2 Pág. 1 de 2

Actividad formativa: 8207P03 Asistencia y participación en congresos y workshops

Tipo: **Optativa** Horas realizadas:**225.00 h.** **Actividad superada**

Curso	Descripción	Documento justificativo	Horas
2021/22	Attendance certificate for scientific session	C5156.pdf	25.00
2021/22	Attendance certificate for scientific session	C4171.pdf	25.00
2021/22	Attendance certificate for session for international protection	C2033.pdf	25.00
2021/22	Attending workshop In how to get benefits from open access journ	C2810.pdf	25.00
2021/22	certificado de reconocimiento y asistencia a una conferencia sob	Certificate1-34- converted.pdf	25.00
2021/22	confirmation of attendance of international congress(Warsaw)	confirmation_of_attendance_Abdelrhman_M...pdf	50.00
2021/22	Speaker at Warsw Conference on Sudan studies	Letter_Mr._Abdelrhman_Fahmy.pdf	50.00

Actividad formativa: 8207P04 Movilidad y estancias de investigación

Tipo: **Optativa** Horas realizadas:**2025.00 h.** **Actividad superada**

Curso	Descripción	Documento justificativo	Horas
2021/22	ERASMUS KA107 SMS entre la universidad de el cairo y la univers	informe_movilidad_EG_ABDELRHMAN_MUHAMED...pdf	450.00
2021/22	Estancia 3 meses en Polonia- Ersamus	Esctancia_Polonia.pdf	450.00
2021/22	Estancia un mes en Polonia de SEA- EU	CERTIFICADOS_PARTICIPANTES_Abdelrhman.pdf	150.00
2021/22	Research stay at Sofía University, Bulgaria	IMG_20210725_160504.pdf	450.00
2022/23	Certificado de estancia en Reino Unido, Universidad de Leicester	Leicester_University_research_stay_.pdf	525.00

Actividad formativa: 8207P06 Colaboraciones en la organización de reuniones y eventos científicos

Tipo: **Optativa** Horas realizadas:**20.00 h.** **Actividad superada**

Curso	Descripción	Documento justificativo	Horas
2021/22	Editing and marketing comiitee member at ASE	Screenshot_20210114_001143.pdf	20.00

Actividad formativa: 8207P08 Participación en campañas o actividades arqueológicas

Tipo: **Optativa** Horas realizadas:**40.00 h.** **Actividad superada**

Curso	Descripción	Documento justificativo	Horas
2021/22	Participation in Archeological campaign	IMG_20210529_100526_1_.pdf	40.00

Actividad formativa: 8207P11 Aprendizaje de la aplicación GIS en el análisis de los paisajes

Tipo: **Optativa** Horas realizadas:**40.00 h.** **Actividad superada**

Curso	Descripción	Documento justificativo	Horas
2021/22	Curso básico de SIG y Teledetección aplicados a la gestión de pr	8205001_20_21_02_Calificaciones_Finales.pdf	40.00

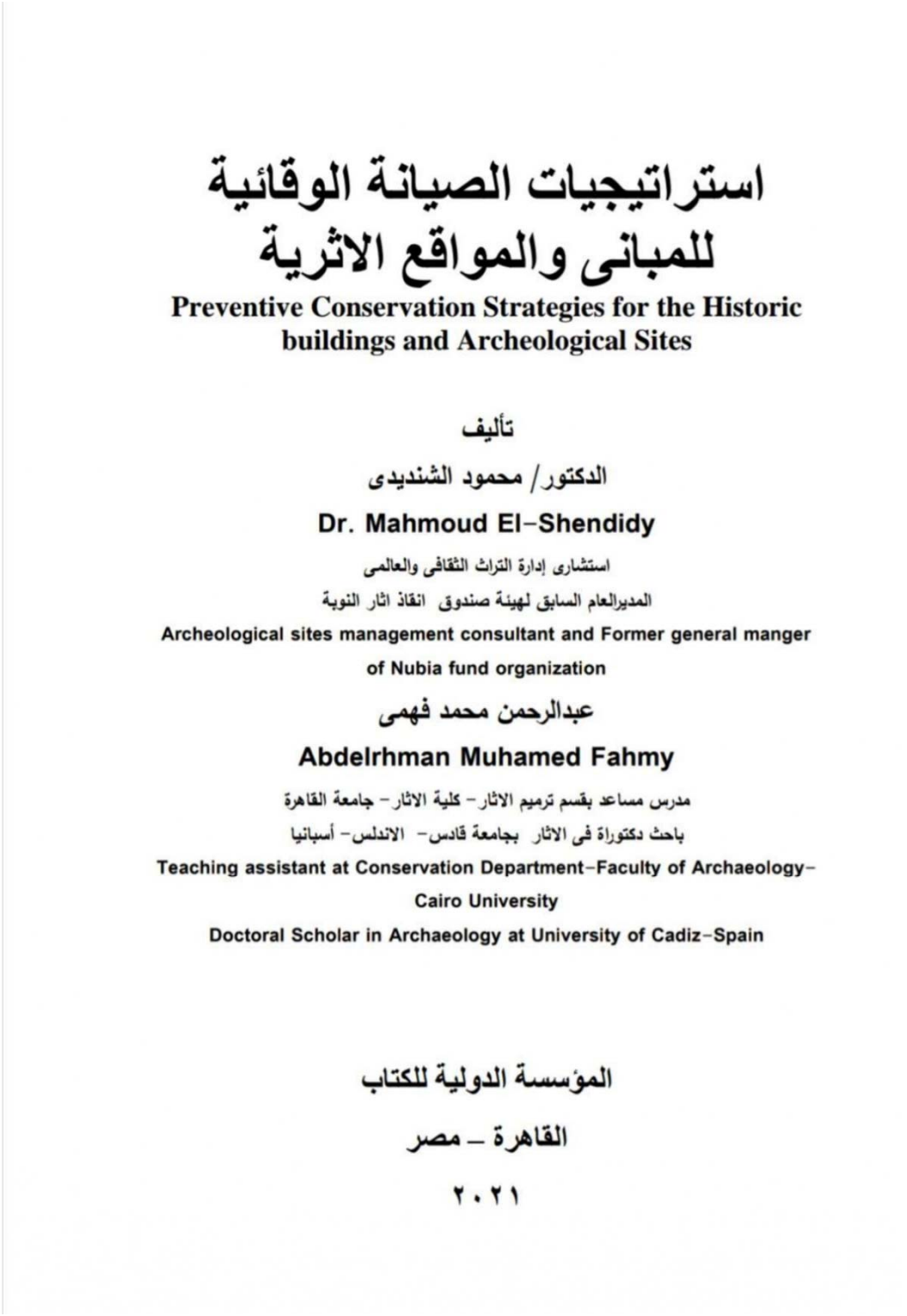
Total horas actividades formativas completadas: 3819.00

El estudiante ha completado todos los requisitos de su plan de estudios para la superación de las actividades formativas.

Cádiz, a 19 de enero de 2023

DAF10919100230126d99118030.2/2 Pág. 2 de 2

3.1 Published book in Arabic language and titled (Preventive Conservation Strategies for the historic Buildings and Archaeological Sites). The book cover is attached as follows:



استراتيجيات الصيانة الوقائية للمبانى والمواقع الاثرية

Preventive Conservation Strategies for the Historic buildings and Archeological Sites

تأليف

الدكتور/ محمود الشنديدى

Dr. Mahmoud El-Shendidy

استشارى إدارة التراث الثقافى والعالمى

المديرالعام السابق لهيئة صندوق انقاذ اثار النوبة

Archeological sites management consultant and Former general manger of Nubia fund organization

عبدالرحمن محمد فهمى

Abdelrhman Muhamed Fahmy

مدرس مساعد بقسم ترميم الاثار - كلية الاثار - جامعة القاهرة

باحث دكتوراة فى الاثار بجامعة قادس- الاندلس- أسبانيا

Teaching assistant at Conservation Department-Faculty of Archaeology-Cairo University

Doctoral Scholar in Archaeology at University of Cadiz-Spain

المؤسسة الدولية للكتاب

القاهرة – مصر

٢٠٢١


استراتيجيات الصيانة الوقائية
للمباني والمواقع الاثرية
Preventive Conservation Strategies
For the Historic Buildings and Archeological Sites
تأليف
الدكتور/ محمود الشنديدي
عبد الرحمن محمد فهمي
2021
International foundation
For monuments
الوقاية خير من العلاج
المؤسسة الدولية للكتاب
Mohamedabdelazem2013@yahoo.com

الكتاب: استراتيجيات الصيانة الوقائية للمبانى والمواقع الاثرية
تأليف – د / محمود الشنديدى - عبدالرحمن محمد فهمى
الناشر: المؤسسة الدولية للكتاب

حقوق النشر محفوظة للمؤسسة الدولية للكتاب، ولا يجوز نشر أي جزء من هذا الكتاب أو اختزان مادته بطريقة الاسترجاع أو نقله على أي نحو أو بأية طريقة سواء كانت الكترونية أو ميكانيكية أو خلاف ذلك إلا بموافقة الناشر على هذا كتابة ومقدماً

رقم الايداع: ٢٢٤٨٦ / ٢٠٢٠
الترقيم الدولى: ٥ - ٢١ - ٦٨٠٩ - ٩٧٧ - ٩٧٨

الطبعة الأولى ٢٠٢١



الناشر : المؤسسة الدولية للكتاب
٧٠ شارع الصفا والمروة – الطوابق – فيصل– الجيزة – مصر .
موبايل : ٠٠٢٠١٠٠١٤٥٢٦٩٦ – ٠٠٢٠١٠٠٢٣٧٠٩٣٤
ت.ف / ٠٠٢٠٢٣٣٨٨٤٧٨

3.2 Conferences

CENTRUM ARCHEOLOGII ŚRÓDZIEMNOMORSKIEJ
UNIWERSYTETU WARSZAWSKIEGO

POLISH CENTRE OF MEDITERRANEAN ARCHAEOLOGY
UNIVERSITY OF WARSAW

Warsaw, June 23rd, 2022

To Whom It May Concern:

From 29th August to 4th September 2022, the Polish Centre of Mediterranean Archaeology of the University of Warsaw will be hosting the 15th International Conference for Nubian Studies (https://nubianstudies2022.uw.edu.pl). The conference is a quadrennial meeting of archaeologists, historians, anthropologists and scholars working on the cultural heritage of ancient and modern Nubia, Egypt and Sudan.

We attest that the participation of Abdelrhman Muhamed Fahmy Sayed Ahmed has been accepted by the organizing committee and we anticipate that his contribution will be a valuable asset to the success of the event.

Full name Abdelrhman Muhamed Fahmy Sayed Ahmed

Date of birth 08.03.1993

Place of birth Giza

Nationality Egyptian

Passport number A20325343

Place of residence Egypt

In case of any questions, please do not hesitate to contact us by writing to nubianstudies2022@uw.edu.pl

With kind regards,

Centrum Archeologii Śródziemnomorskiej
Uniwersytetu Warszawskiego

Artur Obłuski

pcma@uw.edu.pl
00-838 Poland, Warszawa, ul. Prosta 69
T (+48 22) 553 13 28, 826 52 16
Fx (+48 22) 628 45 23

cairo.pcma@uw.edu.pl
Research Centre in Cairo
Cairo–Heliopolis, Egypt
11, Mahalla T (+202) 22 904 459
14, Nazih Khalifa T (+202) 24 159 898

www.pcma.uw.edu.pl
NIP 525-001-12-66
REGON 000001258

UNIVERSITY OF WARSAW

CENTRUM ARCHEOLOGII ŚRÓDZIEMNOMORSKIEJ
UNIWERSYTETU WARSZAWSKIEGO

POLISH CENTRE OF MEDITERRANEAN ARCHAEOLOGY
UNIVERSITY OF WARSAW

Warsaw, 20.07.2021

From:

Polish Centre of Mediterranean Archaeology
University of Warsaw

To:

Mr. Abdelrhman Fahmy
Department of Earth Sciences,
Faculty of Sciences,
University of Cadiz,
Campus Río San Pedro,
Cadiz, Spain

To Whom It May Concern,

I confirm that the proposal of podium presentation entitled 'Geo-hazards assessment for the pyramids of Meroe, Al Bagrawiya archaeological site, Sudan' submitted by Mr. Abdelrhman Fahmy has been accepted by the Organisation Committee of the Sudan Studies International Conference, Warsaw Edition. The conference will be held in the National Museum in Warsaw in 4-5.09.2021.

On behalf of the Organisation Committee,

Dr Mariusz Drzewiecki

MARIUSZ DRZEWIECKI

Elektronicznie podpisany przez MARIUSZ DRZEWIECKI
Data: 2021.07.21 13:00:59 +02'00'

pcma@uw.edu.pl
00-838 Polska, Warszawa,
ul. Prosta 69,
T (+48) 22 55 313 15,
T (+48) 22 55 313 28

cairo.pcma@uw.edu.pl
Research Centre in Cairo
Cairo–Heliopolis, Egypt
11, Mahalla T (+202) 22 904 459
14, Nazih Khalifa T (+202) 24 159 898

www.pcma.uw.edu.pl

NIP 525-001-12-66

REGON 000001258

UNIVERSITY OF WARSAW


University of Sharjah Libraries
CERTIFICATE
OF ATTENDANCE
الحماية الدولية للتراث الثقافي في زمن السلم والنزاعات المسلحة
PROUDLY PRESENTED TO
Abdelrhman Muhamed
Virtual Session - Zoom
10/4/2021
Director of the Libraries
LIBRARIES DEPARTMENT

جامعة الشارقة
UNIVERSITY OF SHARJAH

إدارة المكتبات
LIBRARIES DEPARTMENT

CERTIFICATE OF ATTENDANCE

PROUDLY PRESENTED TO

Abdelrhman Muhamed Fahmy

FOR ATTENDING

Sayed Ahmed

كيف تستفيد المكتبات الجامعية والبحثية من الوصول المفتوح للمعرفة

Virtual Session - Zoom

25-October-2021

NADIA MASOUD

DIRECTOR OF UOS LIBRARIES



UCA | Universidad de Cádiz

Durability problems of the archaeological construction materials in aqueous and subaerial environments, with applications for restoration and conservation in Egypt and Sudan

جامعة الشارقة
UNIVERSITY OF SHARJAH

إدارة المكتبات
LIBRARIES DEPARTMENT

CERTIFICATE OF ATTENDANCE

THIS CERTIFICATE IS AWARDED TO

Abdelrhman Muhamed Fahmy Ahmed

جمع وصون التراث الثقافي غير المادي

قدمها الأستاذ الدكتور عبدالعزيز المسلم

Virtual Session - Zoom

10-January-2022



NADIA MASOUD
DIRECTOR OF UOS LIBRARIES
UNIVERSITY OF SHARJAH

Certificate ID: 4171

جامعة الشارقة
UNIVERSITY OF SHARJAH

إدارة المكتبات
LIBRARIES DEPARTMENT

CERTIFICATE OF ATTENDANCE

THIS CERTIFICATE IS AWARDED TO

Abdelrhman Muhamed

"Storytelling"

قدمها الأستاذ الدكتور عصام النجدي

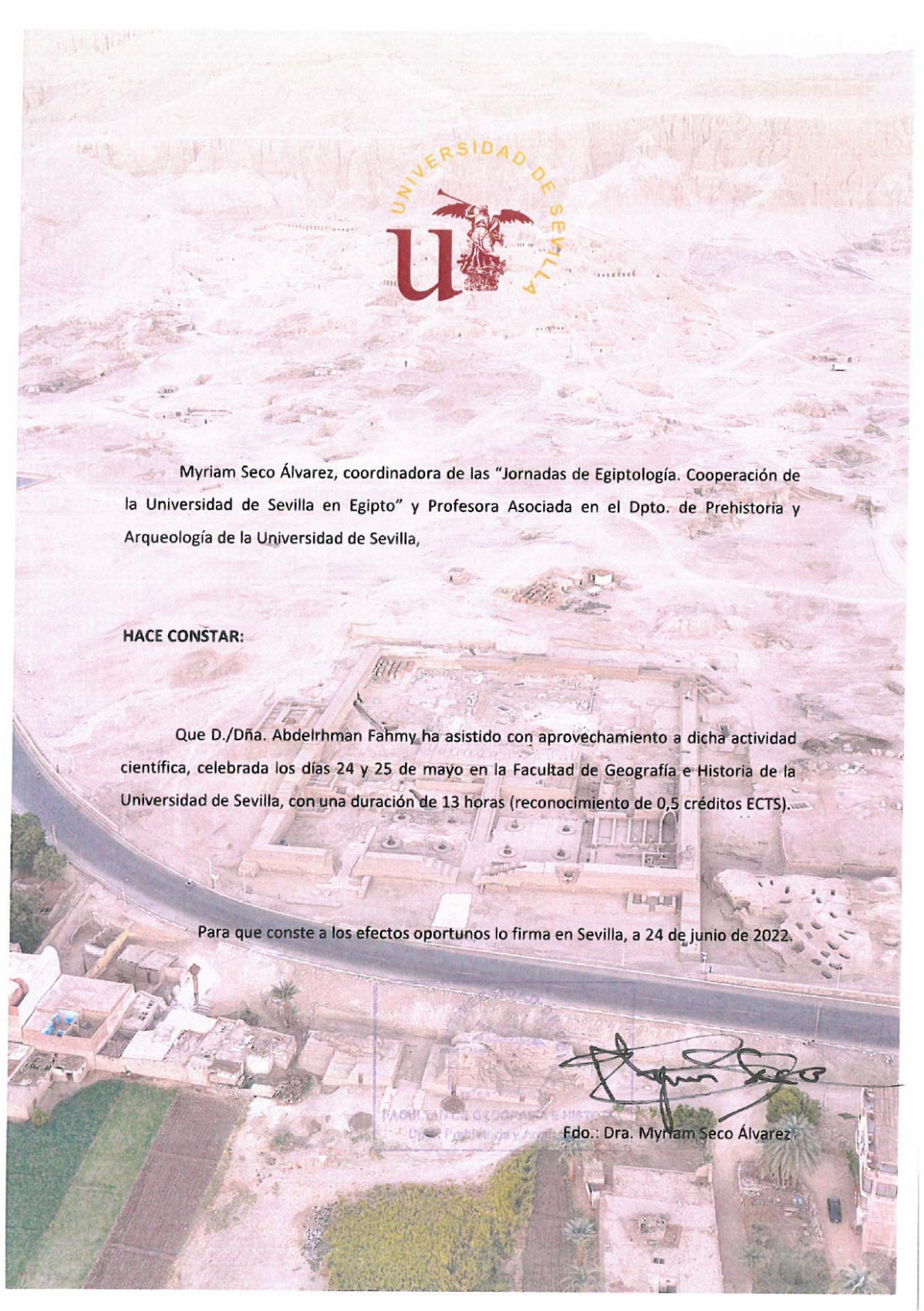
Virtual Session - Zoom

07-February-2022



NADIA MASOUD
DIRECTOR OF UOS LIBRARIES
UNIVERSITY OF SHARJAH

Certificate ID: 5156



UNIVERSIDAD DE SEVILLA

Myriam Seco Álvarez, coordinadora de las "Jornadas de Egiptología. Cooperación de la Universidad de Sevilla en Egipto" y Profesora Asociada en el Dpto. de Prehistoria y Arqueología de la Universidad de Sevilla,

HACE CONSTAR:

Que D./Dña. Abdelrhman Fahmy ha asistido con aprovechamiento a dicha actividad científica, celebrada los días 24 y 25 de mayo en la Facultad de Geografía e Historia de la Universidad de Sevilla, con una duración de 13 horas (reconocimiento de 0,5 créditos ECTS).

Para que conste a los efectos oportunos lo firma en Sevilla, a 24 de junio de 2022.

Fdo.: Dra. Myriam Seco Álvarez

3.3. Fieldwork and committee partications



National Archaeological Institute with Museum -
Bulgarian Academi of Sciences
1892 - 1921 - 1948

CERTIFICATE OF PARTICIPATION

This certificate is presented to

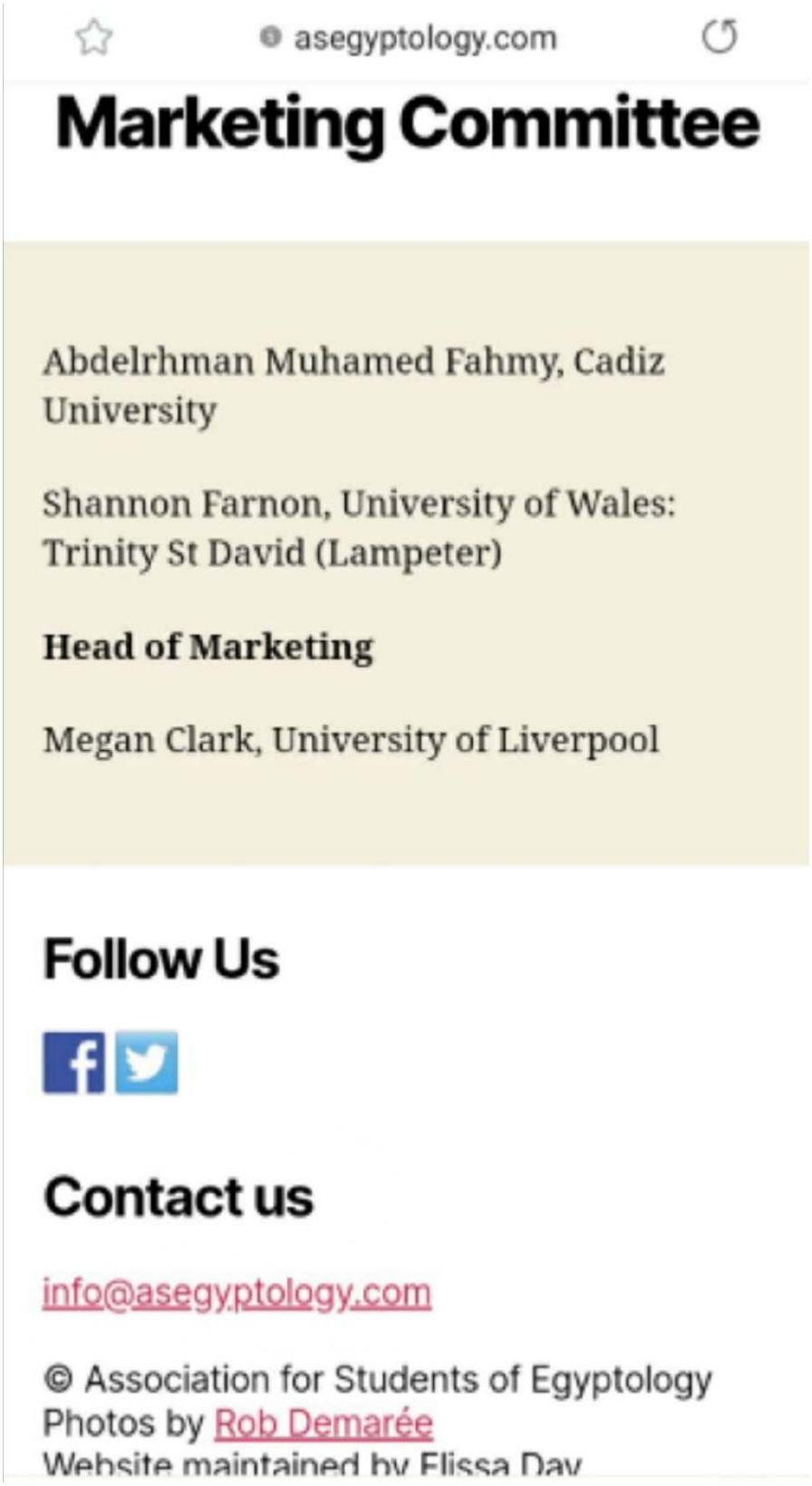
Abdelrhman Muhamed Fahmy

With passport number A20325343 for participating in the excavation of Site 85-2-North-AM Hemus with documentation and digging works from 20th to 29th of May 2021

Given this on 29th of May 2021.

Обект 85-2 Север
АМ Хемус 2021
р-л Андрей Аладжов

Andrey Aladzhov
Scientific chairman of Archaeological Mission


asegyptology.com

Marketing Committee

Abdelrhman Muhamed Fahmy, Cadiz University

Shannon Farnon, University of Wales: Trinity St David (Lampeter)

Head of Marketing

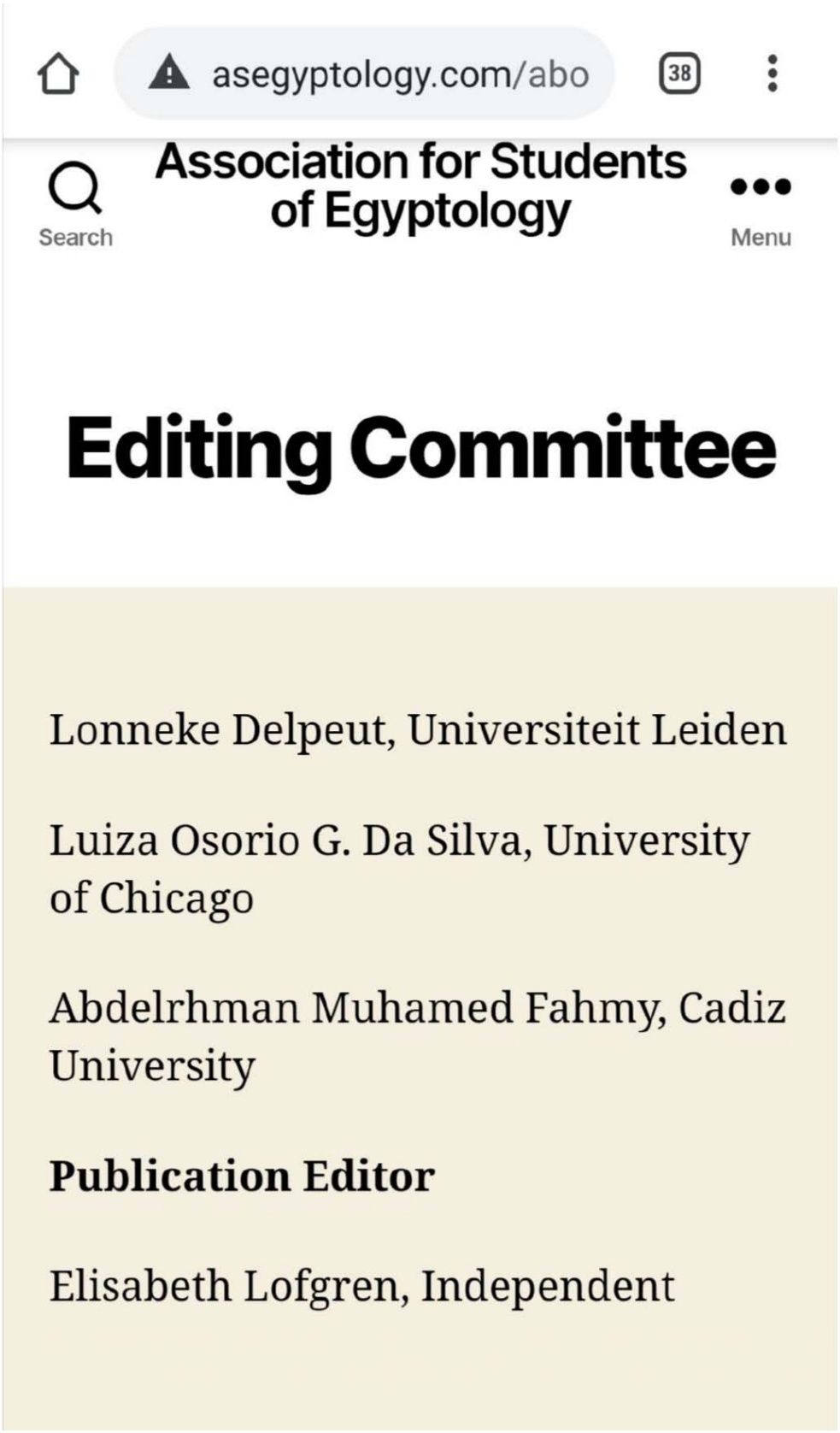
Megan Clark, University of Liverpool

Follow Us

Contact us

info@asegyptology.com

© Association for Students of Egyptology
Photos by Rob Demarée
Website maintained by Elissa Day


asegyptology.com/abo
38
Search
Association for Students of Egyptology
Menu
Editing Committee
Lonneke Delpeut, Universiteit Leiden
Luiza Osorio G. Da Silva, University of Chicago
Abdelrhman Muhamed Fahmy, Cadiz University
Publication Editor
Elisabeth Lofgren, Independent

3.4. Courses and workshops

Nº AF00036197

Escuela de Doctorado de la Universidad de Cádiz

JOSE MARIA GONZALEZ MOLINILLO, Director de la Escuela de Doctorado de la Universidad de Cádiz

Hace constar que:

D. ABDELRHMAN MUHAMED FAHMY SAYED , con Pasaporte A20325343, ha superado el curso ***"Jornadas Doctorales específicas (Artes y Humanidades)"*** (8201P04_004), organizado por Comisión Académica Programa Artes y Humanidades, habiendo obtenido la calificación de **Apto**.

El curso se ha impartido en la Universidad de Cádiz del 3 de diciembre de 2020 al 4 de diciembre de 2020, con una duración global de **20** horas.

Cádiz, a 4 de diciembre de 2020.

El Director de la Escuela de Doctorado
de la Universidad de Cádiz

Fdo.: José María González Molinillo

Pág. 1 de 1

Nº AF00036192

Escuela de Doctorado de la Universidad de Cádiz

JOSE MARIA GONZALEZ MOLINILLO, Director de la Escuela Internacional de Doctorado en Estudios del Mar

Hace constar que:

D. ABDELRHMAN MUHAMED FAHMY SAYED , con Pasaporte A20325343, ha superado el curso ***"VI JORNADAS DOCTORALES EIDEMAR (CON SALIDA DE CAMPO)"*** (8200P004-20B), organizado por EIDEMAR, Escuela Internacional de Doctorado en Estudios del Mar, habiendo obtenido la calificación de **Apto**.

El curso se ha impartido en la Universidad de Cádiz del 1 de diciembre de 2020 al 2 de diciembre de 2020, con una duración global de **15** horas.

Cádiz, a 18 de enero de 2021.

El Director de la Escuela Internacional de Doctorado
en Estudios del Mar

Fdo.: José María González Molinillo

Nº AF00036617

Escuela de Doctorado de la Universidad de Cádiz

JOSE MARIA GONZALEZ MOLINILLO, Director de la Escuela Internacional de Doctorado en Estudios del Mar

Hace constar que:

D. ABDELRHMAN MUHAMED FAHMY SAYED , con Pasaporte A20325343, ha superado el curso ***"Curso básico de SIG y Teledetección aplicados a la gestión de proyectos en el medio marino, terrestre y la protección de"*** (5600780-4-20), organizado por Comisión Académica Programa Ciencias y Tecnologías Marinas, habiendo obtenido la calificación de **Apto**.

El curso se ha impartido en la Universidad de Cádiz del 9 de diciembre de 2020 al 15 de febrero de 2021, con una duración global de **40** horas.

Cádiz, a 23 de marzo de 2021.

El Director de la Escuela Internacional de Doctorado
en Estudios del Mar

Fdo.: José María González Molinillo

Pág. 1 de 1

Nº AF00037498

Escuela de Doctorado de la Universidad de Cádiz

JOSE MARIA GONZALEZ MOLINILLO, Director de la Escuela de Doctorado de la Universidad de Cádiz

Hace constar que:

D. ABDELRHMAN MUHAMED FAHMY SAYED , con Pasaporte A20325343, ha superado el curso ***"Jornada de Recepción para nuevos doctorandos UCA"*** (8200T009_virtual), organizado por EDUCA, Escuela de Doctorado de la Universidad de Cádiz, habiendo obtenido la calificación de **Apto**.

El curso se ha impartido en la Universidad de Cádiz del 23 de febrero de 2021 al 23 de febrero de 2021, con una duración global de **5** horas.

Cádiz, a 22 de marzo de 2021.

El Director de la Escuela de Doctorado
de la Universidad de Cádiz

Fdo.: José María González Molinillo

Nº AF00037071

Escuela de Doctorado de la Universidad de Cádiz

JOSE MARIA GONZALEZ MOLINILLO, Director de la Escuela de Doctorado de la Universidad de Cádiz

Hace constar que:

D. ABDELRHMAN MUHAMED FAHMY SAYED , con Pasaporte A20325343, ha superado el curso ***"Búsqueda, gestión y comunicación de la información científica"*** (8200T002_virt), organizado por EDUCA, Escuela de Doctorado de la Universidad de Cádiz, habiendo obtenido la calificación de **Apto**.

El curso se ha impartido en la Universidad de Cádiz del 18 de enero de 2021 al 22 de febrero de 2021, con una duración global de **35** horas.

Cádiz, a 9 de abril de 2021.

El Director de la Escuela de Doctorado
de la Universidad de Cádiz

Fdo.: José María González Molinillo

Pág. 1 de 1

Nº AF00037638

Escuela de Doctorado de la Universidad de Cádiz

JOSE MARIA GONZALEZ MOLINILLO, Director de la Escuela de Doctorado de la Universidad de Cádiz

Hace constar que:

D. ABDELRHMAN MUHAMED FAHMY SAYED , con Pasaporte A20325343, ha superado el curso ***"Seminario de Metodología de la Investigación en Artes y Humanidades - Modalidad virtual"*** (8201S001B), organizado por Comisión Académica Programa Artes y Humanidades, habiendo obtenido la calificación de **Apto**.

El curso se ha impartido en la Universidad de Cádiz del 22 de febrero de 2021 al 2 de marzo de 2021, con una duración global de **50** horas.

Cádiz, a 8 de mayo de 2021.

El Director de la Escuela de Doctorado
de la Universidad de Cádiz

Fdo.: José María González Molinillo

The Ecole Doctorale des Sciences de la Mer et du Littoral, Université de Bretagne Occidentale certifies that

Abdelrhman Muhamed FAHMY SAYED AHMED

UCA - CADIZ

has participated to the meeting

SEA-EU DOC training event
Career development for doctoral students
17 to 21 May 2021 – ONLINE

Brest, on May 25, 2021

UNIVERSITE / SCIENCES BRETAGNE / DE LA MER LOIRE / ET DU LITTORAL
ECOLE DOCTORALE SCIENCES DE LA MER ET DU LITTORAL
DOCTORAL SCHOOL IN MARINE AND COASTAL SCIENCES
UNIVERSITE DE BRETAGNE OCCIDENTALE
UNIVERSITY OF WESTERN BRITTANY
Rue D. d'Urville - 29280 PLOUZANE - France
https://ed-sml.u-bretagneloire.fr/
edsml-brest@univ-brest.fr

Nº AF00038850

Escuela de Doctorado de la Universidad de Cádiz

JOSE MARIA GONZALEZ MOLINILLO, Director de la Escuela de Doctorado de la Universidad de Cádiz

Hace constar que:

D. ABDELRHMAN MUHAMED FAHMY SAYED , con Pasaporte A20325343, ha superado el curso ***"Iniciación a los Estudios de Doctorado (Modalidad no presencial)"*** (8200T001NP), organizado por EDUCA, Escuela de Doctorado de la Universidad de Cádiz, habiendo obtenido la calificación de **Apto**.

El curso se ha impartido en la Universidad de Cádiz del 11 de mayo de 2021 al 8 de junio de 2021, con una duración global de **25** horas.

Cádiz, a 18 de junio de 2021.

El Director de la Escuela de Doctorado
de la Universidad de Cádiz

Fdo.: José María González Molinillo

Pág. 1 de 1

CERTIFICADO DE PARTICIPACIÓN

D.FIDEL MARÍA ECHEVARRÍA NAVAS, Delegado del Rector para la Universidad Europea de los Mares y Coordinador General de la Alianza,

INFORMA

que **Abdelrhman Muhamed Fahmy Sayed Ahmed** ha participado en el "Curso intensivo: Estrategia y Responsabilidad Social Corporativa desde una Perspectiva Internacional", celebrado los días **24, 26 y 28 de mayo de 2021**.

Fdo.: D. Fidel Mª Echevarría Navas

Delegado del Rector para la Universidad Europea de los Mares

Fecha de emisión: **25/10/2021**

CERTIFICATE OF COMPLETION

Mr. FIDEL MARÍA ECHEVARRÍA NAVAS, Rector's Delegate for the European University of the Seas and General Coordinator of SEA-EU

INFORMS

that: **Abdelrhman Muhamed Fahmy Sayed Ahmed** has participated in the "Intensive course: Strategy and Corporate Social Responsibility from an International Perspective" delivered the days **24th, 26th and 28th of May 2021.**

Signed: Mr. Fidel Mª Echevarría Navas

Delegate of the Rector for the European University of the Seas

Issue date: **25/10/2021**

CSV (Código de Verificación Segura)	IV7F6XLIJAE7JXG5U5QGPZLD64	Fecha	25/10/2021 11:07:25
Normativa	Este documento incorpora firma electrónica reconocida de acuerdo a la ley 6/2020, de 11 de noviembre, reguladora de determinados aspectos de los servicios electrónicos de confianza	Validez del documento	Original
Firmado por	FIDEL MARIA ECHEVARRIA NAVAS		
Url de verificación	https://sede.uca.es/verifirma/code/IV7F6XLIJAE7JXG5U5QGPZLD64	Página	4/7

C | A | U Kiel University | Graduate Center

SEA EU

1 December 2021

Certificate of attendance

Abdelrhman Muhamed Fahmy Sayed Ahmed

has participated in the course

Slidewriting & Storylining

held by **Dr. Markus Burger**

The course took place **online**

22 & 23 November 2021, daily from 09:00 a.m. – 01:00 p.m.

The following topics were covered:

- Convince your audience with well-structured slides and presentations
- Condense your complex research findings to the short time-span of a presentation
- Save time and effort crafting easy to-grasp slides

Graduiertenzentrum der
Christian-Albrechts-Universität zu Kiel
Leibnizstraße 3, 24118 Kiel

Stamp

Dr. Sabine Milde, Graduate Center's managing director

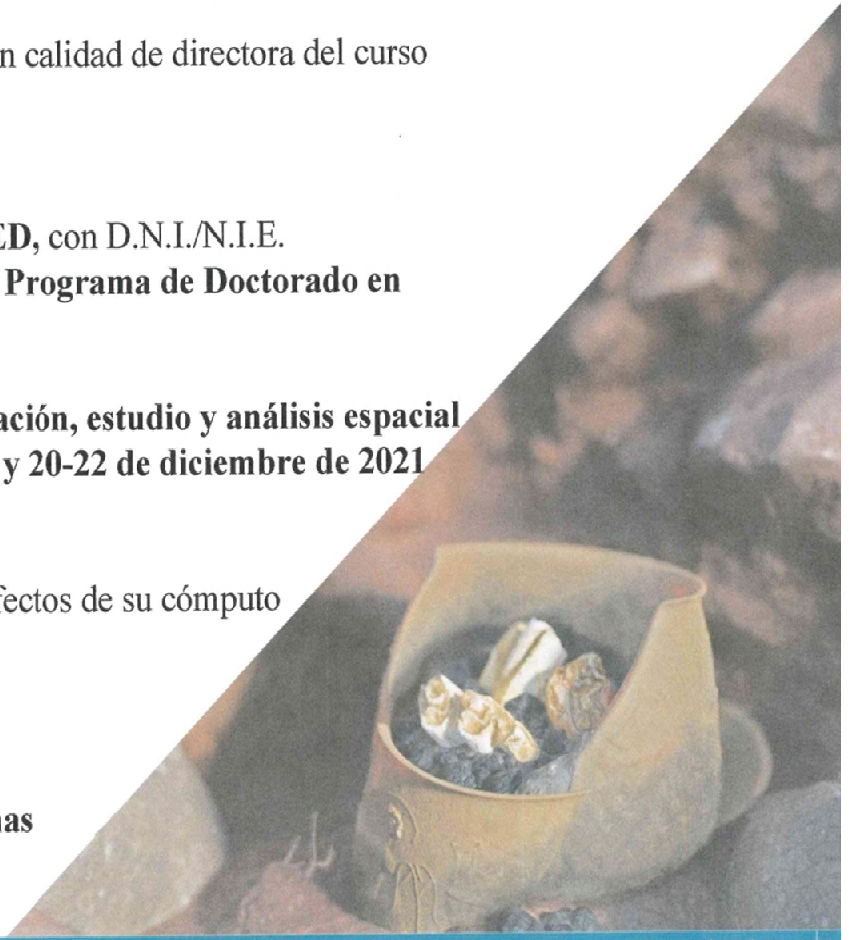
Dña. Ana María Niveau de Villedary y Mariñas en calidad de directora del curso

INFORMA QUE:

D. ABDELRHMAN MUHAMED FAHMY SAYED, con D.N.I./N.I.E. **Y8196167Q,** ha asistido a la actividad formativa del **Programa de Doctorado en Historia y Arqueología Marítimas (8207)**

Curso**: Nuevas tecnologías aplicadas a la digitalización, estudio y análisis espacial del registro arqueológico**, celebrado los días **16-17 y 20-22 de diciembre de 2021** por un total de **50 horas**

De lo que se informa a solicitud del interesado/a a efectos de su cómputo como ACCIONES FORMATIVAS



Fdo.: **Dña. Ana María Niveau Villedary y Mariñas**

Cádiz, 22 de diciembre de 2021

eide·mar escuela internacional de doctorado en estudios del mar campus de excelencia internacional del mar

cei·mar campus de excelencia internacional del mar

SEA EU

UCA Universidad de Cádiz

SPONSORED BY THE Federal Ministry of Education and Research

DAAD Deutscher Akademischer Austauschdienst German Academic Exchange Service

Co-funded by the Erasmus+ Programme of the European Union

CERTIFICATE OF PARTICIPATION

The European University of the Seas (SEA-EU) certifies that

Abdelrhman Muhamed Fahmy Sayed Ahmed

of the University of Cádiz has participated in the following 'SEA-EU Joint PhD Course' organised by Kiel University:

'Paper Writing Academy'

The course was delivered as an 8-week digital programme from 22.11.2021 to 28.01.2022 by Dr Gunther Tress of TRESS ACADEMIC, Munich, Germany, and covered 90 hours with the following learning objectives:

- Getting started and pre-writing (paper topic, audience, ethics, authorship, journal selection)
- Start the paper writing (productive writing strategies, paper objectives, structure, introduction, literature review, title)
- Writing the core sections (methods, results, discussion, conclusion, tables & figures)
- Writing support sections (abstract, keywords, acknowledgments, appendix, references)
- Editing the paper (content & developmental, format, language & style as well as external feedback)
- Peer-review process (submission, review systems, review criteria, reviewer selection, preselection, revision, editorial decision, proof stage)
- Paper promotion

01.03.2022, digitally signed on 01.03.22 by Dr. Jonathan Durgadoo

Date, name & signature

La Universidad Nacional de Educación a Distancia

considerando que

ABDELRHMAN MUHAMAD FAHMY SAYED AHMED

con NIF nº Y8196167Q

ha participado con aprovechamiento en el curso

De Egipto a Gadir. Arte y rituales en el mundo antiguo

Organizado por el Centro Asociado de la UNED en Cádiz, del 28 al 30 de marzo de 2022, según el programa que figura en el reverso de este documento, le expide el presente

CERTIFICADO DE EXTENSIÓN UNIVERSITARIA

Madrid a 3 de mayo de 2022

Jesús de Andrés Sanz
Vicerrector de Centros Asociados
Este documento está firmado digitalmente (*).

Nº de horas: 10 horas

Nº de registro: 10519

Este título se otorga como propio de la UNED y no tiene el carácter oficial establecido en el nº 30 de la Ley Orgánica 4/2007 que modifica el art. 34 de la Ley Orgánica 6/2001 de Universidades.

Ámbito: DAC - La autenticidad, validez e integridad de este documento puede ser verificada mediante el "Código Seguro de Verificación (CSV)" en la dirección https://sede.uned.es/valida/
8F4C0F5B6E2FFA5B260A91B12FA2C0A1

Programa

lunes, 28 de marzo

16:00-18:00 h. "Ceremonia y simbolismo en los enterramientos fenicio-púnicos de la necrópolis de Ibiza".

Ana Mezquida Orti *Profesora-tutora del C.A. UNED Illes Balears. Doctora en Historia.*

18:30-20:30 h. "La necrópolis fenicio-púnica de Gadir: Espacio funerario y rituales de paso".

Paloma Bueno Serrano *Profesora-Tutora del Centro Asociado UNED Cádiz, Doctora en Geografía e Historia.*

martes, 29 de marzo

16:00-18:00 h. "El ritual funerario y los banquetes en las tumbas del antiguo Egipto"

Inmaculada Vivas Sainz *Profesora contratada-doctora. UNED, Dpto. Historia del Arte.*

18:30-20:30 h. "Morir mirando al mar. Ritual y tumbas en la Creta minoica".

Inmaculada Vivas Sainz *Profesora contratada-doctora. UNED, Dpto. Historia del Arte.*

miércoles, 30 de marzo

17:00-19:00 h. VISITA AL MUSEO DE CÁDIZ

Paloma Bueno Serrano *Profesora-Tutora del Centro Asociado UNED Cádiz, Doctora en Geografía e Historia.*

La UNED, por acuerdo del Consejo de Gobierno, de 21 de abril de 2022, reconoce para este curso **0.5 créditos ECTS**(*)
Créditos ECTS: reconocibles como créditos por actividades universitarias culturales en los Grados de la UNED y en los de universidades y centros con convenio de mutuo reconocimiento.

Ámbito: DAC - La autenticidad, validez e integridad de este documento puede ser verificada mediante el "Código Seguro de Verificación (CSV)" en la dirección https://sede.uned.es/valida/
8F4C0F586E2FFA5B260A91B12FA2C0A1

Nº AF00042292

Escuela de Doctorado de la Universidad de Cádiz

JOSE MARIA GONZALEZ MOLINILLO, Director de la Escuela Internacional de Doctorado en Estudios del Mar

Hace constar que:

D. ABDELRHMAN MUHAMED FAHMY SAYED , con Pasaporte A20325343, ha superado el curso ***"La erosión costera: efectos en el litoral y modalidades de respuesta"*** (5600800-1-22), organizado por Comisión Académica Programa Ciencias y Tecnologías Marinas, habiendo obtenido la calificación de **Apto**.

El curso se ha impartido en la Universidad de Cádiz del May 18th, 2022 al May 25th, 2022, con una duración global de **25** horas.

Cádiz, a July 26th, 2022.

El Director de la Escuela Internacional de Doctorado
en Estudios del Mar

Fdo.: José María González Molinillo

Pág. 1 de 1

صدرت بتاريخ: 30 مارس 2021.

شكـــر وتقديـــر

تتقـدم

هيئـــة الشارقـــة للآثـــار

بجزيل الشكر والعرفان لـ

Abdelrhman Muhamed Fahmy Sayed Ahmed

على مشاركتكم الفعالة في إنجاح محاضرة:

« الجزائر 2.4 مليون سنة من الوجود »

والتي قدمتها **د. فايزة رياش**،

والمنعقدة يوم الاثنين الموافق 29 مارس 2021.

مع أخلـص التمنيات لكـم بالتوفيـق والسـداد.



د. صباح عبود جاسم
المديـر العـام

CERTIFICADO DE PARTICIPACIÓN

D.FIDEL MARÍA ECHEVARRÍA NAVAS, Delegado del Rector para la Universidad Europea de los Mares y Coordinador General de la Alianza,

INFORMA

que **ABDELRHMAN MUHAMED** ha participado en el Webinar Internacional "Cambio global y sus efectos en nuestras costas", celebrado los días **23 y 24 de septiembre de 2021**.

Fdo.: D. Fidel Mª Echevarría Navas

Delegado del Rector para la Universidad Europea de los Mares

Fecha de emisión: **06/10/2021**

CERTIFICATE OF COMPLETION

Mr. FIDEL MARÍA ECHEVARRÍA NAVAS, Rector's Delegate for the European University of the Seas and General Coordinator of SEA-EU

INFORMS

that: **ABDELRHMAN MUHAMED** has participated in the International Webinar "Global change and its effects on our coast" delivered from **23 to 24 of September 2021**.

Signed: Mr. Fidel Mª Echevarría Navas

Delegate of the Rector for the European University of the Seas

Issue date: **06/10/2021**

CSV (Código de Verificación Segura)	IV7FSGB3L5JLRKF7CENH4ZCXAY	Fecha	06/10/2021 18:17:59
Normativa	Este documento incorpora firma electrónica reconocida de acuerdo a la ley 6/2020, de 11 de noviembre, reguladora de determinados aspectos de los servicios electrónicos de confianza	Validez del documento	Original
Firmado por	FIDEL MARIA ECHEVARRIA NAVAS		
Url de verificación	https://sede.uca.es/verifirma/code/IV7FSGB3L5JLRKF7CENH4ZCXAY	Página	12/22

3.5. Assessments of research stays

UNIVERSITY OF LEICESTER
School of Archaeology and Ancient History
University of Leicester
University Road
Leicester
LE1 7RH
United Kingdom

12/12/2022

To Whom it May Concern,

Report on Visiting Scholar: Abdelrhman Muhamed Fahmy Sayed Ahmed

School of Archaeology and Ancient History (SAAH) at University of Leicester confirms that Abdelrhman Muhamed Fahmy Sayed Ahmed with NIE Number: Y8196167Q and Passport Number: A20325343 has fulfilled his activities and research stay successfully.

Mr Abdelrhman Fahmy was hard working, highly-engaged and had enthusiasm for learning new skills during his stay. A summary evaluation of the student is as follows

Scale of evaluation: 1. Poor 2. Acceptable 3. Good 4. Very good 5. Excellent

	1	2	3	4	5
Attendance					X
Fulfilment of the research stay					X
The student has fulfilled the required activities					X
The student has fulfilled the tasks successfully					X
The student skills have improved					X
Motivation					X
Initiative					X
Willingness to learn					X
Responsibility					X
Creativity					X
Teamwork					X
Capacity to learn					X

The overall evaluation grade is **(5)**

Professor Ruth Young
Director of Research
School of Archaeology & Ancient History

UNIVERSITY OF LEICESTER
School of Archaeology and Ancient History

School of Archaeology and Ancient History
University of Leicester
University Road
Leicester
LE1 7RH
United Kingdom

12/12/2022

Report of Supervisor

I, **Professor Ruth Young** write in my capacity as Head of Research and on the recommendation of Dr Laura Basell, named host for the doctoral student Abdelrhman Muhamed Fahmy Sayed Ahmed (NIE Number: Y8196167Q and Passport Number: A20325343) to confirm that he fulfilled his research stay successfully. During the course of his stay he completed the following activities:

1. Delivered a presentation for the induction sessions of postgraduate students.
2. Attended research seminars organized by School of Archaeology and Ancient History.
3. Attended the courses of Remote sensing (GY7705 Remote Sensing 2022-23 SEM1) and GIS (GY7701 & GY4471 Fundamentals of GIS 2022-23 SEM1).
4. Attended the training courses organized by School of Archaeology and Ancient History.
5. Attended the course of Academic Speaking (EL7060) and Academic Writing Lectures (EL7030) in the English language support programme.
6. Presented an occasional lecture at School of Archaeology and Ancient History (SAAH) about building materials and decay of Osiris Temple (Abaton Temple) in Aswan, Egypt.
7. Worked with members of the School including the host, on an article entitled "Monitoring the Nile water level fluctuations and its impact at Philae archaeological site (Aswan, Egypt)" for submission to a peer reviewed journal.
8. Discussed with staff and worked with the host on postdoctoral funding applications.

All these activities have enhanced his skills in scientific research, will contribute to his doctoral thesis, future career and personal development. His enthusiasm and cheerful demeanour have meant that it has been a pleasure to have him study here.

Yours sincerely

Professor Ruth Young
Professor of Archaeology and Director of Research
School of Archaeology and Ancient History
University of Leicester

School of Archaeology and Ancient History

MOVILIDAD INTERNACIONAL A CENTROS DE EXCELENCIA PARA ESTUDIANTES DE DOCTORADO. CEI·MAR 2021

INFORME DE ACTIVIDADES REALIZADAS

1º APELLIDO:	2º APELLIDO:	NOMBRE:
Muhamed	Fahmy sayed Ahmed	Abdelrhman

Detailed programme of the traineeship period including tasks carried out by the trainee:

1. Familiarizing with the Department of Environmental Technology group and thr equipments for the characterization of nanomaterials.
2. Presenting lecture entitled (Nano materials in consolidation of archaeological construction materials in marine and fluvial environments in Egypt).
3. Presenting lecture entitled (Pyramids of Egypt and Sudan).
4. Understanding of synthesis of nanomaterials.
5. Preparation and characterization of novel photocatalysts with different methods.
6. Carrying out a practical application for the nanomaterials on the surfaces of experimental and archaeological samples.
7. Characterization of obtained nanomaterials using XRD technique (crystal structure and phase composition), UV-Vis spectroscopy (absorption spectra and bang gap energy), photoluminescence spectra, SEM/TEM analysis (size, shape, surface topography), FTIR analysis.
8. Measurement of photocatalytic activity.
9. Characterization of physical and mechanical properties for treated and untreated experimental and archaeological samples.

13/06/2022

KIEROWNIK KATEDRY
Katedra Technologii Środowiska
prof. dr hab. inż. Adriana Zaleska-Medynska

FIRMA Y SELLO DEL RESPONSABLE DE LA INSTITUCIÓN DE DESTINO

SIGNATURE AND STAMP OF THE HEAD OF THE DESTINATION INSTITUTION

cei·mar 10AÑOS
campus de excelencia internacional del mar

MOVILIDAD INTERNACIONAL A CENTROS DE EXCELENCIA PARA ESTUDIANTES DE DOCTORADO. CEI·MAR 2021

CERTIFICADO FINAL DE ESTANCIA / CERTIFICATE OF ATTENDANCE

Institución de Acogida / Host Institution

Sr.-Sra. / Mr. - Ms:	**Prof. dr hab. Adriana Zaleska-Medynska**
Cargo / Position:	**Professor** **adriana.zaleska-medynska@ug.edu.pl** **+48 58 523 52 20**
Institución de acogida / Host Institution:	**Faculty of Chemistry- Environmental Technology Department** **University of Gdansk** **https://en.ug.edu.pl/**

Certifica que / Certifies that:

Sr.-Sra. / Mr. – Ms:	Abdelrhman Muhamed Fahmy Sayed Ahmed
Con NIF-NIE número / with ID number:	NIE/ Y8196167Q Passport No/ A20325343
Ha realizado una estancia en esta Institución / Has carried out a stay at our Institution Desde el / from : 01 / 09 / 2021 Hasta el / to: 30 / 11 /2021	

Lugar / Place: **Gdansk**

Fecha / Date(*): (13/06/2022)

KIEROWNIK KATEDRY Katedra Technologii Środowiska prof. dr hab. inż. Adriana Zaleska-Medynska	Uniwersytet Gdański Wydział Chemii Katedra Technologii Środowiska ul. Wita Stwosza 63 80-308 Gdańsk
Firma del responsable de la movilidad / Signature of the person responsible for the mobility	**Sello de la Institución de destino / Stamp of the Host Institution**

(*) La fecha de firma no puede ser anterior a la fecha de fin de estancia / The date of signature should not be before the date of departure. Cumplimentar este documento con firma y sello de la institución de acogida a la finalización de la estancia y remitir el documento a proyectos@fundacionceimar.com en un plazo no superior a ***10 días hábiles*** *desde su finalización.*

Erasmus+

Higher Education:
Learning Agreement form
Abdelrhman Muhamed
Fahmy Sayed Ahmed
Academic Year 2021/2022

During the Mobility

Table A2 - Exceptional Changes to the Traineeship Programme at the Receiving Organisation/Enterprise
(to be approved by e-mail or signature by the student, the responsible person in the Sending Institution and the responsible person in the Receiving Organisation/Enterprise)

Planned period of the mobility: from 01/09/2021 till 30/11/2021

Traineeship title: ...	**Number of working hours per week: ...**
Nano materials in consolidation of archaeological limestone and sandstones construction materials in marine and fluvial environments in Egypt	**Full time/ Doctoral work**

Detailed programme of the traineeship period:

- Familiarizing with the Department of Environmental Technology group and equipment for the characterization of nano materials.
- Review of the scientific literature regarding synthesis method of nanomaterials.
- Nano materials in consolidation of archaeological limestone and sandstones construction materials in marine and fluvial environments in Egypt.

The main objective of this research is to study and evaluate nanomaterials to protect two different kinds of natural stones (limestone and sandstone) exposed to marine environments. And the specific objectives of the proposal are:

1. Specify the initial physical and mechanical properties of treated stones.
2. Carry out ageing cycles to evaluate the efficiency of the developed nanomaterials in consolidation of limestone in marine environments and sandstone in fluvial envir
3. Specify the physical and mechanical properties of aged stones after treatment.

The scientific methodology for the research will rely on experimental and testing studies with different techniques and measurements for evaluation/assessment of cor materials before and after treatment with nano materials. The proposed methodology is:

- Preparation of stone samples (sandstone and limestone).
- Preparation of materials in nanoscales.
- Application of nano materials for consolidation of sandstone and limestone (treatment).
- Characterization of the petrophysical properties of the treated sandstone and limestone.
- Artificial ageing after treatment.
- Characterization of petrophysical properties of the treated and stone and limestone after ageing

Knowledge, skills and competences to be acquired by the end of the traineeship (expected Learning Outcomes):

i) Developing new nanostructures, (ii) Knowledge of various methods for the synthesis of nano materials (hydrothermal, solvothermal, hot injection method, sol-gel The expected results are getting and improving nano materials which enhance the consolidation and preservation of archaeological sandstone and limestone constru materials. This conservation work using the produced nano materials will enhance and encourage the tourism movement towards those important buildings and ma cultural heritage to new generations.

Monitoring plan:

- Weekly meetings with the co-Supervisor.
- Monthly meetings with the academic tutor

Evaluation plan:

- Monthly report to the co-Supervisor.
- Final report to the co-supervisor and academic tutor

After the Mobility

Table D - Traineeship Certificate by the Receiving Organisation/Enterprise

Name of the trainee: Abdelrhman Muhamed Fahmy Sayed Ahmed

Name of the Receiving Organisation/Enterprise: Faculty of Chemistry, Environmental Technology Department, Gdansk University

Sector of the Receiving Organisation/Enterprise: Faculty of Chemistry, Environmental Technology Department, Gdansk University

Address of the Receiving Organisation/Enterprise[street, city, country, phone, e-mail address], **website:**
80-309 Gdansk Jana Bażyńskiego 8, Poland Department of Environmental Technologies University of Gdansk adriana.zaleska-medynska@ug.edu.pl
https://en.ug.edu.pl/

Erasmus+

Higher Education:
Learning Agreement form
Abdelrhman Muhamed
Fahmy Sayed Ahmed
Academic Year 2021/2022

Start date and end date of traineeship: from [01/09/2021] ..... to [30/11/2021] .....

Traineeship title:

Nano materials in consolidation of archaeological limestone and sandstones construction materials in marine and fluvial environments in Egypt

Detailed programme of the traineeship period including tasks carried out by the trainee:

1. Familiarizing with the Department of Environmental Technology group and thr equipments for the characterization of nanoamaterials.
2. Presenting lecture entitled (Nano materials in consolidation of archaeological construction materials in marine and fluvial environments in Egypt).
3. Presenting lecture entitled (Pyramids of Egypt and Sudan).
4. Understanding of synthesis of nanomaterials.
5. Preparation and characterization of novel photocatalysts with different methods.
6. Carrying out practical application for the nanomaterials on the surfaces of experimental and archaeological samples.
7. Characterization of obtained nanomaterials using XRD technique (crystal structure and phase composition), UV-Vis spectroscopy (absorption spectra and bang gap energy), photoluminescence spectra, SEM/TEM analysis (size, shape, surface topography), FTIR analysis.
8. Measurement of photocatalytic activity.
9. Characterization of physical and mechanical properties of treated and untreated experimental and archeological samples.

Knowledge, skills (intellectual and practical) and competences acquired (achieved Learning Outcomes):

(i) Developing new nanostructures, *(ii)* Knowledge of various methods for the synthesis of nano materials (hydrothermal, solvothermal, hot injection method, sol-ge The expected results are getting and improving nano materials which enhance the consolidation and preservation of archaeological sandstone and limestone constru materials. This conservation work using the produced nano materials will enhance and encourage the tourism movement towards those important buildings and ma cultural heritage to new generations.

Evaluation of the trainee:

MR. Abdelrhman Muhamed Fahmy Sayed Ahmed was a conscientious, hard-working intern. During the intership he skillfully prepared and characterized novel photocatalysts with different methods (such as: sol-gel, hydrothermal and solvothermal). He is familiar with the techniques of characterization of nanomaterials (X-ray diffraction (XRD) analyses, UV-Vis spectroscopy, photoluminescence spectra, scanning electron microscopy analysis (SEM), FTIR analysis). Overall grade: very good

Date: 10.06.2022

Name and signature of the Supervisor at the Receiving Organisation/Enterprise:

KIEROWNIK KATEDRY
Katedra Technologii Środowiska

prof. dr hab. inż. Adriana Zaleska-Medynska

Uniwersytet Gdański
Wydział Chemii
Katedra Technologii Środowiska
ul. Wita Stwosza 63
80-308 Gdańsk

FUNDACIÓN cei·mar campus de excelencia internacional del mar

Junta de Andalucía Consejería de Economía, Conocimiento, Empresas y Universidad

Cofinanciado por el programa Erasmus+ de la Unión Europea

Erasmus+ CEI·MARPrácticas

INFORME DE EVALUACIÓN DEL PERIODO DE PRÁCTICAS ERASMUS + CURSO 2020/21
INTERSHIP EVALUATION OF PLACEMENT PERIOD ERASMUS + ACADEMIC YEAR 2020/2021

1.- DATOS GENERALES / GENERAL INFORMATION

Nombre del Estudiante / Name of the student:	Abdelrhman Muhamed Fahmy Sayed Ahmed
D.N.I. / ID Card:	Y8196167Q
Área de Estudios / Study Area:	8207 Historia y Arqueología Marítimas (Archaeometry) University of Cádiz
Nombre de la entidad de destino / Name of the Host Organisation:	University of Gdansk – https://en.ug.edu.pl/
Nombre y Cargo del Tutor / Name and Position of Mentor:	prof. dr hab. Adriana Zaleska-Medynska adriana.zaleska-medynska@ug.edu.pl +48 58 523 52 20
Fecha de Inicio / Starting Date:	Fecha de Regreso / Final Date: 01/09/2021
Número Total de Horas Trabajadas / Total Working Hours:	Full time/ 3 months

Tareas Realizadas / Tasks Performed:

1. Familiarizing with the Department of Environmental Technology group and thr equipments for the characterization of nanoamaterials.
2. Presenting lecture entitled (Nano materials in consolidation of archaeological construction materials in marine and fluvial environments in Egypt).
3. Presenting lecture entitled (Pyramids of Egypt and Sudan).
4. Understanding of synthesis of nanomaterials.
5. Preparation and characterization of novel photocatalysts with different methods.
6. Carrying out practical application for the nanomaterials on the surfaces of experimental and archaeological samples.
7. Characterization of obtained nanomaterials using XRD technique (crystal structure and phase composition), UV-Vis spectroscopy (absorption spectra and bang gap energy), photoluminescence spectra, SEM/TEM analysis (size, shape, surface topography), FTIR analysis.
8. Measurement of photocatalytic activity.
9. Characterization of physical and mechanical properties for treated and untreated experimental and archeological samples.

UNIVERSIDAD DE ALMERÍA · UNIVERSIDAD DE GRANADA · UCA Universidad de Cádiz · Universidad de Huelva · UNIVERSIDAD DE MÁLAGA

Cofinanciado por el programa Erasmus+ de la Unión Europea

2.- EVALUACIÓN / EVALUATION.-

Marque con una X el valor más adecuado, teniendo en cuenta la siguiente escala: / Tick the mostappropiateoptionaccording to the followingscale:

1: Bajo / Poor; 2: Aceptable / Fair; 3: Bueno / Good; 4: Muy bueno / VeryGood; 5: Excelente / Excellent.

Cumplimiento de las Obligaciones / Fulfilment of obligations:					
	1	2	3	4	5
Asistencia / Attendance:					X
Cumplimiento del Programa de prácticas / Fulfilment of the Traineeships:					X
Realización de las tareas / Execution of the Tasks:					
	1	2	3	4	5
El estudiante llevó a cabo las actividades previstas / The student has fulfiled the required activities					X
El estudiante realizó las tareas satisfactoriamente / The student has fulfiled the tasks successfully					X
El estudiante avanzó en el dominio de las técnicas, herramientas y metodologías necesarias en el puesto de trabajo / The student's level of mastery of techniques, tools and methodology needed in this post has improved					X
El estudiante mejoró sus aptitudes y capacidades profesionales / The student has improved his/her professional aptitudes and skills					X

Cofinanciado por el programa Erasmus+ de la Unión Europea

Aptitudes / Aptitudes:					
	1	2	3	4	5
Integración en la Institución / Level of the integration in the organization:					X
Motivación / Motivation:					X
Iniciativa / Initiative:					X
Responsabilidad / Responsibility:					X
Creatividad / Creativity:					X
Predisposición para aprender / Willingness to learn:					X
Trabajo en equipo / Teamwork:				X	
Capacidad de aprendizaje / Capacity of learning:					X
Receptividad de las críticas / Receptivity to criticism:				X	

Evaluación Global / Global Evaluation:				
1	2	3	4	5
				X

Observaciones Generales / General Remarks:

Mr Abdelrhaman Muhamed Fahmy Sayed Ahmed, doctoral student, University of Cadiz, Spain has spent his research stay for three months at Department of Environmental Technology. Student was characterized a very high quality of work regularly delivered. Intern had enthusiasm for work and assignments. Intern displayed aptitude and enthusiasm for learning. Overall performance was exemplary.

Cofinanciado por el programa Erasmus+ de la Unión Europea

Signatures below

Nombre del Tutor / Name of Mentor: KIEROWNIK KATEDRY Katedra Technologii Środowiska prof. dr hab. inż. Adriana Zaleska-Medynska

Firma / Signature:

Sello / Stamp: Uniwersytet Gdański Wydział Chemii Katedra Technologii Środowiska ul. Wita Stwosza 63 80-308 Gdańsk

Lugar y Fecha / Place and Date: Gdańsk, 10.06.2022

FUNDACIÓN cei·mar campus de excelencia internacional del mar

Junta de Andalucía Consejería de Economía, Conocimiento, Empresas y Universidad

Cofinanciado por el programa Erasmus+ de la Unión Europea

Programme Erasmus+ KA103 SMP

Erasmus+ CEI·MAR Prácticas

CERTIFICADO FINAL DE ESTANCIA / CERTIFICATE OF ATTENDANCE

Institución de Acogida / Host Institution

Sr.-Sra. / *Mr. - Ms:*	**Prof. dr hab. Adriana Zaleska-Medynska**
Cargo / *Post:*	Professor adriana.zaleska-medynska@ug.edu.pl +48 58 523 52 20
Institución de acogida / *Host Institution*:	Faculty of Chemistry- Environmental Technology Department University of Gdansk https://en.ug.edu.pl/

Certifica que / Certifies that:

Sr.-Sra. / *Mr. – Ms*:	**Abdelrhman Muhamed Fahmy Sayed Ahmed**
con NIF-NIE número / *with ID number*:	NIE/ Y8196167Q Passport No/ A20325343
Ha realizado una estancia en esta Institución / Has carried out a stay at our Institution Desde el / from 01 / 09 / 2021 Hasta el / to: 30 / 11 / 2021	

Lugar / Place: Gdansk

Fecha / *Date (*)*: (09/12/2021)

KIEROWNIK KATEDRY Katedra Technologii Środowiska prof. dr hab. inż. Adriana Zaleska-Medyńska	Uniwersytet Gdański Wydział Chemii Katedra Technologii Środowiska ul. Wita Stwosza 63 80-308 Gdańsk
Firma del responsable de la movilidad de prácticas en la entidad/ *Signature of the person responsible of the traineeships in the host institution*	**Sello de la Institución de acogida /** *Stamp of the Host Institution*

(*) La fecha de firma no puede ser anterior a la fecha de fin de estancia / The date of signature shouldnot be before the date of departure. Cumplimentar este documento con firma y sello de la institución de acogida a la finalización de la estancia y remitir el documento a internacional@fundacionceimar.com

UNIVERSIDAD DE ALMERIA · UNIVERSIDAD DE GRANADA · UCA Universidad de Cádiz · Universidad de Huelva · UNIVERSIDAD DE MÁLAGA

3.6. Spanish Language certificates



UCA
Universidad de Cádiz

Vicerrectorado de Política Educativa

DIPLOMA DE APROVECHAMIENTO

La Vicerrectora de Política Educativa

Hace constar que:

D. **Abdelrhman Muhamed Fahmy Ahmed** , con pasaporte **A20325343**, ha superado el curso con modalidad semipresencial **Español como Lengua Extranjera. Nivel A1**, organizado por el Centro Superior de Lenguas Modernas de la Universidad de Cádiz y aprobado por la Comisión de Ordenación Académica, Profesorado y Alumnos de 6 de marzo de 2019, habiendo obtenido la calificación de **Sobresaliente (9.6)**.

El curso se ha celebrado en el Campus Universitario de Cádiz, del **28 de septiembre de 2020** al **9 de diciembre de 2020**, y tiene una duración global de **180** horas **(ordenación de la docencia 7 ECTS)**.

Los contenidos de este curso se corresponden con los exigidos para la obtención del nivel A1 del Marco Común Europeo de Referencia para las Lenguas.

Cádiz, 16 de diciembre de 2020

V.B. de la Universidad de Cádiz
La Vicerrectora de Política Educativa
(P.D.F. Resolución UCA/R84REC/2019, de 29 de julio, BOUCA nº 292)

Fdo.: Eva Garrido Pérez

Director General de Política Lingüística

Fdo. Javier de Cos Ruiz

Nº Registro: 82271

Gestionado por: fueca

Fundación docente privada sin ánimo de lucro, declarada de "interés público" por Orden de la Consejería de Educación y Ciencia de la J.A.de 9-XII-98 (BOJA nº 148 de 29 de diciembre, pg. 15.898) e inscrito en el Registro de Fundaciones de Andalucía con el nº CA/664



UCA Universidad de Cádiz

Fundación docente privada sin ánimo de lucro, declarada de "interés público" por Orden de la Consejería de Educación y Ciencia de la J.A.de 9-XII-98 (BOJA nº 148 de 29 de diciembre, pg. 15.898) e inscrito en el Registro de Fundaciones de Andalucía con el nº CA/664

Vicerrectorado de Política Educativa

DIPLOMA DE APROVECHAMIENTO

La Vicerrectora de Política Educativa

Hace constar que:

D. **Abdelrhman Muhamed Fahmy Ahmed** , con pasaporte **A20325343**, ha superado el curso con modalidad semipresencial **Español como Lengua Extranjera. Nivel A2**, organizado por el Centro Superior de Lenguas Modernas de la Universidad de Cádiz y aprobado por la Comisión de Ordenación Académica, Profesorado y Alumnos de 21 de abril de 2020, habiendo obtenido la calificación de **Notable (7.4)**.

El curso se ha celebrado en el Campus Universitario de Cádiz, del **2 de marzo de 2021** al **14 de mayo de 2021**, y tiene una duración global de **180** horas **(ordenación de la docencia 7 ECTS)**.

Los contenidos de este curso se corresponden con los exigidos para la obtención del nivel A2 del Marco Común Europeo de Referencia para las Lenguas.

Cádiz, 19 de mayo de 2021

V.B. de la Universidad de Cádiz
La Vicerrectora de Política Educativa
(P.D.F. Resolución UCA/R84REC/2019, de 29 de julio, BOUCA nº 292)

Fdo.: Eva Garrido Pérez

Director General de Política Lingüística

Fdo. Javier de Cos Ruiz

Nº Registro: 84808

AENOR ER Empresa Registrada — IQNet

Gestionado por: fueca Fundación Universidad-Empresa de la Provincia de Cádiz

UCA
Universidad de Cádiz

Vicerrectorado de Política Educativa

DIPLOMA DE APROVECHAMIENTO

La Vicerrectora de Política Educativa

Hace constar que:

D. **Abdelrhman Muhamed Fahmy Sayed Ahmed**, con pasaporte **A20325343**, ha superado el curso que se detalla a continuación:
Español como Lengua Extranjera. Nivel B2.1

Modalidad:	Semipresencial
Lugar:	Campus Cádiz
Fechas:	del **10 de enero de 2022** al **27 de enero de 2022**
Duración:	90 horas
Calificación:	**Aprobado (6.4)**

Curso organizado por el Centro Superior de Lenguas Modernas de la Universidad de Cádiz. **(ordenación de la docencia 3.5 ECTS)**.

Curso aprobado por la comisión de Ordenación Académica, Profesorado y Alumnos de 21 de abril de 2020.

La superación de este curso no implica la obtención de la acreditación del nivel idiomático expresado.

El curso de Español nivel B2.1 del Centro Superior de Lenguas Modernas equivale a una instrucción de hasta 90 horas de las 180 requeridas en el CSLM para cursar los contenidos del nivel B2 del Marco Común Europeo de Referencia para las Lenguas.

Cádiz, 10 de marzo de 2022

V.B. de la Universidad de Cádiz
La Vicerrectora de Política Educativa
(P.D.F. Resolución UCA/R84REC/2019, de 29 de julio, BOUCA nº 292)

Fdo.: Eva Garrido Pérez

Director General de Política Lingüística

Fdo. Javier de Cos Ruiz

Nº Registro: 88425

Fundación docente privada sin ánimo de lucro, declarada de "interés público" por Orden de la Consejería de Educación y Ciencia de la J.A.de 9-XII-98 (BOJA nº 148 de 29 de diciembre, pg. 15.898) e inscrito en el Registro de Fundaciones de Andalucía con el nº CA/664

AENOR ER Empresa Registrada · IQNet

Gestionado por: fueca Fundación Universidad-Empresa de la Provincia de Cádiz

UCA
Universidad de Cádiz

Vicerrectorado de Política Educativa

DIPLOMA DE APROVECHAMIENTO

La Vicerrectora de Política Educativa

Hace constar que:

D. **Abdelrhman Muhamed Fahmy Sayed Ahmed**, con pasaporte **A20325343**, ha superado el curso que se detalla a continuación:
Español como Lengua Extranjera. Nivel B2.2

Modalidad:	Semipresencial
Lugar:	Campus Cádiz
Fechas:	del **18 de julio de 2022** al **4 de agosto de 2022**
Duración:	90 horas
Calificación:	**Sobresaliente (9.3)**

Curso organizado por el Centro Superior de Lenguas Modernas de la Universidad de Cádiz. **(ordenación de la docencia 3.5 ECTS).**

Curso aprobado por la comisión de Ordenación Académica, Profesorado y Alumnos de 21 de junio de 2021.

La superación de este curso no implica la obtención de la acreditación del nivel idiomático expresado.

Los contenidos de este curso se corresponden con los exigidos en el CSLM para la obtención del nivel B2 del Marco Común Europeo de Referencia para las Lenguas.

Cádiz, 29 de agosto de 2022

V.B. de la Universidad de Cádiz
La Vicerrectora de Política Educativa
(P.D.F. Resolución UCA/R84REC/2019,
de 29 de julio, BOUCA nº 292)

Fdo.: Eva Garrido Pérez

Director General de Política Lingüística

Fdo. Javier de Cos Ruiz

Nº Registro: 93104

Fundación docente privada sin ánimo de lucro, declarada de "interés público" por Orden de la Consejería de Educación y Ciencia de la J.A.de 9-XII-98 (BOJA nº 148 de 29 de diciembre, pg. 15.898.) y registrada en su protectorado con el Registro de Fundaciones de Andalucía con el nº CA/664

AENOR GESTIÓN DE LA CALIDAD ISO 9001 ER-0466/2004

Gestionado por: fueca Fundación Universidad-Empresa de la Provincia de Cádiz

Annex 4: List of Publications and contributions

4.A Abdelrhman Fahmy, Eduardo Molina-Piernas, Javier Martínez-López, Philip Machev, and Salvador Domínguez-Bella. 2022. "Coastal Environment Impact on the Construction Materials of Anfushi's Necropolis (Pharos's Island) in Alexandria, Egypt". *Minerals* 12, no. 10: 1235. https://doi.org/10.3390/min12101235

4.A.1 Author Contributions

A F, E M P, J M L and S D B contributed to the conception and design of this study. **A F**, E M P and S D B carried out the laboratory tests. **A F** wrote the first draft of the manuscript. E M P J M L and S D B contributed to the discussion of the results and collaborated in the writing of the different sections of the manuscript. E M P and S D B contributed to the funding acquisition. PM took part in the scanning electron microscopy and thin section preparations. All authors have read and agreed to the published version of the manuscript.

4.A.2. Journal Metrics (Web of Science)

Indicadores

JCR (Journal Impact Factor)

(Indicador correspondiente al último año disponible en este portal, año 2021)

- Año 2021
- Factor de impacto de la revista: 2.818
- Factor de impacto sin autocitas: 2.298
- Article influence score: 0.515
- Cuartil mayor: Q2
- Área: MINERALOGY Cuartil: **Q2** Posición en el área: **11/30** (Edicion: SCIE)
- Área: MINING & MINERAL PROCESSING Cuartil: **Q2** Posición en el área: **8/20** (Edicion: SCIE)
- Área: GEOCHEMISTRY & GEOPHYSICS Cuartil: **Q2** Posición en el área: **42/87** (Edicion: SCIE)

SCImago Journal Rank

(Indicador correspondiente al último año disponible en este portal, año 2021)

- Año 2021
- Impacto SJR de la revista: 0.522
- Cuartil mayor: Q2
- Área: Geology Cuartil: **Q2** Posición en el área: **104/275**
- Área: Geotechnical Engineering and Engineering Geology Cuartil: **Q2** Posición en el área: **78/205**

Scopus CiteScore

(Indicador correspondiente al último año disponible en este portal, año 2021)

- Año 2021
- CiteScore de la revista: 3.7
- Área: Geology Percentil: **71**
- Área: Geotechnical Engineering and Engineering Geology Percentil: **66**

Journal Citation Indicator (JCI)

(Indicador correspondiente al último año disponible en este portal, año 2021)

- Año 2021
- JCI de la revista: 0.78
- Cuartil mayor: Q2
- Área: MINING & MINERAL PROCESSING Cuartil: **Q2** Posición en el área: **8/31**
- Área: GEOCHEMISTRY & GEOPHYSICS Cuartil: **Q2** Posición en el área: **40/100**
- Área: MINERALOGY Cuartil: **Q2** Posición en el área: **10/31**

4. A.3. Consent of co-authors

Edificio Hospital Real
Plaza Falla nº 8
11003 Cádiz
http://escueladoctoral.uca.es/
escuela.doctoral@uca.es

Modelo de consentimiento de coautores para inclusión de trabajos en la modalidad de tesis por compendio de publicaciones

Los investigadores/as:

SALVADOR DOMÍNGUEZ BELLA, EDUARDO MOLINA PIERNAS, JAVIER MARTINEZ LOPEZ, PHILIP MACHEV

como coautores/as del artículo: **Coastal Environment Impact on the Construction Materials of Anfushi's Necropolis (Pharos's Island) in Alexandria, Egypt**, publicado en **Minerals. MDPI**, por la presente dan su consentimiento para que esta publicación sea incorporada a la tesis doctoral titulada: Durability problems of the archaeological construction materials in aqueous and subaerial environments, with applications for restoration and conservation in Egypt and Sudan. // Problemas de durabilidad de los materiales de construcción arqueológicos en ambientes acuosos y subaéreos, con aplicaciones a la restauración y conservación en Egipto y Sudán.

cuyo autor/a es Abdelrhman Muhamed Fahmy Sayed Ahmed, renunciando a presentar estos resultados como parte de otra tesis doctoral en cualquier Universidad.

En Cadiz, a 10 de enero de 2023

Fdo. Salvador Domínguez Bella

Fdo. Eduardo Molina Piernas

Fdo. Javier Martínez López

Fdo. Philip Machev

4-A-4. Acceptance Letter



minerals

an Open Access Journal by MDPI

CITESCORE 3.7 SCOPUS

IMPACT FACTOR 2.818

CERTIFICATE OF ACCEPTANCE

Certificate of acceptance for the manuscript (**minerals-1922306**) titled:

Marine dynamics impact and the construction materials of Anfushi's Necropolis (Pharos Island) in Alexandria, Egypt

Authored by:

Abdelrhman Fahmy; Eduardo Molina-Piernas; Javier Martínez-López; Philip Machev; Salvador Domínguez-Bella

has been accepted in *Minerals* (ISSN 2075-163X) on 25 September 2022

MDPI Academic Open Access Publishing since 1996

Basel, September 2022



minerals

an Open Access Journal by MDPI

Coastal Environment Impact on the Construction Materials of Anfushi's Necropolis (Pharos's Island) in Alexandria, Egypt

Abdelrhman Fahmy; Eduardo Molina-Piernas; Javier Martínez-López; Philip Machev; Salvador Domínguez-Bella

Minerals 2022, Volume 12, Issue 10, 1235

4.B. Abdelrhman Fahmy, Javier Martínez-López, Ángel Sánchez-Bellón, Salvador Domínguez-Bella, and Eduardo Molina-Piernas. 2022. "Multianalytical Diagnostic Approaches for the Assessment of Materials and Decay of the Archaeological Sandstone of Osiris Temple (the Abaton) in Bigeh Island, Philae (Aswan, Egypt)." Journal of Cultural Heritage 58 (November): 167–78. https://doi.org/10.1016/j.culher.2022.09.025

4. B.1. Author Contributions

AF, JML, EMP, ASB, and SDB contributed to the conception and design ofthis study. **AF**, EMP, and SDB carried out the laboratory tests. **AF** wrote the first draft of themanuscript. **AF**, JML, EMP, ASB, and SDB contributed to the discussion ofthe results and collabo- rated in the writing of the differentsections of the manuscript. EMP and SDB contributed to the funding acquisition. All authors con- tributed to the reading and review of the manuscript and approved the submitted version.

4.B.2. Journal Metrics (Web of Science)

Indicadores

JCR (Journal Impact Factor)

(Indicador correspondiente al último año disponible en este portal, año 2021)

- Año 2021
- Factor de impacto de la revista: 3.229
- Factor de impacto sin autocitas: 3.015
- Article influence score: 0.627
- Cuartil mayor: Q2
- Área: CHEMISTRY, ANALYTICAL Cuartil: **Q2** Posición en el área: **42/87** (Edicion: SCIE)
- Área: GEOSCIENCES, MULTIDISCIPLINARY Cuartil: **Q2** Posición en el área: **92/202** (Edicion: SCIE)
- Área: SPECTROSCOPY Cuartil: **Q2** Posición en el área: **12/43** (Edicion: SCIE)
- Área: MATERIALS SCIENCE, MULTIDISCIPLINARY Cuartil: **Q3** Posición en el área: **202/345** (Edicion: SCIE)

SCImago Journal Rank

(Indicador correspondiente al último año disponible en este portal, año 2021)

- Año 2021
- Impacto SJR de la revista: 0.722
- Cuartil mayor: Q1
- Área: Conservation Cuartil: **Q1** Posición en el área: **4/100**
- Área: Archeology (arts and humanities) Cuartil: **Q1** Posición en el área: **30/353**
- Área: History Cuartil: **Q1** Posición en el área: **36/1492**
- Área: Chemistry (miscellaneous) Cuartil: **Q1** Posición en el área: **110/453**
- Área: Economics, Econometrics and Finance (miscellaneous) Cuartil: **Q1** Posición en el área: **55/416**
- Área: Anthropology Cuartil: **Q1** Posición en el área: **42/448**
- Área: Spectroscopy Cuartil: **Q2** Posición en el área: **20/75**
- Área: Computer Science Applications Cuartil: **Q2** Posición en el área: **246/729**
- Área: Materials Science (miscellaneous) Cuartil: **Q2** Posición en el área: **174/591**

CIRC

- Ciencias Sociales: A
- Ciencias Humanas: A+

Scopus CiteScore

(Indicador correspondiente al último año disponible en este portal, año 2021)

- Año 2021
- CiteScore de la revista: 6.1
- Área: Conservation Percentil: **99**
- Área: Archeology (arts and humanities) Percentil: **98**
- Área: Economics, Econometrics and Finance (all) Percentil: **97**
- Área: Chemistry (miscellaneous) Percentil: **87**
- Área: Materials Science (miscellaneous) Percentil: **79**
- Área: Computer Science Applications Percentil: **77**
- Área: Spectroscopy Percentil: **75**

Journal Citation Indicator (JCI)

(Indicador correspondiente al último año disponible en este portal, año 2021)

- Año 2021
- JCI de la revista: 2.29
- Cuartil mayor: Q1
- Área: GEOSCIENCES, MULTIDISCIPLINARY Cuartil: **Q1** Posición en el área: **4/245**
- Área: ARCHAEOLOGY Cuartil: **Q1** Posición en el área: **2/156**
- Área: CHEMISTRY, ANALYTICAL Cuartil: **Q1** Posición en el área: **3/99**
- Área: SPECTROSCOPY Cuartil: **Q1** Posición en el área: **3/46**
- Área: MATERIALS SCIENCE, MULTIDISCIPLINARY Cuartil: **Q1** Posición en el área: **19/414**
- Área: ART Cuartil: **Q1** Posición en el área: **4/141**

4. B.3. Consent of co-authors

Edificio Hospital Real
Plaza Falla nº 8
11003 Cádiz
http://escueladoctoral.uca.es/
escuela.doctoral@uca.es

Modelo de consentimiento de coautores para inclusión de trabajos en la modalidad de tesis por compendio de publicaciones

Los investigadores/as:

JAVIER MARTINEZ LOPEZ, ÁNGEL SANCHEZ-BELLON, SALVADOR DOMÍNGUEZ BELLA, EDUARDO MOLINA PIERNAS.

como coautores/as del artículo: **Multianalytical diagnostic approaches for the assessment of materials and decay of the archaeological sandstone of Osiris Temple (The Abaton) in Bigeh Island, Philae (Aswan, Egypt)**, publicado en **Journal of Cultural Heritage**. **Elsevier**, por la presente dan su consentimiento para que esta publicación sea incorporada a la tesis doctoral titulada: Durability problems of the archaeological construction materials in aqueous and subaerial environments, with applications for restoration and conservation in Egypt and Sudan. // Problemas de durabilidad de los materiales de construcción arqueológicos en ambientes acuosos y subaéreos, con aplicaciones a la restauración y conservación en Egipto y Sudán.

cuyo autor/a es Abdelrhman Muhamed Fahmy Sayed Ahmed, renunciando a presentar estos resultados como parte de otra tesis doctoral en cualquier Universidad.

En Cádiz, a 10 de enero de 2023

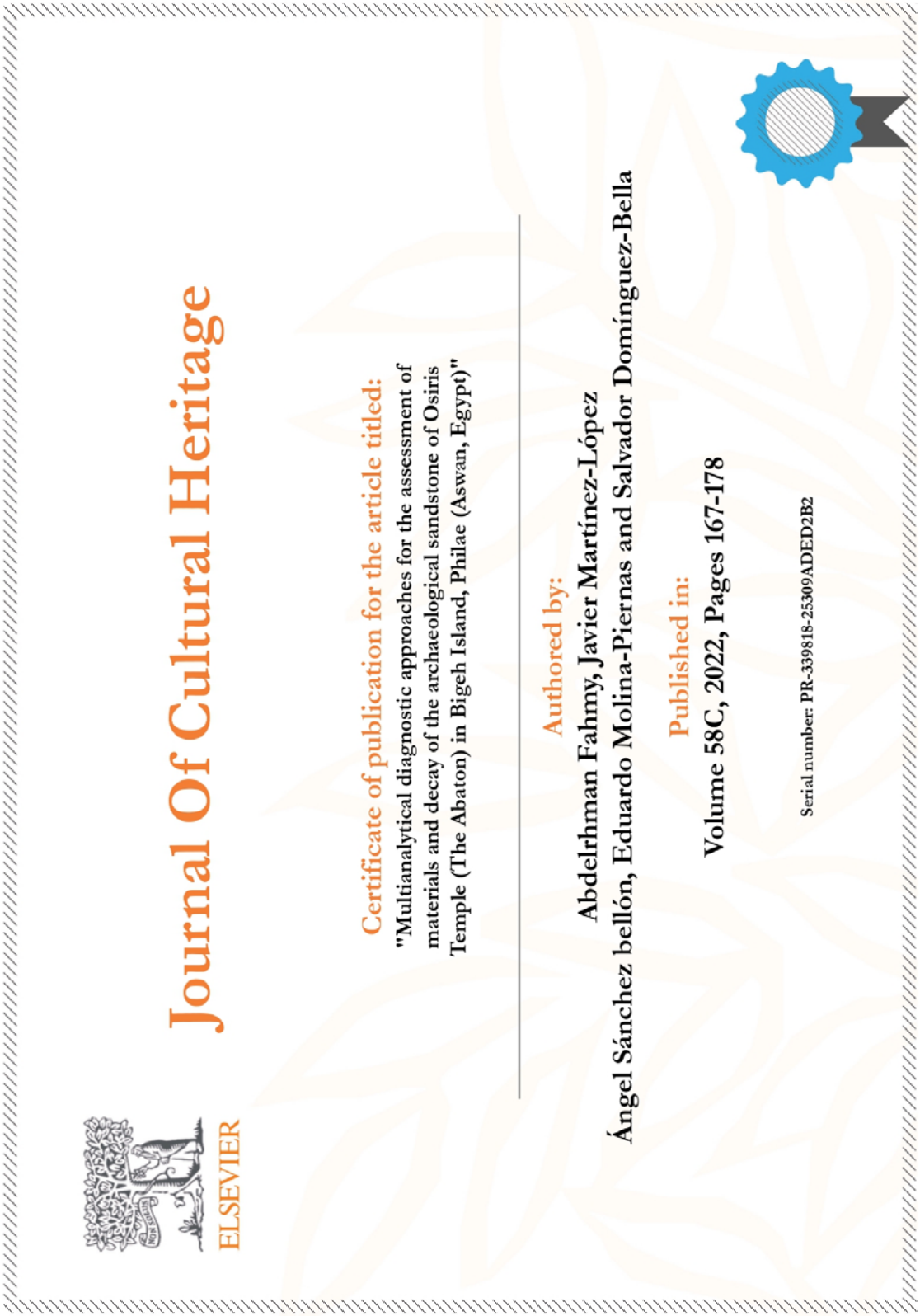
Fdo. Salvador Domínguez Bella

Fdo. Eduardo Molina Piernas

Fdo. Javier Martínez López

Fdo. Ángel Sánchez-Bellón

4-B-4. Acceptance Letter



Journal Of Cultural Heritage

ELSEVIER

Certificate of publication for the article titled:

"Multianalytical diagnostic approaches for the assessment of materials and decay of the archaeological sandstone of Osiris Temple (The Abaton) in Bigeh Island, Philae (Aswan, Egypt)"

Authored by:

Abdelrhman Fahmy, Javier Martínez-López

Ángel Sánchez bellón, Eduardo Molina-Piernas and Salvador Domínguez-Bella

Published in:

Volume 58C, 2022, Pages 167-178

Serial number: PR-339818-25309ADED2B2

4.C. Abdelrhman Fahmy, Eduardo Molina-Piernas, Salvador Domínguez-Bella, Javier Martínez-López, and Fatma Helmi. 2022. "Geoenvironmental Investigation of Sahure's Pyramid, Abusir Archeological Site, Giza, Egypt." Heritage Science 10 (1). https://doi.org/10.1186/s40494-022-00699-1

4.C.1. Author Contributions

The whole database construction, investigation, and analysis are presented in the manuscript and were carried out by the first author. Other authors reviewed and supervised the paper. All authors read and approved the final manuscript.

4.C.2. Journal Metrics (Web of Science)

Indicadores

JCR (Journal Impact Factor)
(Indicador correspondiente al último año disponible en este portal, año 2021)

- Año 2021
- Factor de impacto de la revista: 2.843
- Factor de impacto sin autocitas: 2.373
- Article influence score: 0.603
- Cuartil mayor: Q2
- Área: SPECTROSCOPY Cuartil: **Q2** Posición en el área: **14/43** (Edicion: SCIE)
- Área: CHEMISTRY, ANALYTICAL Cuartil: **Q3** Posición en el área: **48/87** (Edicion: SCIE)
- Área: MATERIALS SCIENCE, MULTIDISCIPLINARY Cuartil: **Q3** Posición en el área: **217/345** (Edicion: SCIE)

SCImago Journal Rank
(Indicador correspondiente al último año disponible en este portal, año 2021)

- Año 2021
- Impacto SJR de la revista: 0.634
- Cuartil mayor: Q1
- Área: Conservation Cuartil: **Q1** Posición en el área: **7/100**
- Área: Archeology (arts and humanities) Cuartil: **Q1** Posición en el área: **38/353**
- Área: Archeology Cuartil: **Q1** Posición en el área: **37/315**
- Área: Chemistry (miscellaneous) Cuartil: **Q2** Posición en el área: **130/453**
- Área: Spectroscopy Cuartil: **Q2** Posición en el área: **28/75**
- Área: Computer Science Applications Cuartil: **Q2** Posición en el área: **285/729**
- Área: Materials Science (miscellaneous) Cuartil: **Q2** Posición en el área: **201/591**

CIRC

- Ciencias Sociales: A
- Ciencias Humanas: A+

Scopus CiteScore
(Indicador correspondiente al último año disponible en este portal, año 2021)

- Año 2021
- CiteScore de la revista: 3.6
- Área: Conservation Percentil: **95**
- Área: Archeology (arts and humanities) Percentil: **93**
- Área: Archeology Percentil: **92**
- Área: Materials Science (miscellaneous) Percentil: **68**
- Área: Chemistry (miscellaneous) Percentil: **59**
- Área: Computer Science Applications Percentil: **58**
- Área: Spectroscopy Percentil: **44**

Journal Citation Indicator (JCI)
(Indicador correspondiente al último año disponible en este portal, año 2021)

- Año 2021
- JCI de la revista: 2.33
- Cuartil mayor: Q1
- Área: CHEMISTRY, ANALYTICAL Cuartil: **Q1** Posición en el área: **2/99**
- Área: HUMANITIES, MULTIDISCIPLINARY Cuartil: **Q1** Posición en el área: **22/402**
- Área: SPECTROSCOPY Cuartil: **Q1** Posición en el área: **2/46**
- Área: MATERIALS SCIENCE, MULTIDISCIPLINARY Cuartil: **Q1** Posición en el área: **18/414**

4. C.3. Consent of co-authors

Edificio Hospital Real
Plaza Falla nº 8
11003 Cádiz
http://escucladoctoral.uca.es/
escuela.doctoral@uca.es

Modelo de consentimiento de coautores para inclusión de trabajos en la modalidad de tesis por compendio de publicaciones

Los investigadores/as:
EDUARDO MOLINA PIERNAS, SALVADOR DOMÍNGUEZ BELLA, JAVIER MARTINEZ LOPEZ, FATMA HELMI
como coautores/as del artículo: **Geoenvironmental investigation of Sahure's pyramid, Abusir archeological site, Giza, Egypt**, publicado en **Heritage Science. Springer Nature**, *por la presente dan su consentimiento para que esta* publicación sea incorporada a la tesis doctoral titulada: Durability problems of the archaeological construction materials in aqueous and subaerial environments, with applications for restoration and conservation in Egypt and Sudan. // Problemas de durabilidad de los materiales de construcción arqueológicos en ambientes acuosos y subaéreos, con aplicaciones a la restauración y conservación en Egipto y Sudán.
cuyo autor/a es Abdelrhman Muhamed Fahmy Sayed Ahmed, renunciando a presentar estos resultados como parte de otra tesis doctoral en cualquier Universidad.

En Cádiz, a 10 de enero de 2023

Fdo. Salvador Domínguez Bella

Fdo. Eduardo Molina Piernas

Fdo. Javier Martínez López

Fdo. Fatma Helmi

4-C-4. Acceptance Letter

Date: 21 Apr 2022
To: "Abdelrhman Fahmy" abdelrhmanmuhammedfahmy@gmail.com
From: "Richard Brereton" heritage.science.journal@gmail.com
Subject: Decision has been reached on your submission to Heritage Science - HSCI-D-22-00003R2

HSCI-D-22-00003R2
Geoenvironmental investigation of Sahure's pyramid, Abusir Archeological site, Giza, Egypt
Abdelrhman Fahmy; Eduardo Molina; Salvador Domínguez-Bella; Javier Martínez-López; Fatma Helmi
Heritage Science

Dear PhD student Fahmy,

I am pleased to inform you that your manuscript "Geoenvironmental investigation of Sahure's pyramid, Abusir Archeological site, Giza, Egypt" (HSCI-D-22-00003R2) has been accepted for publication in Heritage Science.

Before publication, our production team will check the format of your manuscript to ensure that it conforms to the standards of the journal. They will be in touch shortly to request any necessary changes, or to confirm that none are needed.

Articles in this journal may be held for a short period of time prior to publication. If you have any concerns please contact the journal.

Any final comments from our reviewers or editors can be found, below. Please quote your manuscript number, HSCI-D-22-00003R2, when inquiring about this submission.

We look forward to publishing your manuscript and I do hope you will consider Heritage Science again in the future.

Best wishes,

Richard Brereton
Heritage Science
https://heritagesciencejournal.springeropen.com/

Editorial Comment

Please make the small corrections above when you check the proofs.

****

This letter contains confidential information, is for your own use, and should not be forwarded to third parties.

Recipients of this email are registered users within the Editorial Manager database for this journal. We will keep your information on file to use in the process of submitting, evaluating and publishing a manuscript. For more information on how we use your personal details please see our privacy policy at https://www.springernature.com/production-privacy-policy. If you no longer wish to receive messages from this journal or you have questions regarding database management, please contact the Publication Office at the link below.

_____
In compliance with data protection regulations, you may request that we remove your personal registration details at any time. (Use the following URL: https://www.editorialmanager.com/hsci/login.asp?a=r). Please contact the publication office if you have any questions.

4.D. Abdelrhman Fahmy, Eduardo Molina-Piernas, Javier Martínez-López, and Salvador Domínguez-Bella. 2022. "Salt Weathering Impact on Nero/Ramses II Temple at El-Ashmonein Archaeological Site (Hermopolis Magna), Egypt". Heritage Science 10 (1). https://doi.org/10.1186/s40494-022-00759-6

4.D.1. Author Contributions

The whole database construction, investigation, and analysis are presented in the manuscript and were carried out by the first author. Other authors reviewed and supervised the paper. All authors read and approved the final manuscript.

4.D.2. Journal Metrics (Web of Science)

Indicadores

JCR (Journal Impact Factor)
(Indicador correspondiente al último año disponible en este portal, año 2021)

- Año 2021
- Factor de impacto de la revista: 2.843
- Factor de impacto sin autocitas: 2.373
- Article influence score: 0.603
- Cuartil mayor: Q2
- Área: SPECTROSCOPY Cuartil: **Q2** Posición en el área: **14/43** (Edicion: SCIE)
- Área: CHEMISTRY, ANALYTICAL Cuartil: **Q3** Posición en el área: **48/87** (Edicion: SCIE)
- Área: MATERIALS SCIENCE, MULTIDISCIPLINARY Cuartil: **Q3** Posición en el área: **217/345** (Edicion: SCIE)

SCImago Journal Rank
(Indicador correspondiente al último año disponible en este portal, año 2021)

- Año 2021
- Impacto SJR de la revista: 0.634
- Cuartil mayor: Q1
- Área: Conservation Cuartil: **Q1** Posición en el área: **7/100**
- Área: Archeology (arts and humanities) Cuartil: **Q1** Posición en el área: **38/353**
- Área: Archeology Cuartil: **Q1** Posición en el área: **37/315**
- Área: Chemistry (miscellaneous) Cuartil: **Q2** Posición en el área: **130/453**
- Área: Spectroscopy Cuartil: **Q2** Posición en el área: **28/75**
- Área: Computer Science Applications Cuartil: **Q2** Posición en el área: **285/729**
- Área: Materials Science (miscellaneous) Cuartil: **Q2** Posición en el área: **201/591**

CIRC

- Ciencias Sociales: A
- Ciencias Humanas: A+

Scopus CiteScore
(Indicador correspondiente al último año disponible en este portal, año 2021)

- Año 2021
- CiteScore de la revista: 3.6
- Área: Conservation Percentil: **95**
- Área: Archeology (arts and humanities) Percentil: **93**
- Área: Archeology Percentil: **92**
- Área: Materials Science (miscellaneous) Percentil: **68**
- Área: Chemistry (miscellaneous) Percentil: **59**
- Área: Computer Science Applications Percentil: **58**
- Área: Spectroscopy Percentil: **44**

Journal Citation Indicator (JCI)
(Indicador correspondiente al último año disponible en este portal, año 2021)

- Año 2021
- JCI de la revista: 2.33
- Cuartil mayor: Q1
- Área: CHEMISTRY, ANALYTICAL Cuartil: **Q1** Posición en el área: **2/99**
- Área: HUMANITIES, MULTIDISCIPLINARY Cuartil: **Q1** Posición en el área: **22/402**
- Área: SPECTROSCOPY Cuartil: **Q1** Posición en el área: **2/46**
- Área: MATERIALS SCIENCE, MULTIDISCIPLINARY Cuartil: **Q1** Posición en el área: **18/414**

4. D.3. Consent of co-authors

Edificio Hospital Real
Plaza Falla nº 8
11003 Cádiz
http://escueladoctoral.uca.es/
escuela.doctoral@uca.es

Modelo de consentimiento de coautores para inclusión de trabajos en la modalidad de tesis por compendio de publicaciones

Los investigadores/as:
EDUARDO MOLINA PIERNAS, JAVIER MARTINEZ LOPEZ, SALVADOR DOMÍNGUEZ BELLA,
como coautores/as del artículo: **Salt weathering impact on Nero/Ramses II Tempie at El-Ashmonein archaeological site (Hermopolis Magna), Egypt,** publicado en **Heritage Science**. **Springer Nature**, por la presente dan su consentimiento para que esta publicación sea incorporada a la tesis doctoral titulada: Durability problems of the archaeological construction materials in aqueous and subaerial environments, with applications for restoration and conservation in Egypt and Sudan. // Problemas de durabilidad de los materiales de construcción arqueológicos en ambientes acuosos y subaéreos, con aplicaciones a la restauración y conservación en Egipto y Sudán.
cuyo autor/a es Abdelrhman Muhamed Fahmy Sayed Ahmed, renunciando a presentar estos resultados como parte de otra tesis doctoral en cualquier Universidad.

En Cádiz, a 10 de enero de 2023

Fdo. Salvador Domínguez Bella Fdo. Eduardo Molina Piernas

Fdo. Javier Martínez López

4-D-4. Acceptance Letter

Heritage Science: Decision on your manuscript

Emisor: Heritage Science <rashmi.jenna@springernature.com> a través de **<bounces-17638-1813@sp-bounce.springer.com>**
Destinatario: abdelrhman.fahmy@uca.es
Fecha: 27 de julio de 2022 21:28:17
Información Seguridad
Ref: Submission ID 14e8f512-dc63-435f-a04e-6d9883ed7439

Dear Dr Fahmy,

Re: "Contaminated water impact upon Nero/Ramses II Temple at El-Ashmonein archaeological site (Hermopolis Magna), Egypt."

We're delighted to let you know that your manuscript has been accepted for publication in Heritage Science.

Editor comments
Looking forward to your next paper!

Prior to publication, our production team will check the format of your manuscript to ensure that it conforms to the journal's requirements. They will be in touch shortly to request any necessary changes, or to confirm that none are needed.

Checking the proofs

Once we've prepared your paper for publication, you will receive a proof. At this stage, please check that the author list and affiliations are correct. For the main text, only errors that have been introduced during the production process, or those that directly compromise the scientific integrity of the paper, may be corrected.

As the corresponding (or nominated) author, you are responsible for the accuracy of all content, including spelling of names and current affiliations.

To ensure prompt publication, your proofs should be returned within two working days.

Publication policies

Acceptance of your manuscript is conditional on all authors agreeing to our publication policies at: https://www.springernature.com/gp/policies/editorial-policies

Article Processing Charge

You will shortly receive an email asking you to confirm your institutional affiliation and arrange payment of your article-processing charge (APC), if applicable. To find out more about APCs, visit our support portal: https://support.springernature.com/en/support/solutions/6000138386

Once again, thank you for choosing Heritage Science, and we look forward to publishing your article.

Kind regards,

Richard Brereton
Editor
Heritage Science

4.E. Abdelrhman Fahmy, Eduardo Molina-Piernas, Javier Martínez-López, and Salvador Domínguez-Bella. Sand dunes movement and flooding risk analysis for the pyramids of Meroe, Al Bagrawiya archaeological site, Sudan. (**Under revision**, submitted to International Journal of Architectural Heritage).

4.E.1. Author Contributions

The whole database construction, investigation, and analysis are presented in the manuscript and were carried out by the first author. Other authors reviewed and supervised the paper. All authors read and approved the final manuscript.

4.E.2. Journal Metrics (Web of Science)

Indicadores

JCR (Journal Impact Factor)

(Indicador correspondiente al último año disponible en este portal, año 2021)

- Año 2021
- Factor de impacto de la revista: 3.0
- Factor de impacto sin autocitas: 2.586
- Article influence score: 0.568
- Cuartil mayor: Q2
- Área: CONSTRUCTION & BUILDING TECHNOLOGY Cuartil: **Q2** Posición en el área: **31/68** (Edicion: SCIE)
- Área: ENGINEERING, CIVIL Cuartil: **Q2** Posición en el área: **66/138** (Edicion: SCIE)

SCImago Journal Rank

(Indicador correspondiente al último año disponible en este portal, año 2021)

- Año 2021
- Impacto SJR de la revista: 0.64
- Cuartil mayor: Q1
- Área: Conservation Cuartil: **Q1** Posición en el área: **6/100**
- Área: Visual Arts and Performing Arts Cuartil: **Q1** Posición en el área: **10/588**
- Área: Architecture Cuartil: **Q1** Posición en el área: **13/148**

CIRC

- Ciencias Sociales: A
- Ciencias Humanas: A+

Scopus CiteScore

(Indicador correspondiente al último año disponible en este portal, año 2021)

- Año 2021
- CiteScore de la revista: 5.5
- Área: Visual Arts and Performing Arts Percentil: **99**
- Área: Conservation Percentil: **98**
- Área: Architecture Percentil: **96**

Journal Citation Indicator (JCI)

(Indicador correspondiente al último año disponible en este portal, año 2021)

- Año 2021
- JCI de la revista: 2.75
- Cuartil mayor: Q1
- Área: ARCHITECTURE Cuartil: **Q1** Posición en el área: **6/93**
- Área: ENGINEERING, CIVIL Cuartil: **Q1** Posición en el área: **1/175**
- Área: CONSTRUCTION & BUILDING TECHNOLOGY Cuartil: **Q1** Posición en el área: **1/89**

4. E.3. Consent of co-authors

Edificio Hospital Real
Plaza Falla nº 8
11003 Cádiz
http://escueladoctoral.uca.es/
escuela.doctoral@uca.es

Modelo de consentimiento de coautores para inclusión de trabajos en la modalidad de tesis por compendio de publicaciones

Los investigadores/as:
SALVADOR DOMÍNGUEZ BELLA, EDUARDO MOLINA PIERNAS, JAVIER MARTINEZ LOPEZ,
como coautores/as del artículo: **Sand dunes movement and flooding risk analysis for the pyramids of Meroe, Al Bagrawiya archaeological site, Sudan**, subido a **International Journal of Architectural Heritage. Taylor & Francis**, por la presente dan su consentimiento para que esta publicación sea incorporada a la tesis doctoral titulada: Durability problems of the archaeological construction materials in aqueous and subaerial environments, with applications for restoration and conservation in Egypt and Sudan. // Problemas de durabilidad de los materiales de construcción arqueológicos en ambientes acuosos y subaéreos, con aplicaciones a la restauración y conservación en Egipto y Sudán.
cuyo autor/a es Abdelrhman Muhamed Fahmy Sayed Ahmed, renunciando a presentar estos resultados como parte de otra tesis doctoral en cualquier Universidad.

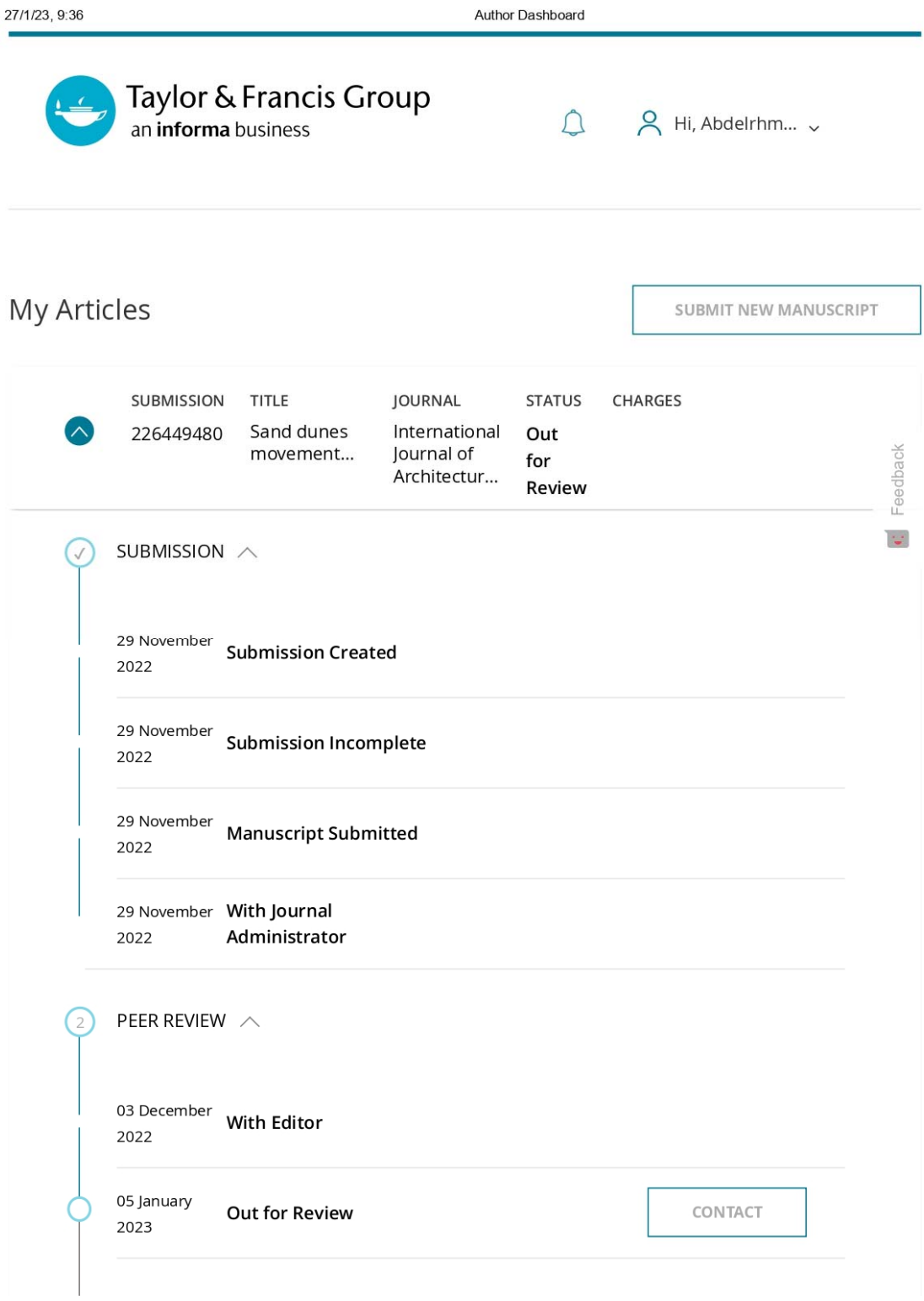
En Cadiz, a 10 de enero de 2023

Fdo. Salvador Domínguez Bella

Fdo. Eduardo Molina Piernas

Fdo. Javier Martínez López

4-E-4. Status of the article



4.F. Abdelrhman Fahmy, Anna Gołąbiewska, Wiktoria Wojnicz, Alicja Stanisławska, Jakub Kowalski, Justyna Łuczak, Adriana Zaleska-Medynska, Salvador Domínguez-Bella, Javier Martínez-López and Eduardo Molina-Piernas. Multi-functional monodispersed SiO_2-TiO_2 NPs and TEOS in the consolidation of archaeological lime mortars surfaces. (**Under revision**, submitted to Journal of Construcrion and Building materials).

4.F.1. Author Contributions

AF, AG, SDB, JML, and EMP contributed to the conception and design of this study. **AF**, AG, WW, AS, JK, JŁ, AZM, SDB, JML, and EMP collaborated in carrying out the laboratory tests. **AF** wrote the first draft of the manuscript. AG, WW, AS, JK, JŁ, AZM, SDB, JML, and EMP contributed to the discussion of the results, supervision and review of the article.

4.F.2. Journal Metrics (Web of Science)

Indicadores

Citas recibidas

- Citas en Scopus: 0 (22-01-2023)

JCR (Journal Impact Factor)

(Indicador correspondiente al último año disponible en este portal, año 2021)

- Año 2021
- Factor de impacto de la revista: 7.693
- Factor de impacto sin autocitas: 5.464
- Article influence score: 0.894
- Cuartil mayor: Q1
- Área: CONSTRUCTION & BUILDING TECHNOLOGY Cuartil: **Q1** Posición en el área: **6/68** (Edicion: SCIE)
- Área: MATERIALS SCIENCE, MULTIDISCIPLINARY Cuartil: **Q1** Posición en el área: **76/345** (Edicion: SCIE)
- Área: ENGINEERING, CIVIL Cuartil: **Q1** Posición en el área: **5/138** (Edicion: SCIE)

SCImago Journal Rank

(Indicador correspondiente al último año disponible en este portal, año 2021)

- Año 2021
- Impacto SJR de la revista: 1.777
- Cuartil mayor: Q1
- Área: Building and Construction Cuartil: **Q1** Posición en el área: **8/193**
- Área: Civil and Structural Engineering Cuartil: **Q1** Posición en el área: **17/328**
- Área: Materials Science (miscellaneous) Cuartil: **Q1** Posición en el área: **54/591**

Scopus CiteScore

(Indicador correspondiente al último año disponible en este portal, año 2021)

- Año 2021
- CiteScore de la revista: 10.6
- Área: Civil and Structural Engineering Percentil: **95**
- Área: Building and Construction Percentil: **94**
- Área: Materials Science (all) Percentil: **87**

Journal Citation Indicator (JCI)

(Indicador correspondiente al último año disponible en este portal, año 2021)

- Año 2021
- JCI de la revista: 1.44
- Cuartil mayor: Q1
- Área: CONSTRUCTION & BUILDING TECHNOLOGY Cuartil: **Q1** Posición en el área: **9/89**
- Área: MATERIALS SCIENCE, MULTIDISCIPLINARY Cuartil: **Q1** Posición en el área: **52/414**
- Área: ENGINEERING, CIVIL Cuartil: **Q1** Posición en el área: **13/175**

4. E.3. Consent of co-authors

UCA
Escuela de Doctorado UCA
Edificio Hospital Real
Plaza Falla nº 8
11003 Cádiz
http://escueladoctoral.uca.es/
escuela.doctoral@uca.es

Modelo de consentimiento de coautores para inclusión de trabajos en la modalidad de tesis por compendio de publicaciones

Los investigadores/as:

Anna Gołąbiewska, Wiktoria Wojnicz, Alicja Stanisławska, Jakub Kowalski, Justyna Łuczak, Adriana Zaleska-Medynska, Salvador Domínguez-Bella, Javier Martínez-López, Eduardo Molina-Piernas,

como coautores/as del artículo: **Multi-functional monodispersed SiO_2-TiO_2 NPs and TEOS in the consolidation of archaeological lime mortars surfaces**, subido a **Construction and Building Materials. Elsevier,** por la presente dan su consentimiento para que esta publicación sea incorporada a la tesis doctoral titulada: Durability problems of the archaeological construction materials in aqueous and subaerial environments, with applications for restoration and conservation in Egypt and Sudan. // Problemas de durabilidad de los materiales de construcción arqueológicos en ambientes acuosos y subaéreos, con aplicaciones a la restauración y conservación en Egipto y Sudán.

cuyo autor/a es Abdelrhman Muhamed Fahmy Sayed Ahmed, renunciando a presentar estos resultados como parte de otra tesis doctoral en cualquier Universidad.

En Cadiz, a 10 de enero de 2023

Fdo. Anna Gołąbiewska
Fdo. Wiktoria Wojnicz
Fdo. Alicja Stanisławska
Fdo. Jakub Kowalski
Fdo. Justyna Łuczak
Fdo. Adriana Zaleska-Medynska
Fdo. Salvador Domínguez Bella
Fdo. Eduardo Molina Piernas
Fdo. Javier Martínez López

4-E-4. Status of the article

ELSEVIER

Track your submission

This is a new submission-tracking service.

Thank you, could you tell us more?

Peer review status

Multi-functional monodispersed SiO2-TiO2 NPs and TEOS in the consolidation of archaeological lime mortars surfaces.

- Reviews completed: 0
- Review invitations accepted: 2+
- Review invitations sent: 2+

Under Review

Last review activity: 1st January 2023

Watch to learn what we're doing behind the scenes

Journal:
Construction and Building Materials

Corresponding author:
Abdelrhman Fahmy

First author:
Abdelrhman Fahmy

Annex 5: Plan of the Investigation

UCA Universidad de Cádiz	**ESTUDIOS DE DOCTORADO**

PLAN DE INVESTIGACIÓN DE TESIS DOCTORAL

R.D. 99/2011

A. MEMORIA DEL PLAN DE INVESTIGACIÓN DE TESIS DOCTORAL

(A cumplimentar por el doctorando

Apellidos: **Muhamed Fahmy Sayed Ahmed** Nombre: **Abdelrhman**

D.N.I./Pasaporte: **A20325343** Programa de doctorado: **8207 Historia y Arqueología Marítimas**

Escuela de Doctorado: Escuela **Internacional de Doctorado en Estudios del Mar (EIDEMAR)**

Título de la tesis: **Durability problems of the archaeological construction materials in aqueous and subaerial environments, with applications for restoration and conservation in Egypt and Sudan.**

Problemas de durabilidad de los materiales de construcción arqueológicos en ambientes acuosos y subaéreos, con aplicaciones a la restauración y conservación en Egipto y Sudán.

Director/es Prof. Dr. D. **SALVADOR DOMÍNGUEZ BELLA**

Dr. D. **EDUARDO MOLINA PIERNAS**

1.Resumen

(Indicar los aspectos más relevantes, los objetivos propuestos y los resultados esperados)

(Máximo 3500 caracteres)

Los entornos marino y fluvial pueden afectar de forma distinta a la durabilidad de los materiales arqueológicos de construcción costeros, ya estén sumergidos en agua y/o en contacto con esta. La interacción entre el agua marina o fluvial y los materiales de construcción arqueológicos de los edificios históricos seleccionados tiene un impacto en el deterioro de estos materiales y juega un papel clave por la erosión fisicoquímica de la piedra natural constituyente de los edificios arqueológicos. En Egipto, la antigua puerta del templo Abaton de Osiris (isla Bigeh) en Asuán es un edificio arqueológico parcialmente sumergido en el río Nilo y sufre los efectos severos y acumulados tanto de las condiciones ambientales como de los impactos del agua. Por otro lado, la necrópolis de Al Anfushi, ambos en Alejandría y adyacentes a la línea de costa del Mar Mediterráneo, están expuestos a un ambiente costero, el cual suele ser más agresivo con la durabilidad de los materiales. Además, la investigación estudiará algunos sitios seleccionados en el desierto (pirámide de Sahure en Egipto y las pirámides de Meroe en Sudan) y entornos urbanos (Templo de Nerón en Minia, Egipto). Los objetivos esenciales de esta investigación son: 1) analizar y evaluar los riesgos y peligros geográficos en los materiales de construcción expuestos a diferentes ambientes acuáticos y terrestres, 2) determinar las características fisicoquímicas de los materiales de construcción arqueológicos 3) proponer un plan de conservación y gestión para proteger los edificios arqueológicos rodeados de entornos acuáticos y, 4) desarrollar nuevos nanomateriales multifuncionales para proteger los edificios de piedra y mortero sometidos a las condiciones del agua. Este proyecto de tesis se llevará a cabo mediante el trabajo de laboratorio y el análisis de los materiales de construcción para detectar los problemas de durabilidad de estos en entornos diferentes, utilizando para ello diferentes tipos de técnicas y herramientas analíticas avanzadas.

1. Abstract

Marine and river environments have different impacts on the durability of the archaeological submerged construction materials which they are either submerged in water and/or contacted to water. The interaction between the saline and fluvial water and the archaeological construction materials of the selected archaeological buildings has impacts in decay of the construction materials and has played a damaged role in physic-chemical weathering of the natural stones of the archaeological buildings. In Egypt, the old gate of Abaton temple of Osiris (Bigeh island) in Aswan is considered a partial submerged archaeological building in the Nile River and suffer the severe and accumulated effects of the environmental conditions and water impacts. On the other hand, Al Anfushi necropolis, adjacent to coastline (Mediterranean Sea) in Alexandria and where coastal environment is usually more aggressive with the building materials. In addition, the research is going to study some selected sites in the desert (pyramid of Sahure in Egypt and the pyramids of Meroe in Sudan) and urban environments (Temple of Nero in Minia, Egypt). The essential objectives of this research are: 1) to analyse and assess the risks and geohazards on the construction materials of different locations and environments, 2) determine the physical and chemical characteristics of the archaeological construction materials 3) to put a conservation, management plan to protect the archaeological buildings surrounded by water environments and 4) to develop new multi-functional nanomaterials to protect the stone and mortar building subjected to water conditions. The assessment study is going to be carried out through laboratory approach and analysis of the construction materials to detect the durability problem of the construction materials in these different environments by utilizing different kinds of advanced techniques and analytical tools.

2.- Antecedentes y estado actual del tema

(Exponer los antecedentes y el estado actual de los conocimientos científico-técnicos de la materia específica del proyecto, incluyendo, en su caso, los resultados previos del grupo de investigación en el que se integre el doctorando y los de otros grupos que trabajen en la misma línea.) (Máximo 16000 caracteres)

2.1 Antecedentes

The different ancient cultural heritage is part of who we are as it is the memory of our past; it leads us for better future. In addition, heritage and history influence on how we develop, transferring knowledge for next generations, and provide a basis for tradition and value [VV.AA., 2015][2] [Viejo-Rose, 2015][3]. It is in this spirit that we must safeguard the cultural heritage with scientific studies and investigation to understand the cultural materials and manage us to preserve and restore it scientifically.

Underwater archaeology is a significant trend all over the world nowadays as a great part of human past/history and it is related with marine, oceanic and river environments, and many of the remains of the built heritage or vestiges of past cultures can be found submerged totally, partially, or existing in surrounding water environments. General terms which have been utilized to express water archaeology are maritime archaeology, marine archaeology, sunken archaeology, submerged heritage, or underwater cultural heritage. According to UNESCO code of ethics, "*underwater cultural heritage encompasses all traces of human existence having a cultural, historical or archaeological character, lying under water. Over the centuries, thousands of ships, entire cities, and even landscapes have been swallowed by the waves. They constitute a precious heritage that needs to be protected*" [UNESCO, website][4] *or "underwater cultural heritage is all traces of human existence having a cultural, historical or archaeological character which have been partially or totally under water, periodically or continuously, for at least 100 years such as sites, structures, buildings, artefacts and human remains*" [UNESCO, website][5]. Underwater cultural heritage (UCH) has a powerful potentiality in achieving of sustainable development and opens the doors to new kind of tourism opportunities with economic benefits and key for urban development.

[2] VV.AA. (2015). *Heritage for Peace and Reconciliation*.

[3] Viejo-Rose, D. (2015). Cultural heritage and memory: untangling the ties that bind. *Culture & History Digital Journal*, *4*(2), e018. https://doi.org/10.3989/chdj.2015.018

[4] *http://www.unesco.org/new/en/culture/themes/underwater-cultural-heritage/divers/code-of-ethics/*

[5] http://www.unesco.org/new/en/culture/themes/underwater-cultural-heritage/underwater-cultural-heritage/definition-of-underwater-cultural-heritage

Consequently, we need a concerted effort to protect our underwater cultural heritage from climate, environmental and decay causes and put a clear suitable plan for preservation of this kind of heritage and keep their wonderful landscape for future generation.

Underwater cultural heritage (UCH) has become a day talk globally, especially in excavations, finding of archaeological finds and preservation of this type of archaeology. Many authors and international organizations in archaeology and marine sciences presented a great effort to publish many international reports, charters, papers and books about the excavations works in oceans and seas, materials and preservation of this kind of heritage. In this sense, e.g. [Wessman, 2011][6] illustrated the environmental impacts for underwater cultural heritage. [Khakzad, 2008][7] studied the damage assessment and conservation of UCH relics in Belgium and suggested an excellent presentation in her case study. In 1987, Florida started to develop the underwater parks to show shipwrecks and other historic sites. The preserved shipwreck has become popular attractions for skin and scuba diving visitors to witness a part of Florida's history first-hand [Florida department of state, website][8]. In 2014, UNESCO issued a conference book to present the underwater cultural heritage from the First World War and their threats and challenges as a step for taking initiatives and programs to protect them for next generations [UNESCO, 2014][9]. In a step towards preserving the underwater cultural heritage International Center of Archaeology in cooperation with another authors and UNESCO, they issued a code of ethics

[6] Mann, H. (2011). The Appearance of New Bacteria (titanic bacterium) and Metal Corrosion. *UNESCO Scientific Colloquium on Factors Impacting Underwater Cultural Heritage*, *December*, 44–51. https://www.academia.edu/7243168/UNESCO_SCIENTIFIC_COLLOQUIUM_ON_FACTORS_IMPACTING_UNDERWATER_CULTURAL_HERITAGE?email_work_card=view-paper

[7] Khakzad, S. (2008). *Conservation, and Presentation of Underwater Cultural Heritage to the Public Case study: The current projects in Belgium Leuven*. 146. https://www.academia.edu/3677467/Underwater_Cultural_Heritage_Conservation_and_Presentation_to_the_Public_Master_Thesis?email_work_card=view-paper

[7] https://dos.myflorida.com/historical/archaeology/underwater/underwater-preserves/

[9] UNESCO. (2014). Underwater Cultural Heritage from World War I. In *Scientific conference on the occasion of the centenary of World War I* (Issues 26 & 27 June). https://www.academia.edu/13991579/The_Underwater_Cultural_Heritage_of_World_War_I._Proceedings_of_the_Scientific_Conference_on_the_Occasion_of_the_Centenary_of_World_War_I_Bruges_Belgium_26_and_27_June_2014?email_work_card=minimal-title

for drivers to protect the underwater heritage from damage [Centre, I., Archaeology et al, 2015][10]. [Hassan, et al, 2000][11] presented a study on underwater cultural heritage, conservation management for marine artefacts and shipwrecks, pollution and erosion impacts on coastal heritage and remote sensing in marine archaeology upon Alexandria. [Eld *et al.*, 2016][12] authored a manual book with guidelines to present conservation and site management plan, documentation techniques and impacts of offshore activities on underwater cultural heritage. [Forrest & Jeffery, 2018][13] [Body, 2001][14]presented a study on safeguarding underwater cultural heritage by mapping projects and programs and identify the gaps to be addressed in order to strengthen the underwater cultural heritage UCH protection for sustainable development. By protection of underwater cultural heritage, we can achieve so many benefits from economy and tourism point of views and achieving urban and sustainable development for the site. [Prott, 2007][15] explained the natural and human impacts on underwater cultural heritage and showed simple and cheap methods to protect the underwater cultural heritage. [Khakzad, 2015] [16] [Khakzad, *et al.*, 2015] [17] presented a management study for coastal cultural heritage with potentials and obstacles. [Carper, 2019][18] presented proceedings for underwater archaeology in geophysical

[10] Centre, I., Archaeology, U., Ferenčić, N., Brugman, F., Villegas, T., Dromgoole, S., Sataloff, R. T., Johns, M. M., Kost, K. M., UNESCO, Guérin, U., SCHWARZ, G., VV.AA., Favis, R. L., Manders, M. R., Underwood, C. J., Goter, P. W., Mann, H., Body, T. A., … Williams, S. (2015). *International Journal of Nautical Archaeology*, *152*(2), 1–6.

[11] Hassan, M., Grimal, N., & Nakashima, D. (2000). *Underwater Archaeology and Coastal Management focus on Alexandria*. ISSN: 9231037307, UNESCO.

[12] Maarleveld, T. J., Guérin, U., & Egger, B. (2016). *Manual for Activities directed at Underwater Cultural Heritage, Guidelines to the Annex of the UNESCO 2001 Convention, in Arabic*. www.unesco.org/en/underwater-cultural-heritage

[13] Craig Forrest & Bill Jeffery, (2018). *Underwater cultural heritage (UCH) related legislation and programme review in the five countries in Micronesia - UNESCO Biblioteca Digital.pdf*. (UNESCO).

[14] Body, T. A. (2001). *The Benefit of the Protection of Underwater Cultural Heritage for Sustainable Growth, Tourism and Urban Development*.

[15] Prott, L. (2007). Underwater Cultural Heritage at Risk: Managing Natural and Human Impacts. In *International Journal of Nautical Archaeology* (Vol. 36, Issue 2, pp. 429–431). https://doi.org/10.1111/j.1095-9270.2007.163_2.x

[16] Khakzad, S. (2015). Integrated Approach in Management of Coastal Cultural Heritage. *Dissertation*, *June*, 236.

[17] Khakzad, S., Pieters, M., & Van Balen, K. (2015). Coastal cultural heritage: A resource to be included in integrated coastal zone management. *Ocean and Coastal Management*, *118*, 110–128. https://doi.org/10.1016/j.ocecoaman.2015.07.032

[18] Carper, R. G. (2007). Underwater Archaeology. *Current Anthropology*, *48*(6), 779–779. https://doi.org/10.1086/521536

investigations to find the Wreck of an iconic Upper Missouri River Mountain Packet Steamboat, Wood Analysis from the Spring Break Wreck, Launching the Submerged Heritage Monitoring Scouts Florida Program, Using Archaeological Lenses and Conservation Assessment Tools to Influence Curation and in Situ Digital Documentation of the 1559 Emanuel Point Shipwrecks. [Steffy, 2001] in the conference proceedings under title "A Mediterranean ship construction database; dating and classifying shipwrecks by their hull remains" many authors presented topics on underwater cultural heritage such as excavations works at Alexandria searching for the lighthouse of Alexandrian and an assessment of maritime conditions, coastal aspects and the suitability of selected second millennium BC anchorages of the eastern Mediterranean, etc. [Schwarz, 2018][19] presented a study on safeguarding of underwater cultural heritage in the Pacific: report on good practice in the protection and management of World War II. [Hairy, 2020][20] presents a significant study about Qaitbay underwater site at Alexandria with surveying methodology for the site using GIS and photogrammetry. [Tallet, 2014][21] the French mission leaded by them had discovered the harbour of king Khufu on the red seacoast with so much stone blocks(anchors), potteries and papyrus. [Abd-el-Maguid, 2012][22] presented a study on underwater archaeology in Egypt and its protection and mentioned the various international and local institutes and missions who have worked in underwater archaeology in Egypt such as Institut European d'Archéologie Sous-Marine, Centre d'Études Alexandrines, Institute of Nautical Archaeology, Hellenic Institute of Ancient and Mediaeval Alexandrian Studies, In Situ Institute, University of Torino, DUA's foundation and Nile Archaeological Mapping Project (NAMP).

[19] Schwarz, G. (2018). Safeguarding Underwater Cultural Heritage in the Pacific: report on good practice in the protection and management of World War II-related underwater cultural heritage. In *International Journal of Nautical Archaeology* (Vol. 47, Issue 2, pp. 495–496). https://doi.org/10.1111/1095-9270.12315

[20] Hairy, I. (2020). *The Qaitbay Underwater Site at Alexandria, Egypt: The evolution of surveying techniques*. *October 2017*.

[21] Pierre Tallet, & Gregory Marouard. (2014). THE HARBOR OF KHUFU on the Red Sea Coast at Wadi al-Jarf, Egypt. *Near Eastern Archaeology*, *77*(1), 4-14. doi:10.5615/neareastarch.77.1.0004

[22] Abd-el-Maguid, M. M. (2012). Underwater Archaeology in Egypt and the Protection of its Underwater Cultural Heritage. *Journal of Maritime Archaeology*, *7*(1), 193–207. https://doi.org/10.1007/s11457-012-9098-5

From previous literature, it can be concluded that although many studies have been carried out, there are still many gaps and lackage in topics of archaeometrical studies because most of studies only focus on archaeological excavations for the underwater findings without looking after the archaeological matters and their characteristics, problems and conservation, especially for the stone-based monuments and existed in underwater conditions. Furthermore, most studies have focused or continue to focus on coastal, marine and oceanic archeological sites, but for river underwater archaeology there is hardly any study. In this sense, in Egypt, all archaeological studies are concentrated in Mediterranean Sea and Red Sea but related to the Nile River still without any archaeometrical studies for underwater findings and buildings along with the comparison with subaerial environments at El Ashmoenin archaeological site (Nero Temple, Egypt), Abusir archaeological site (Sahure pyramid, Egypt) and Al Bagrawyia archeological site (Pyramids of Meroe, Sudan). That is why; the presented research is entitled "Durability problems of the archaeological construction materials in aqueous and subaerial environments, with applications for restoration and conservation in Egypt and Sudan".

Egypt is located in north-eastern of Africa continent and south-western of Asia with coordinates 27°N, 30°E, occupies an area of 1 million km^2 and bordered by Mediterranean Sea in the north, Sudan in the south, Libya in the west and red sea in the east (Figure 1). Egypt has very significant archaeological sites above the ground and underwater heritage, contains one of the world's notable and old sites such as the great pyramid which is one of the seven world's wonders. Egypt has two kinds of sunken or submerged monuments one of them related to seawater in Mediterranean Sea and Red Sea and the second kind with Nile River (freshwater) from south to north of Egypt. In fact, plenty of archaeological artefacts and built heritage are under water such as old cities and old harbours, for example, Wadi Al–Jarf port, Qaitbay fort, Al-Shatby, Mamoura Bay, Saadana Island, Eastern harbour, Abu Quir Bay and Aswan. In addition, to may rock cut and subareial archaeological sites such as Giza pyramids, Temple of Luxor, Temple of Hatshepsut, Valley of nobles, Beni Hassan Tombs, etc.

Sudan is located between Egypt and Eritrea (north-eastern of Africa) It is bordered by the Red Sea in northeast, Libya in northwest, Chad in west, the Central African Republic in southwest, South Sudan in south and Ethiopia in southeast (Figure 1)[23]. Sudan contains many significant archaeological sites and monuments such as pyramids of Meroe, Temple of Amun, Old Dongola, Nuri Pyramids, Jebel Barkal, etc. Most of the buildings there are in the desert and urban environments.

2.2 Sites of study

Figure 1 shows the different locations of the selected archaeological sites in Egypt: Necropolis of Anfushi (Alexandria), Sahure Pyramid (Abusir), Nero Temple (Minia, El Ashmoenin archaeological site), and Abaton Temple (Aswan) and, in Sudan, the Pyramids of Meroe (Al Bagrawyia archeological site).

The presented research is an analytical and comparative study between different selected sites in Alexandria (Al-Anfushy tombs) exposed to coastal environment, and the second located in Aswan (Abaton temple of Osiris near to Philae temple) as (river environment) partially submerged cultural heritage. On the other hand, subaerial environments, Sahure Pyramid (Abusir) and Pyramids of Meroe (Al Bagrawyia archeological site) were selected as desert environment, Nero Temple (Minia, El Ashmoenin archaeological site) as urban environment. The coastal environment represents the subaerial marine archaeology causes many erosions impacts on the archaeological buildings contacted to the marine environments due to saline water action and salt decay. On the other hand, the river environments also have different impact upon the archaeological buildings totally or partially submerged in Nile River. Furthermore, the desert environment shows the geoenvironmental impacts on the durability of the construction material and in the urban environment the subsurface water is the main hazard of the building materials decay. Generally, this study is a pioneer study because all previous archaeometrical studies were

[23] https://www.nationsonline.org/oneworld/map/sudan_map.htm#:~:text=The%20Republic%20of%20the%20Sudan%20is%20located%20in%20north%2Deastern,by%20Ethiopia%20in%20south%20east.

upon aerial stone archaeological buildings in the deserts or above the ground. In addition, this study compares between different aqueous and subaerial environments and their impacts on the conservation state of the selected building materials. Therefore, our study is focusing mainly on archaeometrical and materials studies for archaeological buildings in all different selected sites. To achieve the main goals, this approach will be carried out in two main stages: the first part will consist of the analytical study by means of destructive and non-destructive analytical techniques of the construction materials of the selected archaeological sites to assess and evaluate the sustainability problems due to environmental impacts. Secondly, to reach to final proposal for the preservation and restoration of this kind of heritage in Egypt by using nanomaterials for surfaces protection of the building materials, especially for the joint mortars.



Figure 1. The locations of the selected archaeological sites in Egypt (Anfushi Necropolis, Sahure pyramid, Nero Temple and Abaton Temple) and Sudan (Pyramids of Meroe) (from Google Earth pro).

2.2.1 Aswan (Egypt): Abaton temple of Osiris, Philae complex

Aswan is a big city in south of Egypt with coordinates 24°05'20"N / 32°53'59"E and 194 m.a.s.l., and it is considered the border between Egypt and Sudan. A lot of fascinating archaeological sites are existing in Aswan such as Wadi Allaqui, Abu Simbel, Elephantine, Philae, El Nabatat Island, Kalabsha temple, Tombs of nobles, Nubia, Banu Kanz and Coptic Diocese of Syene, among others.

Our case study is related to Abaton temple of Osiris related and near to Philae complex (figure 2) which it is located on Agilkia Island on Nile River. Nile river is the world's longest river, the Nile runs 6,695 km from its source in Burundi, in Central Africa, to the Mediterranean Sea, most of the water contributed to the Nile comes from the Blue Nile, which originates at Lake Tana in Ethiopia, the average flow of the Nile River is about 50 million cubic meters per day., During the rainy season, however, the three branches of the Nile River increase their flow to just over 700 million cubic meters per day [Stephenson, 2010][24].

The research focuses on the Abaton temple of Osiris, south to Philae complex which is situated on north side of Aswan dam as shown in (figure 2). Abaton temple of Osiris is a very clear example for the effects of freshwater environment (Nile River) and atmospheric environment. Figure 3 shows the effects of Nile River oscillation levels upon archaeological buildings in Aswan, where the bluish and reddish colours mean the Nile River and rocks around, respectively.

This temple was constructed by ancient Egyptians under *Ptolemaic* era and was devoted as mausoleum to the Osiris god (god of fertility, agriculture, afterlife and death), considered as the most important sacred place in Egypt because it was the tomb of Osiris. This current

[24] Stephenson, J. (2010). People and Place. *Planning Theory and Practice*, *11*(1), 9–21. https://doi.org/10.1080/14649350903549878

remained gate was constructed in the entrance of this tomb and now is located in Bigeh Island but previously was situated in west side of Philae Island (figure 3).

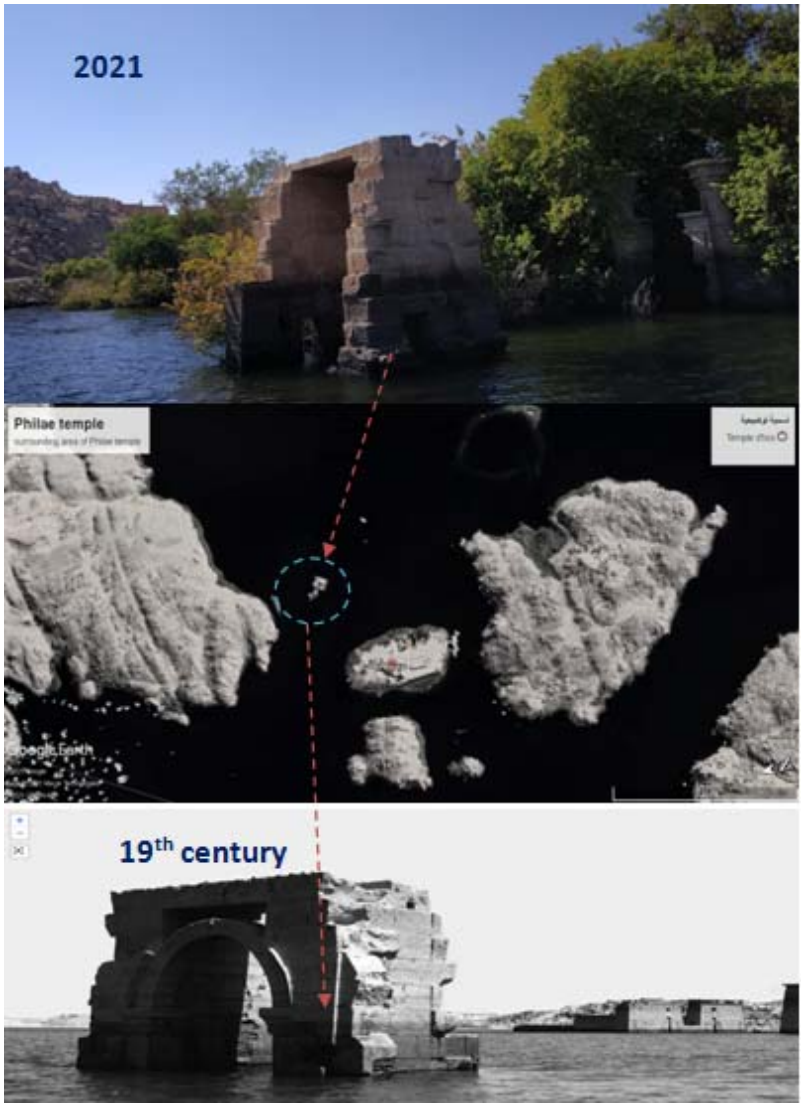


Figure 2. Abaton temple of Osiris in Aswan (Bigeh Island), represents partially submerged heritage in fluvial environments (UNESCO archives).

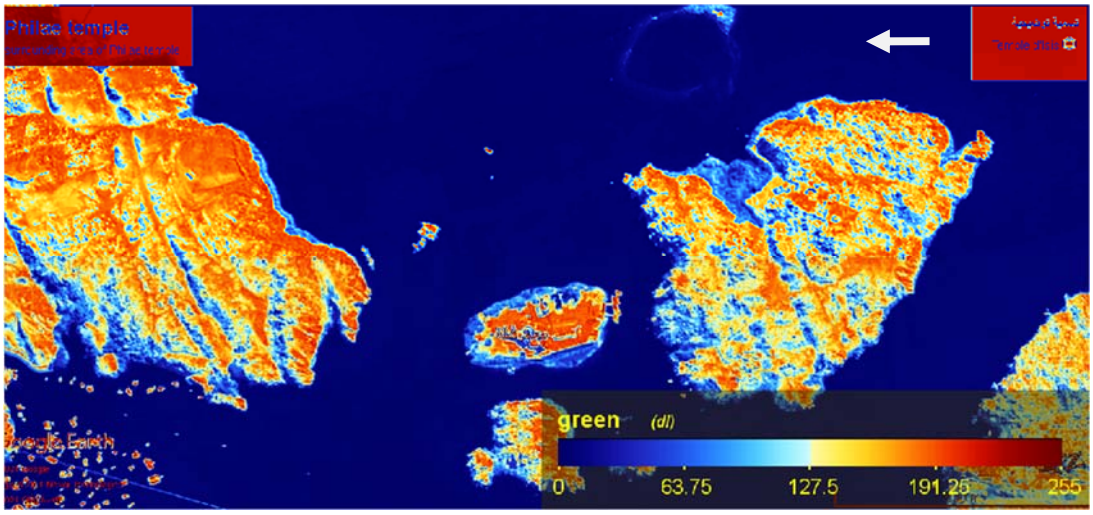


Figure 3. Map of archaeological site of Philae temple and Abaton temple of Osiris in Aswan and Nile water surrounding and covering parts of the archaeological buildings such as Abaton temple of Osiris, (Blue: Nile water; yellow and red: dry rocks).

2.2.2 Alexandria (Egypt): Al-Anfushi Necropolis

The research will focus on the marine archaeological buildings exposed to saline water environment in Alexandria, such as Al-Anfushi Necropolis.

In 1901, the Anfushi Tombs were discovered by Giuseppe Botti who is the director of the Greco-Roman museum, he was the first to discover the tombs and publish about them. After his death, in 1903, Evaristo Breccia and Achille Adriani, his successors in the directorship of the museum, continued the work of Botti. Only five tombs from the overall complex are visible today, dating from the mid of second century, from these tombs, Anfushi I, II, and V will be studied. Each of them consists of two burial units, both approached directly by the court, having also subsidiary rooms. The main characteristic of these tombs is the bilingual character of its decoration, which emerged with the redecoration of the tomb. During this process, Greek decorative elements were retained in the anteroom, while Egyptian elements were added, probably onto plaster previously unpainted, we should also be aware of the fact that the necropolis was located in a district where the majority of the population was Egyptian. In addition, Anfushi II was the only

structure of a Ptolemaic Alexandrian tomb with Egyptian-style views, such as the priest painted in the mural painting of the stairs headed to the court. A comparison with other types of material evidence indicates the important role of Egyptian priesthood throughout the Ptolemaic Period [Savvopoulos, 2013][25] [Savvopoulos, 2011][26] [website][27].

In this necropolis, the study will focus on archaeometrical and petrophysical studies for the construction materials of those tombs and their durability problems due to the coastal environment and effect of subsurface water which led to severe degradation and decay to the structural, architectural and decoration elements of the tombs, with advanced techniques for analysis and investigation to assess the durability of the stone construction material (Figure 4).

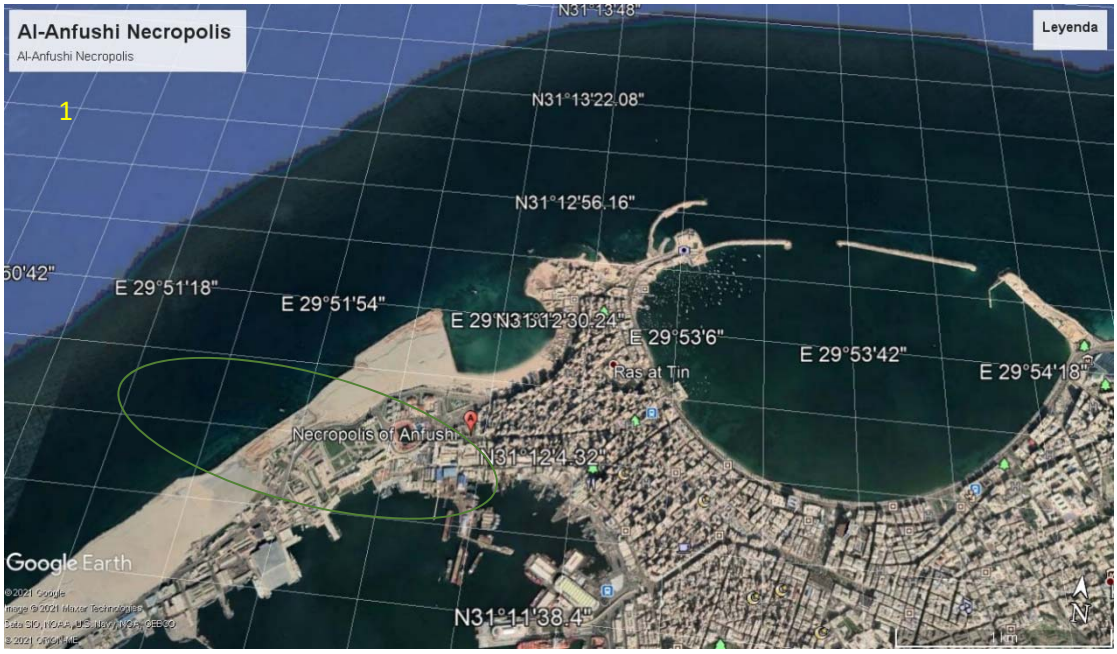
Figure 4. Al Anfushi tombs, 1) Google Earth image for the location of Al Anfushi tombs, 2) general view of Al Anfushi tombs, 3) and 4) durability problems (salt decay) of the elements and the construction materials of Al Anfushi tombs.

(The figure is in the next page)

[25] Kyriakos Savvopoulos (2013). The Polyvalent Nature of the Alexandrian Elite Hypogea: a case study in the Greco-Egyptian Cultural Interaction in the Hellenistic and Roman Periods. The Polyvalent Nature of the Alexandrian Elite Hypogea: a case study in the Greco-Egyptian Cultural Interaction in the Hellenistic and Roman Periods.Porto.

[26] Kyriakos Savvopoulos (2011). *Alexandrea in Aegypto. The Role of the Egyptian Tradition in the Hellenistic and Roman Periods: Ideology, Culture, Identity, and Public Lif*. PHD THESIS, FACULTY OF ARCHAEOLOGY, UNIVERSITEIT LEIDEN,

[27] http://www.alexandria.gov.eg/Alex/english/ANFUSHY%20NECOPOLIS.html


Al-Anfushi Necropolis
Al-Anfushi Necropolis
Leyenda
1
N31°13'48"
N31°13'22.08"
N31°12'56.16"
50'42"
E 29°51'18"
E 29°51'54"
E 29°53'6"
E 29°53'42"
E 29°54'18"
Ras at Tin
Necropolis of Anfushi
N31°12'30.24"
N31°12'4.32"
N31°11'38.4"
Google Earth
N
1 km


TOMB 2
2

4


3


4

2.2.3 Abusir (Giza, Egypt): Sahure pyramid

Of the sixty villages named Abusir in Egypt, only one is an archaeological site of first-class importance. It is located in the southern direction of the Giza Plateau and north of the Saqqara archaeological site and is considered one of the most enriched archaeological sites of the Memphis necropolis (**Figure 5**). The ancient name of Abusir is called Busiri "the house or temple of the Osiris". In this site, the work will focus on the study of the archaeologic construction materials of Sahure's pyramids and their durability.



Figure 5. (1) Location of the site on global earth map. (2) The map of Abusir area and its monuments. (3) General view for Sahure pyramid.

2.2.4 El-Ashmonein archaeological site (Minia, Egypt: Nero Temple

El-Ashmonein is a small village located in Mellway District of Minia governate, which is about 246 km from Cairo, situated on the western bank of Nile River, 27 m elevation and one of the ancient Egyptian metropolis capitals of the fifteenth century of Upper Egypt is called the “hare” (Figure 6). In this site, we will study the impact of agricultural and urban environment of the archaeological construction materials on Nero’s temple (Figure 8).

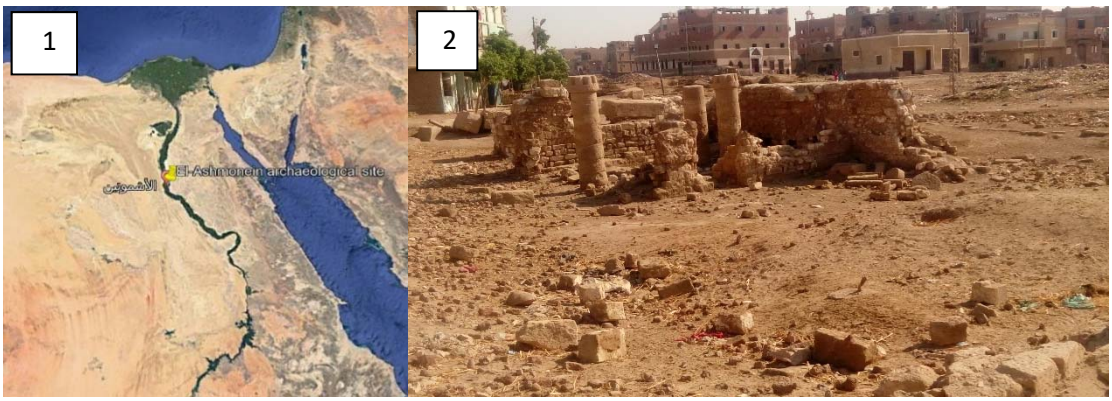


Figure 6. (1) Location of El-Ashmonein site on Egypt map. (2) General view for Nero’s temple.

2.2.5 Al Bagrawiya archaeological site (Sudan): Pyramids of Meroe

Al Bagrawiya archaeological site is a World Heritage Site with significant pyramid-shaped structures of the Meroe kingdom. Meroe was an ancient city in Sudan, and it was the seat of the government and the royal palace. The pyramids of Meroe back to the kingdom of Kush, between the 8th century BC and 4th century AD and were devoted as a necropolis site for the kings and queens of Meroe (Figure 7). In this part, the impact of sand dunes and flooding on the pyramids of Meroe will be carried out.

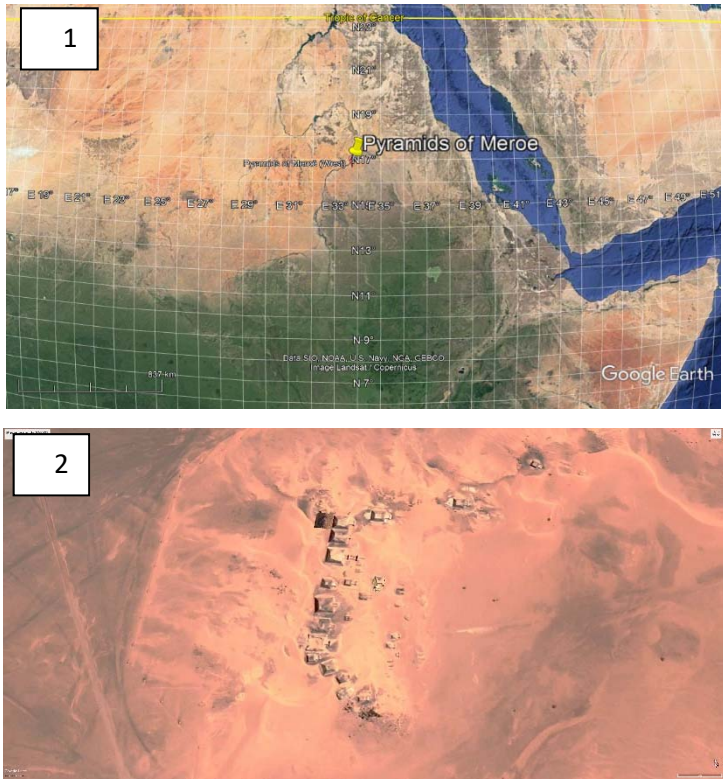


Figure 7. (1) Yellow pin is the location of Al Bagrawiya archaeological site. (2) General view for the pyramids of Meroe.

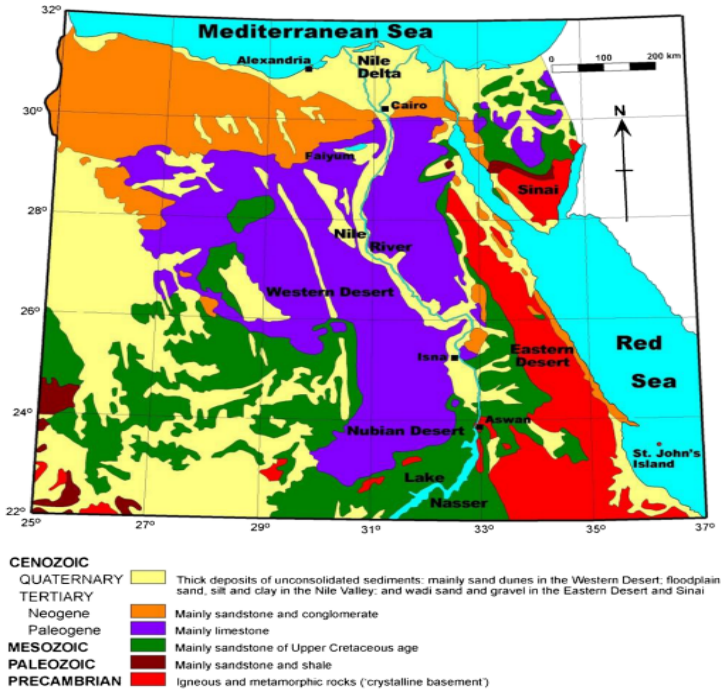
3. Regional geological context of the selected sites

Egypt covers 1000000 km^2 and it is classified into four major physical regions: Nile Valley and Nile Delta, Western Desert, Eastern Desert and Sinai Peninsula. Geologically, In Egypt there are mainly 5 types of lithologies in addition to unconsolidated Quaternary sediments (Figure 8-1), Egypt is composed of thick deposits of loose sediments mainly sand dunes in the western desert, flood plain, silty and clay in the Nile valley and sand and gravel in the eastern desert and Sinai, in the north west is mainly composed of sandstone and conglomerate, western and eastern desert are mainly composed of limestone with some formations in the eastern and western desert with mainly sandstone of upper cretaceous age and little formations in the south western desert are mainly from sandstone and shale and basement rocks and basement complex, are terms that are commonly applied to igneous and metamorphic rocks, overlaid by sedimentary strata. In the eastern and

southeastern desert, there are crystalline basement from igneous and metamorphic rocks [Hosny *et al*., 2014][28] [El-Sharkawi *et al*., 2020][29].

Sudan occupies 1,886,068 km^2 and its geological features ranges from Precambrian crystalline basement rocks to Quaternary unconsolidated alluvial deposits. The lithology of Sudan consists of Unconsolidated sedimentary deposits (Quaternary and Late Tertiary to Quaternary), Igneous Volcanic (Tertiary), Mesozoic Sedimentary Rocks - mainly Cretaceous (Upper Jurassic to Lower Cenozoic, mainly Cretaceous) and Precambrian Basement (Precambrian) [Worrall, 1957][30] (Figure 8-2).

1



[28] Hosny, A., Ali, S. M., & Abed, A. (2014). Study of the 26 December 2011 Aswan earthquake, Aswan area, South of Egypt. *Arabian Journal of Geosciences*, *7*(11), 4553–4562. https://doi.org/10.1007/s12517-013-1098-8

[29] El-Sharkawi M. et al. (2020) History of the Geological Research in Egypt. In: Hamimi Z., El-Barkooky A., Martínez Frías J., Fritz H., Abd El-Rahman Y. (eds) The Geology of Egypt. Regional Geology Reviews. Springer, Cham. https://doi.org/10.1007/978-3-030-15265-9_1

[30] Worrall, G. A. (1957). A simple introduction to the geology of the Sudan. Sudan Notes and Records, 38, 2–9. http://www.jstor.org/stable/41710729

Figure 8. (1) Geological map of Egypt (from Hosny *et al.*, 2014)[31]. (2) Geological map of Sudan (from Schlüter, 2008)[31].

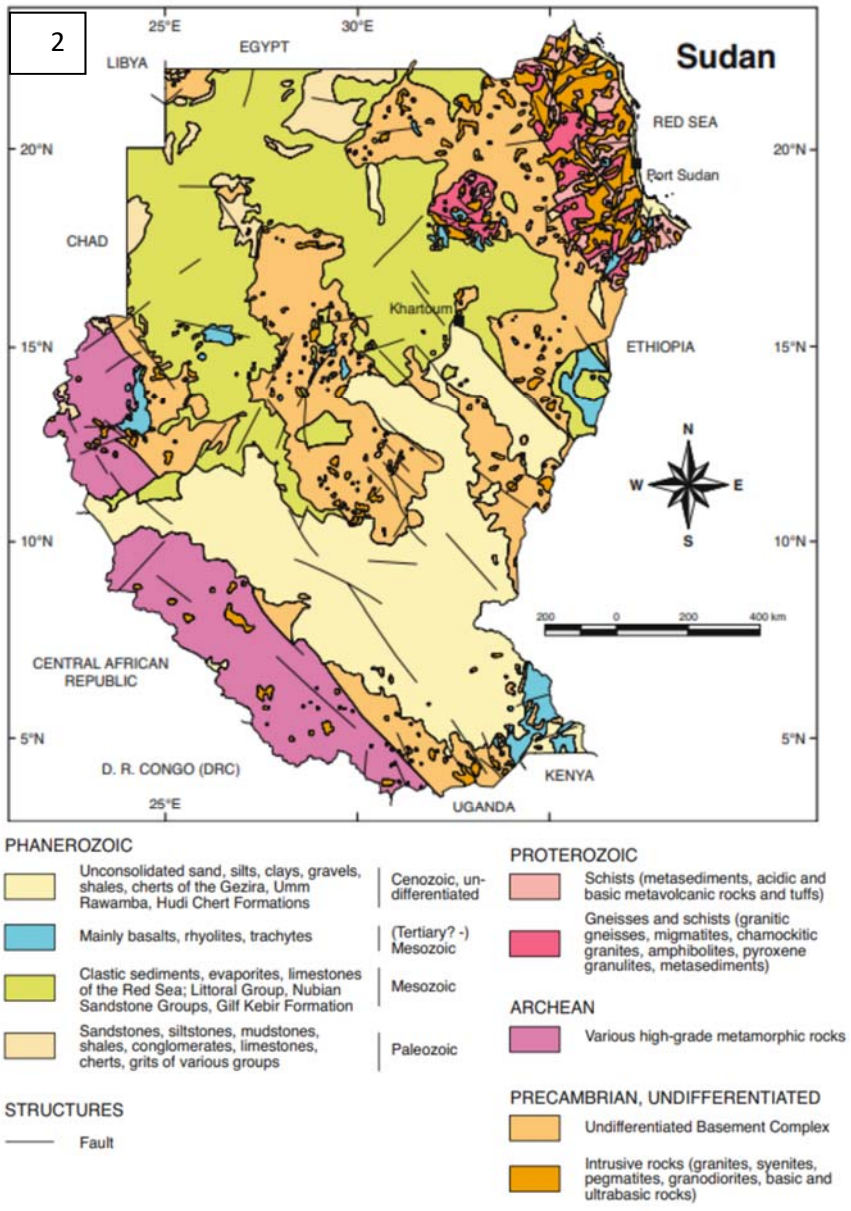


Figure 8. ***Cont*.**

[31] Schlüter, T. (2008). Geological Atlas of Africa. Springer Berlin, Heidelberg. https://doi.org/10.1007/978-3-540-76373-4

3.1 Aswan (Egypt)

Abaton temple of Osiris is situated at a short distance upstream from the First Cataract of the Nile, about 9 kilometers to the South of Aswan town. The underground of this region is formed by various rocks belonging to the Basement Complex, for instance granites, schists and gneisses, meta dolerites, aplites, pegmatites, and late minor dykes and neck intrusions, the coarse variety of the granite is the famous ornamental and building stone, the quarrying of which started more than 5000 years ago during the fourth dynasty of ancient Egypt. The Basement Complex is overlaid by sandstones of the Nubian formation (Upper Cretaceous) [Voûte, 1963][32] (Figure 9).

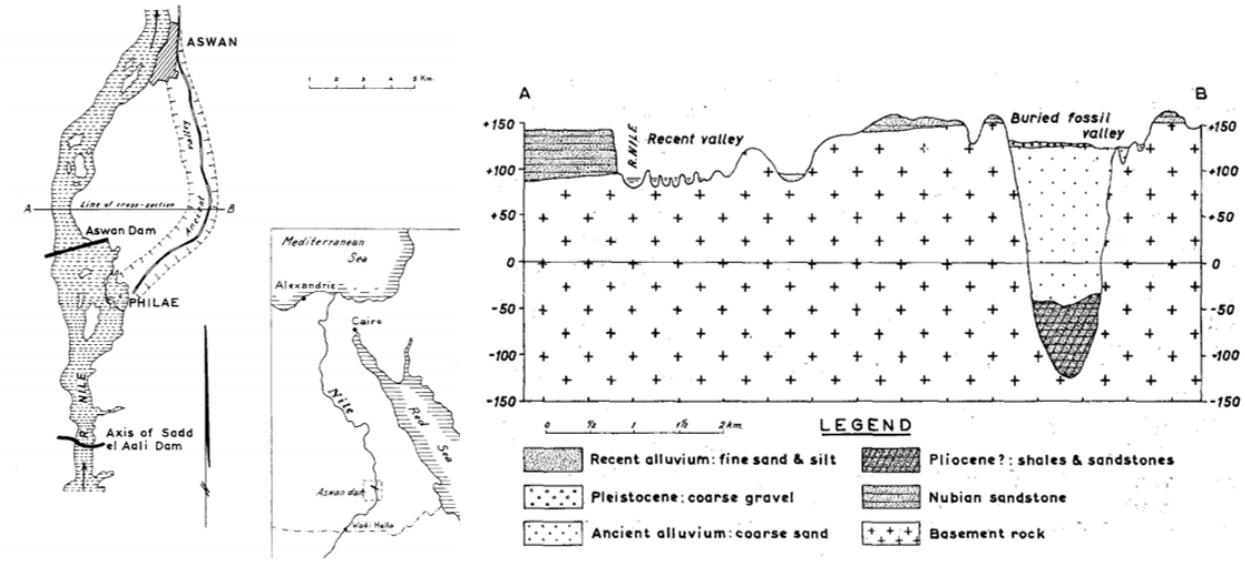


Figure 9. Regional geological setting of Philae area, Aswan [El-Sharkawi *et al*., 2020][33].

[32]Voûte, C. (1963). Some geological aspects of the conservation project for the Philae Temples in the Aswan Area. *Geologische Rundschau*, *52*(2), 665–675. https://doi.org/10.1007/BF01821149

[33] El-Sharkawi M. et al. (2020) History of the Geological Research in Egypt. In: Hamimi Z., El-Barkooky A., Martínez Frías J., Fritz H., Abd El-Rahman Y. (eds) The Geology of Egypt. Regional Geology Reviews. Springer, Cham. https://doi.org/10.1007/978-3-030-15265-9_1

3.2 Alexandria (Egypt)

Lithographically, Alexandria coastline is featured as unconformity surface and is composed of soil sediments, oolitic sand and clay, oolitic limestone, grey shelly dolomite, marly dolomite, oncolitic limestone and dolomite, shelly limestone and core sections comprise largely bioclastic (shelly) and muddy carbonate sand strata interbedded with fine-grained sandy silt, silty mud, and dark organic-rich layers [Ibrahim & Mansour, 2002][34] [Stanley *et al.,* 2006][35] (Figure 10).

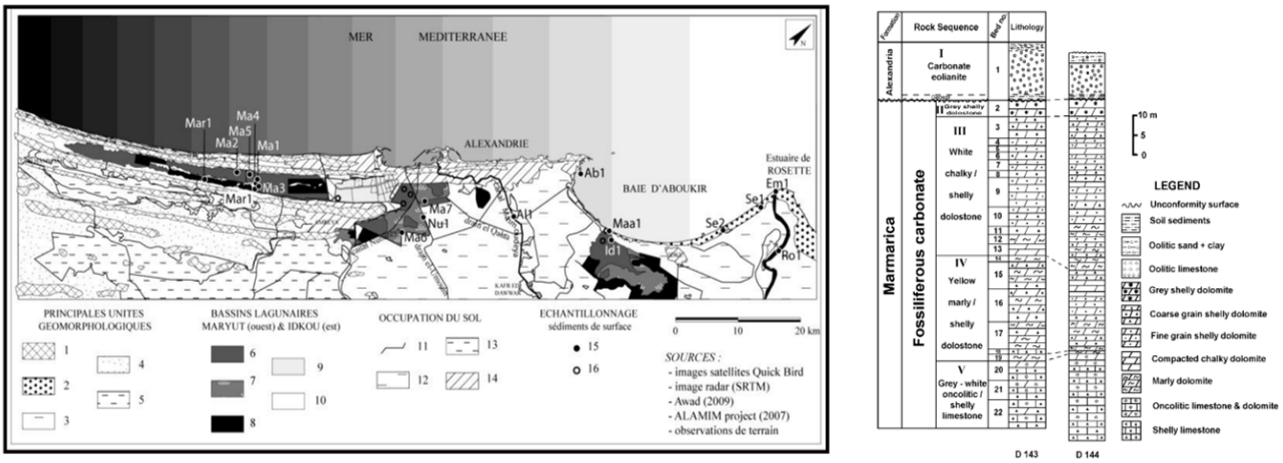


Figure 10. Geomorphological units of Alexandria and its lithology [Torab, 2013][36] [Ibrahim & Mansour, 2002].

[34] Ibrahim, M. I. A., & Mansour, A. M. S. (2002). Biostratigraphy and palaeoecological interpretation of the Miocene–Pleistocene sequence at El-Dabaa, northwestern Egypt. *Journal of Micropalaeontology*, *21*(1), 51–65. https://doi.org/10.1144/jm.21.1.51

[35]Stanley, J. D., Jorstad, T. F., & Goddio, F. (2006). Human impact on sediment mass movement and submergence of ancient sites in the two harbours of Alexandria, Egypt. *Norsk Geologisk Tidsskrift*, *86*(3), 337–350.

[36] Torab, M. M. (2013). Paleo-geomorphological map of Alexandria site, Egypt by using submerged archaeological and other evidence. *International Conference on Agriculture, Science and Engineering*, 16.

[36] Fielding, L., Najman, Y., Millar, I., Butterworth, P., Ando, S., Padoan, M., Barfod, D., & Kneller, B. (2016) A detrital record of the Nile River and its catchment. Journal of the Geological Society, 174(2), 301–317. https://doi.org/10.1144/jgs2016-075

3.3 Abusir (Giza, Egypt)

Generally, the Memphis area consists of different geological features, such as Nile silts, which are located on the eastern and western sides of the Nile River and adjacent to the archaeological sites in Memphis, Wadi (Valley). In addition, deposits include neonile deposits, pronile deposits, undifferentiated pronile deposits, limestone intercalated with shale stones, and Cretaceous formations [Barta, 2015][37] (Figure 11). Specifically, Abusir geological formations are considered from the Late Eocene, and Maadi limestone, clay-limestone, and marls crop out (tafla).

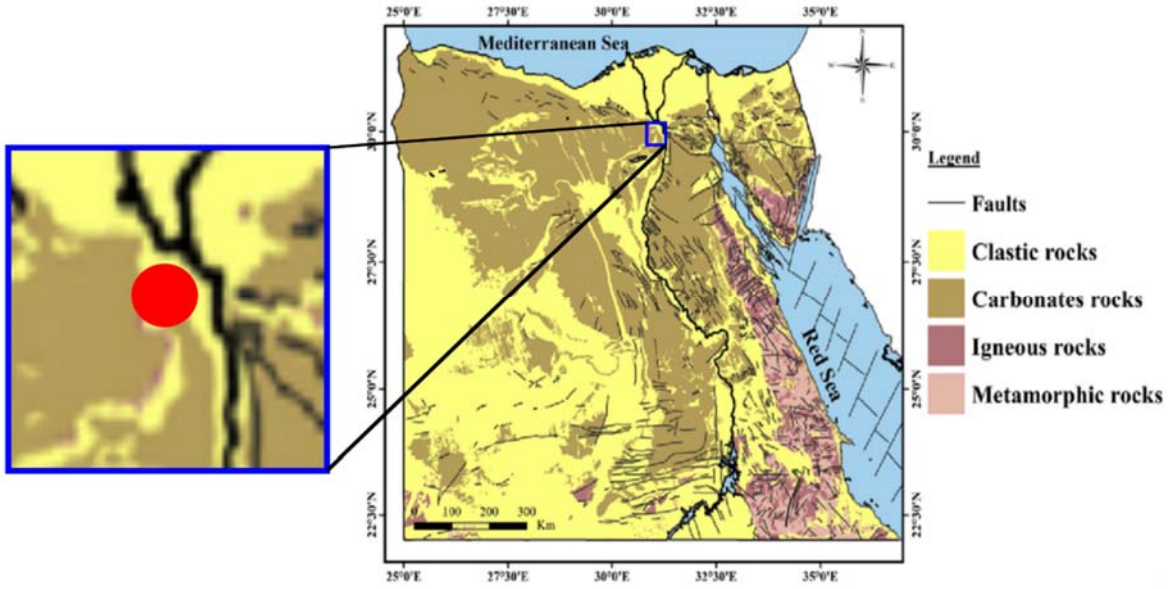


Figure 11. General map of Egypt including the geological setting of the studied area in Abusir in red circle (edited after Abdel Zaher et al., 2018)[38].

[37] Bárta M. Abusir in the Third Millennium BC. https://cegu2.ff.cuni.cz/en/research/projects/field-projects/abusir/abusir-in-the-third-millennium-bc/ (2015). Accessed 08 Mar 2022.

[38] Abdel Zaher, M., Elbarbary, S., El-Shahat, A., Mesbah, H., & Embaby, A. (2018). Geothermal resources in Egypt integrated with GIS-based analysis. *Journal of Volcanology and Geothermal Research*, *365*, 1–12. https://doi.org/https://doi.org/10.1016/j.jvolgeores.2018.09.013

3.4 El-Ashmonein archaeological site, Minia (Egypt)

Minia is featured by sedimentary successions geologically. The sedimentary boundaries range from the Middle Eocene to Pleistocene and Holocene (Figure 12). Limestone (fissured, chalky, silicified, and nummulitic belong to Eocene rocks. In addition, Oligocene sands and gravels, Pliocene dark clays, Pleistocene alluvial deposits (sand, gravel) and Holocene Nile silt belong to post-Eocene deposits (Ibrahim and Lyons, 2017)[39]. Geomorphologically, the El-Ashmonein archaeological site is formed by the annual deposition of river sediments (mud and silt) during flooding events between August and October. This type of soil represents most of the territory of Minia governorate and its villages near the border of the eastern highlands and western desert, while the calcareous soil covers the land available for eastern highlands, near Maghagha and Bani Mazar cities [Moneim et al., 2017] [40].

[39] Ibrahim, R.G.M., Lyons, W.B. (2017). Assessment of the Hydrogeochemical Processes Affecting Groundwater Quality in the Eocene Limestone Aquifer at the Desert Fringes of El Minia Governorate, Egypt. Aquat Geochem 23, 33–52. https://doi.org/10.1007/s10498-016-9298-y

[40] Moneim, A.A.A., Fernández-Álvarez, J.P., Abu El Ella, E.M., Masoud, A.M., (2016). Groundwater management at West El-Minia Desert Area, Egypt using numerical modelling. J Geosci Environ Prot; 04:66–76. https://doi.org/10.4236/gep.2016.47008.

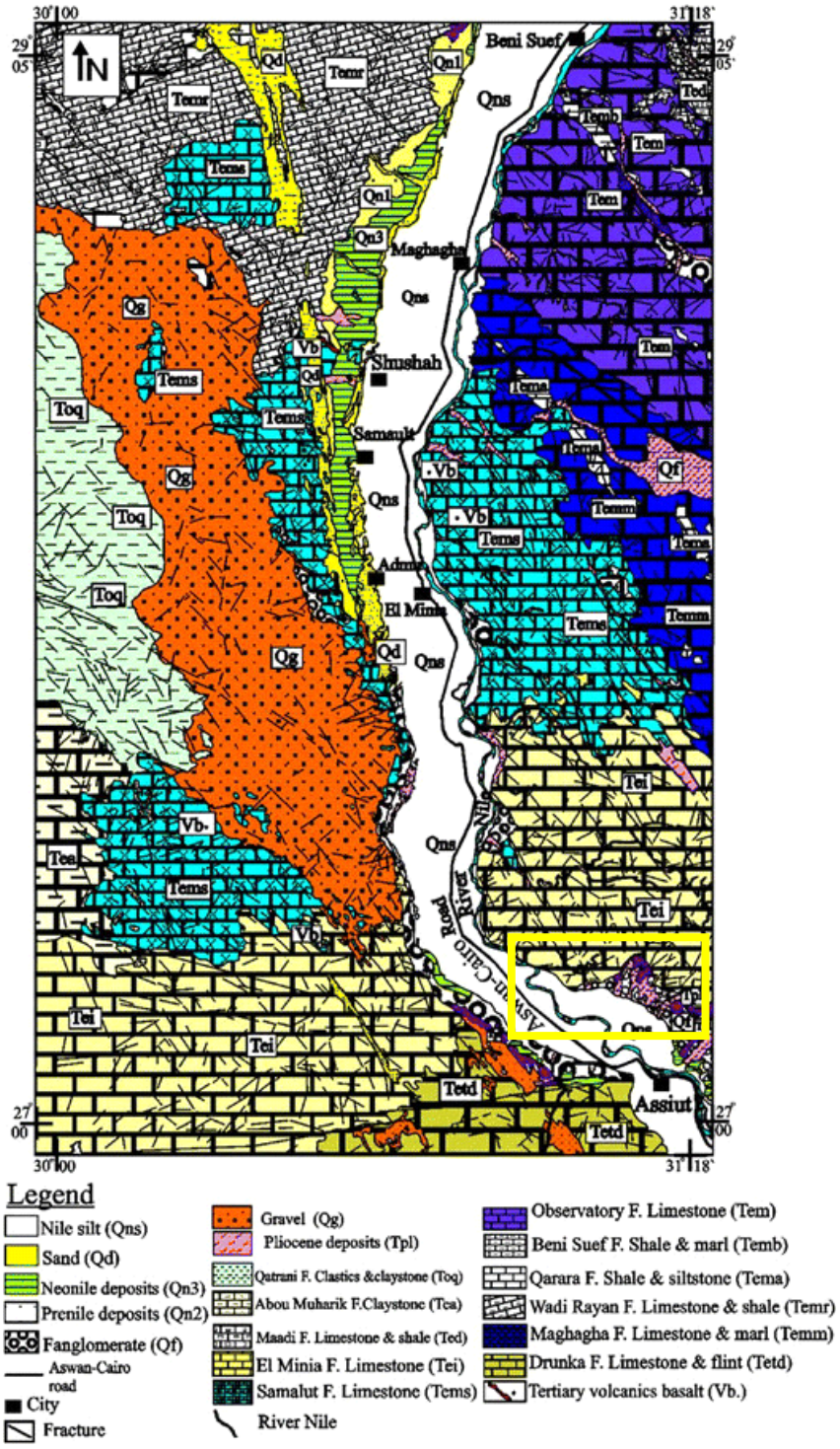
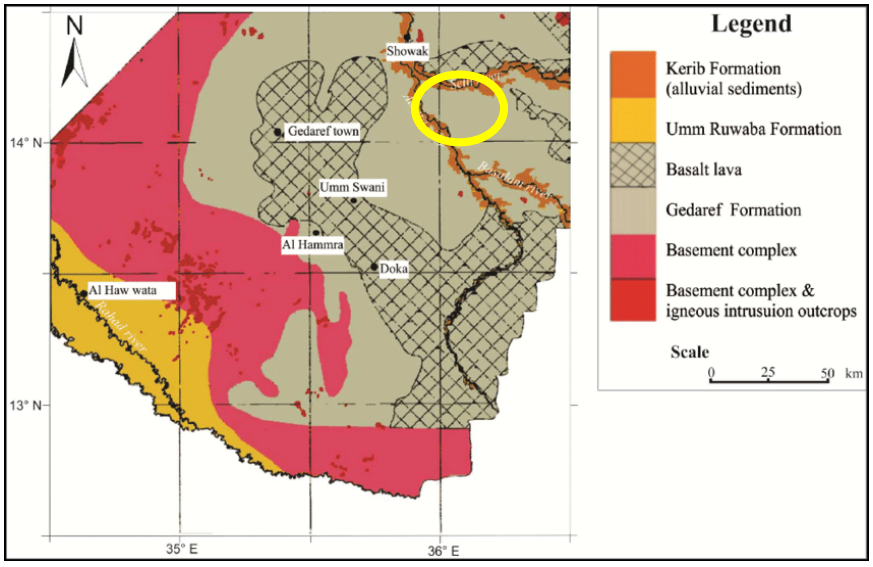


Figure 12. Geologic map of El Minia (from Ibrahim and Lyons, 2017). Yellow rectangle is Mellawy center which includes El-Ashmonein archaeological site.

3.5 Al Bagrawiya archaeological site (Sudan)

The Sudan plain consists of dark clays and red-brown sands [Whiteman, 1966][41]. The general geological column of Sudan is composed of coastal plain deposits, Nubian formations, Paleozoic sandstone formations, and a basement complex (mainly Precambrian). Deposition of the fluvial and marine sediments overlying the amalgamated terranes, from the Cambrian onwards was because of the erosion of the Trans- Gondwanan Mountain belt and subsequent recycling of the eroded detritus during later inversion tectonics [Fielding et al., 2016][42]. The geology of Al Bagrawiya archaeological site consists mainly of four formations: 1) the basement complex; 2) the Nubian series; 3) the alluvium; and 4) the surface deposits of wind-blown sand [Whiteman, 1966] (Figure 13).



[41] Whiteman, A. J. (1966) 'GEOLOGY AND SCENERY OF THE SUDAN. Sudan Notes and Records, vol. 47.pp. 137–44, http://www.jstor.org/stable/44947310. Accessed 25 Apr. 2022.

[42] Fielding, L., Najman, Y., Millar, I., Butterworth, P., Ando, S., Padoan, M., Barfod, D., & Kneller, B. (2016) A detrital record of the Nile River and its catchment. Journal of the Geological Society, 174(2), 301–317. https://doi.org/10.1144/jgs2016-075

Figure 13. Geological map of studied area in yellow circle (from Osman et al., 2016)[43].

3.- Hipótesis y Objetivos

3.1 Hypotheses

The main scientific questions to answer and hypotheses are:

- Nile river water has effective role in damaging of underwater construction materials or contacted to water?

Hypothesis 1: The archaeometrical studies through examination, investigation and analysis will be carried out to evaluate the influence of Nile River water upon the total and partial submerged archaeological building.

- Does coastal environment influence on archaeological buildings characteristics adjacent to sea?

Hypothesis 2: The saline water influence on the physical (porosity and density) and mechanical (compressive strength) properties of construction materials due to the salt attack from the sea (Mediterranean Sea at Alexandria) and this assessment study is going to be carried out throughout investigative, analytical, and testing studies.

- Is the desert environment aggressive to archaeological construction materials?

Hypothesis 3: The geoenvironmental impact of the desert can be aggressive especially the variations of temperature degrees, wind and rains on the construction materials. The

[43] Osman, A. F. I., Ibrahim, A., Abuobida, Y., Eisawi, A. A. M., & Alhadi, M. (2016). *Sedimentary Facies and Depositional Environment of the Gedaref Formation, Sedimentary Facies and Depositional Environment of the Gedaref Formation, Eastern Sudan*. *April*. https://doi.org/10.13140/RG.2.1.4000.5521

research will address monitoring study for the climate and environmental data in the sites and their impact on the building materials through analysis and microscopic studies.

- What is the impact of the urban environment on the durability of the construction materials?

Hypothesis 4: The urban environments can affect the construction materials especially through the subsurface water coming from the near houses and agricultural activities. The assessment of the urban area of the urban area will be conducted through analysis of the construction materials and their alteration types.

- Are there preservation strategies should be done to protect the archaeological underwater stone construction materials?

Hypothesis 5: The research is going to present conservation, restoration, and management plan for the cultural heritage in different environmental sites through development some nanomaterials which used in protection of stone surfaces subjected to water and development of structural pins to repair the damaged stone block of the underwater archaeological buildings.

3.2 Objectives

The main objective of the research is to compare and assess the durability problems of the selected archaeological buildings related with aqueous ambient (Nile River or Mediterranean Sea), comparing with aerial ambient (desert and urban environment). And the specific objectives are:

1. Identify the construction materials of the selected archaeological buildings.
2. Specify the geochemical, petrophysical characterizations for the selected buildings in different sites.
3. Study the deterioration processes of different construction materials in different environments: marine, fluvial, desertic, and urban.

4. Analyze and assess the risks and geo hazards of the selected sites with different environments.

5. Develop promising Nano multi-functional materials for conservation especially for the mortars as building material.

3.3 Significance

The most significant outputs of the doctoral research will be 1) contributing to understand how can aqueous and subaerial environments affecting the Egyptian cultural heritage; 2) getting new information for the construction materials used for the selected submerged building in Aswan; 3) evaluating the impact of different water environments upon selected archaeological buildings; 4) study the construction materials and their decay in the urban and desert environments, as well; 5) using non-destructive methods for assessment of the underwater archaeological construction materials; 6) getting new nano-composite multi-functional materials for stone and mortar surfaces protection from water and environmental impacts; and, finally, 7) contributing to preservation of world cultural heritage in different environmental challenges.

4- Metodología

The scientific methodology for the research will rely on analytical, testing and experimental studies with destructive (DT) and non-destructive techniques (NDT) for evaluation/assessment of construction materials of the selected archaeological buildings and their decay patterns, practically all of these equipment and techniques are found both in the laboratory of Geoarchaeology and Archaeometry (UGEA-PHAM) at Department of Earth Sciences, INHARMAR and SCiCYT, Faculty of Sciences, University of Cadiz. Additionally, a stay in an international research center is proposed to complete the doctoral studies.

- **Chemical and mineralogical analysis:**

1. X-Ray Fluorescence (XRF)

1.1 X-Ray micro-fluorescence (mXRF)

1.2 Portable X-ray fluorescence (pXRF)

X Ray florescence is a usual chemical elemental analysis for the archaeological (inorganic) materials. X-ray micro-fluorescence is a quantitative elemental analysis for the identification of major and some trace elements. The presence of some elements can be the responsible for the chemical alteration of the archaeological stone blocks in the Nile River or in coastal environment or to detect the by-products as result of chemical reactions between the substrate and environment. In the current study, XRF portable is going to be used as an advanced and non-destructive tool especially for the archaeological matters.

2. X-ray diffraction (XRD)

X-Ray Diffraction is a qualitative analytical technique, and it is an important tool in archaeometric studies to identify the mineral compositions of the archaeological matters and detect different original minerals of the substrate and altered minerals of as result of alterations and weathering impacts upon the archaeological underwater buildings.

3. Micro Raman spectroscopy (portable)

Raman spectroscopy is a quantitative powerful non-destructive technique for determination of the chemical compositions of the archaeological materials and give more information about phase, polymorphs, crystallinity, and molecular interactions of the archaeological matters.

4. Fourier-transform infrared spectroscopy (FTIR) (portable)

Fourier-transform infrared spectroscopy is very powerful tool to determine the compounds of the archaeological materials such as stone surfaces and crusts and widely used in organic archaeological materials and in inorganic materials.

5. Optical binocular

Simple optical or digital binocular is perfect tool for examining the morphology of the stone surfaces and detect the problems and weathering aspects and decay forms of the natural stones submerged in water or subjected to water environment.

6. Optical polarized-light microscope

It is a petrological microscope used with transmitted light to identify the minerals and the alteration products as well. Petrological study enhances the archaeometrical studies of the archaeological stone buildings and identify their intrinsic and extrinsic interactions.

7. Scanning electron microscope (SEM)

It uses a focused high energy of electrons over the samples to scan the surface and to see morphological and compositional aspects of the grains and their problems related with decay in perfect due to salt and their crystallizations processes. SEM with EDX detector will be used as elemental analysis for the samples.

8. Cathodoluminescence Microscopy

Cathodoluminescence is an electromagnetic radiation ranging from UV to NIR on electromagnetic spectrum when an electron beam from scanning electron microscope or filament interacts with material, a multitude of processes occur which can have employed for various kinds of microscopy [website][44]. This advanced microscope is very adequate to investigate internal structures with ultrahigh spatial resolution of the natural stone which used in built heritage.

- **Physical properties**

1. Bulk and apparent density.

Density, as applied to any kind of homogeneous monophasic material of mass (M) and volume (V), is expressed as the ratio of M to V. Under specified conditions, this definition leads to unique values that represent a well-defined property of the material. For

[44] https://www.delmic.com/en/techniques/cathodoluminescence

heterogeneous and multiphasic materials, such as porous media, however, application of this definition can lead to different results, depending on the exact way the mass and volume of the system are defined [Sataloff & Kost, 2015][45]. Density gives an indication to the degradation state of the stone-built heritage.

2. Spectrophotometry (Colour analysis).

This is a basic process to measure and detect the change in colours of the archaeological stone heritage visually. Naturally, the minimum inhomogeneity depends on colour diversity of the scanned material, spatial distribution of this diversity (soft, long-range transitions or sharp, abrupt colour changes), rock texture, colour, and size of embedded grains, but also of shape and size of the sampling window and the number of "bins" used during data aggregation. Generally, the inhomogeneity is "sufficient" as long as the peaks remain above the significance lines ("white noise" lines) of the Lomb periodogram (90–95%) [Halász & Halmai, 2015][46].

- **Hydric properties**

1. Water absorption.

Water absorption (WA) is considered an important hydric attribute/test of stone-built heritage, WA reflects the mechanical and physical characteristics of the stone-built heritage and generally the durability of the natural stones. Lower water absorption generally correlates to a greater durability, as it restricts the passage of deleterious solutions, but a larger pore size can assist with durability by reducing the pressure applied by salt or ice crystallization on the walls of the pore, in order to better evaluate the water absorption

[45] Sataloff, R. T., Johns, M. M., & Kost, K. M. (2015).*data collection handbook to support modelling impacts of radioactive material in soil and building structures, environmental science division* .Argonne national laborator.USA

[46] Halász, A., & Halmai, Á. (2015). *The color analysis method applied to homogeneous rocks*. *4*, 233–239. https://doi.org/10.1515/logos-2015-0019

of stones and drying features, the samples should first tested for real density, apparent density and open and total porosity [Ozcelik & Ozguven, 2014][47].

2. Porosity.

Porosity is the percentage of void space in a rock. It is defined as the ratio pore space divided by volume n= v (volume of the voids)/v (total volume). The porosity of a rock depends on many factors, including the rock type and how the grains of a rock are arranged. For example, crystalline rock such as granite has a very low porosity (<1%) since the only pore spaces are the tiny, long, thin cracks between the individual mineral grains. On the other hand, sandstones, typically, have much higher porosities (10–35%) because the individual sand or mineral grains do not fit together closely, allowing larger pore spaces [website][48].

4.1 : Outline of the proposed methodology for the research:

Chapter 1: Introduction.

Chapter 2: Materials and methodology.

Chapter 3: Geoenvironmental investigation of Sahure's pyramid, Abusir Archeological site, Giza, Egypt.

Chapter 4: Salt weathering impact on Nero/Ramses II Temple at El Ashmonein archaeological site (Hermopolis Magna), Egypt.

Chapter 5: Coastal environment impact on the construction materials of Anfushi's Necropolis (Pharos's Island) in Alexandria, Egypt.

[47] Ozcelik, Y., & Ozguven, A. (2014). Water absorption and drying features of different natural building stones. *Construction and Building Materials*, *63*, 257–270. https://doi.org/10.1016/j.conbuildmat.2014.04.030

[48] https://wgnhs.wisc.edu/maps-data/data/rock-properties/understanding-porosity-density/

Chapter 6: Multianalytical diagnostic approaches for the assessment of materials and decay of the archaeological sandstone of Osiris Temple (The Abaton) in Bigeh Island, Philae (Aswan, Egypt).

Chapter 7: Sand dunes movement and flooding risk analysis for the pyramids of Meroe, Al Bagrawiya archaeological site, Sudan

Chapter 8: Creation of the multifunctional nano materials for the application on archaeological lime mortars on ancient structures

Chapter 9: Conclusions

Bibliography

5- Justificación de recursos disponibles

*(Describir los **materiales, infraestructuras y equipamientos singulares** disponibles que permitirán abordar la metodología propuesta.)*

The previous proposal is going to be carried out in the unit of Geoarchaeology and Archaeometry Applied to Historic and Artistic and Monumental Heritage at Department of Earth Sciences, Faculty of Sciences, University of Cadiz (UGEA-PHAM) (https://politicacientifica.uca.es/unidad-de-geoarqueologia-y-arqueometria-aplicadas-al-patrimonio-historico-artistico-y-monumental-ugea-pham/).

The research will depend on the following sources for data acquisition such as libraries and online libraries, organizations and Museums as following:

- **Universities and institutes libraries in archaeology**

1. Library of French institute for oriental archaeology in Cairo http://bib.ifao.egnet.net/F/?func=file&file_name=find-b

2. Library of Cadiz university at Campus of Cadiz and Campus of Puerto Real (Área de Biblioteca – Portal de la Biblioteca (uca.es)
3. Library of American research centre in Egypt https://www.arce.org/resource-library
4. Library of the Netherlands-Flemish Institute in Cairo (NVIC) http://www.nvic.org.eg/Site/AboutUS.aspx
5. Central library of Cairo University https://librarytechnology.org/library/34870
6. Library of Faculty of Archaeology, Cairo university http://fa-arch.cu.edu.eg/en/EgyLibrary.html
7. The UCL Institute of Archaeology https://www.ucl.ac.uk/archaeology/about-us/library/archaeology-library-faqs
8. Society for American archaeology https://www.saa.org/about-archaeology/knowledge-library
9. Library of Oxford for Archaeology https://libguides.bodleian.ox.ac.uk/archaeology
10. Archaeology data service https://archaeologydataservice.ac.uk/library/
11. Princeton University library https://libguides.princeton.edu/artarchhistarch/archaeology
12. Library of University of Cambridge in archaeology https://libguides.cam.ac.uk/archanth
13. library of Brown university in Archaeology https://libguides.brown.edu/archaeology
14. library of Boston university https://www.bu.edu/library/research/collections/collection-development/cdarch/
15. library of Columbia University https://guides.library.columbia.edu/archaeology_resources_for_research/websites_in_archaeology
16. Library of California University, Berkeley https://ahma.berkeley.edu/resources/libraries
17. Library of The Getty Research Institute https://www.getty.edu/research/library/

18. Library of Pennsylvania University, Penn libraries https://www.library.upenn.edu/collections/subjects/archaeology
19. Library of Oslo University https://www.ub.uio.no/english/libraries/uhs/ark/
20. The Hebrew university of Jerusalem https://archaeology.huji.ac.il/book/library
21. Libraries of Worcestershire County Council https://www.worcestershire.gov.uk/info/20005/libraries_archive_and_archaeology
22. Library of Cincinnati University https://guides.libraries.uc.edu/media/archaeology
23. Library of Clare County https://www.clarelibrary.ie/eolas/coclare/archaeology/index.htm
24. Library of university of Leiden https://www.library.universiteitleiden.nl/subject-guides/archaeology
25. Library of McGill University https://libraryguides.mcgill.ca/anthropology
26. The OA Library (Oxford Archaeology) https://library.thehumanjourney.net/
27. Smith college libraries https://libguides.smith.edu/archaeology
28. Library of Yale university https://guides.library.yale.edu/sb.php?subject_id=153
29. Library of Chicago university https://www.lib.uchicago.edu/about/directory/?view=staff&subject=Archaeology%20-%20Classical
30. Library of Brandeis university https://guides.library.brandeis.edu/archaeology
31. Library of Calgary university https://library.ucalgary.ca/sb.php?subject_id=52599, https://www.torontopubliclibrary.ca/search.jsp?N=4294698419+4293412298
32. Library of Michigan university https://apps.lib.umich.edu/browse/Archaeology

- **Organizations and associations libraries in archaeology**

1. UNESCO Library https://unesdoc.unesco.org/library
2. Library of National archaeological Museum, Greece https://www.namuseum.gr/en/vivliothiki/

3. International council of Museums libraries https://icom.museum/en/committee/international-association-of-libraries-and-museums-of-the-performing-arts/
4. Library of ICOMOS https://www.icomos.org/en/other-libraries-and-databases
5. Society for promotion of the Egyptian museum, Berlin http://www.egyptian-museum-berlin.com/e01.php
6. Society of archaeological science https://socarchsci.org/blog-sas-bulletin.html
7. Royal anthological association https://www.therai.org.uk/publications
8. International association of Egyptologists http://www.iae-egyptology.org/
9. European institute of underwater archaeology https://ieasm.institute/publications.php?lang=fr
10. The Egyptologists electronic forum http://www.egyptologyforum.org/
11. Egypt exploration society https://www.ees.ac.uk/
12. Current research in Egyptology http://cregyptology.org.uk/
13. Egyptology resources https://www.fitzmuseum.cam.ac.uk/er/institutions.html

- **Museums libraries**

1. Museum of Metropolitan library https://www.metmuseum.org/art/libraries-and-research-centers
2. The British Museum library https://www.britishmuseum.org/resources/library-and-archive
3. Museum of London library https://www.museumoflondon.org.uk/collections/access-and-enquiries/museum-london-library
4. National History Museum https://www.nhm.ac.uk/our-science/departments-and-staff/library-and-archives.html
5. Toledo museum of art https://www.toledomuseum.org/education/reference-library
6. Worcester museum https://www.worcesterart.org/collection/library/

7. Canadian museum of civilization https://thediscoverblog.com/tag/canadian-museum-of-civilization/
8. Philadelphia museum of art https://philamuseum.org/library/
9. American museum of natural history https://www.amnh.org/research/research-library
10. Bolton museum of Egyptology https://www.visitbolton.com/bolton-museum-egyptology
11. Petri museum of Egyptian archaeology https://www.ucl.ac.uk/culture/petrie-museum
12. Maidstone museum https://museum.maidstone.gov.uk/explore/collections/ancient-egyptians/
13. National museum of Liverpool https://www.liverpoolmuseums.org.uk/whatson/world-museum/exhibition/ancient-egypt
14. The Fitzwilliam Museum https://www.fitzmuseum.cam.ac.uk/digitalpublications
15. National museum of Scotland https://www.nms.ac.uk/collections-research/
16. Blackburn museum https://blackburnmuseum.org.uk/collections/egyptology/
17. Garstang museum https://www.liverpool.ac.uk/garstang-museum/
18. Macclesfield museum https://macclesfieldmuseums.co.uk/egyptology
19. Arizona state museum https://statemuseum.arizona.edu/visit/collections/library-and-archives

Department of Earth Sciences provides me an office at with computer and all tools of research such as pens and papers and internet. Also, they supported me to give me spaces in the laboratory of geoarchaeological studies to prepare my samples and keep them. Prof. Dr. Salvador Dominguez-Bella and Dr. Eduardo Molina supported me with all potentials of the department to upgrade my research process and doing my thesis and investigation in excellent environment.

For experimental work, University of Cadiz, in the Department of Earth Sciences and SCiCYT gave an access to all laboratories which benefit me in my research, and which is where the techniques and instruments described in the methodology section are located. That equipment consists of the following:

1) X-Ray Fluorescence (XRF)
2) X-Ray Diffraction (XRD)
3) Micro Raman spectroscopy (Portable)
4) Fourier-transform infrared spectroscopy (FTIR)
5) Digital binocular
6) Petrological microscope
7) Scanning electron microscope (SEM)
8) Cathodoluminescence microscope (CM)
9) Sample preparation laboratory

6- Planificación temporal de trabajo

(Exponer la distribución temporal del trabajo, indicando el periodo de ejecución de cada uno de los objetivos propuestos)

The Intended duration for research is 3 years (full time) from December 2020 to December 2023, it is expected that during my doctoral stay at University of Cadiz to publish scientific international papers and will be published according to the outcome and results of my research in cooperation with my supervisors from Earth Sciences Department, Faculty of Science:

Activities	**1st year (Aswan)**				**2nd year (Alexandria)**				**3rd year**			
Doctoral courses												

bibliographic material Acquisition and evaluation of												
Research Stay												
Experimental work												
Thin (polished) section preparation												
Mineralogy and petrographic description												
Optical microscopy (binocular)												
Cathodoluminescence												
SEM (BSE-SE-EDX)												
XRD												
XRF												
Hydric behaviour												
Mechanical test												
Dynamic properties (ultrasounds)												
Density												
Porosity												
Processing and interpretation of data												
Scientific production and reports												
Congresses												
Scientific papers submitted to JRC journals												
Thesis writing												

Defence of thesis												

Notes:

Congress:

1. Conference on Sudan studies in Warsaw (September 2021-Poland).
2. Conference on Nubian studies in Warsaw (August 2022-Poland).
3. Conference on Egyptology in Seville (May 2022- Spain)

Scientific papers:

1. Geoenvironmental investigation of Sahure's pyramid, Abusir Archaeological site, Giza, Egypt Underwater archaeology concepts and its approach for sustainable development.
2. Salt weathering impact on Nero/Ramses II Temple at El Ashmonein archaeological site (Hermopolis Magna), Egypt
3. Coastal environment impact on the construction materials of Anfushi's Necropolis (Pharos's Island) in Alexandria, Egypt
4. Multianalytical diagnostic approaches for the assessment of materials and decay of the archaeological sandstone of Osiris Temple (The Abaton) in Bigeh Island, Philae (Aswan, Egypt)
5. Sand dunes movement and flooding risk analysis for the pyramids of Meroe, Al Bagrawiya archaeological site, Sudan
6. Creation of the multifunctional nano materials for the application on archaeological lime mortars on ancient structures.

7- Implicaciones éticas y/o de bioseguridad de la investigación propuesta.

(Si el proyecto tiene implicaciones éticas y/o de bioseguridad, explicar las consideraciones, procedimientos o protocolos que se aplicarán en cumplimiento de la normativa vigente,

indicar las instalaciones de las que se dispondrá y aportar las autorizaciones preceptivas necesarias para la ejecución del proyecto.)

For this proposal, it is not appropriate to provide any additional information since they do not have any ethical or biosafety implications.

8- Bibliografía.

1. **Affatato, A. (2012).** Underwater Cultural Heritage: Sunken cities.
2. **Favis, R. L., Manders, M. R., & Underwood, C. J. (2012).** Training Manual for the UNESCO Foundation Course on the Protection and Management of Underwater Cultural Heritage in Asia and the Pacific. In Training Manual for the UNESCO Foundation Course on the Protection and Management of Underwater Cultural Heritage in Asia and the Pacific (p. 654).
3. **Veneranda, M. (2017).** Development of novel procedures for the preservation of archaeological irons and mural paintings. 2017(July).
4. **Crisci, G. M., La Russa, M. F., MacChione, M., Malagodi, M., Palermo, A. M., & Ruffolo, S. A. (2010).** Study of archaeological underwater finds: Deterioration and conservation. Applied Physics A: Materials Science and Processing, 100(3), 855–863. https://doi.org/10.1007/s00339-010-5661-9
5. **Amer, M., & Identity, C. (2016).** GoUNESCO Internship – Task 7. November.
6. **Cardell, C., Delalieux, F., Roumpopoulos, K., Moropoulou, A., Auger, F., & Van Grieken, R. (2003).** Salt-induced decay in calcareous stone monuments and buildings in a marine environment in SW France. Construction and Building Materials, 17(3), 165–179. https://doi.org/10.1016/S0950-0618(02)00104-6
7. **Abdel-Halim, A. M., & Aly-Eldeen, M. A. (2016).** Characteristics of Mediterranean Sea water in vicinity of Sidikerir Region, west of Alexandria, Egypt. Egyptian Journal of Aquatic Research, 42(2), 133–140. https://doi.org/10.1016/j.ejar.2016.05.002

8. **Zaghloul, E. A., Authority, N., Sensing, R., Sciences, S., & Zaghloul, E. A. (2016).** Physical geology and historical settlement in North Western Nile delta Region, Egypt. August 2013.
9. **Stanley, J. D., & Bernhardt, C. E. (2010).** Alexandria's Eastern Harbor, Egypt: Pollen, microscopic charcoal, and the transition from natural to human-modified basin. Journal of Coastal Research, 26(1), 67–79. https://doi.org/10.2112/JCOASTRES-D-09-00089.1
10. **Stanley, J. D., Carslon, R. W., Van Beek, G., Jorstad, T. F., & Landau, E. A. (2007).** Alexandria, Egypt, before Alexander the Great: A multidisciplinary approach yields rich discoveries. GSA Today, 17(8), 4–10. https://doi.org/10.1130/GSAT01708A.1
11. **Mohamed, A. A., Helal, A. M. A., Mohamed, A. M. E., Shokry, M. M. F., & Ezzelarab, M. (2016).** Effects of surface geology on the ground-motion at New Borg El-Arab City, Alexandria, Northern Egypt. NRIAG Journal of Astronomy and Geophysics, 5(1), 55–64. https://doi.org/10.1016/j.nrjag.2015.11.005
12. **Machek, M., Roxerová, Z., Janoušek, V., Staněk, M., Petrovský, E., & René, M. (2013).** Petrophysical and geochemical constraints on alteration processes in granites. In Studia Geophysica et Geodaetica (Vol. 57, Issue 4). https://doi.org/10.1007/s11200-013-0923-6
13. **Hemeda, S. (2016).** Non-linear static analysis and seismic performance of modern architectural heritage in Egypt. Mediterranean Archaeology and Archaeometry, 16(3), 1–16. https://doi.org/10.5281/zenodo.35520
14. **Hemeda, S. (2019).** 3D FE Analysis Model for Geotechnical Problems of Historic Masonry Structures (Vol. 2). Springer International Publishing. https://doi.org/10.1007/978-3-030-01923-5_16
15. **Hemeda, S., & Sonbol, A. (2020).** Sustainability problems of the Giza pyramids. Heritage Science, 8(1). https://doi.org/10.1186/s40494-020-0356-9
16. **Hemeda, S. (2019).** Carbon Fiber Reinforced Polymers (CFRP) for Strengthening and Seismic Retrofitting of Historic Circular Masonry Stone Columns (pp. 114–137). https://doi.org/10.1007/978-3-030-01932-7_11
17. **Hemeda, S., Fahmy, A., & Sonbol, A. (2019).** Geo-Environmental and Structural Problems of the First Successful True Pyramid, (Snefru Northern Pyramid) in Dahshur,

Egypt. Geotechnical and Geological Engineering, 37(4), 2463–2484. https://doi.org/10.1007/s10706-018-00769-x

18. **Abdelaziz, M., & Elsayed, M. (2019).** Underwater photogrammetry digital surface model (DSM) of the submerged site of the ancient lighthouse near Qaitbay fort in Alexandria, Egypt. ISPRS Annals of the Photogrammetry, Remote Sensing and Spatial Information Sciences, 42(2/W10), 1–8. https://doi.org/10.5194/isprs-archives-XLII-2-W10-1-2019
19. **Hemeda, S., Fahmy, A., & Sonbol, A. (2019).** Geo-Environmental and Structural Problems of the First Successful True Pyramid, (Snefru Northern Pyramid) in Dahshur, Egypt. Geotechnical and Geological Engineering, 37(4), 2463–2484. https://doi.org/10.1007/s10706-018-00769-x
20. **Adam, O., Hemada, S., & El-Hady, A. (2015).** Durability of decorative stones and other construction materials of Al-Tanbogha Al-Mardany mosque (1340 A.D) 14th century in Cairo. In EJARS" An International peer-reviewed journal published bi-annually (Vol. 5, Issue 1). http://ejars.sohag-univ.edu.eg/
21. **Hemeda, S., & Sonbol, A. (2020).** Sustainability problems of the Giza pyramids. Heritage Science, 8(1), 1–28. https://doi.org/10.1186/s40494-020-0356-9
22. **Hemeda, S. (2019).** Carbon Fiber Reinforced Polymers (CFRP) for Strengthening and Seismic Retrofitting of Historic Circular Masonry Stone Columns (Vol. 2). Springer International Publishing. https://doi.org/10.1007/978-3-030-01932-7_11
23. **A. Ragheb, R. (2014).** Alexandria's Eastern Entrance: Analysis of Qaitbay Waterfront Development. *International Journal of Civil, Environmental, Structural, Construction and Architectural Engineering*, *8*(8), 865–874.
24. **Hosny, A., Ali, S. M., & Abed, A. (2014).** Study of the 26 December 2011 Aswan earthquake, Aswan area, South of Egypt. *Arabian Journal of Geosciences*, *7*(11), 4553–4562. https://doi.org/10.1007/s12517-013-1098-8
25. **Hamdan, M. A., & Hassan, F. A. (2020).** *Quaternary of Egypt*. https://doi.org/10.1007/978-3-030-15265-9_12

26. **Voûte, C. (1963).** Some geological aspects of the conservation project for the Philae Temples in the Aswan Area. *Geologische Rundschau*, *52*(2), 665–675. https://doi.org/10.1007/BF01821149
27. **Stephenson, J. (2010).** People and Place. *Planning Theory and Practice*, *11*(1), 9–21. https://doi.org/10.1080/14649350903549878
28. **Stanley, J. D., Jorstad, T. F., & Goddio, F. (2006).** Human impact on sediment mass movement and submergence of ancient sites in the two harbours of Alexandria, Egypt. *Norsk Geologisk Tidsskrift*, *86*(3), 337–350.
29. **Ibrahim, M. I. A., & Mansour, A. M. S. (200**2). Biostratigraphy and palaeoecological interpretation of the Miocene–Pleistocene sequence at El-Dabaa, northwestern Egypt. *Journal of Micropalaeontology*, *21*(1), 51–65. https://doi.org/10.1144/jm.21.1.51
30. **Torab, M. M. (2013).** Paleo-geomorphological map of Alexandria site, Egypt by using submerged archaeological and other evidences. *International Conference on Agriculture, Science and Engineering*, 16.
31. **July, F. R. (2008).** *Atlas of the stones of Alexandria LightHouse (Egypt)*.
32. **Ozcelik, Y., & Ozguven, A. (2014).** Water absorption and drying features of different natural building stones. *Construction and Building Materials*, *63*, 257–270. https://doi.org/10.1016/j.conbuildmat.2014.04.030
33. **Halász, A., & Halmai, Á. (2015).** *The colour analysis method applied to homogeneous rocks*. *4*, 233–239. https://doi.org/10.1515/logos-2015-0019
34. **Wang, A., Han, J., Guo, L., Yu, J., & Zeng, P. (1994).** Database of Standard Raman Spectra of Minerals and Related Inorganic Crystals. *Applied Spectroscopy*, *48*(8), 959–968. https://doi.org/10.1366/0003702944029640
35. **Ben Mabrouk, K., Kauffmann, T. H., Aroui, H., & Fontana, M. D. (2013).** Raman study of cation effect on sulfate vibration modes in solid state and in aqueous solutions. *Journal of Raman Spectroscopy*, *44*(11), 1603–1608. https://doi.org/10.1002/jrs.4374
36. **Fitzner, B. J. (2016).** Investigation of Weathering Damage on Stone Monuments. *Geonomos*, 21–28. https://doi.org/10.18285/geonomos.v24i2.835
37. **McCabe, S., Smith, B. J., & Warke, P. A. (2007).** Preliminary observations on the impact of complex stress histories on sandstone response to salt weathering: Laboratory

simulations of process combinations. *Environmental Geology*, *52*(2), 269–276. https://doi.org/10.1007/s00254-006-0476-x

38. **Navarro, R., Pereira, D., Arévalo, E. F. De, Sebastián-pardo, E. M., & Rodriguez-navarro, C. (2021).** Weathering of serpentinite stone due to in situ generation of calcium and magnesium sulfates. *Construction and Building Materials*, *280*, 122402. https://doi.org/10.1016/j.conbuildmat.2021.122402
39. **Lopez-Arce, P., Doehne, E., Martin, W., & Pinchin, S. (2008).** Sales de sulfato magnésico y materiales de edificios históricos: Simulación experimental de laminaciones en calizas mediante ciclos de humedad relativa y cristalización de sales. *Materiales de Construccion*, *58*(289–290), 125–142. https://doi.org/10.3989/mc.2008.v58.i289-290.77
40. **Angeli, M., Benavente, D., Bigas, J. P., Menéndez, B., Hébert, R., & David, C. (2008).** Modification of the porous network by salt crystallization in experimentally weathered sedimentary stones. *Materials and Structures/Materiaux et Constructions*, *41*(6), 1091–1108. https://doi.org/10.1617/s11527-007-9308-z
41. **Erić, S., Matović, V., Kremenović, A., Colomban, P., Batoćanin, D. S., Nešković, M., & Jelikić, A. (2015).** The origin of Mg sulphate and other salts formed on pure calcium carbonate substrate - Tufa stone blocks built into the Gradac Monastery, Serbia. *Construction and Building Materials*, *98*, 25–34. https://doi.org/10.1016/j.conbuildmat.2015.08.101
42. **Benavente, D., de Jongh, M., & Cañaveras, J. C. (2021).** Weathering processes and mechanisms caused by capillary waters and pigeon droppings on porous limestones. *Minerals*, *11*(1), 1–16. https://doi.org/10.3390/min11010018
43. **Doehne, E., Selwitz, C., Carson, D., & de Tagle, A. (2001).** Prevention of Salt Damage to Monuments: Esem and Time-Lapse Studies. *Microscopy and Microanalysis*, *7*(S2), 466–467. https://doi.org/10.1017/s1431927600028403
44. **Menéndez, B. (2017).** Estimation of salt mixture damage on built cultural heritage from environmental conditions using ECOS-RUNSALT model. *Journal of Cultural Heritage*, *24*, 22–30. https://doi.org/10.1016/j.culher.2016.11.006

45. **Rodriguez-Navarro, C., & Doehne, E. (1999).** Salt weathering: Influence of evaporation rate, supersaturation and crystallization pattern. *Earth Surface Processes and Landforms*, *24*(2–3), 191–209. https://doi.org/10.1002/(sici)1096-9837(199903)24:3<191::aid-esp942>3.0.co;2-g
46. **Heinrichs, K., & Fitzner, B. (2007).** Stone monuments of the Nemrud Dag sanctuary/Turkey petrographical investigation and diagnosis of weathering damage. *Zeitschrift Der Deutschen Gesellschaft Für Geowissenschaften*, *158*(3), 519–548. https://doi.org/10.1127/1860-1804/2007/0158-0519
47. **Doehne, E., Selwitz, D., Carson, D., & Selwitz, C. (2006).** The damage mechanism of sodium sulfate in porous stone. *European Research on Cultural Heritage: State of the Art Studies: Proceedings of the ARCCHIP Workshops Supported from the EC 5th FP Project No. ICA1-CT-2000-70013. Vol. 5, November 2002*, *5*(January 2002), 127–146. file://localhost/Users/workstation/Documents/Sente/2006 Doehne The Damage Mechanism of Sodium Sulfate in Porous Stone.pdf%5Cnwww.itam.cas.cz/ arcchip/ http://publicationslist.org/data/eric.doehne/ref-129/2002_Doehne_NaSO4_SALTeXPERT.pdf%5Cnwww.itam.cas.cz
48. **Derluyn, H., Vontobel, P., Mannes, D., Derome, D., Lehmann, E., & Carmeliet, J. (2019).** Saline Water Evaporation and Crystallization-Induced Deformations in Building Stone: Insights from High-Resolution Neutron Radiography. *Transport in Porous Media*, *128*, 895-913. https://doi.org/10.1007/s11242-018-1151-x
49. **Watt, D., & Colston, B. (2000).** Investigating the effects of humidity and salt crystallisation on medieval masonry. *Building and Environment*, *35*(8), 737–749. https://doi.org/10.1016/S0360-1323(00)00015-9
50. **Franzoni, E. (2014).** Rising damp removal from historical masonries: A still open challenge. *Construction and Building Materials*, *54*, 123–136. https://doi.org/10.1016/j.conbuildmat.2013.12.054
51. **Kamh, G. M. E., Koltuk, S., & Ismael, H. (2017).** Refinement of categorization and scaling of weathering-related damage to natural stone: case study on oolitic limestone from El-Shatbi Tombs (Egypt). *Bulletin of Engineering Geology and the Environment*, *76*(1), 39–57. https://doi.org/10.1007/s10064-016-0946-7

52. **Doehne, E. (2002).** Geological Society Special Publication Salt Weathering: A Selective Review. *Geological Society Special Publication*, *205*(Flatt), 51–64.
53. **Doehne, E., Selwitz, C., Carson, D., de Tagle, A., & DeTagle, A. (2001).** Damage to monuments from the crystallization of mirabilite, thenardite and halite: mechanisms, environment, and preventive possibilities. *Eleventh Annual V. M. Goldschmidt Conference*, *1*(January), 3212. http://www.csa.com/partners/viewrecord.php?requester=gs&collection=TRD&recid=N0221149AH%5Cnhttp://www.lpi.usra.edu/meetings/gold2001/pdf/3212.pdf
54. **Seck, M. D., Keita, E., & Coussot, P. (2019).** Some Observations on the Impact of a Low-Solubility Ionic Solution on Drying Characteristics of a Model Porous Medium. *Transport in Porous Media*, *128*(3), 915–928. https://doi.org/10.1007/s11242-018-1169-0
55. **Menéndez, B. (2018).** Estimators of the impact of climate change in salt weathering of cultural heritage. *Geosciences (Switzerland)*, *8*(11). https://doi.org/10.3390/geosciences8110401



UCA

Universidad de Cádiz

CULTURAL HERITAGE PRESERVATION IS THE DUTY OF ALL

Doctoral Thesis